



# Étude du rôle des effecteurs de type III évolutivement conservés chez deux bactéries colonisatrices du xylème

Manuel Gonzalez Fuente

## ► To cite this version:

Manuel Gonzalez Fuente. Étude du rôle des effecteurs de type III évolutivement conservés chez deux bactéries colonisatrices du xylème. Interactions entre organismes. Université Paul Sabatier - Toulouse III, 2020. Français. NNT : 2020TOU30071 . tel-03738103

**HAL Id: tel-03738103**

**<https://theses.hal.science/tel-03738103>**

Submitted on 25 Jul 2022

**HAL** is a multi-disciplinary open access archive for the deposit and dissemination of scientific research documents, whether they are published or not. The documents may come from teaching and research institutions in France or abroad, or from public or private research centers.

L'archive ouverte pluridisciplinaire **HAL**, est destinée au dépôt et à la diffusion de documents scientifiques de niveau recherche, publiés ou non, émanant des établissements d'enseignement et de recherche français ou étrangers, des laboratoires publics ou privés.

# THÈSE

**En vue de l'obtention du  
DOCTORAT DE L'UNIVERSITÉ DE TOULOUSE**

**Délivré par l'Université Toulouse 3 - Paul Sabatier**

---

**Présentée et soutenue par  
Manuel GONZALEZ FUENTE**

Le 19 juin 2020

**Étude du rôle des effecteurs de type III évolutivement conservés  
chez deux bactéries colonisatrices du xylème**

---

Ecole doctorale : **SEVAB - Sciences Ecologiques, Vétérinaires, Agronomiques et  
Bioingenieries**

Spécialité : **Interactions plantes-microorganismes**

Unité de recherche :

**LIPM - Laboratoire des Interactions Plantes-Microorganismes**

Thèse dirigée par

**Nemo PEETERS et Laurent D. NOEL**

Jury

**Mme Carmen del Rosario BEUZÓN LÓPEZ, Rapporteure**

**M. Frederik BÖRNKE, Rapporteur**

**M. Ludovic BONHOMME, Rapporteur**

**M. Jean Philippe GALAUD, Examineur**

**M. Nemo PEETERS, Directeur de thèse**

**M. Laurent NOËL, Co-directeur de thèse**

# Acknowledgements

These three years have been one of the most rewarding, challenging, enjoyable and demanding experiences of my life and I would like to thank the people that have contributed to make it possible. First, I wish to express my sincere gratitude to my supervisors Laurent Noël and Nemo Peeters for the trust to take me in, the advice and support throughout this time, and the encouragement when my weird sense of “optimism” was kicking. I entered their lab as a shy and insecure student three years ago and they pushed me to become the much more proactive and autonomous researcher that I am today. I gratefully acknowledge the support from the LabEx TULIP, which funded this work through the “Young Scientists for the Future” program. My sincere thanks as well to Richard Berthomé and Lionel Navarro, members of my PhD committee, for their objective support and insightful advice.

A very special gratitude goes to all the people from the SIX team who have contributed to create such a great and welcoming work environment. All the help, lunch and coffee breaks, scientific and non-scientific discussions, outings, cakes and gossip have made these three years a lot easier and forced me to speak French. Thanks to Matthieu for his always classy humor; Noe for the motivation to continue this project and providing a small Spanish refuge within the team; Corinne for all the help inside and outside of the lab and motivation to do (some) sport; Caroline for the venting and chocolate, Alice for giving me the chance to teach at the University and the needed breaks late in the evening; Carine for her help and all the gossip; Manue for the immeasurable help during these years for which I consider her as the third supervisor of this thesis; Julien for the bureau vicinity, company and long discussions; and Jean-Marc for his gastronomic contribution. I would also like to thank the people that, although are not in the team anymore, contributed to its good environment and whose presence has been greatly missed during the last months: Aude for her help, great advice and empathy even in the distance; Ivanna for her immense humor and integrating me when I first arrived; and David for all the help, the parties and most notably our existential discussions.

My sincere gratitude to all the LIPM for providing a great scientific environment, particularly to the common services (administration, kitchen, informatics, greenhouse...) whose help in everyday work made my work much easier and allowed me to focus on my research. A particular mention to Céline for the hours spent generating all the transgenic lines and teaching me all in the process; Sébastien for developing, debugging (and there was a lot to debug...) and

keeping updated EffectorK; and Fabrice, Claudette, Marine and Anaïs for taking care of all the transgenic and suppressor plants that occupied several modules at certain times.

I would also like to thank several people from the lab whose scientific and personal contribution to this thesis has been of a great importance to me: David and Lea, two of the most valuable friendships I get from Toulouse and who have helped me the most during the worst moments of this thesis; Claire for her infectious energy and motivation and her empathy; Ben, for integrating me from the first day; Antho for the scarce but sincere talks and all the food and beer recommendations; Daniela and Camilo, for all the parties, trips and serious (ant not-so-serious) discussions; Arry; Alex; Eli; Fernanda; Carolina; Nathalie; Jai; Rekha; Lorenzo; Arianne; and many others that I might forget.

I am equally indebted to all my friends and family whose unconditional support, even in the distance, has allowed me to stand where I stand today. In special, I would like to thank my parents Araceli and Tomás who, even if they have not always understood what I was doing, have always supported my choices and valued my efforts. Making them proud has always been one of my major life motivations and I hope the present thesis contributes to this goal. Special thanks as well to my brother Ruben and my cousin Leticia for their continuous support. I would also like to acknowledge the support from all my friends from Burgos, particularly Nuria, Rubén, Javi and Sergio; from Salamanca, particularly Andrés, Jorge, Isa, Janire, Kroten, Loreto and Marina; and from Kiel, particularly Judit, Clara, Pau and Alice. Their messages, phone calls and few visits served always to recharge my batteries when feeling homesick.

And finally, I would also like to express my sincere gratitude to Carmen Rosario Beuzón, Ludovic Bonhomme, Frederik Böncke and Jean Philippe Galaud for having accepted to review this manuscript and participated in the defense jury.



# Remerciements

Ces trois années ont été l'une des expériences les plus enrichissantes, les plus stimulantes, les plus agréables et les plus exigeantes de toute ma vie et je tiens à remercier les personnes qui ont contribué à la rendre possible. Tout d'abord, je tiens à exprimer ma sincère gratitude à mes superviseurs Laurent Noël et Nemo Peeters pour la confiance qu'ils m'ont accordée, les conseils et le soutien qu'ils m'ont apportés tout au long de cette période, et les encouragements que j'ai reçus lorsque mon étrange "optimisme" a pris le dessus. Je suis entré dans leur laboratoire en tant qu'étudiant timide et peu sûr de soi il y a trois ans et ils m'ont poussé à devenir le chercheur beaucoup plus proactif et autonome que je suis aujourd'hui. Je remercie le LabEx TULIP pour son soutien, qui a financé ces travaux dans le cadre du programme "Young Scientists for the Future". Je remercie également Richard Berthomé et Lionel Navarro, membres de mon comité de thèse, pour leur soutien et leurs conseils avisés.

Une gratitude toute particulière va à toutes les personnes de l'équipe SIX qui ont contribué à créer un environnement de travail aussi formidable et accueillant. Toute l'aide, les repas, les pauses café, les discussions scientifiques et non scientifiques, les sorties, les gâteaux et les ragots ont rendu ces trois années beaucoup plus faciles et m'ont obligé à parler français. Merci à Matthieu pour son humour toujours très classe ; à Noe pour la motivation à poursuivre ce projet et pour avoir fourni un petit refuge espagnol au sein de l'équipe ; à Corinne pour toute l'aide apportée à l'intérieur et à l'extérieur du laboratoire et la motivation à faire (un peu) de sport ; à Caroline pour le râlage et le chocolat, à Alice pour m'avoir donné la chance d'enseigner à l'université et les pauses nécessaires tard dans la soirée ; Carine pour son aide et tous les ragots ; Manue pour l'aide incommensurable durant ces années pour laquelle je la considère comme le troisième directeur de thèse ; Julien, compagnon de bureau, pour la compagnie et les longues discussions ; et Jean-Marc pour sa contribution gastronomique. Je tiens également à remercier les personnes qui, bien qu'elles ne fassent plus partie de l'équipe, ont contribué à son bon environnement et dont la présence a beaucoup manqué ces derniers mois : Aude pour son aide, ses conseils et son empathie, même au loin ; Ivanna pour son immense humour (et « l'amour » des fois) et pour m'avoir intégré dès mon arrivée ; et David pour toute l'aide, les fêtes et surtout nos discussions existentielles.

Ma sincère gratitude à tout le LIPM pour avoir fourni un excellent environnement scientifique, en particulier aux services communs (administration, laverie, informatique, serre...)

dont l'aide dans le travail quotidien a facilité mon travail et m'a permis de me concentrer sur mes recherches. Une mention particulière à Céline pour les heures passées à générer toutes les lignées transgéniques et à m'enseigner tout au long du processus ; à Sébastien pour le développement, le débogage (et il y avait beaucoup à déboguer...) et la mise à jour d'EffectorK ; et à Fabrice, Claudette, Marine et Anaïs pour s'être occupés de toutes les plantes transgéniques et suppressives qui occupaient plusieurs modules à certains moments.

Je tiens également à remercier plusieurs personnes du laboratoire dont la contribution scientifique et personnelle à cette thèse a été d'une grande importance pour moi : David et Léa, deux des amitiés les plus précieuses que je reçois de Toulouse et qui m'ont le plus aidé dans les pires moments de cette thèse ; Claire pour son énergie et sa motivation contagieuses et son empathie ; Ben, pour m'avoir intégré dès le premier jour ; Antho, pour les discussions rares mais sincères et toutes les recommandations concernant la nourriture et la bière ; Daniela et Camilo, pour toutes les fêtes, les voyages et les discussions sérieuses (et pas si sérieuses) ; Arry ; Alex ; Eli ; Fernanda ; Carolina ; Nathalie ; Jai ; Rekha ; Lorenzo ; Arianne ; et bien d'autres que j'oublie sûrement.

Je suis également redevable à tous mes amis et à ma famille dont le soutien inconditionnel, même au loin, m'a permis d'arriver là où je suis aujourd'hui. Je tiens à remercier tout particulièrement mes parents Araceli et Tomás qui, même s'ils n'ont pas toujours compris ce que je faisais, ont toujours soutenu mes choix et apprécié mes efforts. Les rendre fiers a toujours été l'une de mes principales motivations dans la vie et j'espère que la présente thèse contribuera à cet objectif. Je remercie aussi mon frère Rubén et ma cousine Leticia pour leur soutien continu. Je tiens également à remercier tous mes amis de Burgos, en particulier Nuria, Rubén, Javi et Sergio ; de Salamanque, en particulier Andrés, Jorge, Isa, Janire, Kroten, Loreto et Marina ; et de Kiel, en particulier Judit, Clara, Pau et Alice. Leurs messages, leurs appels et leurs rares visites m'ont toujours permis de me ressourcer lorsque j'avais le mal du pays.

Enfin, je tiens également à exprimer ma sincère gratitude à Carmen Rosario Beuzón, Ludovic Bonhomme, Frederik Böncke et Jean Philippe Galaud d'avoir accepté d'évaluer ce manuscrit et d'avoir pris part au jury de la soutenance de ma thèse.

# Agradecimientos

Estos tres años han sido una de las experiencias más gratificante, desafiante, agradable y exigente de mi vida y me gustaría agradecer a la gente que ha contribuido a hacerla posible. Primero, me gustaría expresar mi más sincera gratitud a mis supervisores Laurent Noël y Nemo Peeters por haber confiado en mí, los consejos y ayuda en este tiempo, y el ánimo cuando mi particular sentido del “optimismo” hacía de las suyas. Entré en el laboratorio como un estudiante tímido e inseguro hace tres años y ellos me empujaron a convertirme en el investigador proactivo y autónomo que soy hoy. Me gustaría reconocer el apoyo del LabEx TULIP, que ha financiado este trabajo a través de su programa “Jóvenes Científicos para el Futuro”. Gracias también a Richard Bethomé y Lionel Navarro, miembros de mi comité de tesis, por su ayuda objetiva y sus perspicaces consejos.

También quisiera agradecer de manera especial a todo el equipo SIX que ha contribuido a crear un ambiente de trabajo muy acogedor. Toda la ayuda, comidas, pausas de café, charlas científicas y no tan científicas, salidas, pasteles y cotilleo ha hecho que estos tres años se pasen mejor y me han obligado a hablar en francés. Gracias a Matthieu por su humor con estilo; Noe por su motivación para continuar este proyecto y por proveer un pequeño refugio hispanoparlante en el equipo; Corinne por toda la ayuda dentro y fuera del laboratorio y motivarme a hacer (algo de) deporte; Caroline por el desahogo y el chocolate, Alice por haberme permitido dar clases en la universidad y por las necesarias pausas al final del día; Carina por toda la ayuda y los cotilleos, Manue por la ayuda inmensurable durante estos años por la que le considero como la tercera supervisora de mi tesis; Julien por ser compañero de oficina, su compañía y nuestras largas conversaciones; y Jean-Marc por su contribución gastronómica. También me gustaría agradecer a la gente que, aunque ya no esté en el equipo, contribuyó a su buen ambiente y cuya presencia se ha echado mucho de menos en los últimos meses: Aude por su ayuda, consejos y empatía en la distancia; Ivanna por su humor y por haberme integrado en el equipo; y David por toda la ayuda, fiestas y sobretodo, nuestras discusiones existenciales.

Mi más sincera gratitud también a todo el LIPM por proveer un buen ambiente científico, particularmente a los servicios comunes (administración, cocina, informática, invernaderos...) cuya ayuda en el día a día facilita enormemente nuestro trabajo permitiendo centrarnos en la ciencia. Mención especial a Céline por las horas pasadas generando todas las líneas transgénicas y enseñándome a la vez todo el proceso; a Sébastien por desarrollar, arreglar (y mira que había

cosas que arreglar...) y mantener actualizado EffectorK; y a Fabrice, Claudette, Marine y Anaïs por cuidar de todas mis plantas transgénicas y supresores que en algunos momentos llegaron a ocupar varios módulos.

También me gustaría agradecer a varias personas del laboratorio por su contribución científica y personal a esta tesis: David y Lea, dos de las amistades más valiosas que extraigo de Toulouse y que siempre me han ayudado en los peores momentos; Claire por su energía y motivación contagiosas y su empatía; Ben por haberme integrado desde el primer día; Antho por las escasas pero sinceras conversaciones que tuvimos y todas las recomendaciones de comida y cervezas; Daniela y Camilo por todas las fiestas, viajes y conversaciones serias (y no tan series); Arry; Alex; Eli; Fernanda; Carolina; Nathalie; Jai; Rekha; Lorenzo; Arianne; y muchos otros que probablemente me deje.

Igualmente en deuda estoy con mis amigos y familia cuyo apoyo incondicional, incluso a distancia, me ha permitido llegar hasta donde he llegado. En especial, quisiera agradecer a mis padres Araceli y Tomás quienes, a pesar de no haber entendido lo que hacía, siempre han apoyado mis decisiones y valorado mis esfuerzos. Hacer que estén orgullosos de mí ha sido siempre uno de mis objetivos en la vida y espero que esta tesis contribuya a ello. Gracias especiales también a mi hermano Rubén y mi prima Leticia por su ayuda continua. También me gustaría agradecer el apoyo de todos mis amigos de Burgos, particularmente de Nuria, Rubén, Javi y Sergio; de Salamanca, particularmente de Andrés, Jorge, Isa, Janire, Kroten, Loreto y Marina; y de Kiel, particularmente de Judit, Clara, Pau y Alice. Sus mensajes, llamadas telefónicas y visitas esporádicas siempre han servido para recargarme las pilas cuando la morriña aparecía.

Y finalmente, me gustaría también expresar mi más sincera gratitud a Carmen Rosario Beuzón, Ludovic Bonhomme, Frederik Börnke y Jean Philippe Galaud por haber aceptado a revisar este manuscrito y participar en el jurado de su defensa.

# Abstract

*Xanthomonas campestris* pv. *campestris* (*Xcc*), the causal agent of black rot disease on Brassicaceae, and *Ralstonia pseudosolanacearum* (*Rps*), the causal agent of bacterial wilt on a wide variety of hosts, are both devastating xylem-colonizing bacteria. Despite their differences in host range, infection strategy and effectome repertoire, reference strains *Xcc*<sub>8004</sub> and *Rps*<sub>GM11000</sub> share six orthologous type III effectors (T3Es). This provides a valuable opportunity for comparative studies as it is likely that these orthologous T3Es target orthologous processes in the host plants, with focus on *Arabidopsis thaliana*, common host of both pathogens.

In a first part of my PhD project, putative *Arabidopsis* interactors of *Xcc*<sub>8004</sub> and *Rps*<sub>GM11000</sub> T3Es were identified by yeast two-hybrid at the effectome-scale. This allowed us to compare our results with similarly screened plant pathogens to acquire a global image of how effectors interfere with the host proteome. This led to the generation of an interactive knowledge database integrating our results with published *Arabidopsis*-effector interactomic data: “EffectorK” ([www.effectork.org](http://www.effectork.org)). In a second part of the project, the *in planta* effects of single T3Es were dissected by generating inducible transgenic *Arabidopsis* lines. Combining results from these two parts, the most promising T3E candidates were selected for further functional characterization, forming the last part of my work. Altogether, this project contributes to a better understanding of the biological role of conserved T3Es among xylem-colonizing bacteria.

# Résumé

*Xanthomonas campestris* pv. *campestris* (Xcc), l'agent responsable de la pourriture noire chez les Brassicacées, et *Ralstonia pseudosolanacearum* (Rps), l'agent responsable du flétrissement bactérien chez une large variété d'espèces végétales, sont toutes deux des bactéries dévastatrices s'établissant dans le xylème de leur hôte. Malgré les différences dans leur gamme d'hôtes, leur stratégie infectieuse et leur répertoire d'effecteurs, les souches de référence Xcc8004 et RpSGMI1000 partagent six effecteurs de type III (ET3) définis comme orthologues. Cela offre une excellente opportunité de mener des études comparatives puisqu'il est probable que ces six ET3 ciblent des processus orthologues chez les plantes hôtes, notamment chez *Arabidopsis thaliana* qui est un hôte commun aux deux pathogènes.

Dans une première partie de mon projet de thèse, de potentielles protéines d'*Arabidopsis* interagissant avec les ET3 de Xcc8004 et RpSGMI1000 ont été identifiées grâce à un criblage par double hybride. Nous avons ainsi pu comparer nos résultats avec des criblages similaires réalisés chez d'autres phytopathogènes afin d'obtenir une vision plus exhaustive de la façon dont les effecteurs interagissent avec le protéome de l'hôte. Cela a permis de générer une base de données interactive intégrant nos résultats ainsi que des données interactomiques *Arabidopsis*-ET3 déjà publiées : « EffectorK » ([www.effectork.org](http://www.effectork.org)). Dans une deuxième partie du projet, les effets *in planta* de chacun des ET3 ont été étudiés en générant des lignées transgéniques inducibles d'*Arabidopsis*. En croisant les résultats de ces deux premières parties, les ET3 candidats les plus prometteurs ont été sélectionnés pour conduire des expériences de caractérisation fonctionnelle, ce qui a constitué la dernière partie de mon travail. Ce projet participe à une meilleure compréhension du rôle biologique des ET3 conservés parmi les bactéries colonisatrices du xylème.

# Table of contents

<b>Acknowledgements</b>	1
<b>Remerciements (FR)</b>	3
<b>Agradecimientos (ES)</b>	5
<b>Abstract</b>	7
<b>Résumé (FR)</b>	8
<b>Table of contents</b>	9
<b>List of figures</b>	13
<b>List of tables</b>	16
<b>List of abbreviations</b>	17
<b>Chapter 1: Introduction</b>	18
1.1 Plants and associated microorganisms: a complicated relationship	19
1.2 How to be a bad guest: the pathogen side of the story	21
1.2.1 The infectious cycle, step by step	23
1.2.1.1 Step #1: Invading the host	23
1.2.1.2 Step #2: Feeding from the host	24
1.2.1.3 Step #3: Multiplying within the host	24
1.2.1.4 Step #4: Leaving the host	25
1.2.2 Virulence determinants: tools to be a bad guest	27
1.2.2.1 Effectors: the pathogen's Swiss Army knife	29
1.3. How to be a bad host: the plant side of the story	37
1.3.1 "Stay ready" - Constitutive defenses	39
1.3.2 "Get ready" - Inducible defenses	41
1.3.2.1 Perception: how to know that you are not alone?	41
1.3.2.2 Signaling: how to process that you are not alone?	45
1.3.2.3 Execution: what to do when you are not alone?	49
1.3.3 "Tell the others to get ready" - Systemic resistance	52
1.4. The xylem: a barely frequented meeting point	53
1.4.1 Suspect #1: <i>Ralstonia solanacearum</i>	57
1.4.1.1 RSSC previous records	57
1.4.1.2 RSSC criminal charges	59
1.4.1.3 RSSC modus operandi	61

1.4.1.4. RSSC known weapons	63
1.4.2. Suspect #2: <i>Xanthomonas campestris</i> pathovar <i>campestris</i>	65
1.4.2.1 Xcc previous records	65
1.4.2.2 Xcc criminal charges	65
1.4.2.3 Xcc modus operandi	67
1.4.2.4. Xcc known weapons	69
1.4.3. A déjà vu	71
<b>Chapter 2: PhD project</b>	74
<b>Chapter 3: Identification of plant targets of type III effectors from <i>R. pseudosolanacearum</i> and <i>X. campestris</i> pv. <i>campestris</i></b>	77
3.1 Introduction	77
3.2 EffectorK, a comprehensive resource to mine for <i>Ralstonia</i> , <i>Xanthomonas</i> , and other published effector interactors in the <i>Arabidopsis</i> proteome	77
3.3 Rps and Xcc share 19 putative Arabidopsis targets	102
3.4 Few common targets seem to be involved in plant susceptibility to Xcc and Rps	108
3.5 Discussion	114
<b>Chapter 4: Determining the effect of the effectors shared by <i>R. pseudosolanacearum</i> and <i>X. campestris</i> pv. <i>campestris</i></b>	120
4.1 Introduction	122
4.2 Shared T3Es contribute collectively to the bacterial pathogenicity	122
4.3 Expressing individual bacterial T3E genes in planta to study their effects	125
4.3.1 Nine shared T3Es confer different developmental alterations when expressed in Arabidopsis	128
4.3.2 The orthologs RipHI-3 and XopP inhibit plant basal defenses	134
4.4 Discussion	142
<b>Chapter 5: XopAG and RipOI, one of the most promising orthologous pair of candidates</b>	148
5.1 Introduction	150
5.2. XopAG and RipOI belong to a widespread and poorly characterized T3E family	150
5.3. XopAG and in lesser extent RipOI are involved in bacterial pathogenicity	156



5.4. First steps to dissect the genetic bases of <i>xopAG</i> -mediated developmental phenotype in <i>Arabidopsis</i>	160
5.5. XopAG and RipOI co-localize with BRG3 in the nucleus	163
5.6. Discussion	168
<b>Chapter 6: Evolutionary history of XopJ6, a PopP2 ortholog translocated into plants by <i>X. campestris</i> pv. <i>campestris</i> to interfere with plant immunity</b>	174
6.1 Introduction	176
6.2 XopJ6 is a member of the YopJ family closely related to <i>R. solanacearum</i> PopP2	176
6.3 <i>xopJ6</i> is located on a transposon present in one to three copies in <i>Xcc</i> genomes	180
6.4 XopJ6 is regulated by the <i>hrp</i> system and possess a functional T3SS translocation signal	186
6.5 <i>xopJ6</i> copy number is correlated with its expression and pathogenicity	189
6.6 XopJ6, a last minute candidate for the pipeline	190
6.6 Discussion	193
<b>Chapter 7: General discussion</b>	196
7.1 Conclusions: What I have done so far	197
7.2 Perspectives: What I would do if I had more time	201
<b>Chapter 8: Material and methods</b>	206
8.1 Biological material and growth conditions	207
8.1.1 Plants	207
8.1.2 Bacteria	207
8.2 Bioinformatic analyses	208
8.3 Cloning	208
8.4 Plant genotyping	209
8.5 Pathogenicity assays	209
8.5.1 <i>Xcc</i> pathogenicity assays	209
8.5.2 <i>Rps</i> pathogenicity assay	210
8.6 Generation of <i>Xcc</i> polymutant	210
8.7 Plant transformation	211
8.8 Gene expression measurement by qPCR	211

8.9 ROS measurement by luminometry	212
8.10 Protein extraction and detection by Western blot	212
8.11 Suppressor screening	212
8.12 Microscopy	213
8.13 Bacterial growth in vitro	213
8.14 Measurement of GUS activity	213
<b>Bibliography</b>	215
<b>Annexes</b>	245
Annex 1. The large, diverse, and robust arsenal of <i>Ralstonia solanacearum</i> type III effectors and their in planta functions	258
Annex 2. From effectors to effectomes: Are functional studies of individual effectors enough to decipher plant pathogen infectious strategies?	271

# List of figures

**Figure 1.1.** Compatibility and incompatibility in plant-pathogen interactions.

**Figure 1.2.** The infectious cycle.

**Figure 1.3.** Virulence determinants of plant pathogens.

**Figure 1.4.** Modes of action of plant pathogen effectors.

**Figure 1.5.** Constitutive structural defense mechanisms of plants.

**Figure 1.6.** The zigzag model for plant immunity.

**Figure 1.7.** Plant receptors involved in plant immunity.

**Figure 1.8.** Plant defense signaling.

**Figure 1.9.** Phytohormone signaling in plant defense.

**Figure 1.10.** Hypersensitive response (HR) and systemic acquired resistance (SAR).

**Figure 1.11.** Structure of xylem.

**Figure 1.12.** Plant diseases caused by vascular pathogens.

**Figure 1.13.** *Ralstonia solanacearum* species complex (RSSC) bacteria aspect, disease symptoms and geographical distribution.

**Figure 1.14.** Life cycle of the *Ralstonia solanacearum* species complex (RSSC).

**Figure 1.15.** Main virulence determinants of the *Ralstonia solanacearum* species complex (RSSC).

**Figure 1.16.** *Xanthomonas campestris* pv. *campestris* (Xcc) aspect, disease symptoms and geographical distribution.

**Figure 1.17.** Life cycle of *Xanthomonas campestris* pv. *campestris* (Xcc).

**Figure 1.18.** Main virulence determinants of *Xanthomonas campestris* pv. *campestris* (Xcc).

**Figure 3.1.** Interspecific convergence of effector targets among plant pathogenic bacteria.

**Figure 3.2.** Involvement in susceptibility to Xcc of 18 common putative targets.

**Figure 3.3.** Involvement of the three common putative targets of XopAG and RipOI in the in planta growth of Xcc.

**Figure 3.4.** Involvement of four common putative targets in susceptibility to *Rps*.

**Figure 3.5.** RipAJ and XopAC show homology of function, but not of sequence.

**Figure 4.1.** Pathogenicity of T3E gene mutants in *Rps<sub>GM11000</sub>* inoculated on susceptible tomato plants.

**Figure 4.2.** Pathogenicity of T3E gene mutants in *Xcc<sub>8004</sub>* inoculated on Arabidopsis plants.

**Figure 4.3.** Pathogenicity of shared T3E mutants in *Xcc<sub>8004</sub>* inoculated on Arabidopsis plants.

**Figure 4.4.** Examples of phenotypes observed on T3E transgenic Arabidopsis plantlets.

**Figure 4.5.** Transient RipH1, RipH2 and RipH3 expression in *N. benthamiana* inhibits flg22-induced ROS production.

**Figure 4.6.**  $\beta$ -estradiol treatment does not alter the flg22-induced ROS production in Arabidopsis Col-0 plants

**Figure 4.7.** RipH1, RipH2 and RipH3 expression in Arabidopsis does not inhibit flg22-induced ROS production.

**Figure 4.8.** RipH1, RipH2 and RipH3 expression in Arabidopsis does not inhibit flg22-induced ROS production.

**Figure 4.9.** *N. benthamiana* produces more ROS upon flg22 treatment than *A. thaliana*.

**Figure 4.10.** The concentration of flg22 is not the limiting factor for the weak production of ROS in Arabidopsis.

**Figure 4.11.** Transient XopP expression in *N. benthamiana* inhibits flg22-induced ROS production.

**Figure 4.12.** Pathogenicity of different combination of multiple T3E mutants in *Xcc*<sub>8004</sub> inoculated on Arabidopsis.

**Figure 4.13.** XopAM and RipR ortholog in *Erwinia amylovora*, DspA/E, is toxic when expressed in *A. thaliana*.

**Figure 4.14.** Drastic alteration phenotypes are correlated with higher levels of induction.

**Figure 5.1.** Summary of previous results related to *Xcc*<sub>8004</sub> XopAG and *Rps*<sub>GMII000</sub> RipOI.

**Figure 5.2.** Schematic alignment of orthologs of XopAG and RipOI in other bacteria.

**Figure 5.3.** Multiple sequence alignment of AvrGf2, HopG1, RipOI and XopAG.

**Figure 5.4.** Phylogeny of orthologs from XopAG and RipOI in other proteobacteria.

**Figure 5.5.** Pathogenicity of *Xcc* 8004 $\Delta$ xopAG in the  $\Delta$ xopAC background.

**Figure 5.6.** *In vitro* growth curve of *Xcc* 8004 wild type,  $\Delta$ xopAC and  $\Delta$ xopAC-xopAG.

**Figure 5.7.** Pathogenicity of *Rps* GMII000 wild type and  $\Delta$ ripOI strains inoculated on susceptible Arabidopsis plants.

**Figure 5.8.** Transient expression of XopAG but not RipOI inhibits flg22-induced ROS production.

**Figure 5.9.** Phenotype of pER8-xopAG and pER8-ripOI transgenic lines grown in different concentrations of inducer.

**Figure 5.10.** Phenotype of suppressor of xopAG-related phenotype (*sxg*) lines.

**Figure 5.11.** Subcellular localization of XopAG- and RipOI-CFP fusion proteins.

**Figure 5.12.** Nuclear co-localization of XopAG- and RipOI-CFP with BRG3-YFP fusion proteins.

**Figure 5.13.** FRET-FLIM measurements of interactions between BRG3-CFP and XopAG-YFP and RipOI-YFP.

**Figure 6.1.** XopJ6 is an RRS1/RPS4-dependant avirulence factor in Arabidopsis.

**Figure 6.2.** Phylogenetic tree of 25 members of the YopJ family of bacterial effectors.

**Figure 6.3.** Pairwise sequence alignment of PopP2 and XopJ6.

**Figure 6.4.** *xopJ6* is located in Tn6714, a new 9-kb Tn3 family transposon.

**Figure 6.5.** *xopJ6* is found in one to three copies in *Xcc* genomes.

**Figure 6.6.** *xopJ6* was acquired as simple or composite transposon in evolutionary related plasmids and chromosomal insertions.

**Figure 6.7.** Proposed evolution of the *xopJ6* loci within *Xcc* strains.

**Figure 6.8.** pAIO strategy to study regulation and translocation of *xopJ6*.

**Figure 6.9.** *xopJ6* promoter is *hrpG*-regulated.

**Figure 6.10.** The N-terminus of XopJ6 is able to translocate a truncated version of AvrBs1 through the *Xcc* type III secretion system.

**Figure 6.11.** The number of copies of *xopJ6* correlates with its relative expression and pathogenicity on susceptible Arabidopsis ecotype Col-0.

**Figure 6.12.** XopJ6 inhibits flg22-induced ROS production.

# List of tables

**Table 1.1.** Characterized effectors from plant pathogens.

**Table 1.2.** Examples of avirulence and resistance proteins.

**Table 1.3.** Characterized effectors from the *Ralstonia solanacearum* species complex (RSSC).

**Table 1.4.** Characterized effectors from *Xanthomonas campestris* pv. *campestris* (Xcc).

**Table 1.5.** Main similarities and differences between the *Ralstonia solanacearum* species complex (RSSC) and *Xanthomonas campestris* pv. *campestris* (Xcc).

**Table 2.1.** Orthology relationship between shared T3Es from Xcc<sub>8004</sub> and Rps<sub>GMII000</sub>.

**Table 3.1.** GO enrichment test of the 12,000 cDNA-library.

**Table 3.2.** GO enrichment test of the 209 putative targets of T3Es from Xcc<sub>8004</sub> and Rps<sub>GMII000</sub>.

**Table 3.3.** Common putative targets of T3Es from Xcc<sub>8004</sub> and Rps<sub>GMII000</sub>.

**Table 3.4.** Putative targets of orthologous T3Es from Xcc<sub>8004</sub> and Rps<sub>GMII000</sub>.

**Table 4.1.** pER8-T3E transgenic Arabidopsis lines generated.

**Table 4.2.** Validation by qPCR of the transgene expression in several pER8-T3E Arabidopsis transgenic lines.

**Table 4.3.** *In vitro* phenotypes of pER8-T3E transgenic Arabidopsis plantlets.

**Table 5.1.** Distribution of *xopAG* and *ripOI* within *X. campestris* pathovars and RSSC strains.

**Table 6.1.** XopJ6 interacts with RRS1-R and dissociates it from DNA contrary to XopJ6CNI3.

**Table A.1.** Putative Arabidopsis targets of T3Es from Xcc<sub>8004</sub>.

**Table A.2.** Putative Arabidopsis targets of T3Es from Rps<sub>GMII000</sub>.

**Table A.3.** Putative targets of orthologous T3Es from Xcc<sub>8004</sub> and Rps<sub>GMII000</sub>.

**Table A.3.** List of bacterial strains used in this study.

**Table A.5.** List of primers used in this study.

# List of abbreviations

<b>ABA:</b>	Abscisic acid	<b>NASC:</b>	Nottingham Arabidopsis Stock Centre
<b>Avr:</b>	Avirulence	<b>NBS:</b>	Nucleotide-binding domain
<b>Ath:</b>	<i>Arabidopsis thaliana</i>	<b>NLR:</b>	NOD-like receptor
<b>BC2:</b>	Backcrossed hybrid, second generation	<b>NO:</b>	Nitric oxide
<b>CC:</b>	Coiled-coil	<b>OD:</b>	Optical density
<b>CFP:</b>	Cyan fluorescent protein	<b>PAMP:</b>	Pathogen-associated molecular pattern
<b>CFU:</b>	Colony-forming unit	<b>PCD:</b>	Programmed cell death
<b>CNL:</b>	CC-type NLR	<b>Pop:</b>	<i>Pseudomonas</i> outer protein
<b>coA:</b>	Coenzyme A	<b>POX:</b>	Peroxidase
<b>Col-0:</b>	Columbia 0	<b>PR:</b>	Pathogenesis related
<b>Cp:</b>	Crossing point	<b>PRR:</b>	Pattern recognition receptor
<b>CPS:</b>	Capsular polysaccharides	<b>Psy:</b>	<i>Pseudomonas syringae</i>
<b>CWDE:</b>	Cell wall-degrading enzymes	<b>PTI:</b>	PAMP-triggered immunity
<b>Cyp:</b>	Cyclophilin	<b>pv:</b>	Pathovar
<b>DAMP:</b>	Damage-associated molecular pattern	<b>R:</b>	Resistance
<b>DMSO:</b>	Dimethyl sulfoxide	<b>Rip:</b>	<i>Ralstonia</i> injected protein
<b>dpi:</b>	Days post inoculation	<b>RNL:</b>	RPW8-type NLR
<b>DR:</b>	Direct repeats	<b>ROS:</b>	Reactive oxygen species
<b>ECW:</b>	Early Calwonder	<b>Rps:</b>	<i>Ralstonia pseudosolanacearum</i>
<b>EMS:</b>	Ethyl methanesulfonate	<b>RSSC:</b>	<i>Ralstonia solanacearum</i> species complex
<b>EPS:</b>	Exopolysaccharides	<b>SA:</b>	Salicylic acid
<b>ET:</b>	Ethylene	<b>SAR:</b>	Systemic acquired resistance
<b>ETI:</b>	Effector-triggered immunity	<b>Sf-2:</b>	San Feliu 2
<b>ETS:</b>	Effector-triggered susceptibility	<b>sp:</b>	Species
<b>FLIM:</b>	Fluorescence-lifetime imaging microscopy	<b>sRNA:</b>	Small non-coding RNA
<b>FRET:</b>	Fluorescence Resonance Energy Transfer	<b>SUMO:</b>	Small ubiquitin-like modifier
<b>GFP:</b>	Green fluorescent protein	<b>sxg:</b>	Suppressor of <i>xopAG</i> -mediated phenotype
<b>GO:</b>	Gene ontology	<b>T3E:</b>	Type III effector
<b>Gor:</b>	<i>Glovinomyces orontii</i>	<b>T3SS:</b>	Type III secretion system
<b>Hpa:</b>	<i>Hyaloperonospora arabidopsidis</i>	<b>TAL:</b>	Transcription activator-like
<b>HR:</b>	Hypersensitive response	<b>TBDT:</b>	TonB-dependent outer membrane transporter
<b>hrc:</b>	<i>hrp</i> -conserved	<b>TIR:</b>	Toll-interleukin 1 receptor domain
<b>hrp:</b>	Hypersensitive reaction and pathogenicity	<b>TNL:</b>	TIR-type NLR
<b>IP<sub>6</sub>:</b>	Inositol-hexakisphosphate	<b>T-DNA:</b>	Transfer DNA
<b>IR:</b>	Inverted repeats	<b>TF:</b>	Transcription factor
<b>IS:</b>	Insertion sequence	<b>Xcc:</b>	<i>Xanthomonas campestris</i> pv. <i>campestris</i>
<b>ISR:</b>	Induced systemic resistance	<b>Xop:</b>	<i>Xanthomonas</i> outer protein
<b>JA:</b>	Jasmonic acid	<b>Y2H:</b>	Yeast two-hybrid
<b>LPS:</b>	Lipopolysaccharide	<b>YFP:</b>	Yellow fluorescent protein
<b>LRR:</b>	Leucine-rich repeat domain	<b>WT:</b>	Wild type
<b>MAMP:</b>	Microbe-associated molecular pattern		
<b>MAPK:</b>	Mitogen-activated protein kinase		

# Chapter 1

## Introduction

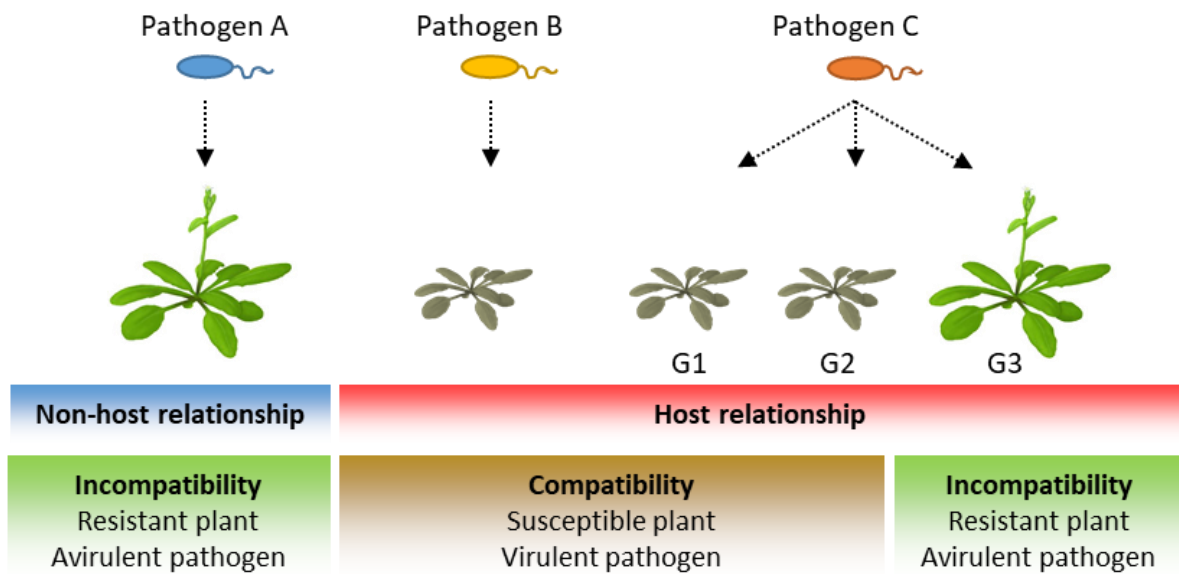


## 1.1 Plants and associated microorganisms: a complicated relationship





Plants, due to their sessile nature, have evolved a wide variety of mechanisms to cope with environmental changes. These include abiotic stresses, such as radiation, extreme temperatures, drought, flooding or salinity; and biotic stresses, such as those caused by viruses, bacteria, oomycetes, fungi, animals and other plants. All these different stresses can significantly reduce the yield and quality of crops, threatening the food security worldwide. It is estimated that biotic stresses are responsible for losses of up to 30-40%, depending on the crop species (Oerke, 2006; Wang *et al.*, 2013). Plants can perceive all these different stresses and generate an adequate response, often involving alterations in gene expression, cellular metabolism and allocation of resources. The severity and duration of the stress determine the ability of the plant to overcome it (Verma, Nizam and Verma, 2013). When the stress is mild or short-lived, plants can face it and are considered tolerant. However, if the stress is severe or prolonged, plants might not be able to overcome it leading to the occurrence of severe symptoms, sterility or ultimately, death. Such plants are considered susceptible.

Biotic stresses are caused by the organisms cohabiting with plants. These organisms establish a symbiotic association with the plant. This definition of symbiosis refers to the original definition coined by German botanist Anton de Bary in 1879 (De Bary, 1879), which did not consider the benefit or harm of the association to the partners. In these relationships, the plant plays the role of “host” or provider of resources while the other organism, called symbiont, play the role of “guest” or consumer of these resources (Pérez-Brocal, Latorre and Moya, 2013). According to the beneficial/detrimental nature for the host, these relationships have been traditionally classified in: 1) Mutualism, when both partners benefit from the interaction. Examples of this kind of relationship are the interactions between nitrogen-fixing rhizobia or mycorrhizal fungi and plants. In these interactions, the rhizobium/fungus provides different nutrients in exchange for carbon sources (Denison and Kiers, 2011). 2) Commensalism, when the symbiont exploits the resources from the host without causing any harm. An example of this kind of relationship are the epiphytes, plants that benefit from other plants for physical support but obtain their nutrients from the air or rain water (Schowalter, 2016). 3) Parasitism, when the exploitation of the host resources by the symbiont is detrimental for the host. The different microorganisms that cause diseases on plants establish this kind of relationships with their hosts. Nevertheless, this traditional classification has been largely debated over the last years as

**A**



**B**

	<i>R</i> gene +	<i>R</i> gene -
<i>Avr</i> gene +	 <b>Incompatibility (resistance)</b>	 <b>Compatibility (disease)</b>
<i>Avr</i> gene -	 <b>Compatibility (disease)</b>	 <b>Compatibility (disease)</b>

**Figure 1.1. Compatibility and incompatibility in plant-pathogen interactions.** (A) Pathogen A is unable to produce the disease in the plant due to non-host resistance. The relationship is therefore incompatible: pathogen A is avirulent and the plant is resistant. Pathogen B is able to produce the disease. The relationship is therefore compatible: pathogen B is virulent and the plant is susceptible. Pathogen C is able to produce disease on the plant genotypes 1 and 2 (G1 and G2) but not on the genotype 3 (G3). The compatibility of the system depends on the plant genotype. Pathogen C is virulent to the susceptible genotypes 1 and 2 and avirulent to the resistant genotype 3. This indicates that genotype 3 present host resistance against pathogen C. (B) Gene-for-gene model of host resistance. When the plant presents the *R* gene (*R* gene +) and the pathogen presents the corresponding *Avr* gene (*Avr* gene +), host resistance occurs and the interaction is incompatible. If any or both of them are missing (*R/Avr* gene -), host resistance does not occur and the interaction is compatible. Adapted from Aude Cerutti PhD thesis, UPS, Toulouse, 2017.

the limits between the different categories have been shown to be less and less clear and often depend heavily on environmental conditions (Hirsch, 2004; Pérez-Brocal, Latorre and Moya, 2013).

Despite the negative impact of biotic stress on yield, only a few species are responsible for plant diseases. The vast majority of microorganisms are not able to infect the majority of plants. This is due to the so-called “non-host resistance”. The latter refers to the resistance of an entire plant species against a parasitic organism (Heath, 2000). It comprises the most durable resistance of plants but the underlying mechanisms remain elusive (Fan and Doerner, 2012; Lee *et al.*, 2017). Non-host resistance is responsible for incompatible interactions, (i.e., interactions that do not end up in disease) in which the plant is called resistant and the associated organism, avirulent (Glazebrook, 2005) (**Figure 1.1A**).

A few organisms can infect the plant, evade the non-host resistance, colonize the plant tissues and ultimately cause disease. These interactions are referred as compatible, the plant is called susceptible, and the pathogen, virulent (Glazebrook, 2005) (**Figure 1.1A**). However, some genotypes from a pathogenic species might not be able to cause disease on certain plant genotypes leading to an incompatible interaction. This is due to “host resistance”, which is restricted to some genotypes of a given plant species (**Figure 1.1A**). Contrary to non-host resistance, host resistance is highly specific and often monogenic, and it is therefore less durable (Gill, Lee and Mysore, 2015). This kind of resistance follows the “gene-for-gene” relationship first described by Henry Flor in 1955 (Flor, 1955) that requires the interaction between the products of an avirulence (*Avr*) gene from the pathogen and a resistance (*R*) gene from the plant. When the pathogen and the host present these genes, the interaction is incompatible but if any of them lacks the corresponding gene, the interaction is compatible (**Figure 1.1B**).

## 1.2 How to be a bad guest: the pathogen side of the story

Pathogens are ubiquitously present in the environment: they can be found in the soil (Hornby, 1998), water (Hong and Moorman, 2005), air (West, Atkins and Fitt, 2009), seeds (Akhtar *et al.*, 2016)) or vector organisms (Eigenbrode, Bosque-Pérez and Davis, 2018). These pathogens will later invade the plant in order to gain a better access to nutrients and shelter to sustain their growth. Once in the plant, the pathogens will need to subvert the host defenses in order to survive, feed and multiply. Ultimately, the pathogen will be released from the plant back into the environment where some pathogens can survive in a resting stage for long periods

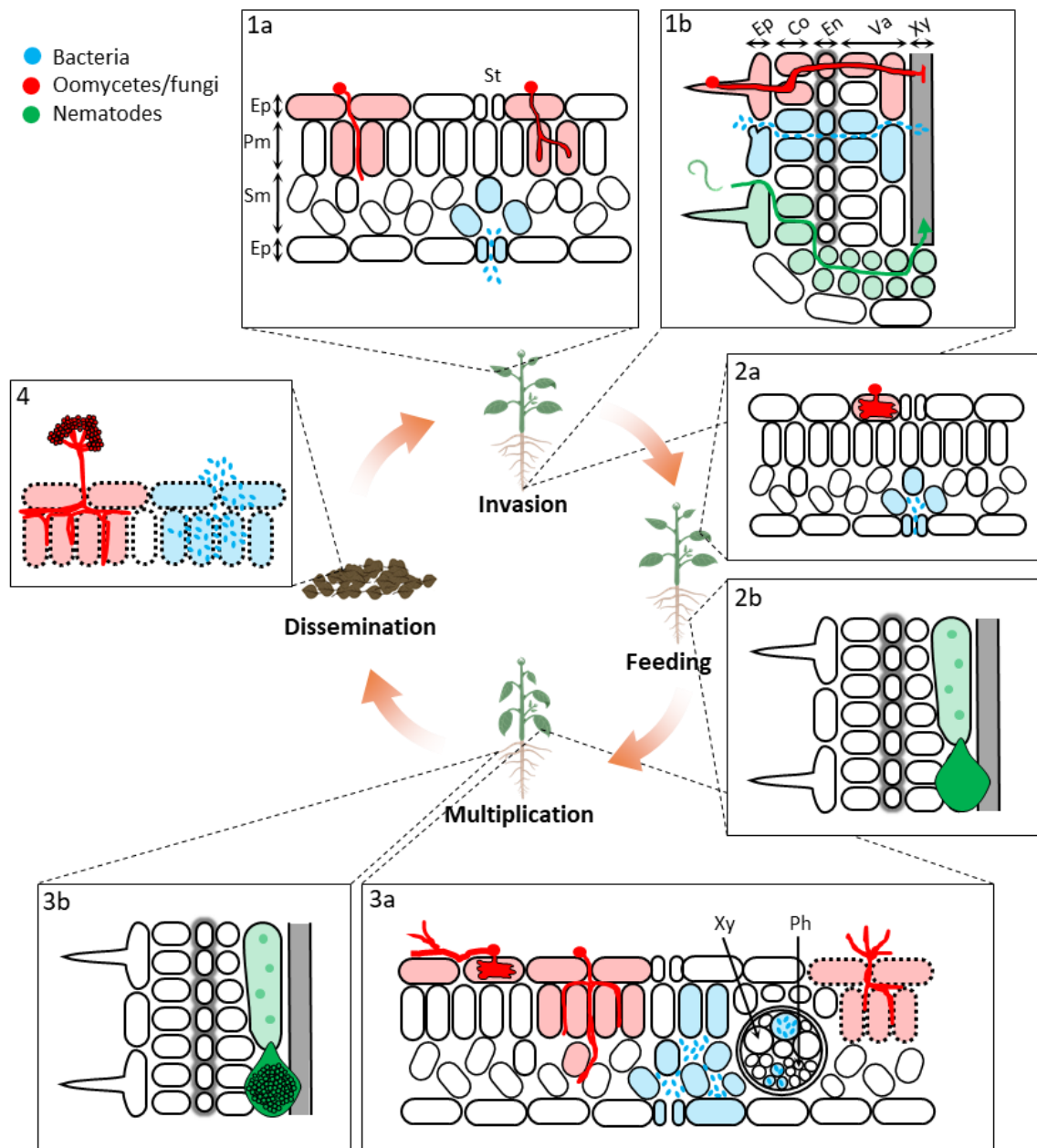


**Figure 1.2. The infectious cycle.** Each mechanism makes the pathogen enter in contact with host cells, shaded in the same color. The first step of the infectious cycle is the invasion. 1a) Aerial pathogens enter inter- or intracellularly or through openings. 1b) Soil pathogens also penetrate the root vasculature inter- or intracellularly and some go to the meristem to avoid passing through the Casparian strip. After invasion, pathogens need to feed and multiply. 2a) Pathogens feed from the apoplast or the symplast (for the latter, filamentous fungi generate haustoria). 2b) Nematodes form multinuclear feeding cell complexes. 3a) Pathogens can grow epiphytically or inside the host. The latter can be in either the apoplast, symplast or vasculature. Necrotrophs kill the host cells (dotted lines) and thrive on dead tissues. 3b) Female nematodes lay eggs. To close the cycle, pathogens are released to the environment. 4) Some pathogens can live on dead tissues and form reproductive structures for dissemination. Abbreviations: epidermis (Ep), palisade mesophyll (Pm), spongy mesophyll (Sm), cortex (Co), endodermis (En), vascular tissue (Va), xylem (Xy), and phloem (Ph). Inspired by Abad and Williamson, 2010; Faulkner and Robatzek, 2012; and Lo Presti *et al.*, 2015.

of time before entering a new infectious cycle (Brown, 1997) (**Figure 1.2**). The mechanisms that the different pathogens employ to invade the host, subvert its defenses, feed from its resources, multiply and disseminate after are neither simple nor uniform.

## 1.2.1 The infectious cycle, step by step

### 1.2.1.1 Step #1: Invading the host

Once pathogens make contact with the plant, they find structural barriers like the epidermis that protects all organs, or the cuticle, that strengthens the aerial parts. Pathogens have developed diverse strategies to penetrate these structural barriers to gain access to the intracellular spaces, the apoplast or the vascular tissues where the nutrients are more abundantly contained. Filamentous pathogens are able to breach through the epidermis at the boundaries of adjacent pavement cells (e.g., oomycete *Hyaloperonospora arabidopsidis*) or directly pierce the epidermal cells thanks to specialized structures called appressoria (e.g., fungus *Magnaporthe oryzae*) (Faulkner and Robatzek, 2012) (**Figure 1.2**). Upon this breach, filamentous pathogens rely on the secretion of a cocktail of enzymes to degrade the cell wall and access the content of the plant cell cytoplasm (Łaźniewska, Macioszek and Kononowicz, 2012). Bacteria lack mechanisms to penetrate the epidermis and rely on pre-existent openings such as the stomata (e.g., *Pseudomonas syringae* pv. *tomato*), hydathodes (e.g., *Xanthomonas campestris* pv. *campestris*) or wounds to gain access to the plant internal parts (Melotto *et al.*, 2006; Cerutti *et al.*, 2019) (**Figure 1.2**). Indeed, some bacteria present chemotactic motility towards molecules secreted in these openings (Kroupitski *et al.*, 2009). Roots are heavily colonized at the cortex but microorganisms rarely penetrate further due to the presence of the endodermal Casparian strip that seals the extracellular space between cells (Schreiber and Franke, 2011). Nevertheless, some bacteria and filamentous pathogens have evolved mechanisms to penetrate the endodermis and access the root vasculature. Some root pathogens enter the intercellular space through wounds or lateral root emergence points (e.g., bacterium *Ralstonia solanacearum*) (Digonnet *et al.*, 2012), while others invade intracellularly the rhizodermis and then move cell-to-cell to avoid the Casparian strip (e.g., fungus *Verticillium longisporum*) (Eynck *et al.*, 2007) (**Figure 1.2**). Plant-parasitic nematodes can also invade the root vasculature by either penetrating the endodermis (cyst nematodes) or by avoiding it passing through the apical meristem instead (root-knot nematodes) (Holbein *et al.*, 2019) (**Figure 1.2**). These strategies are not needed when pathogens are vector-transmitted as they have direct access to internal host tissues (e.g. bacterium *Xylella fastidiosa*) (Purcell and Hopkins, 1996). Vector-borne plant

pathogens include several viruses, bacteria and fungi (Eigenbrode, Bosque-Pérez and Davis, 2018).

#### 1.2.1.2 Step #2: Feeding from the host

Although the plant apoplast contains several nutrients, these are more abundant within the cytoplasm of plant cells, which is protected by the plasma membrane and cell wall. To gain access to these nutrients, pathogens have evolved mechanisms to degrade these protective layers, as observed in necrotrophic pathogens (i.e., pathogens that obtain nutrients mainly from dead cells), or to manipulate living host cells to deliver these nutrients to the pathogen more easily, as employed by biotrophic pathogens (i.e., pathogens that obtain nutrients primarily from living host tissues). Pathogens deploy diverse molecules (e.g., degrading enzymes, phytohormones, toxins or effectors) into the apoplast and inside living host cells allowing the cellular collapse or the reprogramming of host cells to accommodate different feeding structures or facilitate the nutrient uptake (Faulkner and Robatzek, 2012). Bacteria will uptake these nutrients directly from the surrounding medium through passive or active import (**Figure 1.2**). However, bacteria can alter the natural content of their surrounding medium to make it more suitable for bacterial growth (e.g., several *Xanthomonas* species induce sugar transporter gene expression, probably to increase the sugar efflux for the bacterial nutrition) (Chen *et al.*, 2010; Cohn *et al.*, 2014; Cox *et al.*, 2017; Oliva *et al.*, 2019). Conversely, nematodes and filamentous pathogens rely on complex feeding structures for nutrient uptake (**Figure 1.2**). Oomycetes and fungi develop “haustoria”, specialized fungal hyphae that penetrate the plant cell wall and expand within the plant cell surrounded by a thickened derivative of the plant plasma membrane (Szabo and Bushnell, 2001). This structure allows an increase in the nutrient exchange surface with the plant cell. Nematodes migrate within the vascular cylinder upon infection to find competent plant cells for the induction of multinuclear feeding cell complexes. Cyst nematodes produce syncytia (i.e., structures arising from the coordinated cell wall dissolution and subsequent protoplast fusion of several adjacent cells) while root-knot nematodes produce giant cell complexes (i.e., structures generated after cell enlargement and repeated rounds of mitosis without cytokinesis) (Karczmarek *et al.*, 2004).

#### 1.2.1.3 Step #3: Multiplying within the host

Upon favorable conditions, pathogens will start multiplying and colonizing the host. Pathogens can invade practically all plant tissues. Some pathogens can feed from the host but

grow epiphytically on the leaf surface (e.g. fungus *Blumeria graminis*) (Both *et al.*, 2005), but most of them colonize the host internal tissues (**Figure 1.2**). Some bacteria and filamentous pathogens grow intercellularly in the mesophyll apoplast (e.g., bacterium *Pseudomonas syringae* or fungus *Cladosporium fulvum*) (Thomma *et al.*, 2005; Rico and Preston, 2008). Other pathogens are able to grow intracellularly in the mesophyll (e.g., fungus *Ustilago maydis*) (Djamei and Kahmann, 2012) or in the phloem (e.g., several viruses like the *Citrus tristeza virus* and phytoplasmas like *Candidatus Liberibacter asiaticus*) (Bendix and Lewis, 2018). Some pathogens are able to colonize the xylem (e.g. bacterium *Ralstonia solanacearum*) (Digonnet *et al.*, 2012), and even sporulate within the xylem vessels to spread systemically (e.g. fungus *Verticillium longisporum*) (Depotter *et al.*, 2016). Necrotrophic pathogens generally kill epidermal cells by secreting different toxins to feed from and grow on the dying tissues (e.g. fungus *Botrytis cinerea*) (Colmenares *et al.*, 2002) (**Figure 1.2**).

#### 1.2.1.4 Step #4: Leaving the host

To close the infectious cycle, pathogens need to be released back to the environment to infect a new host. The dissemination of pathogens from a diseased plant can occur through diverse mechanisms. Necrotrophic pathogen infection end up in killing the plant. These pathogens are subsequently released on the soil where they can grow saprophytically on the plant debris (e.g., bacterium *Ralstonia solanacearum* or fungus *Sclerotinia sclerotiorum*) (Schell, 2000; Hegedus and Rimmer, 2005) (**Figure 1.2**). Many plant pathogenic bacteria are able to colonize systemically the host plant and reach the reproductive organs where they are transmitted to the seeds (e.g., *Acidovorax citrulli*) (Agarwal and Sinclair, 1996; Dutta *et al.*, 2012). Filamentous fungi and oomycetes develop diverse reproductive structures to disseminate their spores through the air, water or soil (e.g. *Puccinia* spp. fungi or *Phytophthora* spp. oomycetes) (Geagea, Huber and Sache, 1999; Judelson and Blanco, 2005). Plant parasitic nematodes continue growing and feeding from the multinuclear feeding cell complex until they reach maturity and lay eggs (Abad and Williamson, 2010) (**Figure 1.2**). Vector-borne pathogens are reacquired by a new vector organism when feeding from a diseased plant (e.g. bacterium *Xylella fastidiosa*) (Chatterjee, Almeida and Lindow, 2008). These mechanisms are not mutually exclusive and sometimes, a same pathogen species can have different means of dissemination (e.g., *Xanthomonas campestris* pv. *campestris* is released to the soil with the death of the plant but can also colonize systemically the reproductive organs and infect the seeds) (Van Der Wolf and Van Der Zouwen, 2010; Vicente and Holub, 2013).

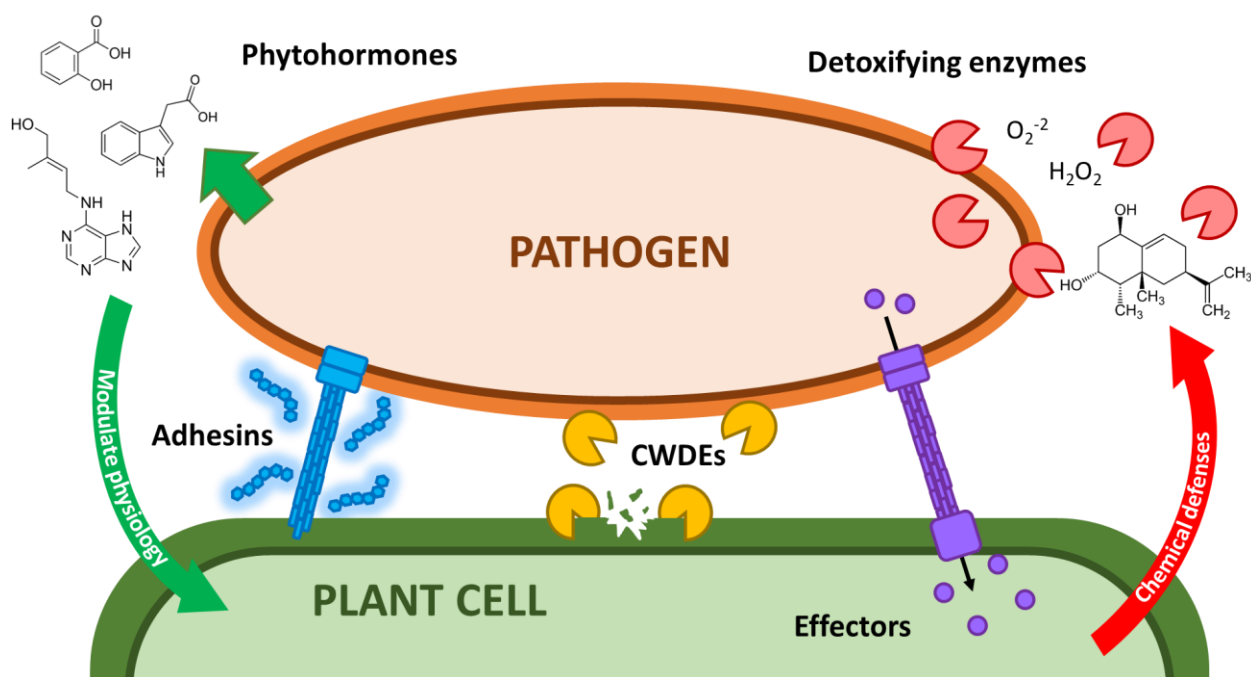


**Figure 1.3. Virulence determinants of plant pathogens.** To facilitate the infection, plant pathogens produce several virulence determinants including adhesins (in blue) that allow the attachment to the plant cell surface, cell wall degrading enzymes (CWDEs, in yellow) that digest the host cell wall, detoxifying enzymes (in red) that allow to subvert the chemical defenses of the plant such as ROS or phytoalexins, phytohormones secreted by the pathogen (green) that can modulate the plant hormone homeostasis in the pathogen's benefit and effectors (in purple), small molecules synthesized by the pathogens that are secreted and modify the plant defenses and physiology.



### 1.2.2 Virulence determinants: tools to be a bad guest

Plants are not passive hosts that accept the colonization by any organisms, but they actively defend themselves against invasions. The molecular bases of plant immunity are further explained in section 1.3. For a successful infection, pathogens rely on several virulence determinants to facilitate the invasion and proliferation within the host and the subversion of the plant defense responses (**Figure 1.3**).

One of the first virulence determinants playing an important role in the plant-pathogen interaction are adhesins. Adhesins are molecules that mediate a relatively specific attachment between a pathogen and its host. Adhesins do not only play an important role in the attachment to the host surfaces, but they are also involved in motility, host penetration, spore germination, exchange of different molecules and biofilm formation (Epstein and Nicholson, 2006; Berne *et al.*, 2015). Adhesins have been extensively characterized in Gram-negative plant pathogenic bacteria. Bacterial adhesins are divided into fimbrial, non-fimbrial and discrete polysaccharide adhesins. Fimbrial adhesins, also referred to as attachment pili, are formed by polymeric protein fibers. Non-fimbrial adhesins are shorter and typically monomeric or trimeric protein structures. Polysaccharide adhesins include polysaccharides firmly associated to the bacterial surface (capsular polysaccharides or CPS) and polysaccharides released by the bacteria (exopolysaccharides or EPS) (Berne *et al.*, 2015). Gram-positive plant pathogenic bacteria adhesins are so far less characterized, but fimbrial adhesins have been also found in spiroplasmas (Davis *et al.*, 2005). Fungal and oomycete adhesins have been largely studied in animal pathogens but less in plant pathogens. Among plant pathogenic fungal adhesins we can find high molecular weight glycoproteins, hydrophobins and glycosylphosphatidylinositol-anchored proteins (Epstein and Nicholson, 2006; Lipke, 2018).

When the pathogen encounters and attaches to the plant, the host cell wall is one of the first important barriers they have to face. Plant cell walls are composed of cellulose microfibrils embedded in a matrix of hemicellulose, pectin and structural proteins. To overcome this barrier, plant pathogens can deploy cell wall-degrading enzymes (CWDEs). CWDEs comprise arabinosidases, cellulases, galactosidases, glucuronidases, glycosidases, mannanases, xylanases, xyloglucanases and accessory enzymes (Kubicek, Starr and Glass, 2014). All these enzymes allow the pathogen not only to weaken the plant cell wall, but also to release mono- and oligosaccharides that can be subsequently catabolized. Different CWDEs are secreted by bacteria (Büttner and Bonas, 2010), filamentous pathogens (Kubicek, Starr and Glass, 2014),

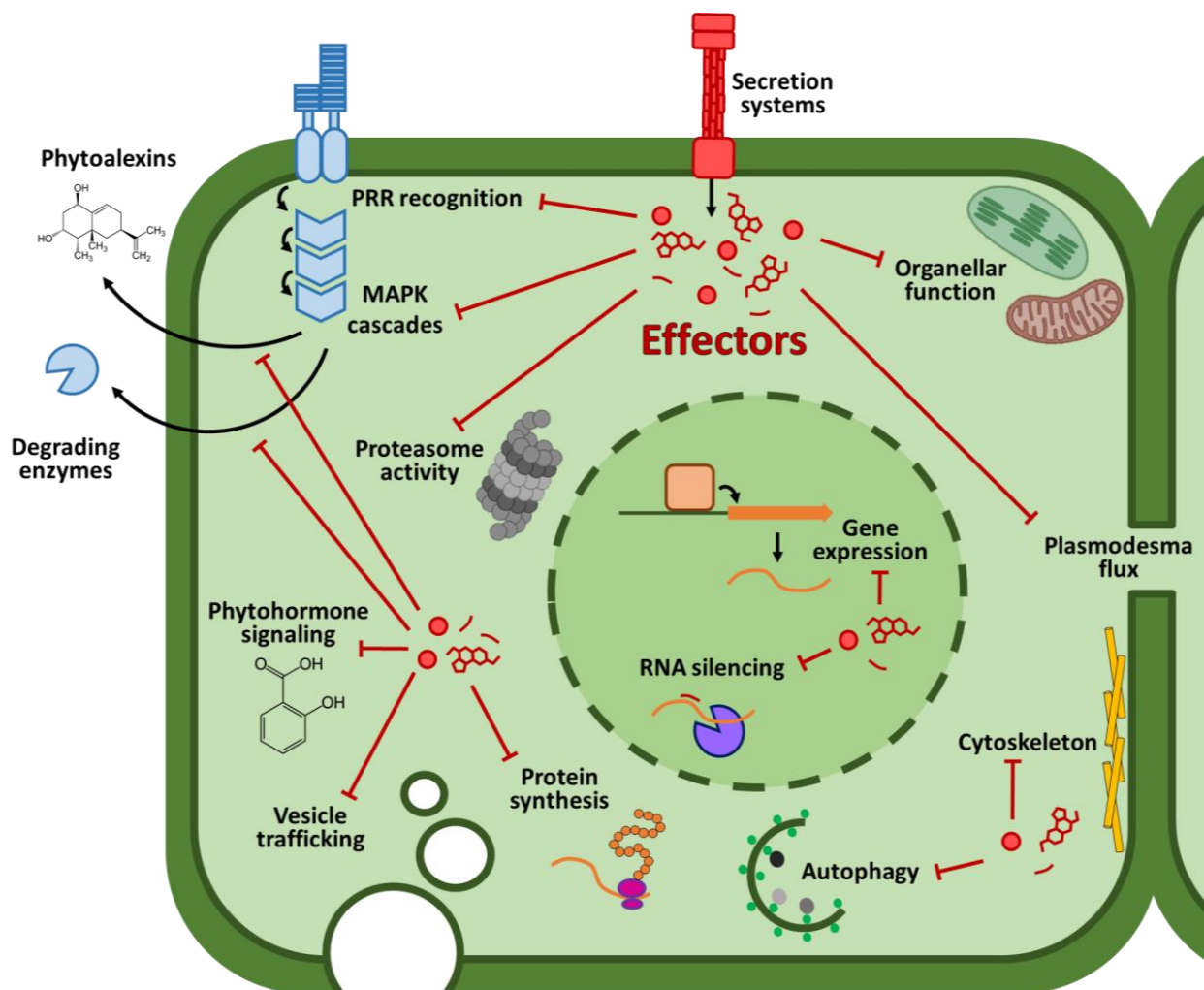


**Figure 1.4. Modes of action of plant pathogen effectors.** Pathogens deploy proteic, chemical and sRNA effectors to modulate the host physiology and subvert the defenses to the pathogen's own benefit. To do so, effectors are known to target many different cellular processes such as the different steps of the early signaling of basal defenses (e.g., recognition of pathogen, signaling cascades or synthesis of chemical defenses), degradative mechanisms such as proteophagy or autophagy, modulation of gene expression, RNA silencing, protein synthesis, vesicle trafficking, phytohormone homeostasis, organellar functions, cytoskeleton or transport through plasmodesmata. An extensive list of effectors targeting all these different cellular processes is presented in **table 1.1**.

nematodes (Davis, Haegeman and Kikuchi, 2011) and insects (Tokuda, 2019). Besides CWDEs, other plant pathogen enzymes can also act as virulence determinants. This is the case of detoxifying enzymes such as peroxidases, cytochrome c oxidases, multi-drug efflux pumps or different phytoalexin-converting enzymes (Genin and Denny, 2012; Pedras and Abdoli, 2017). Additionally, some pathogens are also able to synthesize phytohormones like auxins, cytokinins, abscisic acid, ethylene or salicylic acid to interfere with the plant hormonal homeostasis, which in some cases, can have a direct impact on virulence (De Meutter *et al.*, 2005; Valls, Genin and Boucher, 2006; Kilaru, Bailey and Hasenstein, 2007; Morrison, Emery and Saville, 2015; McClerkin *et al.*, 2018).

#### 1.2.2.1 Effectors: the pathogen's Swiss Army knife

Among all virulence determinants, effectors are probably the ones studied most extensively in many pathosystems over the last decades. Effectors have been classically defined as molecules secreted by the pathogen that manipulate the host physiology and/or subvert the host defense (Göhre and Robatzek, 2008) (**Figure 1.4**). Despite this broad definition, effector biology has focused mainly on effector proteins and has understudied the potentially similar roles played by other small molecules such as secondary metabolites (chemical effectors) or small non-coding RNAs (sRNA effectors) (Collemare, O'Connell and Lebrun, 2019).

Several chemical effectors have been described in different plant pathogens (**Table 1.1** and **figure 1.4**). Different pathovars from the Gram-negative plant pathogenic bacteria *Pseudomonas syringae* secrete several chemical effectors: coronatine, a molecule mimicking jasmonoyl isoleucine to avoid stomatal closure (Zheng *et al.*, 2012); syringolin, an inhibitor of proteasome activity also involved in avoiding stomatal closure (Schellenberg, Ramel and Dudler, 2010); or tabtoxin, phaseolotoxin and mangotoxin, all inhibitors of the protein synthesis (Arrebola *et al.*, 2011). Gram-positive bacterial pathogens also secrete chemical effectors such as thaxtomin, an inhibitor of cellulose synthesis synthesized by *Streptomyces* spp. (Scheible *et al.*, 2003). Fungal and oomycete pathogens possess a wider range of secondary metabolites that can act as chemical elicitors. Many of these metabolites were thought to be cytotoxic but recent transcriptomic analyses show that the enzymes responsible for their biosynthesis are mostly expressed in the early stages of infection suggesting a more probable role as chemical effectors (Collemare, O'Connell and Lebrun, 2019). Among these fungal metabolites, we can find molecules that interfere with the calmodulin signaling

**Table 1.1. Characterized effectors from plant pathogens.** Table summarizing the roles of several characterized protein and nonproteinaceous effectors from plant pathogens involved in virulence classified by their mechanism of action.

Effector <sup>a</sup>	Species (type) <sup>b,c</sup>	Brief description	Reference(s)
<b>Interference with basal plant defense responses</b>			
Avr4	<i>C. flagellaris</i> (F)	Protection against chitinases.	Santos Rezende <i>et al.</i> , 2019
Avr2	<i>C. fulvum</i> (F)	Interacts with cysteine proteases.	van Esse <i>et al.</i> , 2008
Avr4	<i>C. fulvum</i> (F)	Protection against chitinases.	van den Burg <i>et al.</i> , 2006
Tom1	<i>C. fulvum</i> (F)	$\alpha$ -tomatine detoxification.	Ökmen <i>et al.</i> , 2013 ; Osbourn 1996
Ecp6	<i>C. fulvum</i> (F)	Chitin sequestering to prevent PTI.	de Jonge <i>et al.</i> , 2010 ; Sánchez-Vallet <i>et al.</i> , 2013
Cgfl	<i>C. graminicola</i> (F)	Inhibition of plant chitinase activity.	Sanz <i>et al.</i> , 2015
DspA/E	<i>E. amylovora</i> (B)	Inhibits callose deposition	DebRoy <i>et al.</i> , 2004
FBI	<i>F. verticillioides</i> (F)	Protection against $\beta$ -1,3-glucanases.	Sánchez-Rangel <i>et al.</i> , 2012
I6B09	<i>H. glycines</i> (N)	Suppression of host defense responses.	Hu <i>et al.</i> , 2019
GLAND18	<i>H. schachtii</i> (N)	Suppression of host defense responses.	Noon <i>et al.</i> , 2016
4E02	<i>H. schachtii</i> (N)	Inhibition of RD21A-mediated defenses.	Pogorelko <i>et al.</i> , 2019
Slp1	<i>M. oryzae</i> (F)	Chitin sequestering to prevent PTI.	Mentlak <i>et al.</i> , 2012 ; Chen <i>et al.</i> , 2014
Hrip2	<i>M. oryzae</i> (F)	Inhibition of phytoalexin synthesis.	Nie <i>et al.</i> , 2019
TCTP	<i>M. enterolobii</i> (N)	Suppression of PCD.	Zhuo <i>et al.</i> , 2017
01965	<i>M. graminicola</i> (N)	Suppression of host defense responses.	Zhuo <i>et al.</i> , 2018
I6820	<i>M. graminicola</i> (N)	Suppression of host defense responses.	Naalden <i>et al.</i> , 2018
GPP	<i>M. graminicola</i> (N)	Suppression of host defense responses.	Chen <i>et al.</i> , 2017
265	<i>M. hapla</i> (N)	Suppression of host defense responses.	Gleason <i>et al.</i> , 2017
Sp12	<i>M. incognita</i> (N)	Suppression of host defense responses.	Xie <i>et al.</i> , 2016
TTL5	<i>M. japonica</i> (N)	Activation of ROS-scavenging system.	Lin <i>et al.</i> , 2016
ILysM	<i>M. graminicola</i> (F)	Chitin sequestering to prevent PTI.	Marshall <i>et al.</i> , 2011
3LysM	<i>M. graminicola</i> (F)	Chitin sequestering to prevent PTI.	Marshall <i>et al.</i> , 2011
WtsE	<i>P. stewartii</i> (B)	Upregulates the shikimate and phenylpropanoid pathways.	Asselin <i>et al.</i> , 2015
AVRblb2	<i>P. infestans</i> (O)	Prevents secretion of cysteine protease Cl4.	Bozkurt <i>et al.</i> , 2011
EPIC1	<i>P. infestans</i> (O)	Inhibitor of cysteine proteases.	Kaschani <i>et al.</i> , 2010 ; Tian <i>et al.</i> , 2007 ; Song <i>et al.</i> , 2009
EPIC2B	<i>P. infestans</i> (O)	Inhibitor of cysteine proteases.	Kaschani <i>et al.</i> , 2010 ; Tian <i>et al.</i> , 2007 ; Song <i>et al.</i> , 2009

GIP1	<i>P. sojae</i> (O)	Inhibition of endoglucanase EgaseA to prevent PTI.	Rose <i>et al.</i> , 2002
CRN115	<i>P. sojae</i> (O)	Maintenance of proper hydrogen peroxide levels.	Zhang <i>et al.</i> , 2015
CRN63	<i>P. sojae</i> (O)	Destabilization of plant catalases.	Zhang <i>et al.</i> , 2015
CRN70	<i>P. sojae</i> (O)	Suppression of hydrogen peroxide accumulation.	Rajput <i>et al.</i> , 2014
Avh240	<i>P. sojae</i> (O)	Inhibition of plant proteases.	Guo <i>et al.</i> , 2019
AvrB	<i>P. syringae</i> (B)	Phosphorylation of RIN4 and suppression of PTI.	Mackey <i>et al.</i> , 2002
AvrPto	<i>P. syringae</i> (B)	Inhibition of FLS2 and EFR autophosphorylation, BIK1 phosphorylation and dissociation of FLS2-BAK1 complex.	Shan <i>et al.</i> , 2008 ; Xiang <i>et al.</i> , 2008, 2011 ; Zhou <i>et al.</i> , 2014
AvrPtoB	<i>P. syringae</i> (B)	Ubiquitination of EFR and dissociation of FLS2-BAK1 complex.	Göhre <i>et al.</i> , 2008 ; Shan <i>et al.</i> , 2008 ; Cheng <i>et al.</i> , 2011
AvrRpm1	<i>P. syringae</i> (B)	Phosphorylation of RIN4 and suppression of PTI.	Mackey <i>et al.</i> , 2002
HopAO1	<i>P. syringae</i> (B)	Suppression of FLS2-mediated PTI and reduced EFR phosphorylation.	Macho <i>et al.</i> , 2014
HopF2	<i>P. syringae</i> (B)	Suppression of BIK1 phosphorylation.	Wang <i>et al.</i> , 2010 ; Wu <i>et al.</i> , 2011 ; Zhou <i>et al.</i> , 2014
HopZ1a	<i>P. syringae</i> (B)	Suppression of PR1 and PR5 accumulation and SAR.	Macho <i>et al.</i> , 2010
GSRE1	<i>P. striiformis</i> (F)	Inhibition of ROS burst.	Qi <i>et al.</i> , 2019
# Pst-miRNAs	<i>P. striiformis</i> (F)	Silencing of PR2.	Wang <i>et al.</i> , 2017
AGLIP1	<i>R. solani</i> (F)	Suppression of host defense responses.	Li <i>et al.</i> , 2019
RsLysM	<i>R. solani</i> (F)	Suppression of chitin-induced defenses.	Dörfors <i>et al.</i> , 2019
Pepl	<i>U. maydis</i> (F)	Interacts with the maize peroxidase POX12 to suppress ROS signaling	Hemetsberger <i>et al.</i> , 2012 ; Doehlemann <i>et al.</i> , 2013
Pit2	<i>U. maydis</i> (F)	Interacts with cysteine proteases.	Mueller <i>et al.</i> , 2013
Tin2	<i>U. maydis</i> (F)	Inhibition of synthesis of defense-related metabolites.	Tanaka <i>et al.</i> , 2014
XopN	<i>X. euvesicatoria</i> (B)	Stabilization of a TARK1/TFT1 complex and suppression of PTI.	Kim <i>et al.</i> , 2009a ; Taylor <i>et al.</i> , 2012
XopY	<i>X. oryzae</i> (B)	Suppression of CERK1-mediated phosphorylation of RLCK18.	Yamaguchi <i>et al.</i> , 2013
<b>Modulation of MAPK cascade signaling</b>			
AvrLm1	<i>L. maculans</i> (F)	Enhancement of MAPK9 phosphorylation.	Ma <i>et al.</i> , 2018
PexRD2	<i>P. infestans</i> (O)	Interaction with MAPKKKε.	King <i>et al.</i> , 2014
Pi22926	<i>P. infestans</i> (O)	Interaction with MAPKKKε.	Ren <i>et al.</i> , 2019
AvrB	<i>P. syringae</i> (B)	Activation of MPK4.	Cui <i>et al.</i> , 2010
HopAII	<i>P. syringae</i> (B)	Inactivation of MPK3 and MPK6 and reduced kinase activity of MPK4.	Zhang <i>et al.</i> , 2007 ; Zhang <i>et al.</i> , 2012 ; Singh <i>et al.</i> , 2014
HopF2	<i>P. syringae</i> (B)	ADP-ribosylation of MKK5 and interaction with MPK6.	Wang <i>et al.</i> , 2010 ; Singh <i>et al.</i> , 2014
<b>Interference with the proteasome activity</b>			

SAP54	<i>C. phytoplasma</i> (B)	Proteasomal degradation of MTF transcription factors.	McLean <i>et al.</i> , 2014
PM1900185	<i>C. phytoplasma</i> (B)	E3 ligase activity.	Strohmayr <i>et al.</i> , 2019
Rbp-1	<i>G. pallida</i> (N)	Interaction with a HECT-type ubiquitin E3 ligase.	Diaz-Granados <i>et al.</i> , 2020
RHA1B	<i>G. pallida</i> (N)	E3 ligase activity.	Kud <i>et al.</i> , 2019
AvrPiz-t	<i>M. oryzae</i> (F)	Interaction with APIP6, a RING E3 ubiquitin ligase.	Park <i>et al.</i> , 2012
vH6	<i>M. destructor</i> (I)	Contain F-box motif.	Zhao <i>et al.</i> , 2015
vH9	<i>M. destructor</i> (I)	Contain F-box motif.	Zhao <i>et al.</i> , 2015
Avr3a	<i>P. infestans</i> (O)	Stabilize the E3 ligase CMPG1.	Bos <i>et al.</i> , 2010
AvrPtoB	<i>P. syringae</i> (B)	E3 ubiquitin ligase activity.	Göhre <i>et al.</i> , 2008
HopM1	<i>P. syringae</i> (B)	Proteasomal degradation of MIN7 and inhibition of proteasome activity.	Nomura <i>et al.</i> , 2006, 2011 ; Üstün <i>et al.</i> , 2016
HopZ4	<i>P. syringae</i> (B)	Inhibition of proteasome activity.	Üstün <i>et al.</i> , 2014
XopJ	<i>X. euvesicatoria</i> (B)	Inhibition of proteasome activity.	Üstün <i>et al.</i> , 2013, 2015
XopL	<i>X. euvesicatoria</i> (B)	E3 ubiquitin ligase activity.	Singer <i>et al.</i> , 2013
XopP	<i>X. oryzae</i> (B)	Inhibition of OsPUB44 E3 ubiquitin ligase activity.	Ishikawa <i>et al.</i> , 2014 .
<b>Modulation of phytohormone signaling</b>			
Armet	<i>A. pisum</i> (I)	Induces SA accumulation.	Cui <i>et al.</i> , 2019
SAPII	<i>C. phytoplasma</i> (B)	Alteration of JA signaling.	Sugio <i>et al.</i> , 2011
TENGU	<i>C. phytoplasma</i> (B)	Downregulation of JA and auxin signaling.	Minato <i>et al.</i> , 2014
SIX4	<i>F. oxysporum</i> (F)	Activation of JA signaling.	Thatcher <i>et al.</i> , 2012
HARPI	<i>H. armigera</i> (I)	Alteration of JA response.	Chen <i>et al.</i> , 2019
Tyr	<i>H. schachtii</i> (N)	Modulates hormone homeostasis.	Habash <i>et al.</i> , 2017
HaRxL44	<i>H. arabidopsidis</i> (O)	Degradation of MED19A affecting the JA/SA balance.	Caillaud <i>et al.</i> , 2013
MiSSP7	<i>L. bicolor</i> (F)	Block JA-responses.	Plett <i>et al.</i> , 2011
@ LasA	<i>L. mediterranea</i> (F)	JA-Ile precursor.	Chini <i>et al.</i> , 2018
AvrLml	<i>L. maculans</i> (F)	Alteration of SA and ethylene signaling.	Šašek <i>et al.</i> , 2012
Abm	<i>M. oryzae</i> (F)	Hydroxylation of JA.	Miersch <i>et al.</i> , 2008 ; Patkar <i>et al.</i> , 2015
vH24	<i>M. destructor</i> (I)	Probably involved in phytohormone signaling.	Zhao <i>et al.</i> , 2016
ISE5	<i>M. incognita</i> (N)	Alteration of JA signaling.	Shi <i>et al.</i> , 2018
PSE1	<i>P. parasitica</i> (O)	Redistribution of auxin efflux carriers PIN4 and PIN7.	Evangelisti <i>et al.</i> , 2013
Isc1	<i>P. sojae</i> (O)	Isochorismate activity.	Liu <i>et al.</i> , 2014

Avr2	<i>P. infestans</i> (O)	Induces BR signaling.	Turnbull <i>et al.</i> , 2017
Avh238	<i>P. sojae</i> (O)	Inhibits ethylene biosynthesis.	Yag <i>et al.</i> , 2018
PvRXLR131	<i>P. viticola</i> (O)	Alteration of BR signaling.	Lan <i>et al.</i> , 2019
AvrB	<i>P. syringae</i> (B)	Promotion of JAZ and COII interaction.	Mackey <i>et al.</i> , 2002 ; Liu <i>et al.</i> , 2009 ; Cui <i>et al.</i> , 2010 ; Zhou <i>et al.</i> , 2015
AvrRpt2	<i>P. syringae</i> (B)	Promotion of Aux/IAA protein degradation.	Cui <i>et al.</i> , 2013
HopAF1	<i>P. syringae</i> (B)	Required for PAMP-induced ethylene production.	Washington <i>et al.</i> , 2016
HopQ1	<i>P. syringae</i> (B)	Activation of cytokinin signaling.	Hann <i>et al.</i> , 2014
HopX1	<i>P. syringae</i> (B)	JAZ degradation.	Gimenez-Ibanez <i>et al.</i> , 2014
HopZ1a	<i>P. syringae</i> (B)	JAZ degradation.	Jiang <i>et al.</i> , 2013
@ Coronatine	<i>P. syringae</i> (B)	Mimics JA-Ile	Zheng <i>et al.</i> , 2012
@ IaaM	<i>P. graminis</i> (F)	IAA-precursor.	Yin <i>et al.</i> , 2014
PNPi	<i>P. striiformis</i> (F)	Prevents NPR1 interaction with TGA transcription factors.	Wang <i>et al.</i> , 2016
REPAT38	<i>S. exigua</i> (I)	Alteration of JA response.	Chen <i>et al.</i> , 2019
Cmu1	<i>U. maydis</i> (F)	Reduction of SA levels.	Djamei <i>et al.</i> , 2011
lsc1	<i>V. dahliae</i> (F)	Isochorismate activity.	Liu <i>et al.</i> , 2014
SCP41	<i>V. dahliae</i> (F)	Inhibits SA biosynthesis.	Qin <i>et al.</i> , 2018
AvrBs3	<i>X. euvesicatoria</i> (B)	Induced auxin signaling.	Marois <i>et al.</i> , 2002
XopD	<i>X. euvesicatoria</i> (B)	Destabilization of ERF4 and reduced ethylene levels.	Kim, Stork and Mudgett 2013
<b>Modulation of plant gene expression</b>			
@ Depudecin	<i>A. brassicicola</i> (F)	Histone deacetylation.	Wight <i>et al.</i> , 2009
Bsp9	<i>B. tabaci</i> (I)	Interaction with WRKY33 transcription factor.	Wang <i>et al.</i> , 2019
SAPII	<i>C. phytoplasma</i> (B)	Destabilization of TCP transcription factors.	Pecher <i>et al.</i> , 2019
SAP54	<i>C. phytoplasma</i> (B)	Degradation of MTF transcription factors.	McLean <i>et al.</i> , 2014
@ HC-toxin	<i>C. carbonum</i> (F)	Histone deacetylation.	Walton 2006
@ Apicidin	<i>F. fujikuroi</i> (F)	Histone deacetylase inhibitor.	Kim <i>et al.</i> , 2004
SP7	<i>G. intraradices</i> (F)	Interaction with the transcription factor ERF19.	Kloppholz <i>et al.</i> , 2011
30D08	<i>H. schachtii</i> (N)	Interacts with a spliceosomal protein.	Verma <i>et al.</i> , 2018
32E03	<i>H. schachtii</i> (N)	Alteration of plant tRNA gene expression.	Vijayapalani <i>et al.</i> , 2018
GLAND4	<i>H. schachtii</i> (N)	Binding to promoter of lipid transfer protein genes	Barnes <i>et al.</i> , 2018
HsvG	<i>P. agglomerans</i> (B)	DNA binding and activation of plant gene expression.	Nissan <i>et al.</i> , 2006, 2012

Pi03I92	<i>P. infestans</i> (O)	Prevents NTP1 and NTP2 nuclear import.	McLellan <i>et al.</i> , 2013
HopDI	<i>P. syringae</i> (B)	Suppression of NTL9-regulated gene expression during ETI.	Block <i>et al.</i> , 2014
HopUI	<i>P. syringae</i> (B)	Interaction with RNA-binding proteins and reduction of PRR gene expression.	Fu <i>et al.</i> , 2007 ; Jeong <i>et al.</i> , 2011 ; Nicaise <i>et al.</i> , 2013
TAL family	<i>Xanthomonas</i> spp. (B)	Specific DNA-binding and transcriptional activation.	Boch <i>et al.</i> , 2009

#### Interference with the plant cytoskeleton

PFN3	<i>M. incognita</i> (N)	Disruption of actin filaments.	Leelarrasamee <i>et al.</i> , 2018
HopEI	<i>P. syringae</i> (B)	Interaction with calmodulin and microtubule-associated protein MAP65.	Guo <i>et al.</i> , 2016
HopGI	<i>P. syringae</i> (B)	Induces actin filament bundling.	Shimono <i>et al.</i> , 2016
HopWI	<i>P. syringae</i> (B)	Actin cytoskeleton disruption.	Kang <i>et al.</i> , 2014
HopZla	<i>P. syringae</i> (B)	Acetylation of tubulin and destruction of microtubules.	Lee <i>et al.</i> , 2012
@ Cytochalasan	Several species (F)	Actin cytoskeleton disruption.	Kretz <i>et al.</i> , 2019
AvrBsT	<i>X. euvesicatoria</i> (B)	Acetylation of tubulin-binding protein ACIPI.	Cheong <i>et al.</i> , 2014
XopL	<i>X. euvesicatoria</i> (B)	Induces the elimination of stromules.	Erickson <i>et al.</i> , 2018

#### Modulation of organelle function

HopGI	<i>P. syringae</i> (B)	Targets mitochondria to suppress PTI.	Bock <i>et al.</i> , 2010
HopII	<i>P. syringae</i> (B)	Recruitment of cytosolic Hsp70 to chloroplasts.	Jelenska, van Hal and Greenberg 2010
HopKI	<i>P. syringae</i> (B)	Reduced photosynthesis.	Li <i>et al.</i> , 2014
HopNI	<i>P. syringae</i> (B)	Reduced activity of PSII.	Rodriguez-Herva <i>et al.</i> , 2012
XopL	<i>X. euvesicatoria</i> (B)	Relocation of chloroplast near the nucleus.	Erickson <i>et al.</i> , 2018
AvrGf2	<i>X. fuscans</i> (B)	Targets chloroplasts.	Gochez <i>et al.</i> , 2017

#### Interference with molecule trafficking

Avr-Pii	<i>M. oryzae</i> (F)	Interaction with OsExo70-F2 and OsExo70-F3.	Fujisaki <i>et al.</i> , 2015
Avr3a	<i>P. infestans</i> (O)	Interaction with DRP2, involved in endocytosis.	Chaparro-Garcia <i>et al.</i> , 2015
HopWI	<i>P. syringae</i> (B)	Interference with endocytosis	Kang <i>et al.</i> , 2014
HopZla	<i>P. syringae</i> (B)	Interference with vesicle trafficking	Lee <i>et al.</i> , 2012
AvrPtoB	<i>P. syringae</i> (B)	Interaction with EXO70B1.	Wang <i>et al.</i> , 2019
@ Brefeldin A	Several species (F)	Inhibitor of protein ER to Golgi trafficking.	Nebenführ <i>et al.</i> , 2002

#### Interference with RNA silencing

# Bc-sRNAs	<i>B. cinerea</i> (F)	Silencing of Argonaute proteins.	Weiberg <i>et al.</i> , 2013
------------	-----------------------	----------------------------------	------------------------------



PSR1	<i>P. sojae</i> (O)	RNA silencing suppression.	Qiao <i>et al.</i> , 2013, 2015
PSR2	<i>P. sojae</i> (O)	RNA silencing suppression.	Qiao <i>et al.</i> , 2013, 2015
# Vd-sRNAs	<i>V. dahliae</i> (F)	Silencing of DCL proteins.	Wang <i>et al.</i> , 2016
<b>Modulation of autophagy</b>			
PexRD54	<i>P. infestans</i> (O)	Interaction with ATG8CL.	Dagdas <i>et al.</i> , 2016
AVH195	<i>P. parasitica</i> (O)	Interaction with ATG8 and represses autophagy.	Testi <i>et al.</i> , 2019
HopM1	<i>P. syringae</i> (B)	Induced autophagy.	Üstün <i>et al.</i> , 2018
@ Oxalic acid	<i>S. sclerotiorum</i> (F)	Suppression of autophagy.	Kabbage <i>et al.</i> , 2013
<b>Inhibition of protein synthesis</b>			
@ Monorden	<i>C. graminicola</i> (F)	Inhibits protein-folding machinery.	Wicklow <i>et al.</i> , 2009
@ Deoxynivalenol	<i>Fusarium</i> spp. (F)	Binds ribosome and prevents peptidyl transferase activity.	Shifrin and Anderson 1999
@ Mangotoxin	<i>P. syringae</i> (B)	Inhibitors of protein synthesis.	Arrebola <i>et al.</i> , 2011
@ Tenuazonic acid	Several species (F)	Inhibits ribosome activity.	Chen and Qiang 2017
<b>Other mechanisms</b>			
HopOI	<i>P. syringae</i> (B)	Manipulation of plasmodesmata intercellular flux.	Aung <i>et al.</i> , 2019
HopBFI	<i>P. syringae</i> (B)	Inhibition of ATPase activity of HSP90.	Lopez <i>et al.</i> , 2019
@ Tabtoxin	<i>P. syringae</i> (B)	Inhibition of nitrate assimilation.	Arrebola <i>et al.</i> , 2011
@ Phaseolotoxin	<i>P. syringae</i> (B)	Inhibition of one step of the urea cycle.	Arrebola <i>et al.</i> , 2011
@ Thaxtomin	<i>Streptomyces</i> spp. (B)	Inhibition of cellulose synthesis.	Scheible <i>et al.</i> , 2003
@ Ophiobolin	<i>Helminthosporium</i> spp. (F)	Interference with calmodulin signaling.	Au <i>et al.</i> 2000

<sup>a</sup> Protein effector unless otherwise noted (sRNA effectors are preceded by # and chemical effectors by @).

<sup>b</sup> Pathogen types abbreviations: B, bacterium; F, fungus; O, oomycete; N, nematode; and I, insect.

<sup>c</sup> *Ralstonia solanacearum* and *Xanthomonas campestris* pv. *campestris* were excluded from this list as more exhaustive lists on these two pathogens are presented in **tables 1.3** and **1.4**.

(e.g., ophiobolin) (Au, Chick and Leung, 2000), histone acetylation (e.g., depudecin) (Wight *et al.*, 2009), actin polymerization (e.g., cytochalasins) (Skellam, 2017) or different stages of the protein synthesis and secretion (e.g., brefeldin, deoxynivalenol, monorden or tenuazonic acid) (Wang *et al.*, 2002; Wicklow, Jordan and Gloer, 2009; Audenaert *et al.*, 2013)

Recently, it was discovered that pathogen sRNAs can be naturally transferred into the plant cell to silence the endogenous expression of host genes, acting thus as effectors. This first example of cross-kingdom RNA interference was observed between three *Botrytis cinerea* sRNAs that silenced the expression of Argonaute proteins from Arabidopsis and tomato (Weiberg *et al.*, 2013). This same mechanism has been observed later in other fungal pathogens such as *Verticillium dahliae* (Wang *et al.*, 2016) and *Puccinia striiformis* (Wang *et al.*, 2017), and predicted in *Blumeria graminis* (Kusch *et al.*, 2018) and *Sclerotinia sclerotiorum* (Derbyshire *et al.*, 2019) (**Table 1.1** and **figure 1.4**).

Despite the gathered knowledge on chemical and sRNA effectors over the last years, effector proteins are by far the virulence determinants best characterized in plant pathogens. Gram-negative bacterial type III effectors (T3Es) are some of the most extensively studied effectors. T3Es are effector proteins synthesized by the bacterium and translocated through its type III secretion system (T3SS), a sort of molecular syringe, directly into the host cytoplasm (Büttner and He, 2009). There are many examples of bacterial T3Es interfering with the plant basal defenses, mitogen-activated protein kinase (MAPK or MPK) cascade signaling, proteasome activity, phytohormones synthesis and signaling, gene expression, cytoskeleton organization, vesicle trafficking or organelle function (Büttner, 2016; Macho, 2016) (**Table 1.1** and **figure 1.4**). Comparatively less studied are effectors from Gram-positive plant pathogenic bacteria although there are few well-characterized examples such as phytoplasma effectors SAP54 that triggers the proteasomal degradation of plant transcription factors (MacLean *et al.*, 2014), TENGU that downregulates auxin and jasmonic acid signaling (Minato *et al.*, 2015), or SAP11 that interferes with plant transcription factors (Pecher *et al.*, 2019). Effector proteins from filamentous pathogens and nematodes have also been largely studied over the last decades but, although through comparative genomics and transcriptomics, it is now easier to identify putative effectors, the lack of methods for genetic transformation of most species hinders their functional characterization. Similar to bacterial effectors, oomycete, fungal and nematode effectors also interfere with plant basal defenses, phytohormones signaling, gene expression, MAPK cascade signaling, proteasome activity, vesicle trafficking, RNA silencing, epigenetic modifications or

cytoskeleton organization (Sharpee and Dean, 2016; Uhse and Djamei, 2018; Mejias *et al.*, 2019; Vieira and Gleason, 2019) (**Table 1.1** and **figure 1.4**). Work on insect effector manipulation of plant physiology is a relatively new emerging field. However, due to the complexity of the pathogen organisms, functional characterization of insect effectors is not an easy task and therefore, the number of well-characterized insect effectors so far is scarce (Giron *et al.*, 2016) (**Table 1.1**).

Altogether, regardless the type of pathogen they come from or their chemical nature, effectors have some general characteristics: 1) Effector gene expression is regulated in order to save resources. Effector-related genes are usually expressed at low levels in normal conditions and are expressed at higher level specifically during infection (Büttner and Bonas, 2010; Tan and Oliver, 2017). 2) Effectors are secreted. Effector molecules are synthesized in the pathogen and act within the host so they have to be secreted or translocated. Some pathogens secretion mechanisms are well studied such as the bacterial T3SS (Büttner and He, 2009) and T4SS (Voth, Broederdorf and Graham, 2012), fungal sRNA-containing extracellular vesicles (Cai *et al.*, 2019), or nematode and insects stylets (Rodriguez and Bos, 2013; Mejias *et al.*, 2019); whereas other are relatively less known, such as the fungal effector protein secretion mechanisms (Uhse and Djamei, 2018). 3) Effectors from different pathogens modify the plant physiology and immunity by targeting the same similar processes previously mentioned. In order to do so, effectors tend to interact with highly connected host proteins or “hubs” (Mukhtar *et al.*, 2011). These hubs usually occupy key positions in the host regulatory networks and therefore, by interfering with them, the pathogen can maximize its impact (Li, Zhou and Zhang, 2017; Ahmed *et al.*, 2018). 4) As consequence of the previous point, several effectors from a same pathogen might target a same plant target or biological process leading to functional redundancy (Tan *et al.*, 2015). This redundancy ensures a more robust virulence strategy for the pathogen, but complicates the dissection of single effector functions by classical reverse genetics approaches.

### 1.3. How to be a bad host: the plant side of the story

Unlike animals, plants lack an adaptive immune system with highly specialized and motile cells that protect the host against the possible invaders. Instead, each plant cell must be independently capable of defend itself when confronted to a pathogen. Plants have evolved a complex and multilayered immune system (Jones and Dangl, 2006). The long-term maintenance of defense mechanisms is very costly for the plant, limiting the resources otherwise

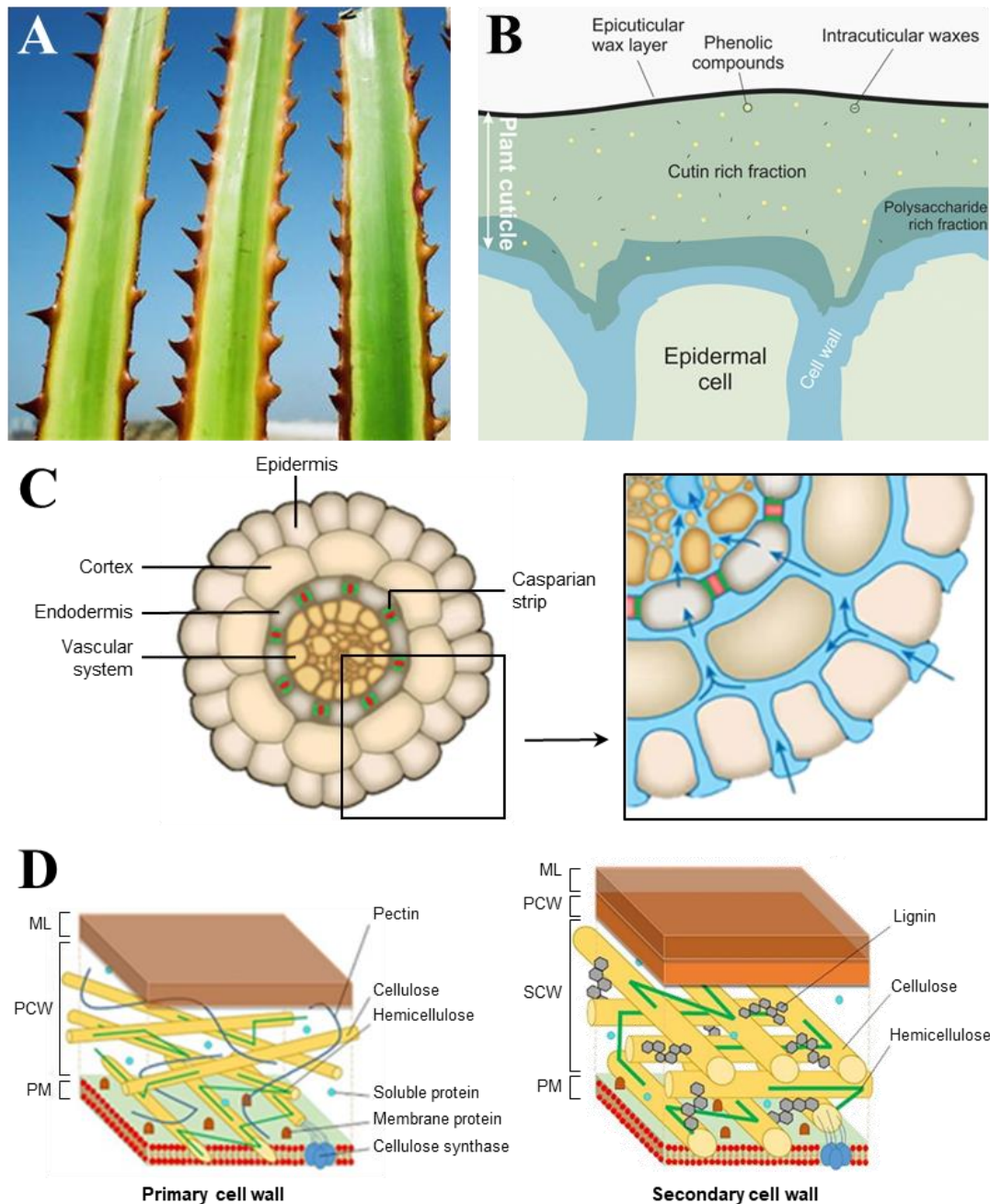


**Figure 1.5. Constitutive structural defense mechanisms of plants.** (A) Aposematic spines along the petioles of fan palms (*Washingtonia filifera*). (B) Scheme of the cross-section of a plant cuticle. The cuticle covers and protect the outermost region of the epidermis in the aerial parts of the plant. (C) Scheme of the cross-section of a root with a close-up of the lower-right quarter of the section depicting the flow of water and nutrients (blue). The Casparian strip act as a selective diffusion barrier preventing the apoplastic flow and forcing a symplastic pass towards the vascular cylinder. (D) Structure and composition of the primary and secondary cell wall of plants. ML: middle lamella, PCW: primary cell wall, PM: plasma membrane, SCW: secondary cell wall. Adapted from Lev-Yadun, 2016 (A); Heredia-Guerrero *et al.*, 2016 (B); Grebe, 2011 (C); and Loix *et al.*, 2017 (D).

available for growth (Huot *et al.*, 2014). This is why most defense mechanisms are tightly regulated and shut down in the absence of biotic stress stimuli prioritizing the allocation of resources towards plant growth (Huot *et al.*, 2014). Nevertheless, plants need to deploy constitutively a minimal set of defense mechanisms to ensure an initial restraint of the pathogen invasion and to gain time to deploy the stronger induced defense mechanisms.

### 1.3.1 “Stay ready” - Constitutive defenses

Among the defense mechanisms constitutively present in the plant, we can find both structural and chemical barriers. Structural barriers can be macroscopic such as thorns, spines and prickles that do not only limit insect herbivory, but they can also present aposematism (i.e., warning coloration) or be colonized by entomopathogenic bacteria and fungi to infect wounded insects (Halpern, Raats and Lev-Yadun, 2007) (**Figure 1.5A**). At the tissue level, we find the cuticle. The cuticle is the barrier covering the outer surface of the epidermis in aerial parts (**Figure 1.5B**). Its composition varies among species but it is generally composed of the polyester cutin covered and interspersed with waxes (Serrano *et al.*, 2014). This barrier allows the plant to prevent the colonization of pathogens and water losses. Precisely due to the impermeability of the cuticle, roots lack this barrier as their main function is water uptake. This could make roots more prone to be colonized by pathogens but this is prevented by the presence of the Casparian strip in the root endoderm (**Figure 1.5C**). This lignified barrier selectively controls the nutrient uptake and prevents the colonization by soilborne pathogens (Naseer *et al.*, 2012). Finally, at the cellular level, plant cells are surrounded by cell wall (**Figure 1.5D**). Cells in expansion present a primary cell wall composed of cellulose, hemicelluloses, pectins, and glycoproteins. In addition to this primary cell wall, cells that have completed their expansion are reinforced with a secondary cell wall mainly formed by cellulose, hemicelluloses and lignins. The cell wall has many essential functions during plant development but also prevents the invasion by many pathogens. The cell wall act thus as a passive barrier that needs to be breached for the progression of the pathogen (Miedes *et al.*, 2014).

In addition to the structural barriers, plants also synthesize constitutively a broad range of secondary metabolites that are toxic to pathogens. Among these secondary metabolites, we can find saponins that degrade cellular membranes, hydrogen cyanide or cardenolides that inhibit respiration, phytic acid that sequesters nutrients, cicutoxin that blocks potassium channels, bismorphine that inhibits pathogen pectinases or glucosionolates that have different deterrent and toxic effects (Wittstock and Gershenzon, 2002; Wittstock *et al.*, 2003). In order

**Table 1.2. Examples of avirulence and resistance proteins.** Table showing several examples of characterized avirulence and resistance proteins.

Effector	Species (kingdom) <sup>a,b</sup>	R protein	Host	Reference
Avr3	<i>B. lactucae</i> (O)	Dm3	Lettuce	Shen <i>et al.</i> , 2001
Avr2	<i>C. fulvum</i> (F)	Cf2	Tomato	Joosten and De Wit, 1999
Avr4	<i>C. fulvum</i> (F)	Cf4	Tomato	Joosten and De Wit, 1999
Avr9	<i>C. fulvum</i> (F)	Cf9	Tomato	de Wit <i>et al.</i> , 1985
ATR1	<i>H. arabidopsidis</i> (O)	RPP1	<i>A. thaliana</i>	Rehmany <i>et al.</i> , 2005
ATR5	<i>H. arabidopsidis</i> (O)	RPP5	<i>A. thaliana</i>	Bailey <i>et al.</i> , 2011
HaRxLI03	<i>H. arabidopsidis</i> (O)	RPP4	<i>A. thaliana</i>	Asai <i>et al.</i> 2018
AvrLm2	<i>L. maculans</i> (F)	Rlm2	<i>B. napus</i>	Ghanbarnia <i>et al.</i> , 2014
AvrLm1	<i>L. maculans</i> (F)	Rlm1	<i>B. napus</i>	Gout <i>et al.</i> , 2006
AvrLm11	<i>L. maculans</i> (F)	Rlm11	<i>B. napus</i>	Balesdent <i>et al.</i> , 2013
AvrLm3	<i>L. maculans</i> (F)	Rlm3	<i>B. napus</i>	Plissonneau <i>et al.</i> , 2015
AvrLm4-7	<i>L. maculans</i> (F)	Rlm4-7	<i>B. napus</i>	Parlange <i>et al.</i> , 2009
AvrLm6	<i>L. maculans</i> (F)	Rlm6	<i>B. napus</i>	Fudal <i>et al.</i> , 2007
AvrLmj1	<i>L. maculans</i> (F)	Rlmj1	<i>B. juncea</i>	Van de Wouw <i>et al.</i> , 2014
vH13	<i>M. destructor</i> (I)	H13	Wheat	Aggarwal <i>et al.</i> , 2014
vH24	<i>M. destructor</i> (I)	H24	Wheat	Aggarwal <i>et al.</i> , 2014
vH6	<i>M. destructor</i> (I)	H6	Wheat	Aggarwal <i>et al.</i> , 2014
vH9	<i>M. destructor</i> (I)	H9	Wheat	Aggarwal <i>et al.</i> , 2014
AvrL567	<i>M. lini</i> (F)	L5, L6 and L7	Flax	Dodds <i>et al.</i> , 2004
AvrM	<i>M. lini</i> (F)	M	Flax	Catanzariti <i>et al.</i> , 2006
AvrP4	<i>M. lini</i> (F)	P4	Flax	Catanzariti <i>et al.</i> , 2006
Avr-Pii	<i>M. oryzae</i> (F)	Pii	Rice	Tsunematsu <i>et al.</i> , 2000
AvrPiz-t	<i>M. oryzae</i> (F)	Piz-t	Rice	Li <i>et al.</i> , 2009
Avr3a	<i>P. infestans</i> (O)	R3a	Potato	Huang <i>et al.</i> , 2005
AVRblb2	<i>P. infestans</i> (O)	Rbi-blb2	<i>S. bulbocastanum</i>	Oh <i>et al.</i> , 2009
AvrB	<i>P. syringae</i> (B)	RPM1	<i>A. thaliana</i>	Mackey <i>et al.</i> , 2002
AvrPphB	<i>P. syringae</i> (B)	RPS5	<i>A. thaliana</i>	Shao <i>et al.</i> , 2003
AvrPto	<i>P. syringae</i> (B)	Prf/Pto	Tomato	Scofield <i>et al.</i> , 1996 ; Kim <i>et al.</i> , 2002
AvrPtoB	<i>P. syringae</i> (B)	Prf/Pto	Tomato	Kim, Lin and Martin 2002
AvrRpm1	<i>P. syringae</i> (B)	RPM1	<i>A. thaliana</i>	Mackey <i>et al.</i> , 2002
AvrRps4	<i>P. syringae</i> (B)	RRS1/RPS4	<i>A. thaliana</i>	Sarris <i>et al.</i> , 2015
AvrRpt2	<i>P. syringae</i> (B)	RPS2	<i>A. thaliana</i>	Axtell <i>et al.</i> , 2003
HopA1	<i>P. syringae</i> (B)	RPS6	<i>A. thaliana</i>	Kim <i>et al.</i> , 2009
HopZ1a	<i>P. syringae</i> (B)	ZAR1	<i>A. thaliana</i>	Lewis <i>et al.</i> , 2013
HopQ1	<i>P. syringae</i> (B)	Roq1	<i>N. benthamiana</i>	Schultink <i>et al.</i> , 2017
ToxA	<i>P. tritici-repentis</i> (F)	Tsn1	Wheat	Ciuffetti <i>et al.</i> , 2010 ; Faris <i>et al.</i> , 2010
ToxB	<i>P. tritici-repentis</i> (F)	Tsc2	Wheat	Effertz <i>et al.</i> , 2002 ; Singh <i>et al.</i> , 2010
AvrBs3	<i>X. euvesicatoria</i> (B)	Bs3	Pepper	Bonas <i>et al.</i> , 1989
AvrBs4	<i>X. euvesicatoria</i> (B)	Bs4	Tomato	Ballvora <i>et al.</i> , 2001
XopQ	<i>X. euvesicatoria</i> (B)	Roq1	<i>N. benthamiana</i>	Schultink <i>et al.</i> , 2017
AvrHah1	<i>X. gardneri</i> (B)	Bs3	Pepper	Schornack <i>et al.</i> , 2008

<sup>a</sup> Pathogen types abbreviations: B, bacterium; F, fungus; O, oomycete; N, nematode; and I, insect.

<sup>c</sup> *Ralstonia solanacearum* and *Xanthomonas campestris* pv. *campestris* were excluded from this list as more exhaustive lists on these two pathogens are presented in **tables 1.3** and **1.4**.

to save resources, constitutive chemical defenses are spatially regulated and accumulate in organs that are under a higher risk of attack while lower-risk organs present rather inducible defenses (Zangerl and Rutledge, 1996).

### 1.3.2 “Get ready” - Inducible defenses

Contrary to constitutive defenses, inducible defense mechanisms require a tight regulation that ensures their inactive state under normal conditions and a quick and effective activation upon the pathogen infection. In order to trigger this kind of defense mechanisms, plants have thus to perceive the presence of the pathogen, activate the adequate signaling pathway and execute the corresponding responses.

#### 1.3.2.1 Perception: how to know that you are not alone?

Pathogen-derived signal molecules have been traditionally classified in two groups: the conserved “pathogen-” or “microbe-associated molecular patterns” (PAMPs or MAMPs) and the pathogen-specific effectors. PAMPs are typically small molecules relatively conserved among different microorganisms (e.g., bacterial flagellin, elongation factor Tu, peptidoglycan or lipopolysaccharide, or fungal chitin or ethylene-induced xylanase) and are responsible for the activation of the first layer of defenses, the “PAMP-triggered immunity” (PTI). PTI comprises a wide variety of responses such as the generation of reactive oxygen species (ROS) and the expression of immune-related genes, and is usually enough to prevent the infection of most microorganisms (Boller and Felix, 2009). It is noteworthy to mention that this kind of defense responses can also be triggered by plant molecules released as consequence of the pathogen attack referred as “damage-associated molecular patterns” (DAMPs) (e.g., systemin, oligogalacturonides or cutin monomers) (Newman *et al.*, 2013). Effectors, in addition to their mentioned role as virulence determinants, can also serve as pathogen attack markers and trigger stronger defense responses collectively known as “effector triggered immunity” (ETI). This makes effectors a double-edge sword as they can act as both virulence and resistance determinants (**Tables 1.1** and **1.2**). ETI responses are a similar but amplified version of the PTI responses and are often associated with local cell death called “hypersensitive response” (HR) that prevents the further expansion of the pathogen.

These two layers of plant immunity, together with the pathogen ability to overcome them, constitute a co-evolutionary arm race between the host and the pathogen known as the

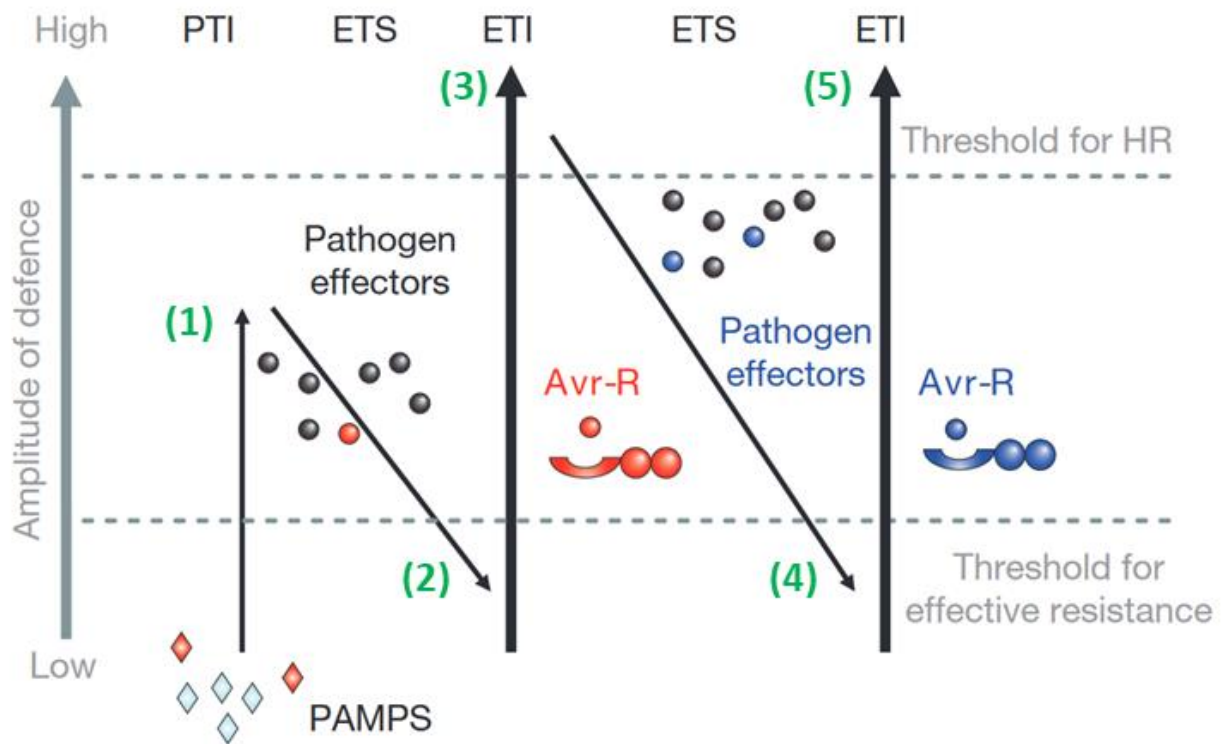


**Figure I.6. The zigzag model for plant immunity.** Classical zigzag model: The output of the plant-pathogen interaction is determined by the contribution of PTI, ETS and ETI. 1) Conserved PAMPs from the pathogen are recognized by the plant triggering PTI. 2) Effectors from an adapted pathogen can subvert the PTI leading to ETS. 3) The plant can recognize one of the pathogen effectors (in red) leading to an avirulence factor-resistance (Avr-R) gene-for-gene ETI. 4) Other effectors from an adapted pathogen can also subvert the ETI leading to ETS. 5) The plant can also recognize new effectors (in blue) and trigger the ETI. Adapted from Jones & Dangl, 2006.



zigzag model (Jones and Dangl, 2006) (**Figure 1.6**): Conserved molecules from different pathogens are recognized by the plant to trigger PTI leading to a basal resistance. However, some pathogens can secrete effectors that inhibit these defenses leading to the so-called effector triggered susceptibility (ETS). Plants, on the other hand, can also evolve to perceive some of these effectors and trigger the stronger ETI leading to full resistance. Nevertheless, pathogens can also evolve new effectors able to block the ETI leading back to susceptibility; until the plant evolves to recognize a new effector and to trigger back ETI, and so on and so forth.

It has been traditionally proposed that the recognition of PAMP/DAMPs and effectors is performed by extracellular and intracellular receptors respectively (Jones and Dangl, 2006). However, this dichotomy between PAMPs and effectors (and therefore, between PTI and ETI) has been challenged due to several limitations, exceptions and incongruities (Cook, Mesarich and Thomma, 2015). Extracellular receptors, also referred as “pattern recognition receptors” (PRR), are surface-localized receptor-like kinases, comprising an extracellular ligand-binding domain and an intracellular kinase domain; or receptor-like proteins, lacking the intracellular kinase domain (Macho and Zipfel, 2014). PRRs are able to homo- or heterodimerize or multimerize (e.g., the chitin receptor CERK1 in Arabidopsis, the flagellin receptor complex FLS2-BAK1 in Arabidopsis, or the chitin receptor complex CEBiP-CERK1 in rice, respectively) to perceive extracellular signals and transduce the signal into the cytoplasm (Chinchilla *et al.*, 2007; Shimizu *et al.*, 2010; Liu *et al.*, 2012) (**Figure 1.7A**). Intracellular receptors belong to the “nucleotide-binding oligomerization domain (NOD)-like receptor” (NLR) family. These modular receptors typically present a C-terminal leucine-rich repeat (LRR) domain, a central nucleotide-binding site (NBS) and an additional N-terminal domain. This N-terminal can be either coiled-coil (CC), Toll-interleukin 1 receptor (TIR), or RPW8-like domain at the N-terminus. Depending on this domain, NLRs are classified as CC-type NLRs (CNLs), TIR-type NLRs (TNLs) or RPW8-type NLRs (RNLs) (Monteiro and Nishimura, 2018). NLRs can recognize pathogen signals directly or indirectly through a guard protein (**Figure 1.7B**). The recognition of these signals usually triggers a conformational change that allows the transduction of the signal. Often these NLRs require the association with helper NLRs such as NRG1, a helper of several TNLs (Collier, Hamel and Moffett, 2011), or the NRC family, helpers of CNLs (Wu *et al.*, 2017).

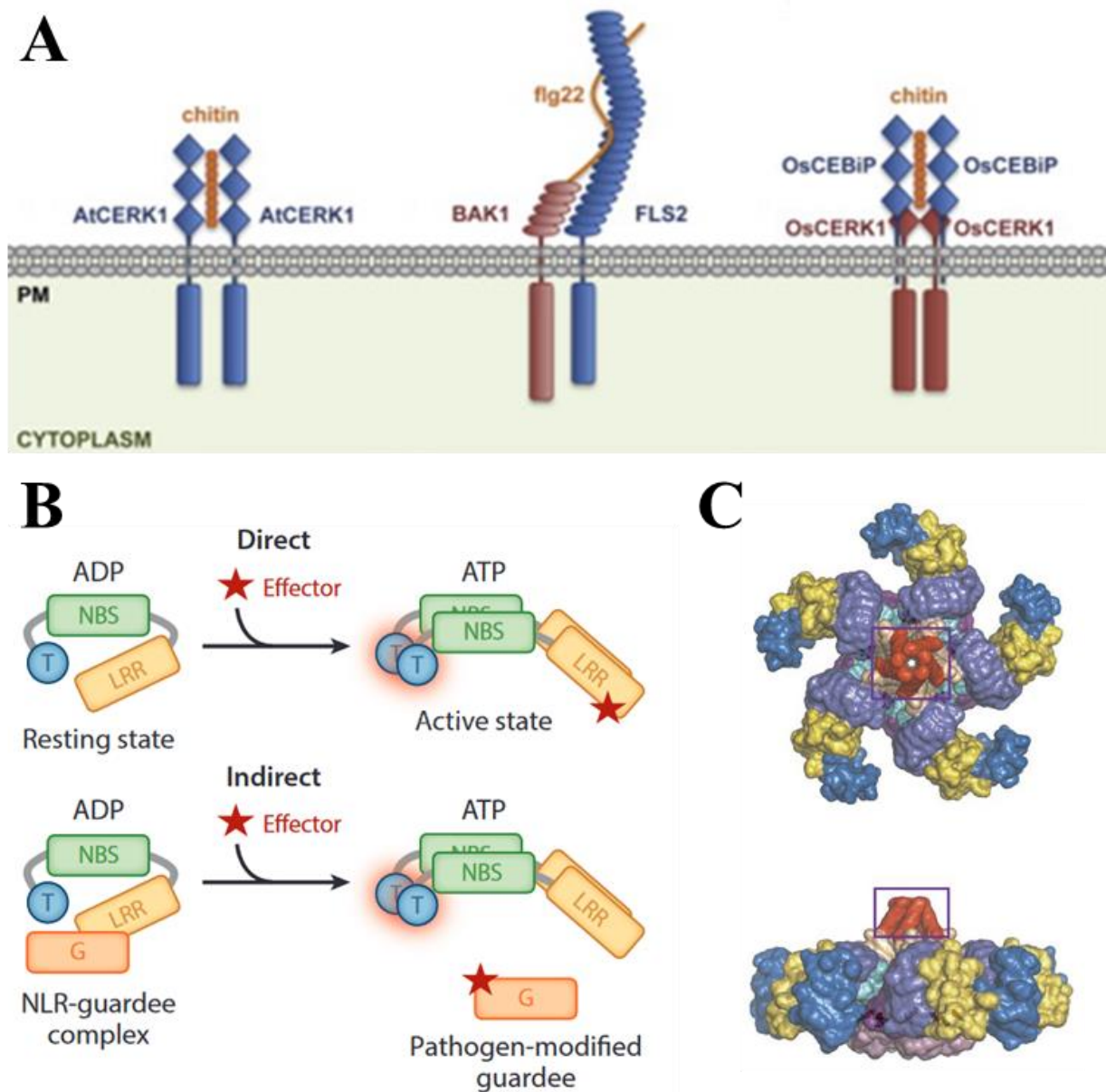


**Figure 1.7. Plant receptors involved in plant immunity.** (A) Extracellular receptors are pattern recognition receptors (PRRs, in blue and red) localized at the plasma membrane (PM). PRRs are able to recognize PAMPs (in orange) through homodimerization (AtCERK1), heterodimerization (FLS2-BAK1) or multimerization (OsCEBiP and OsCERK1). (B) Intracellular receptors are NOD-like receptors (NLRs) that present a variable N-terminus (T, in blue), a nucleotide binding site (NBS, in green) and a leucine-rich-repeat (LRR, in yellow). Upon recognition of an effector (red star), the NLR can change its conformation and transduce the signal. This recognition can be direct or indirect through a guard protein (G, in orange). (C) ZARI resistosome formed upon effector-triggered union and pentamerization of ZARI, RKS1 and PBL2. The N-termini of ZARI form a funnel-shaped structure (squared in purple) that could potentially anchor the resistosome to the PM triggering the ETI through drastic alteration of ion fluxes. Adapted from Macho & Zipfel, 2014 (A); Monteiro & Nishimura, 2018 (B); and Wang *et al.* 2019 (C).

### 1.3.2.2 Signaling: how to process that you are not alone?

Upon recognition of pathogen molecules by the mentioned receptors, several signals coordinately act in the plant cytoplasm to trigger the inducible defense mechanisms. These signals include alterations in the ion fluxes, generation of ROS and nitric oxide (NO), activation of MAPK cascades, modulation of hormone signaling and transcriptional reprogramming (Peng, van Wersch and Zhang, 2018) (**Figure 1.8**).

One of the first signals observed upon infection is a rapid increase of calcium ( $\text{Ca}^{2+}$ ) concentration in the cytoplasm. This increase is not constant and depending on its frequency, amplitude or cellular distribution, it might code for different pathogen signals or “ $\text{Ca}^{2+}$  signatures” (McAinsh and Hetherington, 1998). These signatures are transduced by  $\text{Ca}^{2+}$  binding proteins or  $\text{Ca}^{2+}$  sensors such as calmodulins, calmodulin-like proteins or  $\text{Ca}^{2+}$ -dependent protein kinases by binding or phosphorylation of their respective targets (Aldon *et al.*, 2018) (**Figure 1.8**).

Another rapid signal of pathogen detection is the generation of ROS such as superoxide anion, hydrogen peroxide and hydroxyl radicals. Apoplastic ROS are mainly synthesized by plasma membrane NADPH oxidases and cell wall peroxidases while cytoplasmic ROS are generated mostly in chloroplasts, peroxisomes and mitochondria (Qi *et al.*, 2017) (**Figure 1.8**). Due to their cytotoxicity, ROS do not only play an important role in signaling, but they have also a direct antimicrobial effect. However, to avoid self-cytotoxicity, plants possess efficient ROS scavenging systems including catalases, oxidases, peroxidases, superoxide dismutases and different antioxidants (Mittler *et al.*, 2004; Foyer and Noctor, 2005). ROS signaling is perceived by direct modification of proteins that present sulfur-containing amino acids or indirect modification of targets through redox molecules although yet little is known about these ROS-regulated target proteins (Qi *et al.*, 2017). NO is a reactive nitrogen species also quickly generated upon infection that can interact with  $\text{Ca}^{2+}$ , ROS as well as post-translationally modify proteins to transduce and modulate the biotic stress signal (Besson-Bard, Pugin and Wendehenne, 2008; Malerba and Cerana, 2015).

The recognition of pathogen molecules also triggers the activation of plant MAPK cascades that transduce the signal in form of phosphorylation of a wide range of target proteins with different roles in plant physiology and immunity (Meng and Zhang, 2013). These cascades are formed by successive rounds of phosphorylation of MAPK kinase kinases (MAPKKKs or

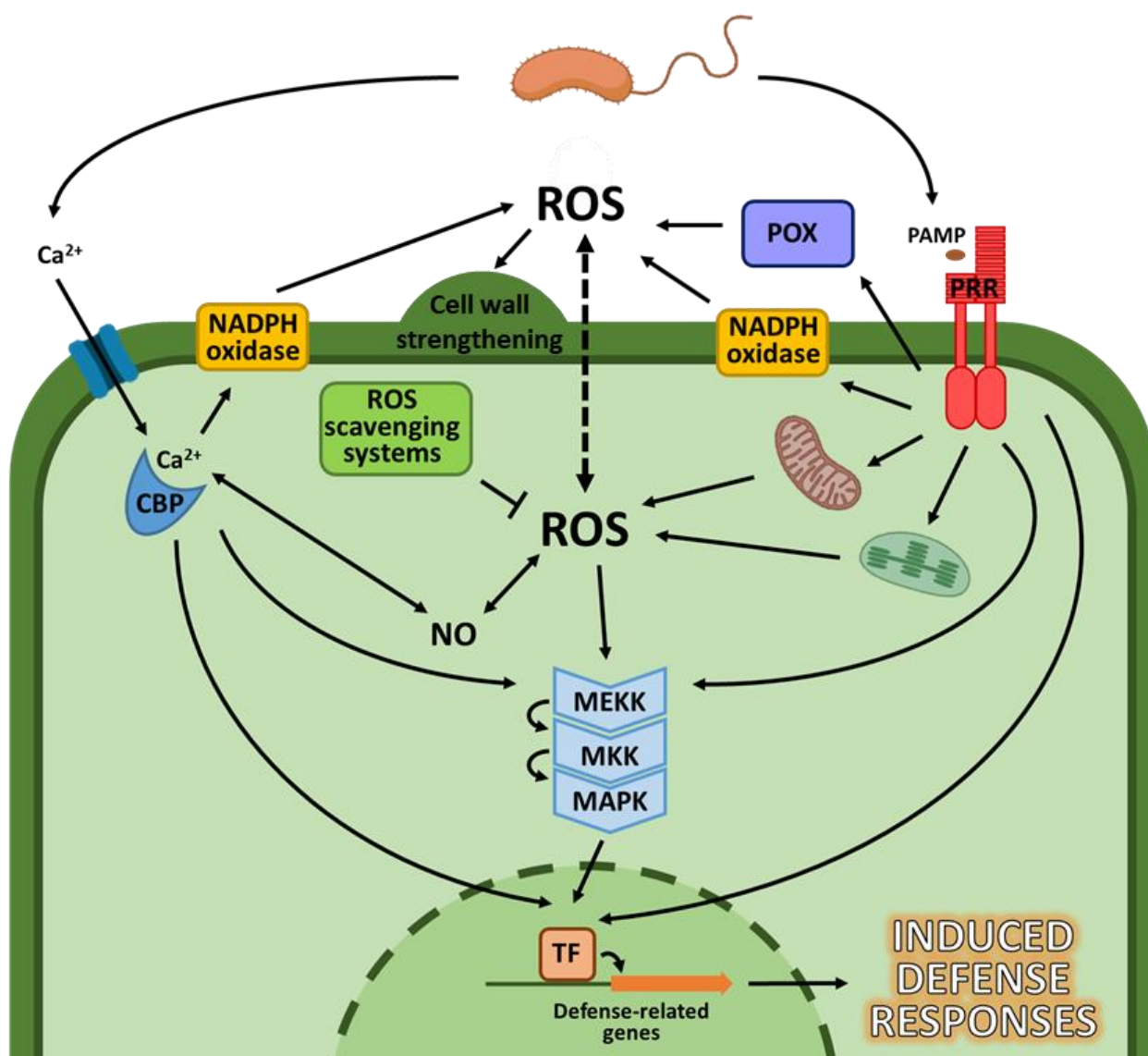


**Figure 1.8. Plant defense signaling.** The presence of the pathogen on the apoplast is perceived by an increase in the cytoplasmic  $\text{Ca}^{2+}$  sensed by calcium binding proteins (CBP) and PAMP binding to extracellular receptors (PRR). This induces the production of ROS in the apoplast via NADPH oxidases and peroxidases (POX) and in the cytoplasm via chloroplasts and mitochondria.  $\text{Ca}^{2+}$ , PAMP and ROS signaling can activate, directly or indirectly via MAPK cascades (MEKK, MKK and MAPK), different transcriptional factors (TF) that will induce the expression of defense-related genes. Additionally, ROS also induce NO synthesis that can interact with  $\text{Ca}^{2+}$  and ROS signaling. To avoid the cytotoxic effect of ROS, plant present different scavenging systems.

MEKKs), MAPK kinases (MAPKKs or MKKs) and MAPKs (**Figure 1.8**). Two important MAPK cascades have been characterized for their role in Arabidopsis immunity: 1) The MAPKKK3/5-MKK4/5-MPK3/6 cascade, which is involved in the biosynthesis of the ethylene, camalexin and glucosinolates and the closure of stomata. 2) The MEKK1-MKK1/2-MPK4 cascade, which is involved in other basal defense responses (Thulasi Devendrakumar, Li and Zhang, 2018).

As in any other physiological process, phytohormones, particularly salicylic acid (SA), jasmonic acid (JA) and ethylene, also play a pivotal role in plant immunity. Generally, biotrophic pathogens tend to induce the SA pathway while necrotrophic pathogens and wounding (herbivores) upregulate the JA and ethylene pathways (**Figure 1.9**). Enhanced diseases susceptibility 1 (EDS1) and Phytoalexin deficient 4 (PAD4) induce the synthesis of SA mostly by the Isochorismate Synthase 1 (ICS1) pathway. The increase in SA triggers the monomerization and subsequent nuclear import of Non-expressor of PR genes 1 (NPR1), the master regulator of the SA signaling pathway. Once in the nucleus, NPR1 interacts with TGA transcription factors to induce the expression of SA-responsive genes (Vlot, Dempsey and Klessig, 2009). JA is synthesized from membrane-released linolenic acid and then conjugated in many different forms although only jasmonoyl-l-isoleucine (JA-Ile) and in lesser extent methyl jasmonate (MeJA) are active. Upon infection, JA-Ile binds and changes the conformation of Coronatine Insensitive 1 (COI1) allowing its association with Jasmonate Zinc-finger expressed in inflorescence meristem (ZIM) (JAZ)-domain transcriptional repressor proteins in the nucleus. This association leads to JAZ protein proteasomal degradation and the arrest of the repression of MYC transcription factors that induce the JA-responsive genes (Antico *et al.*, 2012). Similarly, JAZ proteins also repress Ethylene Insensitive 3 (EIN3) and EIN3-like 1 (EIL1) which control other sets of JA- and ethylene-responsive genes connecting both hormone signaling pathways (Zhu *et al.*, 2011). It has been reported that the JA and SA signaling pathways are antagonist with SA inhibiting the JA pathway via NPR1 or JA inhibiting SA synthesis by inhibition of ICS1 expression (Spoel *et al.*, 2003; Zheng *et al.*, 2012). Ethylene is synthesized from S-adenosyl methionine. Upon infection, ethylene binds its receptors leading to an inactivation of Constitutive Triple Response 1 (CTR1) allowing EIN2 to protect EIN3/EIL from proteasomal degradation and therefore, inducing the expression of ethylene-responsive genes (Zhang *et al.*, 2018). In addition to SA, JA and ethylene, other phytohormones also present minor roles in immunity: Absciscic acid is involved in stomatal closure upon infection (Melotto *et al.*, 2006), gibberellins influence

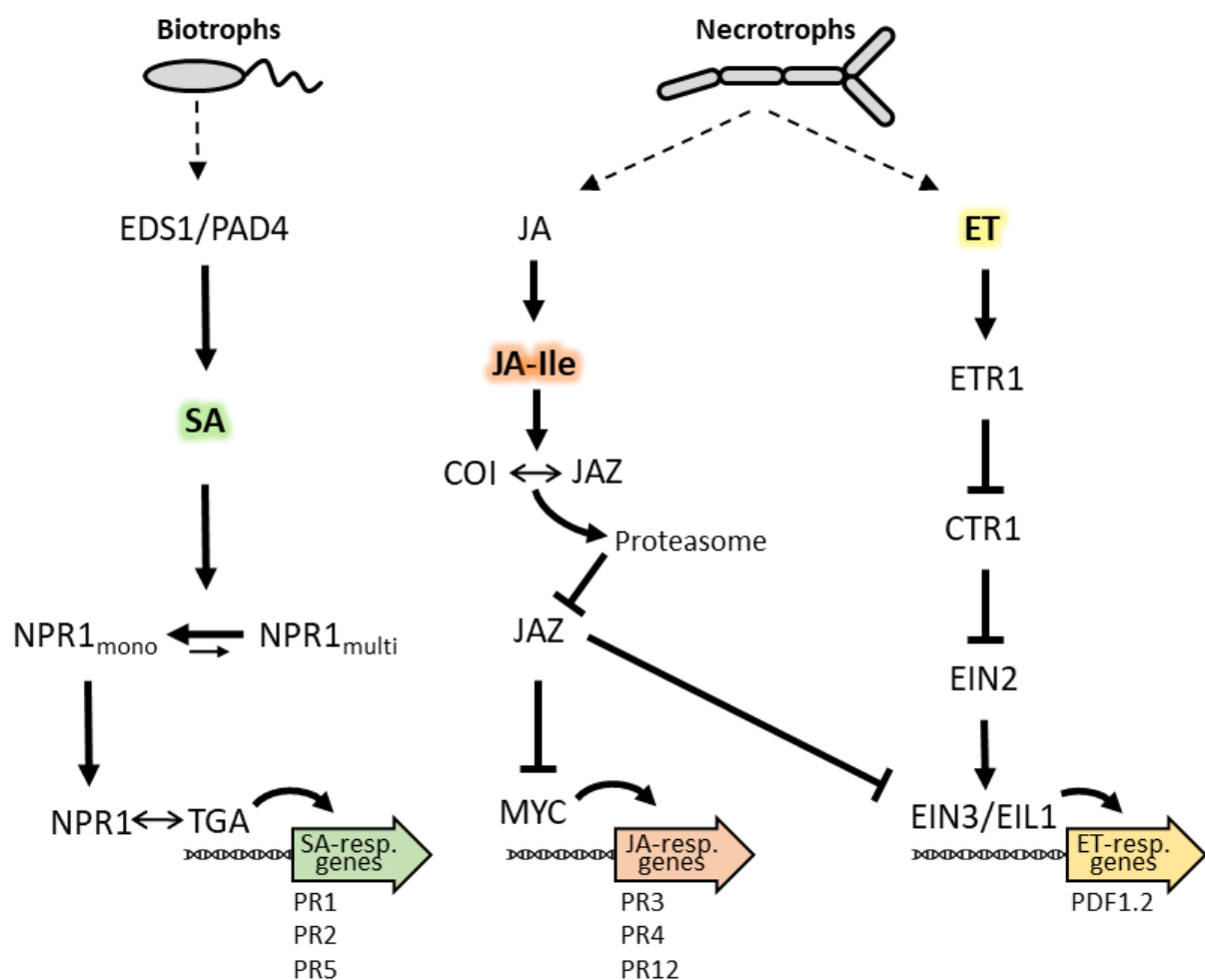


**Figure 1.9. Phytohormone signaling in plant defense.** Biotrophic pathogens induce the salicylic acid (SA) pathway whereas necrotrophic pathogens and wounds induce the jasmonic acid (JA) and ethylene (ET) pathways. Upon perception of a biotrophic pathogen, EDS1 and PAD4 are activated and induce the synthesis of SA. SA triggers a redox change that allow the monomerization of NPR1. Monomeric NPR1 can go to the nucleus where it interacts with TGA transcription factors to induce the expression of SA-responsive genes such as PR1, PR2 and PR5. Upon perception of a necrotrophic pathogen, the synthesis of JA and ET are enhanced. JA is conjugated into its most active forms such as JA-Ile. Ja-ILE induces the interaction of COI with JAZ proteins leading to the proteasomal degradation of the latter. This stops the JAZ-protein-inhibition of MYC transcription factors which is the steady state, allowing thus the expression of JA-responsive genes such as PR3, PR4 and PR12. ET is recognized by ET receptors such as ETR1 that inactivate CTR1. In normal conditions CTR1 inhibits EIN2. Therefore, ET indirectly activates EIN2, which subsequently activates EIN3 and EIL1 transcription factors that control the expression of ET-responsive genes such as PDF1.2. EIN3/EIL1 action is also repressed by JAZ proteins and are therefore equally controlled by JA.

negatively the JA pathway (Robert-Seilaniantz, Grant and Jones, 2011), and auxins and cytokinins can suppress and potentiate SA signaling respectively (Zhang *et al.*, 2018).

Regardless the elicitor molecule or the signaling pathway, most signals end up modulating gene expression through interaction with transcriptional regulators. Members from several plant transcription factor families such as the Apetala2/Ethylene-response element binding factor (AP2/ERF), basic-helix-loop-helix (bHLH), TGA/basic domain leucine zipper (TGA/bZIP), MYB, No apical meristem (NAM)/*Arabidopsis thaliana* activating factor 1 and 2 (ATAF1-2)/Cup-shaped cotyledon 2 (CUC2) (NAC); Teosinte branched 1/Cycloidea/PCF (TCP) or WRKY families are involved in plant immunity (Tsuda and Somssich, 2015). These transcription factors can be targeted directly by immune receptors (e.g., the NLR Mildew locus *ml0*, MLA10, interacts directly with barley transcription factors HvWRKY1 and 2) (Shen *et al.*, 2007); or indirectly through MAPK cascade activation (e.g., *Arabidopsis* AtWRKY33 is a target of the MAPKKK3/5-MKK4/5 -MPK3/6 cascade) (Mao *et al.*, 2011), or  $Ca^{2+}$  sensors (e.g., *Arabidopsis* Calmodulin-binding transcription activator 3, AtCAMTA3) (Galon *et al.*, 2008). Plants can even exploit their own transcription factors as decoys to recognize pathogen effectors (e.g., *Arabidopsis* RRS1 recognizes *R. solanacearum* PopP2) (Le Roux *et al.*, 2015).

### 1.3.2.3 Execution: what to do when you are not alone?

Similar to constitutive defenses, among the defense mechanisms induced by the pathogen signals we also find structural and chemical defenses. Induced structural defenses are related to the reinforcement of the previously described constitutive barriers. In this way, upon infection, plant cells can strengthen their cell wall with the secretion of callose or lignin and expression of extensins and proline-rich proteins (Brisson, Tenhaken and Lamb, 1994; Merkouropoulos and Shirsat, 2003; Underwood, 2012). Another important inducible structural defense is the closure of stomatal pores to prevent the penetration of pathogen through them (Melotto *et al.*, 2006).

Among the chemical inducible defense mechanisms, we can find mainly the synthesis of phytoalexins, the expression of pathogenesis related (PR) proteins and the accumulation of ROS. Phytoalexins are a heterogeneous group of secondary metabolites that show biological activity against pathogens. Phytoalexins have been described in many different botanical families such as dicots Brassicaceae (e.g., *Arabidopsis*, rapeseed or cabbage), Fabaceae (e.g., peanut or pea), Vitaceae (e.g., vine) or Solanaceae (e.g., tomato or pepper) or monocots Poaceae (e.g., maize or

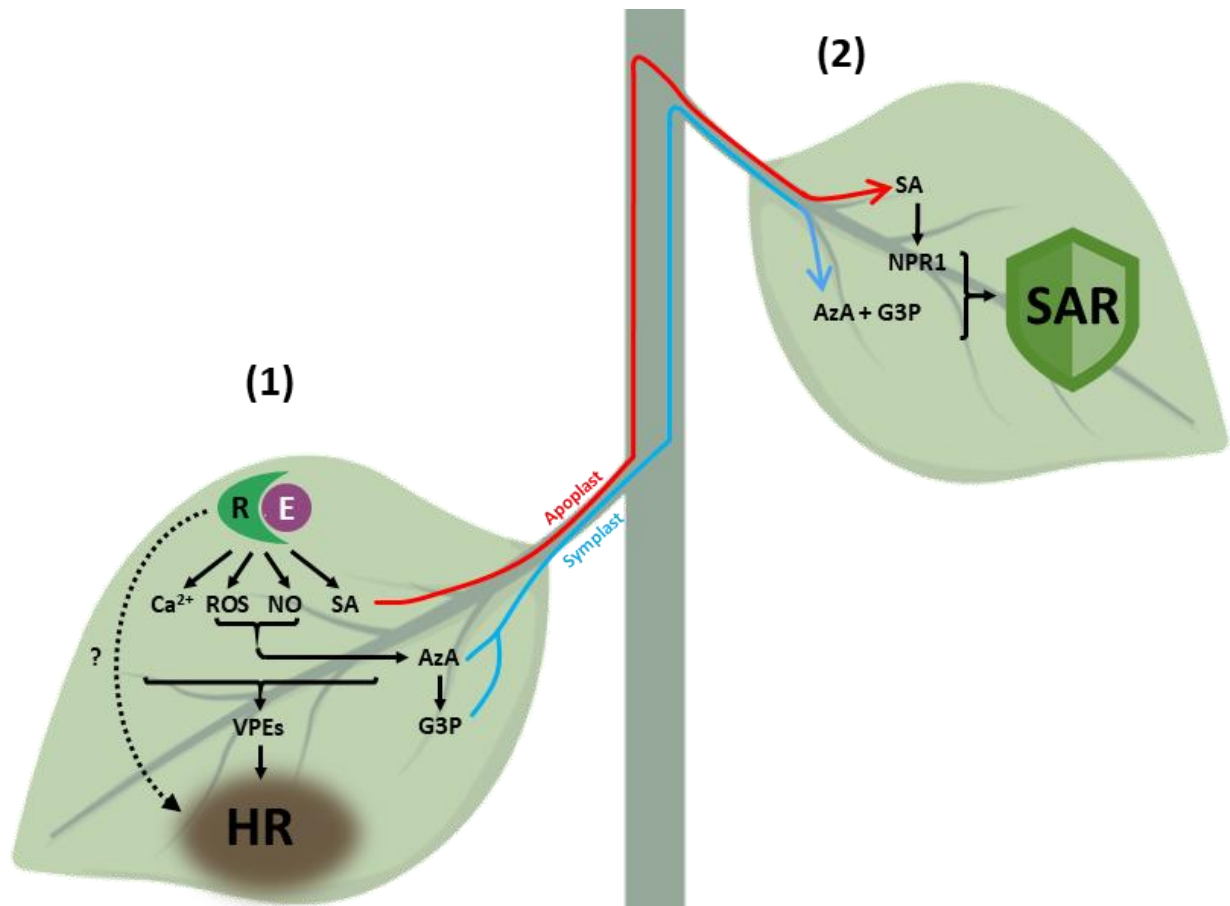


**Figure 1.10. Hypersensitive response (HR) and systemic acquired resistance (SAR).** 1) The recognition of a pathogen effector (E) by a plant resistance protein (R) triggers an increase in cytoplasmic  $\text{Ca}^{2+}$ , ROS, NO and SA. All these signals collectively activate vacuolar processing enzymes (VPEs) which will trigger a local and programmed cell death called HR. This HR prevents the proliferation of pathogens. Recently, an alternative model has been proposed in which the recognition of an effector protein can change the conformation of the R protein and allow its multimerization into “resistosomes” (see **figure 1.7C**) which might trigger their HR directly altering the membrane permeability and ion flux. Upon recognition, SA is formed which can be transported systemically through the apoplast reaching distal tissues where, via NPR1, can trigger SAR. Another SAR-pathway is controlled by azelic acid (AzA), which is synthesized upon a NO-ROS feedback loop, and glycerol-3-phosphate (G3P). These two signal molecules can be transported through the phloem symplast and reach equally distal tissues where they can activate SAR.



oat) (Ahuja, Kissen and Bones, 2012). Often, the molecular mechanisms ruling their regulation, biosynthesis and cytotoxicity are unknown. One of best characterized phytoalexin is camalexin, which possesses *in vitro* antimicrobial activity and that is involved in resistance against necrotroph pathogens (Kliebenstein, Rowe and Denby, 2005). PR proteins englobes a diverse group of proteins that are expressed upon infection. They are grouped into 17 families mainly based on their amino acid sequence similarities, enzymatic activities and other biological features: antifungal proteins (PR1 and PR17), glucanases (PR2), chitinases (PR3, PR4, PR8 and PR11), thaumatin-like proteins (PR5), proteinase inhibitors (PR6), endoproteinases (PR7), peroxidases (PR9), ribonuclease-like proteins (PR10), defensins (PR12), thionins (PR13), lipid-transfer proteins (PR14), oxalate oxidases (PR15) and oxidase-like proteins (PR16) (Sels *et al.*, 2008). Some PR proteins are actively expressed during infection by biotrophs such as PR1, PR2 and PR5 while the expression of others is rather induced upon infection by necrotrophs such as PR3, PR4 and PR12 (Ali *et al.*, 2018). As previously mentioned, ROS production is one of the most rapid signals of pathogen attack and in addition to their role as signaling molecules, ROS also possess antimicrobial effects (Heller and Tudzynski, 2011). However, ROS actions are complex and not yet fully understood as they depend on the type, timing, concentration and interaction with others of each ROS (Hückelhoven and Kogel, 2003).

Another well-characterized inducible defense mechanism, typically associated with ETI, is HR. The term HR refers to a rapid and local cell death in the infection area that prevents totally or partially the progression of the infection (Goodman and Novacky, 1994). Although caused upon infection, HR is an active form of programmed cell death controlled by the host (Mur *et al.*, 2008). HR is a widespread phenomenon found in most higher plants and is induced by all kind of pathogens: viruses, bacteria, oomycetes, fungi, nematodes, insects and even parasitic plants (Balint-Kurti, 2019). HR is typically triggered upon recognition of the products of a pathogen *Avr* gene and the host *R* gene following the gene-for-gene model previously described (Flor, 1955). *Avr* genes typically encode effector proteins and *R* genes, NLRs, although this is not always the case (Kourelis and van der Hoorn, 2018). This recognition leads somehow to the accumulation of  $\text{Ca}^{2+}$ , ROS, NO, SA that will in term activate vacuolar processing enzymes ultimately leading to tonoplast rupture and subsequent cell death (Mur *et al.*, 2008) (**Figure 1.10**). Alternatively, this tonoplast rupture might also be caused by NLR activation and oligomerization generating the so-called “resistosome” structures that can be docking sites for HR signaling proteins and/or membrane spanning pores as recently reported for the Arabidopsis CNL ZAR1 (J. Wang, Hu, Wang, *et al.*, 2019) (**Figure 1.7C and 1.10**). However, despite being a

plant defense mechanisms, HR can be also exploited by necrotroph pathogens as they grow on and feed from host dead tissues (Govrin and Levine, 2000; Lorang, 2019).

### 1.3.3 “Tell the others to get ready” - Systemic resistance

Infection of plants by pathogens or the colonization of plant roots by certain microbes cause the induction of “priming”, a physiological state in which the whole plant displays an either faster, stronger or both, activation of the defense-related cellular processes (Conrath *et al.*, 2006). Systemic acquired resistance (SAR) is the plant priming state induced upon local infection with a pathogen that confers resistance against a broad spectrum of attackers (Ryals *et al.*, 1996). This systemic induction requires the generation and transport through the vasculature of certain systemic signal molecules organized in two parallel branches: one regulated by SA preferentially transported through the apoplast, and another one regulated by azelic acid (AzA) and glycerol-3-phosphate (G3P) transported through the symplast (Singh, Lim and Kachroo, 2017) (**Figure 1.10**). SA-dependent SAR, similar to local response SA-mediated defense responses, also rely on NPR1 monomerization and nuclear import for functioning (Cao *et al.*, 1997; Spoel *et al.*, 2009). Aza-G3P-dependant SAR requires a positive feedback loop between NO and ROS upon infection that triggers the hydrolysis of unsaturated C18 fatty acids into AzA. Aza itself is already a SAR inducer but it also triggers the synthesis of G3P, another SAR inducer (Yu *et al.*, 2013; Wang *et al.*, 2014). These signals trigger defense-related responses in distal tissues producing thus the priming effect. SAR does not only protect systemically the plant after a pathogen attack, but is also epigenetically inherited in the next generation in a SA- and NPR1-dependent manner through hypomethylation of DNA (Luna *et al.*, 2012).

The root colonization by non-pathogenic microorganisms can also trigger a priming effect through a process called induced systemic resistance (ISR). Similar to SAR, ISR also confers resistance against a broad spectrum of pathogen although contrary to SAR, ISR depends on the JA and ethylene pathways (Pieterse *et al.*, 2002). Interestingly, although ISR is SA-independent, it requires NPR1 indicating that NPR1 is able to differentially regulate both SA-dependent SAR and JA/ethylene-dependent ISR (Pieterse *et al.*, 1998). SAR and ISR act thus independently and the simultaneous induction of both have an additive effect potentially exploitable for biocontrol (van Wees *et al.*, 2000). In addition to SAR and ISR, other forms of plant priming can be achieved chemically with  $\beta$ -aminobutyric acid or certain volatile organic compounds released upon herbivory damage (Conrath *et al.*, 2006).

## 1.4. The xylem: a barely frequented meeting point

While many pathogens are adapted to colonize the relatively nutrient-rich apoplast or symplast, some pathogens thrive in the vascular tissues. Plant vasculature is composed of xylem vessels, tracheary elements that transport water and mineral absorbed by the roots (xylem sap) to the photosynthetic organs, and phloem elements, living cells that transport photoassimilates. Paradoxically, although the phloem contain more nutrients, most vascular pathogen colonize xylem vessels because phloem living cells present a high osmotic pressure while xylem dead tracheary elements present a low osmotic pressure. Still, a few pathogens such as viruses, rickettsias, spiroplasmas and phytoplasmas are able to colonize the phloem (Hipper *et al.*, 2013; Yadeta and Thomma, 2013). Hereafter, vascular pathogens will refer exclusively to xylem-colonizing pathogens.

The xylem structure is determined by the size, shape and distribution of the different cell types and respective cell walls that form it. These cells are tracheids and vessel members (collectively known as tracheary elements), parenchyma and fibers (**Figure 1.11**). Tracheary elements correspond to the main conductive tissue. Tracheids appear earlier during the plant development and function as single cellular units connected through large and radial pits whereas vessel elements appear later and are connected end-to-end through large perforations in their ends. Mature tracheary elements are dead cells with not cytoplasmic content and consist only of a thin primary cell wall and a thickened secondary cell wall. Parenchyma cells are the only metabolically active and serve to store water and nutrients. Xylem fibers usually present thickened and lignified cell wall and provide additional support (Myburg, Lev-Yadun and Sederoff, 2013).

Nutritionally, xylem sap is relatively poor which could explain why not so many pathogens thrive on it although the few that can, do it with almost no competition (McCully, 2001). Xylem sap is relatively rich in several inorganic anions such as nitrate, sulfate, and phosphate as well as in several cations like calcium, potassium, magnesium, and manganese (Nakamura *et al.*, 2008). Among its organic composition we can find low concentrations of certain amino acids (Ala, Arg, Asp, Glu, Gln, Ile, Leu, Met, Pro, Thr, Tyr and Val), sugars (glucose, fructose, mannitol, myo-inositol and sucrose), organic acids (formic, fumaric and succinic acid) and alcohols (ethanol and methanol) (Fuente *et al.*, 2017). However, the nature and concentration of these metabolites vary among species, seasons, time or growth conditions (Siebrecht *et al.*, 2003). In addition to the xylem sap, vascular pathogens can feed from products

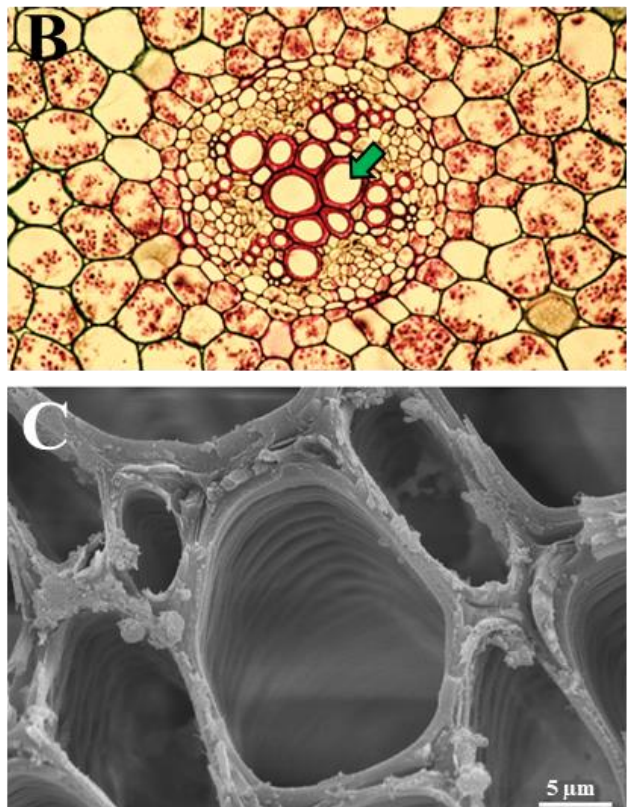
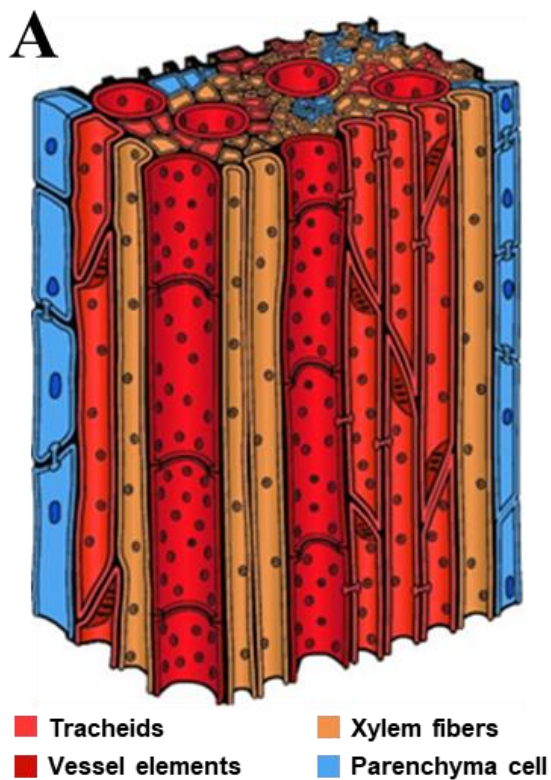


**Figure 1.II. Structure of xylem.** (A) Representation of a cross-section of xylem showing tracheids and vessel elements interconnected via pits, xylem fibers and parenchyma cells. (B) Micrograph of a cross-section of young roots from pea. Xylem vessels in the center are pointed with a green arrow. (C) Micrograph from electron microscopy of xylem vessels from a gerbera flower stem fractured in liquid nitrogen (bar=5  $\mu\text{m}$ ). Adapted from Graf *et al.*, 2015 (A); Spricigo *et al.*, 2015 (B); and Myburg *et al.*, 2013 (C).

of the enzymatic digestion of plant cell walls, invading neighboring parenchyma cells or inducing nutrient leakage from surrounding tissues (Divon *et al.*, 2005; Möbius and Hertweck, 2009; Klosterman *et al.*, 2011).

Among the pathogens genera that colonize the xylem (and their respective hosts) we can find several fungi such as *Ceratocystis* (oak, cocoa and eucalyptus), *Ophiostoma* (elm tree), *Verticillium* and *Fusarium* (broad host range); several bacteria such as *Clavibacter* (Solanaceae), *Curtobacterium* (beans), *Erwinia* (cucurbits), *Pantoea* (cotton), *Xanthomonas* (Brassicaceae, rice and barley), *Ralstonia* and *Xylella* (broad host range); and a oomycete genus: *Pythium* (broad host range) (Yadeta and Thomma, 2013) (**Figure 1.12**). The diseases caused by these pathogens are generally quite hard to control: infected plant cannot be treated and need therefore to be eradicated, the responsible pathogens produce resting structures able to survive for many years, and their broad host range makes classical control measures such as crop rotation inefficient. The resting structures in the soil are the desirable target for chemical control, but the ban on these measures due to possible public and environmental health problems makes resistance breeding the optimal long-term and sustainable control measure (Yadeta and Thomma, 2013).

Plant defense mechanisms against vascular pathogens might differ from those against non-vascular pathogens (van Esse *et al.*, 2009). These defense mechanisms can be structural, mainly focused on preventing the pathogen progression, or chemical, mostly dedicated to kill the pathogen or inhibit its growth. A classical structural defense mechanisms against vascular pathogens is the generation of tyloses, gel-coated protuberances of xylem parenchyma cells that invade and proliferate within tracheary elements through pits blocking thus the spread of pathogen (Clérivet *et al.*, 2000; Fradin and Thomma, 2006). Another observed mechanism against vascular pathogens is the *de novo* formation of xylem to compensate the compromised water transport (Reusche *et al.*, 2012). The coating of the vascular wall covering pit membranes, primary walls and parenchyma cells around the infected site and adjacent cells is another structural defense against vascular pathogens (Rahman, Abdullah and Vanhaecke, 1999). AvrAC/XopAC, a T3E from *Xanthomonas campestris* pv. *campestris*, is only able to confer resistance in Arabidopsis when inoculated in the xylem and not in the mesophyll indicating that ETI responses can also occur specifically in the xylem (Xu *et al.*, 2008a). The chemical defense mechanisms against vascular pathogens depend on the metabolically active xylem parenchyma that pour their content in the xylem sap. Among the substances found in the xylem sap upon



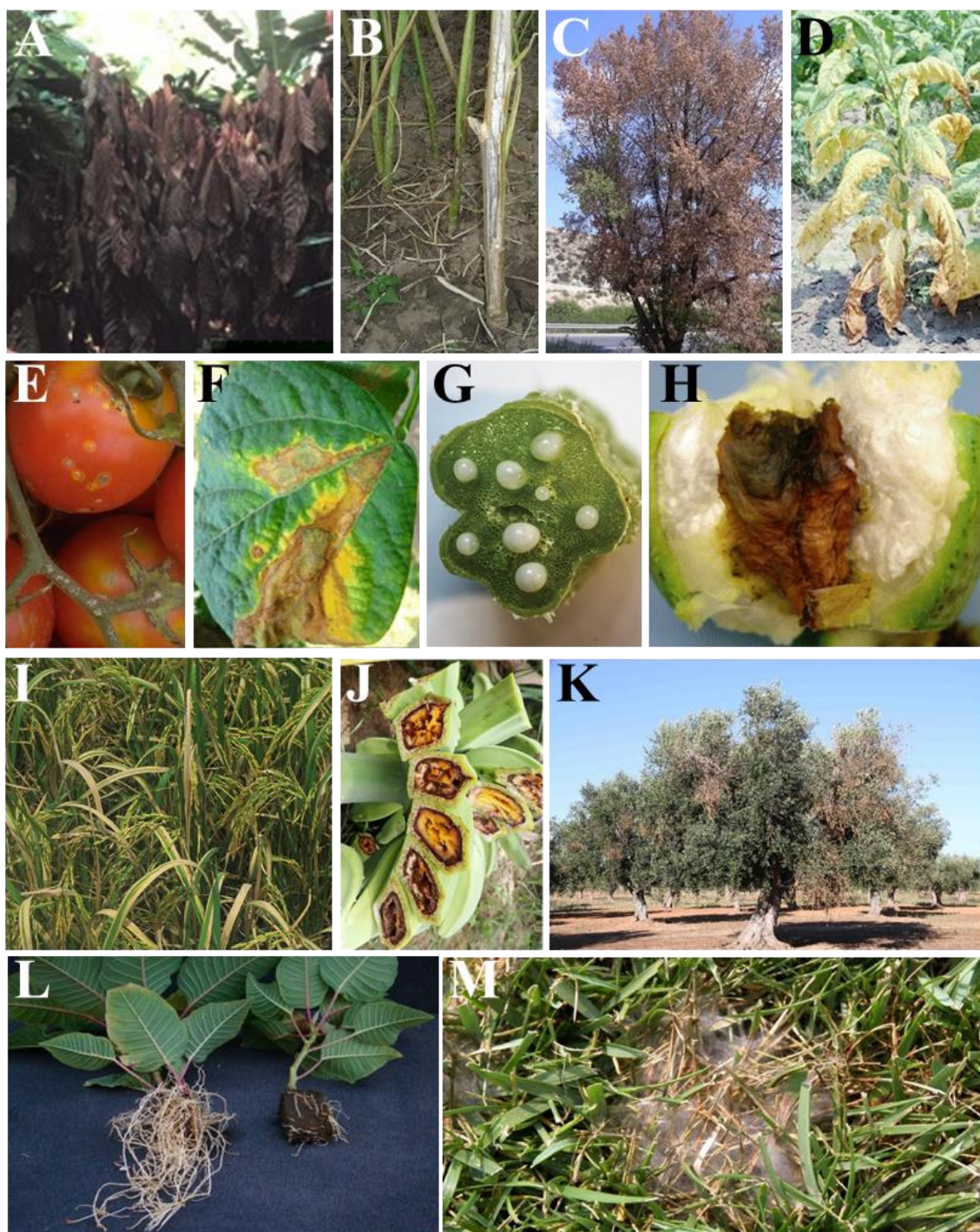


**Figure 1.12. Plant diseases caused by vascular pathogens.** Fungal diseases: (A) *Ceratocystis cacaofunesta*, (B) *Verticillium longisporum*, (C) Dutch elm disease (*Ophiostoma ulmi*) and (D) *Fusarium* wilt of tobacco (*Fusarium oxysporum*). Bacterial diseases: (E) canker of tomato (*Clavibacter michiganensis*), (F) bacterial wilt of bean (*Curtobacterium flaccumfaciens*), (G) bacterial wilt of cucumber (*Erwinia tracheiphila*), (H) boll rot of cotton (*Pantoea agglomerans*), (I) bacterial leaf blight of rice (*Xanthomonas oryzae*), (J) Banana blood disease (*Ralstonia syzygii*) and (K) Olive quick decline syndrome (*Xylella fastidiosa*). Oomycete diseases: (L) Root rot of poinsettia (*Pythium aphanidermatum*) and (M) *Pythium* blight of turf (*P. aphanidermatum*). Photos courtesy of A. von Tiedemann, T.C. Harrington, Ayto. de Aracena, USDA/Clemson U., Heinz, F. Mohammadipanah, R. Kolter, E.G. Medrano, N. Cattlin, A. Drenth, J.A. Navas-Cortes, J. Kerns and M. Hausbeck.

infection there are several peroxidases (Hilaire *et al.*, 2001), PR proteins (Rep *et al.*, 2002), phenolic compounds (Báidez *et al.*, 2007), and phytoalexins (Alvarez *et al.*, 2008).

### 1.4.1 Suspect #1: *Ralstonia solanacearum*

*Ralstonia solanacearum* is a soilborne and vascular plant pathogenic  $\beta$ -proteobacteria responsible for bacterial wilt disease on more than 250 plant species, Moko disease on banana and brown rot on potato (**Figure 1.B**). Due to its lethality, persistence and broad host range and geographical distribution, *R. solanacearum* is the most devastating plant pathogenic bacteria (Elphinstone, 2005; Mansfield *et al.*, 2012). *R. solanacearum* taxonomy is complex and has evolved substantially over the last years, reason why the term “*R. solanacearum* species complex” (RSSC) will be used hereafter.

#### 1.4.1.1 RSSC previous records

Wilting-causing bacteria were first described in 1896 by Erwin F. Smith as two different species, “*Burkholderia solanacearum*” and “*Pseudomonas solanacearum*” that were merged and renamed as “*Ralstonia solanacearum*” a century later (Smith, 1896; Yabuuchi *et al.*, 1995; Kelman, 1998). Efforts to describe and classify the diversity within the RSSC started with the division of the back then *P. solanacearum* in five races based on their host and five biovars based on their sugar/alcohol catabolism (Hayward, 1991). This classification did not reflect properly the RSSC phylogeny so a decade later, a classification of the RSSC in four phylotypes was proposed (Fegan and Prior, 2005). This classification also reflects the geographical origin as the phylotypes I-IV corresponded to RSSC strains isolated mostly in Asia, the Americas, Africa and Japan-Oceania respectively. However, this phylotype classification does not correspond to the host species they were isolated from (Lebeau *et al.*, 2011). Thanks to the later availability of sequenced genomes, the until then known as *R. solanacearum* species was split in three new species: *R. pseudosolanacearum*, including former *R. solanacearum* phylotypes I and III; *R. syzygii*, including phylotype IV; and *R. solanacearum*, now containing only former phylotype II (Safni *et al.*, 2014; Prior *et al.*, 2016).

The correspondence between phylogeny and geographical distribution suggests that geographical isolation has been one of the main driver of RSSC evolution. The reconstruction of the RSSC phylogeny revealed that the origin of the RSSC might be in what it is nowadays Oceania, where *R. syzygii* originates. The possible ancestors of what it is today *R. pseudosolanacearum* and *R. solanacearum* might have diverged from subgroups from this region



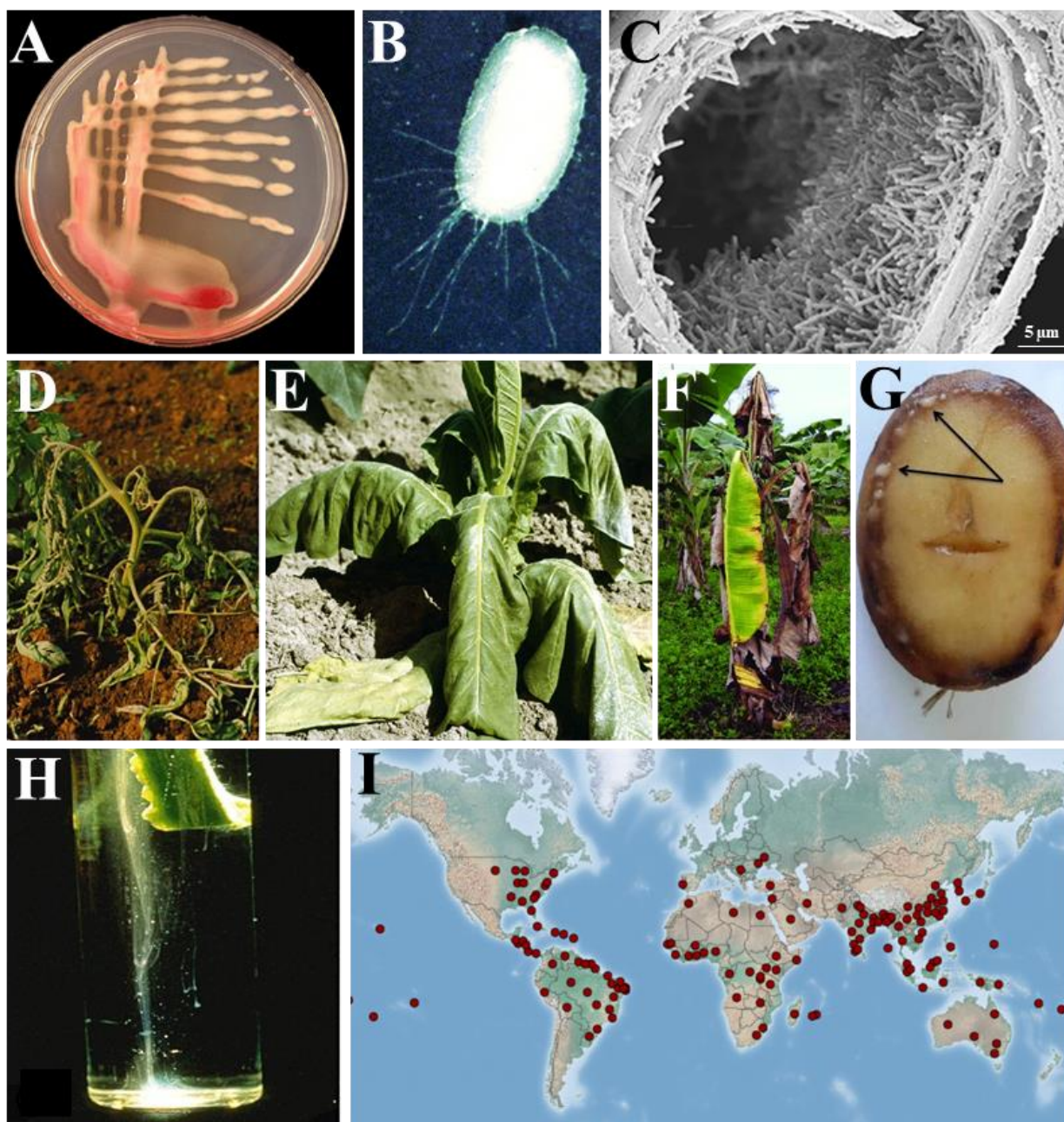


**Figure 1.B. *Ralstonia solanacearum* species complex (RSSC) bacteria aspect, disease symptoms and geographical distribution.** (A) RSSC bacteria cultured on TZC agar medium. (B) Micrograph of a RSSC bacterium observed with electron microscopy. (C) Scanning electron micrograph of stem xylem vessels colonized by RSSC bacteria from inoculated tomato plants. Bacterial wilting symptoms on tomato (D) and tobacco (E). (F) Moko disease of banana. (G) Brown rot of potato. Black arrows point bacterial exudate from vascular ring. (H) Bacteria oozing on water from a tomato cut stem. (I) Geographical distribution of RSSC according to the Centre for Agricultural Bioscience International (CABI). Red dots indicate report of presence of RSSC. Image courtesy of P. Champoiseau (U. Florida) (A); USDA/Clemson U (E); and CABI (I). Adapted from Mansfield *et al.*, 2012 (B, D and H); Lowe-Power *et al.*, 2018 (C); Álvarez *et al.*, 2015 (F); Popovic *et al.* 2016 (G).



and spread through Austral-Eastern Africa and Madagascar, and South America respectively, probably before the separation of Gondwana (Castillo and Greenberg, 2007; Wicker *et al.*, 2012).

#### 1.4.1.2 RSSC criminal charges

Bacterial strains from the RRSC are responsible for bacterial wilt on more than 250 species from both monocot and dicot botanical families, Moko and blood disease on banana and brown rot on potato (Elphinstone, 2005; Peeters, Guidot, *et al.*, 2013). Due to its ability to grow in tropical, subtropical and temperate regions, RRSC is worldwide distributed affecting food, vegetables and fruit crops in all continents (Hayward, 1991; Janse *et al.*, 1998; Poussier, Vandewalle and Luisetti, 1999; Kim *et al.*, 2003; Morais *et al.*, 2015; Safni, Subandiyah and Fegan, 2018) (**Figure 1.13H**). Both the broad host range and the geographical distribution hinder the accurate estimation of yield losses and thus the evaluation of the corresponding economic impact. For potato alone, RSSC is estimated to be responsible for 1 billion dollars worldwide annual losses (Elphinstone, 2005). The incidence of the disease is particularly dramatic in developing intertropical countries in which RSSC is endemic, but it is also problematic in areas in which RSSC has a quarantine status due to its strict regulatory eradication and restriction of production on contaminated land (Mansfield *et al.*, 2012).

Bacterial wilt is characterized by browning of the xylem, foliar epinasty and rapid and drastic wilting of the full plant caused by vascular clogging (**Figure 1.13**). Symptom appearance is enhanced by temperature and humidity (Mew, 1977). Another distinctive symptom, often used for a quick *in situ* diagnosis, is the bacterial oozing when an infected tissue is cut (**Figure 1.13H**). Bacterial wilt is particularly devastating on Solanaceae crops such as tomato, tobacco, pepper or eggplant; but they are problematic in other crops such as peanut (Yu *et al.*, 2011), ginger (M. Liu *et al.*, 2005), clove tress (Safni, Subandiyah and Fegan, 2018), or ornamental plants (Tjou-Tam-Sin, van de Bilt, Westenberg, Gorkink-Smits, *et al.*, 2017). Although RSSC has been largely studied for more than a century now, new host species are still being reported every year (e.g., chard, fig tree or roses) (Lin, Chuang and Wang, 2015; Jiang *et al.*, 2016; Tjou-Tam-Sin, van de Bilt, Westenberg, Bergsma-Vlami, *et al.*, 2017) indicating an alarming ability of RSSC to jump hosts. An increase in plant product trade together with the rapid adaptation potential of RSSC can results in major outbreaks (Genin and Boucher, 2004; Tjou-Tam-Sin, van de Bilt, Westenberg, Gorkink-Smits, *et al.*, 2017). Model plants *Arabidopsis thaliana* and *Medicago truncatula* can also be infected by RSSC, what led to the establishment of RSSC as model for bacterial-root pathogenesis (Deslandes *et al.*, 1998; Vailleau *et al.*, 2007).

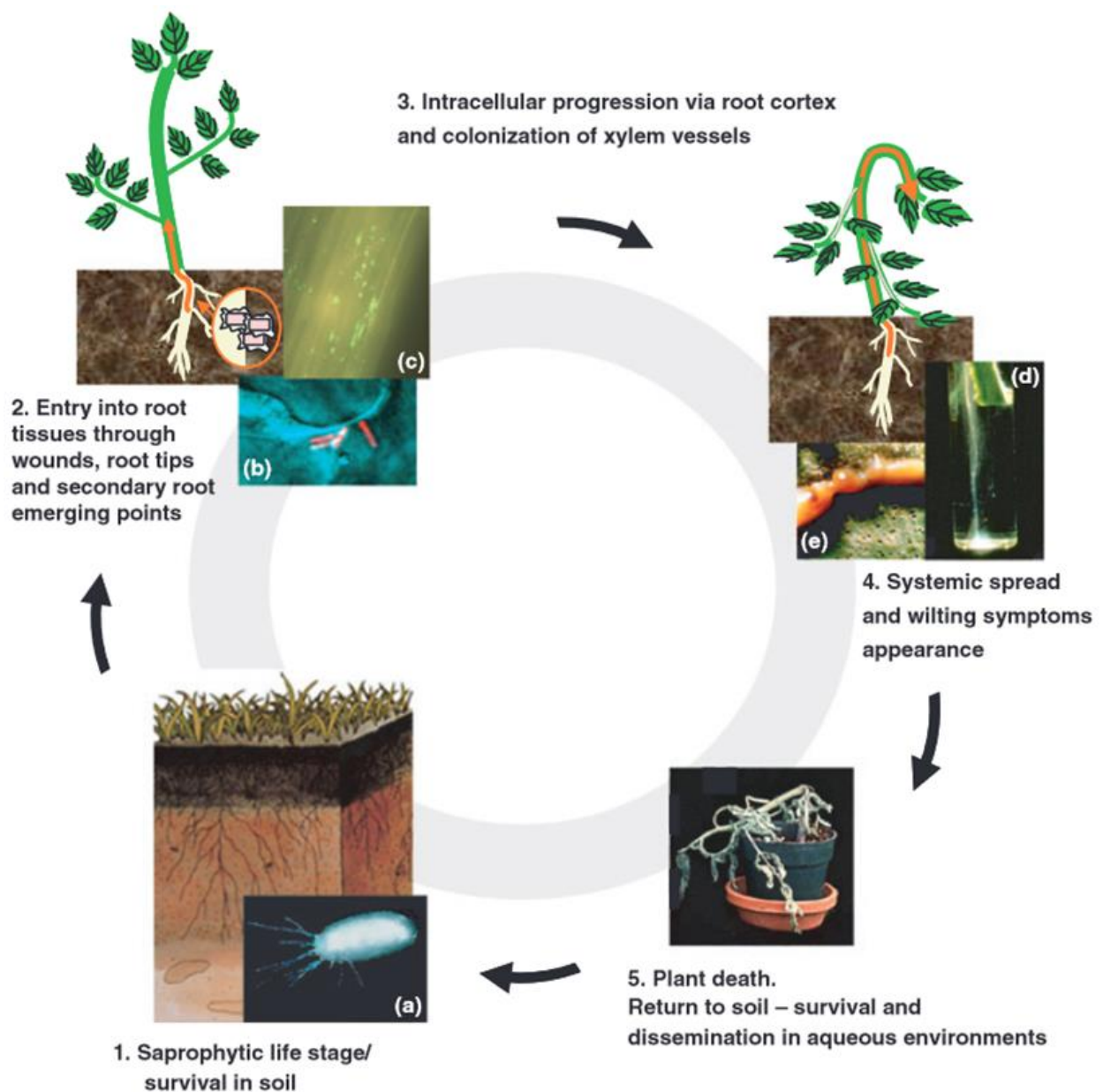


**Figure 1.14. Life cycle of the *Ralstonia solanacearum* species complex (RSSC).** 1. Bacteria can live saprophytically on soil or plant debris from a previous infection even for long periods of time. (a) RRSC bacterium observed by electronic microscopy. 2. Bacteria enter in the root through wound, root tips or secondary root emerging points. (b) RRSC bacteria attached to root surface observed by confocal microscopy. (c) GFP-tagged RSSC bacteria in tomato roots on the surface of tomato roots. 3. Colonization of the xylem and systematic spread of the bacteria produce the characteristic wilting symptoms. (d) Bacterial oozing on water from a cut infected stem. (e) Exopolysaccharide secretion at the section of an infected tissue. 5. When the water uptake is critically impaired, plants die and the bacteria are released back to the soil where they can start a new infectious cycle on a new host. From Genin, 2010.

RSSC is also responsible for great losses due to Moko and blood diseases of banana in America and Indonesia respectively (Denny, 2007; Safni, Subandiyah and Fegan, 2018). Both diseases present relatively similar symptoms: chlorosis and wilting of leaves and premature development of fruits which are also internally rotten (**Figure 1.12J**). Similar to bacterial wilts, Moko diseased plants also produce bacterial oozing when an infected stem is cut. RRSC is also the causal agent of the black rot of potato, which is an additional symptom to the bacterial wilting of potato (**Figure 1.13G**). A particularity of the potato infection by RRSC is that it can occur at lower temperatures than typical RRSC bacterial wilt, as it has been reported in western Europe (Janse *et al.*, 1998), or in elevated regions of the Andes (Gutarra *et al.*, 2017).

As a vascular pathogen, treatment of infected plants is impossible leaving eradication as the only solution for diseased plants (Yadeta and Thomma, 2013). As a soilborne pathogen, RRSC-infected soils can barely be reused, not even after crop rotation, because of RSSC ability survive on soils or in neighboring symptomless hosts (Peeters, Guidot, *et al.*, 2013). Biocontrol alternatives could potentially be used against RSSC as shown with certain strains of *Ralstonia picketti* (Wei *et al.*, 2013), *Bacillus* spp. (Cao *et al.*, 2018; N. Wang, Wang, *et al.*, 2019) or *Flavobacterium* spp. (Kwak *et al.*, 2018); inactivated strains of the RSSC (Hanemian *et al.*, 2013); or phagotherapy (Álvarez, López and Biosca, 2019). However, the most efficient control strategy remains resistance breeding with examples of gene-for-gene resistance observed in eggplant (e.g., PopP2/RE-bw or RipAX2/EBWR9 locus) (Xi'ou *et al.*, 2015; Morel *et al.*, 2018), as well as tolerance-associated QTLs in pepper (Lafortune *et al.*, 2005) or eggplant (Salgon *et al.*, 2017).

#### 1.4.1.3 RSSC *modus operandi*

RSSC bacteria can live saprophytically in the soil or water for long periods of time until they make contact with a suitable host (Denny, 2007) (**Figure 1.14**). After an initial contact, RSSC bacteria penetrate the root surface through small wounds or possibly also at the emergence points of lateral roots. Then, bacteria progress towards the xylem vessels in a highly directed and centripetal manner helped by the cellular collapse of pericycle cells. Once in a xylem vessel, RSSC bacteria start to multiply and colonize neighboring vessels by degradation of pit membranes. (Digonnet *et al.*, 2012). When the concentration of bacteria is elevated, the xylem clogging caused by the bacteria themselves and the EPS they secrete, prevents the plant water uptake leading to wilting and eventually death (Lowe-Power, Khokhani and Allen, 2018). The death of the host releases the bacteria to the soil, where they can thrive on the resulting debris until they find a new host.

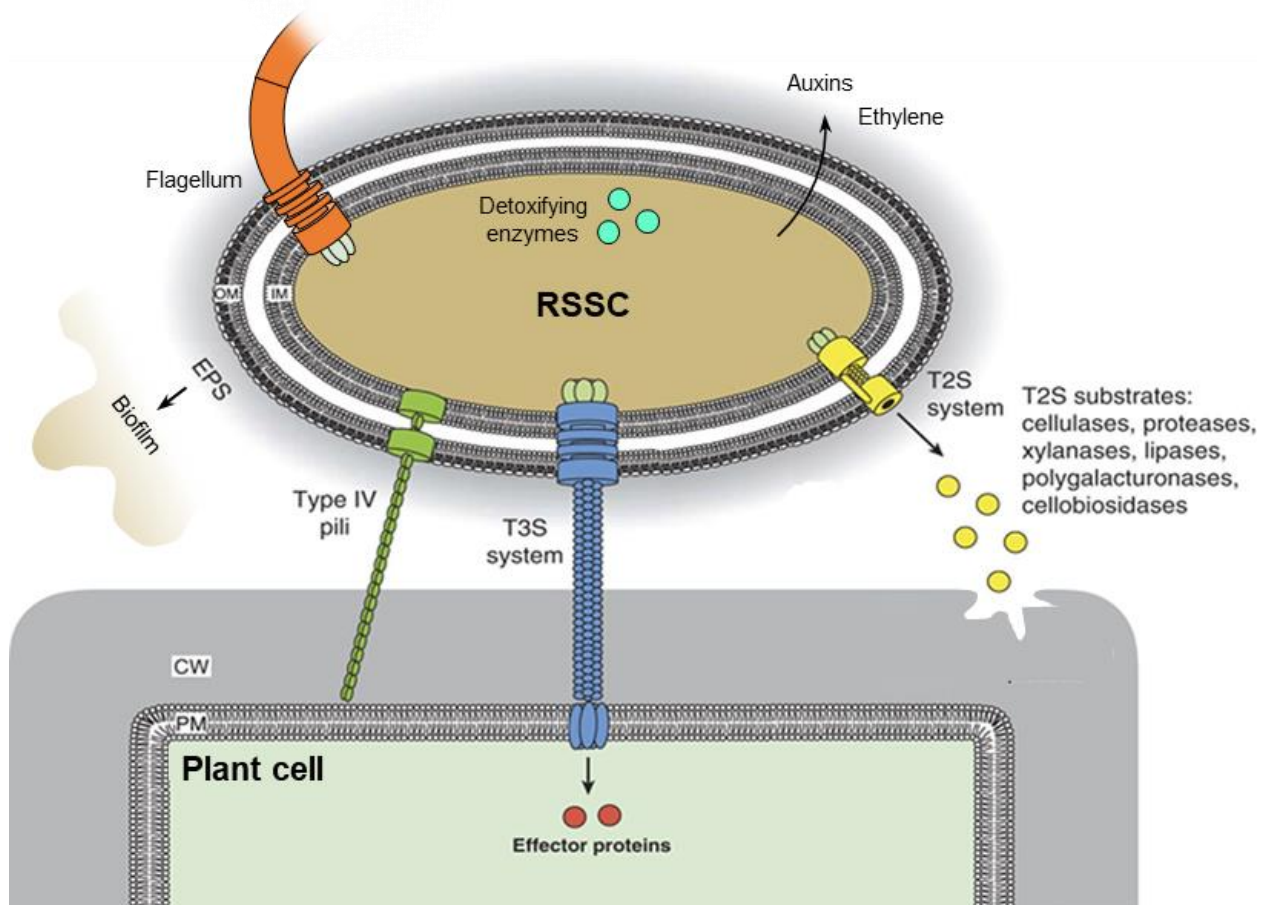


**Figure 1.15. Main virulence determinants of the *Ralstonia solanacearum* species complex (RSSC).** The main virulence determinants of RSSC are the EPS, which contribute to xylem clogging and biofilm formation. Flagellar and type IV pili-driven motilities are also RSSC virulence determinants. RSSC can deploy detoxifying enzymes to avoid the toxicity of certain plant defense compounds. Additionally, RSSC can synthesize phytohormones such as auxins and ethylene although their role in virulence is yet poorly understood. RSSC also present T2SS and T3SS to secrete and translocate cell wall degrading enzymes and effector proteins respectively. Adapted from Büttner and Bonas, 2010; and Genin and Denny, 2012.

#### 1.4.1.4. RSSC known weapons

RSSC bacteria display a wide array of virulence factors to facilitate the plant infection: production of EPS, motility, detoxification systems, production of phytohormones, secretion of CWDEs through the T2SS and translocation of T3Es through the T3SS (Genin and Denny, 2012) (**Figure 1.15**). One of the most important RSSC virulence factors is the secretion of high molecular weight EPS as shown by the *eps* mutant difficulties to wilt the host, even when directly inoculated in the xylem (Saile *et al.*, 1997). RSSC motility has also been described as an important virulence factor. Flagellar motility is required in the early stages of root colonization, but not once the bacteria are located in the xylem (Tans-Kersten, Huang and Allen, 2001). However, type-4-pili-driven motility is required for virulence in all infection stages (Kang *et al.*, 2002). To overcome the stressful environment generated upon elicitation of plant defenses responses, RSSC presents a wide variety of detoxifying systems that include peroxidases (Flores-Cruz and Allen, 2009), DNA binding proteins (Colburn-Clifford, Scherf and Allen, 2010), multidrug efflux pumps (Brown, Swanson and Allen, 2007), polyphenol oxidases (Hernández-Romero, Solano and Sanchez-Amat, 2005), and cytochrome *c* oxidases (Colburn-Clifford and Allen, 2010). RSSC production of auxins and ethylene is regulated by the virulence master regulator HrpG, and in the case of ethylene, this production has been observed *in planta*; however, the impact of this production in virulence is not clear as mutants do not necessarily show reduced virulence (Valls, Genin and Boucher, 2006; Denny, 2007). RSSC also presents approximately 30 extracellular CWDEs (notably cellulases and pectinases) that can be translocated through its T2SS and that are also essential for virulence (H. Liu *et al.*, 2005).

One of the most important and better studied RSSC virulence determinants is the T3SS and associated T3Es (Boucher, Barberis and Demery, 1985; Coll and Valls, 2013). RSSC T3SS constitutes a “molecular syringe” that crosses both bacterial and plant cell walls and plasma membranes and allows the translocation to the plant cell of T3Es synthesized in the bacteria. RSSC effectomes (50-70 T3E referred as *Ralstonia* injected proteins, Rips, per strain) (Sabbagh *et al.*, 2019) is considerably larger than those of other Gram-negative plant pathogenic bacteria such as *X. campestris* (15-30 T3Es per strain) (Roux *et al.*, 2015) or *P. syringae* (30-50 T3Es per strain) (Dillon *et al.*, 2019). The distribution of the different Rips in different RSSC strains do not reflect a clear association with host adaption, although this is hard to conclude due to the unavailability of host compatibility data. Less ambiguous is the association between RSSC species and presence of certain of Rips with only 8 of them present in mostly all strains and 14

**Table 1.3. Characterized effectors from the *Ralstonia solanacearum* species complex (RSSC).** Table summarizing the roles of several characterized protein effectors from RSSC.

Effector	Description	Host(s)	Reference(s)
RipA (AWR) family	Collective contribution to virulence in eggplant, tomato and negative contribution to virulence in Arabidopsis.	<i>Arabidopsis thaliana</i> , <i>Lycopersicum esculentum</i> , <i>Solanum melongena</i>	Solé <i>et al.</i> , 2012
RipA2	Major contribution to virulence in eggplant and Arabidopsis and cell death induction in <i>Nicotiana</i> spp.	<i>Arabidopsis thaliana</i> , <i>Nicotiana</i> spp., <i>Solanum melongena</i>	Solé <i>et al.</i> , 2012
RipA5	Cell death induction and inhibition of TOR-dependent nitrate reductase activity.	<i>Nicotiana</i> spp.	Solé <i>et al.</i> , 2012 ; Popa <i>et al.</i> , 2016
RipAA (AvrA)	Cell death induction in different <i>Nicotiana</i> spp. (major contribution in <i>N. benthamiana</i> and <i>N. tabacum</i> ).	<i>Nicotiana</i> spp.	Pouemyro <i>et al.</i> , 2009 ; Chen <i>et al.</i> , 2018
RipAL	Induces JA signaling pathway to suppress SA-related defenses.	<i>Nicotiana benthamiana</i>	Nakano & Mukaiharu 2018
RipAX2 (Rip36)	Avirulence factor.	<i>Solanum melongena</i> , <i>Solanum torvum</i>	Nahar <i>et al.</i> , 2014 ; Morel <i>et al.</i> , 2018
RipAY	Degradation of plant glutathione and suppression of defenses.	<i>Nicotiana benthamiana</i>	Fujiwara <i>et al.</i> , 2016 ; Mukaihara <i>et al.</i> , 2016 ; Sang <i>et al.</i> , 2018
RipB	Induction of RoqI-mediated ETI.	<i>Nicotiana</i> spp.	Nakano <i>et al.</i> , 2019
RipF1 (PopF1)	Virulence factor in tomato and cell death induction in tobacco.	<i>Lycopersicum esculentum</i> , <i>Nicotiana tabacum</i>	Meyer <i>et al.</i> , 2006
RipF2 (PopF2)	Cell death induction in tobacco.	<i>Nicotiana tabacum</i>	Meyer <i>et al.</i> , 2006
RipG (GALA) family	Collective contribution to virulence in Arabidopsis, tomato and eggplant and interaction with ASK proteins.	<i>Arabidopsis thaliana</i> , <i>Lycopersicum esculentum</i> , <i>Solanum melongena</i>	Angot <i>et al.</i> , 2006 ; Remigi <i>et al.</i> , 2011
RipG4	Inhibition of callose deposition.	<i>Arabidopsis thaliana</i>	Remigi <i>et al.</i> , 2011
RipG7	Host specificity factor.	<i>Medicago truncatula</i>	Angot <i>et al.</i> , 2006
RipH (HLK) family	Collective contribution to virulence in tomato and suppression of defenses.	<i>Solanum lycopersicum</i>	Chen <i>et al.</i> , 2013 ; Morel 2018
RipN	Alteration of the plant NADH/NAD <sup>+</sup> ratio and suppression of defenses.	<i>Arabidopsis thaliana</i>	Yun <i>et al.</i> , 2019
RipP1 (PopP1)	Cell death induction in different <i>Nicotiana</i> spp. (major contribution in <i>N. glutinosa</i> ).	<i>Nicotiana</i> spp.	Pouemyro <i>et al.</i> , 2009 ; Chen <i>et al.</i> , 2018
RipP2 (PopP2)	Acetylation of WRKY transcription factors to inhibit defenses and RRSI-R to induce ETI.	<i>Arabidopsis thaliana</i>	Deslandes <i>et al.</i> , 2003 ; Tasset <i>et al.</i> , 2010 ; Le Roux <i>et al.</i> , 2015
RipR (PopS)	Inhibition of SA-dependent defenses.	<i>Solanum lycopersicum</i> , <i>Solanum tuberosum</i>	Jacobs <i>et al.</i> , 2013
RipTAL (BrgII)	Plant EBE binding and induction of synthesis of polyamines.	<i>Arabidopsis thaliana</i>	de Lange <i>et al.</i> , 2013 ; Wu <i>et al.</i> , 2019
RipTPS	Induction of trehalose-6-phosphate in yeast and cell death in <i>Nicotiana tabacum</i> .	<i>Nicotiana tabacum</i>	Pouemyro <i>et al.</i> , 2014

of them whose distribution matches the RSSC species division (Peeters, Carrère, *et al.*, 2013; Sabbagh *et al.*, 2019). Several Rip have been well characterized over the last years and a summary of their mode of actions is listed in **table 1.3**.

#### 1.4.2. Suspect #2: *Xanthomonas campestris* pathovar *campestris*

*Xanthomonas campestris* pv. *campestris* (Xcc), is a seedborne vascular plant pathogenic  $\gamma$ -proteobacteria responsible for the black rot of Brassicaceae, the principal yield-limiting and destructive bacterial disease of brassica crops worldwide (Mansfield *et al.*, 2012; Vicente and Holub, 2013) (**Figure 1.16**).

##### 1.4.2.1 Xcc previous records

The taxonomy of the *Xanthomonas* genus was initially determined based on descriptive characters such as the host specificity, morphological features or biochemical characteristics (Bergey *et al.*, 1939; Van den Mooter and Swings, 1990). Years later, thanks to DNA/DNA hybridization results, *Xanthomonas* species were redefined and *X. campestris* comprised six pathovars including the causal agent of black rot of Brassicaceae, Xcc, and five others (*aberrans*, *armoraciae*, *barbareae*, *incanae* and *raphani*) (Vauterin *et al.*, 1995). Several rearrangements among these pathovars were proposed during the following years (Alvarez *et al.*, 1994; Tamura *et al.*, 1994; Vicente *et al.*, 2001), but the current consensus is that there are three *X. campestris* pathovars (Fargier and Manceau, 2007): *Xc* pv *campestris*, causal agent of black rot of Brassicaceae; *Xc* pv *raphani*, causal agent of bacterial leaf spot of Brassicaceae; and *Xc* pv *incanae*, causal agent of bacterial blight of stock.

Xcc strains have been differentiated into nine races based on the response on several brassica species (Kamoun *et al.*, 1992; Vicente *et al.*, 2001; Fargier and Manceau, 2007). The geographical distribution of Xcc races is not clear and is highly dependent of the host cultivated but generally, race 1 and 4 strains are more abundant than the rest (Vicente and Holub, 2013). Several gene for gene associations has been described and hypothesized to explain this race division (Vicente *et al.*, 2001; Fargier and Manceau, 2007; He *et al.*, 2007; Jensen *et al.*, 2010).

##### 1.4.2.2 Xcc criminal charges

Xcc presents a relatively narrow host range, limited to certain Brassicaceae species including crops (e.g., cabbage, cauliflower, broccoli, radish or mustard), ornamental plants (e.g.,



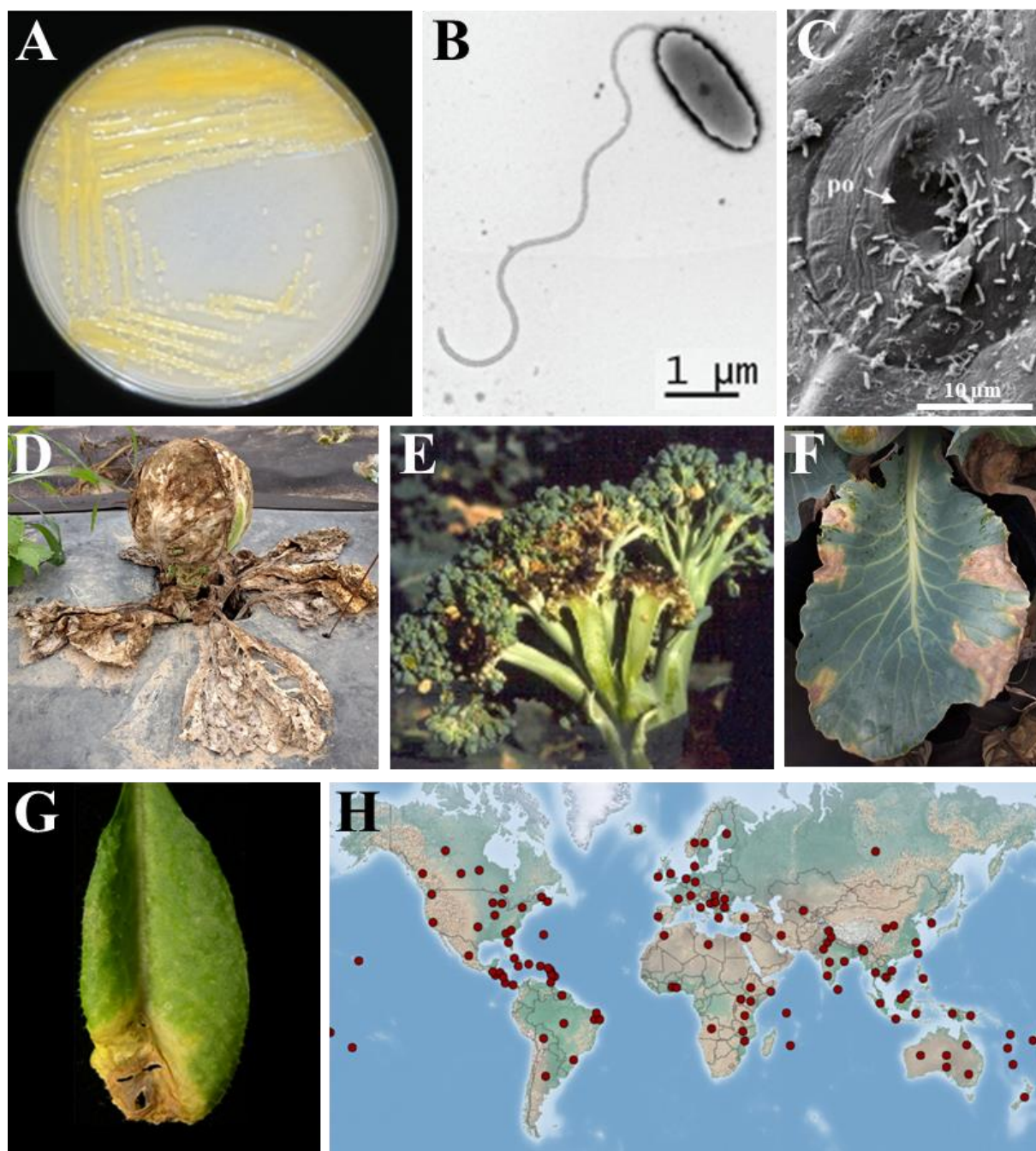


**Figure 1.16. *Xanthomonas campestris* pv. *campestris* (Xcc) aspect, disease symptoms and geographical distribution.** (A) Xcc cultured on Yeast Dextrose Calcium Carbonate medium. (B) Micrograph of a Xcc bacterium observed with electron microscopy. (C) Scanning electron micrograph of an hydathode pore (po) at the surface of a cauliflower leaf. Xcc bacteria are present around and inside the pore. (D) Symptoms of black rot on cabbage (D) and broccoli (E). Close-up symptoms of black rot on leaves from cauliflower (F) or *Arabidopsis thaliana* (G). (H) Geographical distribution of Xcc according to the Centre for Agricultural Bioscience International (CABI). Red dots indicate report of presence of Xcc. Images courtesy of Z. Dubrow (D and F), M. Shurtleff (E), E. Lauber (G) and CABI (H). Adapted from Vicente *et al.*, 2013 (A, B); Cerutti *et al.*, 2017 (C).



flowering kale) and weeds (e.g., pepperweed or swine-cress) (Bain, 1955; Schaad, 1981; Buonauro *et al.*, 2003). It is also able to infect the model plant *A. thaliana*, allowing to use the *Xcc/A. thaliana* pathosystem as a model for plant pathologists (Buell, 2002; Meyer *et al.*, 2005). Despite its relatively narrow host range, limited to just one botanical family, *Xcc* has been found in all continents in which brassica crops are grown (Bradbury, 1986), and it is particularly problematic in intertropical developing countries where it is responsible of up to 10-50% yield losses (Bradbury, 1986; Massomo, Mabagala, *et al.*, 2004; Singh, Dhar and Yadava, 2011) (**Figure 1.16**).

Black rot symptoms and intensity vary considerably depending on the host, age and environmental conditions. Infected seedling will develop into stunted plants with dead cell spots on the cotyledons that will eventually wilt and die. Older plants present the typical chlorotic and/or necrotic V-shaped lesions at the leaf edges, often associated with black veins (**Figure 1.16**). Systemically infected plants might show symptoms anywhere in the leaf, or even in other organs such as stems or curds (Celetti, 2011). The disease is favored by warm and humid environmental conditions and can be rapidly disseminated through rain and irrigation water (Williams, 1980), wind (Kuan, Minsavage and Schaad, 1986), or insects (Van Der Wolf and Van Der Zouwen, 2010)(Williams, 1980; Kuan, Minsavage and Schaad, 1986; Van Der Wolf and Van Der Zouwen, 2010).

Similar to most vascular pathogens, the treatment of infected plants is impossible (Yadeta and Thomma, 2013). The control of the disease relies thus mostly on the use of *Xcc*-free plant material and the eradication of not only infected crop plants but also the surrounding weeds that can act as *Xcc* reservoirs (Williams, 1980; Schaad, 1981). Prophylactic measures to control *Xcc* seed transmission include hot water treatment, but it is not completely efficient and under favorable conditions, even low *Xcc* incidences can result in full epidemics (Roberts *et al.*, 1999; Nega *et al.*, 2003). Biocontrol strategies against *Xcc* have been investigated using antagonist strains of *Bacillus* spp. (Wulff *et al.*, 2002; Massomo, Mortensen, *et al.*, 2004), but the most efficient strategy is again resistance breeding. Major resistance genes and QTLs have been found in *B. rapa* or *B. carinata*, but are scarce in *B. oleracea*, explaining why black rot is particularly devastating on this species (Vicente and Holub, 2013; Singh *et al.*, 2018).

#### 1.4.2.3 *Xcc* *modus operandi*

*Xcc* can survive epiphytically on plant debris for long periods of time (Schultz, Gabrielson and Olson, 1986; López, Haedo and Méndez, 1999). When *Xcc* encounters a host, it

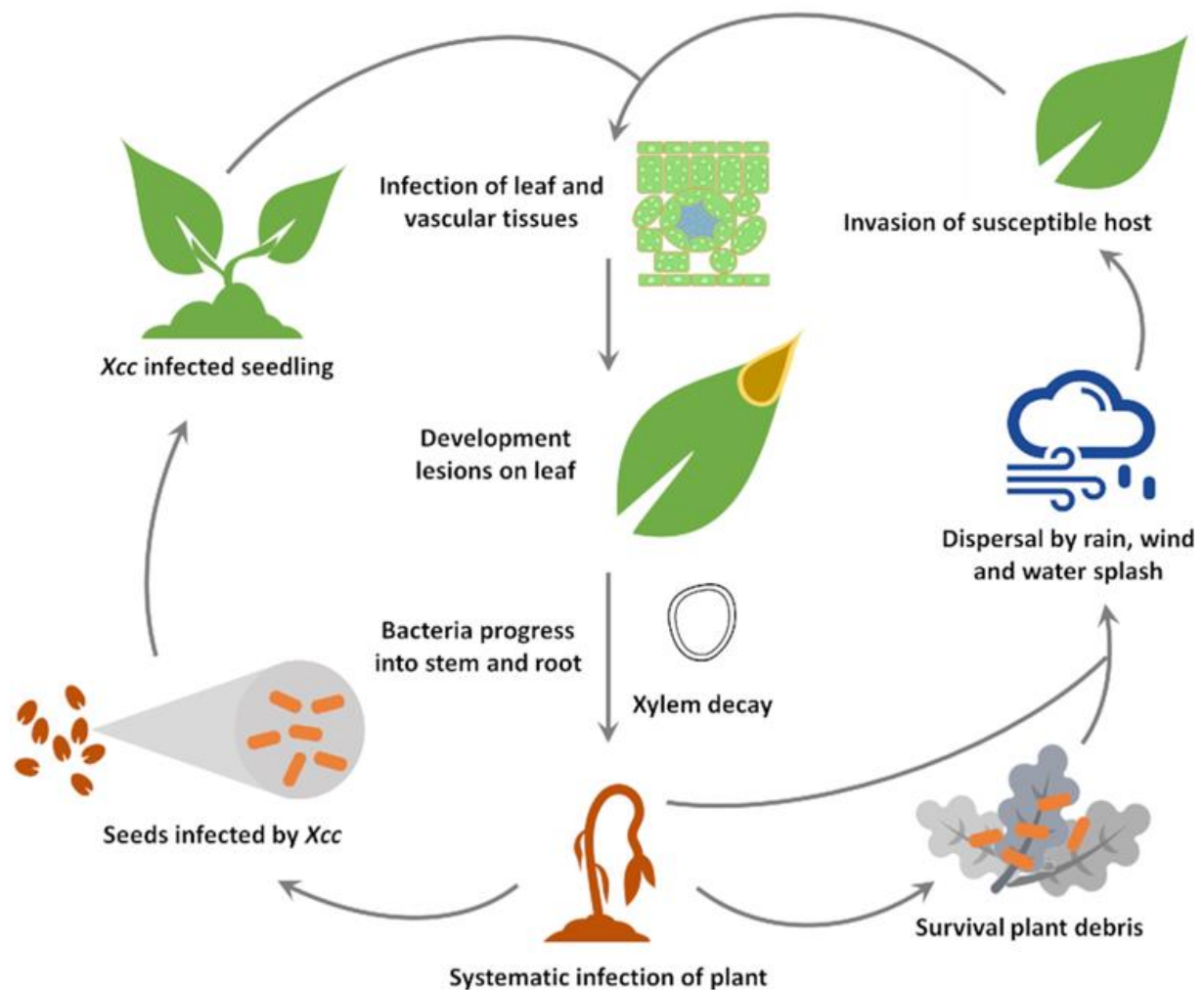


**Figure 1.17. Life cycle of *Xanthomonas campestris* pv. *campestris* (Xcc).** Bacteria can live saprophytically on soil or plant debris for a long period of time until, via wind or water, they reach a susceptible host. They enter the internal tissues through wounds or reabsorption of guttation droplets at the hydathodes. Once inside the plant they invade the xylem vessel where they multiply producing the characteristic chlorotic/necrotic V-shaped lesion. The infection spreads systemically, including reproductive organs, leading to the infection of seeds that, in turn, will germinate producing diseased plants. Adapted from An *et al.*, 2019.

can access the internal tissues by wounds or by the reabsorption of guttation droplets at the hydathodes (Russell, 1898; Shigaki, Nelson and Alvarez, 2000; Cerutti *et al.*, 2017) (**Figure 1.17**). These openings provide an easy access to the xylem vessels from where *Xcc* multiples (Vorhölter, Niehaus and Pühler, 2001; Akimoto-Tomiyama, Furutani and Ochiai, 2014). Upon colonization of the xylem, *Xcc* bacteria can spread systemically through the whole plant leading to the above mentioned symptoms and ultimately, plant death (Kamoun *et al.*, 1992; Akimoto-Tomiyama, Furutani and Ochiai, 2014; An *et al.*, 2019). It is precisely this systemic colonization what allows the invasion of reproductive tissues and subsequently, seeds (Van Der Wolf and Van Der Zouwen, 2010; Kastelein *et al.*, 2014). These seeds will germinate leading to infected seedlings that will equally develop the disease.

#### 1.4.2.4. *Xcc* known weapons

*Xcc* bacteria present several virulence determinants key for the establishment and progression of the infection: synthesis of EPS and lipopolysaccharides (LPS) involved in biofilm formation, adhesins, detoxification system, secretion of CWDEs through the T2SS, TonB-dependent outer membrane transporters (TBDT) and T3SS-dependent translocation of T3Es (Qian *et al.*, 2005; Blanvillain *et al.*, 2007; Büttner and Bonas, 2010) (**Figure 1.18**). *Xcc*, as most *Xanthomonas* spp., produces the well-characterized EPS xanthan, which is involved in bacterial protection due to its consistency (Denny, 1995; Chou *et al.*, 1997; Chan and Goodwin, 1999), clogging of the xylem, and suppression of basal defenses probably through chelation of apoplastic  $\text{Ca}^{2+}$  (Yun *et al.*, 2006; Aslam *et al.*, 2008). In addition to its role in virulence, xanthan is also an interesting molecule used as thickening agent in the food, drug and oil industries. Another polysaccharide, LPS, are also involved in virulence (Dow *et al.*, 1995). LPS are major components of the bacterial cell wall and the genes involved in their synthesis are under strong diversifying selection (Lu *et al.*, 2008). This translates in variation in LPS composition which presumably affect the bacteria ability to evade plant recognition because, as previously mentioned, LPS is also a known PAMP (Dow, Newman and von Roepenack, 2000; Hung, Wu and Tseng, 2002). The role of adhesins has been poorly studied in *Xcc* although in other *Xanthomonas* it is known that both fimbrial and non-fimbrial adhesins present roles in virulence (Büttner and Bonas, 2010; Burdman *et al.*, 2011). In *Xcc*, it has been shown that a mutant from the type IV pilus component *pilA* is moderately impaired in virulence (McCarthy *et al.*, 2008). Collectively, EPS, LPS and adhesins contribute to the formation of biofilms, protective and attachment matrixes, whose impact on virulence, although proven, is poorly understood

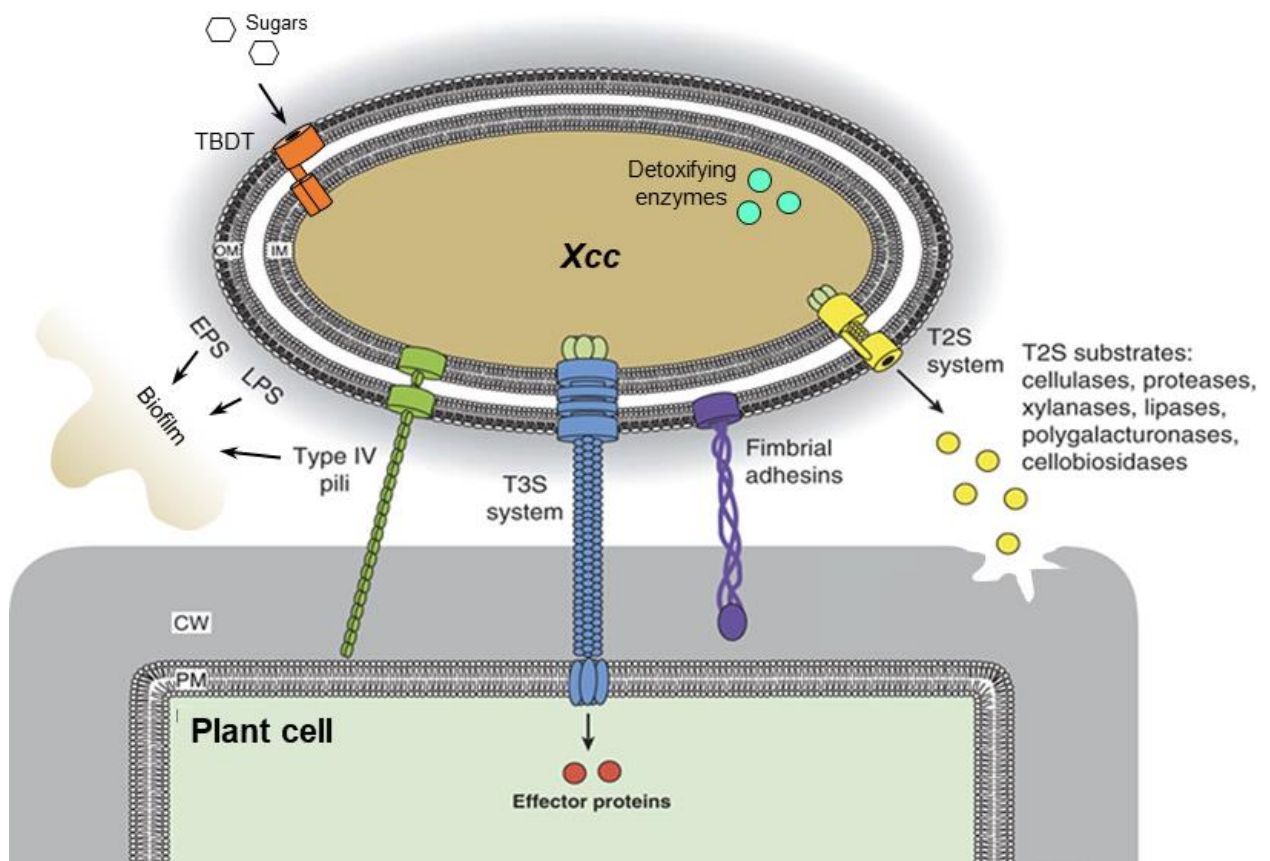


**Figure 1.18. Main virulence determinants of *Xanthomonas campestris* pv. *campestris* (Xcc).** The main virulence determinants of Xcc are the polysaccharides EPS and LPS and adhesins (type IV pili and other fimbrial adhesins), which collectively contribute to the formation of biofilm. Xcc also deploys sugar transporters (TBBDTs) to optimize the nutrient uptake from poor environments and detoxifying enzymes to counter plant chemical defenses. Xcc is also able to secrete cell wall degrading enzymes and effector proteins through the T2SS and T3SS respectively. CWDE disrupt the plant cell wall and effector proteins, once translocated into the plant cytoplasm, are able to modulate the plant physiology and subvert the plant defenses. TBBDT: TonB-dependent transporter. EPS: exopolysaccharide, LPS: lipopolysaccharide, T3S: type III secretion, OM: Outer membrane, IM: Internal membrane. CW: cell wall and PM: plasma membrane. Adapted from Büttner and Bonas, 2010.

(Stoodley *et al.*, 2002; Büttner and Bonas, 2010). *Xcc* strains possess several detoxification enzymes such as glutathione S-transferases, peroxidases, catalases that can counteract the toxic effect of certain plant compounds allowing them to thrive in the plant (Qian *et al.*, 2005). Another problem of the plant environment in which *Xcc* thrives is the low content of assimilable nutrients. To maximize the nutrient uptake, *Xcc* can deploy effective transporters such as certain TBDTs that are able to import sucrose or *N*-acetylglucosamine-containing compounds required for full *Xcc* virulence (Blanvillain *et al.*, 2007; Boulanger *et al.*, 2014). *Xcc* presents two different T2SSs, *xps* and *xcs*, although virulence has been associated to only the *xps* one (Qian *et al.*, 2005). This system allows the secretion to the apoplast of CWDEs such as cellulases, cellobiosidases, lipases, xylanases, endo-glucanases, polygalacturonases and proteases (Büttner and Bonas, 2010).

As for the RSSC, one of *Xcc* main virulence determinants is its T3SS and associated T3Es (Arlat *et al.*, 1991; Qian *et al.*, 2005; Büttner and Bonas, 2010). As previously mentioned, the effectome of *Xcc* (typically 15-30 T3Es or *Xanthomonas* outer proteins, Xops, per strain) (Roux *et al.*, 2015) is smaller than those of other plant pathogenic bacteria such as *P. syringae* (30-50 T3Es per strain) (Dillon *et al.*, 2019) or the RRSC (50-70 Rips per strain) (Sabbagh *et al.*, 2019). Only three Xops are present in all strains from all three *X. campestris* pathovars: XopFl, XopP and XopAlI constituting interesting breeding targets to achieve broad-spectrum protection against *X. campestris* (Roux *et al.*, 2015). Within the *campestris* pathovar, the conservation is larger with 12 Xops out of the total 26 described in *Xcc*, present in at least 95% of sequenced strains. This indicates that *Xcc* effectome is highly polymorphic (Guy *et al.*, 2013), similar to other *Xanthomonas* spp. (Cohn *et al.*, 2014), the RSSC (Sabbagh *et al.*, 2019), or *P. syringae* (Dillon *et al.*, 2019). The role of the *Xcc* Xops characterized up to date is described in **table 1.4**.

### 1.4.3. A déjà vu

After reading the description of both bacteria, one might have the impression of repetition. Indeed, these two species have many aspects in common: they are devastating vascular pathogens that cause problems worldwide, particularly in developing countries; efficient control measures against them are scarce; they deploy similar virulence determinants; or they are extensively studied pathosystems. Nevertheless, they also present strong differences as *Xcc* is an aerial pathogen while RSSC bacteria are soilborne, their symptoms and host range differ substantially or their effectome sizes are quite different. The main similarities and differences between these two bacteria are summarized in **table 1.5**.

**Table 1.4. Characterized effectors from *Xanthomonas campestris* pv. *campestris* (Xcc).** Table summarizing the roles of several characterized protein effectors from Xcc.

Effector	Description	Host	Reference(s)
AvrBs1	Avirulence factor in mustard and HR on nonhost pepper.	<i>Brassica rapa</i> , <i>Capsicum annum</i>	Rongqi <i>et al.</i> , 2006 ; He <i>et al.</i> , 2007
AvrBs2	Virulence factor.	<i>Raphanus sativus</i> , <i>Brassica oleracea</i>	Rongqi <i>et al.</i> , 2006
Tall2a	Virulence factor.	<i>Brassica oleracea</i>	Denancé <i>et al.</i> , 2018
Tall5a	Virulence factor.	<i>Brassica oleracea</i>	Denancé <i>et al.</i> , 2018
XopAC (AvrAC)	Inhibition of PTI (uridylation of BIK1) and induction of ETI (uridylation of PBL2 and complex formation with RKS1 and ZARI)	<i>Arabidopsis thaliana</i>	Xu <i>et al.</i> , 2008 ; Feng <i>et al.</i> , 2012 ; Guy <i>et al.</i> , 2013 ; Wang <i>et al.</i> , 2015 ; Wang <i>et al.</i> , 2019
XopAH (AvrXccC)	Avirulence factor in mustard and induction of ABA signaling in Arabidopsis.	<i>Arabidopsis thaliana</i> , <i>Brassica juncea</i>	He <i>et al.</i> , 2007 ; Ho <i>et al.</i> , 2013
XopAM	Partial avirulence factor.	<i>Arabidopsis thaliana</i>	Guy <i>et al.</i> , 2013
XopD	Interaction with DELLA proteins (GA signaling) and deSUMOylation of HFR1 (photomorphogenesis) to promote disease tolerance.	<i>Arabidopsis thaliana</i>	Tan <i>et al.</i> , 2014, 2015
XopE2 (AvrXccE1)	Avirulence factor.	<i>Brassica juncea</i>	He <i>et al.</i> , 2007
XopJ (AvrXccB)	Interaction with S-adenosyl-L-methionine-dependent methyltransferases 1 and 2 (SAM-MT1 and 2) and suppresses plant basal defenses.	<i>Arabidopsis thaliana</i>	Liu <i>et al.</i> , 2017
XopL	Inhibition of PTI in a MAPK-independent manner.	<i>Arabidopsis thaliana</i>	Yan <i>et al.</i> , 2019
XopN	Virulence factor.	<i>Raphanus sativus</i>	Jiang <i>et al.</i> , 2008

**Table 1.5. Main similarities and differences between the *Ralstonia solanacearum* species complex (RSSC) and *Xanthomonas campestris* pv. *campestris* (Xcc).**

Similarities	
Gram-negative plant pathogenic bacteria	
Vascular pathogens (xylem)	
Economic importance (crop diseases)	
Difficult and inefficient control measures	
Tropical and intertropical areas (special incidence in developing countries)	
Worldwide distribution	
Entry through wounds	
Model pathosystems ( <i>A. thaliana</i> )	
Easily cultivable <i>in vitro</i>	
Extensive genomic resources (several genomes sequenced)	
<i>R</i> genes discovered (e.g., RSSC <i>rrsI</i> or Xcc <i>zarl</i> )	
Epiphytic phase with potential long time survival	
Virulence determinants: EPS (biofilm), T2SS (CWDEs), detoxification systems, type IV pili and T3SS (T3Es)	
Highly polymorphic effectome within species	
Differences	
RSSC	Xcc
β-proteobacteria	γ-proteobacteria
Soilborne	Seedborne
Entry through root openings	Entry through hydathodes
Wilting symptoms	Localized V-shaped chlorotic/necrotic symptoms
Broad range (>50 botanical families)	Narrow range (Brassicaceae)
Virulence determinants: motility, phytohormones	Virulence determinants: T3BDTs
Large effectome (50-70 Rips/strain)	Small effectome (15-30 Xops/strain)
Quarantine organism	No

# Chapter 2

## PhD project



**Table 2.1. Orthology relationship between shared T3Es from *Xcc8004* and *RpsGM11000*.** Table summarizing the orthology relationship between T3Es from *Xcc8004* and *RpsGM11000* (blastp E-value <  $10^{-20}$ ) as defined by full-length protein sequence blastp querying the full effectome of *Xcc8004* against the full effectome of *RpsGM11000*.

<i>Xcc</i> T3E	<i>Xcc8004</i> accession	<i>Rps</i> T3E	<i>RpsGM11000</i> accession	blastp E-value	Identity	Query coverage
XopAG	XC_0563	RipOI	RSp0323	$7.5 \cdot 10^{-149}$	46.4%	88.2%
XopQ	XC_3177	RipB	RSc0245	$8.2 \cdot 10^{-130}$	47.4%	94.1%
XopP	XC_2994	RipH1	RSc1386	$4.1 \cdot 10^{-93}$	34.6%	80.9%
		RipH2	RSp0215	$1.0 \cdot 10^{-77}$	29.9%	96.1%
		RipH3	RSp0160	$4.0 \cdot 10^{-110}$	35.8%	84.6%
XopAM	XC_3160	RipR	RSp1281	$5.8 \cdot 10^{-96}$	27.2%	76.7%
HrpW	XC_3023	RipW	RSc2775	$1.3 \cdot 10^{-64}$	47.9%	71.7%
XopG	XC_0967	RipAX1	RSc3290	$2.1 \cdot 10^{-21}$	48.3%	88.8%
		RipAX2	RSp0572	$2.0 \cdot 10^{-21}$	44.4%	96.9%

As previously mentioned, the T3SS and associated T3Es are among the most important virulence factors of both *Xcc* and the RSSC. Despite their differences in effectome size and composition (Guy *et al.*, 2013; Sabbagh *et al.*, 2019), reference strains *Ralstonia pseudosolanacearum* (*Rps*) GMII000 and *Xcc* 8004 share nine *Rps* T3Es corresponding to six *Xcc* T3Es (**Table 2.1**). This provides a valuable opportunity for comparative studies and opens several questions: 1) Do orthologous T3Es in these two species work similarly? 2) What are the roles of these evolutionary conserved T3Es in these two vascular pathogens? In order to answer these questions, an integrated approach combining protein-protein interaction screenings, physiological analyses of transgenic plants, genetic screens and classical reverse genetics approaches was conducted aiming at identifying “biologically relevant” interactors of these shared T3Es, focusing on *Arabidopsis thaliana*, a common host of both pathogens.

The results of this thesis are structured in four parts: chapter 3 to chapter 6. In chapter 3, the results of two large-scale yeast two-hybrid screenings that allowed the identification of putative *Arabidopsis* targets of *Xcc*<sub>8004</sub> and *Rps*<sub>GMII000</sub> T3Es are presented and discussed. These results served to compare the effector targeting profiles of *Xcc* and *Rps* to those of previously screened pathogens (Mukhtar *et al.*, 2011; Weßling *et al.*, 2014). These meta-analyses together with the interactive knowledge database generated to explore them (EffectorK, available at [www.effectork.org](http://www.effectork.org)), are presented under the form of article draft. In chapter 4, results on the determination of the effects of individual T3Es using bacterial mutants and heterologous expression in model plants *A. thaliana* and *Nicotiana benthamiana* are presented and discussed. Chapters 5 and 6 present the results concerning the functional characterization of the most promising candidates. Chapter 7 will summarize and integrate the main conclusions discussed throughout the different results chapters as well as provide with some hints for the future and analyze the contribution of the present work to the global picture.

# Chapter 3

Identification of plant targets of type III effectors from *R. pseudosolanacearum* and *X. campestris* pv. *campestris*

## 3.1 Introduction

This first chapter of results compiles all the work related to the identification and characterization of Arabidopsis targets of T3Es from *Xcc*<sub>8004</sub> and *Rps*<sub>GM11000</sub>. To this end, several large-scale yeast two-hybrid screenings were conducted similarly to what had been previously done for other plant pathogens such as *Pseudomonas syringae*, *Hyaloperonospora arabidopsidis* or *Glovinomyces orontii* (Mukhtar *et al.*, 2011; Weßling *et al.*, 2014). For this reason, in addition to providing biologically relevant information for the *Xcc* and *Rps* pathosystems, our results can also be integrated into a larger Arabidopsis-effector interactomic dataset for further meta-analyses. This allowed us to extract general conclusions about how plant pathogen effectors interfere with the host proteome and motivated us to generate a public and interactive knowledge database to centralize and make accessible not only our results but also most published Arabidopsis-effector interactomic data. This first part is presented in the form of a research article. In a second part of the chapter, I will present the targets of *Xcc*<sub>8004</sub> and *Rps*<sub>GM11000</sub> T3Es identified in our screenings with a special focus on the common targets of these two pathogens. In the last part, I will present the first results on the characterization of the role of some of the common targets of *Xcc*<sub>8004</sub> and *Rps*<sub>GM11000</sub> in plant immunity.

## 3.2 EffectorK, a comprehensive resource to mine for *Ralstonia*, *Xanthomonas*, and other published effector interactors in the *Arabidopsis* proteome











### Contribution

The first part of this chapter, corresponding to the article, was a team effort involving not only the host Laboratory of Plant-Microbe Interactions, but also the Institute of Plant Sciences at Paris Saclay; University of Alabama at Birmingham and Carleton College at Northfield. This work started with two large-scale yeast two-hybrid screenings performed at the InterATOME platform of the Institute of Plant Sciences at Paris Saclay. The first screening, with 28 T3Es from *Xcc*<sub>8004</sub>, was performed prior to my arrival whereas the second one, with 50 T3Es from *Rps*<sub>GM11000</sub>, was conducted during my PhD. My contribution to this second screening was the preparation and quality check of the samples as well as cloning of some recalcitrant samples. Regarding “EffectorK”, the public database generated during this work, I contributed to the feeding and updating of the server. I also performed an extensive literature review to compile and integrate most published Arabidopsis-effector interactomic data. Regarding the article, I conducted all the analyses presented and wrote the original draft.

## **Research article**

The article “EffectorK, a comprehensive resource to mine for *Ralstonia*, *Xanthomonas*, and other published effector interactors in the *Arabidopsis* proteome” was published in *Molecular Plant Pathology* (submission date: 25/03/2020; acceptance date: 26/05/2020). The research article, as published (doi: 10.1111/mpp.12965), is attached.

# EffectorK, a comprehensive resource to mine for *Ralstonia*, *Xanthomonas*, and other published effector interactors in the *Arabidopsis* proteome

Manuel González-Fuente <sup>1</sup> | Sébastien Carrère <sup>1</sup> | Dario Monachello <sup>2,3</sup> | Benjamin G. Marsella<sup>4</sup> | Anne-Claire Cazalé <sup>1</sup> | Claudine Zischek<sup>1</sup> | Raka M. Mitra <sup>5</sup> | Nathalie Rezé<sup>2,3</sup> | Ludovic Cottret <sup>1</sup> | M. Shahid Mukhtar <sup>4</sup> | Claire Lurin <sup>2,3</sup> | Laurent D. Noël <sup>1</sup> | Nemo Peeters <sup>1</sup>

<sup>1</sup>Laboratoire des Interactions Plantes Micro-organismes, INRAE, CNRS, Université de Toulouse, Castanet-Tolosan, France

<sup>2</sup>Institut des Sciences des Plantes de Paris Saclay, UEVE, INRAE, CNRS, Université Paris Sud, Université Paris-Saclay, Gif-sur-Yvette, France

<sup>3</sup>Université de Paris, Gif-sur-Yvette, France

<sup>4</sup>Department of Biology, University of Alabama at Birmingham, Birmingham, AL, USA

<sup>5</sup>Department of Biology, Carleton College, Northfield, MN, USA

## Correspondence

Nemo Peeters and Laurent D. Noël, Laboratoire des Interactions Plantes Micro-organismes, INRAE, CNRS, Université de Toulouse, F-31326 Castanet-Tolosan, France. Email: nemo.peeters@inrae.fr and laurent.noel@inrae.fr

## Funding information

Agence Nationale de la Recherche, Grant/Award Number: ANR-10-LABX-41 and ANR-11-IDEX-0002-02

## Abstract

Pathogens deploy effector proteins that interact with host proteins to manipulate the host physiology to the pathogen's own benefit. However, effectors can also be recognized by host immune proteins, leading to the activation of defence responses. Effectors are thus essential components in determining the outcome of plant-pathogen interactions. Despite major efforts to decipher effector functions, our current knowledge on effector biology is scattered and often limited. In this study, we conducted two systematic large-scale yeast two-hybrid screenings to detect interactions between *Arabidopsis thaliana* proteins and effectors from two vascular bacterial pathogens: *Ralstonia pseudosolanacearum* and *Xanthomonas campestris*. We then constructed an interactomic network focused on *Arabidopsis* and effector proteins from a wide variety of bacterial, oomycete, fungal, and invertebrate pathogens. This network contains our experimental data and protein-protein interactions from 2,035 peer-reviewed publications (48,200 *Arabidopsis*-*Arabidopsis* and 1,300 *Arabidopsis*-effector protein interactions). Our results show that effectors from different species interact with both common and specific *Arabidopsis* interactors, suggesting dual roles as modulators of generic and adaptive host processes. Network analyses revealed that effector interactors, particularly "effector hubs" and bacterial core effector interactors, occupy important positions for network organization, as shown by their larger number of protein interactions and centrality. These interactomic data were incorporated in EffectorK, a new graph-oriented knowledge database that allows users to navigate the network, search for homology, or find possible paths between host and/or effector proteins. EffectorK is available at [www.effectork.org](http://www.effectork.org) and allows users to submit their own interactomic data.

Manuel González-Fuente and Sébastien Carrère contributed equally to this work.

This is an open access article under the terms of the Creative Commons Attribution License, which permits use, distribution and reproduction in any medium, provided the original work is properly cited.

© 2020 The Authors. *Molecular Plant Pathology* published by British Society for Plant Pathology and John Wiley & Sons Ltd

## KEYWORDS

database, effectors, interactomics, network, *Ralstonia*, *Xanthomonas*

## 1 | INTRODUCTION

Plants are continuously confronted with a wide variety of pathogens, including bacteria, oomycetes, fungi, nematodes, and insects. To prevent their proliferation, plants have evolved a complex multi-layered immune system (Jones and Dangl, 2006). Plants are able to recognize highly conserved pathogen-associated molecular patterns (PAMPs) through pattern-recognition receptors triggering induced defence responses collectively known as PAMP-triggered immunity (PTI) (Zipfel, 2014). These responses are usually enough to prevent most potential invaders; however, some pathogens secrete effector proteins to subvert the defence responses and alter diverse cellular processes to ease their proliferation (Ma *et al.*, 2018). Plants, moreover, have evolved several intracellular nucleotide-binding site-leucine-rich repeat (NBS-LRR) receptors recognizing these effectors and activating potent defence responses collectively known as effector-triggered immunity (ETI) (Cui *et al.*, 2015).

Although the interactors and molecular functions of some effectors have been characterized (Büttner, 2016; Giron *et al.*, 2016; Sharpee and Dean, 2016; Vieira and Gleason, 2019), for most effectors they are still unknown. The main factors complicating the large-scale identification and characterization of effector–host protein interactions are the wide diversity of pathosystems, the difficulty in identifying bona fide effector genes, the collective contribution of effector proteins, the complexity of the host responses, and the lack of robust high-throughput techniques. For the model species *Arabidopsis thaliana* (Ath), to our knowledge, there are only two studies in which systematic effector–host protein interactions at the effectome-scale have been identified (Mukhtar *et al.*, 2011; Weßling *et al.*, 2014). In these studies plant interactors of effector proteins from *Pseudomonas syringae* (Psy, bacterium), *Hyaloperonospora arabidopsidis* (Hpa, oomycete), and *Glovinomyces orontii* (Gor, fungus) were identified by yeast two-hybrid (Y2H) assays. They reported that the effectors of these species converged onto a limited set of Ath proteins. These studies also demonstrated that many effector interactors are important for plant immunity and showed that their importance correlates with the level of effector convergence.

Bacterial wilt, caused by *Ralstonia pseudosolanacearum* (*Ralstonia solanacearum* phylotype I, Rps), and black rot, caused by *Xanthomonas campestris* pv. *campestris* (Xcc), are listed among the top 10 scientifically and economically important plant bacterial diseases (Mansfield *et al.*, 2012). Both Rps and Xcc are xylem-colonizing bacteria able to infect the model plant Ath (Deslandes *et al.*, 1998; Buell, 2002). They both rely on their type III secretion system for full virulence (Arlat *et al.*, 1991, 1992). This “molecular syringe” allows the pathogen to deliver type III effector proteins (T3Es) directly into the host cell in order to promote disease. The roles of several of their T3Es have been characterized (White *et al.*, 2009; Coll and Valls, 2013), but most knowledge on T3E functions comes from the study of Psy,

which resides on leaf surfaces and in the leaf apoplast (Lindeberg *et al.*, 2012; Büttner, 2016). Focusing mainly on a few species offers a partial view of effector biology. It is therefore crucial to expand our studies to other species to grasp the existing diversity of effector proteins and pathogen lifestyles.

To obtain a deeper understanding of the global Ath–effector protein interactome, we conducted three systematic large-scale screenings with T3Es from Rps and Xcc, the first vascular pathogens screened in this manner. Additionally, we conducted an extensive literature survey to gather published Ath interactors of effector proteins from pathogens from four different kingdoms of life: Bacteria, Chromista, Fungi, and Animalia. Combining all these data allowed us to identify 100 new “effector hubs” (i.e., Ath proteins interacting with two or more effectors). Together with Ath–Ath protein interactions retrieved from public databases, we generated an Ath–effector protein network that captures the wide diversity of Ath pathogens. This network allowed us to detect general trends of effector interference with the host proteome. We have created a publicly available interactive knowledge database called EffectorK (for Effector Knowledge) that allows users to access and augment this network.

## 2 | RESULTS

### 2.1 | Systematic identification of *Arabidopsis* interactors of *R. pseudosolanacearum* and *X. campestris* effectors

Three Y2H screenings were performed to identify Ath interactors of Rps and Xcc effector proteins. In a first screening, we identified 42 Ath interactors for 21 out of 56 T3Es from Rps strain GM100 screened against a library of more than 8,000 full-length Ath cDNAs (8K space). The choice of the 56 Rps T3Es was guided by the available clones at the time of screening. In the second and third screenings, we identified 176 Ath interactors for 32 out of 48 T3Es from Rps strain GM1000 and 52 Ath interactors for 18 out of 25 T3Es from Xcc strain 8,004 screened against an extended version of the previous library containing more than 12,000 Ath full-length cDNAs (12K space) (Figure S1 and Table S1). Here the choice of Rps T3Es was constrained by a pool maximum imposed by the screening method (see Materials and Methods). T3Es were picked according to their highest degree of conservation within the species complex (Peeters *et al.*, 2013). On average, 10.7 and 5.7 Ath interactors were found per Rps and Xcc T3E. These Ath cDNA libraries had been previously used to test interactions with 57 and 32 effector proteins from Hpa and Psy, respectively, (8K space) and 46 effector proteins from Gor (12K space) (Mukhtar *et al.*, 2011; Weßling *et al.*, 2014). The subset of interactions of effectors from Rps, Xcc, and Gor in the 8K space was used to compare with previously published Hpa and Psy data

(Figure 1). In general, Rps effectors interacted on average with more Ath proteins than the other screened species; however, this difference is only statistically significant when compared to Gor effectors (one-tailed Wilcoxon signed-rank test  $p < .001$ ). These data show that effector proteins from these five different species, on average, tend to interact with a similar number of Ath proteins regardless of kingdom, life style, or effectome size.

## 2.2 | Effectors converge onto a limited set of *Arabidopsis* proteins

We compared the Rps and Xcc effector interactors identified in our screenings with the interactors previously identified for Hpa, Psy, and Gor effector proteins (Mukhtar *et al.*, 2011; Weßling *et al.*, 2014). To avoid bias related to the size of the screened library, we considered only the subset of effector interactors present in the 8K space (Figure S2). At the kingdom level, Bacteria was the kingdom with the highest number of kingdom-specific interactors, with 158 exclusive interactors out of a total of 217 interactors (72.8%), followed by Chromista, with 31 out of 117 (51.7%), and Fungi, with 16 out of 45 (35.6%). In total, 235 out of 299 effector interactors (78.6%) were kingdom-specific. At the species level, when comparing all five pathogens, the percentage of species-specific interactors was 58.9% for Psy, 58.7% for Rps, 51.7% for Hpa, 48.8% for Xcc, and 35.6% for

Gor. The total number of species-specific effector interactors was 221 out of 299 (73.9%). These data show that most effector interactors are kingdom- and species-specific.

To evaluate whether Rps and Xcc effectors interact randomly or converge onto a common set of Ath proteins we performed simulations rewiring effector–Ath protein interactions within the 8K space. In these simulations, each effector was assigned randomly as many Ath proteins as it had interacted with in our screenings. Then, the number of interactors found on all simulations was plotted and compared with the experimental data (Figure 2a). The number of effector interactors observed in our screenings was significantly lower than the numbers obtained in the random simulations for both Rps and Xcc. Similar results had been reported for effectors from Hpa, Psy, and Gor (Mukhtar *et al.*, 2011; Weßling *et al.*, 2014). This shows that, similarly to other species, both Rps and Xcc effectors also interact with a common subset of Ath proteins (i.e., intraspecific convergence).

These random rewiring simulations also allowed us to determine whether effectors from different species interact randomly or convergently with Ath proteins. For this, the number of common interactors of effectors from different species was compared with the experimental data (Figure 2b). When comparing all three kingdoms, the number of common interactors observed was significantly higher than expected by random rewiring. We then analysed all possible binary, ternary, quaternary, and quinary combinations of species and in all cases the number of common interactors observed was higher than expected randomly (Figure 2c). These differences were all statistically significant except for the common interactors of effectors from Psy and Xcc ( $p = .058$ ; Figure S3). This could indicate that these two species are the most different in terms of effector targeting. However, considering that Psy and Xcc are precisely the two species with the lowest number of effectors for which interactors have been identified (Psy: 32 and Xcc: 18 effector proteins), it is likely that the high  $p$  value is caused by the limited sample size. This shows that effectors from all these five species interact with a common subset of Ath proteins (i.e., interspecific convergence).

Altogether, our data indicate that Rps and Xcc effectors converge both intra- and interspecifically onto a set of limited Ath proteins, behaving similarly to effectors from other previously screened pathogen species. This suggests the existence of a convergent set of effector interactors common to evolutionarily distant pathogens that might have a predominant role in the general modulation of the host responses.

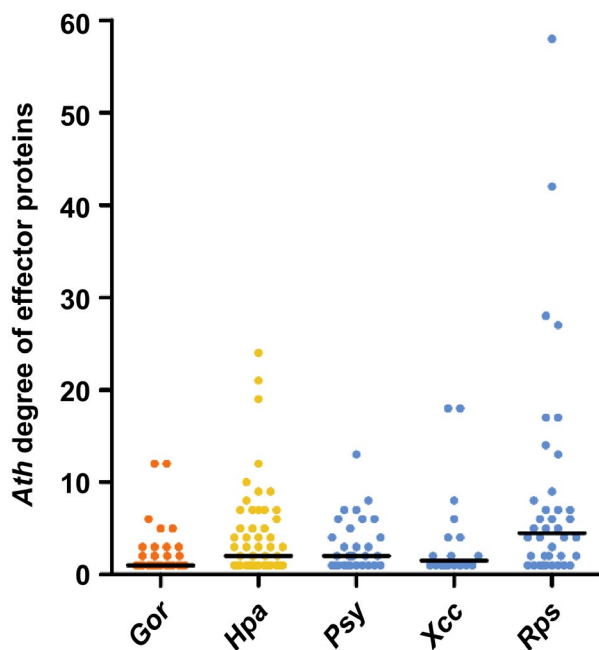


**FIGURE 1** *Arabidopsis thaliana* (Ath) degree of effector proteins from *Glovinomyces orontii* (Gor), *Hyaloperonospora arabidopsidis* (Hpa), *Pseudomonas syringae* (Psy), *Xanthomonas campestris* pv. *campestris* (Xcc), and *Ralstonia pseudosolanacearum* (Rps). Comparison of the Ath degree (i.e., number of Ath interactors per effector) of effector proteins from Gor, Hpa, Psy, Xcc, and Rps found in the 8,000-Ath-cDNA collection (8K space). Horizontal black bars represent the median. Colours represent the kingdom (orange: Fungi, yellow: Chromista, and blue: Bacteria)

## 2.3 | Manual curation of the literature to compile *Arabidopsis*–effector protein interactions

In order to gather more knowledge on Ath–effector protein interactions, we conducted an extensive literature search compiling data from a wider spectrum of bacterial, fungal, oomycete, and invertebrate effector proteins. We only considered published direct protein–protein interactions that had been confirmed by classic techniques such as Y2H, co-immunoprecipitation, pull-down,



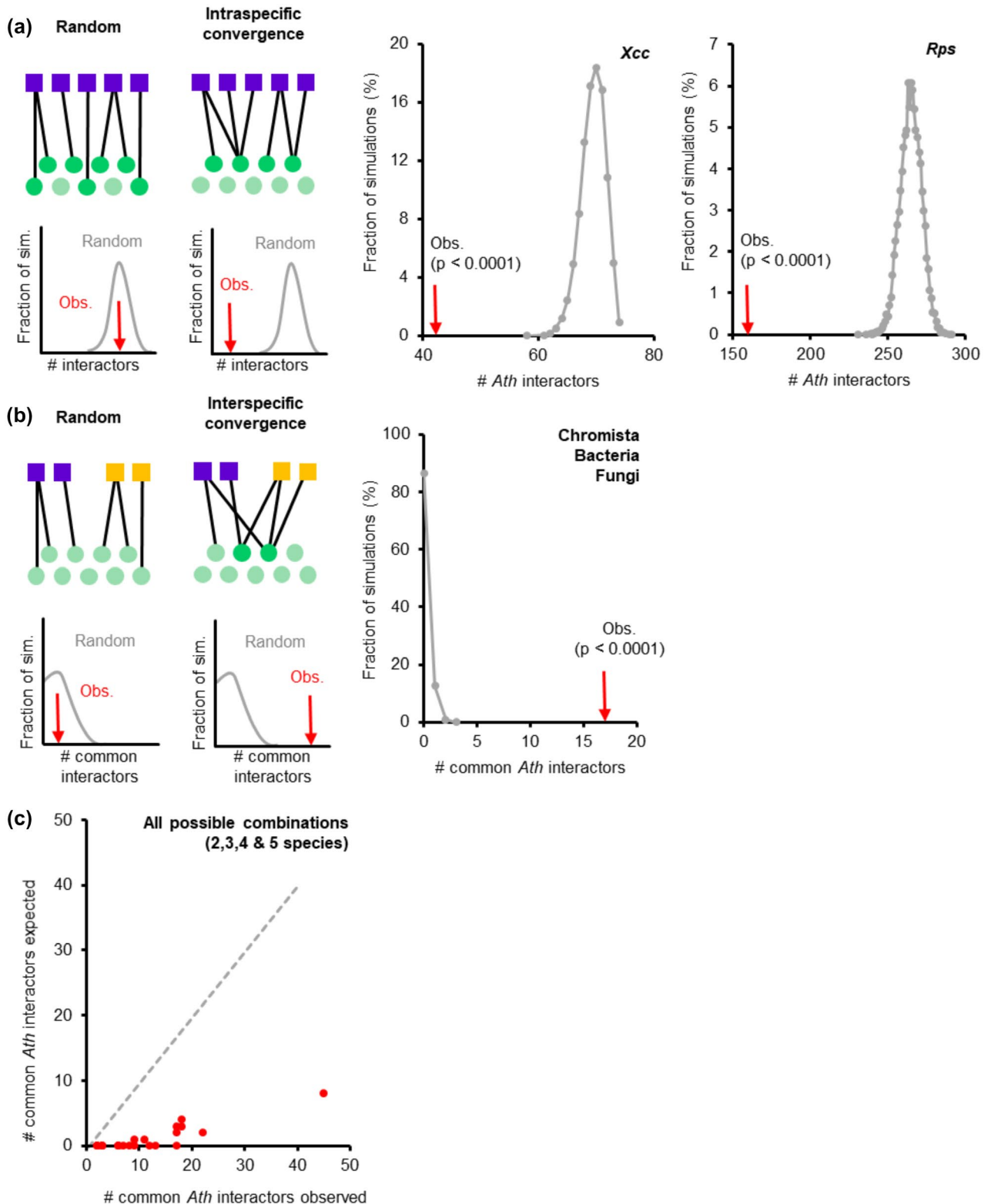


**FIGURE 2** Effectors converge intra- and interspecifically onto a common set of *Arabidopsis thaliana* (Ath) proteins. (a) Left: random and intraspecific convergent interactions of effectors (purple squares) with Ath proteins (green circles) can be distinguished by random network rewiring and simulation. Adapted from Weßling *et al.* (2014). Middle and right: number of Ath interactors in the 8K space of effectors from *Xanthomonas campestris* pv. *campestris* (Xcc) strain 8,004 and *Ralstonia pseudosolanacearum* (Rps) strain GMI1000 found in 10,000 degree-preserving simulations (grey) versus the observed number (red arrow). (b) Left: random and interspecific convergent interactions of effectors from different species (purple and orange squares) with Ath proteins (green circles) can be distinguished by random network rewiring and simulation. Right: number of common Ath interactors in the 8K space of effectors from Chromista, Bacteria, and Fungi found in 10,000 simulations (grey) versus the observed number (red arrow). (c) Scatterplot of observed versus simulated number of common Ath interactors between all binary, ternary, quaternary, and quinary combinations of species.  $x = y$  regression is represented with a dashed grey line

protein-fragment complementation, fluorescence resonance energy transfer, or mass spectrometry. We compiled 287 interactions found in 80 peer-reviewed publications involving 218 *Ath* proteins and 72 effectors from 22 pathogen species (Table S2). Among these 22 pathogens, there were nine bacterial species, mostly proteobacteria but also a phytoplasma species; eight invertebrate species, including both nematodes and insects; four oomycete, and one fungal species. While this collection of species does not represent the full diversity of *Ath* pathogens, it covers the majority of pathogens for which effector interactors have been reported. We can see that, despite being one of the major pathogen classes, few studies have described fungal effector interactors. This illustrates one of the current gaps in our knowledge of effector interactors in *Ath*.

## 2.4 | Identification of one hundred new “effector hubs”

To compare experimental and published data, we combined all the interactions curated from the published data together with data from our large-scale Y2H screenings. This resulted in a total of 564 different *Ath* proteins interacting with pathogen effectors. Our screenings on Rps and Xcc effectors identified 235 interactors. Similar published screenings on Psy, Gor, or Hpa effectors had identified 200 interactors (Mukhtar *et al.*, 2011; Weßling *et al.*, 2014). The literature curation allowed us to identify 218 effector interactors. From the 235 Rps and Xcc effectors interactors found in our screening, 166 were new, which represents 29.4% of the total interactors compiled in this study (Figure 3). This highlights the potential of such systematic and high-throughput large-scale screenings in identifying novel effector interactors. The average effector degree (i.e., the number of effectors interacting with a given *Ath* protein) was 2.3 but it was unevenly distributed among the 564 interactors, with 350 of them interacting with only one effector (62%) and 14 interacting with more than 10 effectors (2.5%) (Figure S4). The contribution of our experimental data was important in the identification of single interactors as we identified 93 out of the 350 (26.6%). More remarkable was the contribution in the identification of “effector hubs,” defined here as *Ath* proteins interacting with two or more effectors (Figure 4). The definition of “hub” has been debated and it has been traditionally associated with proteins that are highly connected in interactomic networks (Vandereyken *et al.*, 2018). Our definition of “effector hub” came from the need to designate the *Ath* proteins that interact with several effectors and is based exclusively on the number of interacting effector proteins. We identified 100 new effector hubs and increased the degree of 42 previously described effector hubs (Table S3).

To evaluate the potential relevance of the newly identified effector hubs in plant immunity, we conducted a second literature survey to check if the corresponding *Ath* genes had previously reported functions in plant immunity or in pathogen fitness in planta (Table 1).

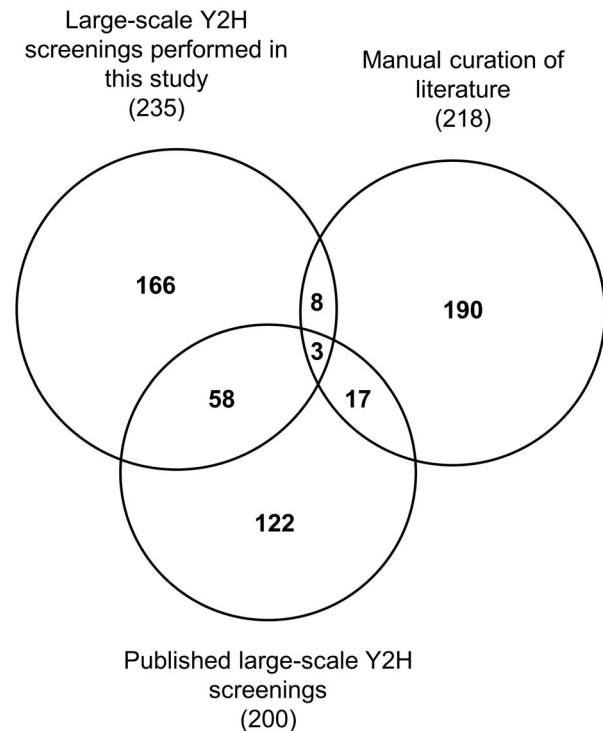


**FIGURE 3** Overlap among effector interactors depending on the origin of the data set. Area-proportional Venn diagram showing the overlap among effector interactors identified in the large-scale yeast two-hybrid (Y2H) screenings performed in this study, in similar large-scale Y2H already published, and in the manual curation of the literature. The total number of effector interactors coming from each dataset is indicated in parentheses

Sixteen out of the 100 new effector hub genes have already been described for their altered infection or other immunity-related phenotype when mutated, silenced or overexpressed. Additionally, the orthologs of three other new hubs in other plant species also produced altered infection phenotypes when silenced or overexpressed. A total of 19 out of the 100 newly identified effector hubs have already been shown to be involved in biotic stress responses. Considering that many of the remaining newly defined effector hubs have been poorly characterized (e.g., hypothetical proteins or descriptions based on homology or belonging to a protein family), it is likely that the number of effector hubs involved in immunity was underestimated. This constitutes a valuable source of novel candidates for further functional characterization.

In terms of organism of origin, most of the 564 interactors are bacterial effector interactors, as could be expected considering that 132 out of the 266 total effectors compiled came from bacteria (Figure S4). In the case of effector hubs, it is noteworthy that 133 out of the 214 hubs described in this work interact with effectors from a single kingdom while there are only 64, 16, and one hubs interacting with effectors from two, three or four different kingdoms, respectively (Table S3). Although biased by the structure of the data, this could suggest kingdom specificity of effector targeting.

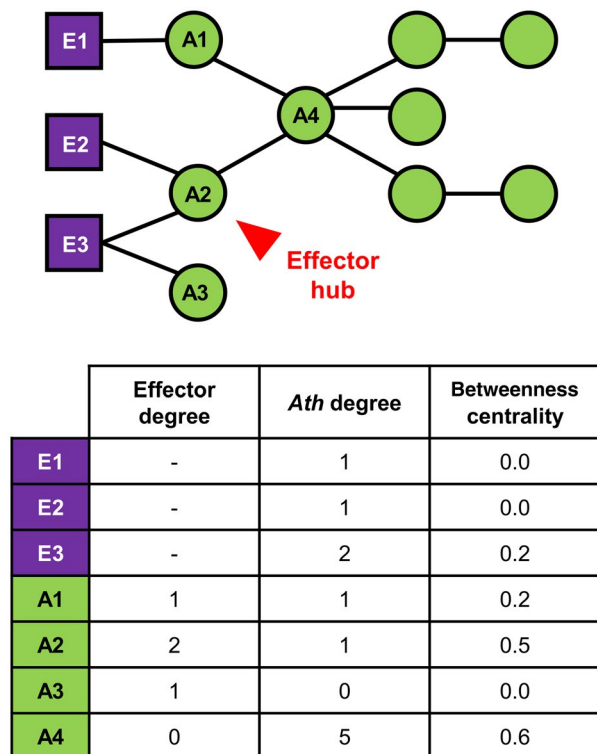


**FIGURE 4** Network topology parameters. Example of a simple interactomic network of three effector proteins (purple squares) and nine *Arabidopsis thaliana* (Ath) proteins (green circles) to illustrate our definition of “effector hub” (i.e., Ath protein interacting with two or more effectors; highlighted in red) and the three network topology parameters analysed in this study. 1, Effector degree: number of effectors that interact with a given Ath protein; 2, Ath degree: number of Ath proteins that interact with a given effector or Ath protein; 3, Betweenness centrality: fraction of all shortest paths connecting two proteins from the network that pass through a given protein

## 2.5 | Construction of an interaction network involving *Arabidopsis* and effector proteins

We constructed an Ath–effector protein interaction network compiling the previously described experimental and literature-compiled data with Ath–Ath protein interactions from public databases and the literature (Stark *et al.*, 2006; Dreze *et al.*, 2011; Orchard *et al.*, 2014; Smakowska-Luzan *et al.*, 2018). From the total of 49,500 interactions compiled in this study, 48,597 were grouped into a single connected component constituting what we defined as our Ath–effector interactomic network (Table S4). This network was constituted of 47,314 Ath–Ath and 1,283 Ath–effector protein interactions between 8,036 Ath proteins and 245 effector proteins. Effectors came from 23 different species, including bacteria (128 effectors), oomycetes (61 effectors), fungi (46 effectors), and invertebrates (10 effectors). The uneven distribution of effectors among kingdoms highlights the contribution of the large-scale screenings in the identification of effector interactors as 1,002 out of 1,283 Ath–effector protein interactions came from either our experimental data or previous screenings of the same library (Mukhtar *et al.*, 2011; Weßling *et al.*, 2014).

## 2.6 | Effector interactors tend to occupy key positions in the *Arabidopsis*–effector protein interaction network

To further investigate the potential impact of effectors on the plant interactome, we evaluated the importance of their interactors for the organization of the network. We focused on two main network topology parameters: “degree” and “betweenness centrality” (Figure 4). The “degree” of a protein represents the number of proteins that it interacts with. In this study we differentiated two types of degrees depending on the nature of the interacting proteins: the Ath degree of a given effector or Ath protein (i.e. the number of interacting Ath proteins) and the effector degree for a given Ath protein (i.e. the number of interacting effector proteins). The “betweenness centrality” of a protein is the fraction of all shortest paths connecting two proteins from the network that pass through it. There are two main types of key proteins in a network (Li *et al.*, 2017): (a) proteins important for local network organization, typically showing high degree, and (b) proteins important for the global diffusion of the information through the network, characterized by high betweenness centrality. It had been previously reported in more limited networks that effectors tend to interact with host proteins with high degree and high centrality (Memišević *et al.*, 2015; Li *et al.*, 2017; Ahmed *et al.*, 2018). We then analysed whether this was the case in our network comparing effector interactors with the rest of the Ath proteins (Figure 5). The fraction of proteins decreased rapidly as the Ath degree increased. This indicates that most Ath proteins present low Ath degree and only a few of them show high Ath degree values. This tendency was significantly shifted towards higher Ath degree values in effector interactors compared to the rest of Ath proteins. To represent this tendency shift we estimated and compared the area under the curve values of the cumulative distribution of the Ath degree for effector interactors and the rest of Ath proteins (Table 2). Effectively, the area under the curve value of effector interactors was higher than the value of the rest of the Ath proteins. This indicates that effector interactors present generally higher Ath degree than the rest of the Ath proteins. Similarly, we compared the betweenness centrality of these two groups of proteins (Table 2 and Figure S5). Effector interactors also presented significantly higher betweenness centrality values than the rest of the Ath proteins. Altogether, these results indicate that effectors preferentially interact with Ath proteins that are more connected to other Ath proteins and that occupy more central positions in the interactomic network as reported for smaller networks (Li *et al.*, 2017; Ahmed *et al.*, 2018).

## 2.7 | Effector hubs are better connected and more central than single effector interactors in the *Arabidopsis*–effector interaction network

We then wanted to test if the Ath degree and betweenness centrality values differed among distinct types of effector interactors (Table 2 and Figure S5). First, we compared multipathogen and pathogen-specific interactors as previously described (Figure S2). Multipathogen effector

**TABLE 1** List of 19 new effector hubs involved in plant immunity

Effector hub	Protein name	Effector degree <sup>a</sup>	Description of observed phenotype	Reference
AT1G58100	TCP domain protein 8 (TCP8)	13	Triple <i>tcp8 tcp14 tcp15</i> mutant showed enhanced <i>Pseudomonas syringae</i> strain DC3000 $\Delta$ avrRps4 growth	Kim <i>et al.</i> (2014)
AT1G71230 <sup>b</sup>	COP9-signalosome 5B (CSN5B)	8	Wheat <i>TaCSN5</i> mutant showed enhanced disease symptoms caused by <i>Puccinia triticina</i>	Zhang <i>et al.</i> (2017)
AT3G12920	BOI-related gene 3 (BRG3)	7	<i>brg3</i> mutant showed increased <i>Botrytis cinerea</i> lesion size	Luo <i>et al.</i> (2010)
AT5G08330 <sup>b</sup>	TCP domain protein 21 (TCP21)	7	Rice <i>OsTCP21</i> silenced and overexpressing plants showed enhanced and reduced disease symptoms caused by rice rust stunt virus (RRSV), respectively	Zhang <i>et al.</i> (2016)
AT5G61010	Exocyst subunit EXO70 family protein E2 (EXO70E2)	6	<i>exo70e2</i> mutant showed reduced flg22-induced callose deposition.	Redditt <i>et al.</i> (2019)
AT4G00270	STOREKEEPER-related 1 (STKR1)	6	<i>STKR1</i> overexpressing plants showed reduced <i>Hyaloperonospora arabidopsidis</i> spore formation	Nietzsche <i>et al.</i> (2018)
AT3G01670	SIEVE ELEMENT OCLUSSION-related 2 (SEOR2)	4	<i>Myzus persicae</i> feeding from <i>seor2</i> mutant showed reduced progeny	Anstead <i>et al.</i> (2012)
AT5G17490	RGA-like protein 3 (RGL3)	3	<i>rgl3</i> mutant showed reduced <i>P. syringae</i> growth and increased SA content upon infection	Li <i>et al.</i> (2019)
AT3G54230	Suppressor of <i>abi3-5</i> (SUA)	3	<i>sua</i> mutant showed enhanced <i>P. syringae</i> growth and reduced chitin-induced ROS production	Zhang <i>et al.</i> (2014)
AT3G11410	Protein phosphatase 2CA (PP2CA)	3	<i>pp2ca</i> mutant showed reduced <i>P. syringae</i> colonization and stomatal aperture. <i>PP2CA</i> overexpressor showed enhanced stomatal aperture	Lim <i>et al.</i> (2014)
AT2G17290	Calcium-dependent protein kinase 6 (CPK6)	3	Double <i>cpk5-cpk6</i> mutant showed enhanced <i>P. syringae</i> growth and reduced flg22-induced ROS production	Boudsocq <i>et al.</i> (2010)
AT5G41410 <sup>b</sup>	Homeobox protein BEL1 homolog (BELL1)	3	Rice <i>OsBIHD1</i> mutant and overexpressing plants showed increased and reduced <i>Magnaporthe oryzae</i> lesion area, respectively	Liu <i>et al.</i> (2017)
AT4G26750	LYST-interacting protein 5 (LIP5)	2	<i>lip5</i> mutant showed enhanced <i>P. syringae</i> growth and disease symptoms and reduced endosomal structure formation upon infection	Wang <i>et al.</i> (2014)
AT4G35090	Catalase-2 (CAT2)	2	<i>cat2</i> mutant showed increased ROS accumulation upon infection with incompatible <i>P. syringae</i> strain	Simon <i>et al.</i> (2010)
AT3G02870	Inositol-phosphate phosphatase (VTC4)	2	<i>vtc4</i> mutant showed reduced <i>P. syringae</i> growth	Mukherjee <i>et al.</i> (2010)
AT5G53060	Regulator of CBF gene expression 3 (RCF3)	2	<i>rcf3</i> mutant showed reduced percentage of diseased plants and higher percentage of plant survival upon <i>Fusarium oxysporum</i> infection	Dagdas <i>et al.</i> (2016)
AT3G02540	RAD23 family protein C (RAD23C)	2	<i>rad23BCD</i> mutant (and not <i>rad23BD</i> ) did not show <i>Candidatus Phytoplasma</i> -induced flower virescence and phyllody	MacLean <i>et al.</i> (2014)
AT5G38470	RAD23 family protein D (RAD23D)	2	<i>rad23D</i> mutant did not show flower virescence and phyllody upon transgenic expression of <i>C. phytoplasma</i> SAP54 effector	MacLean <i>et al.</i> (2014)
AT2G37630	Asymmetric leaves 1 (AS1)	2	<i>as1</i> mutant showed reduced lesion size caused by <i>B. cinerea</i> and <i>Alternaria brassicicola</i> and enhanced <i>Pseudomonas fluorescens</i> and <i>P. syringae</i> growth	Nurmberg <i>et al.</i> (2007)

<sup>a</sup>Ranked in decreasing order.<sup>b</sup>Orthologous gene in other plant species, as defined by EnsemblPlants (Kersey *et al.*, 2018), characterized for a role in immunity.

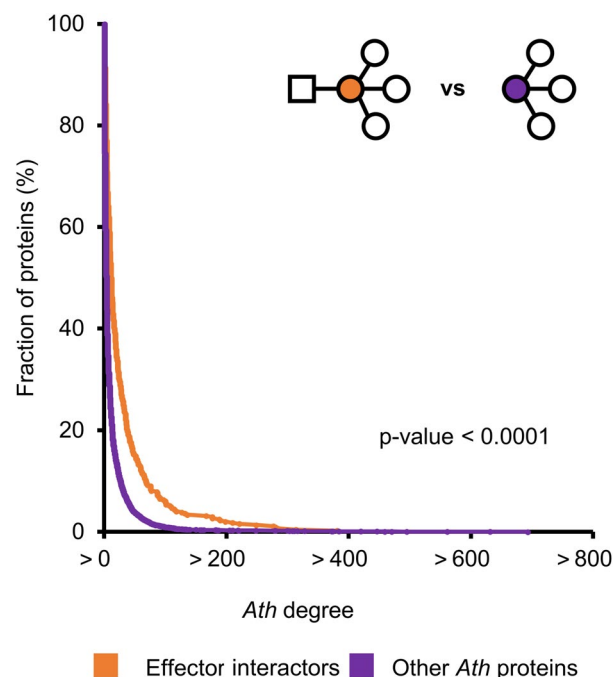


**FIGURE 5** Ath degree of Ath proteins interacting or not with effectors. Cumulative distribution of Ath degree of Ath proteins interacting (orange) or not (purple) with effectors. The significance of the difference was validated by one-tailed Wilcoxon signed-rank test. The illustration in the upper right corner represents each compared group. Effectors are represented by squares, Ath proteins by circles and the colour code matches the cumulative distribution graph

interactors presented significantly higher Ath degree and betweenness centrality compared to pathogen-specific effector interactors. We also compared effector hubs with single effector interactors. Similarly, effector hubs also showed higher betweenness centrality and Ath degree than single effector interactors. This last observation implies that an Ath protein that interacts with several effectors tends also to interact with more Ath proteins. To evaluate whether this is biologically relevant or a bias of the “stickiness” of a protein, we compared the Ath and effector degree values of all effector interactors. Our results showed that these two parameters are not correlated (Pearson correlation coefficient = 0.3221; Figure S6). This suggests that effector hubs interact with more Ath proteins than single effector interactors and that this is not due to a higher stickiness of these proteins. Altogether, these results show that the general tendencies of effector interactors (i.e. more connected to other Ath proteins and more central in the *Arabidopsis*–effector interaction network) are stronger among effector hubs compared to single interactors, and among multipathogen effector interactors compared to pathogen-specific interactors. This reflects the importance of interfering with key position proteins for the modulation of host–pathogen interactions.

## 2.8 | Bacterial core T3Es interact with more connected and central Ath proteins

Our work on Rps and Xcc together with previous work on Psy T3Es (Mukhtar *et al.*, 2011) provided a large amount of interactomic data

**TABLE 2** Cumulative Ath and effector degrees and betweenness centrality of different groups of effector interactors

	Area under the curve <sup>a</sup>		Figure <sup>b</sup>	p value <sup>c</sup>
	Effector interactors	Other Ath proteins		
Ath degree	2,737	1,010	5	<.0001
Betweenness centrality	0.23	0.033	S5A	<.0001
	Multipathogen effector interactors	Pathogen-specific effector interactors		
Ath degree	5,344	1,790	S5B	<.0001
Betweenness centrality	0.657	0.136	S5C	<.0001
	Effector hubs	Single effector interactors		
Ath degree	4,067	1,810	S5D	<.0001
Betweenness centrality	0.407	0.118	S5E	<.0001
	Bacterial core T3Es	Rest of bacterial T3Es		
Ath degree	656	712	S7A	0.4571
Betweenness centrality	0.072	0.074	S7B	0.9198
	Bacterial core T3E interactors	Other bacterial T3Es interactors		
Effector degree	347	123	S7C	<.0001
Ath degree	3,610	2,714	S7D	0.0131
Betweenness centrality	0.369	0.239	S7E	0.0007

<sup>a</sup>Estimated area under the curve of the cumulative distribution of Ath degree, effector degree, and betweenness centrality for each group of proteins as represented in Figures 5, S5, and S7. Estimation based on numerical integration using Simpson's rule.

<sup>b</sup>Figure illustrating the cumulative distribution graphic from which the areas under the curve compared were calculated.

<sup>c</sup>One-tailed Wilcoxon signed-rank test p value of the comparison of the Ath degree, effector degree or betweenness centrality values of all proteins from each compared group.



on bacterial pathogen species for which other resources have been generated, particularly in terms of abundance and diversity of sequenced genomes and thus curated T3E repertoires (Lindeberg *et al.*, 2012; Guy *et al.*, 2013; Peeters *et al.*, 2013; Roux *et al.*, 2015; Dillon *et al.*, 2019; Sabbagh *et al.*, 2019). The most conserved set of T3Es, or “core effectome,” from each of the three bacterial species has been previously defined (Guy *et al.*, 2013; Dillon *et al.*, 2019; Sabbagh *et al.*, 2019). We then tested whether these subsets of T3Es behaved differently from the rest of bacterial T3Es in terms of interaction with host proteins (Table 2 and Figure S7). Our data showed that core and variable T3Es from the three species do not differ in Ath degree nor betweenness centrality. We then tested if there were any differences between the network properties of the interactors of core T3Es and the other bacterial T3E interactors. Core T3Es interactors showed higher effector degree, Ath degree, and betweenness centrality than the rest of interactors of bacterial T3Es. This suggests that, although core T3Es in general do not have more interactors than the rest of bacterial T3Es, they do interact with more highly connected and central Ath proteins. This might imply that core T3Es have a larger potential to interfere with the host interactome, which could explain the selective pressure to maintain them in the majority of strains.

## 2.9 | EffectorK, an online interactive knowledge database to explore the *Arabidopsis*–effector interactomic data

In order to facilitate the access and exploration of all the data presented in this work, we have generated EffectorK (for “Effector Knowledge”), an interactive web-based knowledge database freely available at [www.effectork.org](http://www.effectork.org). The latest version (2 October 2019) contains 49,875 interactions for 8,617 proteins coming from 2,035 publications. Of these, 1,300 are Ath–effector protein interactions. Searches can be done based on a wide range of supported identifiers such as different protein names, NCBI or TAIR accession numbers, PubMed identifiers, and InterPro terms. Additionally, users can also query nucleotide or amino acid sequences directly with BLAST or use accession numbers from other model and crop plants to find homologs within the database. All proteins found by query are then listed in tabular format and hyperlinked to the corresponding interactomic data, external resources, and amino acid sequences. Interactomic data for a given protein can be then explored and downloaded in tabular or graphical format. The graphical representation of the interactomic data depicts proteins interacting with other proteins as nodes interconnected by edges (Figure 6). The size of a node is proportional to the number of interacting proteins, whereas the thickness of an edge represents the confidence of the interaction (i.e. whether the interaction has been detected by one [narrow] or several independent [thick] techniques). This visual interface allows users to expand or re-centre a local subnetwork based on a given protein, get information and access to external resources linked to either a protein (node) or an interaction (edge), or modify the layout and the position of the elements for optimal visualization.

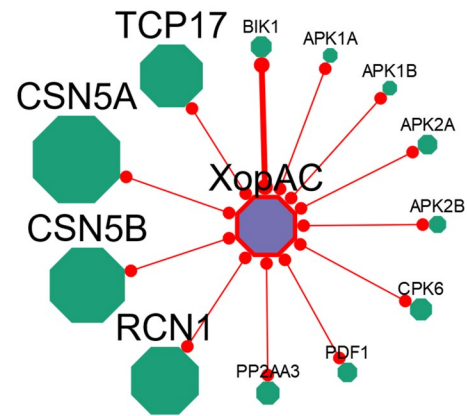


**FIGURE 6** Graphical representation of interactomic data on EffectorK. Graphical representation of interactomic data from Xcc effector XopAC (AvrAC). XopAC, in purple, interacts with 36 Ath proteins, in green (only 12 shown for better visualization). The size of a protein node is proportional to its degree (e.g. CSN5B interacts with 50 proteins, BIK1 with six, and APK1A only with XopAC). The thickness of the connecting edges indicates the level of confidence: narrow edges represent physical interaction detected by only one technique, whereas thick edges indicate that the interaction has been detected by at least two independent techniques (e.g. XopAC interaction with BIK1 has been detected by co-immunoprecipitation and pulldown assays, whereas the interaction with APK1A, only by Y2H)

Additionally, EffectorK also allows users to find the shortest paths between two queried proteins in the network.

In order to update, expand, and further improve EffectorK, we encourage users to submit their own interactomic data by filing in and sending a dedicated template available on the site. These data will be verified by the curator team prior to their incorporation in the database. More information about usage, content, and data submission is accessible online, under the tabs “Help” and “Contribute” of the database web server. Please contact us if you have any question or suggestions by email via [contact@effectork.org](mailto:contact@effectork.org).

## 3 | DISCUSSION

In this study we identified systematically Ath interactors of effectors from the vascular bacterial pathogens Rps and Xcc. We combined this information with other Ath interactors identified in similar experimental setups. Additionally, we conducted an extensive literature review to gather published Ath interactors of effectors from a wide variety of pathogens, including other bacterial species and also oomycete, fungal, and invertebrate pathogens. Studying this combined interactomic dataset allowed us to identify new trends of how effectors interfere with the plant proteome and evaluate whether previously described network principles were still supported on a wider scale. We showed that there are no substantial differences in terms of connectivity among the effectomes of five different pathogen species screened systematically (Figure 1). We have reinforced previously described intra- and interspecific convergence of effector

targeting with effectors from two new species (Mukhtar *et al.*, 2011; Weßling *et al.*, 2014), and showed at the same time that most effector interactors are pathogen specific (Figure 2 and S2). Our analyses also supported the previously described tendency of effectors to interact with plant proteins better connected and central in the network (Li *et al.*, 2017; Ahmed *et al.*, 2018), and showed that this tendency is even stronger among effector hubs, multipathogen interactors, and bacterial core T3E interactors (Table 2 and Figure S5).

### 3.1 | The balance between interactor specificity and convergence

Our data showed that most effector interactors were pathogen-specific (Figure S2) but at the same time effectors converge inter-specifically onto a small subset of Ath proteins (Figure 2B,C). These a priori contradictory observations pose an interesting question: what is the balance between the specificity and convergence of effector interactors? At this point, it is impossible to assert whether this specificity is merely caused by the limited number of pathogens screened at the effectome-scale or if it is a reflection of the different and unique ways that each pathogen has evolved to interfere with the host physiology and immunity. This issue can only be addressed by increasing the number of pathogen effectors screened thoroughly and at a large scale. Comparing large datasets of effector interactors of a wider and more diverse set of pathogens would allow evaluating where the balance is between specificity and convergence: (a) If the interactor specificity decreased, it would mean that the effectomes from the different pathogens tend to interact similarly with the host proteome. This was the case when we compared the percentage of species-specific interactors of effectors from Hpa, Psy, and Gor that passed from being 73.9%, 64.9%, and 46.7% in previous works (Mukhtar *et al.*, 2011; Weßling *et al.*, 2014), to 51.7%, 58.9%, and 35.6%, respectively, in the present study (Figure S2). Nevertheless, a total of five screened species is probably not powerful enough to sustain this claim. (b) If, in contrast, the interactor specificity increased with the number of screened species, it would mean that the different pathogens have evolved unique ways to modulate the interaction with the host. If this were the case, deeper analyses comparing related pathogens (e.g. species with similar lifestyle or from the same kingdom) could allow identifying trait-specific interactors (e.g. effector interactors exclusive among vascular pathogen effectors). In any case, to better understand the similarities and particularities on how effectors modulate host processes, it is essential to increase the number of pathogen species screened for effector interactors at the effectome-scale.

### 3.2 | Large-scale screenings fill the gap in the identification of effector interactors

Including manually curated data from literature has allowed us to broaden significantly the diversity of plant pathogen species compared to similar studies. However, 346 out the 564 described

*Arabidopsis* effector interactors have been identified exclusively through large-scale Y2H screenings against partial libraries of Ath cDNAs. As with any other large-scale screening, the technical limitations together with the incompleteness of the library might have led to an underestimation of the plant-effector interactome of the five screened species (Brückner *et al.*, 2009). The relatively small overlap between the large-scale Y2H screenings and manually curated literature data sets might be a consequence of this limitation (Figure 3). This small overlap illustrates the current knowledge gap in the characterization of the full plant interactome of pathogen effectors. Extensive work will be required to characterize further effector-host protein interactions in other pathosystems. As one of the simplest yet powerful high-throughput techniques for protein-protein interaction detection, our work, like others before, highlights the potential of such large-scale Y2H screenings in the identification of novel effector interactors in an easy, cheap, and systematic manner.

### 3.3 | EffectorK, an entry point to explore and make sense of plant-effector interactomics

To conclude, our work also provides valuable resources for the plant-pathogen interaction community. We described 540 new Ath-Rps and Ath-Xcc effector protein interactions that allowed us to identify 166 new effector interactors (Table S1). We also manually curated several publications to assemble a collection of 287 Ath-effector protein interactions from a wide variety of pathogens (Table S2). All this allowed us to identify 100 novel effector hubs (Table S3). The contribution to plant immunity of these effector hubs has been described for 19 of them, but remains untested for the majority (Table 1). This constitutes a list of promising candidates for further functional characterization. All these data were integrated in EffectorK, a knowledge database where users can have easy access to the Ath-effector protein interactions and explore the resulting interactomic network visually and interactively. While major efforts were made to capture the maximal diversity on the pathogen side, we limited our work to the *Arabidopsis* plant model. Thanks to the built-in homology search tools available, users can also use their own data as query regardless of the species studied. It is therefore feasible to use EffectorK as a starting point to build on and extend to crop plant-effector protein interactomics. In the long term, these data could be exploited to better understand how pathogens interact with these crops with the prospect of selecting breeding candidates for improved tolerance or resistance against pathogens.

## 4 | EXPERIMENTAL PROCEDURES

### 4.1 | Cloning of Rps and Xcc T3E genes

All the cloning of the T3E genes from Rps and Xcc was performed by BP gateway BP or TOPO cloning (Thermo Fisher Scientific,

Waltham, MA, USA) to generate pENTRY plasmids, which were later transferred into the appropriate Y2H plasmids (Mukhtar *et al.*, 2011) using the LR gateway reaction (Thermo Fisher Scientific). Table S5 contains all the PCR primers and final plasmid identities describing the collection of plasmids used in this study. Gene sequence information from Rps strain GMI1000 (GenBank accessions: NC\_003295 and NC\_003296) (Salanoubat *et al.*, 2002) can be obtained from www.ralsto-T3E.org (Sabbagh *et al.*, 2019) and from the published genome of Xcc strain 8,004 (NC\_007086) (Qian, 2005).

## 4.2 | Y2H screenings

The Y2H screening was performed in semi-liquid ("8K space" screening) and liquid ("12K space" screening) media as recently reported (Monachello *et al.*, 2019), which is an adaptation of a previously developed Y2H-solid pipeline (Dreze *et al.*, 2010). In both protocols the same low copy number yeast expression vectors and the two yeast strains, *Saccharomyces cerevisiae* Y8930 and Y8800, were used. The expression of the *GAL1-HIS3* reporter gene was tested with 1 mM 3AT (3-amino-1,2,4-triazole, a competitive inhibitor of the *HIS3* gene product) unless described otherwise. Prior to Y2H screening, DB-X strains were tested for auto-activation of the *GAL1-HIS3* reporter gene in the absence of AD-Y plasmid. In case of auto-activation, DB-X were physically removed from the collection of baits and screened against the (DB)-Ath-cDNA collections using their AD-X constructs. Briefly, DB-X baits expressing yeasts were individually grown (30 °C for 72 hr) in 50-ml polypropylene conical tubes containing 5 ml of fresh selective media (Sc-leucine, Sc-Leu). Pools were created by mixing a maximum of 72 and 50 individual bait yeast strains for the "8K space" and "12K space", respectively. Subsequently, 120 and 50 µl of these individual pools were plated into 96-well and 384-well low-profile microplates for Ath-cDNA "8K space" and "12K space" collections, respectively. Glycerol stocks of the (AD)-Ath-cDNA "8K space" and "12K space" collections were thawed, replicated by hand-picking or using a colony picker Qpix2 XT into 96-well and 384-well plates filled with 120 and 50 µl of fresh selective media (Sc-tryptophan, Sc-Trp), respectively, and incubated at 30 °C for 72 hr. Culture plates corresponding to the DB-baits pools and AD-collection were replicated into mating plates filled with YEPD media and incubated at 30 °C for 24 hr. In liquid Y2H case ("12K space" screening), mating plates were then replicated into screening plates filled with 50 µl of fresh Sc-Leu-Trp-histidine + 1 mM 3AT media and incubated at 30 °C for 5 days. In order to identify primary positives, the OD<sub>600</sub> of the 384-well screening plates was measured using a microplate reader Tecan Infinite M200 PRO (Tecan, Männedorf, Switzerland). In semi-liquid Y2H case ("8K space" screening), mated yeast were spotted onto Sc-Leu-Trp-histidine + 1 mM 3AT media agar plates, and incubated at 30 °C for 3 days. Protein pairs were identified by de-pooling of DB-baits in a similar targeted matricial liquid or semi-liquid assays in which all the DB-baits were individually tested against all the previously identified AD-proteins. Identified pairs were picked and checked by PCR and DNA sequencing.

## 4.3 | Database content and manual curation

Binary interactions between Ath proteins with each other and with pathogen effector proteins were compiled on tabular form keeping track of the protein names and accessions, species and ecotypes/strains of origin, techniques used to detect the interactions and the reference. Ath-Ath protein interactions were compiled from the Arabidopsis Interactome (Dreze *et al.*, 2011; Smakowska-Luzan *et al.*, 2018) and the public databases BioGrid (www.thebiogrid.org [Stark *et al.*, 2006], downloaded in September 2019) and IntAct (www.ebi.ac.uk/intact [Orchard *et al.*, 2014], downloaded in September 2019). We only kept the direct interactions with the evidence codes "co-crystal structure," "FRET" (fluorescence resonance energy transfer), "PCA" (protein-fragment complementation assay), "reconstituted complex" or "two-hybrid" on BioGrid and "physical association" on IntAct. Ath-effector protein interactions were gathered from our experimental Y2H data together with the similarly produced data on Hpa, Psy, and Gor effectors (Mukhtar *et al.*, 2011; Weßling *et al.*, 2014). In addition, an extensive keyword search on effector-*Arabidopsis* literature was done to retrieve interactions from 80 published articles. A confidence level was assigned to each interaction depending on the number of independent techniques used in a publication for validation: "1" if the interaction was detected by only one technique and "2" if the interaction was validated by at least a second technique. Some interactions lacked important information but, in order to maximize the extent of our network, several assumptions were taken instead of discarding useful data. First, gene models for Ath proteins were rarely mentioned on publications so we assumed the first gene model available on the latest version of the *Arabidopsis* genome (Araport11 (Cheng *et al.*, 2017)). Second, when the ecotype/strain of the organism was not explicitly stated, a generic "NA" (not available) was assigned.

## 4.4 | In silico analysis

### 4.4.1 | Computational simulations of random targeting of Ath proteins by single pathogen effectors (intraspecific convergence)

Significance of the intraspecific convergence was tested, comparing our experimental data with random simulations as previously published (Weßling *et al.*, 2014). Briefly, for each effector of Xcc and Rps we assigned randomly the same number of Ath interactors as experimentally observed from the degree-preserved list of 8K proteins. The distribution obtained from 10,000 simulations was plotted and compared to the experimentally obtained data. The *p* value of the experimental data were calculated as follows: number of simulations where the number of interactors is lower than or equal to experimentally observed is divided by the number of simulations. When the number of simulations with fewer interactors than observed was zero, the *p* value was set to <.0001.



$$p \text{ value} = \frac{\text{number of simulations where the number of interactors} \leq \text{experimentally observed number of interactors}}{\text{number of simulations}} \quad (1)$$

#### 4.4.2 | Computational simulations of random targeting of Ath proteins by several pathogen effectors (interspecific convergence)

The significance of the interspecific convergence was tested by comparing our experimental data and previously published data with random simulations as published (Mukhtar *et al.*, 2011; Weßling *et al.*, 2014). Briefly, for each effector of all compared pathogens we assigned the same number of Ath interactors as experimentally observed/published from the list of 8K proteins. The distribution obtained from 10,000 simulations was plotted and compared to experimentally and published data. The *p* values of the experimental data were calculated as follows: number of simulations where the number of common interactors between species was higher or equal than the experimentally observed is divided by the number of simulations. When the number of simulations with more common interactors than observed was zero, the *p* value was set to <.0001.

$$p \text{ value} = \frac{\text{number of simulations where the number of common interactors} \geq \text{experimentally observed number of common interactors}}{\text{number of simulations}} \quad (2)$$

#### 4.4.3 | Overlap of effector interactors

The overlap of effector interactors from the different datasets was calculated without limiting the screening space. For representation of the data, Venn diagrams were generated using the Venn Diagrams tool from VIB-UGent Center for Plant Systems Biology ([www.bioinformatics.psb.ugent.be/webtools/Venn/](http://www.bioinformatics.psb.ugent.be/webtools/Venn/)). The overlap of effector interactors from the different datasets were calculated not limiting to any limited space. For an area-proportional representation of the data, a Venn diagram was generated using BioVenn (Hulsen *et al.*, 2008).

#### 4.4.4 | Network topology analyses

The topology parameters of the Ath-effector interactomic network were calculated on Cytoscape 3.7.2 (Shannon, 2003). Our analyses focused on two key node parameters: degree and betweenness centrality. The degree of a protein is a measure of its connectivity and denotes the number of proteins interacting with it. Throughout this work, we have differentiated two kinds of degrees: (a) effector degree (i.e. number of interacting effector proteins) and (b) Ath degree (i.e. number of interacting Ath proteins). The betweenness centrality measures the proportion of shortest pathways between two proteins that passes through a given node. These parameters were compared against different subsets of data and statistical tests were performed in R language (R Core Team, 2019). The cumulative distributions of these parameters among different subset of data were plotted and the area under

the curve was estimated using Simpson's rule with the "Bolstad2" package (Bolstad, 2009).

#### 4.5 | Database construction

The databases were built using the software architecture recently described (Carrère *et al.*, 2019). The files submitted by the curator team were automatically checked for typographic mistakes using ad hoc Perl scripts and loaded into a Neo4J database and indexed in an ElasticSearch search engine. Each release was rebuilt from scratch. Data were made accessible through a web interface (see Results and Discussion) built on Cytoscape.js library (Franz *et al.*, 2016). The raw data used for the database setup are available in the "Data" section of [www.effectork.org](http://www.effectork.org) and the source code is available at <https://framagit.org/LIPM-BIOINFO/KGBB>.

#### ACKNOWLEDGMENTS

We wish to thank Alberto Macho and Laurent Deslandes for the contribution of RipS3, RipP1, and RipP2 containing plasmids. M.G.F. was supported by a PhD fellowship from the French Laboratory of Excellence project "TULIP" (ANR-10-LABX-41; ANR-11-IDEX-0002-02). This work was supported by the National Science Foundation (IOS-1557796) to M.S.M. The L.I.P.M. is supported by the French Laboratory of Excellence project "TULIP" (ANR-10-LABX-41; ANR-11-IDEX-0002-02). The IPS2 is supported by the French Laboratory of Excellence project "SPS" (ANR-10-LABX-0040-SPS).


#### CONFLICT OF INTEREST

None of the authors has a conflict of interest to declare.

#### DATA AVAILABILITY STATEMENT

The data that support the findings of this study are openly available in EffectorK at [www.effectork.org](http://www.effectork.org).

#### ORCID

Manuel González-Fuente  <https://orcid.org/0000-0003-2960-2657>  
 Sébastien Carrère  <https://orcid.org/0000-0002-2348-0778>  
 Dario Monachello  <https://orcid.org/0000-0001-7551-0214>  
 Anne-Claire Cazalé  <https://orcid.org/0000-0002-6822-7186>  
 Raka M. Mitra  <https://orcid.org/0000-0002-2798-2038>  
 Ludovic Cottret  <https://orcid.org/0000-0001-7418-7750>  
 M. Shahid Mukhtar  <https://orcid.org/0000-0002-1104-6931>  
 Claire Lurin  <https://orcid.org/0000-0003-3516-4438>  
 Laurent D. Noël  <https://orcid.org/0000-0002-0110-1423>  
 Nemo Peeters  <https://orcid.org/0000-0002-1802-0769>

## REFERENCES

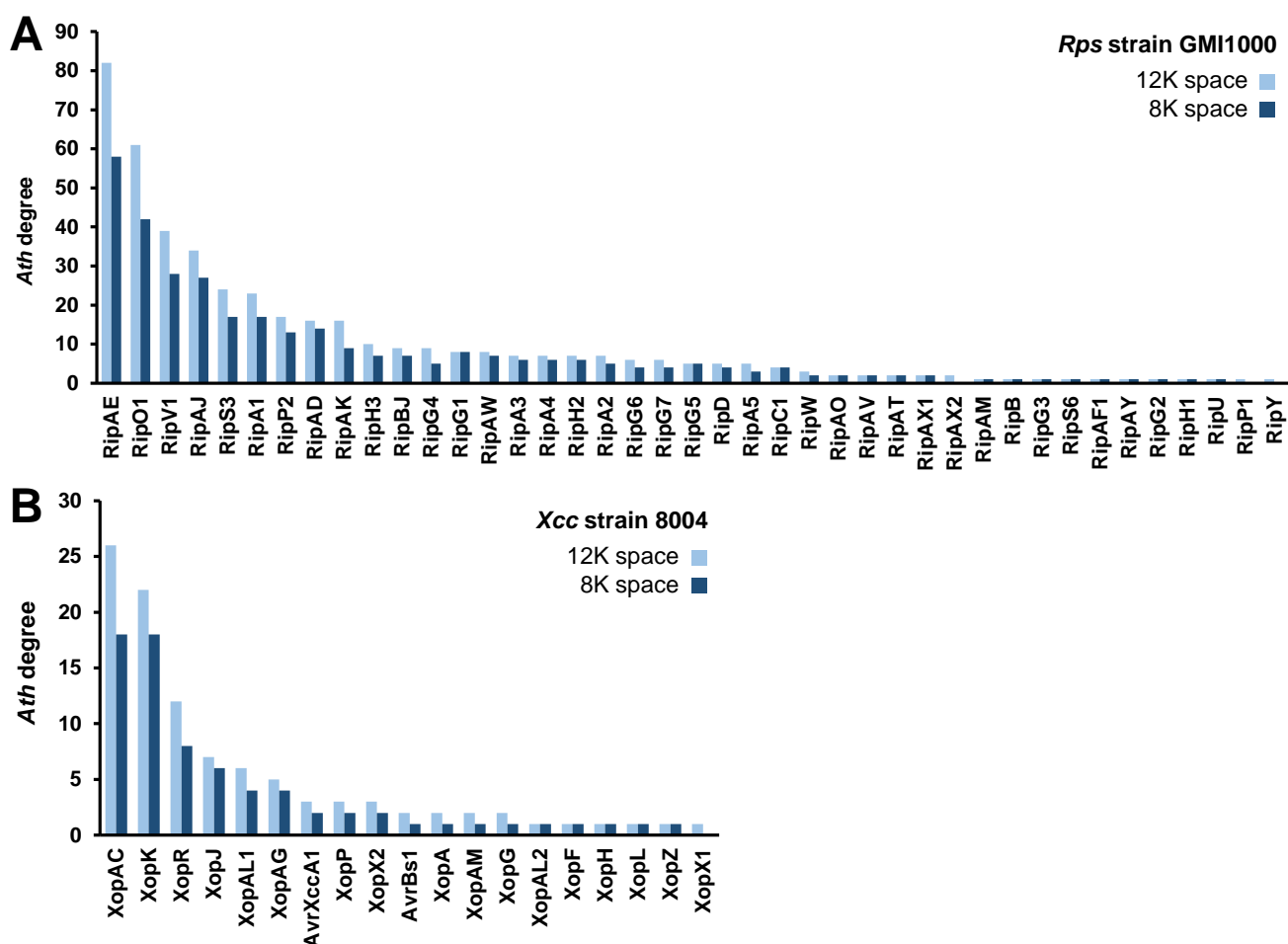
- Ahmed, H., Howton, T.C., Sun, Y., Weinberger, N., Belkhadir, Y. and Mukhtar, M.S. (2018) Network biology discovers pathogen contact points in host protein–protein interactomes. *Nature Communications*, 9, 2312.
- Anstead, J.A., Froelich, D.R., Knoblauch, M. and Thompson, G.A. (2012) Arabidopsis P-protein filament formation requires both AtSEOR1 and AtSEOR2. *Plant & Cell Physiology*, 53(6), 1033–1042. <https://doi.org/10.1093/pcp/pcs046>.
- Arlat, M., Gough, C.L., Barber, C.E., Boucher, C. and Daniels, M.J. (1991) *Xanthomonas campestris* contains a cluster of *hrp* genes related to the larger *hrp* cluster of *Pseudomonas solanacearum*. *Molecular Plant-Microbe Interactions*, 4(6), 593–601. <https://doi.org/10.1094/mpmi-4-593>
- Arlat, M., Gough, C.L., Zischek, C., Barberis, P.A., Trigalet, A. and Boucher, C.A. (1992) Transcriptional organization and expression of the large *hrp* gene cluster of *Pseudomonas solanacearum*. *Molecular Plant-Microbe Interactions*, 5(2), 187. <https://doi.org/10.1094/MPMI-5-187>
- Bolstad, W.M. (2009) *Understanding Computational Bayesian Statistics*. Hoboken, NJ, USA: John Wiley & Sons, Inc. <https://doi.org/10.1002/9780470567371>
- Boudsocq, M., Willmann, M.R., McCormack, M., Lee, H., Shan, L., He, P. et al. (2010) Differential innate immune signalling via Ca(2+) sensor protein kinases. *Nature*, 464(7287), 418–422. <https://doi.org/10.1038/nature08794>.
- Brückner, A., Polge, C., Lentze, N., Auerbach, D. and Schlattner, U. (2009) Yeast two-hybrid, a powerful tool for systems biology. *International Journal of Molecular Sciences*, 10(6), 2763–2788. <https://doi.org/10.3390/ijms10062763>
- Buell, C.R. (2002) Interactions between *Xanthomonas* species and *Arabidopsis thaliana*. *The Arabidopsis Book*, 1, e0031. <https://doi.org/10.1199/tab.0031>
- Büttner, D. (2016) Behind the lines-actions of bacterial type III effector proteins in plant cells. *FEMS Microbiology Reviews*, 40(6), 894–937. <https://doi.org/10.1093/femsre/fuw026>
- Carrère, S., Verdenaud, M., Gough, C., Gouzy, J. and Gamas, P. (2019) LeGOO: an expertized knowledge database for the model legume *Medicago truncatula*. *Plant and Cell Physiology*, <https://doi.org/10.1093/pcp/pcz177>
- Cheng, C.Y., Krishnakumar, V., Chan, A.P., Thibaud-Nissen, F., Schobel, S. and Town, C.D. (2017) Araport11: a complete reannotation of the *Arabidopsis thaliana* reference genome. *The Plant Journal*, 89(4), 789–804. <https://doi.org/10.1111/tpj.13415>
- Coll, N.S. and Valls, M. (2013) Current knowledge on the *Ralstonia solanacearum* type III secretion system. *Microbial biotechnology*, 6(6), 614–620. <https://doi.org/10.1111/1751-7915.12056>
- Cui, H., Tsuda, K. and Parker, J.E. (2015) Effector-triggered immunity: from pathogen perception to robust defense. *Annual Review of Plant Biology*, 66(1), 487–511. <https://doi.org/10.1146/annurev-arplant-050213-040012>
- Dagdas, Y.F., Belhaj, K., Maqbool, A., Chaparro-Garcia, A., Pandey, P., Petre, B. et al. (2016) An effector of the Irish potato famine pathogen antagonizes a host autophagy cargo receptor. *eLife*, 5, e10856. <https://doi.org/10.7554/eLife.10856>.
- Deslandes, L., Pileur, F., Liaubet, L., Camut, S., Can, C., Williams, K. et al. (1998) Genetic characterization of RRS1, a recessive locus in *Arabidopsis thaliana* that confers resistance to the bacterial soilborne pathogen *Ralstonia solanacearum*. *Molecular Plant-Microbe Interactions* MPMI, 11(7), 659–667. <https://doi.org/10.1094/MPMI.1998.11.7.659>
- Dillon, M.M., Almeida, R.N.D., Laflamme, B., Martel, A., Weir, B.S., Desveaux, D. et al. (2019) Molecular evolution of *Pseudomonas syringae* type III secreted effector proteins. *Frontiers in Plant Science*, 10, <https://doi.org/10.3389/fpls.2019.00418>
- Dreze, M., Monachello, D., Lurin, C., Cusick, M.E., Hill, D.E., Vidal, M. et al. (2010) High-quality binary interactome mapping. In Guthrie, C., Fink, G. and Weissman, J. (Eds.) *Methods in Enzymology* (Vol. 470, pp. 281–315). San Diego, CA: Academic Press. [https://doi.org/10.1016/S0076-6879\(10\)70012-4](https://doi.org/10.1016/S0076-6879(10)70012-4)
- Dreze, M., Carvunis, A.-R., Charlotiaux, B., Galli, M., Pevzner, S.J., Tasan, M. et al. (2011) Evidence for network evolution in an Arabidopsis interactome map. *Science*, 333(6042), pp. 601–607. <https://doi.org/10.1126/science.1203877>
- Franz, M., Lopes, C.T., Huck, G., Dong, Y., Sumer, O. and Bader, G.D. (2016) Cytoscape.js: a graph theory library for visualisation and analysis. *Bioinformatics*, 32(2), 309–311. <https://doi.org/10.1093/bioinformatics/btv557>
- Giron, D., Huguet, E., Stone, G.N. and Body, M. (2016) Insect-induced effects on plants and possible effectors used by galling and leaf-mining insects to manipulate their host-plant. *Journal of Insect Physiology*, 84, 70–89. <https://doi.org/10.1016/j.jinsphys.2015.12.009>
- Guy, E., Genissel, A., Hajri, A., Chabannes, M., David, P., Carrere, S. et al. (2013) Natural genetic variation of *Xanthomonas campestris* pv. *campestris* pathogenicity on Arabidopsis revealed by association and reverse genetics. *mBio*, 4(3). <https://doi.org/10.1128/mBio.00538-12>
- Hulsen, T., de Vlieg, J. and Alkema, W. (2008) BioVenn—a web application for the comparison and visualization of biological lists using area-proportional Venn diagrams. *BMC genomics*, 9, 488. <https://doi.org/10.1186/1471-2164-9-488>
- Jones, J.D.G. and Dangl, J.L. (2006) The plant immune system. *Nature*, 444(7117), 323–329. <https://doi.org/10.1038/nature05286>
- Kersey, P.J., Allen, J.E., Allot, A., Barba, M., Boddu, S., Bolt, B.J. et al. (2018) Ensembl genomes 2018: an integrated omics infrastructure for non-vertebrate species. *Nucleic Acids Research*, 46, D802–D808. <https://doi.org/10.1093/nar/gkx1011>.
- Kim, S. H., Son, G. H., Bhattacharjee, S., Kim, H. J., Nam, J. C., Nguyen, P. D. T., et al. (2014). The Arabidopsis immune adaptor SRFR1 interacts with TCP transcription factors that redundantly contribute to effector-triggered immunity. *The Plant Journal*, 78, 978–989. <https://doi.org/10.1111/tpj.12527>
- Li, Y., Yuhua, Y., Yilong, H., Hailun, L., Ming, H., Ziyin, Y. et al. (2019) DELLA and EDS1 form a feedback regulatory module to fine-tune plant growth-defense tradeoff in Arabidopsis. *Molecular Plant*, 12(11), 1485–1498. <https://doi.org/10.1016/j.molp.2019.07.006>.
- Li, H., Zhou, Y. and Zhang, Z. (2017) Network analysis reveals a common host-pathogen interaction pattern in Arabidopsis immune responses. *Frontiers in Plant Science*, 8, 893. <https://doi.org/10.3389/fpls.2017.00893>
- Lim, C.W., Luan, S. and Lee, S.C. (2014) A prominent role for RCAR3-mediated ABA signaling in response to *Pseudomonas syringae* pv. tomato DC3000 infection in Arabidopsis. *Plant & Cell Physiology*, 55(10), 1691–1703. <https://doi.org/10.1093/pcp/pcu100>.
- Liu, H., Dong, S., Gu, F., Liu, W., Yang, G., Huang, M. et al. (2017) NBS-LRR protein Pik-H4 interacts with OsBIHD1 to balance rice blast resistance and growth by coordinating ethylene-brassinosteroid pathway. *Frontiers in Plant Science*, 8, 127. <https://doi.org/10.3389/fpls.2017.00127>.
- Lindeberg, M., Cunnac, S. and Collmer, A. (2012) *Pseudomonas syringae* type III effector repertoires: last words in endless arguments. *Trends in Microbiology*, 20(4), 199–208. <https://doi.org/10.1016/j.tim.2012.01.003>
- Luo, H., Laluk, K., Lai, Z., Veronese, P., Song, F. and Mengiste, T. (2010) The Arabidopsis botrytis susceptible1 interactor defines a subclass of RING E3 ligases that regulate pathogen and stress responses. *Plant Physiology*, 154(4), 1766–1782. <https://doi.org/10.1104/pp.110.163915>.
- Ma, W., Wang, Y. and McDowell, J. (2018) Focus on effector-triggered susceptibility. *Molecular Plant-Microbe Interactions*, 31(1), 5–5. <https://doi.org/10.1094/MPMI-11-17-0275-LE>

- Mansfield, J., Genin, S., Magori, S., Citovsky, V., Sriariyanum, M., Ronald, P. et al. (2012) Top 10 plant pathogenic bacteria in molecular plant pathology. *Molecular Plant Pathology*, 13(6), 614–629. <https://doi.org/10.1111/j.1364-3703.2012.00804.x>
- MacLean, A.M., Orlovskis, Z., Kowitwanich, K., Zdziarska, A.M., Angenent, G.C., Immink, R.G. et al. (2014) Phytoplasma effector SAP54 hijacks plant reproduction by degrading MADS-box proteins and promotes insect colonization in a RAD23-dependent manner. *PLoS Biology*, 12(4), e1001835. <https://doi.org/10.1371/journal.pbio.1001835>
- Memišević, V., Zavaljevski, N., Rajagopala, S.V., Kwon, K., Pieper, R., DeShazer, D. et al. (2015) Mining host-pathogen protein interactions to characterize *Burkholderia mallei* infectivity mechanisms. *PLoS Computational Biology*, 11(3), e1004088. <https://doi.org/10.1371/journal.pcbi.1004088>
- Monachello, D., Guillaumot, D. and Lurin, C. (2019) A pipeline for systematic yeast 2-hybrid matricial screening in liquid culture. <https://doi.org/10.21203/rs.2.9948/v1>
- Mukherjee, M., Larrimore, K.E., Ahmed, N.J., Bedick, T.S., Barghouthi, N.T., Traw, M.B. et al. (2010) Ascorbic acid deficiency in arabidopsis induces constitutive priming that is dependent on hydrogen peroxide, salicylic acid, and the NPR1 gene. *Molecular Plant-Microbe Interactions: MPMI*, 23(3), 340–351. <https://doi.org/10.1094/MPMI-23-3-0340>
- Mukhtar, M.S., Carvunis, A.-R., Dreze, M., Eppe, P., Steinbrenner, J., Moore, J. et al. (2011) Independently evolved virulence effectors converge onto hubs in a plant immune system network. *Science*, 333(6042), pp. 596–601. <https://doi.org/10.1126/science.1203659>
- Nietzsche, M., Guerra, T., Alseekh, S., Wiermer, M., Sonnewald, S., Fernie, A.R. et al. (2018) STOREKEEPER RELATED1/G-element binding protein (STKR1) interacts with protein kinase SnRK1. *Plant Physiology*, 176(2), 1773–1792. <https://doi.org/10.1104/pp.17.01461>
- Nurmeberg, P.L., Knox, K.A., Yun, B.-W., Morris, P.C., Shafiei, R., Hudson, A. et al. (2007) The developmental selector AS1 is an evolutionarily conserved regulator of the plant immune response. *Proceedings of the National Academy of Sciences of the United States of America*, 104, 18795–18800. <https://doi.org/10.1073/pnas.0705586104>
- Orchard, S., Ammari, M., Aranda, B., Breuza, L., Briganti, L., Broackes-Carter, F. et al. (2014) The MIntAct project-IntAct as a common curation platform for 11 molecular interaction databases. *Nucleic Acids Research*, 42(Database issue), pp. D358–D363. <https://doi.org/10.1093/nar/gkt1115>
- Peeters, N., Carrère, S., Anisimova, M., Plener, L., Cazalé, A.-C. and Genin, S. (2013) Repertoire, unified nomenclature and evolution of the Type III effector gene set in the *Ralstonia solanacearum* species complex. *BMC Genomics*, 14, 859. <https://doi.org/10.1186/1471-2164-14-859>
- Qian, W. (2005) Comparative and functional genomic analyses of the pathogenicity of phytopathogen *Xanthomonas campestris* pv. *campestris*. *Genome Research*, 15(6), 757–767. <https://doi.org/10.1101/gr.3378705>
- R Core Team (2019) *R: A Language and Environment for Statistical Computing*. Authors R Core Team. Vienna, Austria. Available at <https://www.r-project.org/>
- Redditt, T.J., Chung, E.H., Zand Karimi, H., Rodibaugh, N., Zhang, Y., Trinidad, J.C. et al. (2019) AvrRpm1 functions as an ADP-ribosyl transferase to modify NOI-domain containing proteins, including Arabidopsis and soybean RPM1-interacting protein 4. *The Plant cell*, tpc.00020.2019. Advance online publication. <https://doi.org/10.1105/tpc.19.00020>
- Roux, B., Bolot, S., Guy, E., Denancé, N., Lautier, M., Jardinaud, M.-F. et al. (2015) Genomics and transcriptomics of *Xanthomonas campestris* species challenge the concept of core type III effectome. *BMC Genomics*, 16(1), 975. <https://doi.org/10.1186/s12864-015-2190-0>
- Sabbagh, C.R.R., Carrere, S., Lonjon, F., Vaillau, F., Macho, A.P., Genin, S. et al. (2019) Pangenomic type III effector database of the plant pathogenic *Ralstonia* spp. *PeerJ*, 7, e7346. <https://doi.org/10.7717/peerj.7346>
- Salanoubat, M., Genin, S., Artiguenave, F., Gouzy, J., Mangenot, S., Arlat, M. et al. (2002) Genome sequence of the plant pathogen *Ralstonia solanacearum*. *Nature*, 415(6871), 497–502. <https://doi.org/10.1038/415497a>
- Shannon, P., Markiel, A., Ozier, O., Baliga, N.S., Wang, J.T., Ramage, D., et al. (2003) Cytoscape: a software environment for integrated models of biomolecular interaction networks. *Genome Research*, 13(11), 2498–2504. <https://doi.org/10.1101/gr.1239303>
- Sharpee, W.C. and Dean, R.A. (2016) Form and function of fungal and oomycete effectors. *Fungal Biology Reviews*, 30(2), 62–73. <https://doi.org/10.1016/j.fbr.2016.04.001>
- Simon, C., Langlois-Meurinne, M., Bellvert, F., Garmier, M., Didierlaurent, L., Massoud, K. et al. (2010) The differential spatial distribution of secondary metabolites in Arabidopsis leaves reacting hypersensitively to *Pseudomonas syringae* pv. tomato is dependent on the oxidative burst. *Journal of Experimental Botany*, 61(12), 3355–3370. <https://doi.org/10.1093/jxb/erq157>
- Smakowska-Luzan, E., Mott, G.A., Parys, K., Stegmann, M., Howton, T.C., Layeghifard, M. et al. (2018) An extracellular network of Arabidopsis leucine-rich repeat receptor kinases. *Nature*, 553(7688), 342–346. <https://doi.org/10.1038/nature25184>
- Stark, C. (2006) BioGRID: a general repository for interaction datasets. *Nucleic Acids Research*, 34(Database issue), pp. D535–D539. <https://doi.org/10.1093/nar/gkj109>
- Vandereyken, K., Van Leene, J., De Coninck, B. and Cammue, B.P.A. (2018) Hub protein controversy: taking a closer look at plant stress response hubs. *Frontiers in Plant Science*, 9, 694. <https://doi.org/10.3389/fpls.2018.00694>
- Vieira, P. and Gleason, C. (2019) Plant-parasitic nematode effectors—Insights into their diversity and new tools for their identification. *Current Opinion in Plant Biology*, 50, 37–43. <https://doi.org/10.1016/j.pbi.2019.02.007>
- Wang, F., Shang, Y., Fan, B., Yu, J.Q. and Chen, Z. (2014) Arabidopsis LIP5, a positive regulator of multivesicular body biogenesis, is a critical target of pathogen-responsive MAPK cascade in plant basal defense. *PLoS Pathogens*, 10(7), e1004243. <https://doi.org/10.1371/journal.ppat.1004243>
- Weßling, R., Eppe, P., Altmann, S., He, Y., Yang, L., Henz, S.R. et al. (2014) Convergent targeting of a common host protein-network by pathogen effectors from three kingdoms of life. *Cell Host & Microbe*, 16(3), 364–375. <https://doi.org/10.1016/j.chom.2014.08.004>
- White, F.F., Potnis, N., Jones, J.B. and Koebnik, R. (2009) The type III effectors of *Xanthomonas*. *Molecular Plant Pathology*, 10(6), 749–766. <https://doi.org/10.1111/j.1364-3703.2009.00590.x>
- Zhang, C., Ding, Z., Wu, K., Yang, L., Li, Y., Yang, Z. et al. (2016) Suppression of jasmonic acid-mediated defense by viral-inducible MicroRNA319 facilitates virus infection in rice. *Molecular plant*, 9(9), 1302–1314. <https://doi.org/10.1016/j.molp.2016.06.014>
- Zhang, Z., Liu, Y., Ding, P., Li, Y., Kong, Q. and Zhang, Y. (2014) Splicing of receptor-like kinase-encoding SNC4 and CERK1 is regulated by two conserved splicing factors that are required for plant immunity. *Molecular Plant*, 7(12), 1766–1775. <https://doi.org/10.1093/mp/ssu103>
- Zhang, H., Wang, X., Giroux, M. J. and Huang, L. (2017) A wheatCOP9 subunit 5-like gene is negatively involved in host response to leaf rust. *Molecular Plant Pathology*, 18, 125–133. <https://doi.org/10.1111/mpp.12467>
- Zipfel, C. (2014) Plant pattern-recognition receptors. *Trends in Immunology*, 35(7), 345–351. <https://doi.org/10.1016/j.it.2014.05.004>

## SUPPORTING INFORMATION

Additional Supporting Information may be found online in the Supporting Information section.

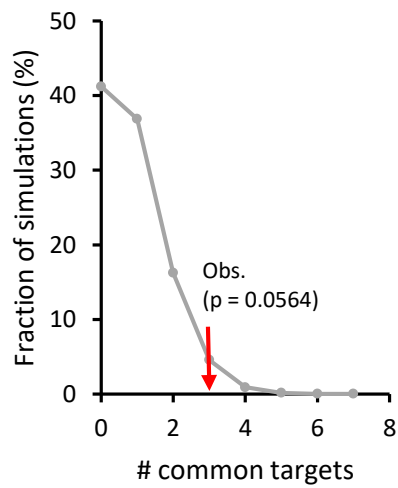
**How to cite this article:** González-Fuente M, Carrère S, Monachello D, et al. EffectorK, a comprehensive resource to mine for *Ralstonia*, *Xanthomonas*, and other published effector interactors in the *Arabidopsis* proteome. *Molecular Plant Pathology*. 2020;00:1–14. <https://doi.org/10.1111/mpp.12965>



**S1 Fig. *Ath* degree of T3E proteins from *Rps* strain GMI1000 and *Xcc* strain 8004.**

*Ath* degree (i.e., number of *Ath* targets per effector) in the in the 12,000 (12K space, light blue) and 8,000 *Ath* cDNA collections (8K space, dark blue) of T3E proteins from *Rps* strain GMI1000 (A) and *Xcc* strain 8004 (B). For *Rps* strain GMI1000: in the first screening RipA3, RipAA, RipAB, RipAC, RipAG, RipAL, RipAM, RipAN, RipAO, RipAP, RipAQ, RipAR, RipAZ1, RipB, RipBA, RipG3, RipG4, RipG6, RipG7, RipH2, RipH3, RipI, RipK, RipM, RipN, RipO1, RipP1, RipQ, RipR, RipS2, RipS6, RipT, RipTPS, RipX and RipZ were screened but no targets were found. In the second screening RipAB, RipAC, RipAI, RipAX1, RipAY, RipBM, RipC1, RipE1, RipH1, RipN, RipR, RipS4, RipU, RipX and RipZ were screened but no targets were found, and RipAN and RipM could not be screened because of recalcitrant problems with yeast transformation. For *Xcc* strain 8004: AvrXccA2, HpaA, HrpW, XopAN, XopN and XopQ were screened but no targets were found, and AvrBs2, XopAH, XopAL2, XopD and XopE2 could not be screened because they showed autoactivation in yeast.

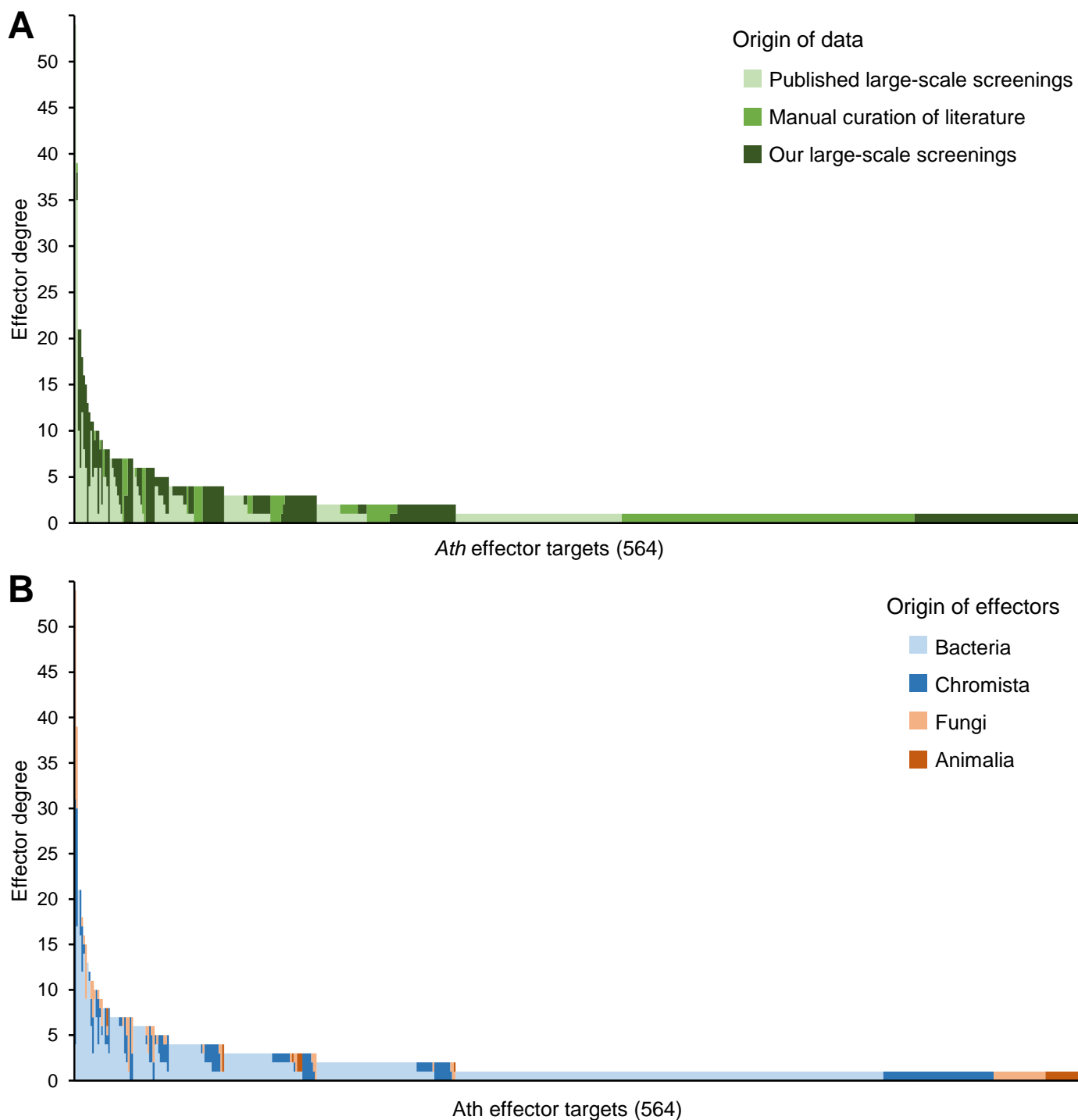




**S3 Fig. Interspecific convergence of *Psy* and *Xcc* effector proteins.**

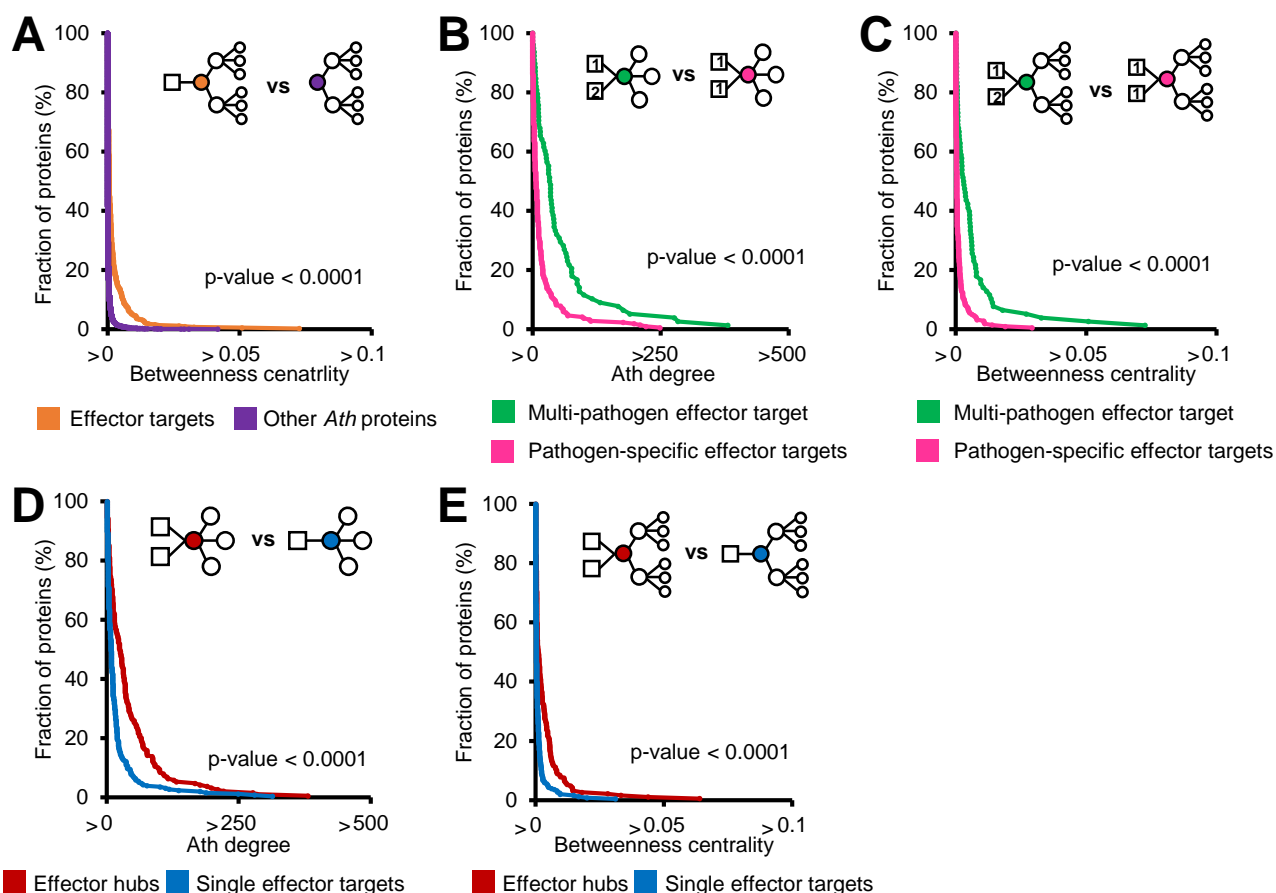
Number of *Ath* targets in the 8K space of effectors from *Psy* and *Xcc* and *Rps* strain found in 10,000 degree-preserving simulations (grey) versus the observed number (red arrow).





**S4 Fig. Effector degree distribution for *Ath* effector targets.**

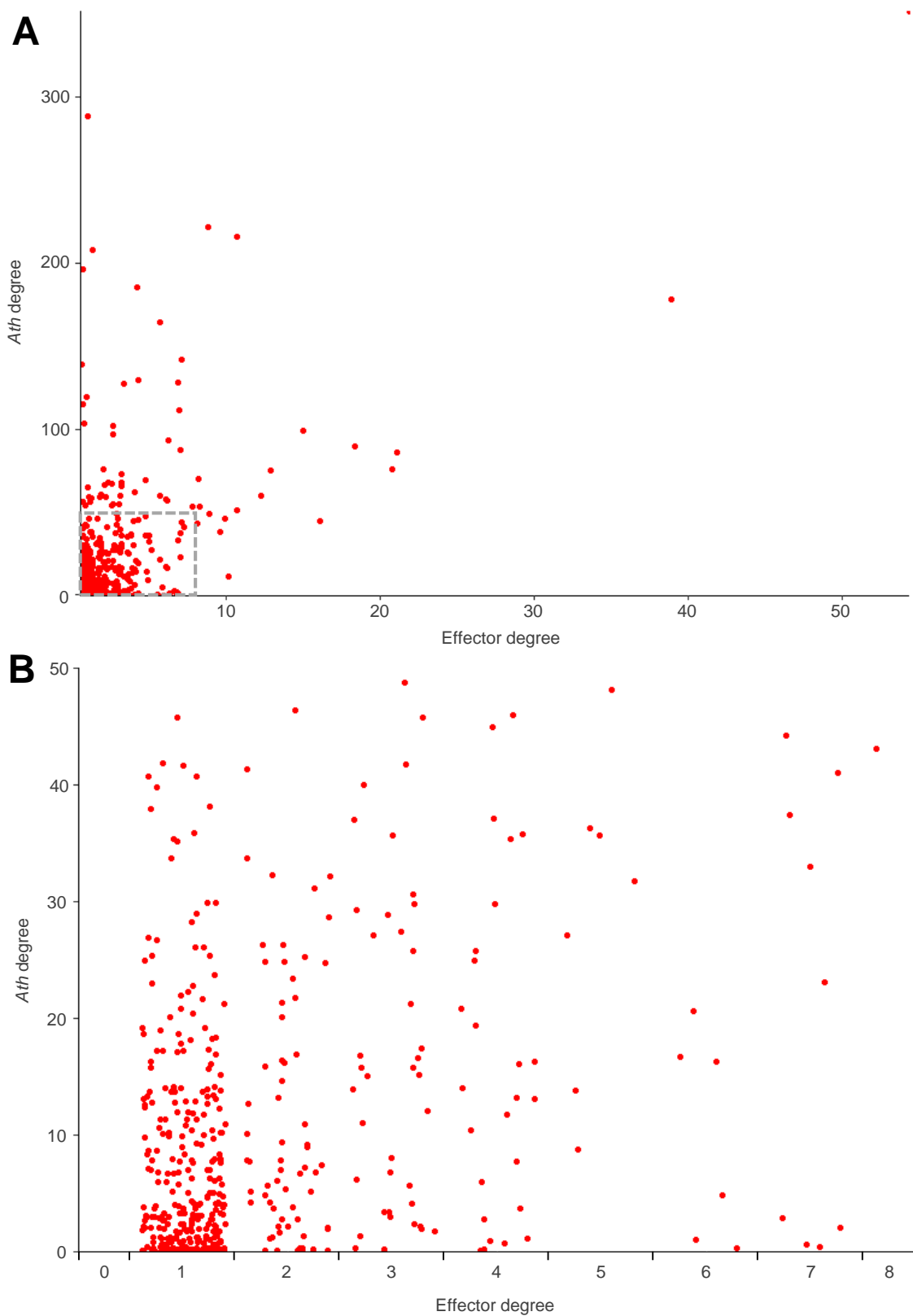
Effector degree (i.e., number of effectors that interact with an *Ath* protein) distribution among the 564 identified *Ath* effector targets (A), according to the origin the data: published large-scale screenings in light green, manual curation of literature in mid-green and this study in dark grey or (B), according to the kingdom of the corresponding effector pathogen: Bacteria in light blue, Chromista in dark blue, Fungi in light orange and Animalia in dark orange.



**S5 Fig. *Ath* degree and betweenness centrality of different groups of *Ath* effector targets.**

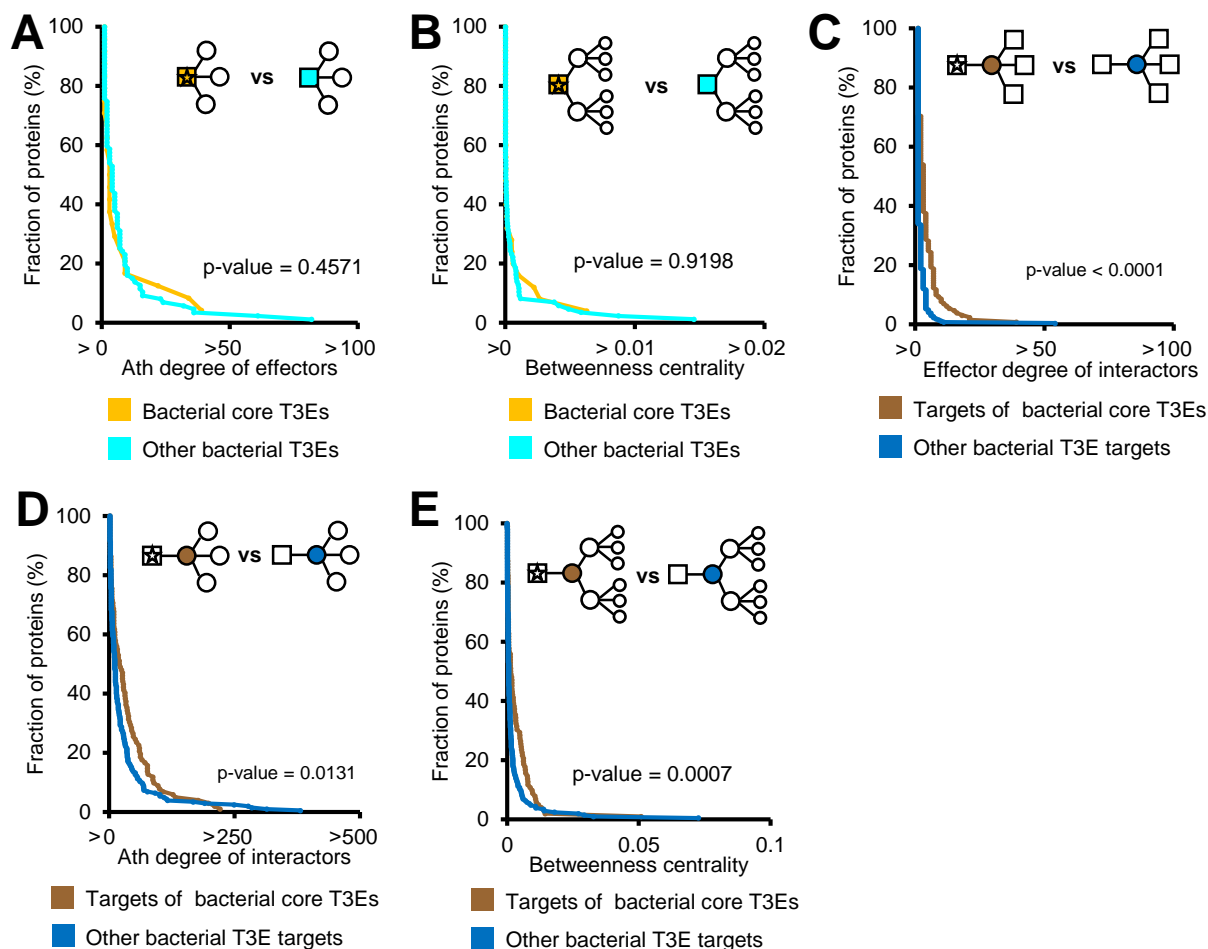
Cumulative distribution of *Ath* degree (B and D) and betweenness centrality (A, C and E) for *Ath* proteins targeted (orange) or not (purple) by effectors (B), multi-pathogen (green) and pathogen-specific (pink) effector targets (B and C) and effector hubs (red) and single effector targets (blue) (D and E). The significance of the differences were evaluated by one-tailed Wilcoxon signed-rank test. The illustration in the upper right corner of each graph represents each compared group: effectors are represented by squares, *Ath* proteins by circles, numbers represent different pathogens species and the color code matches the respective cumulative distribution graph. The estimation of the area under the curve of each distribution is compiled in Table 2.





**S6 Fig. *Ath* and effector degree of effector targets.**

(A) Scatterplot of *Ath* degree versus effector degree of all *Ath* effector targets. Squared in a grey dashed line is the close-up area represented in (B).



**S7 Fig. Degrees and betweenness centrality of bacterial core and non-core T3Es and their targets.**

Cumulative distribution of *Ath* degree (A and D), effector degree (C) and betweenness centrality (B and D) for bacterial core T3Es (yellow) and other bacterial T3Es (cyan) (A and B) and their targets (brown and blue respectively) (C-E). The significance of the differences were evaluated by one-tailed Wilcoxon signed-rank test. The illustration in the upper right corner of each graph represents each compared group: bacterial T3Es are represented by squares, *Ath* proteins by circles and stars represents bacterial core T3Es. The estimation of the area under the curve of each distribution is compiled in Table 2.

**Table 3.1. Gene ontology (GO) enrichment test of the 12,000 cDNA-library.** GO enrichment test of the 12,000-cDNA library used in the large-scale yeast two-hybrid screenings performed to identify targets of *Xanthomonas campestris* pv. *campestris* and *Ralstonia pseudosolanacearum* type III effectors. The full Arabidopsis protein-coding genome was used as reference.

GO class	GO term <sup>a</sup>	Fold change <sup>b</sup>	P-value <sup>c</sup>
Biological process	Response to light stimulus	1.55	$4.23 \cdot 10^{-9}$
Biological process	Oxoacid metabolic process	1.56	$2.11 \cdot 10^{-14}$
Biological process	Response to inorganic substance	1.61	$7.69 \cdot 10^{-16}$
Biological process	Response to temperature stimulus	1.6	$3.29 \cdot 10^{-9}$
Biological process	Response to oxidative stress	1.64	$1.94 \cdot 10^{-6}$
Biological process	Peptide metabolic process	1.56	$1.18 \cdot 10^{-6}$
Biological process	Response to abscisic acid	1.53	$5.49 \cdot 10^{-6}$
Cellular component	Ribonucleoprotein complex	1.51	$1.03 \cdot 10^{-8}$
Cellular component	Cytosol	1.61	$3.27 \cdot 10^{-72}$
Cellular component	Chloroplast stroma	1.72	$2.21 \cdot 10^{-19}$
Cellular component	Chloroplast envelope	1.66	$6.42 \cdot 10^{-14}$
Cellular component	Organelle subcompartment	1.53	$1.82 \cdot 10^{-12}$

<sup>a</sup> Only GO terms associated with a minimum of 500 genes (~ 2% of reference list) in the reference list were considered and hierarchically presented (i.e., when multiple related terms are significant, only the most specific is shown).

<sup>b</sup> Only fold changes inferior to 0.5 or superior to 1.5 are shown.

<sup>c</sup> P-value Bonferroni corrected for multiple testing. Only P-values inferior to  $10^{-3}$  are shown.

**Table 3.2. Gene ontology (GO) enrichment test of the 209 putative targets of T3Es from *Xcc*<sub>8004</sub> and *Rps*<sub>GM11000</sub>.** GO enrichment test of the 209 putative targets (52 putative targets of *Xcc* T3Es and 176 putative targets of *Rps* T3Es) identified in our two large-scale yeast two-hybrid screenings. The 12,000 cDNA-library was used as reference.

GO class	GO term <sup>a</sup>	Fold change <sup>b</sup>	P-value <sup>c</sup>
Biological process	Regulation of biological process	1.8	$5.19 \cdot 10^{-5}$
Molecular function	Protein binding	2.26	$8.32 \cdot 10^{-15}$
Molecular function	DNA-binding transcription factor activity	2.43	$1.92 \cdot 10^{-3}$
Cellular component	Nucleus	1.62	$1.9 \cdot 10^{-11}$

<sup>a</sup> Only GO terms associated with a minimum of 240 genes (~ 2% of reference list) in the reference list were considered and hierarchically presented (i.e., when multiple related terms are significant, only the most specific is shown).

<sup>b</sup> Only fold changes inferior to 0.5 or superior to 1.5 are shown.

<sup>c</sup> P-value Bonferroni corrected for multiple testing. Only P-values inferior to  $10^{-3}$  are shown.

### 3.3 *Rps* and *Xcc* share 19 putative Arabidopsis targets

The 52 putative targets of *Xcc*<sub>8004</sub> T3Es and the 176 putative targets of *Rps*<sub>GM11000</sub> T3Es identified in our large-scale yeast two-hybrid screenings using the 12,000 Arabidopsis cDNA library (12K space) are presented in **tables A.1** and **A.2** respectively. In order to extract some preliminary conclusions about them, gene ontology (GO) enrichment tests were performed. As the cDNA library used for the screenings comprises only around 40% of the total proteome-coding genome, a first enrichment test was performed to check whether there could be any initial composition bias of the library (**Table 3.1**). All the small biases observed were linked to overrepresentation of certain GO terms and never due to underrepresentation, and the fold change values were not particularly high (highest value = 1.72). According to these results, the composition of the cDNA library does not entail any strong biological bias besides the evident partiality.

A second enrichment test was then performed combining the 209 putative T3E targets identified (52 from *Xcc*<sub>8004</sub> T3Es and 176 from *Rps*<sub>GM11000</sub> T3Es) and using the 12K space as reference (**Table 3.2**). The only GO terms associated with biological processes that were enriched were unspecific terms such as “regulation of biological process” (GO ID: 0050789) which did not provide biologically relevant information. More informative were the enriched GO terms associated with molecular functions: “protein binding” (GO ID: 0005515) or “DNA-binding transcription factor activity” (GO ID: 0003700); or cellular components: “nucleus” (GO ID: 0005634). This suggests that *Xcc* and *Rps* T3Es targets tend to interact with other proteins and that many of them present nuclear localization and transcription factor activity. As key regulators of gene expression, transcription factors are ideal targets for modulation of the host cellular processes. Besides this slight enrichment in transcription factors, no other general effector targeting tendencies could be extracted from the enrichment test, probably due to the small sample size.

Crossing the lists of putative targets of T3Es from *Xcc*<sub>8004</sub> and from *Rps*<sub>GM11000</sub>, 19 common targets were found (**Table 3.3**). Among these 19 common targets, nine were also common to other pathogen effectors (*Agrobacterium tumefaciens*, *Glovinomyces orontii*, *Hyaloperonospora arabidopsidis* or *Pseudomonas syringae*) whereas ten were exclusive to *Xcc* and *Rps* T3Es. This indicates that more than half of the common putative effector targets of these two species could be considered as exclusive to these two vascular pathogens. Whether this relatively high specificity of effector targeting is linked to the lifestyle or is an artifact from the low number of

**Table 3.3. Common putative targets of T3Es from *Xcc8004* and *RpsGM11000*.**

Accession	Gene symbol and description	Degree <sup>a</sup>	Interacting Xop(s) <sup>b</sup>	Interacting Rip(s) <sup>b</sup>	Other interacting effector(s) <sup>c</sup>	Immune phenotype <sup>d</sup>	Reference(s)
ATIG13320	(PP2AA3) Protein phosphatase 2A subunit A3	3	XopAC, XopJ	RipAJ	-	-	-
ATIG22920	(CSN5A) COP9 signalosome 5A	37	XopAC	RipAJ, <b>RipO1</b>	( <i>Atu</i> ) VirE3, ( <i>Hpa</i> ) ATR1, ATR13, HARXL10, HaRxLI45, HARXL16, HARXL62, HARXL68, HARXL69, HARXLL108, HARXLL445, HARXLL445_A, HARXLL445_B, HaRxLL518, ( <i>Psy</i> ) AvrB1, AvrB2, AvrB4-1, AvrPto1, AvrPto5, AvrRpm1, HopAO1, HopARI, HopAT1, HopBF1, HopF3, HopOI-2, HopP1, ( <i>Gor</i> ) OEC21, OEC25, OEC61, OEC67, OEC70, OEC71, OEC78, OEC85, OEC89	EDR to <i>Hpa</i> .	Mukhtar <i>et al.</i> 2011
ATIG25490	(RCN1) Roots curl in NPA 1	7	XopAC	RipAJ	( <i>Hpa</i> ) ATR1, HaRxLI45, HARXL16, ( <i>Gor</i> ) OEC119, OEC70	Impaired in stomatal closure.	Saito <i>et al.</i> 2008
ATIG71230	(CSN5B) COP9 signalosome 5B	8	AvrBsl, XopAC, <b>XopG</b> , XopK	RipAJ, RipAM, RipBJ, <b>RipO1</b>	-	-	-
AT2G45680	(TCP9) TCP domain protein 9	15	XopALI, XopK	RipAE, RipAJ, RipAK, RipAW, RipG4, <b>RipO1</b> , RipP2	( <i>Gor</i> ) OEC27, OEC39, OEC49, OEC67, OEC70, OEC76	EDS to <i>Psy</i> .	Wang <i>et al.</i> 2015
AT3G08530	(CHC2) Clathrin heavy chain 2	11	XopL, XopR	RipAD, RipAE, RipP2	( <i>Hpa</i> ) ATR13, HARXL73, HaRxLL515, ( <i>Gor</i> ) OEC45, OEC63	EDR to <i>Gci</i> .	Wu <i>et al.</i> 2015
AT3G12920	(BRG3) BOI-related gene 3	7	XopAC, <b>XopAG</b> , XopALI	RipA1, RipAE, <b>RipO1</b> , RipV1	-	EDS to <i>Bci</i> .	Luo <i>et al.</i> 2010
AT3G25800	(PP2AA2) Protein phosphatase 2A subunit A2	3	XopAC	RipAJ	( <i>Gor</i> ) OEC119	-	-
AT3G27960	(KLCR2) Kinesin light chain-related 2	21	XopAC, <b>XopAG</b> , XopF, XopZ	RipA1, RipA2, RipA4, RipA5, RipAD, RipAE, RipG4, <b>RipO1</b> , RipS3, RipS6, RipV1	( <i>Hpa</i> ) ATR13, HARXL30, HARXL73, HARXL79, HARXLL60, ( <i>Psy</i> ) HopAB1	EDS to <i>Hpa</i> .	Mukhtar <i>et al.</i> 2011
AT3G54000	TIP41-like protein	3	XopALI	RipAK, <b>RipO1</b>	-	-	-
AT4G01090	Hypothetical protein	9	<b>XopAG</b> , XopR	RipA2, RipAE, RipP2, RipS3, RipV1	( <i>Hpa</i> ) HaRxLL515, ( <i>Gor</i> ) OEC45	-	-
AT4G09060	Hypothetical protein	3	XopK	RipAE, <b>RipO1</b>	-	-	-
AT4G17680	SBP (S-ribonuclease binding protein) family protein	16	XopAC, <b>XopAG</b> , XopALI, <b>XopP</b>	RipAD, RipAE, RipAK, <b>RipO1</b>	( <i>Hpa</i> ) ATR1, ( <i>Psy</i> ) AvrB1, AvrB2, AvrB4-1, HopAB1, HopR1, AvrC, ( <i>Gor</i> ) OEC61	EDR to <i>Hpa</i> .	Mukhtar <i>et al.</i> 2011

AT4G26660	Kinesin-like protein	2	XopR	RipAE	-	-	-
AT5G02020	(SIS) Salt induced serine rich	2	XopR	<b>RipO1</b>	-	-	-
AT5G08070	(TCP17) TCP domain protein 17	7	XopAC, XopK, XopR	RipAE, RipAJ, RipAK, <b>RipO1</b>	-	-	-
AT5G26720	Ubiquitin carboxyl-terminal hydrolase-like protein	4	XopAC, XopJ, XopK	RipAJ	-	-	-
AT5G51110	(SDIRIP1) SDIR1-interacting protein 1	3	XopK	<b>RipO1</b>	(Hpa) ATR1	-	-
AT5G51440	(HSP23.5) HSP20-like chaperones superfamily protein	7	XopAC, XopAL1	RipAE, RipAK, RipAW, <b>RipH3</b> , <b>RipO1</b>	-	-	-

<sup>a</sup> Effector degree (number of interacting effector proteins) in EffectorK database.

<sup>b</sup> Effectors with orthology between *Xcc*<sub>8004</sub> and *Rps*<sub>GM11000</sub> are highlighted in bold. When both orthologous effectors interact with a same Arabidopsis protein, the effectors are underlined and the full row is colored in grey.

<sup>c</sup> Other plant pathogen effectors interacting with the same putative target of *Xcc* and *Rps* effectors preceded by the species in brackets. *Atu*, *Agrobacterium tumefaciens*; *Gor*, *Glovinomyces orontii*; *Hpa*, *Hyaloperonospora arabidopsidis*; and *Psy*, *Pseudomonas syringae*.

<sup>d</sup> Published immune-related phenotypes characterized on Arabidopsis T-DNA insertion mutant lines. EDR, enhanced diseases resistance; EDS, enhanced disease susceptibility; *Bcy*, *Botrytis cinerea* and *Gci*, *Glovinomyces cichoracearum*.

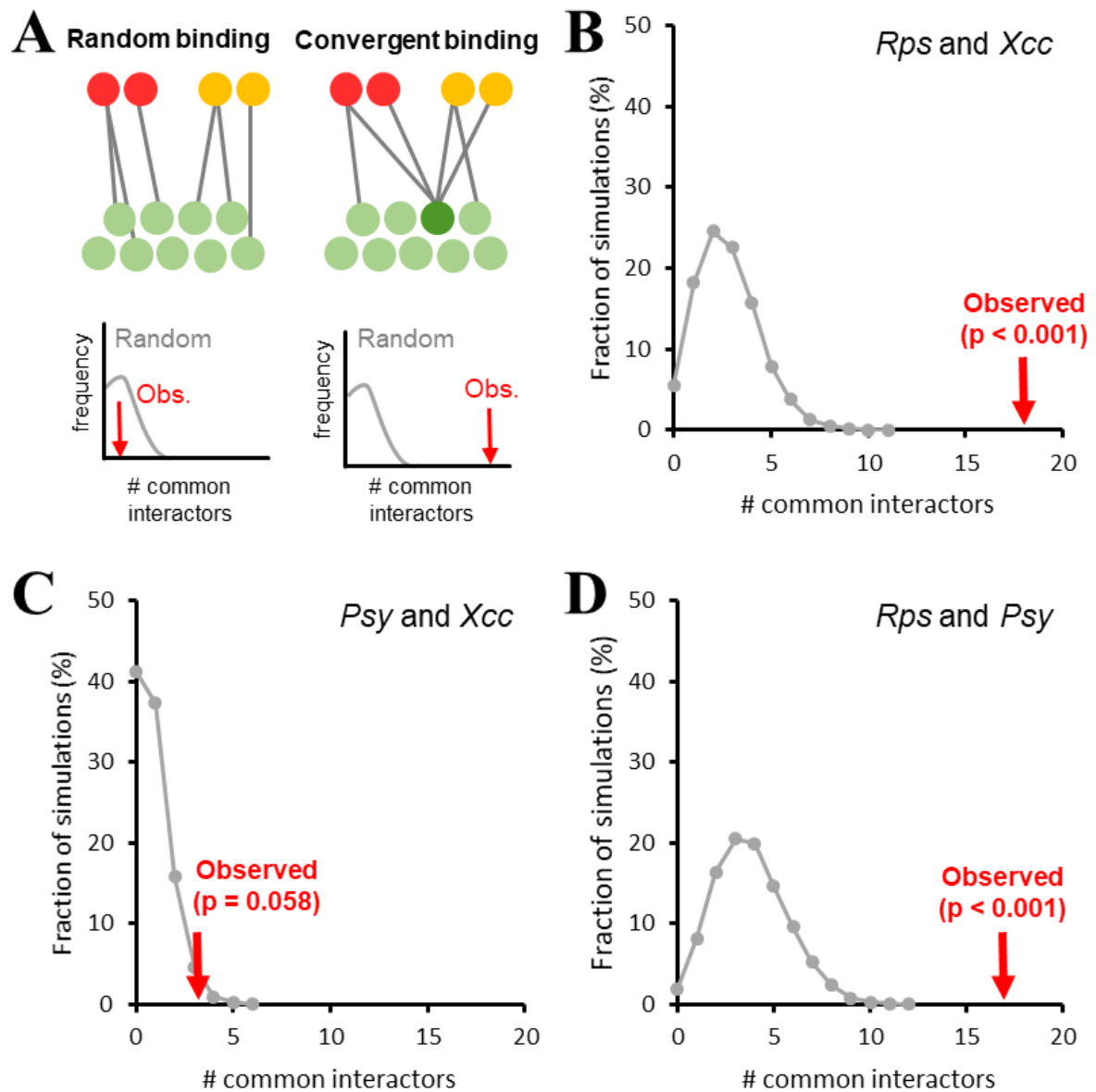


**Figure 3.1. Interspecific convergence of effector targets among plant pathogenic bacteria.** (A) Random or convergent targeting of effectors from two different species (red and yellow circles) with *Arabidopsis* proteins (green circles) can be distinguished by random network rewiring and simulation. Comparison of the number of observed (red arrow) versus 10,000-simulation-expected (grey curve) common targets of effectors from *Rps* and *Xcc* (B), *Psy* and *Xcc* (C) and *Rps* and *Psy* (D). Adapted from González-Fuente *et al.*, 2019 (A and C).

species screened is difficult to assess at this stage. As presented in the previous section, random rewiring simulations showed that effectors from different pathogens have more putative targets than expected by chance (**Figure 3.1A**). When comparing pairwise all three pathogenic bacteria screened at the effectome-scale (i.e., *Psy*, *Rps* and *Xcc*), the biggest difference between the observed number of common effector targets and the expected by random simulation, is observed precisely between *Rps* and *Xcc*, the two vascular pathogens (**Figure 3.1B**), and the smallest difference is between *Xcc* and the mesophyll pathogen *Psy* (**Figure 3.1C**). This could indicate that the convergence of effector targeting is more pronounced among pathogens with similar lifestyles. However, the difference between *Psy* and *Rps* is similar to that of *Rps* and *Xcc* (**Figure 3.1B** and **3.1D**), undermining this hypothesis. It is more likely that the differences in the level of convergence are due to the number of effectors screened rather than due to the lifestyle of the pathogen as discussed in the article.

From the functional point of view, among these 19 common putative targets of T3Es from *Xcc*<sub>8004</sub> and *Rps*<sub>SGMII000</sub> (**Table 3.3**), there are six proteins involved in ubiquitin-mediated signaling: COP9 signalosome components (CSN5A and CSN5B), SBP family proteins (BRG3 and AT4GI7680), an ubiquitin hydrolase-like protein (AT5G26720) and a target of an E3 ubiquitin ligase (SDIRIP1). There are also two transcription factors from the same family: TCP9 and TCP17. The three subunits of the protein phosphatase 2A (RCN1, PP2AA2 and PP2AA3) are also targeted by effectors from *Xcc* and *Rps*. The remaining common targets are proteins related to the cytoskeleton (KLRC2 and AT4G26660), membrane trafficking (CHC2), response to abiotic stress (SIS and HSP23.5) and hypothetical proteins of unknown function (AT3G54000, AT4G01090 and AT4G09060).

The involvement in plant immunity has already been demonstrated for seven out of the 19 common putative targets of *Xcc*<sub>8004</sub> and *Rps*<sub>SGMII000</sub> T3Es (**Table 3.3**). This proven involvement serves as indirect evidence of the potential of the cognate *Xcc* and *Rps* T3Es to modulate plant immunity. This also highlights the lack of knowledge for most of the identified putative targets, and the subsequent potential for further experimental validation. Interestingly, most of the proteins that have not been characterized in immunity yet are exclusive targets of *Rps* and *Xcc*. This could indicate that these exclusive targets might be novel and important proteins for specific plant responses against vascular pathogens, although it is also possible that this is simply caused by the low number of pathogen effectomes thoroughly screened.



**Table 3.4. Putative targets of orthologous T3Es from *Xcc8004* and *RpsGM11000*.** For each T3E from the set of orthologs between *Xcc8004* and *RpsGM11000*, the number of identified targets (if any) is presented. Common targets of both members of each orthologous groups are also indicated.

<i>Xcc8004</i> T3Es (Xops)	Xop targets identified (number)	<i>RpsGM11000</i> T3Es (Rips)	Rip targets identified (number)	Common targets (number) <sup>a</sup>
XopAG	Yes (5)	RipOI	Yes (61)	<u>Yes (3)</u>
XopQ	No	RipB	Yes (1)	No
XopP	Yes (3)	RipH1	No	No
		RipH2	Yes (7)	<u>No</u>
		RipH3	Yes (10)	<u>No</u>
XopAM	Yes (2)	RipR	No	No
HrpW	No	RipW	Yes (2)	No
XopG	Yes (2)	RipAX1	No	No
		RipAX2	Yes (2)	<u>No</u>

<sup>a</sup> Underlined if targets identified for both members of each ortholog pair.

If the orthology relationships between *Xcc*<sub>8004</sub> and *Rps*<sub>GMII000</sub> T3Es are considered, there are 13 targets of common T3Es but only three of them interact with both partners of an ortholog pair (**Table 3.3**). This *a priori* low number of common targets of orthologous T3Es might be the product of the lack of identified targets of several T3Es. Indeed, from the nine possible ortholog T3E pairs, only in four of them targets were identified for both of members (XopAG/RipOI, XopP/RipH2, XopP/RipH3 and XopG/RipAX2) (**Table 3.4**). From these four ortholog pairs, common targets were only found in one: XopAG/RipOI (**Tables 3.3** and **3.4**). These three common targets of XopAG and RipOI are BRG3, a putative E3 ubiquitin ligase involved in immunity against necrotrophic fungus *Botrytis cinerea* (Luo *et al.*, 2010); KLCR2 and AT4G17680, both hub proteins involved in immunity against the oomycete *Hyaloperonospora arabidopsidis* (Mukhtar *et al.*, 2011).

### 3.4 Few common targets seem to be involved in plant susceptibility to *Xcc* and *Rps*

To evaluate the involvement of the identified 19 common putative targets of effectors of *Xcc*<sub>8004</sub> and *Rps*<sub>GMII000</sub> in Arabidopsis immunity against these two pathogens, several T-DNA insertion lines for each of the 19 targets were requested from authors or ordered from public collections (**Table A.3**). When not directly available, homozygous mutant plants were obtained from a heterozygous population through PCR genotyping (O'Malley, Barragan and Ecker, 2015). The growth of all these mutant lines up to 4 weeks was similar to the Col-0 wild type except for *csn5a* mutants (MGF323 and MGF336) that were considerably smaller as previously reported (Gusmaroli *et al.*, 2007). For this reason, these lines were excluded from the following experiments. The mutants for the remaining 18 putative common targets of *Xcc*<sub>8004</sub> and *Rps*<sub>GMII000</sub> were first screened for disease susceptibility to *Xcc* using the strain 8004Δ*xopAC*. This strain was used instead of the wild type because, in the Arabidopsis ecotype Col-0 in which the mutants were generated, *xopAC* triggers resistance (Xu *et al.*, 2008b). 4-weeks-old Arabidopsis plants were wound-inoculated with *Xcc* bacteria and the disease symptoms were scored at 10 days post inoculation (**Figure 3.2**). Only four mutant lines produced altered symptom development: MGF249 and MGF370 mutant alleles of *SIS* both showed enhanced disease susceptibility. MGF309, one of the mutant alleles of *RCNI*, and MGF346, one of the mutant alleles of *BRG3*, showed reduced disease susceptibility. In parallel, the growth *in planta* of *Xcc* was also measured in Col-0 and some of the initially most interesting candidates: the three common targets of XopAG and RipOI (i.e., KLCR2, AT4G17680 and BRG3).

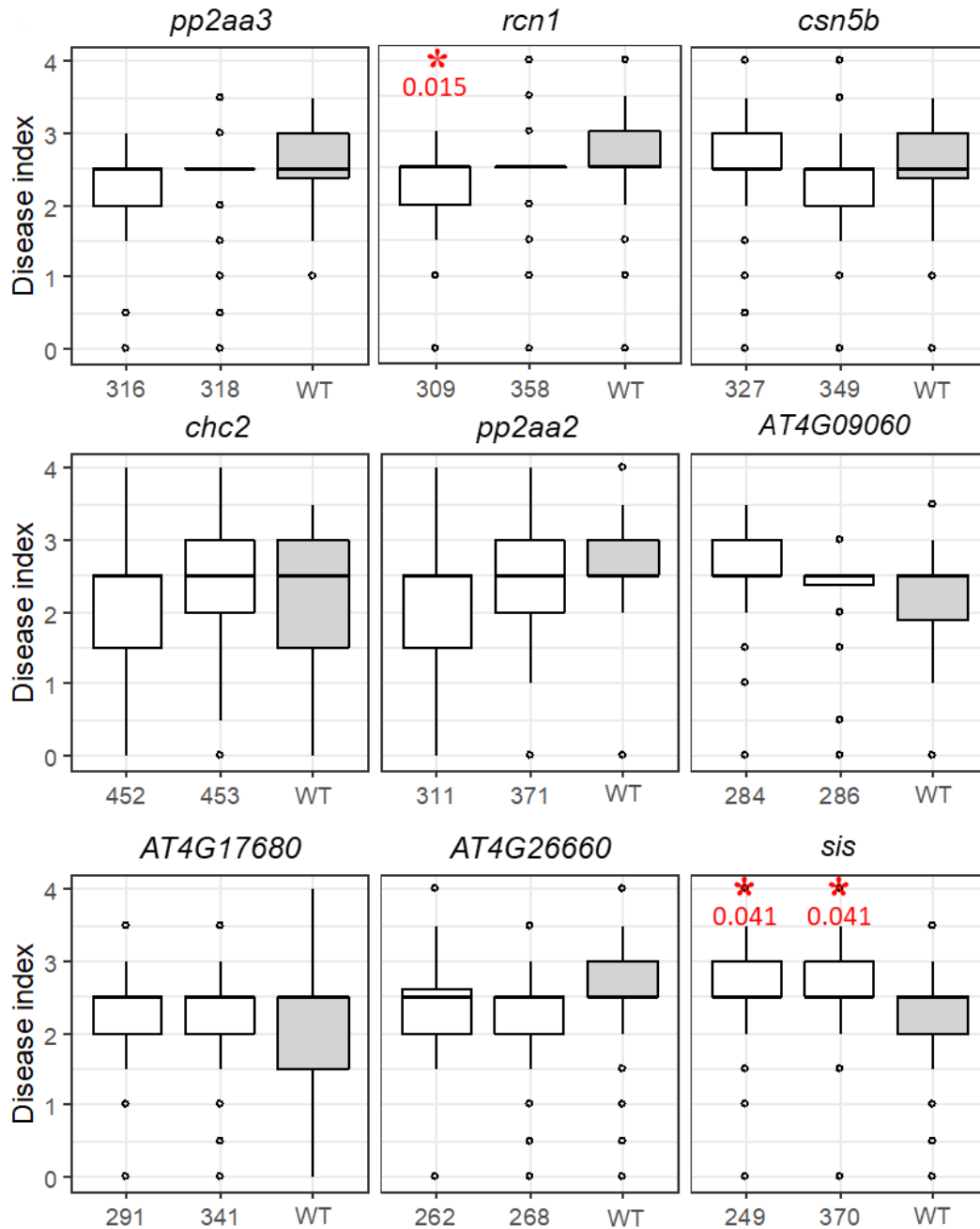


**Figure 3.2 (1/2). Involvement in susceptibility to *Xcc* of 18 common putative targets.** Boxplot representation of disease index scored at 10 days post wound-inoculation on *A. thaliana* ecotype Col-0 wild-type (WT, in grey) and mutant (given name in table 3.7, in white) plants. Disease index is as follows: 0-1, no symptoms; 1-2, weak chlorosis around the inoculation sites; 2-3, stronger and extended chlorosis; and 3-4, necrosis. Inoculation was done with the *Xcc* strain 8004 $\Delta$ *xopAC* at  $10^8$  CFU/ml. Six plants (four leaves per plant) were inoculated per condition. Two independent experiments were performed and the results were combined. Red asterisks indicate that the difference with the Col control is statistically significant (one-tailed Wilcoxon signed-rank test p-value < 0.05, exact value indicated below). Boxplot representation: thick bar, median; box limits, highest and lowest value within  $1.5 \cdot$  inter-quartile range; and circles, outliers.

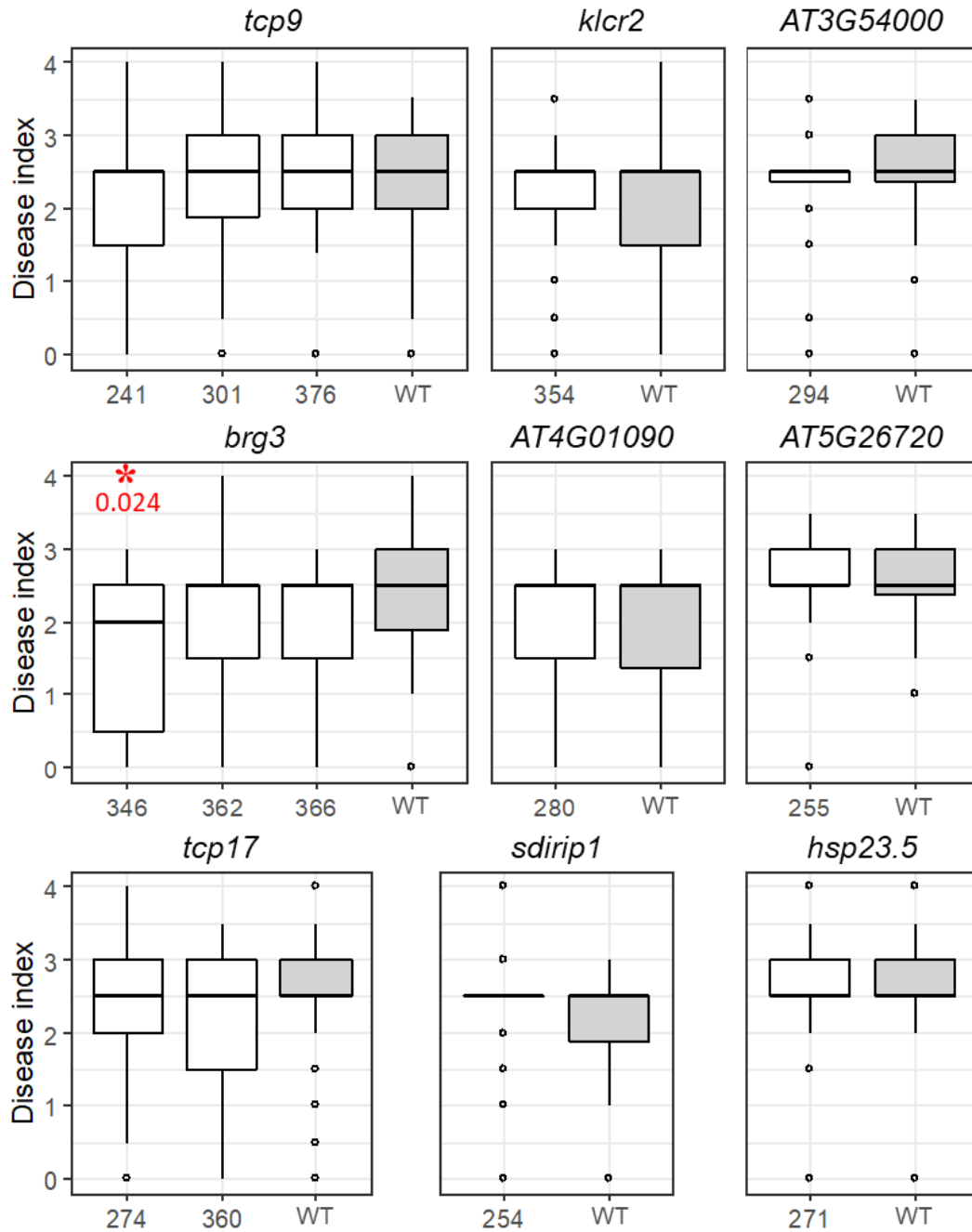


**Figure 3.2 (2/2). Involvement in susceptibility to Xcc of 18 common putative targets.** Boxplot representation of disease index scored at 10 days post wound-inoculation on *A. thaliana* ecotype Col-0 wild-type (WT, in grey) and mutant (given name in table 3.7, in white) plants. Disease index is as follows: 0-1, no symptoms; 1-2, weak chlorosis around the inoculation sites; 2-3, stronger and extended chlorosis; and 3-4, necrosis. Inoculation was done with the *Xcc* strain 8004 $\Delta$ *xopAC* at  $10^8$  CFU/ml. Six plants (four leaves per plant) were inoculated per condition. Two independent experiments were performed and the results were combined. Red asterisks indicate that the difference with the Col control is statistically significant (one-tailed Wilcoxon signed-rank test p-value < 0.05, exact value indicated below). Boxplot representation: thick bar, median; box limits, highest and lowest value within  $1.5 \cdot$  inter-quartile range; and circles, outliers.

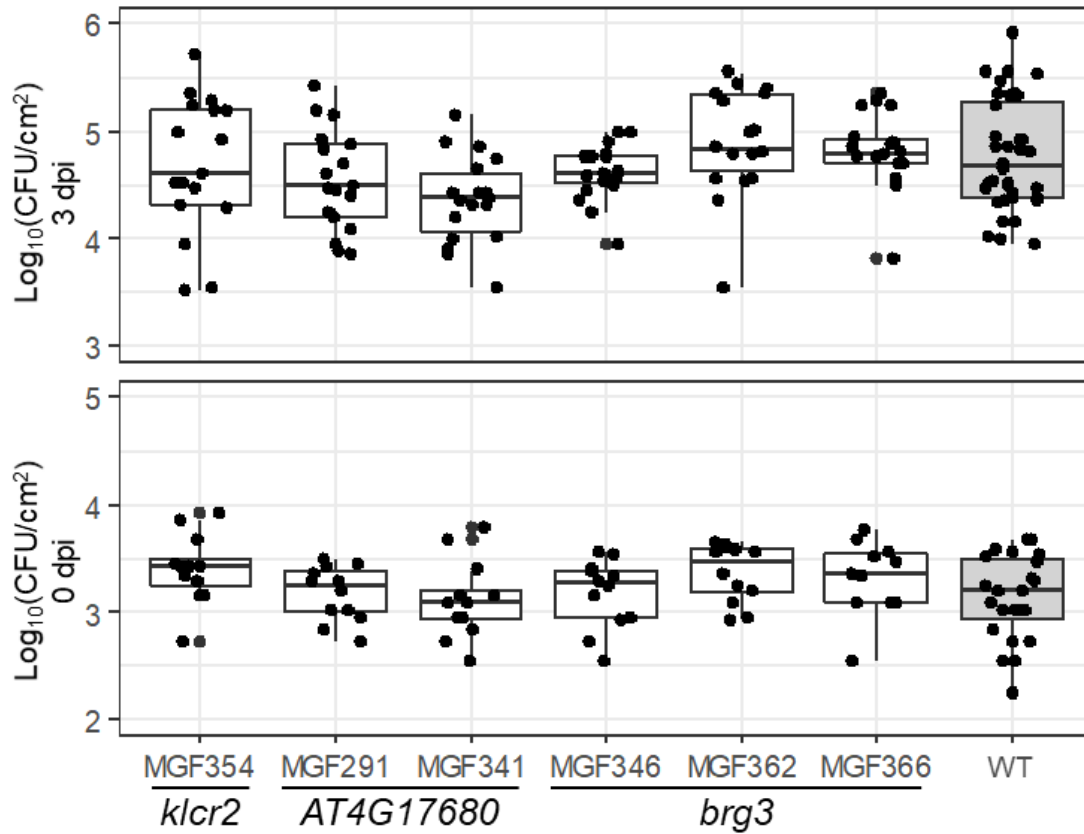


**Figure 3.3. Involvement of the three common putative targets of XopAG and RipOI in the *in planta* growth of *Xcc*.** Boxplot representation of bacterial population of *Xcc* strain 8004 $\Delta$ *xopAC* in *A. thaliana* ecotype Col-0 wild-type (WT, in grey) and mutant (given name in **table 3.7**, in white) leaves at 0 (bottom) and 3 (top) days post inoculation. Inoculation was done by infiltration of a bacterial suspension at  $10^5$  CFU/ml with a needleless syringe. Six and nine samples from six plants were randomly corrected at 0 and 3 dpi respectively. Two independent experiments were performed and the results were combined. No statistically significant differences were observed between the different groups (one-tailed Wilcoxon signed-rank test  $p$ -value  $< 0.05$ ). Boxplot representation: black dots, raw values; thick bar, median; and box limits, highest and lowest value within  $1.5 \cdot$  inter-quartile range.

*Xcc* strain 8004  $\Delta xopAC$  bacteria were infiltrated in the mesophyll and counted immediately after the inoculation and three days later (**Figure 3.3**). No significant differences between the screened mutants and the Col-0 control were observed, not even for MGF346, one of the mutant lines that had previously shown reduced disease susceptibility. This suggests that small alterations in symptom appearance might not necessarily be correlated with bacterial growth alterations *in planta*.

Due to space constraints at the time, only the most promising candidates were screened for involvement in disease susceptibility to *Rps*: the three common targets of XopAG and RipOI (i.e., KLCR2, AT4GI7680 and BRG3) because they are the only common targets of an ortholog pair of T3Es, and SIS because two independent mutant alleles had shown enhanced disease susceptibility to *Xcc* (**Figure 3.2**). 4-weeks-old Arabidopsis plants were soil-drenched in *Rps* wild-type strain GMII000 bacterial suspension and the percentage of plants still alive was scored daily up to 10 days (**Figure 3.4A**). These results, although quite variable, showed that most of the mutant alleles screened were not significantly different from Col-0 controls. Only two mutant alleles showed statistically significant differences in one of the experiments: MGF354 (*klcr2*) showed enhanced disease susceptibility whereas MGF362 (*brg3*), showed reduced disease susceptibility. The difference of MGF354 with Col-0 plants in the first experiment was not observed in the other two; however, the tendency was the same as evidenced by their hazard ratio higher than one (i.e., mutant plants die proportionally faster than the control) in all experiments (**Figure 3.4B**). This could suggest that KLCR2 might be implicated in susceptibility to *Rps* although three experiments were not statistically powerful enough to evidence this. Conversely, the difference of MGF362 with Col-0 was not only not observed again in the other two experiments, but the tendencies were actually reversed (**Figure 3.4B**). Indeed, if considered all three different *brg3* mutant alleles (i.e., MGF346, MGF362 and MGF366), the general tendency is enhanced disease susceptibility, as shown by their hazard ratios slightly higher than one (**Figure 3.4B**). Whether this is coincidence or evidence of a minor role in susceptibility cannot be assessed with the number of experiments performed. The mutant alleles of the remaining screened genes (*AT4GI7680* and *SIS*) did not show any significant difference to the Col-0 controls and the curve tendencies were contradictory among alleles from a same gene and among independent experiments (**Figure 3.4A and 3.4B**).

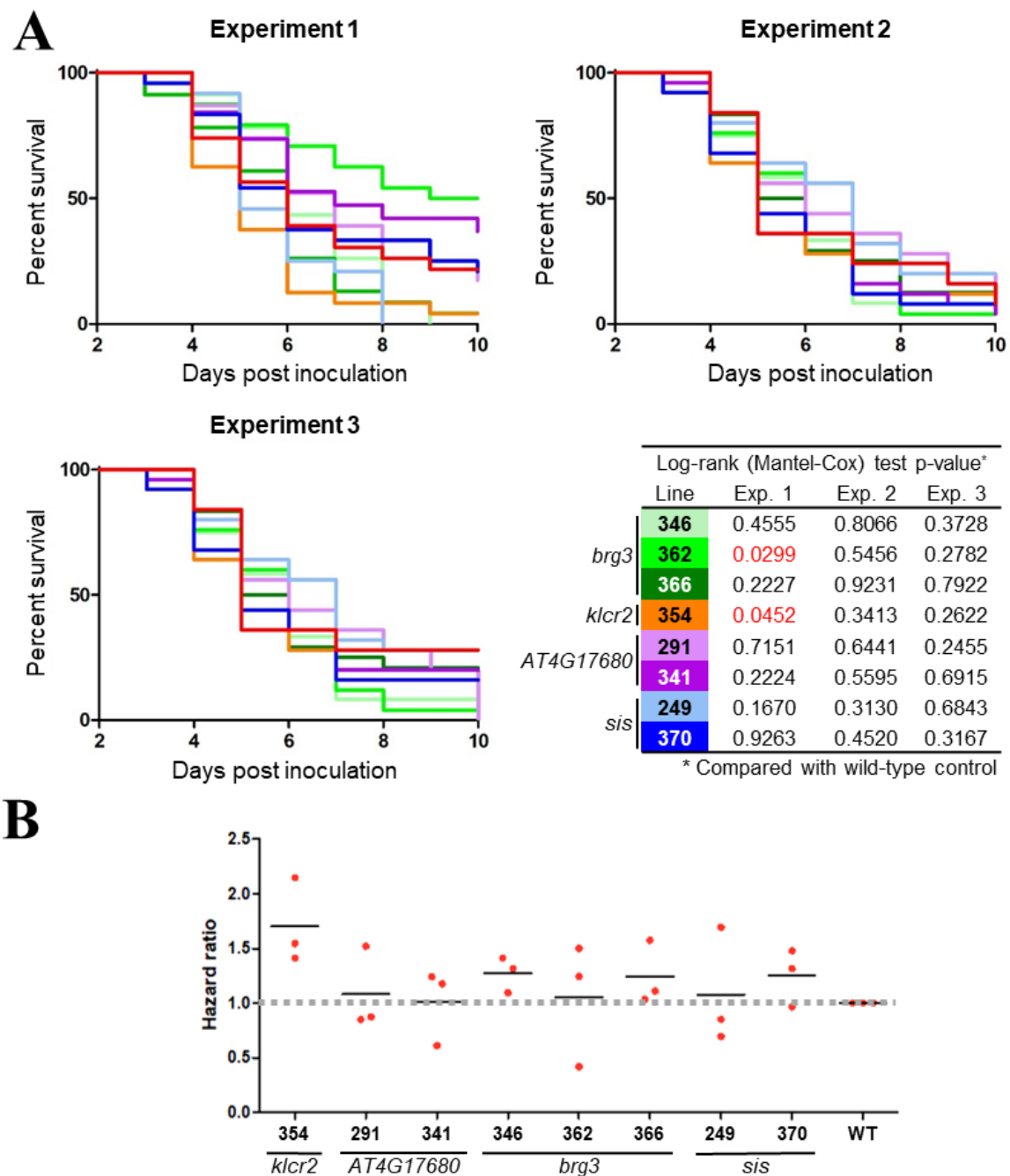


**Figure 3.4. Involvement of four common putative targets in susceptibility to *Rps*.** (A) Survival curves scored for 10 days after soil-drenching inoculation of *A. thaliana* ecotype Col-0 wild-type (red) and mutant (color code in adjacent table) plants with *Rps* strain GMII000 at  $10^8$  CFU/ml. Twenty plants were inoculated per line and experiment and the results of three independent experiments are shown. Statistically significant differences to the wild type curve are highlighted in red (Mantel-Cox logrank test p-value < 0.05). (B) Dotplot representing the hazard ratio of each survival curve using the wild type (WT) as reference. Results from the three independent experiments are shown. Black lines indicate the mean and the grey dotted line is located at a constant ratio of 1 for reference.

## 3.5 Discussion

### ***Rps* and *Xcc* T3Es behave like most plant pathogen effectors**

In this first part of results, the systematically identified putative targets of several effectors from vascular pathogens *Xcc*<sub>8004</sub> and *Rps*<sub>SGMII000</sub> were presented (**Tables A.1 and A.2**). This allowed the comparison of the effector interactomes of these two species with other *Arabidopsis* pathogens previously screened in a similar manner (Mukhtar *et al.*, 2011; Weßling *et al.*, 2014). This evidenced that the effectors of *Xcc* and *Rps* behave similarly to those of other plant pathogens: 1) Effectors from a same species tend to interact with a limited set of *Arabidopsis* proteins indicating intraspecific convergence (**Article figure 2A**). 2) Effectors from different species tend to have more common targets than it could be expected by chance, indicating interspecific convergence (**Article figures 2B and 2C**). 3) Effector interact preferentially with *Arabidopsis* proteins highly connected to other plant proteins (**Article figure 5**). 4) Effector targets occupy central positions in the *Arabidopsis* interactomic network (**Article table 2**). Altogether, these results indicate that effectors tend to interact with host proteins with higher potential to modulate the organization of the plant interactomic network.

From a functional point of view, it was also shown that *Xcc* and *Rps* T3Es target similar plant processes to other pathogen effectors. *Xcc* and *Rps* T3E targets were significantly enriched in proteins with transcription factor activity and nuclear localization (**Table 3.2**). Indeed, several examples of effectors targeting plant transcription factors have been reported in other plant pathogens including other bacteria (MacLean *et al.*, 2014; Yang *et al.*, 2017), oomycetes (McLellan *et al.*, 2013), fungi (Qin *et al.*, 2018), nematodes (Hewezi *et al.*, 2015) or insects (N. Wang, Zhao, *et al.*, 2019). Among the 19 common putative targets of T3Es from *Xcc*<sub>8004</sub> and *Rps*<sub>SGMII000</sub> there were precisely two transcription factors, both from the same family: TCP9 and TCP17. TCP transcription factors are known to modulate a wide variety of plant processes including responses to biotic stress (Li *et al.*, 2018; Z. Wang, Cui, Liu, *et al.*, 2019). TCP9 is precisely one of these TCP family members involved in plant defense responses as it has been shown that, together with its paralog TCP8, they control the expression of *ICSI*, key enzyme in the biosynthesis of SA (X. Wang *et al.*, 2015). There were also several proteins involved in ubiquitin-mediated signaling. This is in agreement with previous reports of plant pathogen effectors interfering with plant ubiquitination and proteasome functioning (Banfield, 2015; Üstün *et al.*, 2016). PP2A, whose three structural subunits are also targets of *Xcc* and *Rps* effectors, is a key negative regulator of defense responses acting at the PRR phosphorylation, ROS homeostasis, hormone signaling and autophagy levels (Durian *et al.*, 2016). PP2A



constitutes thus an ideal target for pathogen effectors as it has been already shown in other phytopathogenic bacteria (Jin *et al.*, 2016). Other three targets are linked to the cytoskeleton and membrane trafficking, processes highly involved in all levels of immunity. Cytoskeleton components are involved in the PTI and ETI receptor localization and signaling (Mbengue *et al.*, 2016; Postma *et al.*, 2016; Bücherl *et al.*, 2017) or in organellar reorganization during defense responses (Takemoto, Jones and Hardham, 2003; A. S. Kumar *et al.*, 2018). Therefore, cytoskeletal proteins are also targeted by different plant pathogenic bacteria (Lee *et al.*, 2012; Cheong *et al.*, 2014; Erickson *et al.*, 2018) or nematode effectors (Leelarasamee, Zhang and Gleason, 2018), including kinesin family proteins (Shimono *et al.*, 2016), such as two of the common putative targets identified. Altogether, these results corroborate the strong similarities existing among the virulence mechanisms of different pathogen effectors. *Xcc* and *Rps* T3Es do not only behave similarly to other effectors in terms of connectivity and interaction tendencies with *Arabidopsis* proteins, but also in terms of biological processes modulated.

### **Is there a certain effector targeting specificity among vascular pathogen?**

An unanswered question that these results open is: what is the level of pathogen specificity of effector targets? As pointed out in the article, while there are significantly many common effector targets to different pathogens (**Article figure 2**), the majority of them remain specific to each species (**Article figure S2**). Whether this is caused by a true biological specificity of effector targeting or is just an artifact of the low number of pathogens species screened at the effectome level is impossible to assess at this point. This work represents the first systematic screen for interactors of effectors from *Arabidopsis* vascular pathogens. Therefore, the question about pathogen specificity can be extended to lifestyle specificity. Can effector target specificity reflect the pathogen lifestyle? As discussed in this chapter, within the common targets of *Xcc* and *Rps* T3Es, more than half of them were exclusive to these two vascular pathogens (**Table 3.3**). However, the limited number of other species to compare to prevents the assessment of whether this indicates true adaption to vasculature or is just an artifact caused by the low number of species screened. To answer these questions, more large-scale screenings of several effectors from several and varied pathogens would be required to conduct comparative studies with enough power.

## Functional similarities beyond homology

From the 209 T3Es targets identified, 19 were common to effectors from *Xcc*<sub>8004</sub> and *Rp*<sub>SGM11000</sub> (**Table 3.3**). However, considering the orthology relations between T3Es, only three of these targets interacted with orthologous T3Es from the two species. This result is probably underestimated due to the lack of identified targets for some of the T3Es. This prevented the comparison of targets between many of the ortholog pairs (**Table 3.4**). Considering this, testing interaction between T3Es for which no targets were identified, and the identified targets of the orthologous T3E could help to recover possible false negatives (e.g., test interactions between RipR and the identified targets of its *Xcc* ortholog, XopAM). However, even if a few false negatives were recovered, most of the common targets can still interact with sequence-unrelated *Xcc* and *Rps* effectors. This indicates that, besides sequence orthology, there is also a sort of “homology of function”. This refers to effectors that although are not similar in sequence, interact with the same targets. This seems to be the case for example of XopAC and RipAJ which, despite showing only 11% amino acid sequence identity, interact with six common proteins (**Figure 3.5**). Among these six, there are the three structural subunits of PP2A, which did not interact with other Xops or Rips in our screenings (except PP2AA3 that can also interact with XopJ) (**Table 3.3**). *RCN1*, one of these subunits, was precisely one of the few genes for which a mutant allele showed reduced disease susceptibility to a compatible *Xcc* strain, although this difference was not significant in the other *rcn1* allele (**Figure 3.2B**). This could suggest a minor role of *RCN1* in the response against a vascular pathogen. Considering that XopAC and RipAJ interact with *RCN1*, it could also be possible that these T3Es modulate *RCN1* action. Nevertheless, this could not be tested because XopAC triggers resistance in the Col-0 background in which the *rcn1* mutants had been generated.

### Is the lack of infection phenotypes a mark of complex responses or are we dealing with false negatives?

The involvement in plant immunity of the rest of identified common putative targets to a compatible *Xcc* strain was assessed (**Figures 3.2 and 3.3**). However, statistically significant differences were observed only for mutant alleles of four genes. This indicates either that most of them are not involved in the plant responses to *Xcc*, or that the architecture of these responses is too complex to be dissected with single mutants. The fact that the T3E targets were identified uniquely through large-scale yeast two-hybrid screening is an argument in favor of the first assumption. Although powerful, these kind of screenings have limitations and false positives are expected (Brückner *et al.*, 2009). However, even if the identified targets truly interacted with

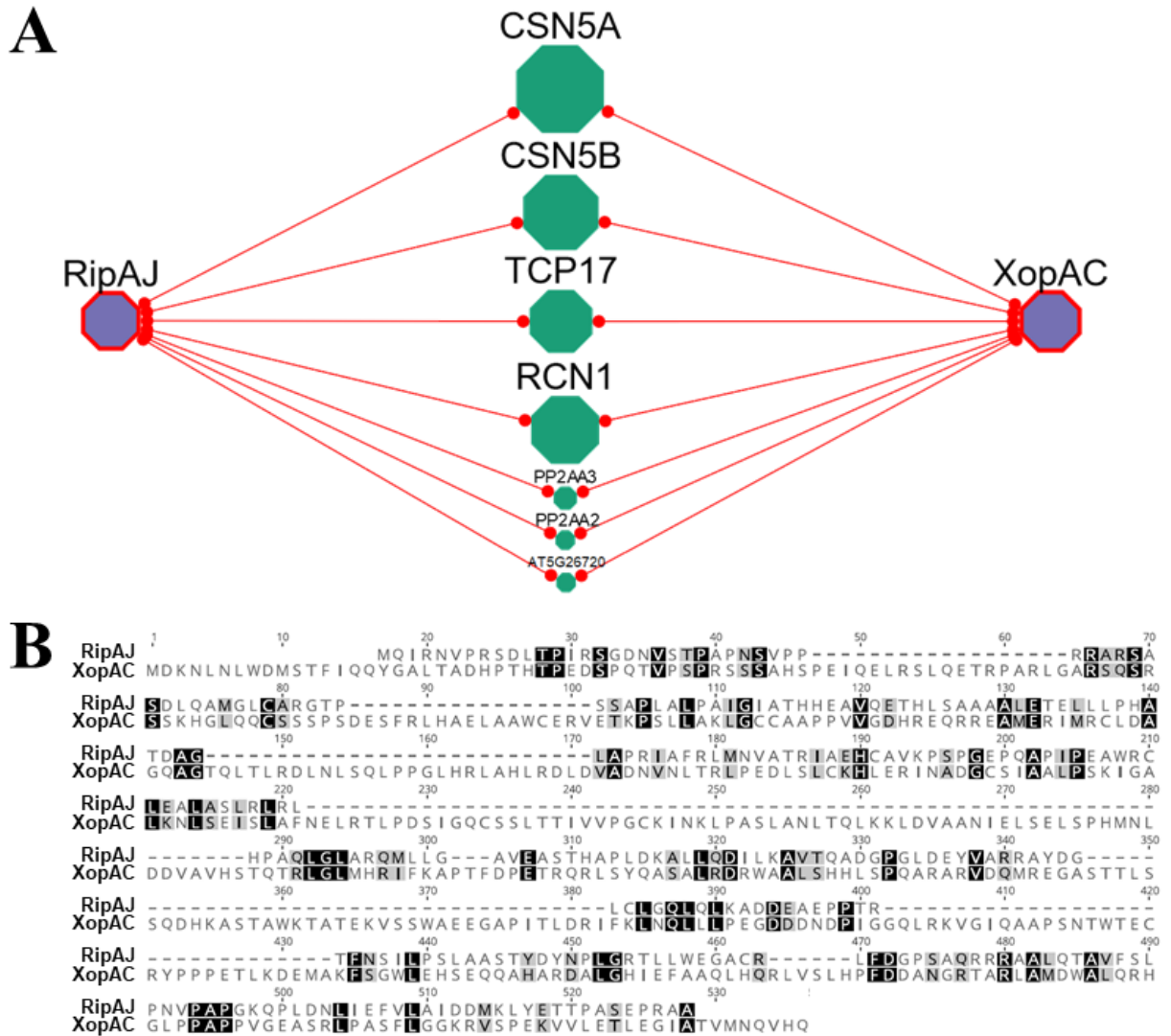


**Figure 3.5. RipAJ and XopAC show homology of function, but not of sequence.** (A) Representation of the six common targets that interact with RipAJ and XopAC. Purple and green octagons represent effector and arabidopsis proteins respectively where as the connecting red lines indicate protein-protein interaction. Obtained by the path finding tool of EffectorK. (B) ClustalW alignment of the full-length amino acid sequence of *Rps*<sub>GMI1000</sub> RipAJ (WP\_011002032) and *Xcc*<sub>8004</sub> XopAC (AFP74845). The background color represents the percentage of similarity based on the BLOSUM62 scoring matrix with a threshold of 1: black, identical; grey, similar; and white, not similar.

T3Es, this would not necessarily imply that they are involved in the plant responses to *Xcc*. Contrary to resistance that is often qualitative and monogenic (i.e., the recognition of one pathogen effector by one plant receptor triggers the resistance), susceptibility is a much more complex trait (i.e., several pathogen effectors, and other virulence determinants, interfere collectively with several plant targets). Therefore, it is not unreasonable to think that even if the targets were involved in the plant responses to *Xcc*, we would still not observe a phenotype. Among the possible reasons to explain this, there are biological and experimental limitations such as functional redundancy, epistasis, low sensitivity of the phenotyping methods or wrong choice of inoculation methods.

Among the genes for which mutant alleles showed phenotype there were the previously discussed *RCN1* and *BRG3* that showed reduced disease susceptibility, and *SIS* that showed enhanced disease susceptibility to *Xcc* (**Figure 3.2**). *SIS* encodes a serine-rich protein of unknown function involved in the response to salt stress as *sis* mutants showed reduced tolerance to salinity (Brinker *et al.*, 2010). Therefore, it seems like *SIS* is a positive regulator of both biotic and abiotic stress responses making it a new convergence point in both stress signaling pathways (Fujita *et al.*, 2006). Whether *Xcc* is able to modulate *SIS* function through its interacting effector, *XopR* would be interesting to test.

*BRG3* encodes a putative RING E3 ubiquitin ligase involved in resistance against necrotroph fungus *Botrytis cinerea* as *brg3* mutants showed increased lesion size (Luo *et al.*, 2010). This work showed that *brg3* mutants are less susceptible to *Xcc*, although this difference was only significant for one of the alleles (**Figure 3.2**). Therefore, *BRG3* could be a positive regulator of the responses against *B. cinerea* and a negative regulator of the responses against *Xcc* evidencing the specificity of the plant responses against different pathogens. As one of the common targets of two orthologous T3Es, *XopAG* and *RipOI*, the bacterial growth *in planta* of *Xcc* was measured in *brg3* mutants (**Figure 3.3**). However, no differences with the Col-0 control were observed, not even for MGF436, the mutant allele that showed significant reduced susceptibility. This evidenced that symptom development upon vascular inoculation and bacterial growth in the mesophyll are not necessarily correlated.

Similar to what was observed in *Xcc*, most of the screened mutants for T3E target genes did not show altered susceptibility phenotypes when inoculated with a compatible *Rps* strain (**Figure 3.4**). Only one mutant allele showed a slight but consistent tendency of enhanced disease susceptibility: *klcr2*. *KLCR2* is an identified effector hub targeted by effectors from *P. syringae* and *H. arabidopsidis* and *klcr2* mutants showed enhanced disease susceptibility to the

latter (Mukhtar *et al.*, 2011). As common target of *Rps* and *Xcc* T3Es, this work reinforces the fact that KLCR2 is indeed a multipathogen effector hub and that could be involved in the plant responses to both *H. arabidopsidis* and *Rps*. Whether *Rps* is able to modulate KLCR2 function in a T3E-dependent manner would be interesting to test. However, as a putative interactor of 11 *Rps* T3Es, identifying which ones, if any, are involved in this modulation would probably require the generation and phenotyping of several combination of bacterial polymutants.

### **Is there also effector targeting specificity between *Rps* and *Xcc*?**

Interestingly, none of the genes with an observable implication in the response to *Xcc* was found to be explicitly involved in the response to *Rps*, and vice versa. This could reflect that the plant defense responses against these two bacteria are substantially different. Considering that *Xcc* infects the aerial parts while *Rps* enter through the root system, it was expected that the plant defense mechanisms against each of them would be different. However, as they are both xylem-colonizing bacteria that spread systematically through the vasculature, it could equally be expected to find some similarities, particularly taking into account the presence of orthologous T3Es in their repertoire. Considering the very low number of mutant lines for which a clear immune phenotype was observed, it is not surprising that there were not coincidences. More repetitions to increase the statistical power of the already produced data could allow discerning true but weak effects from background noise. Additionally, complementary experiments using more sensitive phenotyping methods and/or alternative inoculation procedures could provide additional information to better characterize the implication of all the identified candidates in the plant defense responses. Then and only then, it would be possible to adequately compare these responses in both pathosystems. If any similarity in the response to both bacteria were to be found, it would be equally interesting to test whether this is specific to these two species or if on the contrary, is conserved among other vascular pathogens, among bacteria or among all kinds of plant pathogens

# Chapter 4

Determining the effect of the effectors  
shared by *R. pseudosolanacearum*  
and *X. campestris* pv. *campestris*

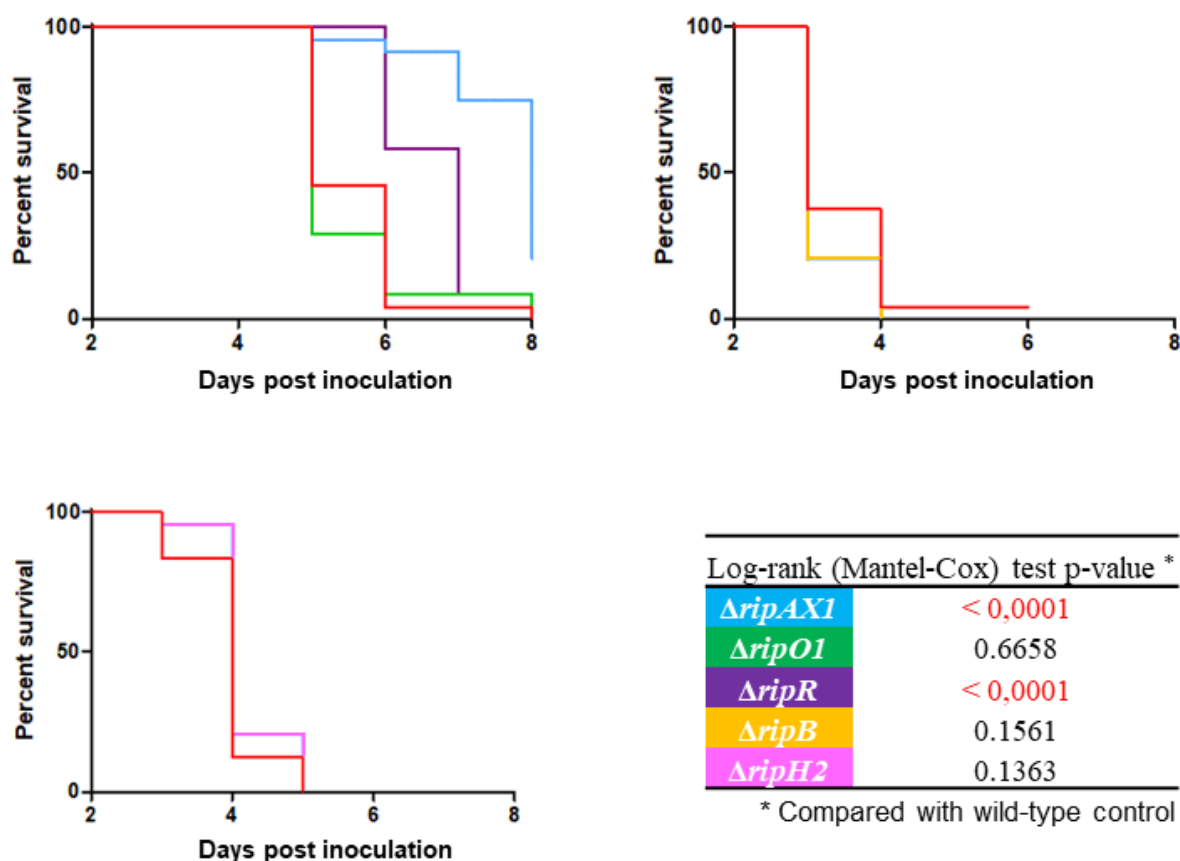


**Figure 4.1. Pathogenicity of T3E gene mutants in *RpsGM11000* inoculated on susceptible tomato plants.** Survival curves scored for up to 8 days after soil-drenching inoculation of tomato cultivar Super Marmande plants with *RpsGM11000* wild type (red) and different single T3E gene mutants (colors as stated in the table). Plants were drenched bacterial suspension at  $10^8$  CFU/ml. 24 plants were inoculated per strain. Only one experiment was performed. Statistically significant differences to the Col-0 curve are highlighted in red (Mantel-Cox logrank test p-value < 0.05). Preliminary results from Patrick Barberis (unpublished).

## 4.1 Introduction

This second chapter of results gathers all the work related to the characterization of the effects in the bacteria and in the plant of the shared T3Es between *Xcc*<sub>8004</sub> and *Rps*<sub>GMI1000</sub>. To this end, a first approach was conducted using different single and multiple bacterial T3E gene mutants to evaluate their contribution to *Xcc* and *Rps* pathogenicity. Considering the collective action of effectors, which often show phenomena of functional redundancy (Kvitko *et al.*, 2009; Zumaquero *et al.*, 2010; Tan *et al.*, 2015) or epistasis (Phan *et al.*, 2016; Rufián *et al.*, 2018), an alternative approach was conducted in parallel: the heterologous expression *in planta* of single bacterial T3E genes. For this, stably transformed Arabidopsis plants and transiently transformed *Nicotiana benthamiana* leaves were generated and phenotyped for developmental alterations and inhibition of basal plant defense responses.

## 4.2 Shared T3Es contribute collectively to the bacterial pathogenicity

As the characterization of the roles of T3Es from *Xcc*<sub>8004</sub> and *Rps*<sub>GMI1000</sub> is one of the main research axes of both host teams, many useful biological resources had been generated previously: all *Xcc*<sub>8004</sub> and *Rps*<sub>GMI1000</sub> T3E genes had been cloned in entry plasmids, or different bacterial mutants had been generated. Most of these bacterial mutants had already been phenotyped previously. In the case of *Rps*<sub>GMI1000</sub>, many T3E single mutants have been phenotyped for virulence when inoculated in susceptible tomato Super Marmande plants. Previous preliminary results showed that most of the single T3E gene mutants did not show differences in pathogenicity with the wild type GMI1000 strain (Patrick Barberis, unpublished data). Among these *Rps*<sub>GMI1000</sub> T3E genes, there were five shared with *Xcc*<sub>8004</sub>: *ripAXI*, *ripB*, *ripH2*, *ripOI* and *ripR* (**Figure 4.1**). From these five, only *ripAXI* and *ripR* showed a significant reduction in pathogenicity.

Similarly, most *Xcc*<sub>8004</sub> single T3E gene mutants had also been phenotyped previously, in this case, in both resistant and susceptible Arabidopsis ecotypes (Guy *et al.*, 2013). In the resistant ecotype Col-0, only five mutants showed significant differences in virulence compared to the 8004 wild-type control (**Figure 4.2A**):  $\Delta xopAC$  and  $\Delta xopAM$  were moderately virulent whereas  $\Delta xopN$ ,  $\Delta xopXI/2$  and  $\Delta xopALI/xopP$  were completely avirulent. Conversely, in the susceptible ecotype Kas, no major differences in virulence were observed for any of the mutants compared to wild-type control (**Figure 4.2B**).



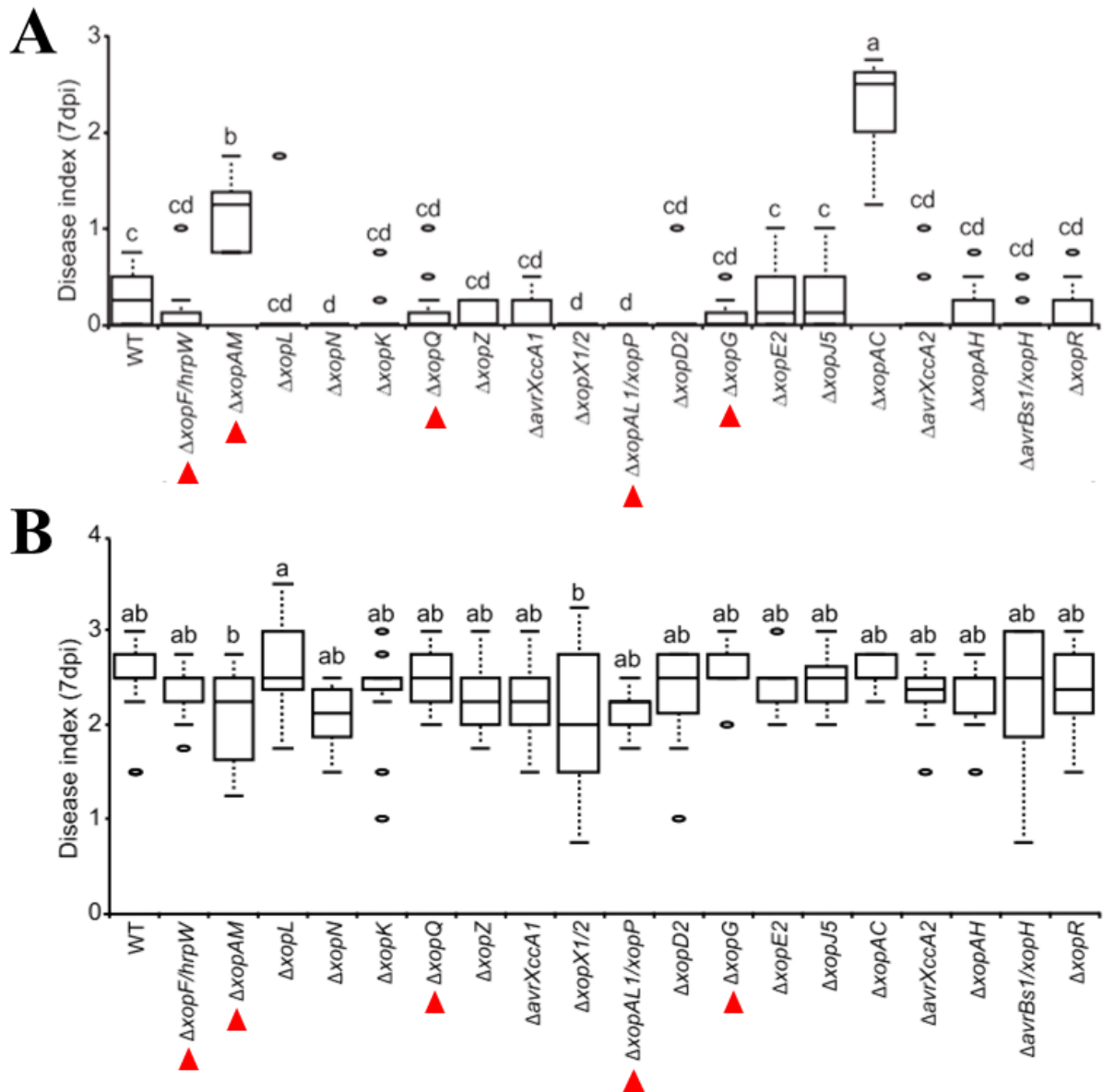


**Figure 4.2. Pathogenicity of T3E gene mutants in *Xcc8004* inoculated on *Arabidopsis* plants.** *Arabidopsis* resistant Col-0 (A) and susceptible Kas (B) ecotype plants were inoculated by piercing in the central vein at a bacterial density of  $10^8$  CFU/ml, and infection symptoms were scored at 7 days post inoculation. The disease index was as follows: 0 to 1, no symptoms; 1 to 2, weak chlorosis; 2 to 3, strong chlorosis; and 3 to 4, necrosis. Box plot representations of symptoms are as follows: middle bar, median; box limit, upper and lower quartiles; and extremes, minimum and maximum values. Statistical groups were determined using a Kruskal-Wallis test ( $p$ -value < 0.001) and are indicated by different letters. Red triangles indicate the single or double mutants for T3E genes shared with *RpsGM1000* (*hrpW*, *xopAM*, *xopQ*, *xopP* and *xopG*. *xopAG* was not tested). Adapted from Guy et al., 2013.

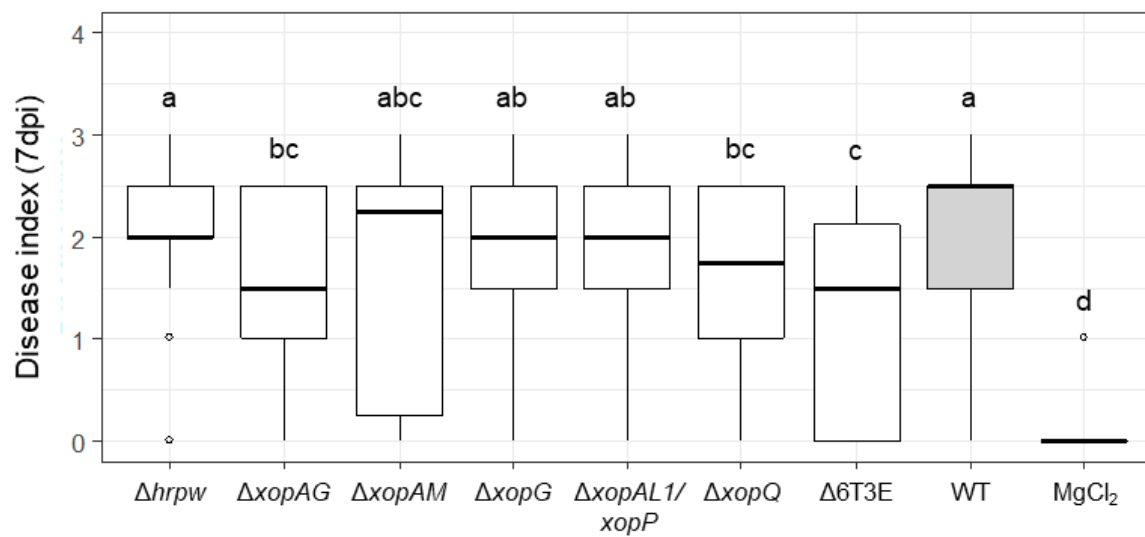


**Figure 4.3. Pathogenicity of shared T3E mutants in *Xcc*<sub>8004</sub> inoculated on *Arabidopsis* plants.** Susceptible ecotype Sf-2 *Arabidopsis* plants were inoculated by piercing in the central vein at a bacterial density of  $10^8$  CFU/ml, and infection symptoms were scored at 7 days post inoculation. Disease index is as follows: 0-1, no symptoms; 1-2, weak chlorosis around the inoculation sites; 2-3, stronger and extended chlorosis; and 3-4, necrosis. *Xcc* 8004 wild type (WT) highlighted in grey for reference. Four plants (four leaves per plant) were inoculated per condition. Two independent experiments were performed and the results were combined. Boxplot representation: thick bar, median; box limits, highest and lowest value within  $1.5 \cdot$  inter-quartile range; and circles, outliers. Statistical groups were determined using a Kruskal-Wallis test (one-tailed Wilcoxon signed-rank test p-value < 0.05) and are indicated by different letters.

As not all single shared T3E gene mutants had been tested in this study, I tested all six shared *Xcc*<sub>8004</sub> T3E mutants in a slightly less susceptible Arabidopsis ecotype, Sf-2 (**Figure 4.3**). Similar to what was observed in Kas (Guy *et al.*, 2013), in Sf-2 neither 8004 $\Delta$ *hrpW*,  $\Delta$ *xopAM* nor  $\Delta$ *xopG* showed any differences in terms of pathogenicity. Conversely, 8004 $\Delta$ *xopQ* showed a significant reduction in pathogenicity. This could indicate that the possible virulence function observed for *xopQ* depends on the Arabidopsis susceptible ecotype. As 8004 $\Delta$ *xopAG* had not been previously screened, this work is the first report of the implication of this effector in *Xcc* virulence.

To test the collective impact of the shared effectors, a sextuple mutant was created in the *Xcc*<sub>8004</sub> background. This mutant showed significantly reduced virulence compared to the wild type and most of the single T3E genes, except for  $\Delta$ *xopAG* and  $\Delta$ *xopQ*, for which the difference were not significant (**Figure 4.3**). Despite this lack of significant differences between the latter, it seems like the sextuple mutant is slightly less virulent than the single  $\Delta$ *xopAG* and  $\Delta$ *xopQ* as evidenced by the fact that these two single mutants are not significantly different to the other single T3E mutants (statistical group “bc”) whereas the sextuple mutant is (statistical group “c”). However, to confidently state this, additional complementation experiments should be performed.

### 4.3 Expressing individual bacterial T3E genes *in planta* to study their effects

In order to generate stable *A. thaliana* transgenic lines, all shared T3E genes from *Xcc*<sub>8004</sub> and *Rp*<sub>SGM11000</sub> were cloned into the chemical-inducible expression vector pER8 (Zuo, Niu and Chua, 2000). This vector allows a tight inducible expression by  $\beta$ -estradiol at low concentrations such as 8 nM, with a higher expression value than the constitutive 35S promoter at 5  $\mu$ M. Concerning the induction time, observable expression of transgene can be achieved after 30 minutes and it peaks after 24 hours. This vector also contains the coding sequence of the hygromycin phosphotransferase II, a selectable marker for plant transformation.

As part of a larger project of the team involving the generation of Arabidopsis transgenic lines for all *Xcc*<sub>8004</sub> T3E genes, most *Xcc*<sub>8004</sub> T3E genes had already been cloned into this vector and transformed in *A. tumefaciens* prior to my arrival. Due to the moderately large-scale of the screening, involving all *Xcc*<sub>8004</sub> and some *Rp*<sub>SGM11000</sub> T3E genes, no tags were added to minimize the chances of observing any kind of phenotype unrelated to the expression of the T3E

**Table 4.1. pER8-T3E transgenic Arabidopsis lines generated.** Number of transformation attempts, independent T1 plants containing T-DNA insertion verified by PCR, independent T2 lines with a 3:1 hygromycin resistance/susceptibility ratio and independent T3 homozygous lines generated per transformation and per construct.

Construct	Transformation code <sup>a</sup>	PCR positive T1 <sup>b</sup>	Segregation 3:1 T2 <sup>c</sup>	Homozygous T3 <sup>d</sup>	Total <sup>e</sup>
pER8- <i>xopG</i>	AT064	4	4	4	9
	AT119	29	12	5	
pER8- <i>xopP</i>	AT070	0	0	0	9
	AT092	31	12	9	
pER8- <i>xopQ</i>	AT071	1	0	0	7
	AT094	31	10	7	
pER8- <i>hrpW</i>	AT077	1	0	0	3
	AT105	1	0	0	
	AT127	0	0	0	
pER8- <i>xopAG</i>	AT146	14	10	3	7
	AT080	20	7	5	
	AT120	37	10	2	
pER8- <i>xopAM</i>	AT083	0	0	0	0
	AT107	0	0	0	
	AT136	0	0	0	
	AT147	1	0	0	
	AT167	0	0	0	
pER8- <i>ripAXI</i>	AT110	0	0	0	2
	AT149	20	9	2	
pER8- <i>ripAX2</i>	AT111	30	17	6	6
pER8- <i>ripB</i>	AT112	3	1	0	1
	AT150	0	0	0	
	AT170	26	3	1	
pER8- <i>ripH1</i>	AT113	3	1	1	6
	AT151	0	0	0	
	AT171	28	6	5	
pER8- <i>ripH2</i>	AT114	12	1	1	6
	AT172	9	6	5	
pER8- <i>ripH3</i>	AT115	14	6	5	10
	AT173	48	6	5	
pER8- <i>ripOI</i>	AT116	23	8	5	5
pER8- <i>ripR</i>	AT117	4	1	1	1
	AT152	0	0	0	
	AT174	4	1	0	
pER8- <i>ripW</i>	AT118	14	6	2	9
	AT175	38	8	7	

<sup>a</sup> Each code refers to one independent transformation experiment.

<sup>b</sup> Number of independent hygromycin-resistant T1 plants PCR-genotyped for the presence of the transgene (T3E-gene-specific primers).

<sup>c</sup> Number of independent T2 lines for which the percentage of hygromycin resistant plants is 60-90% (approximately 3:1 ratio).

<sup>d</sup> Number of independent T3 lines homozygous for hygromycin resistance.

<sup>e</sup> Total number of independent homozygous T3 lines per construct combining all conducted transformations.

**Table 4.2. Validation by qPCR of the transgene expression in several pER8-T3E Arabidopsis transgenic lines.** Raw crossing points (Cp) and fold change values for the expression of some shared T3E genes in 2-week-old transgenic Arabidopsis plantlets incubated for 24 hours in liquid MS supplemented with either 5  $\mu$ M  $\beta$ -estradiol or equivalent DMSO volume.

Construct	Line	Cp (Transgene) <sup>a</sup>		Cp (OXA1) <sup>a</sup>		Cp (GAPC2) <sup>a</sup>		Fold change 1 <sup>b</sup>	Fold change 2 <sup>b</sup>
		-	+	-	+	-	+		
pER8- <i>hrpW</i>	MGF 394	34.3	22.6	28.0	28.0	22.1	22.8	3258.52	5442.30
pER8- <i>hrpW</i>	MGF	>45	34.7	27.8	27.11	22.9	22.9	*	*
pER8- <i>ripH1</i>	MGF396	34.3	30.6	28.1	26.7	21.2	21.9	4.84	21.22
pER8- <i>ripH1</i>	MGF400	36.9	28.5	26.0	25.4	21.6	20.3	232.68	139.53
pER8- <i>ripH1</i>	MGF402	32.5	20.6	26.5	26.0	21.5	22.1	2744.26	5779.68
pER8- <i>ripH2</i>	MGF172	32.2	32.9	27.7	25.8	22.0	20.9	0.17	0.30
pER8- <i>ripH2</i>	MGF410	32.3	21.5	25.8	26.7	21.5	21.1	3230.83	1298.94
pER8- <i>ripH2</i>	MGF415	32.8	20.2	25.3	26.8	21.3	21.7	17506.59	8231.03
pER8- <i>ripH2</i>	MGF420	32.9	20.9	34.5	25.7	ND	20.1	9.39	ND
pER8- <i>ripH3</i>	MGF176	30.7	32.0	25.4	28.0	20.6	21.1	2.45	0.57
pER8- <i>ripH3</i>	MGF177	31.9	31.4	34.1	28.7	34.3	24.1	0.03	0.00
pER8- <i>ripH3</i>	MGF428	25.5	22.6	26.1	26.7	21.6	22.0	11.04	9.71
pER8- <i>ripH3</i>	MGF431	24.7	19.3	26.0	25.9	21.5	21.1	37.83	30.84
pER8- <i>ripOI</i>	MGF185	> 45	21.8	24.4	28.3	19.9	21.4	*	*
pER8- <i>ripOI</i>	MGF192	> 45	23.8	26.5	25.9	21.0	20.6	*	*
pER8- <i>ripOI</i>	MGF205	> 45	16.3	26.6	24.6	22.0	19.7	*	*
pER8- <i>ripOI</i>	MGF206	> 45	17.3	25.9	24.9	21.0	20.2	*	*
pER8- <i>xopAG</i>	MGF222	30.6	29.2	26.0	24.8	23.5	19.9	1.15	0.23
pER8- <i>xopAG</i>	MGF240	27.9	16.0	27.3	24.6	22.1	20.8	606.63	1558.89
pER8- <i>xopAG</i>	MGF29	28.8	16.5	27.1	24.8	22.5	20.6	1002.07	1388.66
pER8- <i>xopAG</i>	MGF34	32.2	16.8	27.5	24.5	ND	19.6	5677.79	ND
pER8- <i>xopAG</i>	MGF 36	35.1	22.3	27.6	27.2	21.8	21.9	5518.27	7858.29
pER8- <i>xopAG</i>	MGF 221	34.5	24.4	28.2	27.0	22.7	22.5	504.95	996.00
pER8- <i>xopG</i>	MGF23	35.9	19.0	ND	26.5	23.4	21.3	ND	30145.71
pER8- <i>xopG</i>	MGF 218	33.4	23.8	25.4	24.8	19.6	20.1	494.56	1112.82
pER8- <i>xopG</i>	MGF 387	33.7	19.3	26.5	27.6	21.3	22.4	45073.75	47314.67
pER8- <i>xopP</i>	MGF 52	40.0	32.5	26.9	27.1	21.5	21.2	202.25	144.01
pER8- <i>xopP</i>	MGF 59	35.7	32.8	25.2	25.6	20.5	20.5	9.19	7.36
pER8- <i>xopP</i>	MGF 77	38.1	28.0	26.7	25.9	21.2	21.8	689.78	1675.06
pER8- <i>xopQ</i>	MGF 88	35.8	37.0	26.9	26.3	21.6	21.1	0.29	0.32
pER8- <i>xopQ</i>	MGF 99	34.9	32.7	28.0	27.6	23.4	23.0	3.34	3.46
pER8- <i>xopQ</i>	MGF 101	34.8	24.8	23.7	24.6	18.9	19.7	1871.53	1746.20
pER8- <i>xopQ</i>	MGF 105	35.6	34.0	24.7	24.8	19.5	19.9	3.32	3.94

<sup>a</sup> Cp values for the amplification of the corresponding transgene and the housekeeping genes *OXA1* (AT5G62050) and *GAPC2* (AT1G13440) in inducing (+) and non-inducing (-) conditions. ND: Not determined.

<sup>b</sup> Fold change of the expression in inducing over non-inducing conditions using the reference housekeeping genes *OXA1* (1) or *GAPC2* (2). When the fold change value is lower than 1.0, the full row is highlighted in grey indicating that the line does not express the transgene inducibly. Asterisks indicate lines for which the transgene induction is perfect as there was no detectable amplification on DMSO treated samples.

transgene. Therefore, after my arrival, the cloning of the shared *Rp<sub>SGMII000</sub>* T3E genes following the same strategy was conducted. The subsequent *A. tumefaciens*-mediated transformation of *A. thaliana* Col-0 plants with all shared *Xcc<sub>8004</sub>* and *Rp<sub>SGMII000</sub>* T3E genes was performed. Homozygous single-copy-insertion plants were selected in the T3 generation after being tested for T-DNA presence by hygromycin resistance and PCR at the T1 and T2 generations, and for a 3:1 segregation ratio typical of single T-DNA insertions at the T2 generation. When possible, several independent transgenic lines for each T3E construct were selected (**Table 4.1**). No transgenic plants were generated for only one of the shared T3E genes after five unfruitful transformation attempts: *Xcc<sub>8004</sub> xopAM*. For other two genes, *Rp<sub>SGMII000</sub> ripB* and *ripR* (the ortholog of *xopAM*), only one homozygous line could be generated. For the rest of T3E genes, 2 to 10 independent homozygous lines were generated. The inducible expression of the transgene in some of the generated transgenic lines was validated by qPCR (**Table 4.2**).

#### 4.3.1 Nine shared T3Es confer different developmental alterations when expressed in Arabidopsis

As the different pER8-T3E-gene transgenic lines were generated, they were first phenotyped *in vitro* to detect any possible macroscopic developmental alteration. To this end, seeds were grown on MS plates supplemented with either 5  $\mu$ M  $\beta$ -estradiol or equivalent dimethylsulphoxide (DMSO) volume for two weeks (**Table 4.3** and **figure 4.4**). For five shared T3E-gene transgenic lines, no differences were observed between the induced and non-induced plants in none of the independent lines: *hrpW*, *ripAX1*, *ripAX2*, *ripB* and *ripW* (**Figures 4.4A, 4.4L-N** and **4.4X**). This indicates that the expression of these five transgenes does not necessarily cause any observable developmental alteration. A drastic growth arrest upon induction was observed on several independent lines of the following transgenes: *xopAG*, *ripH1*, *ripH2* and *ripR* (only one line available for the latter) (**Figures 4.4B, 4.4O, 4.4Q** and **4.4W**). Alterations in root architecture were observed for *xopAG*, *xopG*, *xopQ* and *xopP*. They all showed shorter primary roots (**Figures 4.4C, 4.4E, 4.4H** and **4.4J**), except *xopP* for which several lines also showed an increased number of lateral roots (**Figure 4.4G**). Phenotypes on the aerial parts were observed in *ripH3* and *ripOI* transgenic lines. For four independent *ripH3* transgenic lines, the growth of the aerial parts was blocked at the cotyledon stage (**Figure 4.4S**), whereas several transgenic *ripOI* lines showed chlorosis or early bolting (**Figure 4.4U-V**).

**Table 4.3. *In vitro* phenotypes of pER8-T3E transgenic Arabidopsis plantlets.** Description of the different phenotypes observed on transgenic Arabidopsis lines of the shared T3E genes of *Xcc8004* and *RpSGM11000*. For each construct, a brief description of the phenotype observed after two weeks grown on MS plates supplemented with either 5  $\mu$ M  $\beta$ -estradiol or equivalent DMSO volume, with the corresponding figure panel and number of independent homozygous out of the total number of lines tested.

Construct	Phenotype <i>in vitro</i> <sup>a</sup>	Example figure	Number lines/total <sup>b</sup>
pER8- <i>hrpW</i>	ND	Fig. 4A	2/2
pER8- <i>xopAG</i>	Growth arrest	Fig. 4B	2/7
	Shorter primary roots	Fig. 4C	2/7
	ND	Fig. 4D	3/7
pER8- <i>xopG</i>	Smaller roots	Fig. 4E	1/8
	ND	Fig. 4F	7/8
pER8- <i>xopP</i>	More lateral roots	Fig. 4G	6/9
	Shorter primary roots	Fig. 4H	2/9
	ND	Fig. 4I	1/9
pER8- <i>xopQ</i>	Shorter primary roots	Fig. 4J	2/7
	ND	Fig. 4K	5/7
pER8- <i>ripAX1</i>	ND	Fig. 4L	2/2
pER8- <i>ripAX2</i>	ND	Fig. 4M	6/6
pER8- <i>ripB</i>	ND	Fig. 4N	1/1
pER8- <i>ripH1</i>	Growth arrest	Fig. 4O	2/5
	ND	Fig. 4P	3/5
pER8- <i>ripH2</i>	Growth arrest	Fig. 4Q	3/4
	ND	Fig. 4R	1/4
pER8- <i>ripH3</i>	Blocked at cotyledon stage	Fig. 4S	4/9
	ND	Fig. 4T	5/9
pER8- <i>ripO1</i>	Chlorosis	Fig. 4U	3/5
	Early bolting	Fig. 4V	3/5
pER8- <i>ripR</i>	Growth arrest	Fig. 4W	1/1
pER8- <i>ripW</i>	ND	Fig. 4X	4/4
Col-0 (control)	ND	Fig. 4Y	-

<sup>a</sup> Description of the phenotype observed. ND: No differences observed between induced and non-induced plants.

<sup>b</sup> Number of independent homozygous lines presenting the mentioned phenotype out of the total number of phenotyped lines from the same construct.

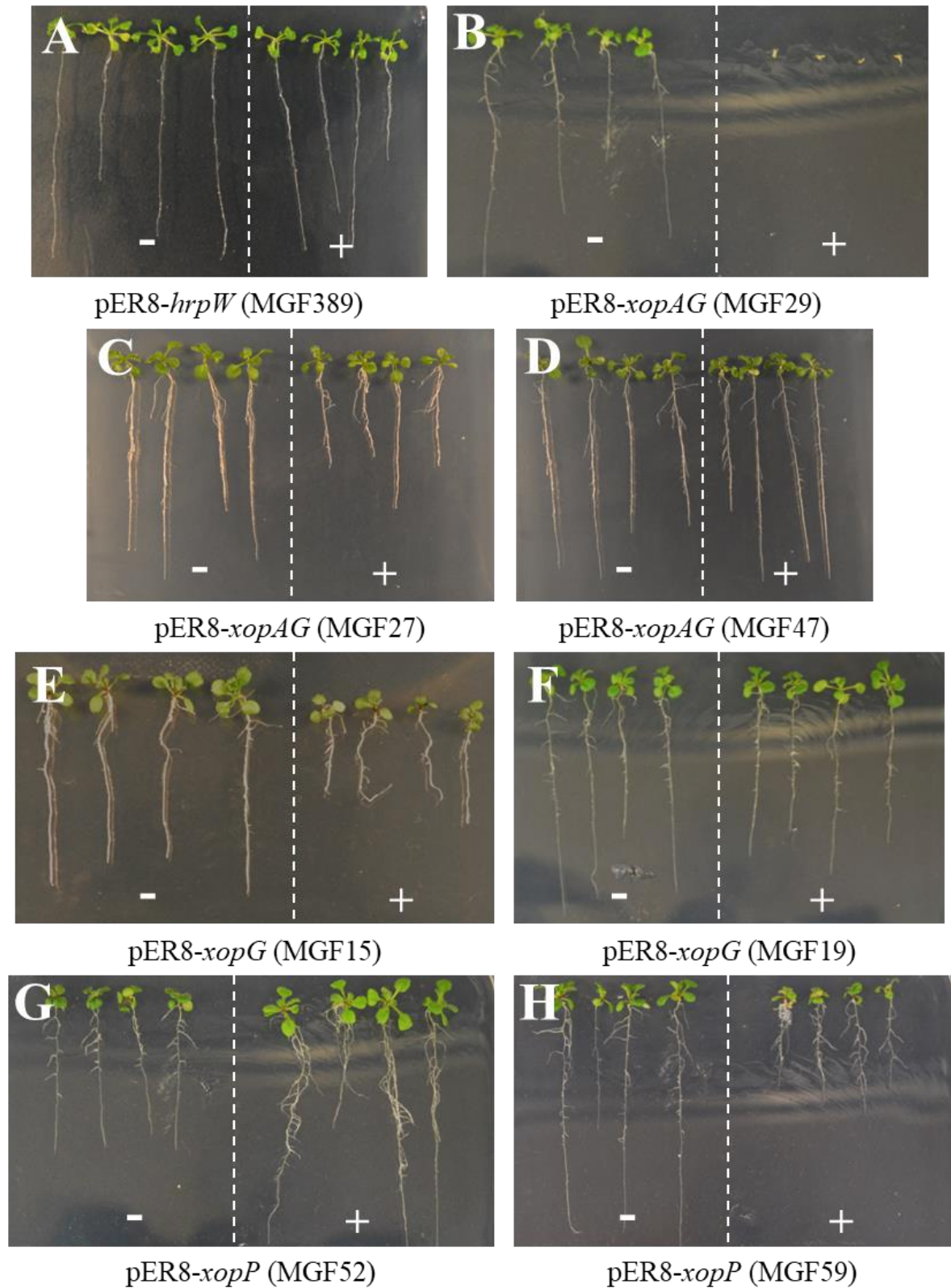


**Figure 4.4 (1/3).** Examples of phenotypes observed on T3E transgenic *Arabidopsis* plantlets. Photos of *Arabidopsis* plantlets grown for 2 weeks on MS-agar plates supplemented with either 5  $\mu$ M  $\beta$ -estradiol (+) or equivalent DMSO volume (-). The number of independent lines per construct showing a similar phenotype is presented in **table 4.2**.



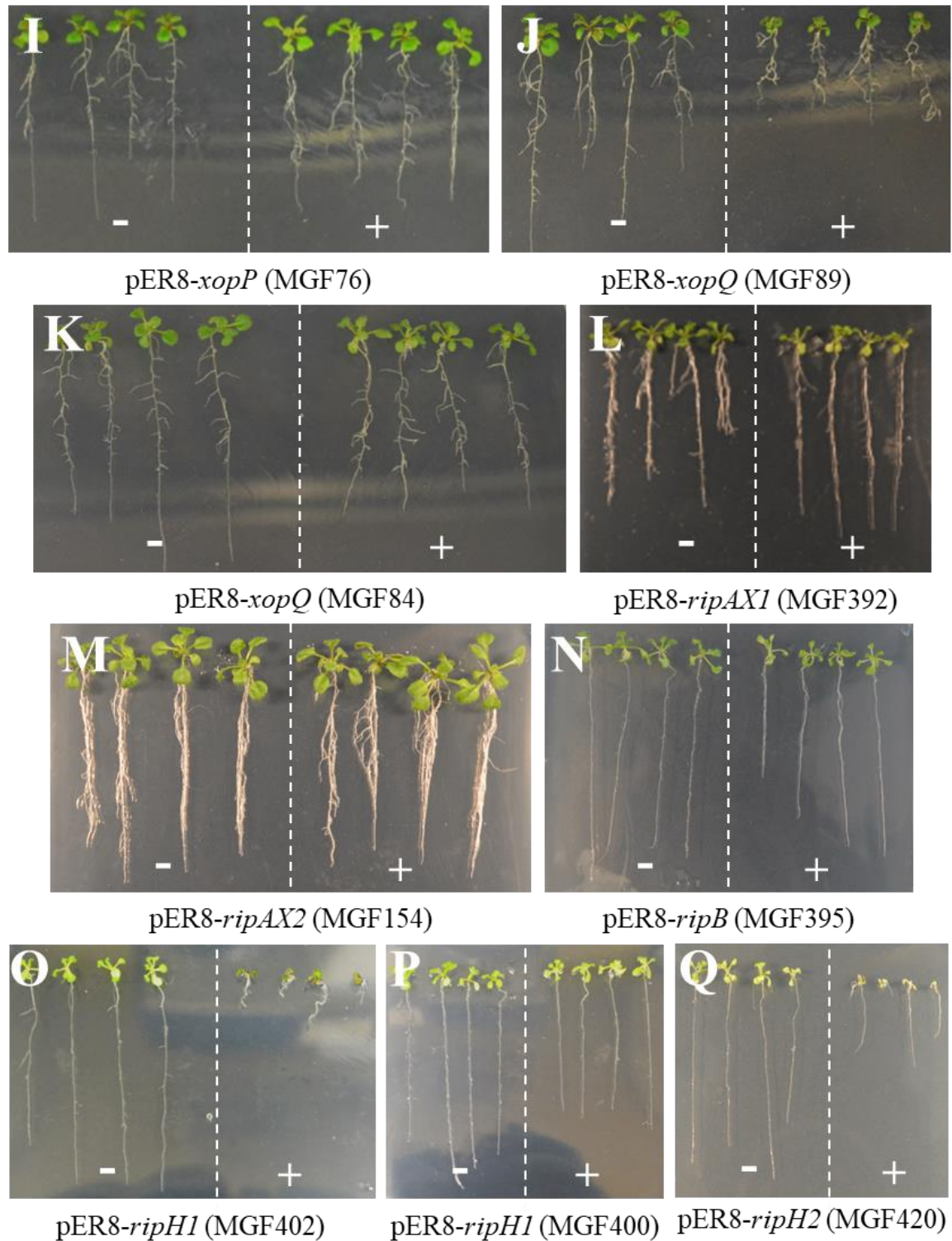


**Figure 4.4 (2/3).** Examples of phenotypes observed on T3E transgenic *Arabidopsis* plantlets. Photos of *Arabidopsis* plantlets grown for 2 weeks on MS-agar plates supplemented with either 5  $\mu$ M  $\beta$ -estradiol (+) or equivalent DMSO volume (-). The number of independent lines per construct showing a similar phenotype is presented in **table 4.2**.

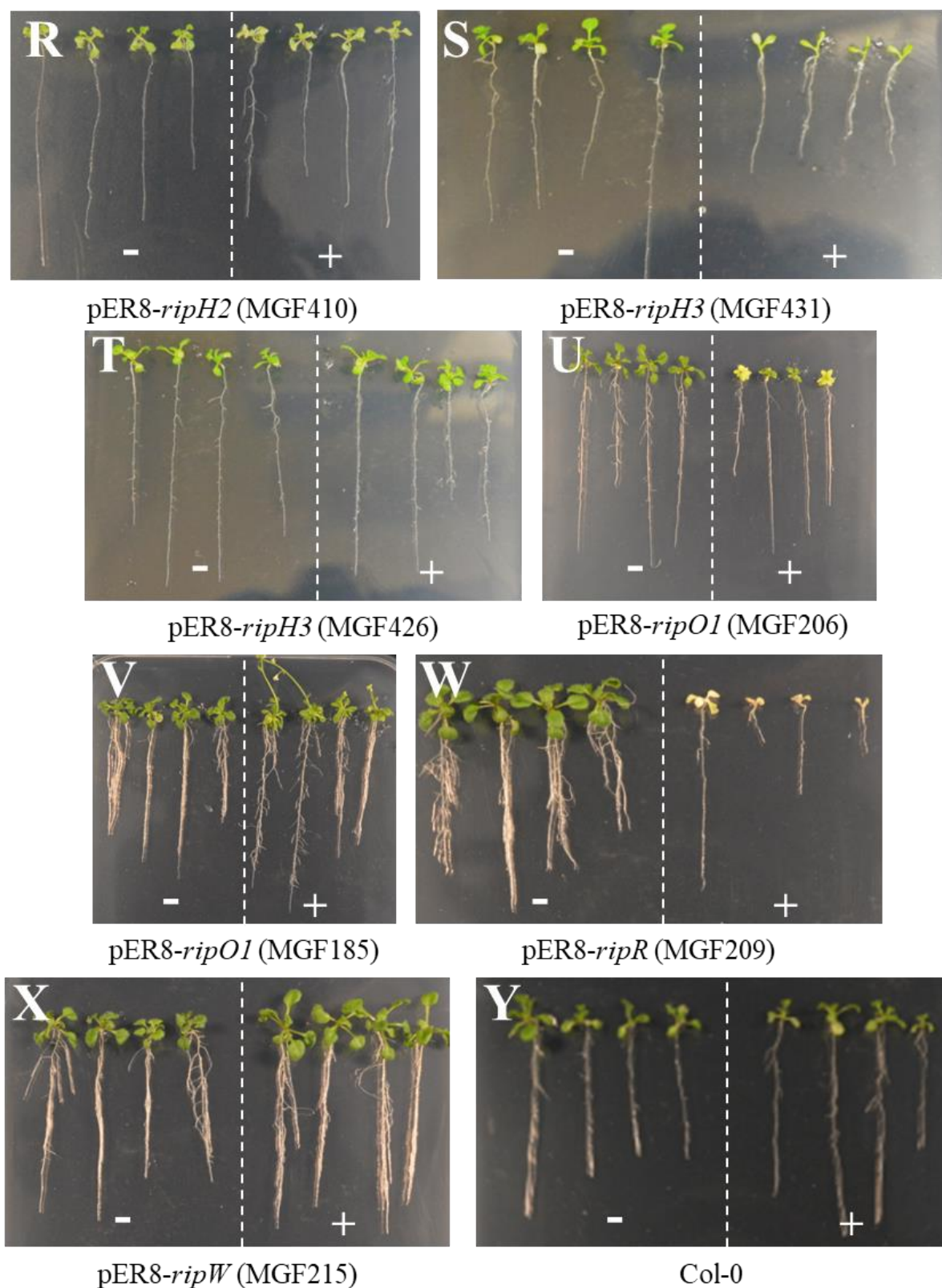


**Figure 4.4 (3/3). Examples of phenotypes observed on T3E transgenic Arabidopsis plantlets.** Photos of Arabidopsis plantlets grown for 2 weeks on MS-agar plates supplemented with either 5  $\mu$ M  $\beta$ -estradiol (+) or equivalent DMSO volume (-). The number of independent lines per construct showing a similar phenotype is presented in **table 4. 2**.

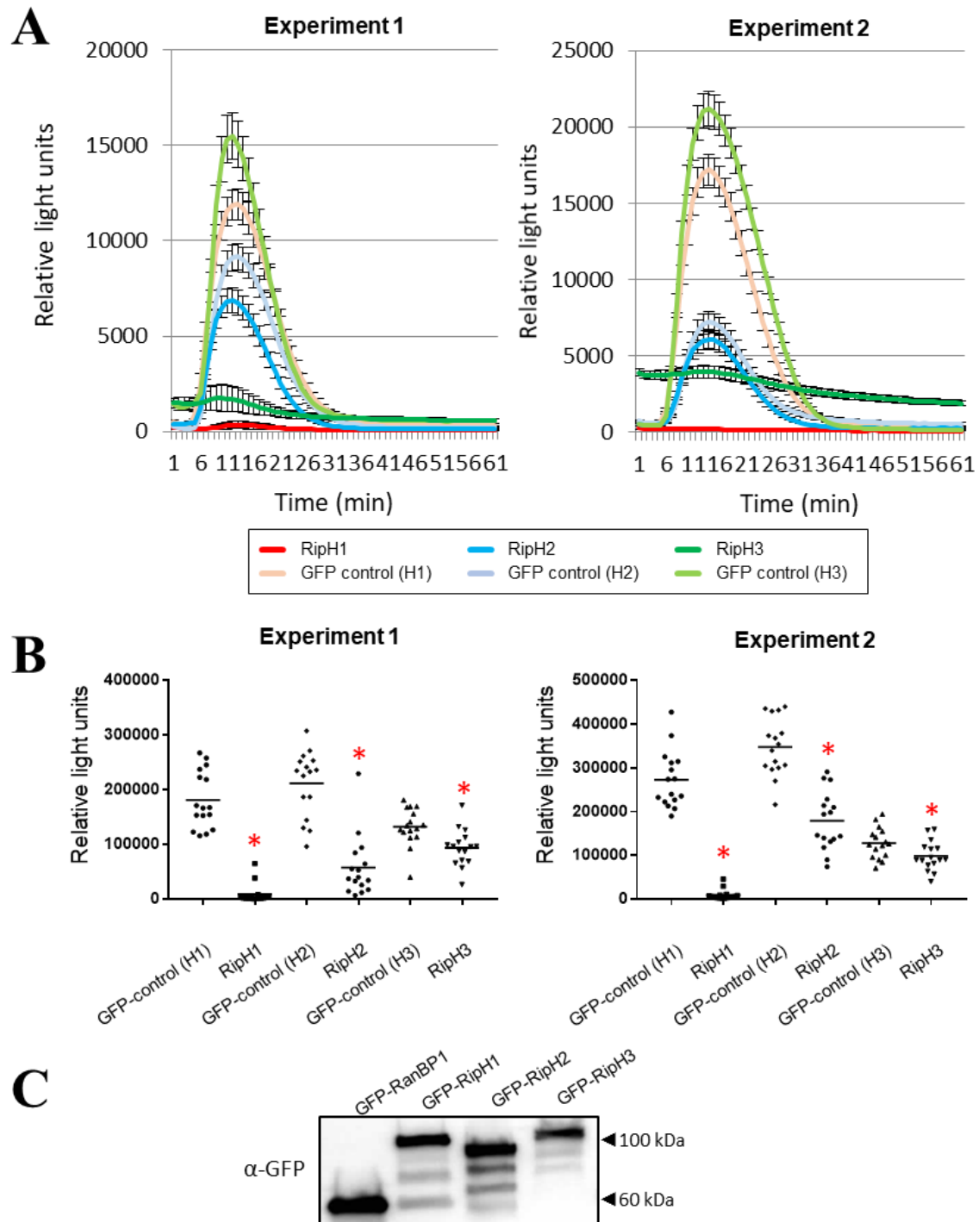


**Figure 4.5. Transient RipH1, RipH2 and RipH3 expression in *N. benthamiana* inhibits flg22-induced ROS production.** Indirect measurement of ROS production after flg22 treatment by luminometry on *N. benthamiana* leaves upon *Agrobacterium tumefaciens*-mediated expression of GFP-RipH1, -RipH2 or -RipH3 (darker colors) or GFP-RanBP1 (control, lighter colors). Measurement of the ROS production over time on average (A) or integrated over one hour (B). Error bars represent the standard error of the mean on 16 leaf disk samples. Horizontal black lines represent the average. Red asterisks indicate significant differences with the respective control (Mann-Whitney test  $p$ -value  $< 0.05$ ). Results from two independent experiments are shown. (C) Western blot showing the expression of GFP-RipH1, -RipH2, -RipH3 and -RanBP1 fusion proteins detected with an anti-GFP antibody. Adapted from Arry Morel PhD thesis, INP, Toulouse, 2018.

### 4.3.2 The orthologs RipH1-3 and XopP inhibit plant basal defenses

To have an idea of the possible involvement of the T3Es in the subversion of plant defense responses, the production of ROS upon flg22 induction, a classical readout of plant early defense responses, was measured by luminometry in some of the generated transgenic Arabidopsis lines (Sang and Macho, 2017). The partial inhibition of the flg22-induced ROS burst had already been described for *ripH1*, *ripH2* and *ripH3* when transiently expressed in *N. benthamiana* (**Figure 4.5**) (Morel, 2018). As transgenic Arabidopsis lines for these three genes had been generated, they were first screened for inhibition of flg22-induced ROS production. To discard any possible effect of the  $\beta$ -estradiol, the ROS production in Arabidopsis Col-0 leaf samples was measured upon  $\beta$ -estradiol or DMSO treatment (**Figure 4.6**). Indeed, the flg22-induced ROS production does not seem to be altered by the  $\beta$ -estradiol treatment indicating that the pER8 transgenic lines can be used in this screening. Two independent qPCR-validated transgenic lines were screened per *ripH* transgene (**Figure 4.7** and **4.8**). Contrary to what was observed in *N. benthamiana*, none of the transgenic Arabidopsis lines showed a clear inhibition of the flg22-induced ROS production upon induction of the transgene expression compared to the DMSO-treated samples.

It is noteworthy that the values of relative luminescence obtained are generally much lower than those observed in *N. benthamiana* leaves. Indeed, when comparing in a same experiment flg22- and water-treated leaf samples from *N. benthamiana* and Arabidopsis, the first produced 12 times more ROS than the latter (**Figure 4.9**). This higher production of ROS provides a larger margin to observe partial inhibition in *N. benthamiana* that would be harder to observe in Arabidopsis. This could potentially explain the lack of coherence between the results in these two species, although it cannot be ruled out that the behavior of the RipH effectors varies according to the plant species. In an attempt to optimize the ROS measurement in Arabidopsis, increasing concentrations of flg22 were tested but the ROS production was not altered indicating that the flg22 is not the limiting factor (**Figure 4.10**).

Considering the better performance of the transient expression in *N. benthamiana* leaves, the T3E-mediated inhibition of the flg22-induced ROS production was no further measured in other Arabidopsis lines. However, given the described inhibition of the flg22-induced ROS production for the three *RpsGM11000* RipH T3Es (Morel, 2018) (**Figure 4.5**), its *Xcc8004* ortholog, XopP, was screened similarly in agroinfiltrated *N. benthamiana* leaves. Similar to RipH1, XopP inhibits almost totally the flg22-induced ROS production (**Figure 4.11**).

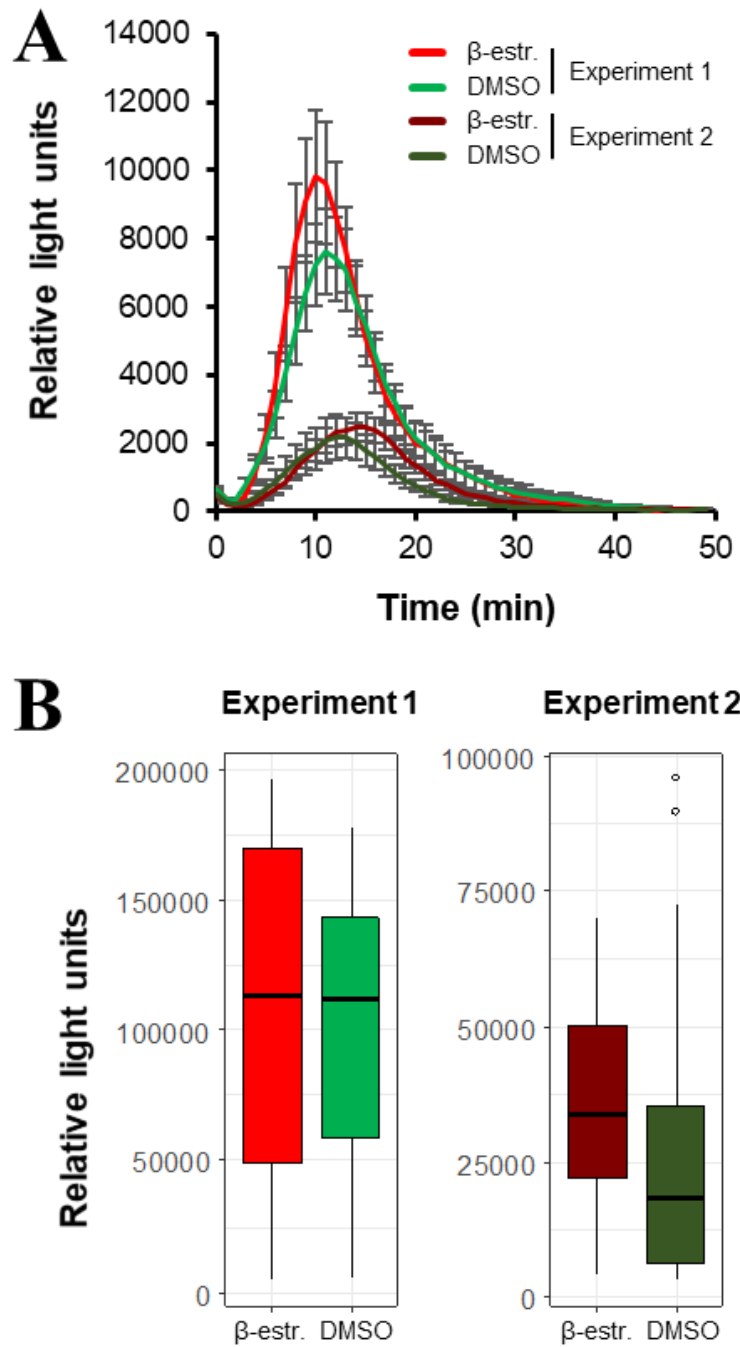


**Figure 4.6.  $\beta$ -estradiol treatment does not alter the flg22-induced ROS production in Arabidopsis Col-0 plants.** Indirect measurement of ROS production upon 50 nM flg22 treatment by luminometry on 4-week-old Arabidopsis Col-0 plants treated for 24 hours with either 5  $\mu$ M  $\beta$ -estradiol (red) or equivalent DMSO volume (green). Measurement of the ROS production over time on average (A) or integrated over one hour (B). Error bars represent the standard error of the average on 16 leaf disk samples. Boxplots representation meaning: thick bar, median; box limits, highest and lowest value within 1.5  $\cdot$  inter-quartile range; and circles, outliers. No significant differences were observed between  $\beta$ -estradiol treated samples and the respective DMSO controls (one-tailed Wilcoxon signed-rank test p-value < 0.05). Results from two independent experiments are shown.



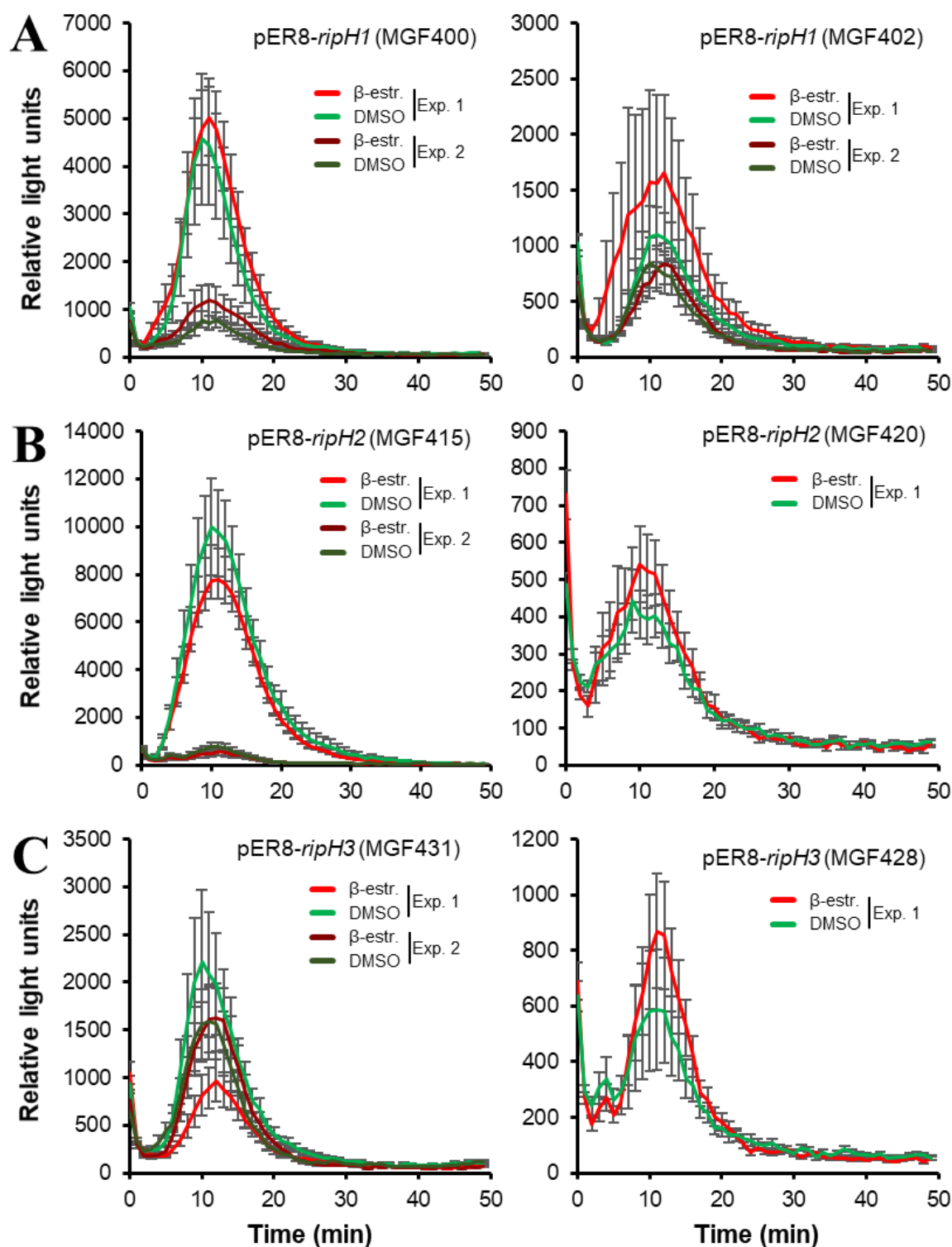


**Figure 4.7. RipH1, RipH2 and RipH3 expression in Arabidopsis does not inhibit flg22-induced ROS production.** Indirect measurement of ROS production over time upon 50 nM flg22 treatment by luminometry on 4-week-old Arabidopsis plants treated for 24 hours with either 5  $\mu$ M  $\beta$ -estradiol (red) or equivalent DMSO volume (green). Two independent lines per construct were tested: pER8-*ripH1* (A), pER8-*ripH2* (B), and pER8-*ripH3* (C). Error bars represent the standard error of the average on 16 leaf disk samples. Results from two independent experiments, when available, are shown.

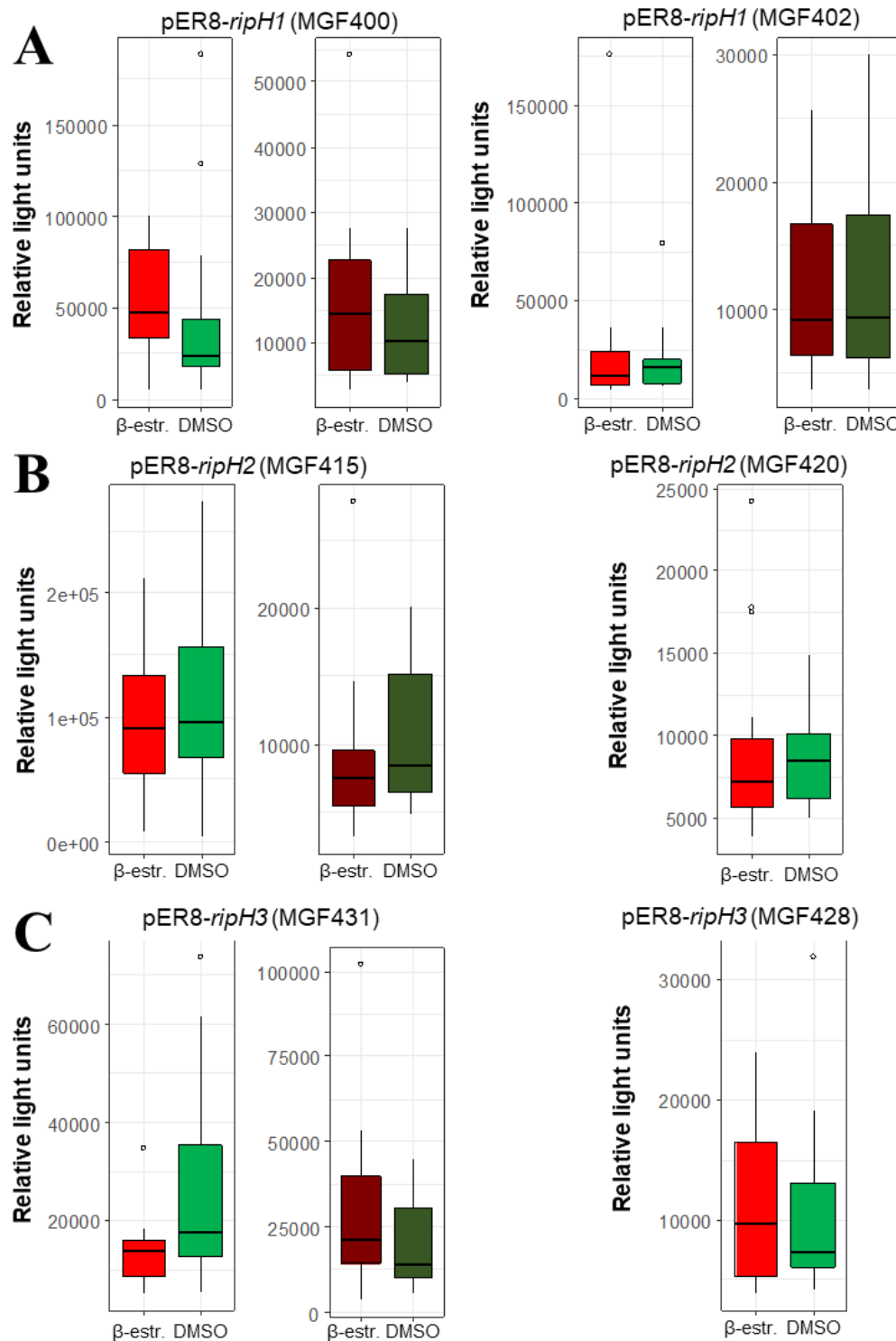


**Figure 4.8. RipH1, RipH2 and RipH3 expression in Arabidopsis does not inhibit flg22-induced ROS production.** Measurement of the ROS production upon 50 nM flg22 treatment integrated over 1 hour as shown in **figure 4.7**. Two independent lines per construct were tested: pER8-ripH1 (A), pER8-ripH2 (B), and pER8-ripH3 (C). Boxplots representation meaning: thick bar, median; box limits, highest and lowest value within  $1.5 \cdot$  inter-quartile range; and circles, outliers. No significant differences were observed between 5  $\mu$ M  $\beta$ -estradiol treated samples and the respective DMSO controls (one-tailed Wilcoxon signed-rank test  $p$ -value  $< 0.05$ ). Results from two independent experiments, when available are, shown.

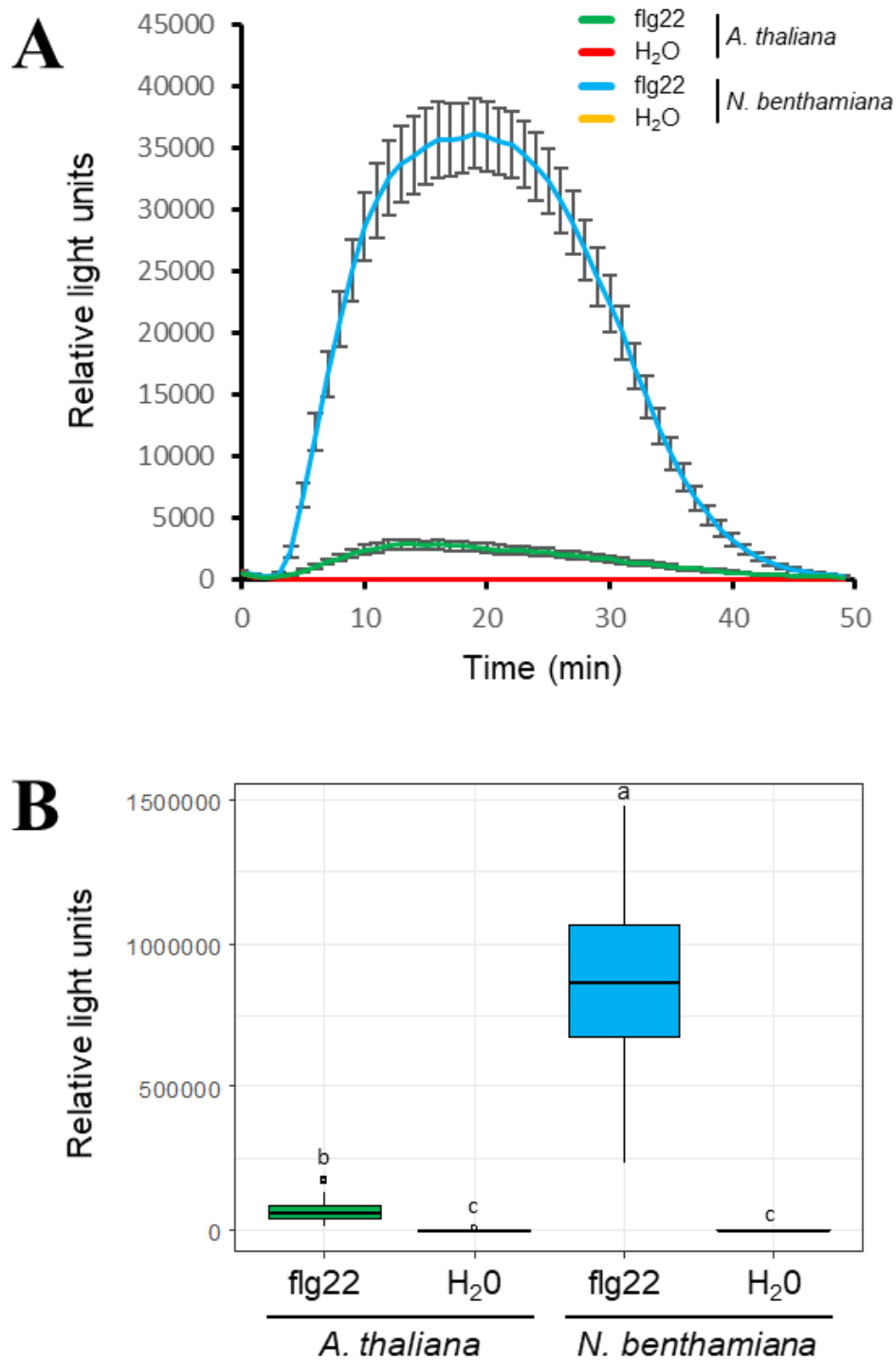


**Figure 4.9. *N. benthamiana* produces more ROS upon flg22 treatment than *A. thaliana*.** Indirect measurement of ROS production upon either 50 nM flg22 or water-mock treatment by luminometry on either 4-week-old *A. thaliana* or *N. benthamiana* leaves. Measurement of the ROS production over time on average (A) or integrated over one hour (B). Error bars represent the standard error of the average on 48 leaf disk samples. Boxplots representation meaning: thick bar, median; box limits, highest and lowest value within  $1.5 \cdot$  inter-quartile range; and circles, outliers. Statistical groups were determined using a Kruskal-Wallis test (one-tailed Wilcoxon signed-rank test  $p$ -value  $< 0.05$ ) and are indicated by different letters.



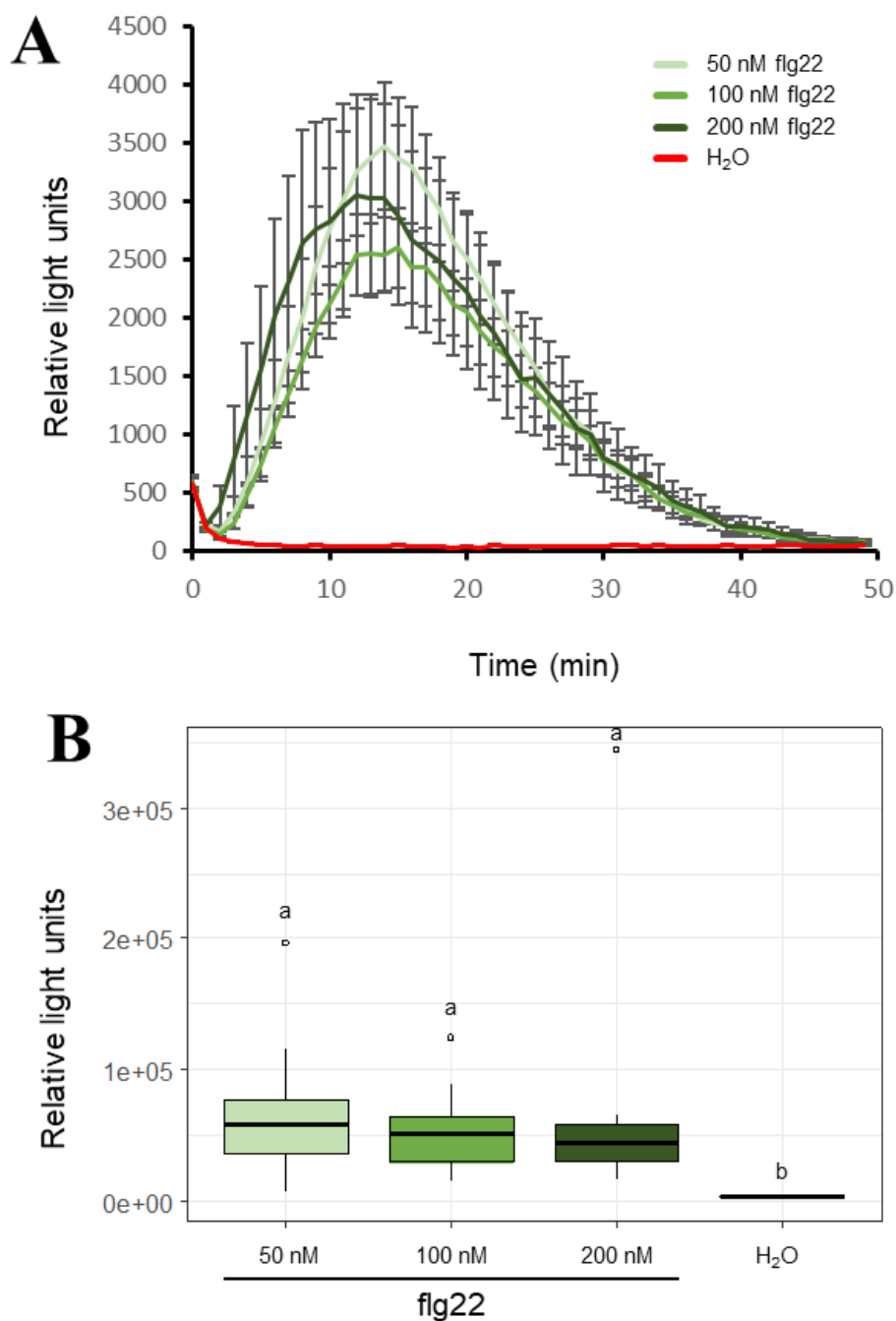


**Figure 4.10. The concentration of flg22 is not the limiting factor for the weak production of ROS in Arabidopsis.** Indirect measurement of ROS production upon either different concentrations of flg22 (different shades of green) or water-mock (red) treatment by luminometry on 4-week-old *A. thaliana* Col-0 plants. 50 nM flg22 is the concentration used in all tests previously presented (figures 5-9). Measurement of the ROS production over time on average (A) or integrated over one hour (B). Error bars represent the standard error of the average on 16 leaf disk samples. Boxplots representation meaning: thick bar, median; box limits, highest and lowest value within 1.5 · inter-quartile range; and circles, outliers. Statistical groups were determined using a Kruskal-Wallis test (one-tailed Wilcoxon signed-rank test p-value < 0.05) and are indicated by different letters.

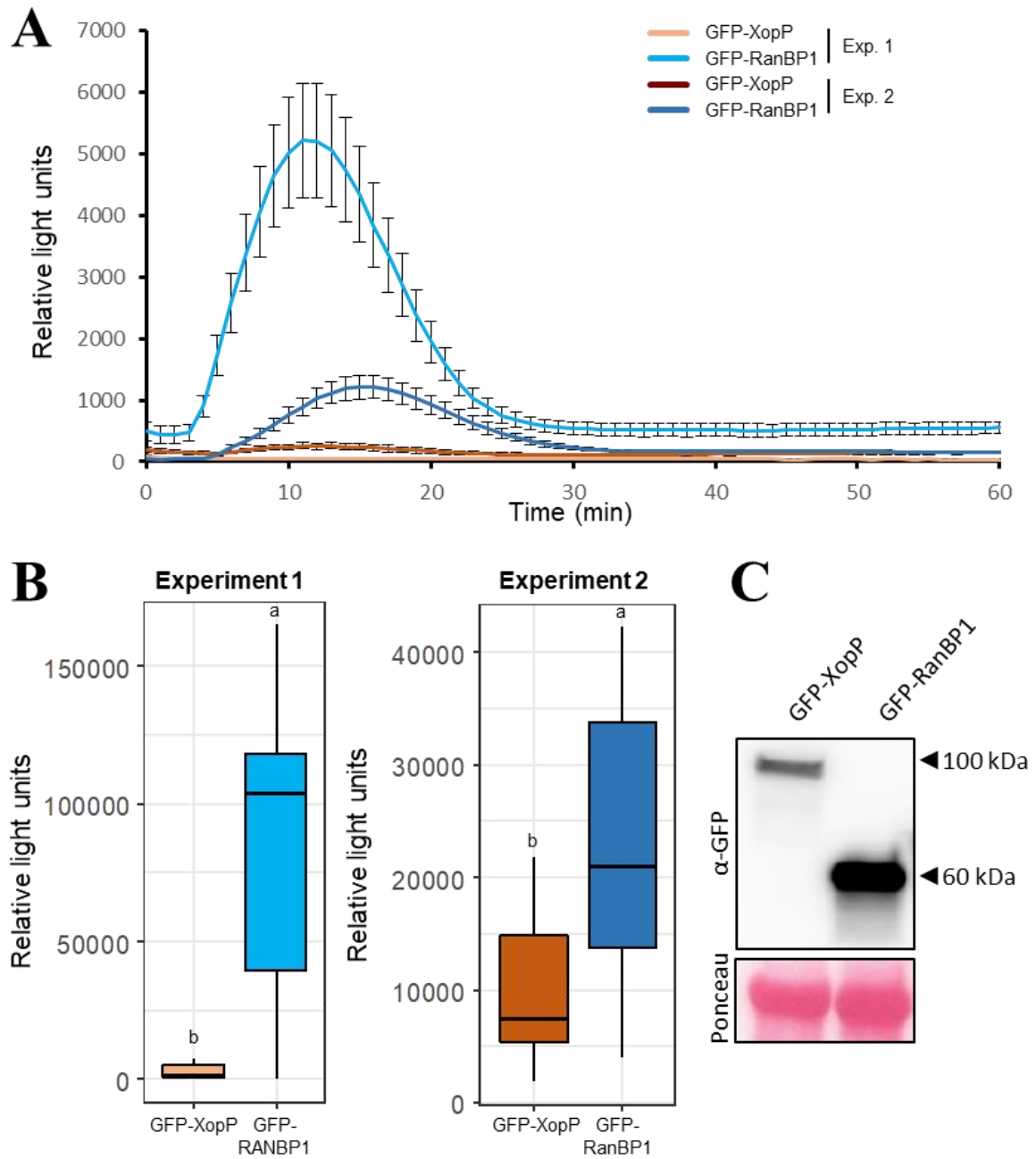


**Figure 4.II. Transient XopP expression in *N. benthamiana* inhibits flg22-induced ROS production.** Indirect measurement of ROS production after 50 nM flg22 treatment by luminometry on *N. benthamiana* leaves upon *A. tumefaciens*-mediated expression of GFP-XopP (orange) or GFP-RanBP1 control (blue). Measurement of the ROS production over time on average (A) or integrated over one hour (B). Error bars represent the standard error of the mean on 16 leaf disk samples. Boxplots representation meaning: thick bar, median; box limits, highest and lowest value within 1.5 · inter-quartile range; and circles, outliers. Statistical groups were determined are indicated by different letters (one-tailed Wilcoxon signed-rank test p-value < 0.05). Results from two independent experiments. (C) Western blot showing the expression of GFP-XopP and GFP-RanBP1 fusion proteins detected with an anti-GFP antibody. Ponceau S staining used as loading control.

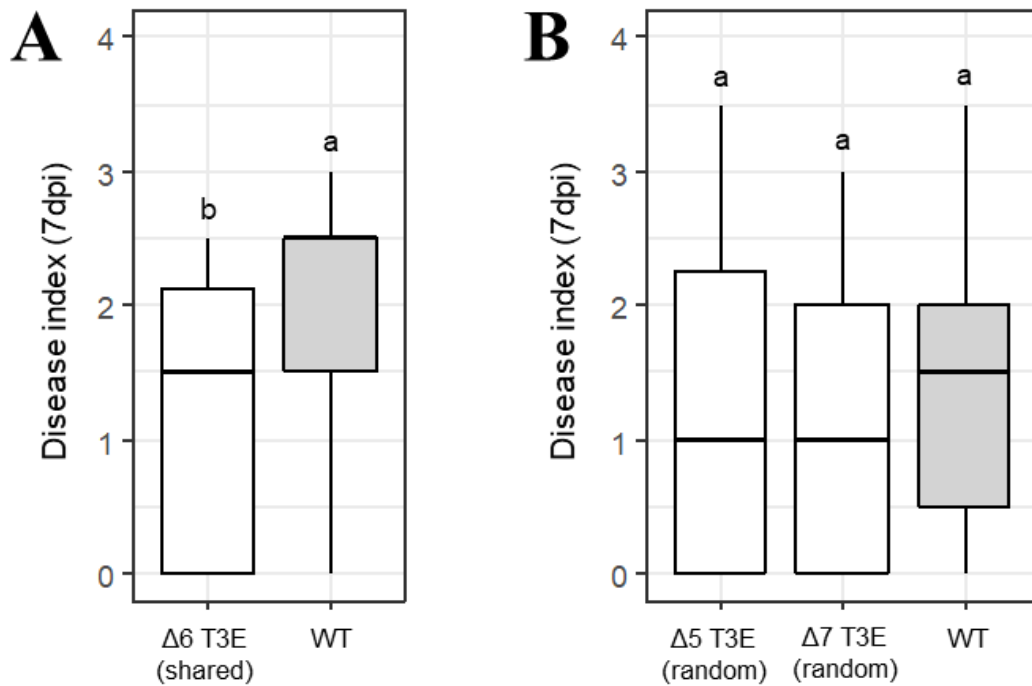


**Figure 4.12. Pathogenicity of different combination of multiple T3E mutants in *Xcc8004* inoculated on *Arabidopsis*.** Susceptible ecotype Sf-2 *Arabidopsis* plants were inoculated by piercing in the central vein at a bacterial density of  $10^8$  CFU/ml, and infection symptoms were scored at 7 days post inoculation. The genes mutated for each polymutant are as follows: Δ6 T3E (shared): *hrpW*, *xopAG*, *xopAM*, *xopG*, *xopP* and *xopQ*; Δ5 T3E (random): *avrBsl*, *xopAC*, *xopH*, *xopXI* and *xopX2*; and Δ7 T3E (random): same as Δ5 plus *hrpW* and *xopF*. Disease index is as follows: 0-1, no symptoms; 1-2, weak chlorosis around the inoculation sites; 2-3, stronger and extended chlorosis; and 3-4, necrosis. *Xcc8004* wild type highlighted in grey for reference. Four plants (four leaves per plant) were inoculated per condition. Two (A) or three (B) independent experiments were performed and the results were combined. Boxplot representation meaning: thick bar, median; box limits, highest and lowest value within  $1.5 \cdot$  inter-quartile range; and circles, outliers. Statistical groups were determined using a Kruskal-Wallis test (one-tailed Wilcoxon signed-rank test  $p$ -value  $< 0.05$ ) and are indicated by different letters. Data from (A), extracted from figure 4.3; and data from random polymutant (B), obtained from E. Lauber (unpublished).

Additionally, other shared T3Es were screened for inhibition of ROS production in *N. benthamiana* leaves but these results are presented and discussed in the chapters five (XopAG and RipOI) and six (XopJ6).

## 4.4 Discussion

### ***Rps* and *Xcc* T3Es work collectively in bacterial pathogenicity**

In this second part of the results, the contribution of the shared T3Es between *Xcc*<sub>8004</sub> and *Rps*<sub>SGM11000</sub> in the bacterial pathogenicity and in the modulation of the plant physiology and defenses was evaluated. The translocation of T3Es through the T3SS is the major pathogenicity determinant on both *Rps* and *Xcc* (Boucher, Barberis and Demery, 1985; Arlat *et al.*, 1991). However, the contribution of single T3Es to the bacterial pathogenicity is negligible for many of them as it has been shown in previously (Cunnac *et al.*, 2004; Guy *et al.*, 2013), and in this work (**Figures 4.1-4.3**). This proves that *Rps* and *Xcc* effectors, like those from other plant pathogens, are “collectively essential but individually dispensable” (Kvitko *et al.*, 2009; Macho *et al.*, 2012). This collective action of *Xcc* T3Es was shown in the present work by the small additive effect of the sextuple mutant lacking all six shared T3Es between *Xcc*<sub>8004</sub> and *Rps*<sub>SGM11000</sub> (**Figure 4.3**). To test whether the random deletion of six other T3Es has the same impact on *Xcc* pathogenicity, this result was compared to a different polymutant generated in the team in the context of a different project (a quintuple and a septuple mutant were used instead because no sextuple mutant had been generated) (**Figure 4.12**). Contrary to the sextuple mutant for the shared effectors, neither the quintuple nor the septuple random mutants showed a significant decrease in *Xcc* pathogenicity. This could suggest that the shared T3Es contribute more to *Xcc* pathogenicity than other randomly picked T3Es. However, to confidently state that the shared T3Es are indeed more important for *Xcc* pathogenicity than the rest of T3Es, more multiple deletion combinations should also be tested. If the contribution to *Xcc* pathogenicity of the shared T3Es were shown to be indeed relevant, it would be interesting to test whether the corresponding nine T3Es in *Rps* also have a similar impact. Another point to discuss about the collective effect of the shared T3Es in *Xcc* pathogenicity is the contribution of *xopQ* and *xopAG*, the only two genes for which single mutants were significantly impaired in pathogenicity (**Figure 4.3**). Is the decreased pathogenicity of the sextuple mutant a product of the deletion of these only two genes or a true collective effect of the six? Single and multiple complementations of

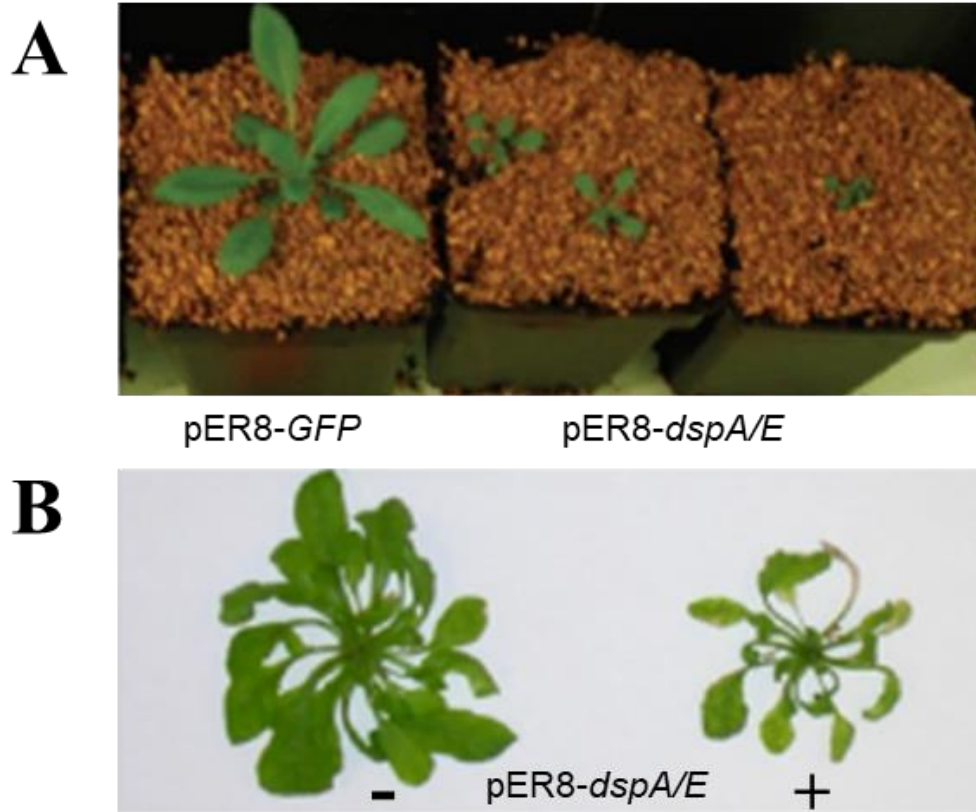


**Figure 4.B. XopAM and RipR ortholog in *Erwinia amylovora*, DspA/E, is toxic when expressed in *A. thaliana*.** (A) Phenotype of four-week-old pER8-GFP and pER8-dspA/E plants grown in non-inducing conditions. (B) Five-week-old pER8-dspA/E transgenic plants were sprayed each day with 5  $\mu$ M  $\beta$ -estradiol (+) or DMSO (-) for 3 weeks. The photograph shows representative plants for each treatment. Adapted from Degraeve *et al.*, 2013.

the different shared T3E genes in the sextuple mutant background would allow answering this question.

This work represents the first report for the involvement of XopQ and XopAG genes in *Xcc* pathogenicity (**Figure 4.3**). XopQ is a known virulence factor in the *X. euvesicatoria*/tomato and pepper (Teper *et al.*, 2014), and *X. oryzae* pv. *oryzae*/rice pathosystems (Deb *et al.*, 2019), targeting plant 14-3-3 proteins in both cases. This virulence mechanism is shared with its ortholog in *P. syringae*, HopQ1, which also targets 14-3-3 proteins in tomato and *N. benthamiana* (Giska *et al.*, 2013; Li *et al.*, 2013). Both XopQ and HopQ1, together with their *Rps* ortholog, RipB, confer resistance in *Nicotiana* spp. in a *Roql*-dependent manner (Adlung *et al.*, 2016; Schultink *et al.*, 2017; Nakano and Mukaihara, 2019). Less known is the involvement of XopAG in virulence, which has not been reported in other *Xanthomonas*. Its *X. fuscans* ssp. *aurantifolii* orthologs, AvrGf1 and AvrGf2, confer avirulence in different citrus through interaction with chloroplastic cyclophilins (Gochez *et al.*, 2015, 2017). Conversely, XopAG ortholog in *P. syringae*, HopG1, is a known virulence factor targeting the mitochondria (Block *et al.*, 2010), and remodeling the actin cytoskeleton (Shimono *et al.*, 2016).

### ***Rps* and *Xcc* T3Es are able to modulate *Arabidopsis* development**

Despite their role in bacterial pathogenicity, the possible effects of the T3Es directly in the plant were dissected through transgenesis. Inducible T3E transgenic *Arabidopsis* lines were generated for fourteen out of the fifteen shared T3Es between *Xcc*<sub>8004</sub> and *Rps*<sub>SGM11000</sub> (**Table 4.1**). The only T3E gene for which no transgenic lines could be generated was XopAM. This gene belongs to the AvrE family of T3Es present in several other Gram-negative plant pathogenic bacteria such as *P. syringae* (AvrE), *Erwinia amylovora* (DspA/E), *Pantoea stewartii* (WtsE) and *Rps* (RipR). These T3Es are important virulence factors inhibiting SA-mediated basal defenses and promoting disease necrosis (DebRoy *et al.*, 2004). *E. amylovora* DspA/E has been shown to be toxic when heterologously expressed in yeast (Siamer *et al.*, 2011), or under inducible expression in *Arabidopsis* where even a residual leaky expression leads to important growth defects (**Figure 4.1B**) (Degrave *et al.*, 2013). *Rps* RipR also seems to affect drastically the growth of *Arabidopsis* (**Figure 4.4W**). The leaky expression of the pER8 system together with the high toxicity of the AvrE T3E family members could explain why no pER8-*xopAM* and only one pER8-*ripR* lines were obtained after several transformation attempts (**Table 4.1**).

In total, the inducible expression of single T3E genes *in planta* led to different developmental phenotypes for nine out of the 14 T3E genes tested (**Table 4.3** and **figure 4.4**).

These differences go from drastic growth impairments such as the phenotypes observed for *xopAG*, *ripHI*, *ripH2* or *ripR* transgenic lines; to more moderate but observable phenotypes in root architecture such as the ones observed for *xopG*, *xopP* or *xopQ* lines; or in the aerial parts, such as the ones observed for *ripH3* and *ripOI* lines. This unveils the potential of *Xcc* and *Rps* T3Es to modulate different aspects of plant physiology. Conversely, the expression of other five T3E genes did not show any developmental phenotype, at least at the stage observed. This suggests that the phenotypes observed for the other nine T3E genes are not caused by the heterologous expression of any given bacterial transgene, but are rather specific of given T3Es.

### **Orthologous T3Es modulate the Arabidopsis development in similar ways**

Considering the orthology relationship between *Xcc*<sub>8004</sub> and *Rps*<sub>GM11000</sub> T3Es, in several cases the phenotypes observed for one T3E gene are mirrored in the ortholog. This is the case of the *hrpW/ripW* and *xopG/ripAXI-2* ortholog pairs which did not show developmental alterations in most of the independent lines generated (**Table 4.3** and **figures 4.4A, 4.4F, 4.4L-M** and **4.4X**). This could also be the case of *xopQ/ripB* which did not show developmental phenotypes in most (5/7) and all (2/2) of the lines respectively, although two independent *xopQ* lines showed reduced root growth and this phenotype was never observed in *ripB* lines (**Table 4.3** and **figures 4.4J-K** and **4.4N**). In the case of *xopAG/ripOI* the phenotypes observed, although not identical, are all related to plant growth impairments. However, this growth is more drastically affected in *xopAG* lines than in *ripOI* lines (**Table 4.3** and **figures 4.4B-C** and **4.4U-V**). Conversely, in the case of *xopP/ripHI-3*, macroscopic phenotypes were observed for the majority of the lines but they do not necessarily mirror the phenotype observed in the corresponding orthologs. While *xopP* lines generally grow more and produce more lateral roots (although in two independent lines the phenotype observed in the opposite), most *ripH* lines are impaired in growth with *ripHI* and *ripH2* being more drastic than *ripH3* (**Table 4.3** and **figures 4.4G-I** and **4.4O-T**). Altogether, it seems like the behavior of most of the different ortholog T3E pairs *in planta* might be similar based on the developmental phenotypes observed.

### **The severity of the Arabidopsis developmental phenotypes depends on the level of transgene expression**

The lack of any protein tag for the generated transgenic lines, while maximizing the chances that the observed phenotypes are linked to the expression of T3E genes, complicates the measurement of the T3E accumulation at the protein level. The transcript accumulation was measured instead as a proxy by qPCR (**Table 4.2**), but this entails a bias as it is known that

transcription and translation levels are not necessarily correlated (Vogel and Marcotte, 2012; Liu, Beyer and Aebersold, 2016). Comparing the results from the transcript accumulation and the developmental phenotype for different independent lines of a same construct, it could be observed that lines showing drastic phenotypes tend to show higher levels of transgene induction than the lines with no developmental phenotypes (**Figure 4.14A**). Indeed, low concentrations of inducer can reverse drastic developmental phenotypes indirectly linking the phenotype with the transgene expression (**Figure 4.14B**).

### **XopP, as RipH1-3, inhibits plant basal defenses: another case of functional similarities between orthologous T3Es**

Due to the sensitivity of the technique and the relatively low production of flg22-induced ROS in *A. thaliana* (**Figure 4.9**), the inhibition of the plant basal defenses was not evaluated in this species but rather in transiently transformed *N. benthamiana* leaves. *Xcc*<sub>8004</sub> XopP showed a strong, almost complete, inhibition of this classical PTI readout (**Figure 4.11**) similar to what had been previously reported with one of its *Rp*<sub>SGMII000</sub> orthologs, RipH1, and in lesser extent, to RipH2 and RipH3 (**Figure 4.5**) (Morel, 2018). On a similar note, XopP from *X. oryzae* pv. *oryzae*, another vascular pathogen, also showed inhibition of basal defense responses, in this case in rice (Ishikawa *et al.*, 2014). This provides an additional example of similarities in the mode of action of orthologous T3Es from different xylem-colonizing bacteria.



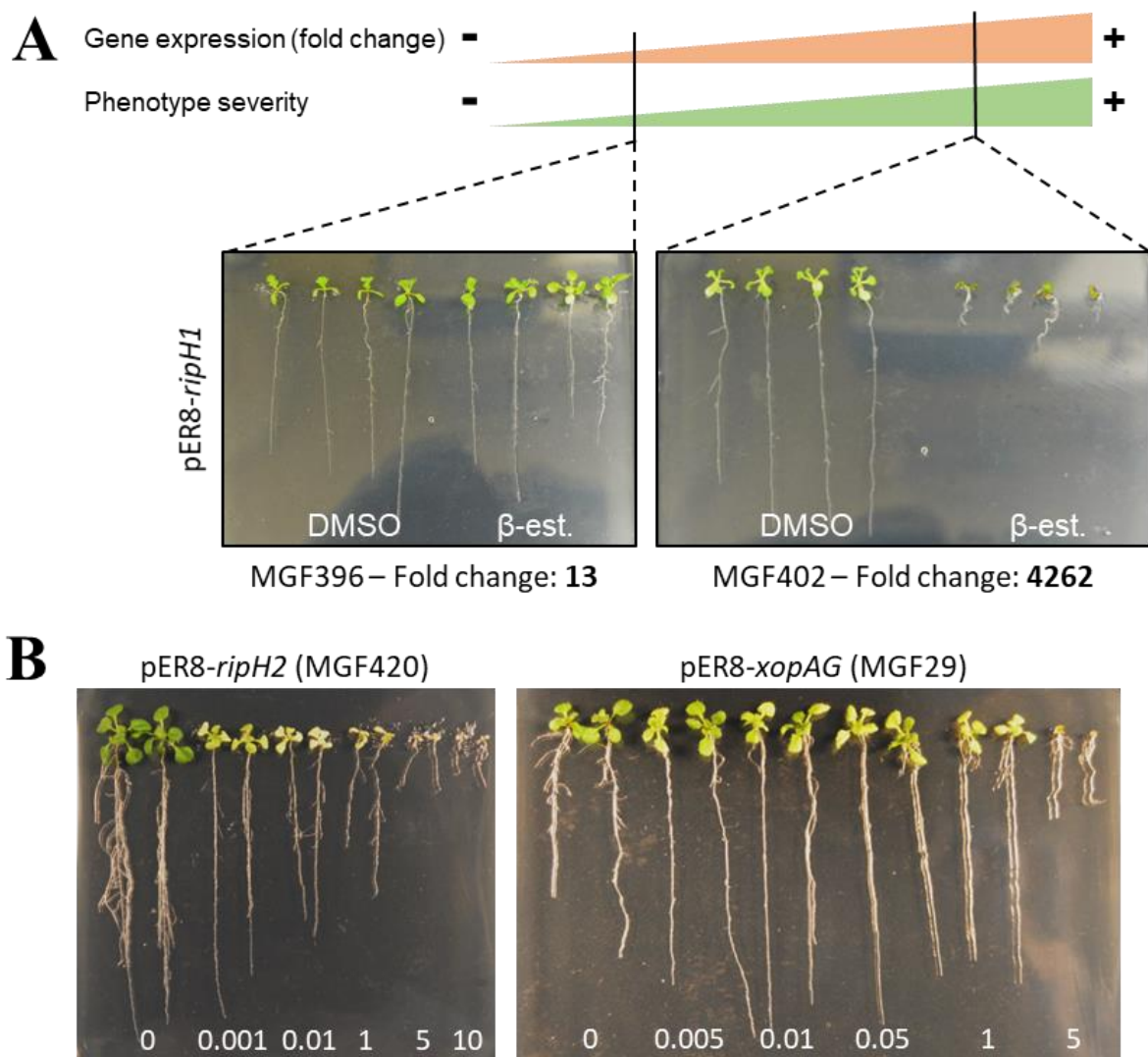


**Figure 4.14. Drastic alteration phenotypes are correlated with higher levels of induction.** (A) Two independent lines from a same construct can show different phenotypes depending on the induction levels (e.g., MGF396 does not show any developmental alteration and it shows a low level of induction whereas MGF402 shows a strong growth impairment and level of induction). Average fold change values of the induction using *OXA1* and *GAPC2* as reference genes (data on table 2). (B) The severity of drastic developmental phenotypes can be reduced by decreasing the concentration of inducer. The numbers at the bottom indicate the concentration ( $\mu$ M) of  $\beta$ -estradiol. Plants were grown for two weeks in MS agar plates supplemented with different concentrations of  $\beta$ -estradiol or equivalent DMSO volume.

# Chapter 5

XopAG and RipO1, one of the most  
promising orthologous pair of  
candidates

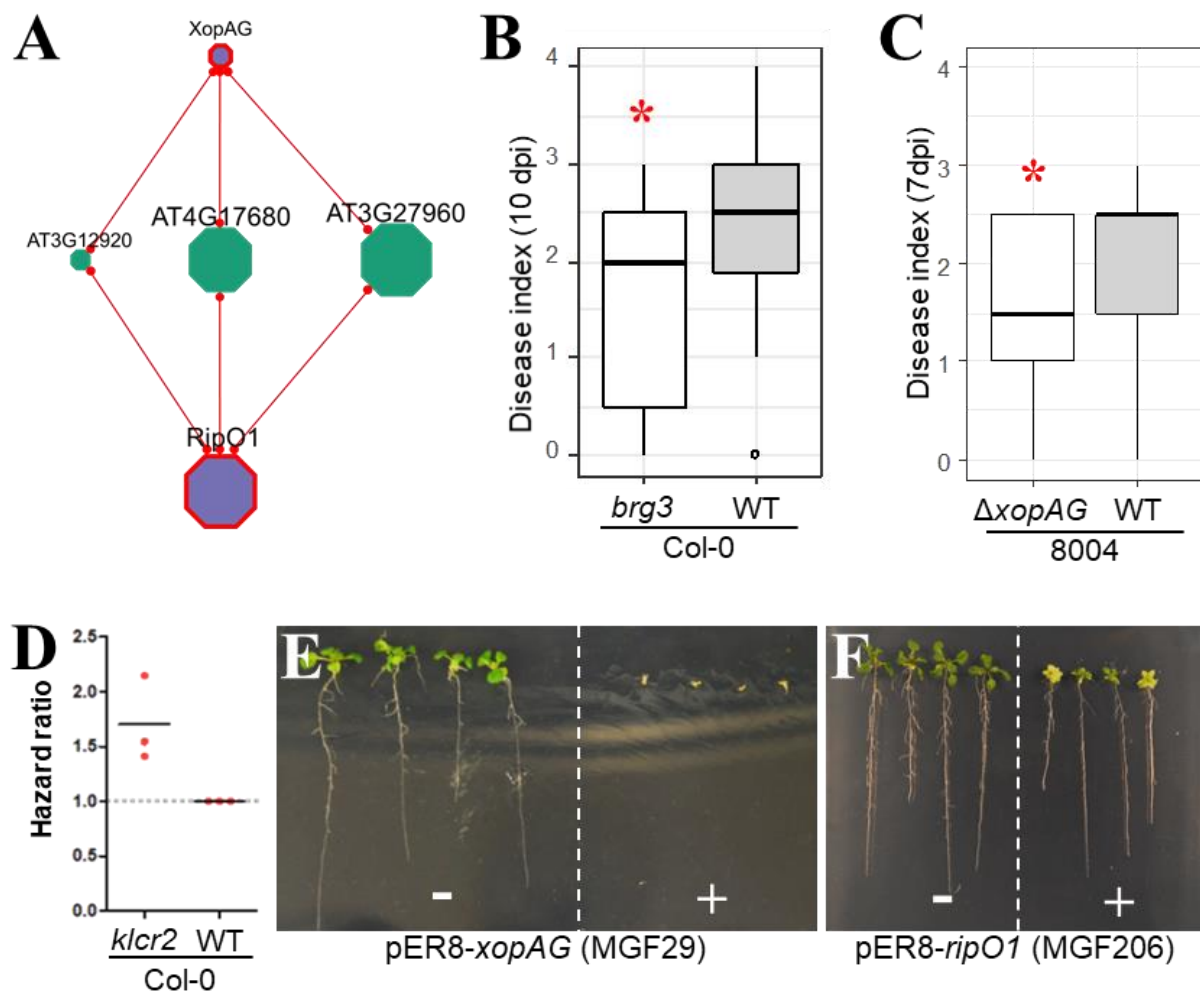


**Figure 5.1. Summary of previous results related to *Xcc*<sub>8004</sub> XopAG and *Rps*<sub>GMII000</sub> RipOI.** (A) XopAG and RipOI are the only orthologous T3Es with three putative common targets: BRG3 (AT3G12920), KLCR2 (AT3G27960) and AT4G17680. Screen capture from EffectorK. (B) Arabidopsis *brg3* mutant shows reduced disease symptoms upon *Xcc* infection. Full image: **Figure 3.2**. (C) *Xcc* 8004 $\Delta xopAG$  mutant is less virulent than the wild type on susceptible Arabidopsis ecotype Sf-2. Full image: **Figure 4.3**. (D) Arabidopsis *klcr2* mutant shows slightly reduced susceptibility to *Rps* (higher hazard ratio). Full image: **Figure 3.4** (E) pER8-*xopAG* and (F) pER8-*ripOI* plants show different developmental alterations when the transgene expression is induced by  $\beta$ -estradiol (+) compared to the DMSO control (-) for 2 weeks.

## 5.1 Introduction

Based on the results presented in the previous chapters, one pair of orthologous T3Es stood out: XopAG<sub>8004</sub> and RipOI<sub>GMI1000</sub>. These orthologs are the only pair sharing three putative targets in Arabidopsis based on the yeast two-hybrid screenings (**Figure 5.1A**): AT4G17680, BRG3 (AT3G12920) and KLCR2 (AT3G27960). From the eighteen putative common targets of Xcc<sub>8004</sub> and Rps<sub>GMI1000</sub> T3Es, only three showed differences in susceptibility to Xcc when mutated in Arabidopsis. One of them is precisely BRG3, common target of XopAG and RipOI, whose mutant showed reduced disease susceptibility (**Figure 5.1B**). Regarding differences in susceptibility to Rps, there were no strong differences, but the only mutant for which a slight but constant tendency of reduced susceptibility was observed was *kler2*, another common target of XopAG and RipOI (**Figure 5.1D**). On the bacterial side, *xopAG* was one of the only two Xcc<sub>8004</sub> T3E genes for which simple deletion mutants showed reduced pathogenicity in a susceptible Arabidopsis ecotype (**Figure 5.1C**). When inducibly expressed in transgenic Arabidopsis lines, both *xopAG* and *ripOI* alter the normal development of the plant. Several independent pER8-*xopAG* lines showed a drastic growth impairment after germination (**Figure 5.1E**) whereas pER8-*ripOI* lines showed chlorosis and a weaker growth impairment (**Figure 5.1F**). Altogether, these results suggest that XopAG and RipOI are able to modulate the plant physiology and might be involved in bacterial pathogenicity and at the same time, some of their common putative targets seems to play a role in susceptibility to Xcc and Rps. For this reason, further studies were conducted to understand better how this pair of orthologous T3Es work. In a first part, the phylogeny of XopAG and RipOI will be analyzed and discussed. Then, the results of the different approaches aiming at functionally characterize this couple of candidates will be presented. This includes the study of their involvement in bacterial pathogenicity through T3E gene mutants in Xcc<sub>8004</sub> and Rps<sub>GMI1000</sub>; the characterization of the developmental phenotypes observed when *ripOI*, and more notably *xopAG*, are heterologously expressed in Arabidopsis; and the determination of their subcellular localization and possible interaction with BRG3, one of their common putative targets.

## 5.2. XopAG and RipOI belong to a widespread and poorly characterized T3E family

Orthologs of XopAG and RipOI were retrieved from public databases by blasting their amino acid sequences. Orthologs were found in several plant- and soil-associated proteobacteria

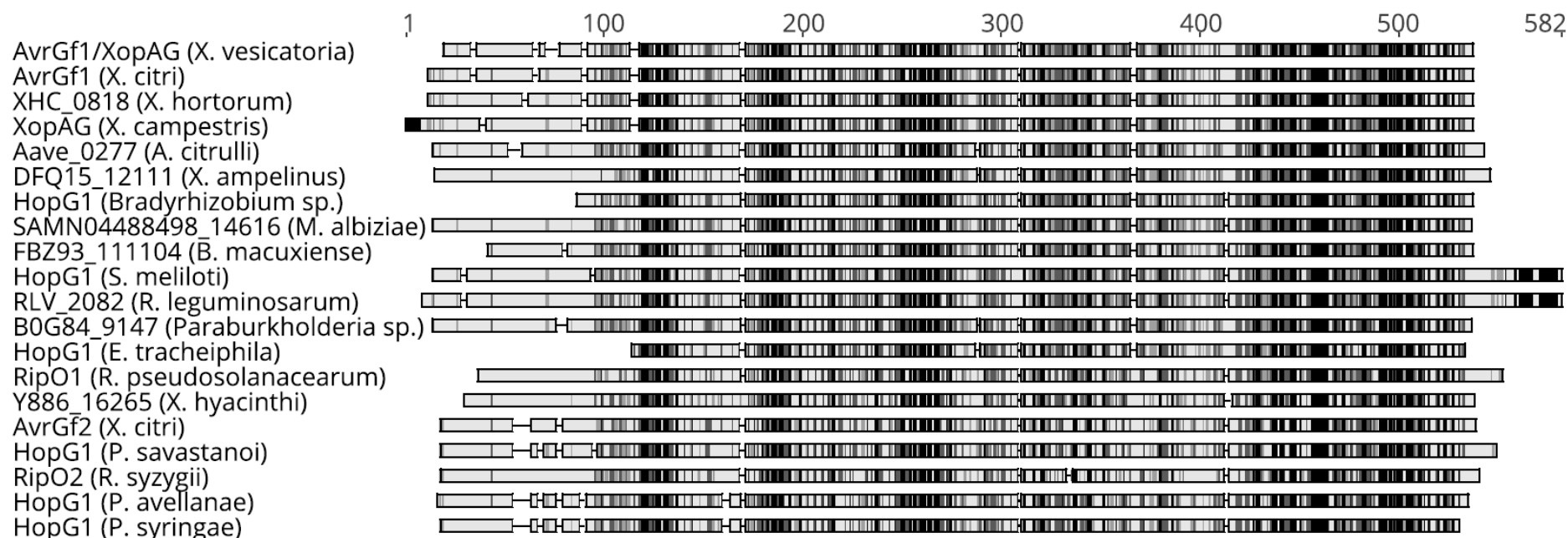


**Figure 5.2. Schematic alignment of orthologs of XopAG and RipO1 in other bacteria.** ClustalW multiple sequence alignment (cost matrix: BLOSUM, gap open/extension penalties: 10/0.1) of 20 XopAG/RipO1 orthologs. The color represents the percentage of similarity based on the BLOSUM62 scoring matrix with a threshold of 1: black, 100%; dark grey, 80-100%; light grey, 60-80%; and white, less than 60% similar). The GenBank accession numbers of the full-length proteins used in the alignment are as follows: EGD09323.1 for AvrGf1/XopAG (*Xanthomonas vesicatoria*), CEJ44051.1 for AvrGf1 (*X. citri*), ETC89650.1 for XHC\_0818 (*X. hortorum*), AAY47644.1 for XopAG (*X. campestris*), ABM30884.1 for Aave\_0277 (*Acidovorax citrulli*), PYE74990.1 for DFQ15\_12111 (*Xylophilus ampelinus*), TCK32019.1 for B0G84\_9147 (*Paraburkholderia* sp. BL8N3), TWB93065.1 for FBZ93\_111104 (*Bradyrhizobium macuxiense*), WP\_160169077.1 for HopG1 (*Bradyrhizobium* sp. Aila-2), SSFL17055.1 for SAMN04488498\_14616 (*Mesorhizobium albiziae*), WP\_146722007.1 for HopG1 (*Sinorhizobium meliloti*), AVC52551.1 for RLV\_2082 (*Rhizobium leguminosarum*), AXF78828.1 for HopG1 (*Erwinia tracheiphila*), CADI7474.2 for RipO1 (*Ralstonia pseudosolanacearum*), KLD77357.1 for Y886\_16265 (*Xanthomonas hyacinthi*), RMU24844.1 for HopG1 (*Pseudomonas avellanae*), AAO58163.1 for HopG1 (*P. syringae*), CCA86847.1 for RipO2 (*R. syzygii*), AIP90071.1 for AvrGf2 (*X. citri*) and KPB44896.1 for HopG1 (*P. savastanoi*). Constructed with MEGA X (Kumar et al., 2018).

including other plant pathogens (e.g., *Xanthomonas*, *Ralstonia*, *Pseudomonas*, *Erwinia* or *Xylophilus* spp.) and nitrogen-fixing rhizobia (e.g., *Rhizobium*, *Sinorhizobium*, *Mesorhizobium* or *Bradyrhizobium* spp.). The degree of conservation among the retrieved sequences was considerably high with global percentages of similarity and identity of 49.4% and 16.9% respectively (**Figure 5.2**). Despite the broad distribution among different proteobacteria, little is known about this family of T3Es. Only three members have been functionally characterized: *P. syringae* HopG1 induces changes in actin organization and inhibits plant defense targeting the plant mitochondria (Block *et al.*, 2010; Shimono *et al.*, 2016). AvrGf1 and AvrGf2 are HR inducers that control the host range of *X. citri* strains among citrus and target the plant chloroplasts (Figueiredo *et al.*, 2011; Gochez *et al.*, 2015, 2017). No functional domains were predicted on RipOI nor XopAG except for a C-terminal cyclophilin (Cyp)-binding motif (Block *et al.*, 2010), conserved in most XopAG and RipOI orthologs (**Figure 5.3**).

The phylogeny of the family of XopAG and RipOI was reconstructed based on the multiple sequence alignment presented. Two main groups could be differentiated (**Figure 5.4**): group I, larger and containing T3Es from plant pathogenic, symbiotic and environmental bacteria; and group II, smaller and containing exclusively plant pathogen T3Es. Previously characterized *P. syringae* HopG1 and *X. citri* AvrGf2 belong to this second group whereas XopAG and RipOI belong to group I. Within the group I, XopAG is located in a monophyletic clade with T3Es from other *Xanthomonas* species such as *X. citri* AvrGf1. This suggests that XopAG and AvrGf1 have a common antecessor present possibly before the speciation of the *Xanthomonas* genus. Within *X. campestris* strains, *xopAG* is practically exclusive to pathovar *campestris* (Roux *et al.*, 2015), but is present in all of this pathovar strains, constituting thus a “core” Xcc T3E (Guy *et al.*, 2013) (**Table 5.1**). This supports an ancient origin of *xopAG* within the Xcc lineage and suggests a possible strong selective pressure. Other *Xanthomonas* effectors such as AvrGf2 from *X. citri* and Y886\_16265 from *X. hyacinthi*, belong to the group II and are not closely related to each other but rather with other *Pseudomonas* effectors, suggesting two independent horizontal gene transfer events in two different *Xanthomonas* species. RipOI also belongs to group I; however, its position within the group is clearly divergent from the rest of members complicating the inference of its possible origin. However, regarding the distribution of *ripOI*, present in the majority of *R. pseudosolanacearum* and *R. solanacearum* strains (**Table 5.1**), it seems likely that the acquisition of *ripOI* occurred early, before the speciation of the RSSC. The other *Ralstonia* member of the family, *R. syzygii* RipO2, belongs to the group II and is more related to *Pseudomonas* and to horizontally-transferred *Xanthomonas* T3Es than to RipOI. It is





**Figure 5.3. Multiple sequence alignment of AvrGf2, HopG1, RipO1 and XopAG.** ClustalW multiple sequence alignment (Cost matrix: BLOSUM, gap open/extension penalties: 10/0.1) of AvrGf2 from *X. citri* pv. *auranaurantifolii* AvrGf2 (AIP90071.1), HopG1 from *P. syringae* pv. *tomato* (AAO58163.1), RipO1 from *Rps* (CADI7474.2) and XopAG from *Xcc* (AAY47644.1) using their full-length amino acid sequences. The background color represents the percentage of similarity based on the BLOSUM62 scoring matrix with a threshold of 1: black, 100%; grey, 60-100%; and white, less than 60% similar). The conserved cyclophilin-binding site (GPxL) is squared in red.

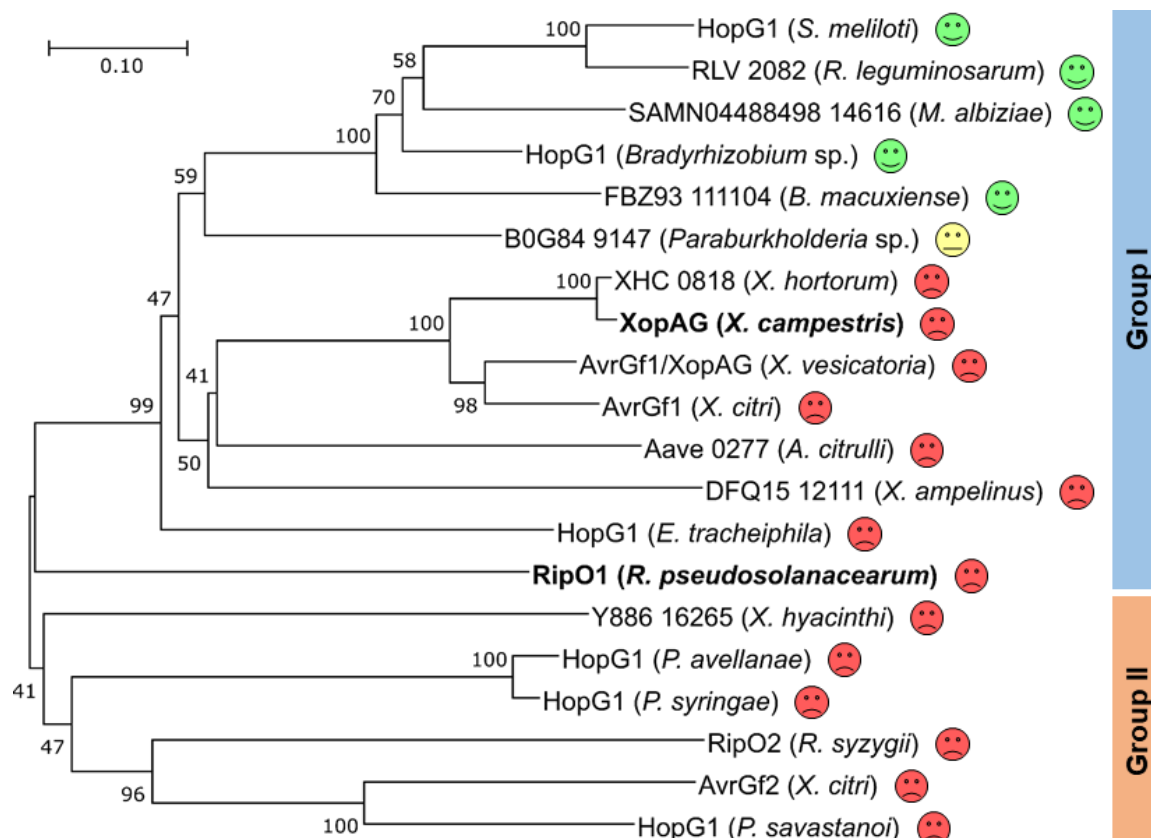


**Figure 5.4. Phylogeny of orthologs from XopAG and RipO1 in other proteobacteria.** Neighbor-Joining tree with bootstrap support values (1000 replicates) indicated above each node. The scale bar indicates the evolutionary distance in number of amino acid substitutions per site computed using the Poisson correction method. XopAG and RipO1 are highlighted in bold. Red, yellow and green faces represent plant pathogenic, environmental and symbiotic bacteria respectively. Groups were determined based on the first bifurcation of the tree. The GenBank accession numbers of the full-length proteins used in the alignment and construction of the tree are indicated in **figure 5.2**. Constructed with MEGA X (Kumar et al., 2018).

**Table 5.1. Distribution of *xopAG* and *ripO1* within *X. campestris* pathovars and the *Ralstonia solanacearum* species complex strains.**

Effector	Species	Present <sup>a</sup>	Absent <sup>a</sup>	Reference
<i>xopAG</i>	<i>X. campestris</i> pv. <i>campestris</i>	45	0	Guy et al. 2013
	<i>X. campestris</i> pv. <i>raphani</i>	0	2	Roux et al. 2015
	<i>X. campestris</i> pv. <i>incanae</i>	1	1	Roux et al. 2015
<i>ripO1</i>	<i>R. pseudosolanacearum</i>	45	17	Sabbagh et al. 2019
	<i>R. solanacearum</i>	55	5	Sabbagh et al. 2019
	<i>R. syzygii</i>	0	21	Sabbagh et al. 2019

<sup>a</sup> Number of strains in which the effector gene is present or absent. For the RSSC strains, only strains sequenced with a level of stringency 2 were considered.



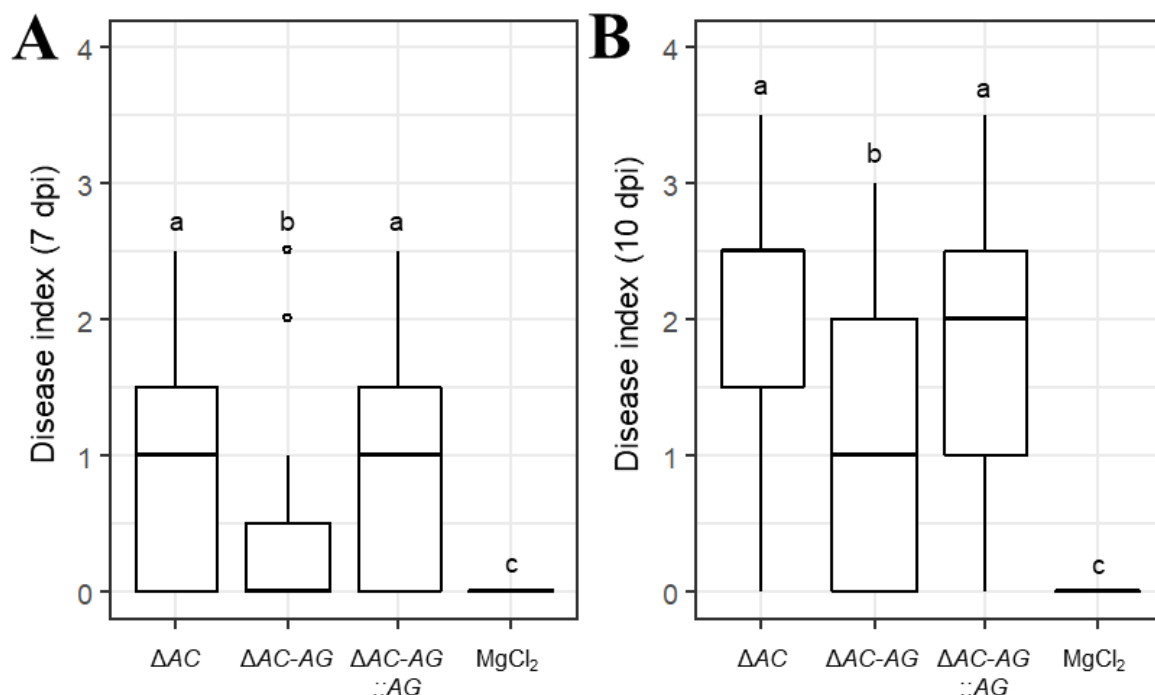


**Figure 5.5. Pathogenicity of *Xcc8004ΔxopAG* in the *ΔxopAC* background.** Arabidopsis Col-0 ecotype plants were inoculated by piercing in the central vein at a bacterial density of  $10^8$  CFU/ml, and infection symptoms were scored at 7 (A) and 10 (B) days post inoculation. The strains tested were *Xcc 8004ΔxopAC* ( $\Delta AC$ ), *ΔxopAC-xopAG* ( $\Delta AC-AG$ ) and *ΔxopAC-xopAG* complemented with a genomic insertion of *xopAG* under the control of its natural promoter ( $\Delta AC-AG::AG$ ). Disease index is as follows: 0-1, no symptoms; 1-2, weak chlorosis around the inoculation sites; 2-3, stronger and extended chlorosis; and 3-4, necrosis. Six plants (four leaves per plant) were inoculated per condition (except  $MgCl_2$  mock control, only two plants). Three independent experiments were performed and the results were combined. Boxplot representation: thick bar, median; box limits, highest and lowest value within  $1.5 \cdot$  inter-quartile range; and circles, outliers. Statistical groups were determined using a Kruskal-Wallis test (one-tailed Wilcoxon signed-rank test  $p$ -value  $< 0.05$ ) and are indicated by different letters.

thus likely that RipOI and RipO2 have had different origins, and that the latter has been horizontally transferred.

### 5.3. XopAG and in lesser extent RipO1 are involved in bacterial pathogenicity

Bacterial single *xopAG* and *ripOI* mutants had been previously tested for pathogenicity in susceptible Arabidopsis and tomato plants respectively. While *Rps* GMII000 $\Delta$ *ripOI* did not show reduced pathogenicity in tomato, *Xcc* 8004 $\Delta$ *xopAG* showed reduced pathogenicity in Arabidopsis (**Figure 5.1C**). As most Arabidopsis resources are available in the resistant ecotype Col-0, the  $\Delta$ *xopAG* mutation was introduced in the compatible *Xcc* strain 8004 $\Delta$ *xopAC*. Similarly to what was observed in Sf-2, 8004 $\Delta$ *xopAC*-*xopAG* mutant showed reduced pathogenicity compared to the single  $\Delta$ *xopAC* mutant (**Figure 5.5**). To test whether the observed difference in pathogenicity was due to bacterial fitness, *in vitro* growth curves in rich and poor media were measured. No differences between *Xcc* 8004 $\Delta$ *xopAC* and  $\Delta$ *xopAC*-*xopAG* were observed in any of the media (**Figure 5.6**). The reduced pathogenicity was restored when *xopAG* was complemented by a genomic insertion under the control of its natural promoter (**Figure 5.5**). Altogether, this proves that the observed reduced pathogenicity of the double mutant is indeed caused by the absence of *xopAG*, evidencing that XopAG is a virulence factor in *Xcc* on Arabidopsis.

To evaluate whether RipOI could act as virulence factor in Arabidopsis similarly to XopAG, *Rps* GMII000 $\Delta$ *ripOI* was inoculated on susceptible Arabidopsis Col-0 ecotype. In two out of three independent experiments performed, there was a slight reduction of pathogenicity compared to the wild-type strain, but in a third experiment, this difference was not observed (**Figure 5.7**). This suggests that, while it is possible that RipOI acts as a virulence factor in Arabidopsis, its effect is too small to be observed with three independent experiments. Additional experiments and/or more sensitive assays would be required to assess RipOI possible virulence function in Arabidopsis.

A typical role of T3E in virulence is the inhibition of the host basal defenses. As a readout of early plant defense responses, the flg22-induced production of ROS was measured while transiently expressing XopAG and RipOI in *N. benthamiana* leaves (Sang and Macho, 2017). XopAG inhibits significantly the ROS burst upon flg22-treatment (**Figures 5.8A-B**). Conversely, RipOI possible inhibition of the ROS burst is much weaker and not statistically significant

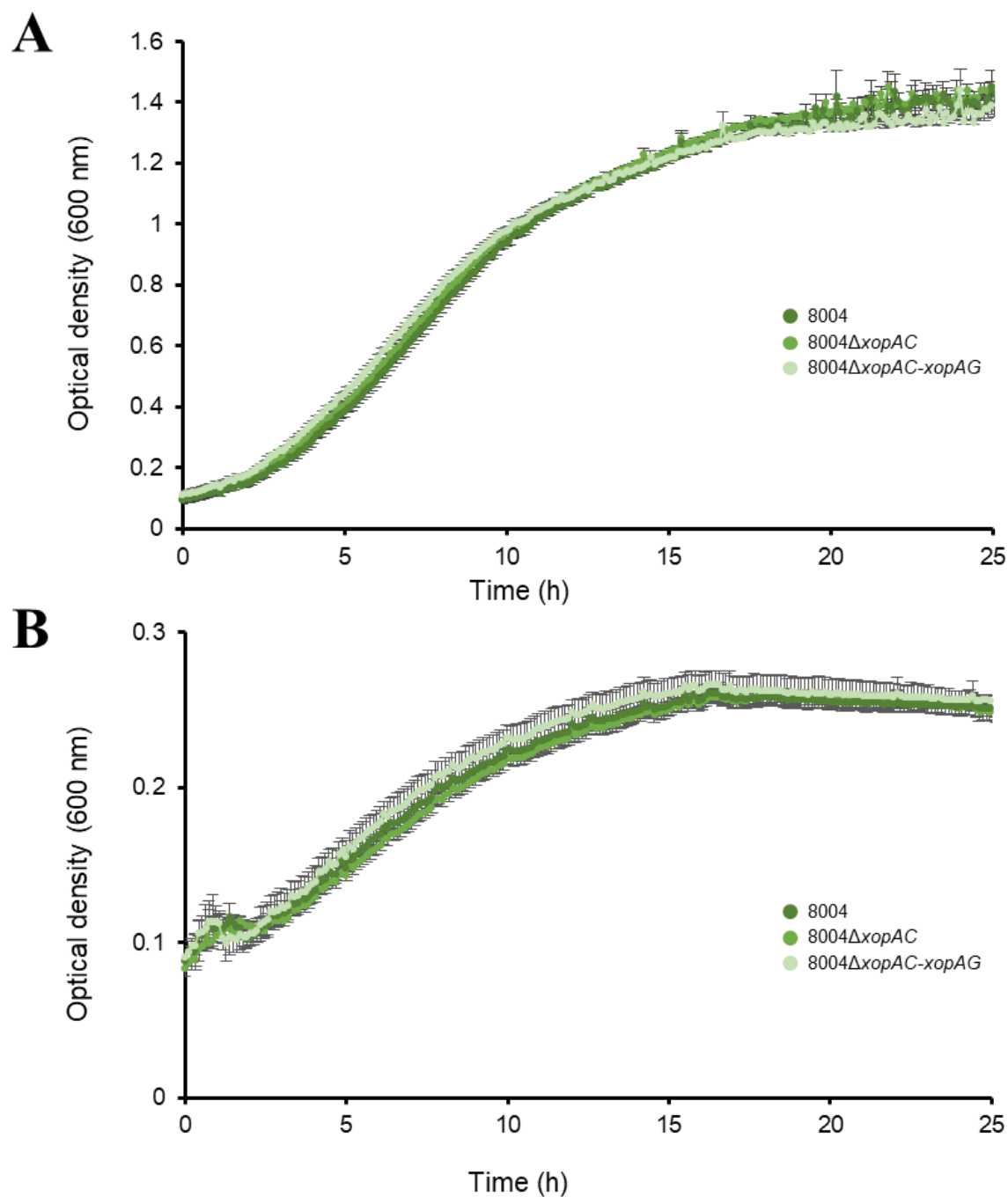


**Figure 5.6.** *In vitro* growth curve of *Xcc* 8004 wild type,  $\Delta$ xopAC and  $\Delta$ xopAC-xopAG. Bacterial growth measured spectrophotometrically (optical density at a wavelength of 600 nm) over 25 hours on Moka (A) and MME (B) medium. Each point represents the mean of eight replicates coming from two independent bacterial pre-cultures. Error bars indicate the standard error of the mean.

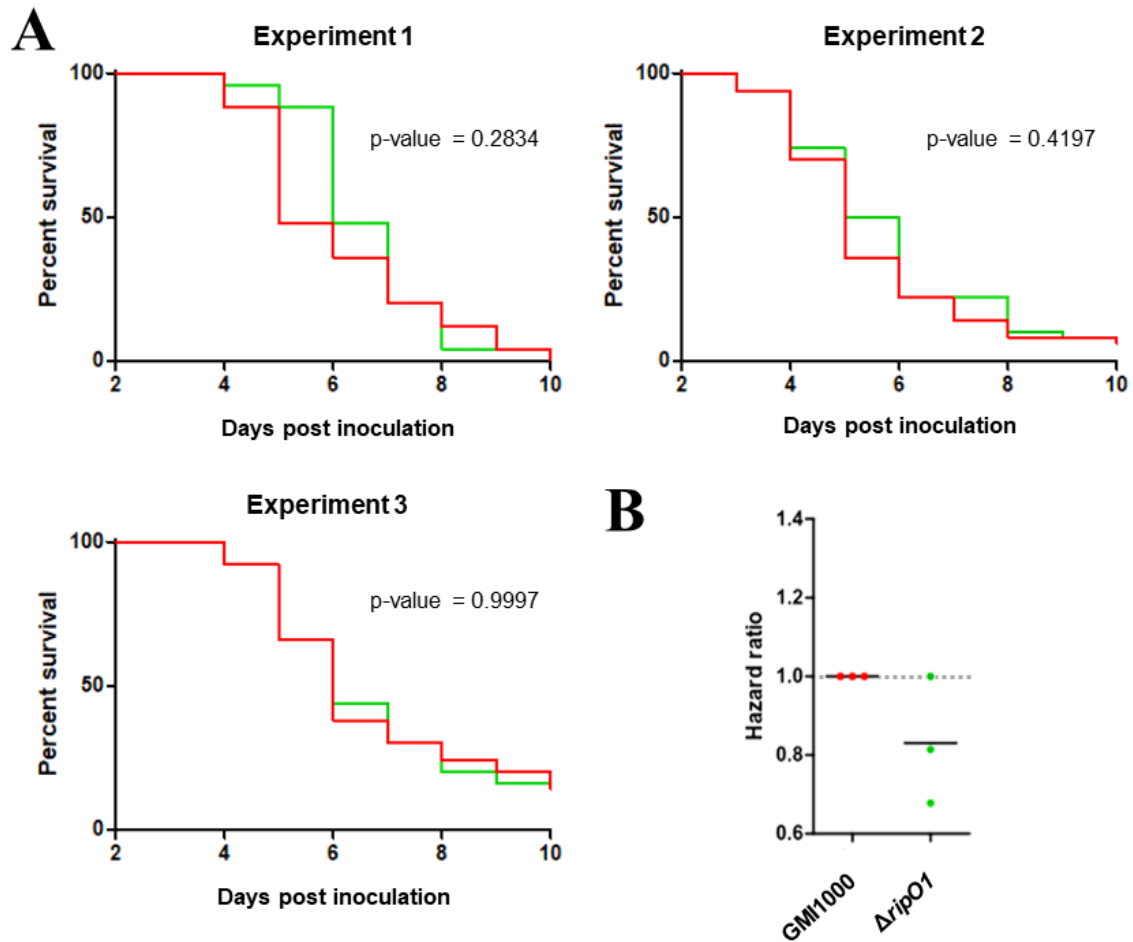


**Figure 5.7. Pathogenicity of *Rps* GMII000 wild type and  $\Delta ripOI$  strains inoculated on susceptible *Arabidopsis* plants.** (A) Survival curves scored for up to 10 days after soil-drenching inoculation of *Arabidopsis* ecotype Col-0 plants with *Rps*<sub>GMII000</sub> wild type (red) and  $\Delta ripOI$  (green). Plants were drenched in bacterial suspension at  $10^8$  CFU/ml. Three independent experiment were conducted with 25 (experiment 1) or 50 (experiments 2 and 3) plants inoculated per strain. The p-value (Mantel-Cox logrank test) of the comparison of the curves of each experiment is indicated in the corresponding graph. (B) Dotplot representing the hazard ratio of each survival curve using GMII000 as reference. Results from the three independent experiments are shown. Black lines indicate the mean and the grey dotted line is located at a constant ratio of 1 for reference. No statistically significant differences were observed (One sample t-test, comparison with Col-0 plants, p-value < 0.05).

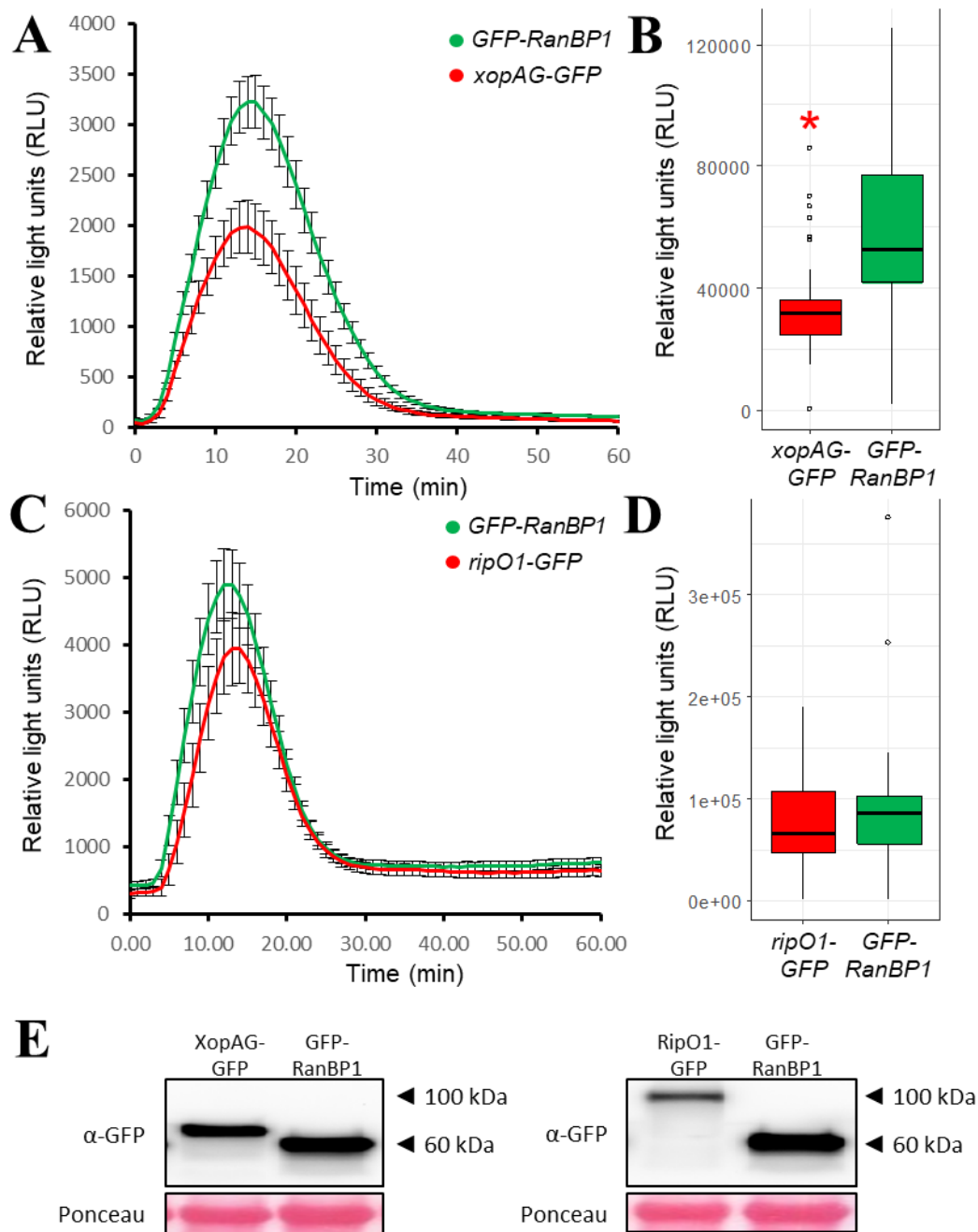


**Figure 5.8. Transient expression of XopAG but not RipOI inhibits flg22-induced ROS production.** Measurement of ROS production after flg22 treatment on *N. benthamiana* leaves upon *A. tumefaciens*-mediated expression of XopAG-GFP (red, A-B) or RipOI-GFP (red, C-D) or GFP-RanBP1 (green). Measurement over time on average (A,C) or integrated over one hour (B,D). Results combined from two independent experiments. Error bars represent the standard error of the mean on 32 leaf disk samples. Boxplots representation meaning: thick bar, median; box limits, highest and lowest value within 1.5 · inter-quartile range; and circles, outliers. Red asterisk indicates difference with GFP control statistically significant (one-tailed Wilcoxon signed-rank test p-value < 0.05). (E) Expression of XopAG/RipOI-GFP and GFP-RanBP1 detected with an anti-GFP antibody by Western blot. Ponceau S staining for loading reference

(**Figure 5.8C-D**). This is in agreement with the previously described role as virulence factor of these two T3Es which has been observed for XopAG, but not (or at least not clearly) for RipOI.

## 5.4. First steps to dissect the genetic bases of *xopAG*-mediated developmental phenotype in Arabidopsis

Several independent *xopAG* and *ripOI* transgenic Arabidopsis lines showed altered developmental phenotypes. These alteration appeared to be stronger in *xopAG* transgenic lines (plants stopped growing after germination on inducing  $\beta$ -estradiol-containing medium) than in *ripOI* lines (plants grew less and were chlorotic) (**Figures 5.1E-F**). When these lines were grown at lower concentrations of  $\beta$ -estradiol, the severity of the developmental alterations was also reduced. pER8-*xopAG* lines could grow after germination at concentrations of 1  $\mu$ M  $\beta$ -estradiol although chlorotic and visibly less than non-induced plants (**Figure 5.9A**). Same growth as non-induced plants and lack of chlorosis were observed only at 0.01 and 0.005  $\mu$ M  $\beta$ -estradiol (**Figure 5.9A**). pER8-*ripOI* grew similarly to non-induced plants at concentrations of 0.01  $\mu$ M  $\beta$ -estradiol but showed chlorosis in all tested  $\beta$ -estradiol concentrations, even at 0.001  $\mu$ M (**Figure 5.9B**). It is therefore possible that the apparently different phenotypes first reported in these two transgenic lines (i.e. *xopAG* drastic growth arrest and *ripOI* chlorosis and slightly reduced growth) might not be that different after all, but rather a similar phenotype shown with different intensity. This could indicate that XopAG and RipOI are able to modulate the plant physiology in a similar manner.

It is precisely due to the strong phenotype observed on certain pER8-*xopAG* lines that a suppressor screening was envisaged, similar to what had been already used in the dissection of the genetic basis of *xopAC*-mediated resistance (G. Wang *et al.*, 2015). Around 13,000 seeds from MGF29 and its sister line MGF34 (pER8-*xopAG*, phenotype in **figure 5.1E**), were EMS-mutagenized and grown on soil. 3,264 of these M1 plants were grown individually. The progeny of 2,502 independent M1 lines were harvested indicating that there was 17% of loss caused by sterility of certain lines and temperature/drought stress linked to technical problems in the greenhouse. Up to date, 1,248 M2 populations (49.9% of the total) have been screened for suppression of *xopAG*-mediated phenotype. 62 possible suppressors from independent M2 populations were identified and grown individually. The suppressor phenotype was confirmed for ten of the resulting M3 populations, hereafter named suppressor of *xopAG*-mediated

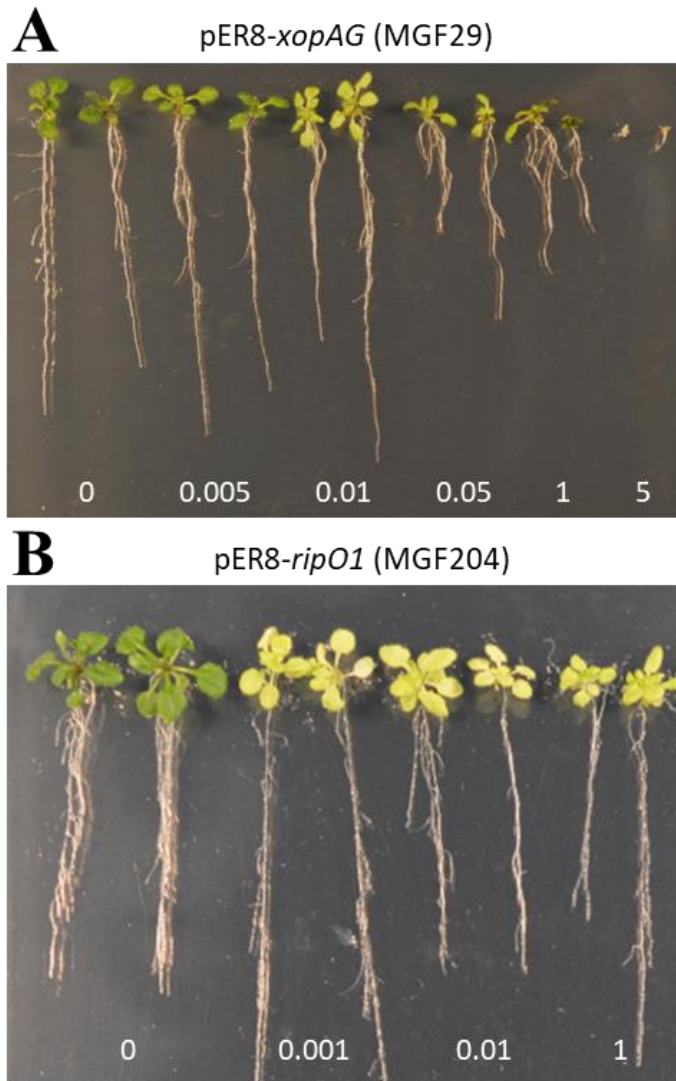


**Figure 5.9. Phenotype of pER8-*xopAG* and pER8-*ripO1* transgenic lines grown in different concentrations of inducer.** Photos of Arabidopsis plantlets grown for two weeks on MS-agar plates supplemented with either different concentrations of  $\beta$ -estradiol (indicated by numbers at the bottom) or equivalent DMSO volume (o).

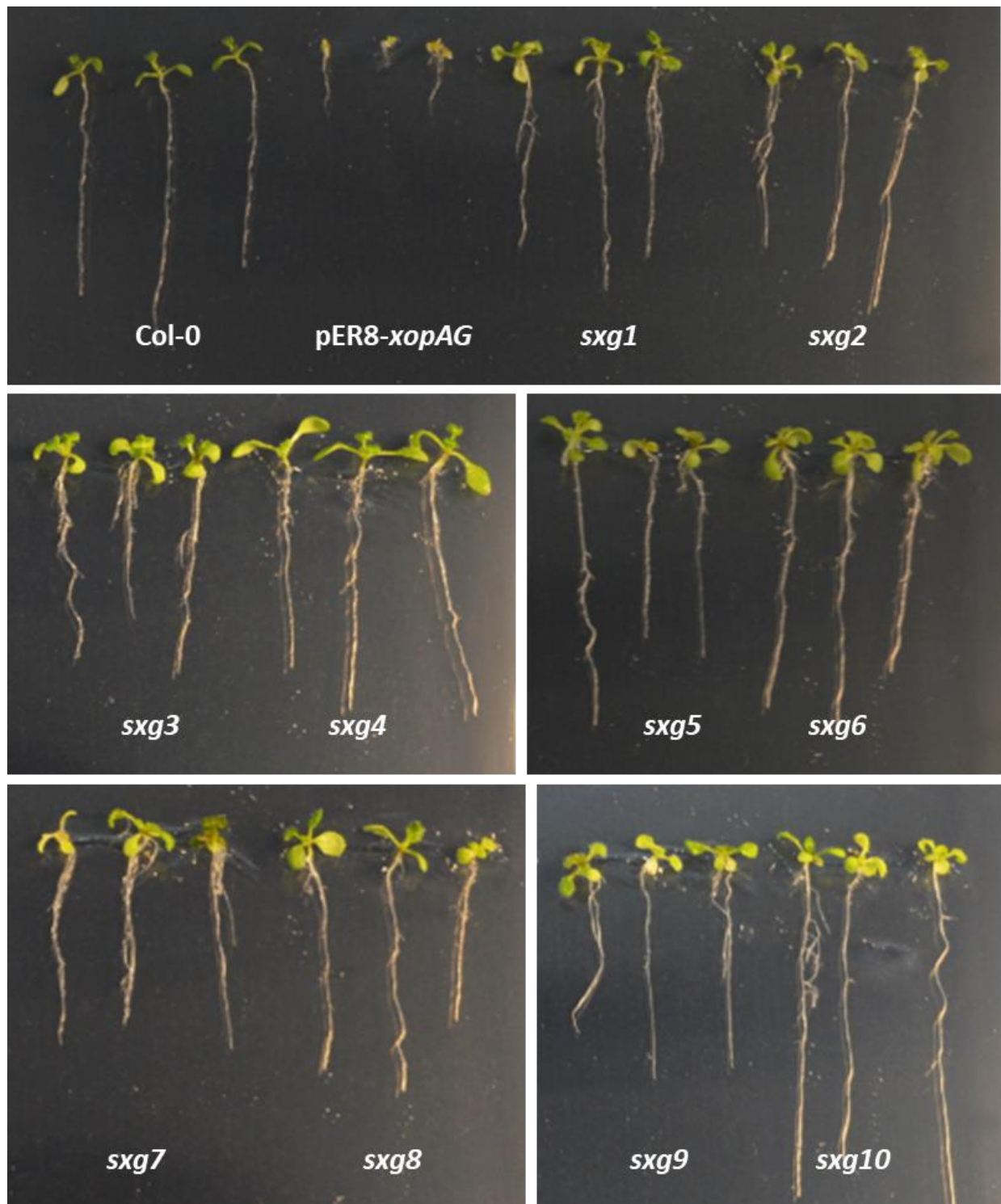


**Figure 5.10. Phenotype of suppressor of *xopAG*-related phenotype (*sxg*) lines.** Photos of Col-0, pER8-*xopAG* (MGF29) and ten independent M3 *sxg* Arabidopsis plants. Plantlets were grown for 12 days on vertical 5  $\mu$ M  $\beta$ -estradiol MS-agar plates.



phenotype (*sxg*) 1-10 (**Figure 5.10**). In addition to its suppression phenotype, *sxg4* showed enhanced growth of cotyledons and *sxg10*, increased root length.

Alternatively, a more straightforward and time-saving strategy was also conducted taking advantage of previously generated results and material. Assuming that the XopAG targets identified previously through yeast two-hybrid truly interact with XopAG *in planta*, it could be possible that they are thus involved in *xopAG*-mediated phenotype. To explore this, one of the pER8-*xopAG* transgenic lines used in the suppressor screening, was crossed with T-DNA mutants of four identified targets of XopAG: the three common targets of XopAG and RipOI; BRG3, KLCR2 and AT4G17680; and an exclusive target of XopAG, AT4G0190, an hypothetical protein involved in wound-induced lateral root formation (Justamante *et al.*, 2019). The resulting F2 populations have been generated and are currently under analysis.

## 5.5. XopAG and RipOI co-localize with BRG3 in the nucleus

To better characterize the function of XopAG and RipOI, C-terminal translational fusions of CFP and YFP with both XopAG and RipOI were generated. These constructs were *A. tumefaciens*-mediated expressed in *N. benthamiana* leaves and observed with a fluorescence microscope. The localization of both XopAG and RipOI in combination with both fluorochromes was always the same: they are both nucleocytoplasmic (**Figure 5.11**). Previously characterized members of the XopAG/RipOI family of T3Es had been described to localize in mitochondria, such as HopG1 (Block *et al.*, 2010); or in chloroplasts, such as AvrGfl (Figueiredo *et al.*, 2011) or AvrGf-2 (Gochez *et al.*, 2017).

The subcellular localization of two of the common putative targets of XopAG and RipOI has been already described: BRG3 is located in the nucleus (Bae *et al.*, 2003) whereas KLCR2 is located in the plasma membrane (Benschop *et al.*, 2007). The nuclear localization of BRG3 together with the phenotype of *brg3* mutant in susceptibility to *Xcc* (**Figure 5.1B**), made it a particularly interesting candidate for further analyses. C-terminal translational fusions of CFP and YFP with *A. thaliana* BRG3 were constructed and transiently co-expressed with the reciprocal XopAG or RipOI construct in *N. benthamiana* leaves. The co-localization of XopAG-CFP and RipOI-CFP with BRG3-YFP at the nucleus was observed by confocal microscopy (**Figure 5.12**). Two types of nuclei were observed in both combinations: nuclei where the fluorescent signal was diffuse throughout all the nucleus except the nucleolus, and nuclei where the signal

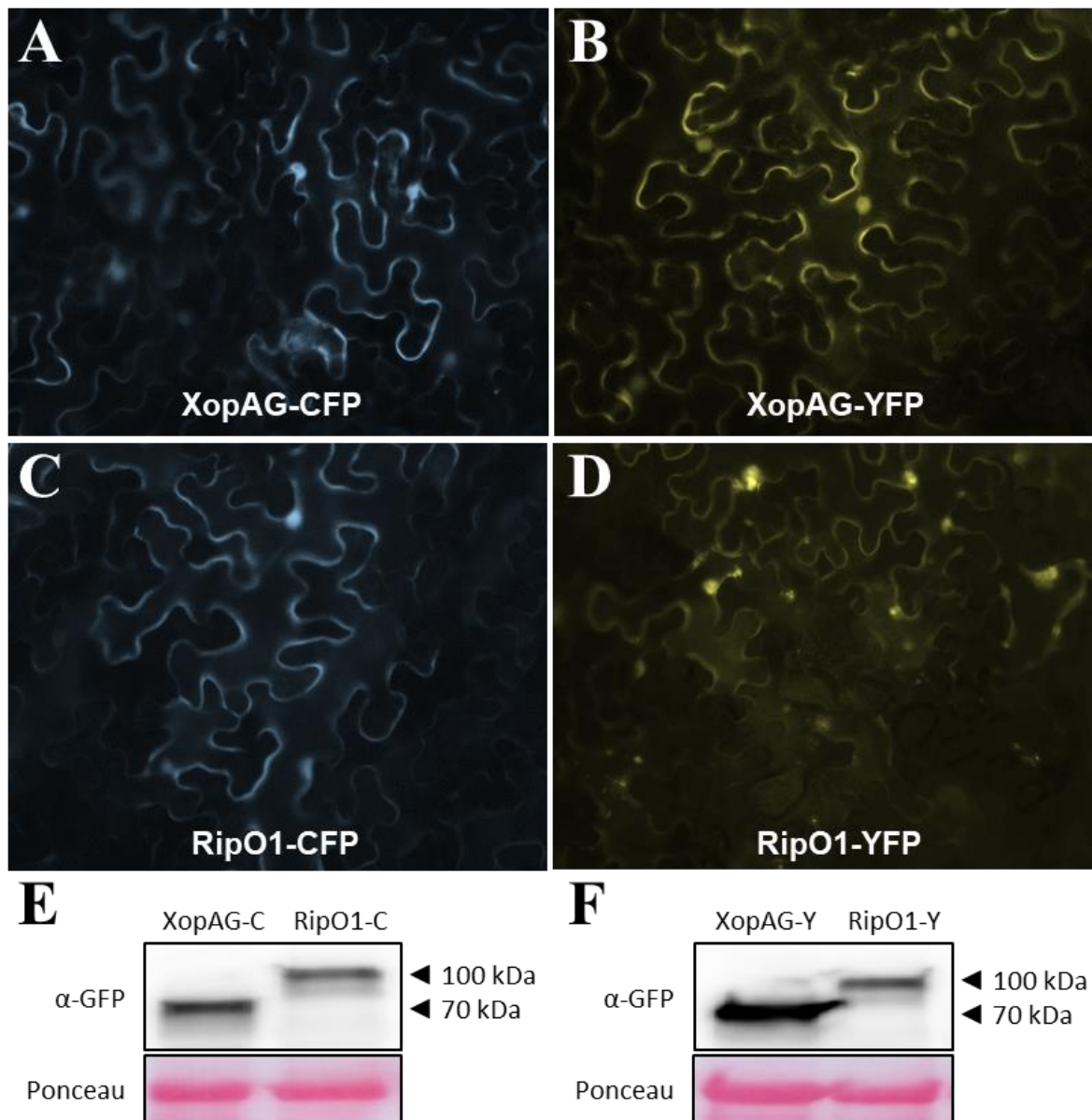


**Figure 5.11. Subcellular localization of XopAG- and RipOI-CFP fusion proteins.** Fluorescence microscopy images of *N. benthamiana* leaves transiently expressing either XopAG (A-B) or RipOI (C-D) fused to either CFP (A, C) or YFP (B, D). Western blot showing the expression of XopAG-CFP and RipOI-CFP (E) and XopAG-YFP and RipOI-YFP (F) fusion proteins with an anti-GFP antibody. Ponceau S staining used as loading control

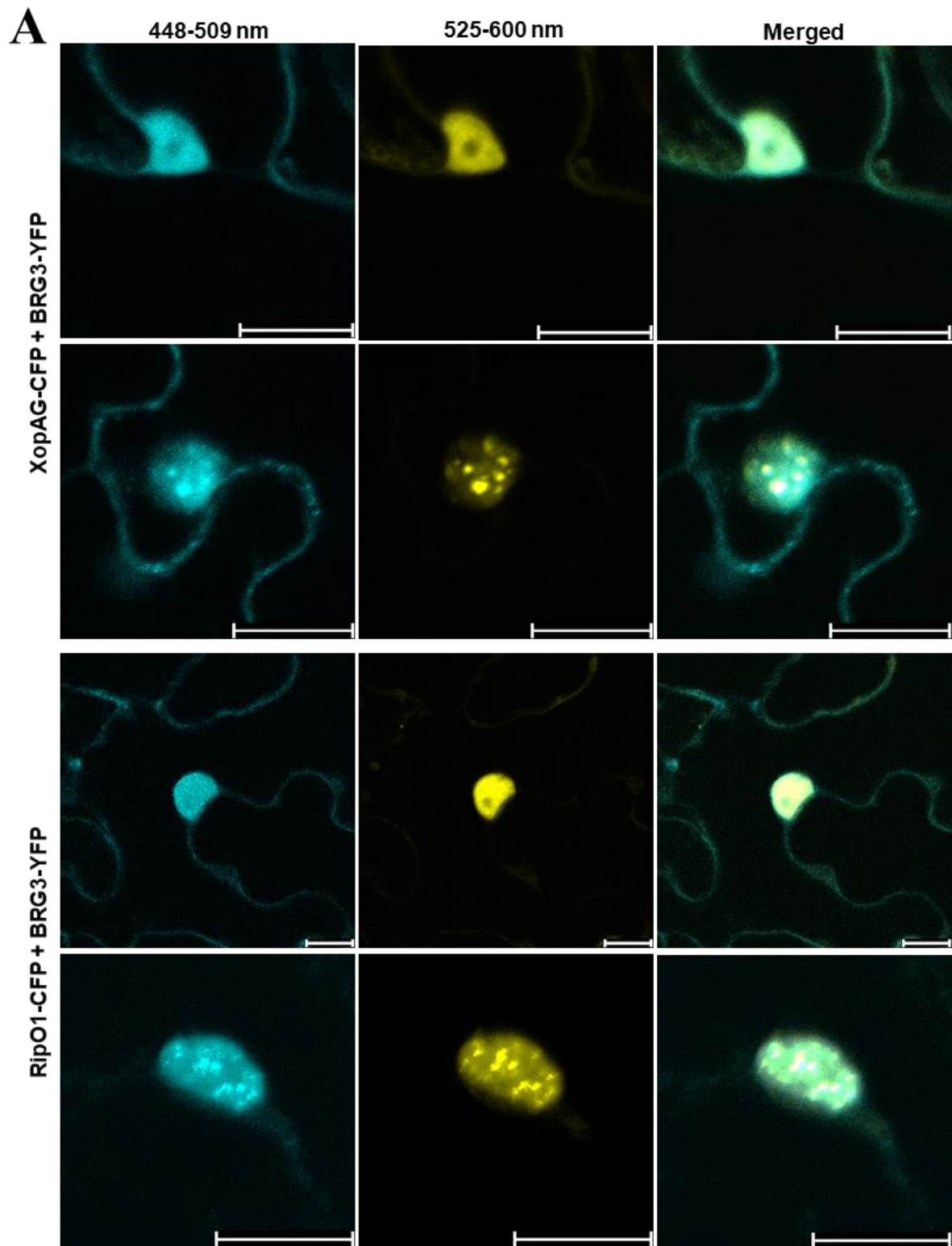


**Figure 5.12 (1/2). Nuclear co-localization of XopAGCF-CFP and RipO1-CFP with BRG3-YFP fusion proteins.** (A) Confocal laser scanning microscopy images of *N. benthamiana* leaves transiently expressing either XopAG-CFP (top) or RipO1-CFP (bottom) and BRG3-YFP. The CFP (wavelength = 448-509 nm) and YFP (wavelength = 525-600 nm) signals are shown in blue and yellow respectively. The white scale bar represents 20  $\mu$ m. (B) Western blot showing the expression of XopAG-CFP, RipO1-CFP and BRG3-YFP and detected with an anti-GFP antibody.

**B**

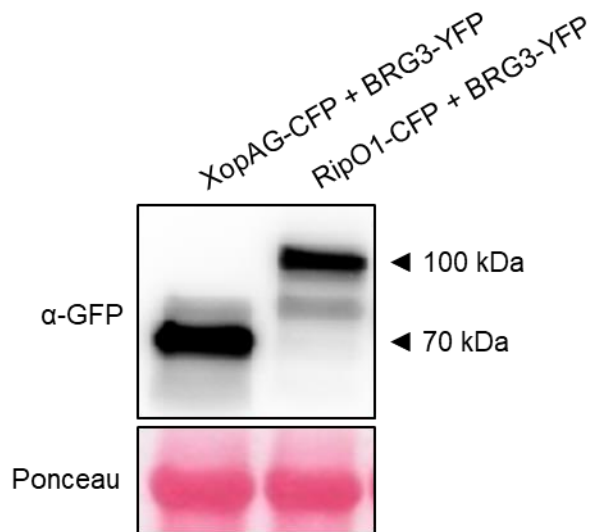


**Figure 5.12 (2/2). Nuclear co-localization of XopAG-CFP and RipOI-CFP with BRG3-YFP fusion proteins.** (A) Confocal laser scanning microscopy images of *N. benthamiana* leaves transiently expressing either XopAG-CFP (top) or RipOI-CFP (bottom) and BRG3-YFP. The CFP (wavelength = 448-509 nm) and YFP (wavelength = 525-600 nm) signals are shown in blue and yellow respectively. The white scale bar represents 20  $\mu$ m. (B) Western blot showing the expression of XopAG-CFP, RipOI-CFP and BRG3-YFP and detected with an anti-GFP antibody. Ponceau S staining for loading reference.

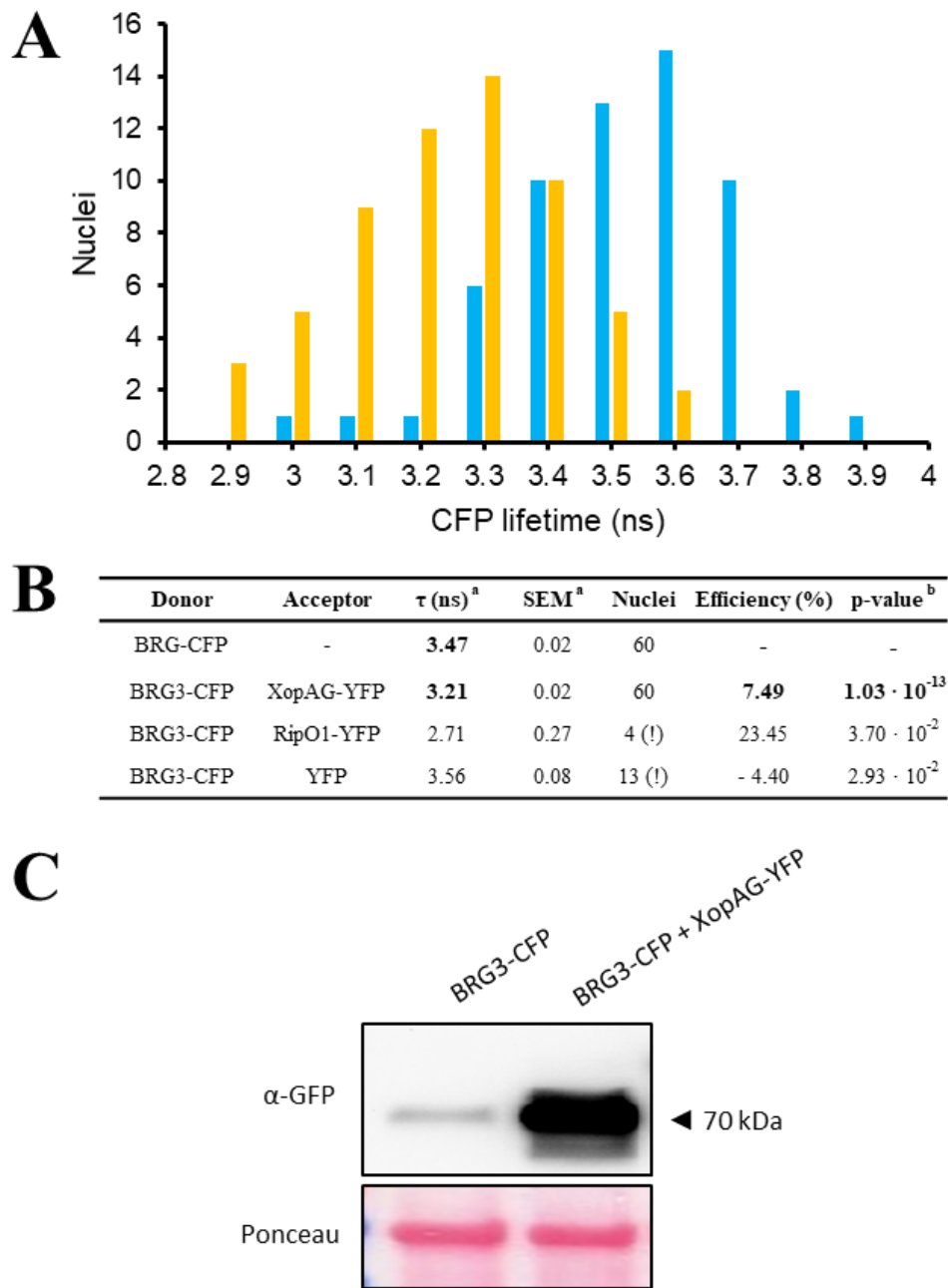


**Figure 5.B. FRET-FLIM measurements of interactions between BRG3-CFP and XopAG-YFP and RipO1-YFP.** (A) Histogram representing the distribution of nuclei according to the measured CFP lifetime of BRG3-CFP fusion protein in the presence (yellow) or absence (blue) of XopAG-YFP fusion protein. Values were obtained from three different foliar discs 48 hours after *A. tumefaciens*-mediated transformation of *N. benthamiana* leaves. Two independent experiments were performed and the results were combined. (B) Results from FRET-FLIM measurements. For each nuclei, average fluorescence decay profiles were plotted and fitted with exponential function using a non linear square estimation procedure and the mean and standard error of the mean lifetime were calculated. The exclamation point indicate preliminary result that needs to be corroborated. <sup>a</sup> For each nucleus, average fluorescence decay profiles were plotted and fitted with exponential function using a non linear square estimation procedure and the mean and standard error of the mean lifetime were calculated. <sup>b</sup> Student's *t* test p-value of the difference between the donor lifetimes in the presence/absence of acceptor. (C) Western blot showing the expression of BRG3-CFP and XopAG-YFP detected with an anti-GFP antibody. Ponceau S staining for loading reference.

was concentrated in aggregates. If left longer, both XopAG and RipOI-transformed plants show chlorosis in the infiltration area (Noe Arroyo Vélez, unpublished data), what could indicate that XopAG and RipOI might trigger cell death in *N. benthamiana*. Whether these aggregates are thus a product of cell-death degradation or true nuclear bodies is hard to assess at this stage.

Given the interaction detected by yeast two hybrid and the nuclear co-localization of BRG3 with both T3Es, the different CFP and YFP constructs generated were used to detect possible protein-protein interaction through fluorescence resonance energy transfer-fluorescence lifetime imaging microscopy (FRET-FLIM) (Fricker, Runions and Moore, 2006). The CFP lifetime of the BRG3-CFP fusion protein was significantly reduced when co-expressed with XopAG-YFP compared to when it was expressed alone (**Figure 5.13**). This indicates that XopAG-YFP and BRG3-CFP physically interact in the nucleus validating through a different technique the yeast two-hybrid detected interaction. The CFP lifetime of BRG3-CFP was also measured in co-expression with RipOI-YFP and YFP alone but due to problems in the expression, not enough co-transformed nuclei could be measured to properly compare with BRG-CFP alone. In the case of the co-expressed YFP control, thirteen nuclei were measured with an average CFP-lifetime of  $3.56 \pm 0.29$  ns, which corresponds approximately to the peak of CFP-lifetime of BRG3-CFP alone. If confirmed, this result would suggest that YFP alone does not interact with BRG3-CFP validating thus the specificity of the interaction between XopAG-YFP and BRG3-CFP. In the case of RipOI-YFP, only four co-expressed nuclei were measured with an average CFP-lifetime of  $2.72 \pm 0.28$  ns, which is even less than when co-expressed with XopAG-YFP. If confirmed, this result would suggest that RipOI also interacts with BRG3.

## 5.6. Discussion

### Is XopAG the “big cousin” of RipOI?

Altogether, the results presented in this third chapter have brought together and expanded what has been done to characterize the roles of the most promising pair of candidates: XopAG and RipOI. XopAG is involved in *Xcc* pathogenicity (**Figure 5.5**), inhibits the flg22-induced ROS burst (**Figures 5.8A-B**), and alters drastically the growth when expressed in transgenic Arabidopsis plants (**Figure 5.9A**). RipOI, on the other hand, might be slightly involved in *Rps* virulence (**Figure 5.7**), inhibits very weakly the flg22-induced ROS burst (**Figures 5.8C-D**), and confers a similar but weaker phenotype than XopAG in Arabidopsis (**Figure 5.9B**). This could indicate either that the mode of action of this pair of orthologs differ substantially, or that it is indeed similar but varies in the level of intensity, stronger in the case

of XopAG compared to RipOI. This second hypothesis opens an interesting question: could it be possible that the differences observed reflect the condition of *Arabidopsis* as a natural host of *Xcc* (Buell, 2002) and not of *Rps*? To assess which hypothesis is true, more insight into the molecular functions of these two effectors would be required. However, certain simple experiments could help to support either one or the other hypothesis in a fast and straightforward manner. One such experiment, which was planned but could not be performed in time, is the cross-complementation of *Xcc* 8004 $\Delta$ xopAG reduced pathogenicity in *Arabidopsis* with *Rps*<sub>GMI1000</sub> *ripOI*. Cross-complementation of orthologous bacterial *hrp* genes has already been used to establish functional similarities and differences (Wei and Beer, 1995; Bogdanove *et al.*, 1998). Equally interesting would be the cross-complementation in the opposite sense. However, considering the weak phenotype of the *Rps*<sub>GMI1000</sub>  $\Delta$ *ripOI* mutant, this would be much harder to detect. If the cross-complementation worked, suggesting that XopAG and RipOI function similarly but with different intensity, this would provide a great opportunity for further functional and structural analyses. Considering the high level of conservation between both (43.4% pairwise identity) (**Figure 5.3**), domain shuffling between XopAG and RipOI could potentially reveal the amino acids responsible for the difference in intensity of the phenotype. In this matter, the differences observed in the inhibition of the flg22-induced ROS burst could be exploited as a quantitative, fast and easy readout of the function intensity of different chimeric XopAG/RipOI T3Es. This would contribute to better characterize functionally XopAG and RipOI, and potentially other members of this poorly characterized family of bacterial T3Es.

### **A sequence-similar but localization- and functionally-diverse T3E family**

Looking at their position in the phylogeny of the family, XopAG and RipOI are not particularly close to each other (**Figure 5.4**). Although they both belong to the group I, RipOI is clearly different from the rest of members whereas XopAG is more closely related to other *Xanthomonas* T3Es, including the chloroplast-localized AvrGf1 from *X. citri*. However, XopAG presented nucleocytoplasmic localization (**Figure 5.11**), indicating that the proximity in the tree does not necessarily reflect a common subcellular localization. This can be at least partially explained by high level of divergence at the N-terminus (**Figures 5.2**), where the signals for the chloroplast localization of AvrG1 and AvrGf2 (Figueiredo *et al.*, 2011; Gochez *et al.*, 2017) and mitochondrial localization of HopG1 were found (Block *et al.*, 2010). The only characterized functional domain of the family is the conserved Cyp-binding motif (**Figure 5.3**), which is required for AvrGf-2 mediated HR and chloroplast localization (Gochez *et al.*, 2017), but not for HopG1 mitochondrial localization (Block *et al.*, 2010). This suggests that despite their strong

sequence homology, different members of the family can present different functions based on their different subcellular localizations. Yet, as XopAG and RipOI are both nucleocytoplasmic (Figure 5.11), this is not a major concern for assuming that they might function similarly.

### **XopAG and RipOI have been probably horizontally acquired and benefited from strong selective pressure**

HopGI was described to be horizontally acquired in *Pseudomonas* and undergo considerably high rates of gene gain/loss within the *P. syringae* species complex (Rohmer, Guttman and Dangl, 2004; Dillon *et al.*, 2019). The lower GC percentage of both *xopAG* (56.7%) and *ripOI* (61.5%) compared to the average of the genomes of *Xcc* (~ 65%) and *Rps* (~ 69%) and the wide distribution among different plant-associated proteobacteria could suggest that both genes have been also acquired horizontally. However, contrary to *hopGI* in the *P. syringae* species complex, *xopAG* and *ripOI* are present in the majority of sequenced *Xcc* and *Rps* strains (Table 5.1). This indicates that the horizontal acquisition of *xopAG* and *ripOI* occurred anciently and that they might have benefited from a relatively strong selective pressure that other orthologs such as HopGI might have not. Further genomic analyses taking advantage of the large number of *Xcc*, *Rps* and *P. syringae* sequenced genomes available would allow to corroborate this hypothesis. If true, this could indicate that the virulence roles of this T3E family are more important to *Xcc* and *Rps* than they are to *P. syringae*. Considering the vascular nature of these two pathogens, this opens the following question: are XopAG/RipOI orthologs particularly important among vascular pathogens? Dissecting the roles of these two effectors could provide meaningful biological sense to this possible higher selective pressure among vascular pathogen.

### **What can we learn about XopAG and RipOI looking at their orthologs?**

Some other members of XopAG and RipOI family had been previously characterized and their molecular functions can provide some clues about the molecular mechanisms for XopAG and RipOI possible virulence function. *X. citri* AvrGf1 and AvrG2 are both able to trigger cell-death in different citrus species controlling thus the host range of the different *X. citri* subspecies (Rybak *et al.*, 2009; Gochez *et al.*, 2015). Both orthologs are localized in the chloroplast (Figueiredo *et al.*, 2011; Gochez *et al.*, 2017). Little is known about AvrGf1 mode of action despite that its chloroplast localization is required for triggering cell-death (Figueiredo *et al.*, 2011). Characterized more in detail is its ortholog AvrGf2, whose interaction with a plant cyclophilin is required for the accumulation of ROS and subsequent cell death (Gochez *et al.*, 2017). To this end, they introduced two modified versions of the Cyp-binding motif that allowed a weak



interaction or the inhibition of the interaction with the plant cyclophilin. Whether this motif is required for XopAG and RipOI virulence functions would be interesting to study but if it is, these two modification could serve to dissect the implication of the interaction with cyclophilins. Nonetheless, no cyclophilin proteins were identified as putative targets of neither XopAG nor RipOI.

*P. syringae* HopGI is able to suppress both PTI and ETI responses by targeting the plant mitochondria reducing the respiration levels and increasing the basal concentration of ROS (Block *et al.*, 2010). They also showed that constitutive expression of *hopGI* in Arabidopsis, tomato and tobacco conferred stunted growth, increased number of leaves and inflorescences and infertility. This is particularly interesting because both *xopAG* and *ripOI* also showed drastic phenotypes when inducibly expressed in Arabidopsis (**Figure 5.9**). However, these phenotypes are different from *hopGI*-mediated phenotypes, indicating that although all three T3Es have the potential to modulate the plant physiology, their mode of action might differ, probably due to their different subcellular localization. In a different study, it was shown that HopGI is responsible for *P. syringae*-induced actin remodeling through interaction with a mitochondrial kinesin (Shimono *et al.*, 2016). Interestingly, a kinesin related protein, KLR2, is one of the three common targets of RipOI and XopAG (**Figure 5.1A**), and the only gene for which a mutant showed a slight decrease in susceptibility to *Rps* (**Figure 5.1D**). While the characterization of this putative target was not prioritized in favor of BRG3, KLCR2 remains an interesting candidate whose interaction with XopAG and RipOI and possible involvement in plant susceptibility are worth studying.

Additionally, HopGI had been also characterized for inhibiting the *P. syringae*-induced reduction of vascular flow into minor veins in *N. benthamiana* leaves (Oh and Collmer, 2005). While this was just exploited as an easy and fast readout for plant basal defenses at the time, it opens a new perspective in the context of vascular pathogens. Indeed, orthologs from HopGI have been identified in many xylem-colonizing bacteria including not only *Xcc* and *Rps*, but also *X. hortorum* (Barel *et al.*, 2015), *X. hyacinthi* (Janse, 2005), *R. syzygii* (Safni, Subandiyah and Fegan, 2018), *Erwinia tracheiphila* (Shapiro *et al.*, 2018), and *Xylophilus ampelinus* (Grall and Manceau, 2003). As vascular pathogens, disease progression relies on the colonization and multiplication within the xylem. Therefore, the plant ability to respond by reducing the xylem flow could prevent or delay the progression of the infection and some pathogens have evolved T3E that are able to inhibit this flow reduction. In the same study where HopGI was identified, other four *P. syringae* T3Es were also identified as inhibitors of the vascular flow reduction (Oh

and Collmer, 2005). Among them there is AvrE, ortholog of XopAM and RipR, another couple of shared T3E between *Xcc*<sub>8004</sub> and *Rps*<sub>GMI1000</sub>. Whether the inhibition of this defense-related reduction of the xylem flow can be achieved by HopGI orthologs from vascular pathogens, notably XopAG and RipOI, is worth studying. If that were the case, it would be interesting to test other orthologs in other species to evaluate whether this is an extended and/or specific strategy among xylem-colonizing bacteria.

### **What can we learn about XopAG and RipOI without looking at their orthologs?**

Although informative clues, it is not sure that XopAG and RipOI behave as previously characterized member of their family. Being guided for what has been described in orthologous T3Es, although it is a straightforward and time-saving strategy, might prevent exploring the full potential mode of action of an effector. For this reason, and taking advantage of the strong phenotype of the transgenic pER8-*xopAG* lines (**Figure 5.1E**), an unbiased suppressor screening was initiated. While it is still ongoing, 10 independent suppressor lines have been already identified (**Figure 5.10**). Although time-consuming, this approach will allow to dissect the genetic bases of the *xopAG*-related phenotypes without any *a priori*. However, at this stage it is not possible to link directly this *xopAG*-related phenotype with XopAG virulence function. Experiments aiming at connecting these two aspects should be a priority as soon as more insight is acquired on either one of them (e.g., testing the impact on susceptibility to *Xcc* of plant genes genetically involved in the *xopAG*-mediated phenotype). Additionally, and as the pER8-*ripOI* phenotype seem to be similar to those of weakly induced pER8-*xopAG* plants, testing whether the future identified suppressor mutations are also able to suppress *ripOI*-mediated phenotype should also be done. If that was the case, this would provide further evidence for the possible functional similarities of these two orthologous T3Es.

While waiting for the results of the suppressor screening, a possible mechanism for XopAG and RipOI virulence based on the results presented in previous chapters is currently being explored: the interaction with Arabidopsis BOI-Related Gene 3 (BRG3). BRG3 co-localizes with XopAG and RipOI in the nucleus (**Figure 5.12**), and interacts with both of them by yeast two-hybrid (**Figure 5.1A**), confirmed in the case of XopAG by FRET-FLIM (**Figure 5.13**). Arabidopsis *brg3* mutants show reduced disease symptoms upon infection with a compatible *Xcc* strain (**Figure 5.1B**), acting thus as an Arabidopsis susceptibility factor. BRG3 belongs to a subclass of RING E3 ubiquitin ligases involved in the defense against necrotrophic fungus *B. cinerea* and salt tolerance (Luo *et al.*, 2010). While the E3 ligase activity *in vitro* has only been confirmed for BOI, the founding member of the BRG family, both BOI and all BRGs (including

BRG3) are positive regulators of the plant defense responses against *B. cinerea* and negative regulators of *P. syringae*-induced cell death (**Figure 5.14**) (Luo *et al.*, 2010). The molecular mechanisms behind this are still unknown although for BOI it is suggested that is linked to the interaction and ubiquitination of the MYB transcription factor *Botrytis Susceptible 1* (BOS1) (Luo *et al.*, 2010). However, none of the BRGs interact with BOS implying that, even if they relied on their putative E3 ligase activity, their targets might differ. Given the impact of BRG3 in susceptibility to *Xcc*, it would be interesting to test whether BRG3 truly possesses E3 ligase activity and if it does, to test if this activity is required for its role in susceptibility and to identify its ubiquitination targets (**Figure 5.14**). Additionally, although the interaction with XopAG has been confirmed, it has not been yet studied whether this interaction modulates somehow BRG3 activity linking thus XopAG virulence and BRG3 susceptibility functions. Considering the functional redundancy among BRGs (Luo *et al.*, 2010), it would also be interesting to test whether XopAG and RipOI can also interact with BOI and other BRGs. Finally, although the virulence function of RipOI might be weaker and the interaction with BRG3 has not yet been corroborated by a different technique, it is possible that the same mechanisms discovered for BRG3-dependendant XopAG virulence apply for RipOI. Therefore, it would also be worth testing.

# Chapter 6

Evolutionary history of XopJ6, a PopP2 ortholog translocated into plants by *X. campestris* pv. *campestris* to interfere with plant immunity

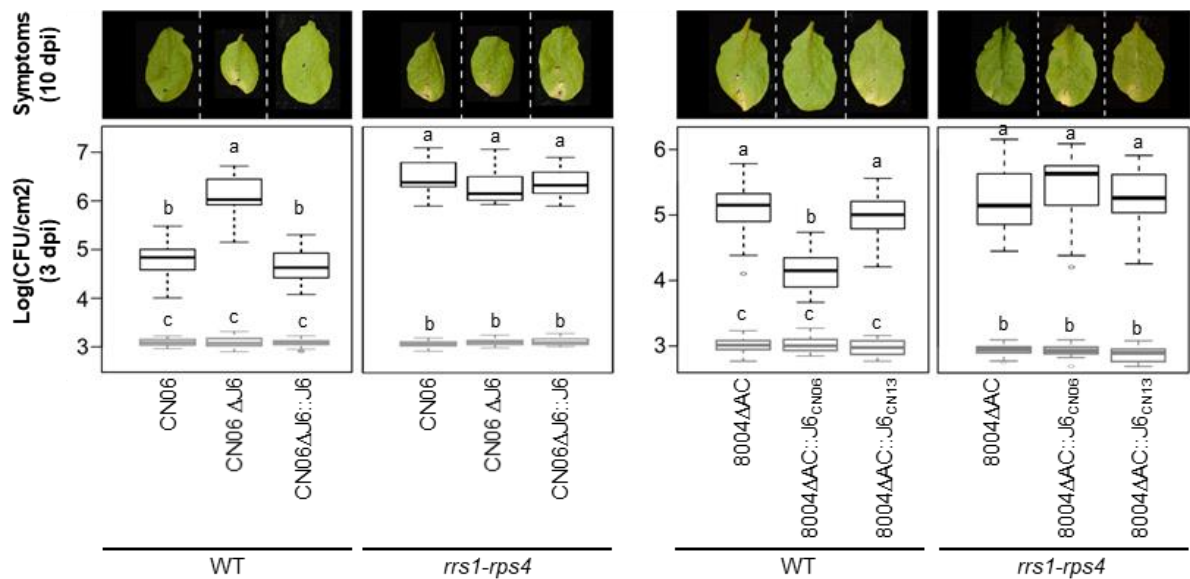


**Figure 6.1. XopJ6 is an RRS1/RPS4-dependant avirulence factor in Arabidopsis.** Disease symptoms at 10 dpi after wound-inoculation (top) and bacterial population at 0 (grey) and 3 (black) dpi after mesophyll infiltration (bottom) on 4-weeks-old Arabidopsis Ws-0 wild-type (WT) and *rrs1-rps4* plants. CN06, CN06Δ*xopJ6* (ΔJ6) and CN06Δ*xopJ6*::*xopJ6* (ΔJ6::J6); and 8004Δ*xopAC* (ΔAC), 8004Δ*xopAC*::*xopJ6*<sub>CN06</sub> and 8004 Δ*xopAC*::*xopJ6*<sub>CN13</sub> bacterial strains were inoculated at 10<sup>8</sup> and 10<sup>5</sup> CFU/ml for wound inoculation and mesophyll-infiltration respectively. Images are representative of the median disease index obtained from 24 leaves from three independent experiments. Boxplots represent the combination of three independent experiments with 17 and 27 values per point at 0 and 3 dpi respectively. Statistical groups were determined using non parametric Kruskal-Wallis test (p-value<0.01) and are indicated by different letters. Results from E. Lauber (LIPM)

**Table 6.1. XopJ6 interacts with RRS1-R and dissociates it from DNA contrary to XopJ6<sub>CN13</sub>.** FRET-FLIM measurements of interactions between RRS1-R-YFP and XopJ6-CFP, XopJ6<sub>C409A</sub>(CA, catalytic mutant)-CFP and XopJ6<sub>CN13</sub>-CFP (top) and between RRS1-R-GFP and Sytox-labelled DNA in the presence of XopJ6-3HA and XopJ6-CA-3HA (bottom) in transiently transformed *N. benthamiana* leaves. Results from L. Deslandes, M. Escouboué, C. Vicedo (LIPM) and C. Pouzet (FRAIB imagery platform).

Donor	Acceptor	$\tau$ (ns) <sup>a</sup>	SEM <sup>a</sup>	Nuclei	Efficiency (%)	p-value <sup>b</sup>
XopJ6-CFP	-	3.703	0.129	80	11.7	5.4 10 <sup>-29</sup>
XopJ6-CFP	RRS1-R-YFP	3.269	0.228	61		
XopJ6CA-CFP	-	3.724	0.138	77	12.1	2.9 10 <sup>-26</sup>
XopJ6CA-CFP	RRS1-R-YFP	3.272	0.254	60		
XopJ6 <sub>CN13</sub> -CFP	-	3.660	0.143	75	0.4	0.5
XopJ6 <sub>CN13</sub> -CFP	RRS1-R-YFP	3.642	0.174	90		
RRS1-R-GFP	-	2.075	0.146	26	-4.9	3.4 10 <sup>-2</sup>
(in co expr. with XopJ6-3HA)	Sytox	2.177	0.191	26		
RRS1-R-GFP	-	2.098	0.183	30	11.5	2.8 10 <sup>-4</sup>
(in co expr. with XopJ6-CA-3HA)	Sytox	1.860	0.291	30		

<sup>a</sup> For each nucleus, average fluorescence decay profiles were plotted and fitted with exponential function using a non linear square estimation procedure and the mean and standard error of the mean lifetime were calculated.

<sup>b</sup> Student's *t* test p-value of the difference between the donor lifetimes in the presence/absence of acceptor.

## 6.1 Introduction

Previous work in the group identified a new *Xcc* avirulence protein recognized by certain *A. thaliana* and cabbage genotypes: the type III effector XopJ6. *xopJ6* encodes a putative acetyl transferase from the YopJ effector family that is closely related to *Rps* PopP2/RipP2, whose recognition and function have been largely studied (Deslandes *et al.*, 1998, 2003; Tasset *et al.*, 2010; Le Roux *et al.*, 2015; Zhang *et al.*, 2017). Emmanuelle Lauber (LIPM) has characterized *xopJ6* avirulence function in *Arabidopsis* showing that is dependent on *RRSI-R/RPS4*, the same R gene pair that recognizes *popP2* (**Figure 6.1A**). She also found a natural variant of XopJ6, XopJ6<sub>CNIB</sub>, which escapes the recognition by *RRSI-R/RPS4*. Additionally, work done by Laurent Deslandes and his group (LIPM) showed that, similar to PopP2 (Deslandes *et al.*, 2003), XopJ6 physically interacts with *RRSI-R* (**Table 6.1**). This interaction is prevented by XopJ6<sub>CNIB</sub>, the natural variant of XopJ6 that does not confer *RRSI-R/RPS4*-mediated resistance, suggesting thus a link between resistance and the physical interaction with *RRSI-R*. Moreover, XopJ6 also seems to prevent *RRSI-WRKY* domain binding to genomic DNA (**Table 6.1**). However, contrary to PopP2, it has not been yet demonstrated that this inhibition is caused by the effector-mediated acetylation of *RRSI* (Le Roux *et al.*, 2015).

### Contribution

This project had been started prior to my arrival, led by Emmanuelle Lauber, Laurent Deslandes and Laurent Noël (LIPM). My contribution to this work has been the study of the phylogeny, regulation, translocation and ROS-burst inhibition by XopJ6, the analysis of its genetic distribution on a variety of *Xcc* strains and the measurement of its expression in diverse wild-type and mutant strains to correlate it with the copy number and pathogenicity. Additionally, I included *xopJ6* in the same work pipeline than the rest of *xop* and *rip* candidate genes. Therefore, it was screened for protein-protein interactions against the *Arabidopsis* cDNA library and inducible *xopJ6* transgenic *Arabidopsis* lines were constructed.

## 6.2 XopJ6 is a member of the YopJ family closely related to *R. solanacearum* PopP2

*xopJ6* was annotated as belonging to the Serine/Threonine acetyltransferase, YopJ family (InterPro identifier: IPR005083). This family comprises evolutionary conserved type III effectors from a wide variety of animal and plant bacterial pathogens as well as nitrogen fixing rhizobia.

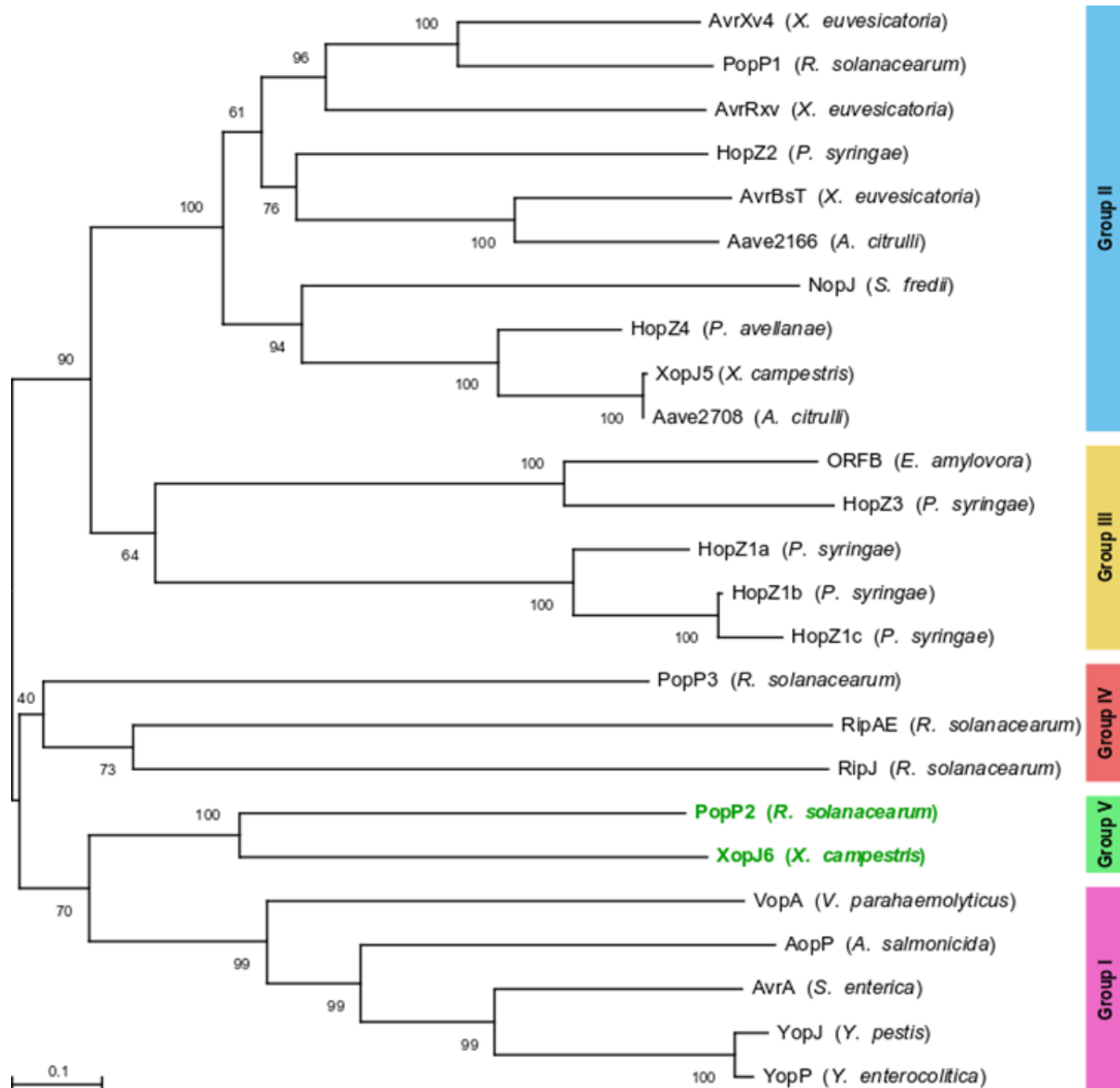


**Figure 6.2. Phylogenetic tree of 25 members of the YopJ family of bacterial effectors.** The position of XopJ6 and its close ortholog PopP2 is highlighted in green. Neighbor-Joining tree with bootstrap support values indicated above each node. The scale bar indicates the evolutionary distance in number of amino acid substitutions per site computed using the Poisson correction method. Division in groups based on a previous report (Ma & Ma, 2016). The GenBank accession numbers of the full-length proteins used to construct the tree are as follows: AAG39033 for AvrXv4 (*Xanthomonas euvesicatoria*), CAF32331 for PopP1 (*Ralstonia solanacearum*), AAA27595 for AvrRxv (*X. euvesicatoria*), CAC16700 for HopZ2 (*Pseudomonas syringae*), AAD39255 for AvrBsT (*X. euvesicatoria*), ABM32744 for Aave2166 (*Acidovorax citrulli*), NP\_443964 for NopJ (*Sinorhizobium fredii*), EKG29639 for HopZ4 (*P. syringae*), WP\_011347382 for XopJ5 (*X. campestris*), ABM33278 for Aave2708 (*A. citrulli*), AAF63400 for ORFB (*Erwinia amylovora*), AAF71492 for HopZ3 (*P. syringae*), AAR02168 for HopZ1a (*P. syringae*), WP\_004661226 for HopZ1b (*P. syringae*), AAL84243 for HopZ1c (*P. syringae*), CAF32358 for PopP3 (*R. solanacearum*), CADI3849 for RipAE (*R. solanacearum*), CADI5839 for RipJ (*R. solanacearum*), CADI4570 for PopP2 (*R. solanacearum*), AAT08443 for VopA (*Vibrio parahaemolyticus*), NP\_710166 for AopP (*Aeromonas salmonicida*), AAL21745 for AvrA (*Salmonella enterica*), AKN09807 for YopJ (*Yersinia pestis*) and AAN37537 for YopP (*Y. enterocolitica*). XopJ6 (*X. campestris*) amino acid sequence is the translation of CN06-G2\_01.2135 in the private annotated version of CN06 (L. Noël, unpublished data). Constructed with MEGA X (Kumar et al., 2018).

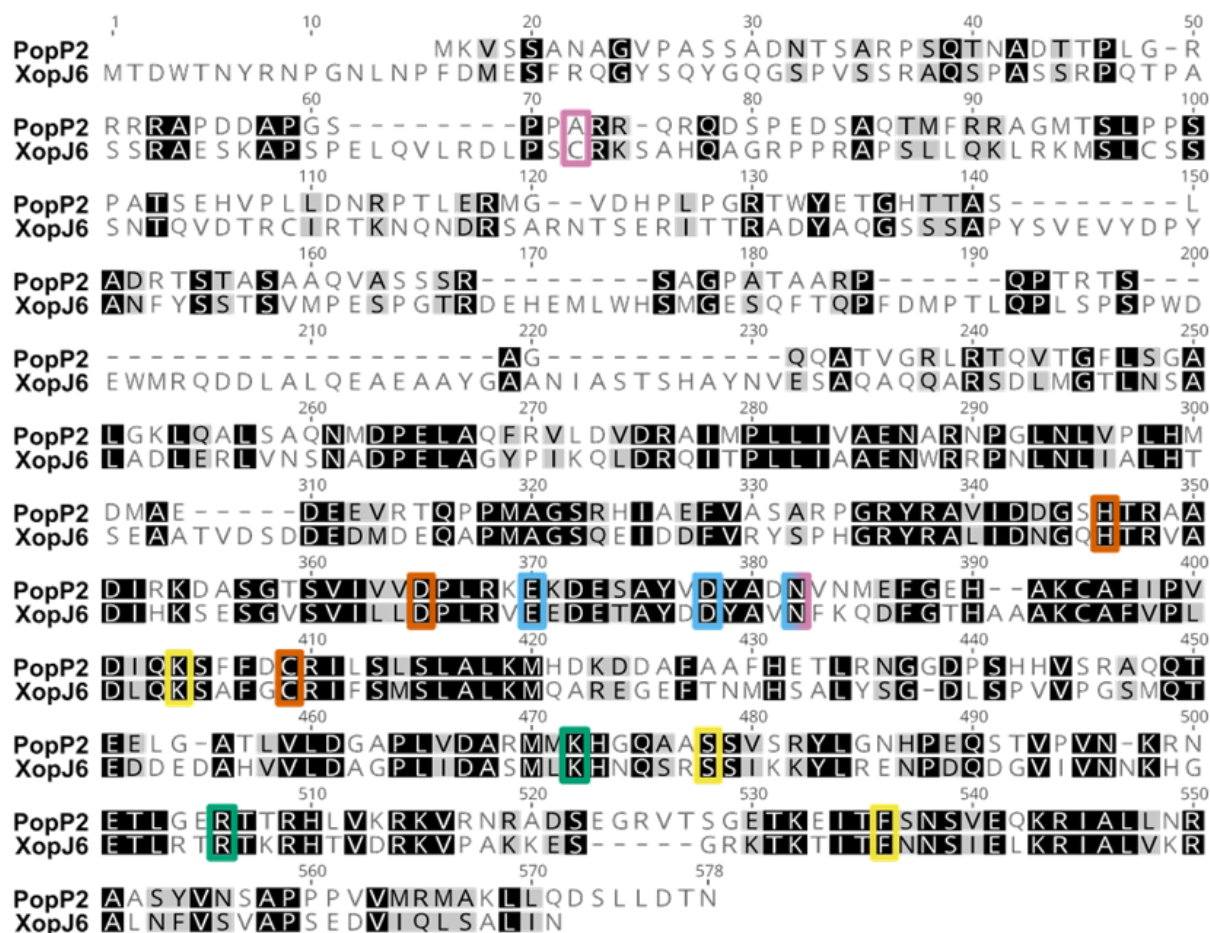


**Figure 6.3. Pairwise sequence alignment of PopP2 and XopJ6.** ClustalW2 alignment using the BLOSUM cost matrix with an open and extension gap penalties of 10 and 0.1 respectively. The background color represents the percentage of similarity based on the mentioned matrix with a threshold of 1 (black: identical, grey: similar, and white: not similar). The amino acids forming the conserved catalytic triad (Orth et al. 2000) are boxed in red, and the residues involved in binding to acetyl-CoA, IP6 and RRSI-R (Tasset et al. 2010, Zhang et al. 2017), in yellow, green and blue respectively. The two amino acid substitutions found in the natural variants XopJ6<sub>CN3</sub> (C72G and N382K) are squared in pink.



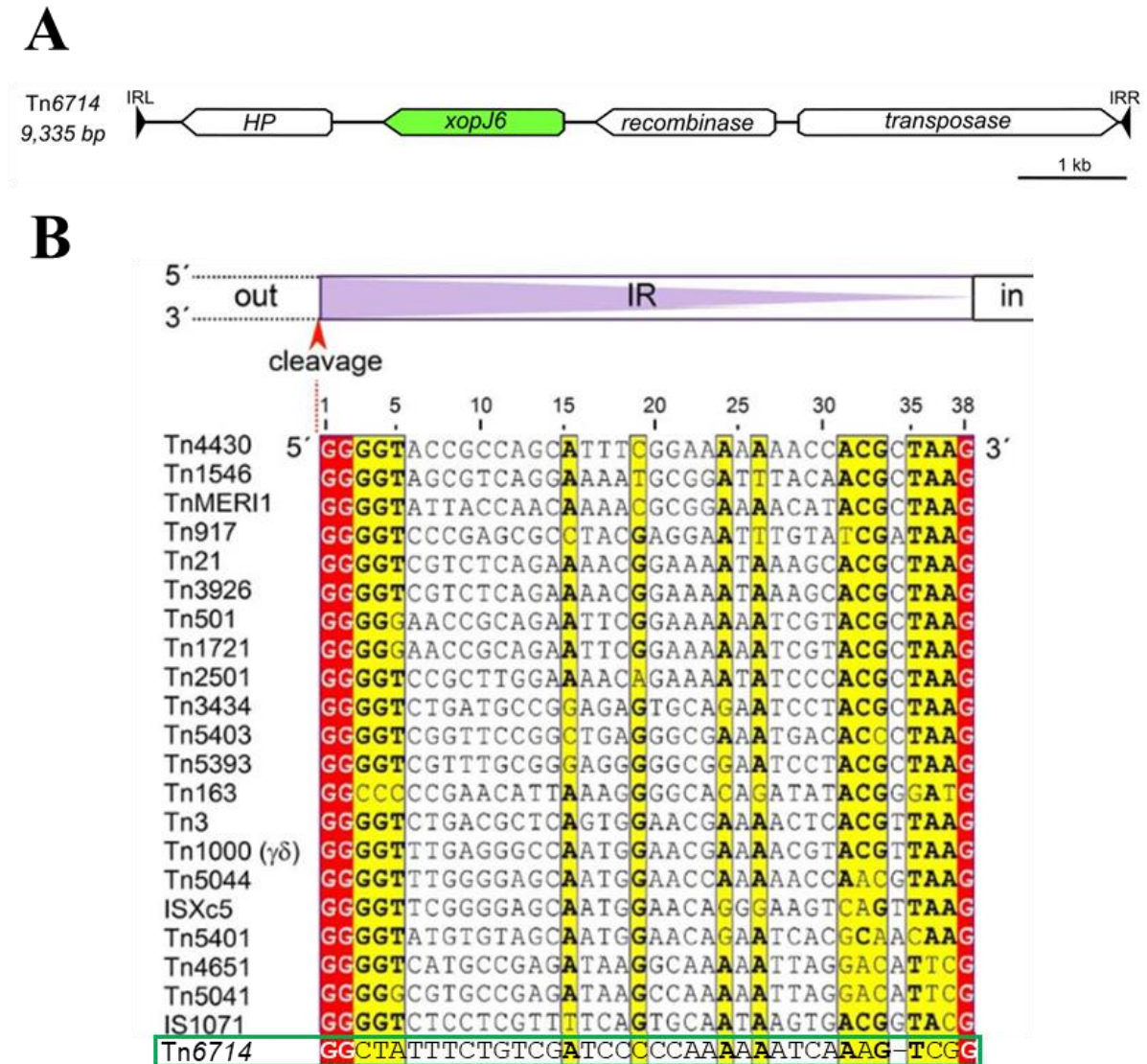


**Figure 6.4. *xopJ6* is located in Tn6714, a new 9-kb Tn3 family transposon.** (A) Genetic organization of Tn6714, the Tn3 family transposon containing *xopJ6*. Genes are represented by pointed squares indicating their orientation. *xopJ6* is highlighted in green. The flanking inverted repeats (IR) are represented by black triangles. The convention used for orientation of the transposon is that the transposase is transcribed from left to right. (B) Sequence comparison of Tn6714 IR, squared in green, with other Tn3 family transposon IRs. Adapted from Nicolas *et al.*, 2015.

To assert whether XopJ6 truly belongs to this family and to study its relationship with other known members, the phylogeny of the family was reconstructed (**Figure 6.2**). Based on the position in the phylogenetic tree, XopJ6 appears to be a true member of the YopJ family. It is closely related to *Rps* PopP2 forming the group V, which is closer to YopJ family members from animal pathogens (group I) and *Ralstonia* effectors (group IV) than to other *Xanthomonas* effectors (groups II and III). XopJ6 and PopP2 are 35.4% identical, with stronger conservation at the C-terminus than at the N-terminus (**Figure 6.3**). The importance of certain amino acids for the normal functioning of PopP2 has been reported: 1) H260, D279 and C321 form the catalytic triad which is conserved not only among YopJ family members, but also among C55 cysteine proteases (Orth *et al.*, 2000). The C321A substitution prevents RRSI-R-mediated resistance and PopP2 acetyl transferase activity (Tasset *et al.*, 2010; Le Roux *et al.*, 2015). 2) E284, D292 and N296 are involved in the physical interaction with RRSI. E284A/D292A/N296A triple substitution prevents the acetylation of RRSI-R and cell-death triggering (Zhang *et al.*, 2017). 3) K383 is a target of PopP2 autoacetylation activity. K383R substitution prevents RRSI-mediated resistance (Tasset *et al.*, 2010). More recently, this same residue has been described to be involved, together with R416, in the interaction with the host cofactor IP<sub>6</sub>. Both K383R and R416E substitutions prevent PopP2 acetyl transferase activity (Zhang *et al.*, 2017). 4) K316, S389 and F446 are important for the interaction with acetyl-CoA. K316A/S389A/F446A triple substitution also prevents PopP2 acetyl transferase activity and cell death triggering (Zhang *et al.*, 2017). All these eleven amino acids are conserved between PopP2 and XopJ6 (**Figure 6.3**), suggesting that XopJ6 could function similarly to PopP2.

### 6.3 *xopJ6* is located on a transposon present in one to three copies in *Xcc* genomes

*xopJ6* had been previously identified in twelve *Xcc* genome-sequenced strains. *xopJ6* location had been mapped in the 5-Mb chromosome of only two of these strains (CN03 and CN06) or in large contigs from other two strains (CFBP6865 and CNI3). In the remaining eight strains, *xopJ6* was located in a 9-kb or smaller contig (CFBP4954, CFBP6943R, CN02, CN07, CN08, CNI2, CNI7 and CNI8). This 9-kb region was highly conserved among the twelve strains. In addition to *xopJ6*, this region also contained other three protein-coding genes: a Tn3-family transposase (IPR002513), a tyrosine recombinase (IPR020876) and another gene coding for a hypothetical protein. This structure is typical of Tn3-family transposons (Nicolas *et al.*, 2015) (**Figure 6.4A**). Effectively, this 9 kb region was flanked by 37-bp inverted repeats (IR) similar to

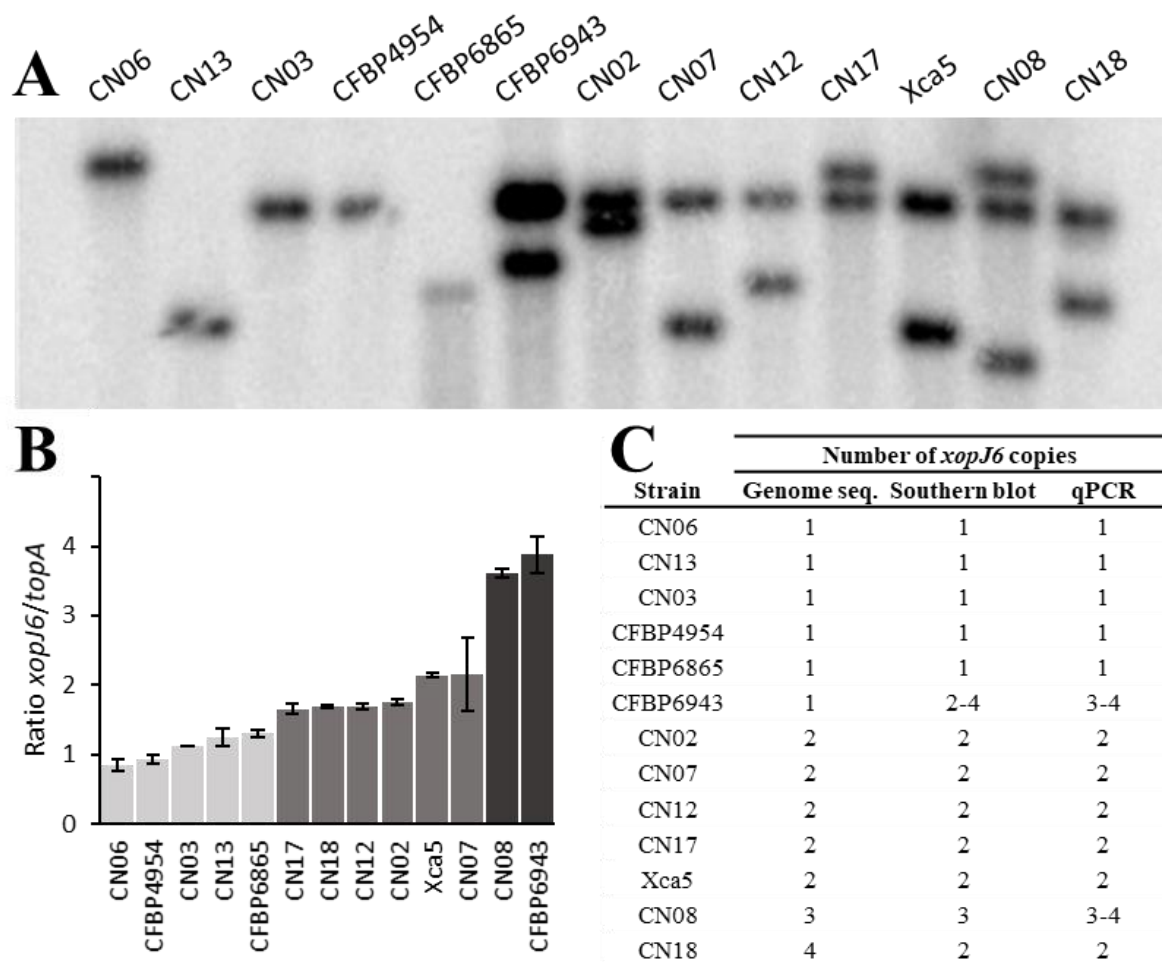


**Figure 6.5. *xopJ6* is found in one to three copies in *Xcc* genomes.** (A) Southern blot analysis of genomic DNA from different *Xcc* strains using a radiolabeled *xopJ6* DNA probe. Performed by Emmanuelle Lauber (LIPM). (B) Ratio between the quantification of products of amplification of *xopJ6* and *topA*, gene found in single copy in *Xcc* genomes. Results from one experiment, three technical replicates. Error bars represent the standard error with two technical replicates. The bar color represents the inferred number of *xopJ6* copies: light grey, one; grey, two; and dark grey, three to four. (C) Summary of the number of *xopJ6* copies in different *Xcc* strains as inferred from the most recent sequenced genome available, Southern blot and qPCR on genomic DNA.

those of other Tn3-family transposons (**Figure 6.4B**). This indicates that *xopJ6* is located within a new Tn3-family transposon that was registered in the Transposon Registry (Tansirichaiya, Rahman and Roberts, 2019), as Tn6714.

Most of the *xopJ6*-containing *Xcc* strains were later resequenced using long-read sequencing technology. This allowed us to detect that *xopJ6* was indeed always present in Tn6714. Yet, this transposon was found in one to three copies in the different genomes and plasmids. This observation was experimentally validated by quantitative real-time PCR (qRT-PCR) using genomic DNA as template and by Southern blot, the latter done by Emmanuelle Lauber (**Figure 6.5**). Tn6714 was found in single copy on CN03 and CN06, precisely the only two strains in which *xopJ6* could have been mapped in the chromosome through the initial short-read sequencing. On CN02, CN07, CN12 and CN17, Tn6714 was found in two copies; and on CN08, in three copies, all in the chromosome. This could explain the assembly problems found in the previous versions of the genomes, sequenced with HiSeq short reads, which led to the presence of *xopJ6* in short contigs. Tn6714 from CN13 was found in single copy on a 186-kb contig, similar size to the plasmid contained in this strain according to a previous report (Guy *et al.*, 2013), indicating Tn6714 is probably located in a single-copy plasmid in this strain. Tn6714 from CFBP6943 and CN18 were found in single and four copies (two in the chromosome and two in two small contigs) respectively, but these results contradicted our experimental data. This is probably due to problems during the genome assembly. In the case of CN18, the two small Tn6714-containing contigs matched entirely or partially the chromosome suggesting that there are only two chromosomal copies of Tn6714, as seen by qPCR and Southern blot, and the small contigs are likely assembly artifacts. In the case of CFBP6943, the fact that Tn6714 was found on a 9-kb contig (like all strains that contain more than one copy) instead of on the chromosome or a plasmid (like all strains that contain only one copy) suggests that there could be more than one *xopJ6* copy, as evidenced later by qPCR and Southern blot. However, the exact number and location of the additional copies could not be exactly mapped and therefore, CFBP6943 was excluded from further analyses. Strains CFBP4954 and CFBP6865 were not resequenced using long-read technologies so the only information about the number and location of Tn6714 comes from the first version of the genomes. In the case of CFBP4964, the location and number is unknown because Tn6714 was found in a 9-kb contig, but according to the qPCR and Southern blot results, there is only a single copy. In the case of CFBP6865, Tn6714 was found in a 62-kb contig, similar size to a 63-kb-long plasmid contained in this strain (Laurent Noël, unpublished data). According to the qPCR and Southern blot results, there is only one copy. However, this

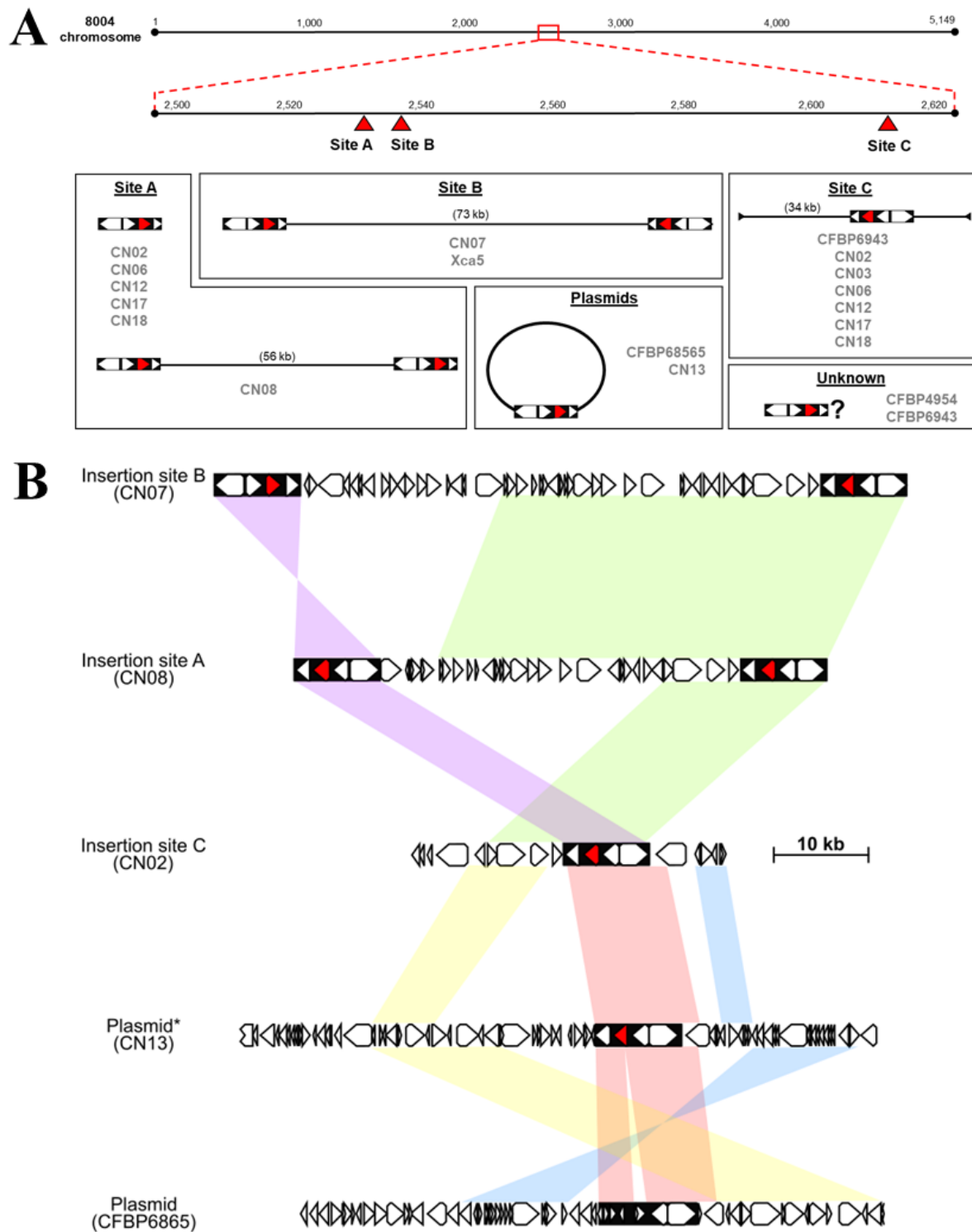


**Figure 6.6. *xopJ6* was acquired as simple or composite transposon in evolutionary related plasmids and chromosomal insertions.** (A) All possible locations of Tn6714 (black box, *xopJ6* highlighted in red) and derived composite transposon on the bacterial genome using the 8004 reference strain chromosome as reference. (B) Synteny between the different Tn6714-containing genomic locations. Because of the large size of the plasmid from CN13, only an extraction of it was represented. Blocks of synteny calculated by progressive MAUVE multiple genome alignment (Darling *et al.*, 2004). Different colors indicate different synteny blocks.

Tn6714 copy presents an 1.2-kb-long IS3-family insertion sequence (IS) inserted precisely within *xopJ6* coding region truncating this gene.

With the known localization of the different copies of Tn6714 in the different genomes, I tried to infer the possible evolutionary story of *xopJ6* within *Xcc* strains. Tn6714 was found as an autonomous transposon or forming different composite transposons (**Figure 6.6A**). In the case of the chromosomal copies of Tn6714, three insertion sites located in a 80-kb window were mapped in the *Xcc* reference strain 8004, hereafter called sites A, B and C. Tn6714 was found in site A as an autonomous transposon in all strains but CN08, where it was found in two copies delimiting a 56-kb composite transposon. The target sequence of the insertion site A is 5'-TAATA-3' found at the end of conjugal transfer protein *trbP* gene (XC\_2105) and the direct repeats (DRs) produced upon integration are 5'-TAGTA-3'. In site B, Tn6714 is found in two opposed copies delimiting a 73-kb composite transposon. The target sequence of the insertion site B is 5'-ATGCA-3' found at the beginning of a hypothetical protein-encoding gene (XC\_2115) and the DRs produced upon integration are 5'-ATGAA-3'. Tn6714 was found in the middle of a 34-kb region flanked by 50-bp inverted repeats. The target sequence of the insertion site C is 5'-GATC-3' found in an intergenic region (between XC\_2164 and XC\_2165) and this same sequence is produced as DR when the 34-kb region is integrated. The target sequences of insertion sites A and B are both 5-bp long and AT-rich matching the target sequences of other Tn3-family members (Nicolas *et al.*, 2015). This indicates that the integration of Tn6714 and derived composite transposons at these sites took place through Tn3-family typical replicative transposition. Conversely, insertion site C is not AT-rich and the DR produced are 4-bp-long and match perfectly the target site, indicating that the integration at this site took place through a different mechanism. In the case of plasmidic copies, there was one on a 186 kb plasmid in the CN13 strain and another one on a 62-kb plasmid in the CFBP6865 strain.

To test whether the different composite transposons and plasmids shared a common origin or if they are completely independent, synteny studies were performed (**Figure 6.6B**). A ~17-kb block of synteny containing Tn6714 was observed between the 34-kb region of the insertion site C and the composite transposons of insertions sites A and B. This block is even larger (~30 kb) when compared the two composite transposons. Similarly, three blocks of synteny (two of ~12 kb, one of them containing Tn6714, and another of ~3 kb) were also found between the 34-kb region of the insertion site C and the plasmids of the CN13 and CFBP6865

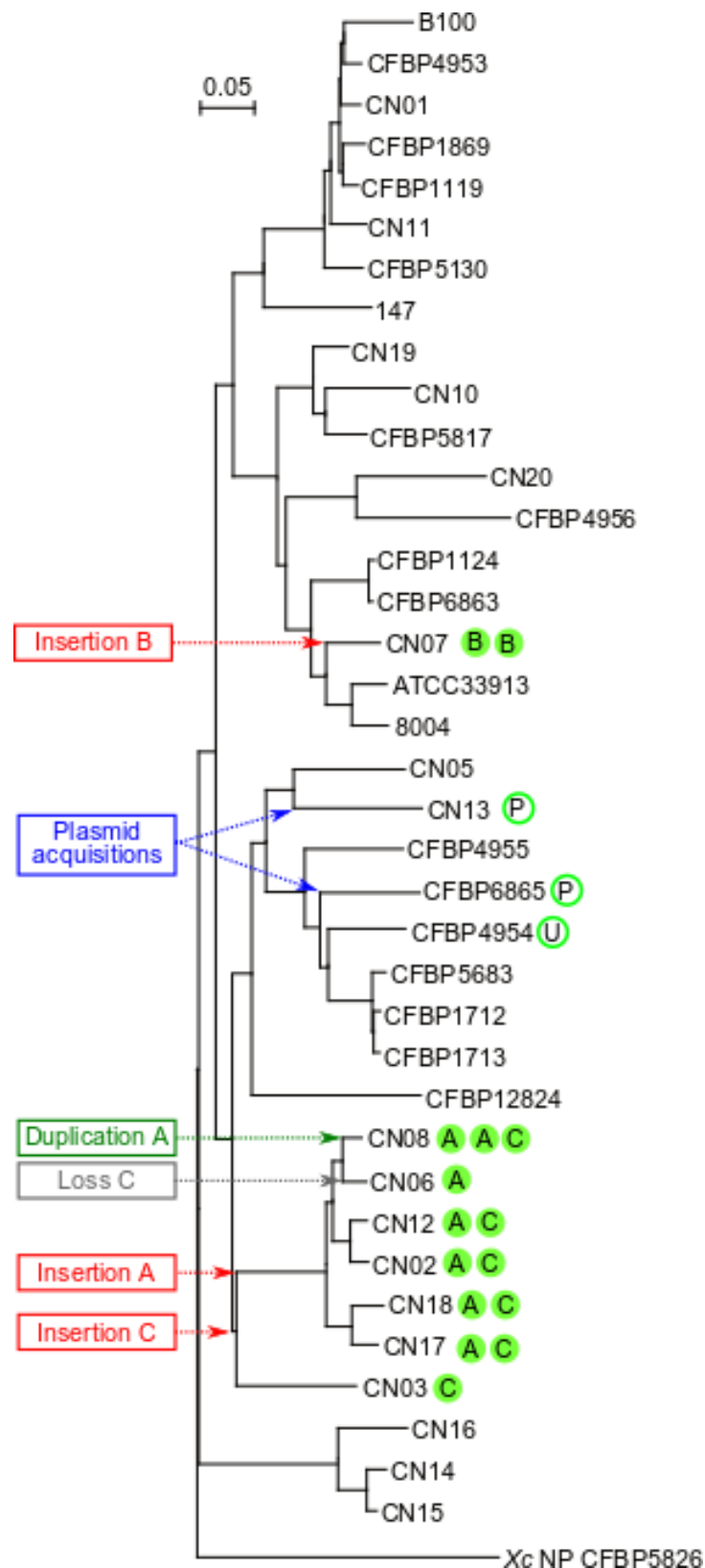


**Figure 6.7. Proposed evolution of the *xopJ6* loci within *Xcc* strains.** The number of Tn67I4 copies is indicated by green circles. Unfilled circles indicate variants of XopJ6 not recognized by RRS1-R. Letters indicate the genomic location of Tn67I4: A, B and C (chromosome insertions sites A, B and C respectively), P (plasmids) or U (unknown). Phylogenetic tree from Denancé *et al.*, 2018.

strains. This could indicate that all these different sequences might have a common origin, suggesting that the different chromosomal insertions and plasmids are somehow related.

Considering the presence and conservation of Tn6714 on the different sites and taking in consideration the phylogeny of these strains (Denancé *et al.*, 2018), the following evolutionary scenario was proposed (**Figure 6.7**): *xopJ6* had been initially acquired horizontally through plasmids, as it has been seen on different plasmids in at least two strains (CFBP6865 and CN13). A first chromosomal insertion was found on the site C in the ancestor of CN02, CN03, CN06, CN08, CN12, CN17 and CN18 strains. This insertion was more recently lost in CN06. Tn6714 could have been inserted in the site A by replicative transposition from the Tn6714 copy in the site C. This could explain why Tn6714 was found in site A as a single or composite transposon only in strains that presented Tn6714 in the site C. This would mean that insertion in the site A was posterior to insertion in the site C, which could explain why CN03, the strain that diverged the earliest from this clade, do not present insertion site A. Another independent and more recent chromosomal insertion occurred in the site B to the common ancestor of CN07 and closely related Xca5, probably by replicative transposition from a possible Tn6714-containing plasmid lost afterwards.

## 6.4 XopJ6 is regulated by the *hrp* system and possess a functional T3SS translocation signal

To study the regulation and translocation of XopJ6, the first 300 bp of its open reading frame were cloned into the suicide vector pAIO (Laurent Noël, unpublished data) generating a translational fusion with *avrBsl*<sub>59-445</sub> (coding for the T3E AvrBsl without its translocation signal) and a HA-strep tag, and transcriptional fusion with the reporter gene *uidA* (*E. coli*  $\beta$ -glucuronidase) (**Figure 6.8**). This construction (hereafter pAIO-J6), through homologous recombination, was later inserted in several variants of the *xopJ6*-containing *Xcc* strain CN06 under the control of its native promoter. The variant strains in which pAIO-J6 was inserted were CN06 wild type, the T3SS mutant  $\Delta hrcV$  (Rossier *et al.*, 1999), a mutated version of master regulator gene *hrpG* (named *hrpG\**, coding for HrpG<sub>E44K</sub>) that renders *hrp* gene expression constitutive (Wengelnik, Van den Ackerveken and Bonas, 1996; Wengelnik, Rossier and Bonas, 1999) and the double mutant *hrpG\**  $\Delta hrcV$ .

To estimate *xopJ6* promoter activity, the GUS activity of *in vitro* bacterial cultures of the different CN06 variants in minimal (MME) and rich (Moka) media was measured by



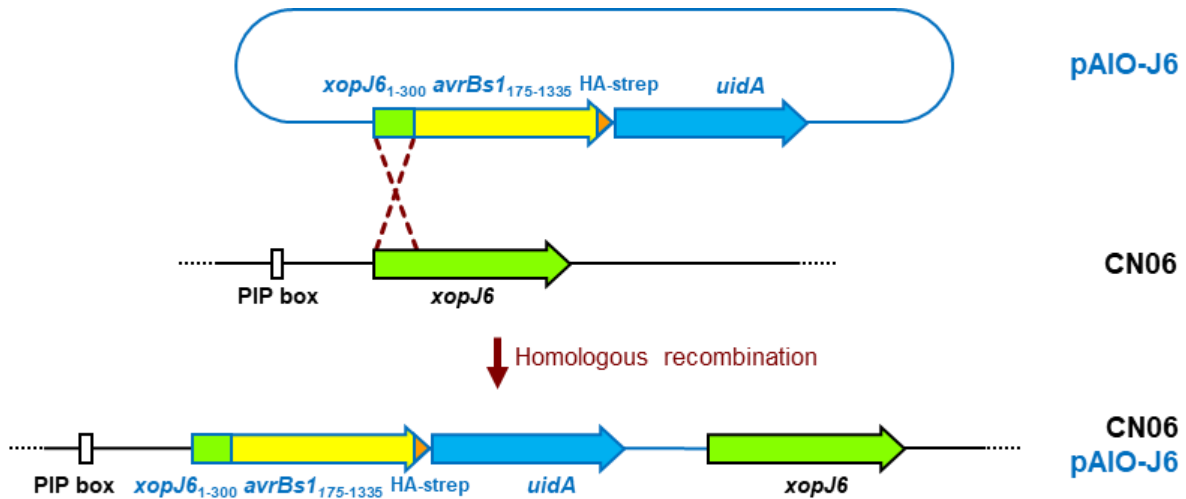


**Figure 6.8. pAIO strategy to study regulation and translocation of *xopJ6*.** The suicide vector pAIO-J6 containing the first 300 bp of *xopJ6* open reading frame in a translational fusion with *avrBs1*<sub>175-1335</sub> and a HA-strep tag and in a transcriptional fusion with *uidA* was generated and transformed in *Xcc* CN06 variant and wild type strains. The homologous recombination between the first 300 bp of *xopJ6* of pAIO-J6 and CN06 genome allows the integration of the full plasmid with the *xopJ6-avrBs1-HA-strep-uidA* cassette under the control of the natural *xopJ6* promoter which contains a PIP-box.

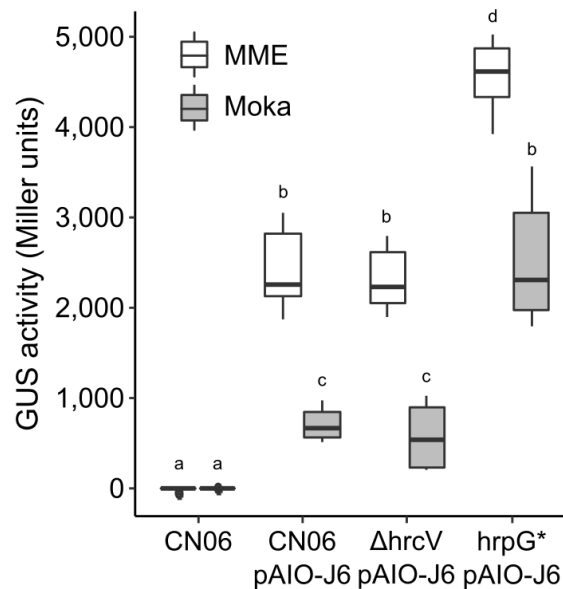


**Figure 6.9. *xopJ6* promoter is *hrpG*-regulated.**  $\beta$ -glucuronidase (GUS) activity of pAIO-J6 in different *Xcc* strain CN06 WT, *hrpG*\* and  $\Delta$ *hrcV* variants. White and grey boxes represent GUS activity of bacterial cultures in poor (MME) and rich (Moka) medium respectively. Combination of three independent experiments. The different letters (a-d) above the boxes indicate statistically different groups (one-tailed Wilcoxon signed-rank test  $p$ -value < 0.0001).

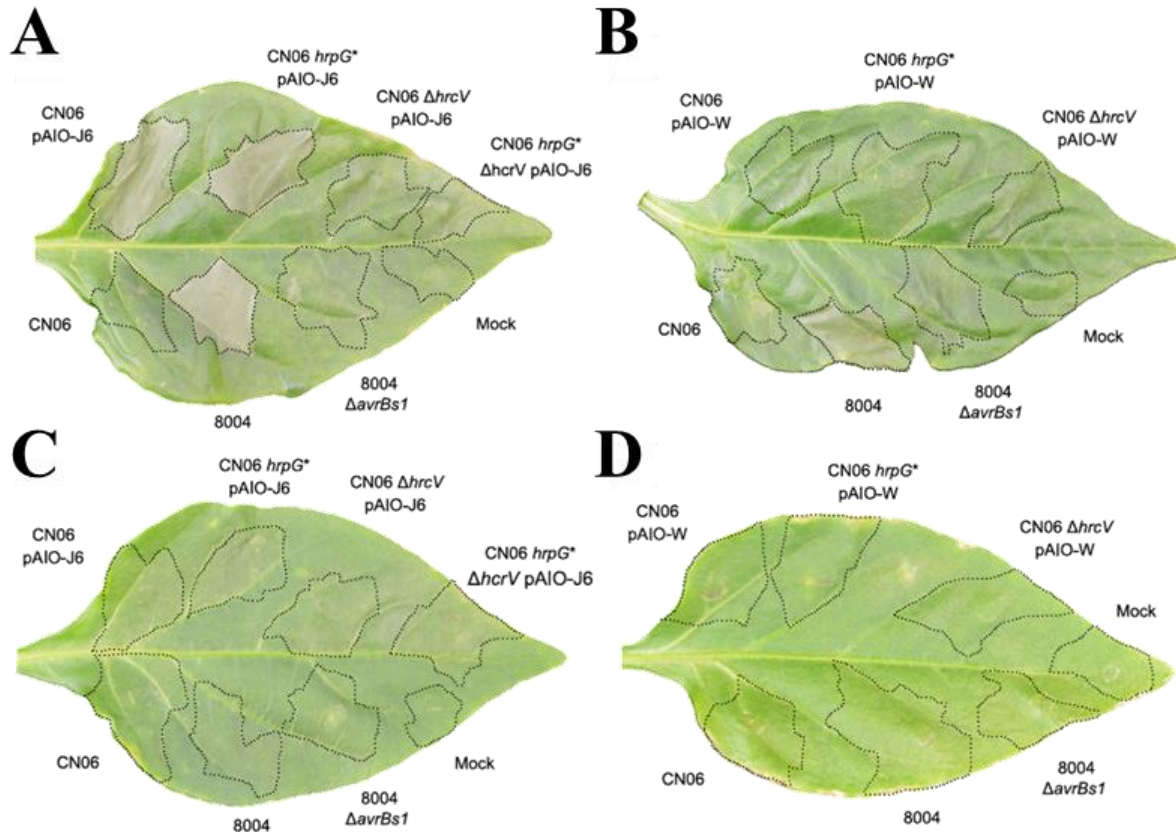


**Figure 6.10. The N-terminus of XopJ6 is able to translocate a truncated version of AvrBs1 through the Xcc type III secretion system.** Translocation experiments in 6-weeks-old ECW-10R (A and B) and ECW (C and D) pepper leaves using *Xcc* strain CN06 WT, *hrpG\** and  $\Delta hrcV$  transformed with the integrative plasmid pAIO containing either *xopJ6*<sub>1-300</sub> (pAIO-J6) or *hrpW*<sub>1-300</sub> (pAIO-W), fused to *avrBs1*<sub>59-445</sub> (coding for AvrBs1 lacking its translocation signal). *Xcc* 8004 WT and  $\Delta avrBs1$  strains and 1 mM MgCl<sub>2</sub> (mock) were used as controls. The symptoms were observed at 48 hours after leaf infiltration with bacterial suspensions at OD<sub>600</sub> = 0.3. The experiment was repeated three times with similar results

colorimetry (**Figure 6.9**). As shown with other *Xanthomonas* T3E and *hrp* genes (Schulte and Bonas, 1992; Jiang *et al.*, 2013), *xopJ6* is less expressed in rich medium compared to minimal medium. The expression in both media is enhanced in the *hrpG*<sup>\*</sup> mutant indicating that *xopJ6* belongs to the *hrpG* regulon. This expression is unaltered in the *hrcV* T3SS mutant.

To test whether XopJ6 contains a T3SS translocation signal, the different CN06 variants were infiltrated into ECW and ECW-10R pepper plants (**Figure 6.10**). These plants only differ in the absence/presence respectively of *Bsl*, an R gene able to recognize *Xanthomonas* AvrBsl (Minsavage *et al.*, 1990). CN06 pAIO-J6 and *hrpG*<sup>\*</sup> pAIO-J6 induced HR on ECW-10R plants similar to the naturally *avrBsl*-containing strain 8004 but this symptom could not be observed in the wild-type CN06 nor any of the  $\Delta hrcV$  mutants, similarly to 8004 $\Delta avrBsl$ . Conversely, this HR was never observed in ECW pepper plants. This indicates that the cell-death observed is *avrBsl/Bsl*-dependen. Therefore, in the CN06 pAIO-J6 and *hrpG*<sup>\*</sup> pAIO-J6, this HR is linked to the translocation of the *xopJ6*<sub>1-300</sub>*avrBsl*<sub>59-445</sub> translational fusion product through the T3SS. To exclude that any other sequence could confer translocation ability; the same CN06 variants were transformed with the previously generated pAIO with the 300 first bp of the hairpin gene *hrpW* (hereafter pAIO-W) which had been shown to be equally *hrpG*-regulated but not translocated through the T3SS (Laurent Noël, unpublished data). Contrary to pAIO-J6, pAIO-W did not cause HR on the CN06 and *hrpG*<sup>\*</sup> backgrounds in ECW-10R plants reinforcing that XopJ6 first 100 amino acid constitute a true T3SS translocation signal. Altogether, the regulation and translocation of XopJ6, together with its belonging to the YopJ family proves that XopJ6 is a true type III effector.

## 6.5 *xopJ6* copy number is correlated with its expression and pathogenicity

Despite being an avirulence factor in certain *Arabidopsis* ecotypes and cabbage varieties, *xopJ6* is present in multiple copies on several *Xcc* strains. This suggests that XopJ6 might have a beneficial role for the bacteria in susceptible plants that has allowed the expansion and conservation of multiple copies through evolution. Due to its tight regulation and its translocation through the T3SS, it is unlikely that this possible beneficial role occurs in the bacteria. It is more likely that XopJ6 could confer a benefit during the infection of the host. As the pathogenicity on susceptible *Arabidopsis* ecotype Col-0 of several *Xcc* strains had been previously evaluated, I checked whether the number of functional copies might correlate with the pathogenicity of the strains (**Figure 6.11A**). Effectively, the disease index scored at 7 dpi is

statistically higher among strains that contain multiple *xopJ6* copies compared to strains containing just one copy, and even higher compared to strains that do not contain *xopJ6*. When plotting the number of functional *xopJ6* copies and the median of the disease index of all these strains, the coefficient of determination of the corresponding linear regression is 0.779 indicating correlation between these two parameters (**Figure 6.IIB**). This suggests that in susceptible ecotypes, XopJ6 might have a virulence function.

Nevertheless, it is yet unclear how multiple identical copies of *xopJ6* could confer increased pathogenicity. The simplest explanation could be that an increase in the number of *xopJ6* copies implies an enhanced expression. To test this, the relative expression of *xopJ6* was measured in bacterial cultures *in vitro* in *hrp* gene- inducing medium. Effectively, the relative expression of *xopJ6* correlates with the number of *xopJ6* copies, with a coefficient of determination of 0.833 (**Figure 6.IIC**). This indicates that presenting multiple copies of *xopJ6* increases its expression. There seems to be also a positive correlation between *xopJ6* expression and pathogenicity (median of the disease index at 7 dpi), with a coefficient of determination of 0.629 (**Figure 6.IID**).

To dig more into a possible virulence function of XopJ6, I evaluated whether XopJ6 could inhibit the plant defense responses. When transiently expressed in *Nicotiana benthamiana* leaves, XopJ6 was able to inhibit significantly the flg22-induced ROS production, a classical readout of PTI responses (Boller and Felix, 2009; Sang and Macho, 2017) (**Figure 6.I2**). This reinforces a possible role of XopJ6 in virulence mediated by the inhibition of the basal plant defenses.

## 6.6 XopJ6, a last minute candidate for the pipeline

As *xopJ6* is not present in reference *Xcc* strain 8004, it was not initially included in the same characterization pipeline followed for the rest of effectors studied in this work. Therefore, it was not included in the first large-scale yeast two-hybrid screening with *Xcc*<sub>8004</sub> T3Es performed prior to my arrival in the lab. However, considering its interest, it was included in the second screening with the *Rp*<sub>SGM11000</sub> T3Es performed during my time in the lab. Only one putative Arabidopsis target of XopJ6 was identified in this screening: AT2G39990, the eukaryotic translation Initiation Factor 3 subunit F (eIF3f). This protein has not been identified as putative target of any other effector in any previous screening.

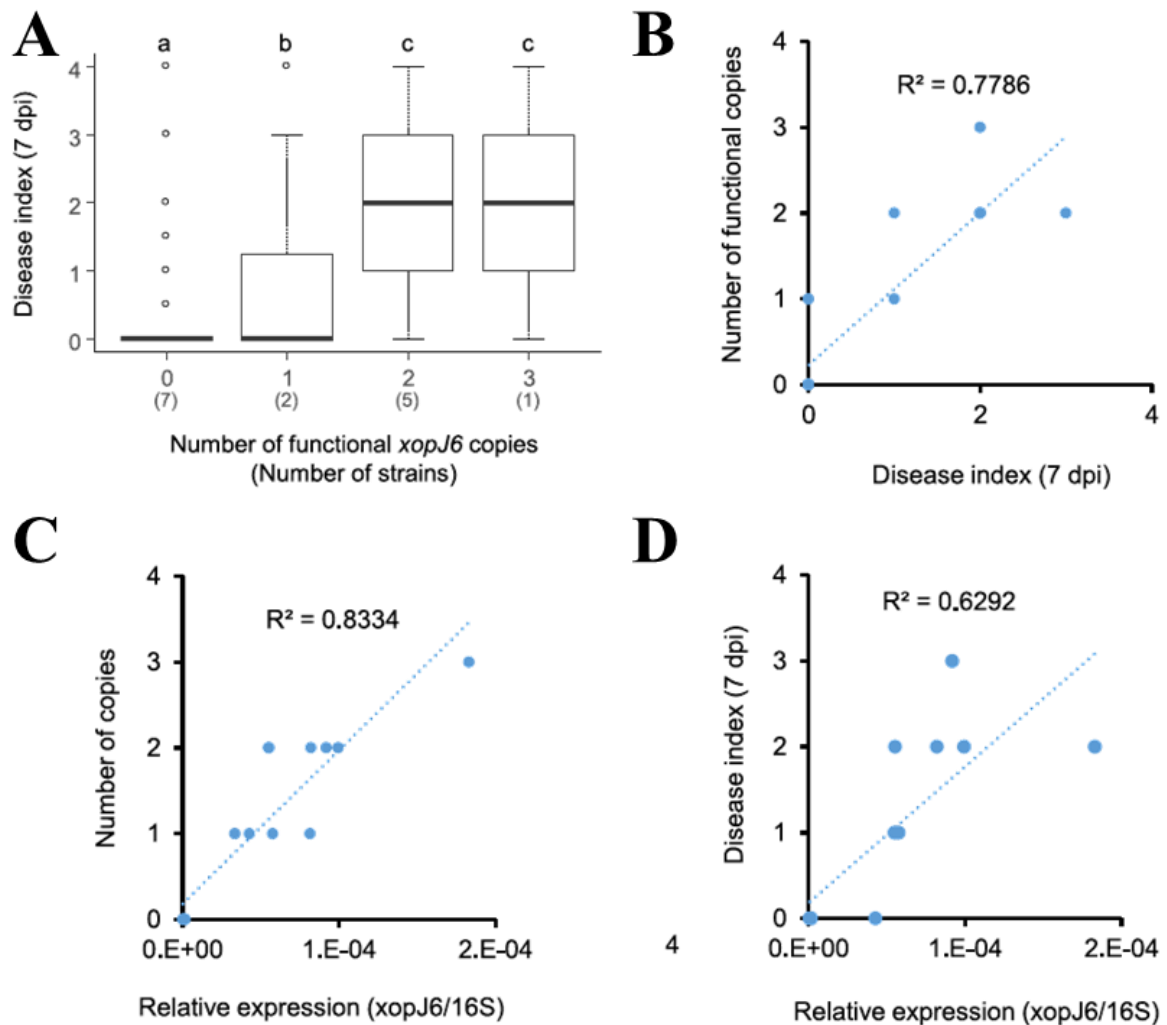


**Figure 6.11. The number of copies of *xopJ6* correlates with its relative expression and pathogenicity on susceptible *Arabidopsis* ecotype Col-0.** (A) Disease index at 7 dpi of different *Xcc* strains lacking *xopAC* and containing a variable number of *xopJ6* copies. The number of strains is marked in brackets below. The different letters (a-c) above the boxes indicate statistically different groups (one-tailed Wilcoxon signed-rank test  $p$ -value  $< 0.0001$ ). Correlation between the number of functional *xopJ6* copies and the median of the disease index at 7 dpi (B), the number of total *xopJ6* copies and the relative expression of *xopJ6* (using 16S rRNA gene as reference) *in vitro* in inducing medium (C) and the median of the disease index (D) among diverse *Xcc* strains lacking *xopAC*. The dotted blue line represents the linear regression whose coefficient of determination ( $R^2$ ) is shown at the top of each scatterplot. Combination of three independent experiments for both pathogenicity tests on Col-0 (performed by Emmanuelle Lauber) and relative expression measurements *in vitro*.

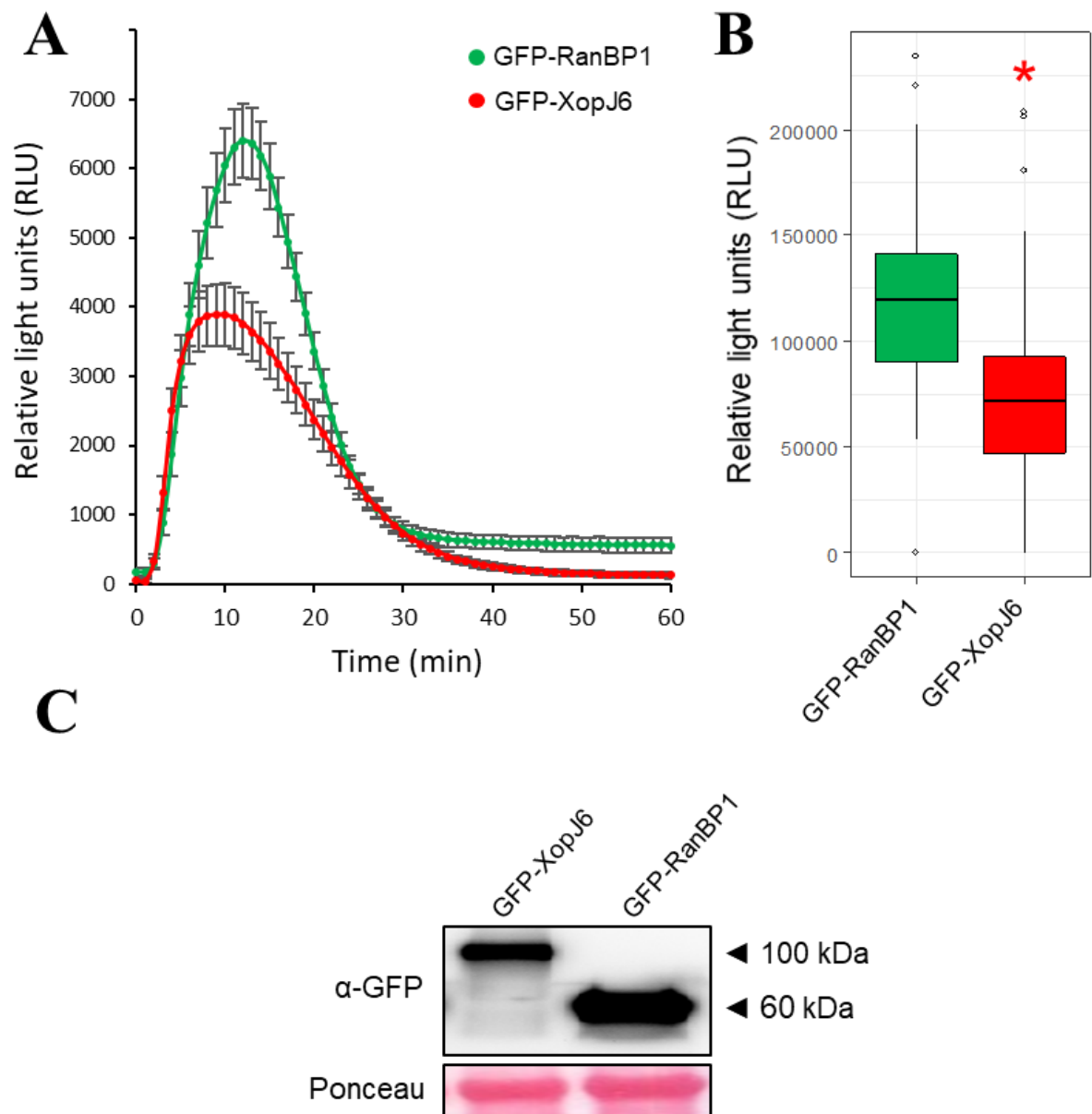


**Figure 6.12. XopJ6 inhibits flg22-induced ROS production.** Indirect measurement of ROS production upon 50 nM flg22 treatment by luminometry on *N. benthamiana* leaves transiently expressing either GFP-RanBP1 (green) in one half of the leaf, or GFP-XopJ6 (red) on the other half. Measurement of the ROS production over time (A) or in total after 1 hour (B). Combination of 32 samples issued from two independent experiments. Error bars represent the standard error. Red asterisk indicates that the difference with the *GFP* control is statistically significant (one-tailed Wilcoxon signed-rank test  $p$ -value < 0.05). Boxplot representation: thick bar, median; box limits, highest and lowest value within  $1.5 \cdot$  interquartile range; and circles, outliers. (C) Western blot showing the expression of GFP-XopJ6 and GFP-RanBP1 fusion proteins detected with an anti-GFP antibody. Ponceau S staining used as loading control.

Simultaneously, inducible pER8-*xopJ6* transgenic Arabidopsis lines were also generated. After three unfruitful *A. tumefaciens*-mediated transformation attempts, 18 PCR-positive T1 plants were generated. From these 18, only three showed around 75% hygromycin resistant segregation pattern in T2 indicating the presence of a single copy of the T-DNA. Plants from these three independent lines are currently being grown to look for possible homozygous lines in the T3 generation.

## 6.6 Discussion

### **XopJ6 and PopP2, a new example of orthologous Xcc and Rps T3Es with similar functions**

My contribution to this project showed that XopJ6 is a *bona fide* T3E based on its phylogeny in the YopJ family, closely related to Rps PopP2, *hrpG*-regulation and functional T3SS translocation signal (**Figures 6.2, 6.9 and 6.10**). All the amino acids important for PopP2 acetyl transferase activity and interaction with RRS1-R and cofactors are conserved between PopP2 and XopJ6 (**Figure 6.3**), suggesting that they might function similarly as it is being currently studied by both Laurent Noël's and Laurent Deslandes' teams. Effectively, similarly to PopP2, XopJ6 seems to be recognized by the NLR pair RRS1-R-RPS4 leading to its dissociation from DNA in an enzymatic activity dependent manner (**Figure 6.1**). This constitutes a perfect example of how two orthologous T3Es from *Rps* and *Xcc* function similarly, one of the initial postulates of my PhD work.

### **Both *xopJ6* and *popP2* were probably acquired horizontally in *Xcc* and *Rps***

This work also showed that *xopJ6* is located within a new Tn3 family transposon, Tn6714, present in several *Xcc* strains (**Figures 6.4, 6.6 and 6.7**). As shown in other *Xanthomonas*, transposable elements allow spreading horizontally pathogenicity determinants such as TALE and other T3E genes among different *Xanthomonas* spp. strains (Noël *et al.*, 2003; Jalan *et al.*, 2013; Ferreira *et al.*, 2015). Unlike *xopJ6*, *popP2* is not located in a Tn3 family transposon; however, it is located in a region with several bacteriophage-related proteins, another classical mechanism of horizontal gene transfer (HGT) of effector genes (Kado, 2009; Boyd, Carpenter and Chowdhury, 2012). Indeed, *xopJ6* and *popP2* GC content (53.9 and 59.7% respectively) are lower than the average of *Xcc* and *Rps* chromosomes (around 65 and 69% respectively), suggesting that both have been horizontally inherited in the respective species. This could explain their isolated position in the YopJ family phylogenetic tree (**Figure 6.2**), closer to animal

pathogen T3Es than to other plant pathogen T3Es. It seems clear that *xopJ6* and *popP2* share a common ancestor. Whether this ancestor effector gene was acquired by a *Xanthomonas-Ralstonia* common ancestor and has evolved differentially in each lineage, or if this common ancestor gene has been acquired independently in two different HGT events in RSSC and *Xcc*, is not known. However, this second hypothesis seems more likely because: 1) the mechanisms of transmission within the species are different between *Xcc* (Tn3 replicative transposition) and RSSC (possibly through bacteriophages). 2) The distribution and conservation among same species strains are quite uneven. While *popP2* is present in 64 out of 155 sequenced RSSC strains from all four phylotypes and presents several sequence polymorphisms (Peeters, Carrère, *et al.*, 2013; Sabbagh *et al.*, 2019), *xopJ6* is present in a lower number of phylogenetically related *Xcc* strains and is highly conserved (Figure 6.3 and 6.7).

### **Copy number variation as a novel strategy to modulate bacterial pathogenicity**

Thanks to the recent long-read sequencing of several *Xcc* strains, we have discovered that *xopJ6* was located in one to three copies highly conserved on the chromosome or different plasmids (Figures 6.5 and 6.6). This variation in the copy number of *xopJ6* is correlated with higher expression *in vitro* and stronger pathogenicity in a susceptible *Arabidopsis* ecotype (Figure 6.11). This suggests a possible role of XopJ6 in virulence, possibly related to its ability to inhibit PTI responses (Figure 6.12). In order to validate this, the possible dosage effect on the virulence function of XopJ6 is currently being studied through reverse genetics in a same genetic background by Emmanuelle Lauber. If corroborated, this would provide the first experimental evidence for such novel mechanism to modulate virulence in bacterial pathogens, similar to what has been suggested in oomycetes (Qutob *et al.*, 2009), and nematodes (Castagnone-Sereno *et al.*, 2019).

In addition to this copy number variation strategy, there seems to be another XopJ6-mediated virulence strategy evolved by *Xcc*. As mentioned in the introduction, although XopJ6 is highly conserved among the different *Xcc* strains, there is an alternative version present only in two strains: CN13 and CFBP4954. This XopJ6 variant presents only two amino acid substitutions: C72G and N382K, the latter occurring at an amino acid important for the physical interaction with RRS1-R (Zhang *et al.*, 2017) (Figure 6.3). Emmanuelle Lauber has shown that this variant does not confer RRS1-mediated resistance and Laurent Deslandes' team has demonstrated that indeed, XopJ6<sub>CN13</sub> is unable to interact with neither RRS1 nor WRKY22 WRKY domains (Table 6.1). This shows that some *Xcc* strains have evolved a XopJ6 variant that is no longer recognized by its plant immune receptor avoiding thus XopJ6-triggered immunity.



Whether XopJ6<sub>CN3</sub> maintains XopJ6 virulence functions has yet to be studied. However, due to the impossibility of XopJ6<sub>CN3</sub> to interact with WRKY domains, these possible virulence mechanisms will most probably be WRKY-independent. Based on our yeast two-hybrid screening, a possible WRKY-independent virulence target candidate of XopJ6 has been identified: eIF3f. Downregulation of protein synthesis is one of the general plant responses against stress and is mediated mainly by eIFs (Immanuel, Greenwood and MacDiarmid, 2012; Dutt *et al.*, 2015). Several eIFs have been shown to be involved in biotic stress responses such as eIF2 (Aparicio *et al.*, 2011; Liu, Afrin and Pajerowska-Mukhtar, 2019), eIF4 (Wang and Krishnaswamy, 2012; Contreras-Paredes *et al.*, 2013; Xu *et al.*, 2017), or eIF5 (Hopkins *et al.*, 2008). Interestingly, *P. syringae* HopZ2, another member of the YopJ family, interacts with eIF2γ (Lewis *et al.*, 2012). Whether XopJ6 is able to interact truly with eIF3 and/or other eIFs and this has any implications in the plant defense responses has not yet been studied. The inducible pER8-*xopJ6* transgenic Arabidopsis lines generated in the susceptible Col-0 background are a powerful tool to explore this, or any other alternative hypothesis about XopJ6-mediated virulence, directly *in planta*.

# Chapter 7

## General discussion

## 7.1 Conclusions: What I have done so far

The main results of my experiments have been discussed at the end of each respective chapter. To refresh the memory and to integrate and make global sense of the different points discussed throughout the different chapters, I would like to summarize here the main conclusions obtained in this work.

### ***Rps* and *Xcc* T3Es behave as most plant pathogen effectors...**

Different large-scale (and “not-so-large-scale”) screenings have allowed to get a global picture of the putative collective action of *Rps*<sub>SGM11000</sub> and *Xcc*<sub>8004</sub> T3Es. Thanks to the yeast two-hybrid screenings, the putative Arabidopsis targets of these two species T3Es were identified and compared to the targets of other plant pathogen effectors. It was shown that *Rps* and *Xcc* T3Es present similar “targeting tendencies” to other pathogens: 1) Preference for Arabidopsis proteins that are highly connected and important for the host interactome organization, indicating a higher potential of interference with the host cellular processes (Li, Zhou and Zhang, 2017; Ahmed *et al.*, 2018). This tendency is even stronger among core T3Es compared to variable T3Es. This could suggest that higher selection pressure to maintain these T3Es is linked to their higher interference potential. 2) Targeting host processes important for plant immunity and physiology. From a functional point of view, the targets of *Rps* and *Xcc* T3Es include several transcription factors, ubiquitin-signaling-related proteins, kinases and phosphatases, cytoskeleton components or proteins involved in vesicle-trafficking; all important signaling and executor components of plant responses against environmental changes and usual targets of other pathogen effectors (Büttner, 2016; Khan *et al.*, 2018). Collectively, these results suggest that *Rps* and *Xcc* T3Es possess the potential to modulate the plant physiology. Indeed, this has been supported through transgenesis as nine out of fourteen T3E transgenic Arabidopsis lines showed developmental alterations when grown *in vitro* in inducing conditions. Two additional *Xcc* T3E genes have also been reported to alter normal development in similar setups (G. Wang *et al.*, 2015; Yan *et al.*, 2019). In the context of a different project, sixteen additional *Xcc* T3E-gene transgenic lines have been screened and similarly, seven of them showed altered developmental phenotypes (Noe Arroyo Vélez, unpublished data). Altogether, this illustrates the ability of *Xcc* and *Rps* T3Es to modulate the plant physiology. Another convergence point between *Xcc* and *Rps* T3Es and other pathogen effectors is the ability to inhibit basal defenses, shown in this work for a few: XopP, similarly to its orthologs RipH1-3 (Morel, 2018); XopJ6, similarly to its ortholog PopP2 (Le Roux *et al.*, 2015); and XopAG. Finally, another common feature of *Xcc*, *Rps* and other pathogens effectors is their collective contribution. Most *Xcc* and

*Rps* single T3E-gene mutants have not shown any impairment in pathogenicity whereas an *Xcc* sextuple mutant has. This evidences functional redundancy and/or epistatic interactions among *Xcc* or *Rps* T3Es, as it has been seen in many other pathogen species (Kvitko *et al.*, 2009; Zumaquero *et al.*, 2010; Phan *et al.*, 2016; Rufián *et al.*, 2018).

### **... yet there are some clues suggesting certain specificity of T3Es from *Rps* and *Xcc***

Despite all the beforementioned similarities found between T3Es of *Xcc* and *Rps*, and other plant pathogen effectors; this work also sheds some light on certain possible particularities of these two bacterial species. Notably, when we compare all the identified putative targets of *Xcc* and *Rps* T3Es to the effector targets of previously characterized species, the majority are specific to *Xcc* and/or *Rps* T3Es. Specifically, from the 235 identified *Xcc/Rps* T3E targets, 166 were exclusive. While this number is likely to be overestimated due to the few species that have been screened systematically at a large-scale, it still provides a large margin for reflecting a true *Xcc-Rps* T3E target specificity. This target specificity becomes particularly intriguing considering that *Rps* and *Xcc* are the first and only vascular pathogens whose effectors have been screened systematically. Therefore, it is possible that the observed target specificity of these two species actually reflects their lifestyle. This would mean that vascular pathogens modulate differently the plant cellular processes compared to other lifestyle pathogens by targeting different sets of plant proteins.

On the bacterial side, a minor detail could potentially reinforce the notion of a vascular-specific way of modulating plant immunity: although most of single T3E mutants did not show alterations in pathogenicity, the few that did are actually shared T3Es between *Xcc* and *Rps*. On previous tomato/*Rps*<sub>GM11000</sub> experiments,  $\Delta$ *ripAX1* and  $\Delta$ *ripAX2* showed reduced pathogenicity; whereas in this work it was shown on *Arabidopsis/Xcc*<sub>8004</sub> experiments that  $\Delta$ *xopQ* and  $\Delta$ *xopAG* were less virulent, the latter confirmed by complementation. This suggests that effectors shared between vascular pathogens are among the most important for pathogenicity in vascular pathogens. Nevertheless, as the impact on virulence has only been corroborated in one case, the previous statement is a mere hypothesis that should be experimentally validated.

### **XopAG/RipO1 and XopJ6/PopP2: The fast-tracked orthologous pairs**

The development of two different stories has been prioritized during my time in the lab, for very different reasons. On the one hand, the first results obtained during this work highlighted a pair of orthologous candidates, XopAG and RipO1: 1) They are the only orthologous

pair for which common targets were identified. 2) Arabidopsis mutants of two of these common targets showed enhanced disease tolerance to *Xcc* (*brg3*) or *Rps* (*klcr2*). 3) pER8-*xopAG* and pER8-*ripOI* Arabidopsis lines showed strong developmental phenotypes, although with different intensity. 4) *Xcc*<sub>8004</sub>  $\Delta$ *xopAG* is one of the two single mutants that showed a reduction in pathogenicity compared to the wild type in susceptible Arabidopsis plants. *Rps*<sub>8004</sub>  $\Delta$ *ripOI* effect, if any, is much weaker and would need further and finer experiments to be corroborated. For these reasons, different approaches were conducted to characterize further this orthologous pair of T3Es. This work showed that they belong to a highly conserved family of effectors that have been largely understudied and from which members have been found in several vascular pathogens. It has also been shown that XopAG inhibit the plant basal defenses, what could potentially explain its observed virulence role. To gain some insight into the molecular bases of this virulence role of XopAG and possibly RipOI, two simultaneous approaches are being followed: 1) Taking advantage of pER8-*xopAG* developmental phenotype, a suppressor screening on an EMS-mutagenized population has been conducted. Up to now, 10 independent homozygous M3 suppressor lines have been identified. 2) Considering the nucleocytoplasmic localization of XopAG and RipOI, and the reduced susceptibility phenotype of *brg3* Arabidopsis mutants, a possible *BRG3*-dependent XopAG and RipOI virulence functions are being explored. Indeed, the physical interaction between BRG3 and XopAG detected by yeast two-hybrid has been validated by FRET-FLIM. However, the different phenotypes on the target and on the effectors size have not been linked yet.

On the other hand, and in the context of a different project, a new candidate effector was discovered in a different *Xcc* strain. This effector, named XopJ6, turned out to be a very close ortholog of the *Rps* “model T3E” PopP2 (Deslandes *et al.*, 1998). This provided an additional pair of *Rps*-*Xcc* orthologous T3Es to study. However, considering how much is already known about the molecular mechanisms of PopP2-mediated virulence and susceptibility (Deslandes *et al.*, 2003; Tasset *et al.*, 2010; Le Roux *et al.*, 2015; Zhang *et al.*, 2017), my work contributed to the characterization of the novel XopJ6. More specifically, this work demonstrated that *xopJ6*, as most T3E genes, is transcriptionally regulated by *hrp* gene regulator HrpG and that its protein product possesses a functional T3SS-translocation signal on the N-terminus. Additionally, thanks to long-read sequencing, it was shown that *xopJ6* is always located in a 9-kb Tn3 family transposon found in one to three almost identical copies on several *Xcc* bacterial chromosomes or plasmids. Precisely this copy number variation was shown to be correlated with *xopJ6* expression and pathogenicity in a susceptible Arabidopsis ecotype. If corroborated, this would constitute a novel strategy for bacteria to modulate their virulence.

## Finally, do orthologous T3Es from *Rps* and *Xcc* work similarly?

The presence of nine/six orthologous T3Es in *Rps/Xcc* respectively provided a great opportunity for comparative studies. However, when dealing with this kind of comparative studies, an immediate question arises: “do orthologous T3Es work similarly?”. Although reasonable to assume, no experimental evidence backed up any kind of functional similarity between orthologous *Xcc* and *Rps* T3Es at the beginning of this work. Examples of orthologous effectors working similarly had been reported previously in other species: *Pseudomonas syringae* *avrE* restores pathogenicity in a *Erwinia amylovora*  $\Delta$ *dspE* (*avrE* ortholog) strain (Bogdanove *et al.*, 1998). *Cladosporium fulvum* Avr4 and Ecp2 and their orthologs in *Mycosphaerella fijiensis* contribute similarly to virulence and are recognized by the same R proteins (Stergiopoulos *et al.*, 2010). *Xanthomonas* sp. XopQ and *Pseudomonas* sp. HopQ1 are also recognized by the same tobacco R protein (Schultink *et al.*, 2017). Nevertheless, several other examples of functional divergence among orthologous effectors had also been described: YopJ family T3Es can act as proteases or as acetyl transferases (Lewis *et al.*, 2011). *P. syringae* HopG1 possesses mitochondrial localization and alters the respiration and cytoskeletal organization (Block *et al.*, 2010; Shimono *et al.*, 2016), whereas its *X. fuscans* ortholog, AvrGf2, its chloroplastic and possesses a cyclophilin-dependent avirulence-role (Gochez *et al.*, 2017). Therefore, it was not initially clear whether orthologous T3Es from *Rps* and *Xcc* could actually function similarly or not. Based on the large-scale yeast two-hybrid screenings results, common targets were only found for one out of the nine possible pairs of orthologous T3Es in *Rps* and *Xcc* (XopAG and RipO1). *A priori*, this result could suggest that the shared T3Es show a completely different targeting profile and therefore we could conclude that they differ functionally. However, for many of the shared T3Es no target were identified in these screenings making thus impossible the comparison with the corresponding ortholog. Therefore, it is likely that this observation has been underestimated (Brückner *et al.*, 2009). Nevertheless, these first results rather supported a scenario in which the orthologous T3Es shared by *Rps* and *Xcc* behave differently. Conversely, when pER8-T3E transgenic lines were generated and phenotyped in a second phase of my PhD, the results were the opposite: most of the pER8-*rip* and orthologous -*xop* combinations showed the same or similar developmental phenotype. This could suggest that orthologous T3Es modulate the plant physiology in a similar manner. These results contradicted somehow the lack of similarities found with the interactomic profile and supported a scenario in which most orthologous T3Es from *Xcc* and *Rps* could behave similarly. Additionally, other smaller-scale experiments pointed out certain similarities between orthologous T3Es as well: 1) XopP inhibits almost completely the flg22-induced ROS burst similarly to its ortholog RipH1 (Morel, 2018). 2) XopJ6 is recognized

by the same NLR pair than its ortholog PopP2 (Deslandes *et al.*, 1998). 3) RipR lines showed a strong developmental impairment when transgenically expressed in Arabidopsis and was hard to transform suggesting a cytotoxic effect similar to that observed with its *E. amylovora* ortholog DspA/E (Degrave *et al.*, 2013). This is probably what occurred with the Xcc ortholog, XopAM, for which it was impossible to generate transgenic lines. 4) XopAG and RipOl co-localize and probably interact with BRG3 in the nucleus. All these details moderately support functional similarities. Therefore, coming back to the original question, “do orthologous T3Es work similarly?” the answer is that, while there are experimental evidences supporting both negative and affirmative answers, most of the results back up the later.

## 7.2 Perspectives: What I would do if I had more time

My PhD project was a pioneer study in the systematic and large-scale screening of *Rps*<sub>GMII000</sub> and *Xcc*<sub>8004</sub> T3Es for both host teams. As previously stated, the biological material generated during this work has allowed us to gain some valuable insight into how *Rps* and *Xcc* T3Es work, with a particular focus on the shared ones between *Rps*<sub>GMII000</sub> and *Xcc*<sub>8004</sub>. However, a lot of the generated material could not be exploited fully within the timeframe of this thesis constituting thus a source of valuable tools for the future characterization of these T3Es, a long-term objective of both host teams.

### **What to do now with all these plants?**

Despite being one of the most time-consuming parts of this work, the generated pER8-T3E transgenic Arabidopsis lines are probably the biological resources most understudied. Nevertheless, this valuable biological resource will be further exploited in the immediate future. More specifically, in the context of a different PhD project, transgenic Arabidopsis lines for most *Xcc*<sub>8004</sub> and some *Rps*<sub>GMII000</sub> T3E genes are being used for systematic screenings of inhibition of plant basal defenses measuring differences between induced and non-induced plants in terms of Ca<sup>2+</sup> signaling and MAPK phosphorylation. Simultaneously, these lines are also going to be molecularly phenotyped through RNA sequencing. This will provide the different transcriptional profiles of each effector when expressed individually *in planta*. The large-scale molecular phenotyping of such a transgenic line collection would represent an innovative and without *a priori* strategy that could allow us to unveil the full potential of T3Es and to exploit in more depth the biological material generated. Collectively, these results would provide an extensive description of the role of all these T3Es, which is something never done to this extent. Additionally, the collective analysis of the transcriptional signatures of each T3E could allow

their functional clustering identifying groups of T3Es targeting similar processes. This information would be key in order to manage functional redundancy and start synthetic biology projects such as the construction and combinatorial complementation of polymutants, strategy successfully used already in model plant pathogen *P. syringae* (Kvitko *et al.*, 2009; Cunnac *et al.*, 2011).

### **Focusing on a couple of stories**

One of the most advanced and yet not finished projects developed during this thesis is the characterization of the virulence role of XopAG and RipOI. On the one hand, the performed suppressor screening has allowed the identification of ten suppressor lines already. The characterization of these lines should be a priority in the determination of the genetic bases of *xopAG*, and potentially *ripOI*, -related phenotypes. For this reason, measuring *xopAG* expression and discarding mutations in the inducer and *xopAG* genes are the first steps required. For the lines that do express a non-mutated version of *xopAG*, backcrosses with the parental pER8-*xopAG* line would ensure cleaning spurious mutations to facilitate the identification of the causal suppressor mutation through bulk genome sequencing of the BC2 progeny. The identified mutations would then need to be validated (e.g., validating the suppressor phenotype with crosses with “clean” T-DNA mutants of the identified gene) and, depending on the biological nature of the candidates, different experiments should be foreseen to functionally characterize and provide biological meaning to the proven genetic link between the genotype and the phenotype. As several Arabidopsis targets of XopAG have been identified, searching for mutations on the corresponding genes in the suppressor lines as well as phenotyping the progeny of the crosses done with pER8-*xopAG* and T-DNA mutants of its targets could serve as more straightforward and time-saving strategies worth to pursue. In parallel, a possible BRG3-mediated role of XopAG and RipOI virulence is already being explored. While promising phenotypes have been observed on both effector and target sides, not a direct link has been yet established between both except for their physical interaction. Experiment that allow linking *xopAG*-related phenotype and pathogenicity with *BRG3* involvement in susceptibility should be thus a priority (e.g., testing if *Xcc* 8004Δ*xopAG* reduced virulence is not observed in *brg3* background).

An additional interesting but less explored story is the further characterization of the *Rps* RipH family, and potentially their *Xcc* ortholog, XopP. *Rps* RipH1-3 have been characterized as being involved in bacterial pathogenicity (Chen *et al.*, 2014), and that they target plant proteins involved in the response against *Rps* (Morel, 2018). My work has shown that all three



RipHs confer strong developmental alterations when transgenically expressed in Arabidopsis. The same strategies followed in the characterization of XopAG could be foreseen for the three RipHs. The drastic developmental phenotypes observed, particularly on pER8-*ripH1* and pER8-*ripH2* lines, could allow additional fast-discerning suppressor screenings to identify the responsible plant genes. Again, similar to XopAG, the identified targets of RipH, not only in Arabidopsis in this case, but also in tomato (Morel, 2018), could provide additional hints for a more straightforward and direct characterization. More specifically, *Chromatine Remodeling Complex Subunit R3* (*CHR3*; AT2G28290), the Arabidopsis ortholog of a described tomato target of RipH3, has been already shown to be involved in susceptibility to *Rps* (Morel, 2018) and resistance to *B. cinerea* (Walley *et al.*, 2008). It would be therefore interesting to test whether a *chr3* mutation could suppress pER8-*ripH3*-mediated phenotype. Similar to RipOI and XopAG, any discovery found on the possible functions of RipHs would be worth testing whether it is also applicable to their Xcc ortholog, XopP.

### **What was left behind**

In addition to the general large-scale analyses conducted (e.g., study of the effector targeting patterns through network analyses on yeast two-hybrid data) or foreseen (e.g., molecular phenotyping through RNA sequencing of the pER8 transgenic lines), and the functional characterization of the most-promising candidates (i.e., XopJ6, XopAG/RipOI or RipHI-3/XopP), this work also provides some clues for additional and potentially interesting stories that I could not explore further within this thesis. This is the case of the homology of function but not of sequence of Xcc XopAC and *Rps* RipAJ, two unrelated T3Es that share six common targets including RCN1, important for Arabidopsis susceptibility to Xcc. This is also the case for a possible KLCR2-dependent virulence function of RipOI and XopAG, as KLCR2 is a common target of these two T3Es and a *kclr2* mutant in Arabidopsis seemed slightly more tolerant to *Rps*. The drastic phenotype of pER8-*ripR* and the impossibility to construct pER8-*xopAM* lines could reflect a strong toxic effect not only observed on these two but also in other species orthologs such as *Erwinia amylovora* DspA/E (Degrave *et al.*, 2013), functionally connecting all of them. The observed involvement of XopQ in Xcc pathogenicity; the role of SIS in the crosstalk between abiotic and biotic stresses (Arabidopsis *sis* mutants showed reduced tolerance to both salt stress (Brinker *et al.*, 2010), and Xcc); or the role of eIF3f, the only identified putative target of XopJ6 by yeast two-hybrid, in Arabidopsis susceptibility to *xopJ6*-containing Xcc strains are other examples of potentially interesting leads to follow in the near future.

## Contribution of this work to the bigger picture

In a general context, this work contributes to the global understanding of effector biology at the molecular level. The systematic identification of targets of T3Es from *Rps* and *Xcc* has allowed performing large-scale meta-analyses comparing different pathogen effectors, including for the first time effectors from vascular pathogens. This served as a starting point for the generation of an open and interactive database: EffectorK ([www.effectork.org](http://www.effectork.org)). This database integrates and makes easily accessible all the otherwise scattered published information about Arabidopsis targets from a wide variety of pathogenic bacterial, oomycete, fungal, nematode and insect effector proteins. EffectorK accepts the contribution of users to expand and update the interactomic dat. For this first version, we limited the scope to Arabidopsis and pathogen effector proteins. However, if the community considers it as a useful tool, it could be foreseen to expand it to other plant hosts (a private version of EffectorK including also tomato interactomic data has already been developed for internal use) and/or effector molecules (e.g., chemical and sRNA effectors), as it has already been suggested when this work was presented in different congresses.

The ensemble of identified targets does not only provide information for fundamental research analyses, but it also constitutes a list of potentially interesting candidates for resistance breeding. Particularly interesting on this regard are the 100 novel effector hubs (i.e., Arabidopsis protein targeted by at least two different effectors) identified in this work. Indeed, a few of them have already been described to be involved in immunity. This could be considered as a sort of validation of the importance that these targets could have in plant immunity. However, the majority of these effector hubs have never been tested for a role in immunity and constitute thus a list of promising candidates for further analysis. All this work has been performed on the model species *A. thaliana*. The involvement of any potentially interesting candidate in plant immunity or susceptibility should also be tested in agronomically relevant crops in order to, in the long term, apply this knowledge in practical breeding schemes. Although not always directly accomplished (Nelissen, Moloney and Inzé, 2014), several successful examples of translational research from Arabidopsis to crops have been reported throughout the years (Rensink and Buell, 2004; Zhang, Creelman and Zhu, 2004; Chopra *et al.*, 2018).

Finally, as already mentioned, several results from this work pointed out a possible vascular-pathogen-specific way of modulating plant processes: most notably the *Rps*- and *Xcc*-specificity of effector targeting, but to a lesser extent also the presence among vascular pathogens of orthologous T3Es that can potentially inhibit the defense-related vascular flow

reduction (Oh and Collmer, 2005), and/or are involved in pathogenicity in vascular tissues. However, at this point it is still impossible to assess whether this vascular specificity is genuine. Similar comparative studies to the ones performed in this work, but with an increased number of vascular and non-vascular pathogen species could shed some light on this matter. If real, this specific ability of vascular pathogens to modulate the plant cellular processes should be further studied in order to, in the long term, design more adequate strategies to fight against these kind of devastating pathogens.

# Chapter 8

## Material and methods

## 8.1 Biological material and growth conditions

### 8.1.1 Plants

*A. thaliana* ecotypes Sf-2 and Col-0 were used. All T-DNA mutant (listed in **table A.3**) and pER8 transgenic lines (listed in **table 4.1**) were obtained/generated in the Col-0 background. For *in vitro* experiments, seeds were surface-sterilized with 25% bleach treatment for 15 minutes and two washing steps with sterile water, and grown in Murashige & Skoog (MS) (Sigma-Aldrich) medium supplemented with 15 g/l agar under long day conditions (16h light; 20°C). When required, medium was supplemented with 50 mg/l hygromycin B or 30 mg/l pimaricin. For inoculation assays, plants were grown individually for 4 weeks on wet Jiffy pellets under short day conditions (9h light; 22°C; relative humidity 70%). *N. benthamiana* plants were grown on wet Jiffy pellets for 3 weeks, then transplanted to bigger soil-filled pots for an additional week under long day conditions (16h light; 21°C; relative humidity 70%). Pepper cultivar ECW and ECW-10R were grown on soil-filled pots for 6 weeks in greenhouse conditions.

### 8.1.2 Bacteria

A list of bacterial strains used in this study is presented in **table A.4**. *E. coli* TGI, DB3.1, TOP10, DH5 $\alpha$  derived strains were grown in Luria-Bertani (LB) medium (5 g/l yeast extract; 10 g/l bacto tryptone and 10 g/l NaCl. For solid medium: 15 g/l agar) at 37°C with shaking when cultured in liquid. When required, medium was supplemented with 100 mg/l carbenicillin or chloramphenicol; 50 mg/l kanamycin or rifampicin; 40 mg/l spectinomycin; 30 g/l pimaricin; or 10 mg/l gentamycin or tetracycline. *Xcc* 8004, CN06 and derived strains were grown in Moka medium (4 g/l yeast extract; 8 g/l casamino acids; 2 g/l K<sub>2</sub>HPO<sub>4</sub> and 0.3 g/l Mg<sub>2</sub>SO<sub>4</sub> · 7 H<sub>2</sub>O. For solid medium: 15 g/l agar) or MME medium (8 g/l casamino acids, 10.5 g/l K<sub>2</sub>HPO<sub>4</sub>; 4.5 g/l K<sub>2</sub>HPO<sub>4</sub>; 1 g/l (NH<sub>4</sub>)<sub>2</sub>SO<sub>4</sub> and 0.3 g/l Mg<sub>2</sub>SO<sub>4</sub> · 7 H<sub>2</sub>O). *Rps* GM1000 and derived strains were grown in  $\phi$  medium (10 g/l bacto peptone; 1 g/l casamino acids; 1 g/l yeast extract. For red staining: 5 g/l glucose and 0.05 g/l triphenyltetrazolium chloride (TTC). For solid medium: 15 g/l agar). *A. tumefaciens* GV3101 and C58 derived strains were grown in LB rich medium. *Xcc*, *Rps* and *A. tumefaciens* strains were grown at 28°C with shaking when cultured in liquid. When required, media were supplemented with same antibiotic concentrations as *E. coli* except for 10 g/l chloramphenicol or 5 g/l tetracycline.

## 8.2 Bioinformatic analyses

PANTHER Overrepresentation Tests on “GO biological process complete”, “GO molecular function complete” and “GO cellular compartment complete” annotation datasets were performed using the AGI codes of the different Arabidopsis gene lists compared (Ashburner *et al.*, 2000; Mi *et al.*, 2019). Fisher’s Exact test with Bonferroni correction for multiple testing was used every time.

Full-length amino acid sequences were retrieved from public databases and ClustalW2.1 multiple sequence alignments (Larkin *et al.*, 2007) using the BLOSUM62 scoring matrix with gap opening/extension penalties of 10 and 0.1 respectively were conducted on Geneious 11.1.4 (<https://www.geneious.com>). Phylogenetic trees were constructed based on ClustalW2.1 alignments using the bootstrap-tested (Felsenstein, 1985) Neighbor-Joining method (Saitou and Nei, 1987) on MEGA X (S. Kumar *et al.*, 2018) with the rest of parameters as default.

The identification of transposon flanking inverted repeats was done with support from the “Inverted Repeats Finder” tool from the Tandem Repeats Database (Gelfand, Rodriguez and Benson, 2007). Once all composing elements of the *xopJ6*-containing transposon were identified, it was registered in the Transposon Registry (Tansirichaiya, Rahman and Roberts, 2019), receiving the number Tn6714. Synteny studies between different genomic, composite transposon or plasmidic sequences were performed using a progressive MAUVE algorithm (Darling *et al.*, 2004) on Geneious 11.1.4 (<https://www.geneious.com>).

## 8.3 Cloning

Different Gateway clonings were performed using “Gateway Cloning kit” (Thermo) following the manufacturer’s instructions. BP reaction was used to generate an entry plasmid for *A. thaliana* *BRG3* using pDONR207. LR reactions were used to generate expression plasmids using different *xop* and *rip* entry plasmids (González-Fuente *et al.*, 2019), and pER8-GW (for  $\beta$ -estradiol-inducible expression *in planta*), pMDC43 (for N-terminal GFP-fusions) and pBIN-GW-CFP/YFP (for C-terminal CFP or YFP fusions) as destination vectors.

The generation of pK18*mobsacB* derivatives for the deletion of *Xcc*<sub>8004</sub> *hrpW* and *xopP* as well as the introduction of the first 300 bp of *Xcc*<sub>06</sub> *xopJ6* into pAIO was done by PCR amplification of the region of interest using genomic DNA from *Xcc* and Golden Gate assembly

(Engler, Kandzia and Marillonnet, 2008). The primers used for the PCR amplification are listed in **table A.5**.

The plasmid for the complementation of *xopAG* was constructed by ligation of BamHI/HindIII (Promega) digestion products of pCZ101, an *Xcc* integrative plasmid, and PCR-amplified *xopAG* full gene (primers used in **table A.5**). The ligation was carried out with T4 DNA Ligase (Promega).

## 8.4 Plant genotyping

Genomic DNA from 1-2 small leaves from 3-5 week-old Arabidopsis plant was extracted following D. Bellstedt's rapid protocol (Bellstedt *et al.*, 2010). The product of the extraction can be directly used as template for PCR. The primers used for genotyping of T-DNA mutants and pER8 transgenic lines are listed in **table A.5**.

## 8.5 Pathogenicity assays

### 8.5.1 *Xcc* pathogenicity assays

For wound-inoculation, 4-week-old Arabidopsis plant leaves were pierced three times with a needle dipped in *Xcc* bacterial suspension at  $10^8$  CFU/ml ( $\sim OD_{600}=0.1$ ) on 1 mM  $MgCl_2$ . Four leaves per plant and four to six plants per condition were tested in each independent experiment. After inoculation, plants were placed in trays covered with pierced plastic film to increase the relative humidity and grown in short day conditions (9h light; 22°C). Different treated plant were randomized within trays to minimize position biases. Disease symptom appearance was scored at 7 and 10 days post inoculation following this index: 0-1, no symptoms; 1-2, weak chlorosis around the inoculation sites; 2-3, stronger and extended chlorosis; and 3-4, necrosis. Results from independent experiments were combined and one-tailed Wilcoxon signed-rank tests were conducted on R version 3.5.2 (<https://www.r-project.org/>).

For *in planta* growth assays, 5-week-old Arabidopsis plants leaves were infiltrated with a needleless syringe with *Xcc* bacterial suspension at  $10^5$  CFU/ml ( $\sim OD_{600}=0.0001$ ) on 1 mM  $MgCl_2$ . Four leaves per plants and four to six plants per condition were tested in each independent experiments. After inoculation, plants were placed in trays covered with plastic film to increase the relative humidity and grown in short day conditions (9h light; 22°C). Different treated plant were randomized within trays to minimize position biases. At 0 and 3 days post inoculation, leaf disks were harvested with a punch and grinded in 100  $\mu$ l sterile water.

5 µl droplets of several dilutions were spotted on selective Moka medium in triplicate and incubated at 28°C for 2 days. Colonies on adequate dilutions were counted to estimate the CFU/cm<sup>2</sup>. Results from independent experiments were combined and one-tailed Wilcoxon signed-rank tests were conducted on R version 3.5.2 (<https://www.r-project.org/>).

For observation of AvrBsl-dependent HR on pepper, 6-week-old pepper plant leaves were infiltrated with a needleless syringe with *Xcc* bacterial suspension at 10<sup>8</sup> CFU/ml (~ OD<sub>600</sub>=0.1) on 1 mM MgCl<sub>2</sub>. Pepper plants were grown in Phytotron under short day conditions (9h light; 22°C; 66% relative humidity). HR symptoms were observed at 24 and 48 hours post inoculation. For discoloration of detached leaves, they were incubated in 80% ethanol at 60-65°C for 24 hours.

### 8.5.2 *Rps* pathogenicity assay

For soil-drenching inoculation, 4-week-old *Arabidopsis* plants grown on Jiffys were drenched in 2l of *Rps* bacterial suspension at 10<sup>8</sup> CFU/ml (~ OD<sub>600</sub>=0.1) in water for 20 minutes. Then, soil was added to soak the remaining bacterial suspension and Jiffys were placed over. Plants were grown under long day conditions (12h light; 27°C; relative humidity 80-85%). Different treated plant were randomized within trays to minimize position biases. Disease symptom appearance was scored daily 3 to 10 days post inoculation following this index: 0, no symptoms; 1, first wilting symptoms; 2, wilting of half of the leaves; 3, wilting of more than half of the leaves; and 4, complete wilting. For survival analyses, plants are considered alive when disease index is lower than 2 and dead when greater or equal than 2. Results from independent experiments were analyzed separately and the survival curves, Mantel-Cox logrank tests and hazard ratios were calculated with GraphPad Prism 5.03 (<https://www.graphpad.com>).

## 8.6 Generation of *Xcc* sextuple effector deletion mutant

The generation of *Xcc*<sub>8004</sub> sextuple mutant (8004ΔxopAM-ΔxopG-ΔxopQ-ΔxopAG-ΔxopP-ΔhrpW) was performed by sequential deletion of single genes by the SacB method (Schäfer et al., 1994). Plasmids for the deletion of single T3E genes were introduced into *Xcc* by triparental mating as previously described (Turner, Barber and Daniels, 1985). Deletions were verified by PCR using the left primer specific to the upstream fragment and the right primer specific to the downstream fragment used to amplify upstream and downstream amplicons in the corresponding deletion primers (Table A.5).



## 8.7 Plant transformation

For stable transformation of *Arabidopsis thaliana*: *Agrobacterium tumefaciens* strain GV3101 pMP90 was transformed by electroporation with the desired plant expression vector. Ecotype Col-0 *A. thaliana* plants were transformed with *A. tumefaciens* bacterial suspension at  $OD_{600} = 0.8$  in 50 g/l sucrose and 100  $\mu$ L/l Silwett by flower dipping (Clough and Bent, 1998). Plants were grown in greenhouse conditions. T1 seeds were surface-sterilized and screened for resistance on solid MS medium (Sigma) supplemented with 50  $\mu$ g/ml hygromycin. Resistant plants were genotyped by PCR with transgene-specific primers (**Table A.5**). T2 seeds from PCR-confirmed resistant T1 lines were screened for resistance on solid MS medium supplemented with 50  $\mu$ g/ml hygromycin. Lines with a percentage of resistance between 60 and 90% were selected and re-genotyped by PCR. T3 seeds from segregation- and PCR-positive T2 lines were screened for resistance on solid MS medium supplemented with 50  $\mu$ g/ml hygromycin to select homozygous lines.

For transient expression in *Nicotiana benthamiana*: *Agrobacterium tumefaciens* strains GV3101 pMP90 and C58 were transformed by electroporation with the desired expression vector. 4-week-old *N. benthamiana* plant leaves were infiltrated with a needleless syringe with *A. tumefaciens* bacterial suspension at  $OD_{600} = 0.25$  in infiltration buffer (10 mM 2-(N-morpholino)-ethanesulfonic acid (MES); 10 mM  $MgCl_2$ ; and 150  $\mu$ M acetosyringone) previously incubated in darkness for 2 hours. Plant were then grown under long day conditions (16h light; 21°C; relative humidity 70%).

## 8.8 Gene expression measurement by qPCR

Material for RNA analysis was ground in liquid nitrogen and total RNA was isolated using the “Nucleospin RNA Plus kit” (Macherey-Nagel) following to the manufacturers’ recommendations. Reverse transcription was performed using 1  $\mu$ g of total RNA with the “Transcriptor Reverse Transcriptase” (Roche) and oligo(dT)<sub>18</sub> primer. Real-time quantitative PCR (qRT-PCR) was performed on a Light Cycler 480 II machine (Roche Diagnostics), using Roche reagents. Primers used for qRT-PCR are listed in **table A.5**. Relative expression was calculated as the  $\Delta C_p$  between each gene and the following reference genes: Glyceraldehyde 3-phosphate dehydrogenase C2, (*GAPC2*; AT1G13440) (Czechowski *et al.*, 2005) and Oxidase Assemble 1 (*OXA1*; AT5G62050) (Hok *et al.*, 2011) for *A. thaliana* and 16S rRNA (XC\_4393) for *Xcc*.

## 8.9 ROS measurement by luminometry

The measurement of flg22-induced ROS production was measured by luminometry as previously described (Sang and Macho, 2017). Briefly, leaf disks (diameter: 4mm) were harvested on OptiPlate-96-well microplates (Perkin Elmer) containing 100  $\mu$ l water and washed for 24 hours. In the case of pER8 transgenic lines, the water was supplemented with 5  $\mu$ M  $\beta$ -estradiol or equivalent volume of DMSO for induction. Then, the washing medium was substituted by 100  $\mu$ l of elicitation medium (20  $\mu$ g/ml horseradish peroxidase (HRP); 100  $\mu$ M luminol; and 50 nM (unless otherwise noted) flg22) and luminescence was measured every minute for 50 minutes on a GloMax Multimode Multiplate Reader (Promega).

## 8.10 Protein extraction and detection by Western blot

Four leaf disks (diameter: 8 mm) from transformed *N. benthamiana* plants were harvested and frozen in liquid nitrogen 24 to 48 hours post inoculation. Leaf disks were grinded and the proteins extracted in Laemli buffer 2X at 95°C for 5 minutes. Immunodetection of proteins were performed by loading 5-15  $\mu$ l of protein extract on precast gels SDS-PAGE (4-15%, Biorad). Migrated proteins were transferred to a nitrocellulose membrane by Transblot turbo (Biorad). Total proteins were revealed with Ponceau S staining. GFP-, CFP- and YFP-tagged proteins were revealed using antibody GFP-HRP (1:3000, Roche).

## 8.11 Bacterial growth *in vitro*

*In vitro* growth curves were generated using the FLUOStar Omega apparatus (BMG Labtech) with four independent replicates as previously described (Boulanger *et al.*, 2010). For each strain, 2 independent overnight precultures in MOKA rich medium were washed in MME minimal medium. Growth rates were measured using 96-well flat-bottom microtiter plates containing 200  $\mu$ l of MOKA or MME containing 10 mM glucose inoculated at an OD<sub>600</sub> of 0.15 with two technical replicates for each preculture. The microplates were shaken continuously at 700 rpm using the linear shaking mode and OD was measured every 5 minutes. Results were given as the mean of the four replicates (2 biological and 2 technical repeats).

## 8.12 Suppressor screening

Seeds were mutagenized with ethyl methanesulfonate (EMS) as previously described (Weigel and Glazebrook, 2002). Individually harvested M2 seeds were vapor-phase-sterilized and screened for suppression of the *xopAG*-mediated growth arrest on 5  $\mu$ M  $\beta$ -estradiol and 30

mg/l pimaricin solid MS medium (Sigma). Lines showing consistent suppressor phenotype were selected and the resulting M3 seeds were re-screened for normal growth in the same conditions.

## 8.13 Microscopy

CFP and YFP fluorescence was analyzed with a confocal laser scanning microscope (TCS SP8; Leica) using a x25 water immersion objective lens (numerical aperture 0.95; HCX PL APO CS2). CFP and YFP fluorescence was excited with the 458/514 nm ray line of the argon laser and recorded in one of the confocal channels in the 465-520/ 525-600nm emission range respectively. The images were acquired in the sequential mode using Leica LAS X software (version 3.0).

Fluorescence lifetime measurements were performed in time domain using a streak camera (Camborde *et al.*, 2017). The light source is a 440 nm pulsed laser diode (PLP-10, Hamamatsu) delivering ultrafast picosecond pulses of light at a fundamental frequency of 2 MHz. All images were acquired with a 60x oil immersion lens (plan APO 1.4 N.A., IR) mounted on an inverted microscope (Eclipse TE2000E, Nikon). The fluorescence emission is directed back into the detection unit through a short pass filter and a band pass filter (490/30 nm). The detector is a streak camera (Streakscope C4334, Hamamatsu) coupled to a fast and high-sensitivity CCD camera (model C8800-53C, Hamamatsu). For each acquisition, average fluorescence decay profiles were plotted and lifetimes were estimated by fitting data with exponential function using a non-linear least-squares estimation procedure (Camborde *et al.*, 2017). Fluorescence lifetime of the donor was experimentally measured in the presence and absence of the acceptor. FRET efficiency was calculated by comparing the lifetime of the donor in the presence or absence of the acceptor. Statistical comparisons between control (donor) and assay (donor + acceptor) lifetime values were performed by Student *t* test.

## 8.14 Measurement of GUS activity

$\beta$ -glucuronidase (GUS) activity was measured using the FLUOStar Omega apparatus (BMG Labtech) with three independent replicates. For each strain, 2 independent overnight precultures in MOKA rich medium were washed in MME minimal medium. 200  $\mu$ l of MME or MOKA were inoculated at an OD<sub>600</sub> of 0.3 and OD<sub>600</sub> of 0.15 respectively with two technical replicates per culture on 96-well flat-bottom microtiter plates and incubated at 28°C with 700 rpm shaking for 5-6 hours. 160  $\mu$ l of bacterial culture were transferred to a new microtiter plate containing 40  $\mu$ l 5X GEB buffer (50 mM NaHPO<sub>4</sub>, pH 7.0; 10 mM  $\beta$ -mercaptoethanol; 10 mM

EDTA, pH 8.0; 0.1% (w/v) Triton X-100; and 0.1% (w/v) sodium lauryl sarcosine) and incubated at 37°C for 30 minutes. Then 2 µl of 100 mg/mL p-nitrophenyl-β-D-glucuronide (pNPG) were added and the OD<sub>415</sub> and OD<sub>550</sub> were measured every 2 minutes during 1 hour at 37°C. The GUS activity was expressed in Miller Units.

# Bibliography

- Abad, P. and Williamson, V. M. (2010) 'Plant Nematode Interaction: A Sophisticated Dialogue.', in, pp. 147–192.
- Adlung, N. *et al.* (2016) 'Non-host Resistance Induced by the *Xanthomonas* Effector XopQ Is Widespread within the Genus *Nicotiana* and Functionally Depends on EDS1.', *Frontiers in plant science*, 7, p. 1796.
- Agarwal, V. K. and Sinclair, J. B. (1996) 'Mechanism of Seed Infection.', in *Principles of Seed Pathology, Second Edition*. CRC Press, pp. 159–178.
- Ahmed, H. *et al.* (2018) 'Network biology discovers pathogen contact points in host protein-protein interactomes.', *Nature communications*. Springer US, 9(1), p. 2312.
- Ahuja, I., Kissen, R. and Bones, A. M. (2012) 'Phytoalexins in defense against pathogens.', *Trends in Plant Science*, 17(2), pp. 73–90.
- Akhtar, J. *et al.* (2016) 'Diagnostics of Seed-Borne Plant Pathogens for Safe Introduction and Healthy Conservation of Plant Genetic Resources.', in, pp. 429–440.
- Akimoto-Tomiya, C., Furutani, A. and Ochiai, H. (2014) 'Real time live imaging of phytopathogenic bacteria *Xanthomonas campestris* pv. *campestris* MAFF106712 in "plant sweet home" ', *PloS one*, 9(4), p. e94386.
- Aldon, D. *et al.* (2018) 'Calcium Signalling in Plant Biotic Interactions.', *International journal of molecular sciences*, 19(3).
- Ali, S. *et al.* (2018) 'Pathogenesis-related proteins and peptides as promising tools for engineering plants with multiple stress tolerance.', *Microbiological Research*, 212–213, pp. 29–37.
- Alvarez, A. M. *et al.* (1994) 'Serological, pathological, and genetic diversity among strains of *Xanthomonas campestris* infecting crucifers.', *Phytopathology*. [St. Paul, Minn., etc.: American Phytopathological Society], 84(12), pp. 1449–1457.
- Álvarez, B., López, M. M. and Biosca, E. G. (2019) 'Biocontrol of the Major Plant Pathogen *Ralstonia solanacearum* in Irrigation Water and Host Plants by Novel Waterborne Lytic Bacteriophages.', *Frontiers in microbiology*, 10, p. 2813.
- Alvarez, S. *et al.* (2008) 'Metabolomic and proteomic changes in the xylem sap of maize under drought.', *Plant, Cell & Environment*, 31(3), pp. 325–340.
- An, S.-Q. *et al.* (2019) 'Mechanistic insights into host adaptation, virulence and epidemiology of the phytopathogen *Xanthomonas* ', *FEMS Microbiology Reviews*.
- Antico, C. J. *et al.* (2012) 'Insights into the role of jasmonic acid-mediated defenses against necrotrophic and biotrophic fungal pathogens.', *Frontiers in Biology*, 7(1), pp. 48–56.
- Aparicio, F. *et al.* (2011) 'A Plant Virus Movement Protein Regulates the Gcn2p Kinase in Budding Yeast.', *PLoS ONE*. Edited by M. Bendahmane, 6(11), p. e27409.
- Arlat, M. *et al.* (1991) '*Xanthomonas campestris* contains a cluster of *hrp* genes related to the larger *hrp* cluster of *Pseudomonas solanacearum* ', *Molecular plant-microbe interactions* :

MPMI, 4(6), pp. 593–601.

Arrebola, E. *et al.* (2011) 'Chemical and Metabolic Aspects of Antimetabolite Toxins Produced by *Pseudomonas syringae* Pathovars.', *Toxins*, 3(9), pp. 1089–1110.

Ashburner, M. *et al.* (2000) 'Gene ontology: tool for the unification of biology. The Gene Ontology Consortium.', *Nature genetics*, 25(1), pp. 25–9.

Aslam, S. N. *et al.* (2008) 'Bacterial polysaccharides suppress induced innate immunity by calcium chelation.', *Current biology : CB*, 18(14), pp. 1078–83.

Au, T. K., Chick, W. S. H. and Leung, P. C. (2000) 'Initial kinetics of the inactivation of calmodulin by the fungal toxin ophiobolin A.', *The international journal of biochemistry & cell biology*, 32(11–12), pp. 1173–82.

Audenaert, K. *et al.* (2013) 'Deoxynivalenol: a major player in the multifaceted response of *Fusarium* to its environment.', *Toxins*, 6(1), pp. 1–19.

Bae, M. S. *et al.* (2003) 'Analysis of the Arabidopsis nuclear proteome and its response to cold stress', *The Plant Journal*, 36(5), pp. 652–663.

Báidez, A. G. *et al.* (2007) 'Dysfunctionality of the xylem in *Olea europaea* L. Plants associated with the infection process by *Verticillium dahliae* Kleb. Role of phenolic compounds in plant defense mechanism.', *Journal of agricultural and food chemistry*, 55(9), pp. 3373–7.

Bain, D. C. (1955) 'Resistance of cabbage to black rot', *Phytopathology*. American Phytopathological Society, 45(1), pp. 35–37.

Balint-Kurti, P. (2019) 'The plant hypersensitive response: concepts, control and consequences.', *Molecular plant pathology*, 20(8), pp. 1163–1178.

Banfield, M. J. (2015) 'Perturbation of host ubiquitin systems by plant pathogen/pest effector proteins', *Cellular microbiology*. 2014/11/25. John Wiley & Sons Ltd, 17(1), pp. 18–25.

Barel, V. *et al.* (2015) 'Virulence and in planta movement of *Xanthomonas hortorum* pv. *pelargonii* are affected by the diffusible signal factor (DSF)-dependent quorum sensing system.', *Molecular plant pathology*, 16(7), pp. 710–23.

De Bary, A. (1879) *Die Erscheinung der Symbiose*. Strassburg: Verlag von Karl J. Trubner.

Bellstedt, D. U. *et al.* (2010) 'A rapid and inexpensive method for the direct PCR amplification of DNA from plants.', *American Journal of Botany*, 97(7), pp. e65–e68.

Bendix, C. and Lewis, J. D. (2018) 'The enemy within: phloem-limited pathogens.', *Molecular Plant Pathology*, 19(1), pp. 238–254.

Benschop, J. J. *et al.* (2007) 'Quantitative phosphoproteomics of early elicitor signaling in Arabidopsis.', *Molecular & cellular proteomics : MCP*, 6(7), pp. 1198–214.

Bergey, D. H. *et al.* (1939) 'Manual of determinative bacteriology.', *Manual of determinative bacteriology*. Fifth Edn. London, Bailliere, Tindall & Cox.

Berne, C. *et al.* (2015) 'Adhesins Involved in Attachment to Abiotic Surfaces by Gram-Negative Bacteria.', *Microbiology spectrum*, 3(4).

Besson-Bard, A., Pugin, A. and Wendehenne, D. (2008) 'New Insights into Nitric Oxide Signaling in Plants.', *Annual Review of Plant Biology*, 59(1), pp. 21–39.

Blanvillain, S. *et al.* (2007) 'Plant carbohydrate scavenging through tonB-dependent receptors: a feature shared by phytopathogenic and aquatic bacteria.', *PloS one*, 2(2), p. e224.

Block, A. *et al.* (2010) 'The *Pseudomonas syringae* type III effector HopG1 targets mitochondria, alters plant development and suppresses plant innate immunity.', *Cellular microbiology*, 12(3), pp. 318–30.

Bogdanove, A. J. *et al.* (1998) 'Homology and functional similarity of an *hrp*-linked pathogenicity locus, *dspEF*, of *Erwinia amylovora* and the avirulence locus *avrE* of *Pseudomonas syringae* pathovar *tomato*.', *Proceedings of the National Academy of Sciences*, 95(3), pp. 1325–1330.

Boller, T. and Felix, G. (2009) 'A renaissance of elicitors: perception of microbe-associated molecular patterns and danger signals by pattern-recognition receptors.', *Annual review of plant biology*, 60, pp. 379–406.

Both, M. *et al.* (2005) 'Gene expression profiles of *Blumeria graminis* indicate dynamic changes to primary metabolism during development of an obligate biotrophic pathogen.', *The Plant cell*, 17(7), pp. 2107–22.

Boucher, C. A., Barberis, P. A. and Demery, D. A. (1985) 'Transposon Mutagenesis of *Pseudomonas solanacearum*: Isolation of Tn5-Induced Avirulent Mutants.', *Microbiology*, 131(9), pp. 2449–2457.

Boulanger, A. *et al.* (2010) 'Identification and Regulation of the N-Acetylglucosamine Utilization Pathway of the Plant Pathogenic Bacterium *Xanthomonas campestris* pv. *campestris*.', *Journal of Bacteriology*, 192(6), pp. 1487–1497.

Boulanger, A. *et al.* (2014) 'The Plant Pathogen *Xanthomonas campestris* pv. *campestris* Exploits N-Acetylglucosamine during Infection.', *mBio*, 5(5).

Boyd, E. F., Carpenter, M. R. and Chowdhury, N. (2012) 'Mobile effector proteins on phage genomes.', *Bacteriophage*, 2(3), pp. 139–148.

Bradbury, J. F. (1986) *Guide to plant pathogenic bacteria*. CAB international.

Brinker, M. *et al.* (2010) 'Linking the Salt Transcriptome with Physiological Responses of a Salt-Resistant *Populus* Species as a Strategy to Identify Genes Important for Stress Acclimation.', *Plant Physiology*, 154(4), pp. 1697–1709.

Brisson, L. F., Tenhaken, R. and Lamb, C. (1994) 'Function of Oxidative Cross-Linking of Cell Wall Structural Proteins in Plant Disease Resistance.', *The Plant cell*, 6(12), pp. 1703–1712.

Brown, D. G., Swanson, J. K. and Allen, C. (2007) 'Two host-induced *Ralstonia solanacearum* genes, *acrA* and *dinF*, encode multidrug efflux pumps and contribute to bacterial



wilt virulence.’, *Applied and environmental microbiology*, 73(9), pp. 2777–86.

Brown, J. F. (1997) ‘Survival and dispersal of plant parasites: general concepts.’, in Brown, J. F. and Ogle, H. J. (eds) *Plant Pathogens and Plant Diseases*. Armidale: Rockvale Publications, pp. 195–206.

Brückner, A. *et al.* (2009) ‘Yeast two-hybrid, a powerful tool for systems biology.’, *International journal of molecular sciences*, 10(6), pp. 2763–88.

Bücherl, C. A. *et al.* (2017) ‘Plant immune and growth receptors share common signalling components but localise to distinct plasma membrane nanodomains.’, *eLife*, 6.

Buell, C. R. (2002) ‘Interactions Between *Xanthomonas* Species and *Arabidopsis thaliana*.’, *The arabidopsis book*, 1, p. e0031.

Buonaurio, R. *et al.* (2003) ‘Occurrence of black rot caused by *Xanthomonas campestris* pv. *campestris* on ornamental kale in Italy.’, *Journal of Plant Pathology*, 85(1), pp. 1–63.

Burdman, S. *et al.* (2011) ‘Involvement of Type IV Pili in Pathogenicity of Plant Pathogenic Bacteria.’, *Genes*, 2(4), pp. 706–35.

Büttner, D. (2016) ‘Behind the lines-actions of bacterial type III effector proteins in plant cells.’, *FEMS microbiology reviews*, 40(6), pp. 894–937.

Büttner, D. and Bonas, U. (2010) ‘Regulation and secretion of *Xanthomonas* virulence factors.’, *FEMS microbiology reviews*, 34(2), pp. 107–33.

Büttner, D. and He, S. Y. (2009) ‘Type III Protein Secretion in Plant Pathogenic Bacteria.’, *Plant Physiology*, 150(4), pp. 1656–1664.

Cai, Q. *et al.* (2019) ‘Small RNAs and extracellular vesicles: New mechanisms of cross-species communication and innovative tools for disease control.’, *PLOS Pathogens*. Edited by C. Zipfel, 15(12), p. e1008090.

Camborde, L. *et al.* (2017) ‘Detection of nucleic acid–protein interactions in plant leaves using fluorescence lifetime imaging microscopy.’, *Nature Protocols*, 12(9), pp. 1933–1950.

Cao, H. *et al.* (1997) ‘The *Arabidopsis* NPR1 gene that controls systemic acquired resistance encodes a novel protein containing ankyrin repeats.’, *Cell*, 88(1), pp. 57–63.

Cao, Y. *et al.* (2018) ‘Antagonism of Two Plant-Growth Promoting *Bacillus velezensis* Isolates Against *Ralstonia solanacearum* and *Fusarium oxysporum*.’, *Scientific reports*, 8(1), p. 4360.

Castagnone-Sereno, P. *et al.* (2019) ‘Gene copy number variations as signatures of adaptive evolution in the parthenogenetic, plant-parasitic nematode *Meloidogyne incognita*.’, *Molecular Ecology*, 28(10), pp. 2559–2572.

Castillo, J. A. and Greenberg, J. T. (2007) ‘Evolutionary Dynamics of *Ralstonia solanacearum*.’, *Applied and Environmental Microbiology*, 73(4), pp. 1225–1238.

- Celetti, M. (2011) *Black Rot Of Crucifer Crops*.
- Cerutti, A. *et al.* (2017) 'Immunity at Cauliflower Hydathodes Controls Systemic Infection by *Xanthomonas campestris* pv *campestris*', *Plant Physiology*, 174(2), pp. 700–716.
- Cerutti, A. *et al.* (2019) 'Mangroves in the Leaves: Anatomy, Physiology, and Immunity of Epithelial Hydathodes.', *Annual Review of Phytopathology*, 57(1), pp. 91–116.
- Chan, J. W. Y. . and Goodwin, P. H. (1999) 'The molecular genetics of virulence of *Xanthomonas campestris*.', *Biotechnology Advances*, 17(6), pp. 489–508.
- Chatterjee, S., Almeida, R. P. P. and Lindow, S. (2008) 'Living in two Worlds: The Plant and Insect Lifestyles of *Xylella fastidiosa*.', *Annual Review of Phytopathology*, 46(1), pp. 243–271.
- Chen, L.-Q. *et al.* (2010) 'Sugar transporters for intercellular exchange and nutrition of pathogens.', *Nature*, 468(7323), pp. 527–32.
- Chen, L. *et al.* (2014) 'Involvement of HLK effectors in *Ralstonia solanacearum* disease development in tomato.', *Journal of General Plant Pathology*, 80(1), pp. 79–84.
- Cheong, M. S. *et al.* (2014) 'AvrBsT acetylates Arabidopsis ACIP1, a protein that associates with microtubules and is required for immunity.', *PLoS pathogens*. United States, 10(2), p. e1003952.
- Chinchilla, D. *et al.* (2007) 'A flagellin-induced complex of the receptor FLS2 and BAK1 initiates plant defence.', *Nature*, 448(7152), pp. 497–500.
- Chopra, R. *et al.* (2018) 'Translational genomics using Arabidopsis as a model enables the characterization of pennycress genes through forward and reverse genetics.', *The Plant Journal*, 96(6), pp. 1093–1105.
- Chou, F.-L. *et al.* (1997) 'The *Xanthomonas campestris gumD* Gene Required for Synthesis of Xanthan Gum Is Involved in Normal Pigmentation and Virulence in Causing Black Rot.', *Biochemical and Biophysical Research Communications*, 233(1), pp. 265–269.
- Clériveret, A. *et al.* (2000) 'Tyloses and gels associated with cellulose accumulation in vessels are responses of plane tree seedlings (*Platanus × acerifolia*) to the vascular fungus *Ceratocystis fimbriata* f. sp *platani*.', *Trees*, 15(1), pp. 25–31.
- Clough, S. J. and Bent, A. F. (1998) 'Floral dip: a simplified method for *Agrobacterium*-mediated transformation of *Arabidopsis thaliana*.', *The Plant journal: for cell and molecular biology*, 16(6), pp. 735–43.
- Cohn, M. *et al.* (2014) 'Xanthomonas axonopodis virulence is promoted by a transcription activator-like effector-mediated induction of a SWEET sugar transporter. in cassava.', *Molecular plant-microbe interactions : MPMI*, 27(11), pp. 1186–98.
- Colburn-Clifford, J. and Allen, C. (2010) 'A *cbb 3*-Type Cytochrome C Oxidase Contributes to *Ralstonia solanacearum* R3bv2 Growth in Microaerobic Environments and to Bacterial Wilt Disease Development in Tomato.', *Molecular Plant-Microbe Interactions*, 23(8), pp. 1042–1052.

Colburn-Clifford, J. M., Scherf, J. M. and Allen, C. (2010) 'Ralstonia solanacearum Dps contributes to oxidative stress tolerance and to colonization of and virulence on tomato plants.', *Applied and environmental microbiology*, 76(22), pp. 7392–9.

Coll, N. S. and Valls, M. (2013) 'Current knowledge on the Ralstonia solanacearum type III secretion system.', *Microbial biotechnology*, 6(6), pp. 614–20.

Collemare, J., O'Connell, R. and Lebrun, M. (2019) 'Nonproteinaceous effectors: the terra incognita of plant–fungal interactions.', *New Phytologist*, 223(2), pp. 590–596.

Collier, S. M., Hamel, L.-P. and Moffett, P. (2011) 'Cell death mediated by the N-terminal domains of a unique and highly conserved class of NB-LRR protein.', *Molecular plant-microbe interactions : MPMI*, 24(8), pp. 918–31.

Colmenares, A. J. *et al.* (2002) 'The putative role of botrydial and related metabolites in the infection mechanism of *Botrytis cinerea*.', *Journal of chemical ecology*, 28(5), pp. 997–1005.

Conrath, U. *et al.* (2006) 'Priming: Getting Ready for Battle.', *Molecular Plant-Microbe Interactions*, 19(10), pp. 1062–1071.

Contreras-Paredes, C. A. *et al.* (2013) 'The absence of eukaryotic initiation factor eIF(iso)4E affects the systemic spread of a Tobacco etch virus isolate in *Arabidopsis thaliana*.', *Molecular plant-microbe interactions : MPMI*, 26(4), pp. 461–70.

Cook, D. E., Mesarich, C. H. and Thomma, B. P. H. J. (2015) 'Understanding Plant Immunity as a Surveillance System to Detect Invasion.', *Annual Review of Phytopathology*, 53(1), pp. 541–563.

Cox, K. L. *et al.* (2017) 'TAL effector driven induction of a *SWEET* gene confers susceptibility to bacterial blight of cotton.', *Nature communications*, 8, p. 15588.

Cunnac, S. *et al.* (2004) 'Inventory and functional analysis of the large Hrp regulon in *Ralstonia solanacearum*: identification of novel effector proteins translocated to plant host cells through the type III secretion system.', *Molecular Microbiology*, 53(1), pp. 115–128.

Cunnac, S. *et al.* (2011) 'Genetic disassembly and combinatorial reassembly identify a minimal functional repertoire of type III effectors in *Pseudomonas syringae*.', *Proceedings of the National Academy of Sciences of the United States of America*, 108(7), pp. 2975–80.

Czechowski, T. *et al.* (2005) 'Genome-Wide Identification and Testing of Superior Reference Genes for Transcript Normalization in *Arabidopsis*.', *Plant Physiology*, 139(1), pp. 5–17.

Darling, A. C. E. *et al.* (2004) 'Mauve: multiple alignment of conserved genomic sequence with rearrangements.', *Genome research*, 14(7), pp. 1394–403.

Davis, E. L., Haegeman, A. and Kikuchi, T. (2011) 'Degradation of the Plant Cell Wall by Nematodes.', in *Genomics and Molecular Genetics of Plant-Nematode Interactions*. Dordrecht: Springer Netherlands, pp. 255–272.

Davis, R. E. *et al.* (2005) 'Cryptic plasmid pSKU146 from the wall-less plant pathogen

*Spiroplasma kunkelii* encodes an adhesin and components of a type IV translocation-related conjugation system.’, *Plasmid*, 53(2), pp. 179–90.

Deb, S. *et al.* (2019) ‘*Xanthomonas oryzae* pv. *oryzae* XopQ protein suppresses rice immune responses through interaction with two 14-3-3 proteins but its phospho-null mutant induces rice immune responses and interacts with another 14-3-3 protein.’, *Molecular Plant Pathology*, 20(7), pp. 976–989.

DebRoy, S. *et al.* (2004) ‘A family of conserved bacterial effectors inhibits salicylic acid-mediated basal immunity and promotes disease necrosis in plants.’, *Proceedings of the National Academy of Sciences*, 101(26), pp. 9927–9932.

Degrave, A. *et al.* (2013) ‘The bacterial effector DspA/E is toxic in *Arabidopsis thaliana* and is required for multiplication and survival of fire blight pathogen.’, *Molecular plant pathology*, 14(5), pp. 506–17.

Denancé, N. *et al.* (2018) ‘Two ancestral genes shaped the *Xanthomonas campestris* TAL effector gene repertoire.’, *New Phytologist*, 219(1), pp. 391–407.

Denison, R. F. and Kiers, E. T. (2011) ‘Life Histories of Symbiotic Rhizobia and Mycorrhizal Fungi.’, *Current Biology*, 21(18), pp. R775–R785.

Denny, T. (2007) ‘Plant pathogenic *Ralstonia* species.’, in *Plant-Associated Bacteria*. Dordrecht: Springer Netherlands, pp. 573–644.

Denny, T. P. (1995) ‘Involvement of bacterial polysaccharides in plant pathogenesis.’, *Annual review of phytopathology*, 33, pp. 173–97.

Depotter, J. R. L. *et al.* (2016) ‘*Verticillium longisporum*, the invisible threat to oilseed rape and other brassicaceous plant hosts.’, *Molecular Plant Pathology*, 17(7), pp. 1004–1016.

Derbyshire, M. *et al.* (2019) ‘Small RNAs from the plant pathogenic fungus *Sclerotinia sclerotiorum* highlight host candidate genes associated with quantitative disease resistance.’, *Molecular plant pathology*, 20(9), pp. 1279–1297.

Deslandes, L. *et al.* (1998) ‘Genetic characterization of RRS1, a recessive locus in *Arabidopsis thaliana* that confers resistance to the bacterial soilborne pathogen *Ralstonia solanacearum*.’, *Molecular plant-microbe interactions : MPMI*, 11(7), pp. 659–67.

Deslandes, L. *et al.* (2003) ‘Physical interaction between RRS1-R, a protein conferring resistance to bacterial wilt, and PopP2, a type III effector targeted to the plant nucleus.’, *Proceedings of the National Academy of Sciences of the United States of America*. United States, 100(13), pp. 8024–9.

Digonnet, C. *et al.* (2012) ‘Deciphering the route of *Ralstonia solanacearum* colonization in *Arabidopsis thaliana* roots during a compatible interaction: focus at the plant cell wall.’, *Planta*. Springer-Verlag, 236(5), pp. 1419–1431.

Dillon, M. M. *et al.* (2019) ‘Molecular Evolution of *Pseudomonas syringae* Type III Secreted Effector Proteins’, *Frontiers in Plant Science*, 10.

Divon, H. H. *et al.* (2005) 'Nitrogen-responsive genes are differentially regulated in planta during *Fusarium oxysporum* f. sp. *lycopersici* infection.', *Molecular plant pathology*, 6(4), pp. 459–70.

Djamei, A. and Kahmann, R. (2012) '*Ustilago maydis*: dissecting the molecular interface between pathogen and plant.', *PLoS pathogens*, 8(11), p. e1002955.

Dow, J. M. *et al.* (1995) 'A locus determining pathogenicity of *Xanthomonas campestris* is involved in lipopolysaccharide biosynthesis.', *Molecular plant-microbe interactions : MPMI*, 8(5), pp. 768–77.

Dow, M., Newman, M.-A. and von Roepenack, E. (2000) 'The Induction and Modulation of Plant Defense Responses by Bacterial Lipopolysaccharides.', *Annual review of phytopathology*, 38, pp. 241–261.

Durian, G. *et al.* (2016) 'Protein Phosphatase 2A in the Regulatory Network Underlying Biotic Stress Resistance in Plants.', *Frontiers in plant science*. Frontiers Media S.A., 7, p. 812.

Dutt, S. *et al.* (2015) 'Translation initiation in plants: roles and implications beyond protein synthesis', *Biologia Plantarum*, 59(3), pp. 401–412.

Dutta, B. *et al.* (2012) 'Location of *Acidovorax citrulli* in infested watermelon seeds is influenced by the pathway of bacterial invasion.', *Phytopathology*, 102(5), pp. 461–8.

Eigenbrode, S. D., Bosque-Pérez, N. A. and Davis, T. S. (2018) 'Insect-Borne Plant Pathogens and Their Vectors: Ecology, Evolution, and Complex Interactions.', *Annual review of entomology*, 63, pp. 169–191.

Elphinstone, J. G. (2005) 'The current bacterial wilt situation: A global overview.', in Allen, C., Prior, P., and Hayward, A. C. (eds) *Bacterial Wilt Disease and the Ralstonia solanacearum Species Complex*. APS Press. St. Paul, MN: American Phytopathological Society, pp. 9–28.

Engler, C., Kandzia, R. and Marillonnet, S. (2008) 'A one pot, one step, precision cloning method with high throughput capability.', *PloS one*, 3(11), p. e3647.

Epstein, L. and Nicholson, R. L. (2006) 'Adhesion and Adhesives of Fungi and Oomycetes.', in *Biological Adhesives*. Berlin, Heidelberg: Springer Berlin Heidelberg, pp. 41–62.

Erickson, J. L. *et al.* (2018) 'The *Xanthomonas* effector XopL uncovers the role of microtubules in stomule extension and dynamics in *Nicotiana benthamiana*.', *The Plant journal : for cell and molecular biology*, 93(5), pp. 856–870.

van Esse, H. P. *et al.* (2009) 'Tomato Transcriptional Responses to a Foliar and a Vascular Fungal Pathogen Are Distinct.', *Molecular Plant-Microbe Interactions*, 22(3), pp. 245–258.

Eynck, C. *et al.* (2007) 'Differential interactions of *Verticillium longisporum* and *V. dahliae* with *Brassica napus* detected with molecular and histological techniques.', *European Journal of Plant Pathology*, 118(3), pp. 259–274.

Fan, J. and Doerner, P. (2012) 'Genetic and molecular basis of nonhost disease resistance:

complex, yes; silver bullet, no.', *Current Opinion in Plant Biology*, 15(4), pp. 400–406.

Fargier, E. and Manceau, C. (2007) 'Pathogenicity assays restrict the species *Xanthomonas campestris* into three pathovars and reveal nine races within *X. campestris* pv. *campestris*.', *Plant Pathology*. Wiley Online Library, 56(5), pp. 805–818.

Faulkner, C. and Robatzek, S. (2012) 'Plants and pathogens: putting infection strategies and defence mechanisms on the map.', *Current Opinion in Plant Biology*, 15(6), pp. 699–707.

Fegan, M. and Prior, P. (2005) 'How complex is the *Ralstonia solanacearum* species complex.', in Allen, C., Prior, Philippe, and Hayward, A. C. (eds) *Bacterial Wilt Disease and the Ralstonia Solanacearum Species Complex*. APS Press. St. Paul, MN: American Phytopathological Society, pp. 449–461.

Felsenstein, J. (1985) 'Confidence Limits on Phylogenies: An Approach using the Bootstrap.', *Evolution; international journal of organic evolution*, 39(4), pp. 783–791.

Ferreira, R. M. *et al.* (2015) 'A TALE of transposition: Tn3-like transposons play a major role in the spread of pathogenicity determinants of *Xanthomonas citri* and other xanthomonads.', *mBio*, 6(1), pp. e02505-14.

Figueiredo, J. F. L. *et al.* (2011) 'Agrobacterium-mediated transient expression in citrus leaves: a rapid tool for gene expression and functional gene assay.', *Plant cell reports*, 30(7), pp. 1339–45.

Flor, H. (1955) 'Host-parasite interaction in flax rust - Its genetics and other implications.', *Phytopathology*, 45, pp. 680–685.

Flores-Cruz, Z. and Allen, C. (2009) '*Ralstonia solanacearum* encounters an oxidative environment during tomato infection.', *Molecular plant-microbe interactions : MPMI*, 22(7), pp. 773–82.

Foyer, C. H. and Noctor, G. (2005) 'Redox Homeostasis and Antioxidant Signaling: A Metabolic Interface between Stress Perception and Physiological Responses.', *The Plant Cell*, 17(7), pp. 1866–1875.

Fradin, E. F. and Thomma, B. P. H. J. (2006) 'Physiology and molecular aspects of *Verticillium* wilt diseases caused by *V. dahliae* and *V. albo-atrum*.', *Molecular Plant Pathology*, 7(2), pp. 71–86.

Fricker, M., Runions, J. and Moore, I. (2006) 'Quantitative Fluorescence Microscopy: From Art to Science.', *Annual Review of Plant Biology*, 57(1), pp. 79–107.

Fuente, L. de la *et al.* (2017) 'Metabolomic characterization of xylem sap of different olive cultivars growing in Spain.', in *European Conference on Xylella*. Palma de Mallorca.

Fujita, M. *et al.* (2006) 'Crosstalk between abiotic and biotic stress responses: a current view from the points of convergence in the stress signaling networks.', *Current Opinion in Plant Biology*, 9(4), pp. 436–442.

Galon, Y. *et al.* (2008) 'Calmodulin-binding transcription activator (CAMTA) 3 mediates

biotic defense responses in Arabidopsis.', *FEBS letters*, 582(6), pp. 943–8.

Geagea, Huber and Sache (1999) 'Dry-dispersal and rain-splash of brown (*Puccinia recondita* f.sp. *tritici*) and yellow (*P. striiformis*) rust spores from infected wheat leaves exposed to simulated raindrops.', *Plant Pathology*, 48(4), pp. 472–482.

Gelfand, Y., Rodriguez, A. and Benson, G. (2007) 'TRDB--the Tandem Repeats Database.', *Nucleic acids research*, 35(Database issue), pp. D80–7.

Genin, S. and Boucher, C. (2004) 'Lessons learned from the genome analysis of *Ralstonia solanacearum*.', *Annual review of phytopathology*, 42, pp. 107–34.

Genin, S. and Denny, T. P. (2012) 'Pathogenomics of the *Ralstonia solanacearum* species complex.', *Annual review of phytopathology*, 50, pp. 67–89.

Gill, U. S., Lee, S. and Mysore, K. S. (2015) 'Host versus nonhost resistance: distinct wars with similar arsenals.', *Phytopathology*, 105(5), pp. 580–7.

Giron, D. *et al.* (2016) 'Insect-induced effects on plants and possible effectors used by galling and leaf-mining insects to manipulate their host-plant.', *Journal of Insect Physiology*, 84, pp. 70–89.

Giska, F. *et al.* (2013) 'Phosphorylation of HopQ1, a type III effector from *Pseudomonas syringae*, creates a binding site for host 14-3-3 proteins.', *Plant physiology*, 161(4), pp. 2049–61.

Glazebrook, J. (2005) 'Contrasting mechanisms of defense against biotrophic and necrotrophic pathogens.', *Annual review of phytopathology*, 43, pp. 205–27.

Gochez, A. M. *et al.* (2015) 'A functional XopAG homologue in *Xanthomonas fuscans* pv. *aurantifolii* strain C limits host range.', *Plant Pathology*, 64(5), pp. 1207–1214.

Gochez, A. M. *et al.* (2017) 'Molecular characterization of XopAG effector AvrGf2 from *Xanthomonas fuscans* ssp. *aurantifolii* in grapefruit.', *Molecular plant pathology*, 18(3), pp. 405–419.

Göhre, V. and Robatzek, S. (2008) 'Breaking the Barriers: Microbial Effector Molecules Subvert Plant Immunity.', *Annual Review of Phytopathology*, 46(1), pp. 189–215.

González-Fuente, M. *et al.* (2019) 'EffectorK, a comprehensive resource to mine for pathogen effector targets in the Arabidopsis proteome.', *bioRxiv*, p. 2019.12.16.878074.

Goodman, R. N. and Novacky, A. J. (1994) *The hypersensitive reaction in plants to pathogens: a resistance phenomenon*. Edited by APS Press. St. Paul, MN.

Govrin, E. M. and Levine, A. (2000) 'The hypersensitive response facilitates plant infection by the necrotrophic pathogen *Botrytis cinerea*.', *Current biology : CB*, 10(13), pp. 751–7.

Grall, S. and Manceau, C. (2003) 'Colonization of *Vitis vinifera* by a Green Fluorescence Protein-Labeled, *gfp*-Marked Strain of *Xylophilus ampelinus*, the Causal Agent of Bacterial Necrosis of Grapevine.', *Applied and Environmental Microbiology*, 69(4), pp. 1904–1912.

Gusmaroli, G. *et al.* (2007) 'Role of the MPN Subunits in COP9 Signalosome Assembly and Activity, and Their Regulatory Interaction with Arabidopsis Cullin3-Based E3 Ligases.', *The Plant Cell*, 19(2), pp. 564–581.

Gutarra, L. *et al.* (2017) 'Diversity, Pathogenicity, and Current Occurrence of Bacterial Wilt Bacterium *Ralstonia solanacearum* in Peru.', *Frontiers in plant science*, 8, p. 1221.

Guy, E. *et al.* (2013) 'Natural Genetic Variation of *Xanthomonas campestris* pv. *campestris* Pathogenicity on Arabidopsis Revealed by Association and Reverse Genetics.', *mBio*. Edited by D. Guttman and F. M. Ausubel, 4(3).

Halpern, M., Raats, D. and Lev-Yadun, S. (2007) 'The Potential Anti-Herbivory Role of Microorganisms on Plant Thorns.', *Plant Signaling & Behavior*, 2(6), pp. 503–504.

Hanemian, M. *et al.* (2013) 'Hrp mutant bacteria as biocontrol agents: toward a sustainable approach in the fight against plant pathogenic bacteria.', *Plant signaling & behavior*, 8(10), p. doi: 10.4161/psb.25678.

Hayward, A. C. (1991) 'Biology and epidemiology of bacterial wilt caused by *Pseudomonas solanacearum*.', *Annual review of phytopathology*, 29, pp. 65–87.

He, Y.-Q. *et al.* (2007) 'Comparative and functional genomics reveals genetic diversity and determinants of host specificity among reference strains and a large collection of Chinese isolates of the phytopathogen *Xanthomonas campestris* pv. *campestris*.', *Genome biology*, 8(10), p. R218.

Heath, M. C. (2000) 'Nonhost resistance and nonspecific plant defenses.', *Current Opinion in Plant Biology*, 3(4), pp. 315–319.

Hegedus, D. D. and Rimmer, S. R. (2005) '*Sclerotinia sclerotiorum*: When “to be or not to be” a pathogen?', *FEMS Microbiology Letters*, 251(2), pp. 177–184.

Heller, J. and Tudzynski, P. (2011) 'Reactive Oxygen Species in Phytopathogenic Fungi: Signaling, Development, and Disease.', *Annual Review of Phytopathology*, 49(1), pp. 369–390.

Hernández-Romero, D., Solano, F. and Sanchez-Amat, A. (2005) 'Polyphenol oxidase activity expression in *Ralstonia solanacearum*.', *Applied and environmental microbiology*, 71(11), pp. 6808–15.

Hewezi, T. *et al.* (2015) 'The cyst nematode effector protein I0A07 targets and recruits host posttranslational machinery to mediate its nuclear trafficking and to promote parasitism in Arabidopsis.', *The Plant cell*. United States, 27(3), pp. 891–907.

Hilaire, E. *et al.* (2001) 'Vascular Defense Responses in Rice: Peroxidase Accumulation in Xylem Parenchyma Cells and Xylem Wall Thickening.', *Molecular Plant-Microbe Interactions*, 14(12), pp. 1411–1419.

Hipper, C. *et al.* (2013) 'Viral and cellular factors involved in Phloem transport of plant viruses.', *Frontiers in plant science*, 4, p. 154.

Hirsch, A. M. (2004) 'Plant-microbe symbioses: A continuum from commensalism to



parasitism.', *Symbiosis*, 37.

Hok, S. *et al.* (2011) 'An *Arabidopsis* (malectin-like) leucine-rich repeat receptor-like kinase contributes to downy mildew disease.', *Plant, cell & environment*, 34(11), pp. 1944–57.

Holbein, J. *et al.* (2019) 'Root endodermal barrier system contributes to defence against plant-parasitic cyst and root-knot nematodes.', *The Plant Journal*, 100(2), pp. 221–236.

Hong, C. X. and Moorman, G. W. (2005) 'Plant Pathogens in Irrigation Water: Challenges and Opportunities.', *Critical Reviews in Plant Sciences*, 24(3), pp. 189–208.

Hopkins, M. T. *et al.* (2008) 'Eukaryotic translation initiation factor 5A is involved in pathogen-induced cell death and development of disease symptoms in *Arabidopsis*.', *Plant physiology*, 148(1), pp. 479–89.

Hornby, D. (1998) 'Diseases caused by soilborne pathogens.', in *The Epidemiology of Plant Diseases*. Dordrecht: Springer Netherlands, pp. 308–322.

Hückelhoven, R. and Kogel, K.-H. (2003) 'Reactive oxygen intermediates in plant-microbe interactions: who is who in powdery mildew resistance?', *Planta*, 216(6), pp. 891–902.

Hung, C.-H., Wu, H.-C. and Tseng, Y.-H. (2002) 'Mutation in the *Xanthomonas campestris xanA* gene required for synthesis of xanthan and lipopolysaccharide drastically reduces the efficiency of bacteriophage (phi)L7 adsorption.', *Biochemical and biophysical research communications*, 291(2), pp. 338–43.

Huot, B. *et al.* (2014) 'Growth–Defense Tradeoffs in Plants: A Balancing Act to Optimize Fitness.', *Molecular Plant*, 7(8), pp. 1267–1287.

Immanuel, T. M., Greenwood, D. R. and MacDiarmid, R. M. (2012) 'A critical review of translation initiation factor eIF2 $\alpha$  kinases in plants - regulating protein synthesis during stress.', *Functional Plant Biology*, 39(9), p. 717.

Ishikawa, K. *et al.* (2014) 'Bacterial effector modulation of host E3 ligase activity suppresses PAMP-triggered immunity in rice.', *Nature Communications*, 5(1), p. 5430.

Jalan, N. *et al.* (2013) 'Comparative genomic and transcriptome analyses of pathotypes of *Xanthomonas citri* subsp. *citri* provide insights into mechanisms of bacterial virulence and host range.', *BMC Genomics*, 14(1), p. 551.

Janse, J. D. *et al.* (1998) 'Experiences with Bacterial Brown Rot *Ralstonia solanacearum* Biovar 2, Race 3 in the Netherlands.', in *Bacterial Wilt Disease*. Berlin, Heidelberg: Springer Berlin Heidelberg, pp. 146–152.

Janse, J. D. (2005) *Phytopathology: Principles and Practice*. CABI Pub. (CABI Publishing Series).

Jensen, B. D. *et al.* (2010) 'Occurrence and Diversity of *Xanthomonas campestris* pv. *campestris* in Vegetable Brassica Fields in Nepal.', *Plant disease*, 94(3), pp. 298–305.

Jiang, G.-F. *et al.* (2013) 'Establishment of an inducing medium for type III effector

secretion in *Xanthomonas campestris* pv. *campestris*.', *Brazilian journal of microbiology: [publication of the Brazilian Society for Microbiology]*, 44(3), pp. 945–52.

Jiang, Y. *et al.* (2016) 'First report of bacterial wilt caused by *Ralstonia solanacearum* on fig trees in China.', *Forest Pathology*. Edited by S. Woodward, 46(3), pp. 256–258.

Jin, L. *et al.* (2016) 'Direct and Indirect Targeting of PP2A by Conserved Bacterial Type-III Effector Proteins.', *PLoS pathogens*, 12(5), p. e1005609.

Jones, J. D. G. and Dangl, J. L. (2006) 'The plant immune system.', *Nature*, 444(7117), pp. 323–9.

Judelson, H. S. and Blanco, F. A. (2005) 'The spores of *Phytophthora*: weapons of the plant destroyer.', *Nature reviews. Microbiology*, 3(1), pp. 47–58.

Justamante, M. S. *et al.* (2019) 'A Genome-Wide Association Study Identifies New Loci Involved in Wound-Induced Lateral Root Formation in *Arabidopsis thaliana*.', *Frontiers in Plant Science*, 10.

Kado, C. I. (2009) 'Horizontal gene transfer: sustaining pathogenicity and optimizing host-pathogen interactions.', *Molecular plant pathology*, 10(1), pp. 143–50.

Kamoun, S. *et al.* (1992) 'A vascular hypersensitive response: role of the *hrpK* locus.', *Mol Plant-Microbe Interact*, 5, pp. 22–33.

Kang, Y. *et al.* (2002) '*Ralstonia solanacearum* requires type 4 pili to adhere to multiple surfaces and for natural transformation and virulence.', *Molecular microbiology*, 46(2), pp. 427–37.

Karczmarek, A. *et al.* (2004) 'Feeding cell development by cyst and root-knot nematodes involves a similar early, local and transient activation of a specific auxin-inducible promoter element.', *Molecular plant pathology*, 5(4), pp. 343–6.

Kastelein, P. *et al.* (2014) 'Transmission of *Xanthomonas campestris* pv. *campestris* in Seed Production Crops of Cauliflower.', *Acta Horticulturae*, (1041), pp. 197–204.

Kelman, A. (1998) 'One Hundred and One Years of Research on Bacterial Wilt.', in *Bacterial Wilt Disease*. Berlin, Heidelberg: Springer Berlin Heidelberg, pp. 1–5.

Khan, M. *et al.* (2018) 'Oh, the places they'll go! A survey of phytopathogen effectors and their host targets', *Plant Journal*, 93(4), pp. 651–663.

Kilaru, A., Bailey, B. A. and Hasenstein, K. H. (2007) '*Moniliophthora perniciosa* produces hormones and alters endogenous auxin and salicylic acid in infected cocoa leaves.', *FEMS microbiology letters*, 274(2), pp. 238–44.

Kim, S. H. *et al.* (2003) '*Ralstonia solanacearum* Race 3, Biovar 2, the Causal Agent of Brown Rot of Potato, Identified in Geraniums in Pennsylvania, Delaware, and Connecticut.', *Plant Disease*, 87(4), pp. 450–450.

Kliebenstein, D. J., Rowe, H. C. and Denby, K. J. (2005) 'Secondary metabolites influence

Arabidopsis/Botrytis interactions: variation in host production and pathogen sensitivity.', *The Plant Journal*, 44(1), pp. 25–36.

Klosterman, S. J. *et al.* (2011) 'Comparative Genomics Yields Insights into Niche Adaptation of Plant Vascular Wilt Pathogens.', *PLoS Pathogens*. Edited by J. L. Dangl, 7(7), p. e1002137.

Kourelis, J. and van der Hoorn, R. A. L. (2018) 'Defended to the Nines: 25 Years of Resistance Gene Cloning Identifies Nine Mechanisms for R Protein Function.', *The Plant cell*, 30(2), pp. 285–299.

Kroupitski, Y. *et al.* (2009) 'Internalization of *Salmonella enterica* in Leaves Is Induced by Light and Involves Chemotaxis and Penetration through Open Stomata.', *Applied and Environmental Microbiology*, 75(19), pp. 6076–6086.

Kuan, T. L., Minsavage, G. V and Schaad, N. W. (1986) 'Aerial dissemination of *Xanthomonas campestris* pv. *campestris* from crucifer weeds.', *Plant Dis*, 70, pp. 409–413.

Kubicek, C. P., Starr, T. L. and Glass, N. L. (2014) 'Plant Cell Wall-Degrading Enzymes and Their Secretion in Plant-Pathogenic Fungi.', *Annual Review of Phytopathology*, 52(1), pp. 427–451.

Kumar, A. S. *et al.* (2018) 'Stromule extension along microtubules coordinated with actin-mediated anchoring guides perinuclear chloroplast movement during innate immunity.', *eLife*, 7.

Kumar, S. *et al.* (2018) 'MEGA X: Molecular Evolutionary Genetics Analysis across Computing Platforms.', *Molecular biology and evolution*, 35(6), pp. 1547–1549.

Kusch, S. *et al.* (2018) 'Small RNAs from cereal powdery mildew pathogens may target host plant genes.', *Fungal biology*, 122(11), pp. 1050–1063.

Kvitko, B. H. *et al.* (2009) 'Deletions in the repertoire of *Pseudomonas syringae* pv. *tomato* DC3000 type III secretion effector genes reveal functional overlap among effectors.', *PLoS pathogens*, 5(4), p. e1000388.

Kwak, M.-J. *et al.* (2018) 'Rhizosphere microbiome structure alters to enable wilt resistance in tomato.', *Nature biotechnology*.

Lafortune, D. *et al.* (2005) 'Partial Resistance of Pepper to Bacterial Wilt Is Oligogenic and Stable Under Tropical Conditions.', *Plant Disease*, 89(5), pp. 501–506.

Larkin, M. A. *et al.* (2007) 'Clustal W and Clustal X version 2.0.', *Bioinformatics (Oxford, England)*, 23(21), pp. 2947–8.

Łażniewska, J., Macioszek, V. K. and Kononowicz, A. K. (2012) 'Plant-fungus interface: The role of surface structures in plant resistance and susceptibility to pathogenic fungi.', *Physiological and Molecular Plant Pathology*, 78, pp. 24–30.

Lebeau, A. *et al.* (2011) 'Bacterial Wilt Resistance in Tomato, Pepper, and Eggplant: Genetic Resources Respond to Diverse Strains in the *Ralstonia solanacearum* Species Complex.',

*Phytopathology*, 101(1), pp. 154–165.

Lee, A. H.-Y. *et al.* (2012) 'A bacterial acetyltransferase destroys plant microtubule networks and blocks secretion.', *PLoS pathogens*, 8(2), p. e1002523.

Lee, H.-A. *et al.* (2017) 'Current Understandings of Plant Nonhost Resistance.', *Molecular plant-microbe interactions : MPMI*, 30(1), pp. 5–15.

Leelarasamee, N., Zhang, L. and Gleason, C. (2018) 'The root-knot nematode effector MiPFN3 disrupts plant actin filaments and promotes parasitism.', *PLoS pathogens*, 14(3), p. e1006947.

Lewis, J. D. *et al.* (2011) 'The YopJ superfamily in plant-associated bacteria.', *Molecular Plant Pathology*, 12(9), pp. 928–937.

Lewis, J. D. *et al.* (2012) 'Quantitative Interactor Screening with next-generation Sequencing (QIS-Seq) identifies *Arabidopsis thaliana* MLO2 as a target of the *Pseudomonas syringae* type III effector HopZ2.', *BMC genomics*, 13, p. 8.

Li, H., Zhou, Y. and Zhang, Z. (2017) 'Network analysis reveals a common host–pathogen interaction pattern in *Arabidopsis* immune responses.', *Frontiers in Plant Science*, 8, p. 893.

Li, M. *et al.* (2018) 'TCP Transcription Factors Interact With NPR1 and Contribute Redundantly to Systemic Acquired Resistance.', *Frontiers in Plant Science*, 9.

Li, W. *et al.* (2013) 'The *Pseudomonas syringae* effector HopQ1 promotes bacterial virulence and interacts with tomato 14-3-3 proteins in a phosphorylation-dependent manner.', *Plant physiology*, 161(4), pp. 2062–74.

Lin, C.-H., Chuang, M.-H. and Wang, J.-F. (2015) 'First Report of Bacterial Wilt Caused by *Ralstonia solanacearum* on Chard in Taiwan.', *Plant Disease*, 99(2), pp. 282–282.

Lipke, P. N. (2018) 'What We Do Not Know about Fungal Cell Adhesion Molecules.', *Journal of fungi (Basel, Switzerland)*, 4(2).

Liu, H. *et al.* (2005) 'Pyramiding unmarked deletions in *Ralstonia solanacearum* shows that secreted proteins in addition to plant cell-wall-degrading enzymes contribute to virulence.', *Molecular plant-microbe interactions : MPMI*, 18(12), pp. 1296–305.

Liu, M. *et al.* (2005) 'Advances in research bacterial wilt of ginger in China.', *Chinese agricultural science bulletin*, 21(6), p. 337—340,357.

Liu, T. *et al.* (2012) 'Chitin-induced dimerization activates a plant immune receptor.', *Science (New York, N.Y.)*, 336(6085), pp. 1160–4.

Liu, X., Afrin, T. and Pajerowska-Mukhtar, K. M. (2019) 'Arabidopsis GCN2 kinase contributes to ABA homeostasis and stomatal immunity.', *Communications Biology*, 2(1), p. 302.

Liu, Y., Beyer, A. and Aebersold, R. (2016) 'On the Dependency of Cellular Protein Levels on mRNA Abundance.', *Cell*, 165(3), pp. 535–550.

López, N. I., Haedo, A. S. and Méndez, B. S. (1999) 'Evaluation of *Xanthomonas campestris* survival in a soil microcosm system.', *International microbiology: the official journal of the Spanish Society for Microbiology*, 2(2), pp. 111–4.

Lorang, J. (2019) 'Necrotrophic Exploitation and Subversion of Plant Defense: A Lifestyle or Just a Phase, and Implications in Breeding Resistance.', *Phytopathology*, 109(3), pp. 332–346.

Lowe-Power, T. M., Khokhani, D. and Allen, C. (2018) 'How *Ralstonia solanacearum* Exploits and Thrives in the Flowing Plant Xylem Environment.', *Trends in Microbiology*. Elsevier Ltd, 26(11), pp. 929–942.

Lu, H. *et al.* (2008) 'Acquisition and Evolution of Plant Pathogenesis-Associated Gene Clusters and Candidate Determinants of Tissue-Specificity in *Xanthomonas*.', *PLoS ONE*. Edited by P. Wang, 3(11), p. e3828.

Luna, E. *et al.* (2012) 'Next-generation systemic acquired resistance.', *Plant physiology*, 158(2), pp. 844–53.

Luo, H. *et al.* (2010) 'The Arabidopsis Botrytis Susceptible Interactor defines a subclass of RING E3 ligases that regulate pathogen and stress responses.', *Plant physiology*, 154(4), pp. 1766–82.

Macho, A. P. *et al.* (2012) 'Genetic Analysis of the Individual Contribution to Virulence of the Type III Effector Inventory of *Pseudomonas syringae* pv. *phaseolicola*.', *PLoS ONE*. Edited by G. Bonaventure, 7(4), p. e35871.

Macho, A. P. (2016) 'Subversion of plant cellular functions by bacterial type-III effectors: beyond suppression of immunity.', *New Phytologist*, 210(1), pp. 51–57.

Macho, A. P. and Zipfel, C. (2014) 'Plant PRRs and the Activation of Innate Immune Signaling.', *Molecular Cell*, 54(2), pp. 263–272.

MacLean, A. M. *et al.* (2014) 'Phytoplasma effector SAP54 hijacks plant reproduction by degrading MADS-box proteins and promotes insect colonization in a RAD23-dependent manner.', *PLoS biology*. Edited by D. Wagner, 12(4), p. e1001835.

Malerba, M. and Cerana, R. (2015) 'Reactive oxygen and nitrogen species in defense/stress responses activated by chitosan in sycamore cultured cells.', *International journal of molecular sciences*, 16(2), pp. 3019–34.

Mansfield, J. *et al.* (2012) 'Top 10 plant pathogenic bacteria in molecular plant pathology.', *Molecular plant pathology*, 13(6), pp. 614–29.

Mao, G. *et al.* (2011) 'Phosphorylation of a WRKY transcription factor by two pathogen-responsive MAPKs drives phytoalexin biosynthesis in Arabidopsis.', *The Plant cell*, 23(4), pp. 1639–53.

Massomo, S. M. S., Mortensen, C. N., *et al.* (2004) 'Biological Control of Black Rot (*Xanthomonas campestris* pv. *campestris*) of Cabbage in Tanzania with *Bacillus* strains.', *Journal of Phytopathology*, 152(2), pp. 98–105.

Massomo, S. M. S., Mabagala, R. B., *et al.* (2004) 'Evaluation of varietal resistance in cabbage against the black rot pathogen, *Xanthomonas campestris* pv. *campestris* in Tanzania.', *Crop Protection*, 23(4), pp. 315–325.

Mbengue, M. *et al.* (2016) 'Clathrin-dependent endocytosis is required for immunity mediated by pattern recognition receptor kinases.', *Proceedings of the National Academy of Sciences of the United States of America*, 113(39), pp. 11034–9.

McAinsh, M. R. and Hetherington, A. M. (1998) 'Encoding specificity in Ca<sup>2+</sup> signalling systems.', *Trends in Plant Science*, 3(1), pp. 32–36.

McCarthy, Y. *et al.* (2008) 'The role of PilZ domain proteins in the virulence of *Xanthomonas campestris* pv. *campestris*.', *Molecular plant pathology*, 9(6), pp. 819–24.

McClerklin, S. A. *et al.* (2018) 'Indole-3-acetaldehyde dehydrogenase-dependent auxin synthesis contributes to virulence of *Pseudomonas syringae* strain DC3000.', *PLOS Pathogens*. Edited by D. Mackey, 14(1), p. e1006811.

McCully, M. E. (2001) 'Niches for bacterial endophytes in crop plants: a plant biologist's view', *Functional Plant Biology*, 28(9), pp. 983–990.

McLellan, H. *et al.* (2013) 'An RxLR effector from *Phytophthora infestans* prevents re-localisation of two plant NAC transcription factors from the endoplasmic reticulum to the nucleus.', *PLoS pathogens*, 9(10), p. e1003670.

Mejias, J. *et al.* (2019) 'Plant Proteins and Processes Targeted by Parasitic Nematode Effectors.', *Frontiers in plant science*, 10, p. 970.

Melotto, M. *et al.* (2006) 'Plant Stomata Function in Innate Immunity against Bacterial Invasion.', *Cell*, 126(5), pp. 969–980.

Meng, X. and Zhang, S. (2013) 'MAPK Cascades in Plant Disease Resistance Signaling.', *Annual Review of Phytopathology*, 51(1), pp. 245–266.

Merkouropoulos, G. and Shirsat, A. H. (2003) 'The unusual *Arabidopsis* extensin gene *atExt1* is expressed throughout plant development and is induced by a variety of biotic and abiotic stresses.', *Planta*, 217(3), pp. 356–66.

De Meutter, J. *et al.* (2005) 'Production of auxin and related compounds by the plant parasitic nematodes *Heterodera schachtii* and *Meloidogyne incognita*.', *Communications in agricultural and applied biological sciences*, 70(1), pp. 51–60.

Mew, T. W. (1977) 'Effect of Soil Temperature on Resistance of Tomato Cultivars to Bacterial Wilt.', *Phytopathology*, 77(7), p. 909.

Meyer, D. *et al.* (2005) 'Optimization of pathogenicity assays to study the *Arabidopsis thaliana*-*Xanthomonas campestris* pv. *campestris* pathosystem.', *Molecular plant pathology*, 6(3), pp. 327–33.

Mi, H. *et al.* (2019) 'PANTHER version 14: more genomes, a new PANTHER GO-slim and improvements in enrichment analysis tools.', *Nucleic acids research*, 47(D1), pp. D419–D426.

Miedes, E. *et al.* (2014) 'The role of the secondary cell wall in plant resistance to pathogens.', *Frontiers in plant science*, 5, p. 358.

Minato, N. *et al.* (2015) 'The phytoplasmal virulence factor TENGU causes plant sterility by downregulating of the jasmonic acid and auxin pathways.', *Scientific Reports*, 4(1), p. 7399.

Minsavage, G. V. *et al.* (1990) 'Gene-For-Gene Relationships Specifying Disease Resistance in *Xanthomonas campestris* pv. *vesicatoria* - Pepper Interactions.', *Molecular Plant-Microbe Interactions*, 3(1), p. 41.

Mittler, R. *et al.* (2004) 'Reactive oxygen gene network of plants.', *Trends in Plant Science*, 9(10), pp. 490–498.

Möbius, N. and Hertweck, C. (2009) 'Fungal phytotoxins as mediators of virulence.', *Current Opinion in Plant Biology*, 12(4), pp. 390–398.

Monteiro, F. and Nishimura, M. T. (2018) 'Structural, Functional, and Genomic Diversity of Plant NLR Proteins: An Evolved Resource for Rational Engineering of Plant Immunity.', *Annual review of phytopathology*, 56, pp. 243–267.

Van den Mooter, M. and Swings, J. (1990) 'Numerical analysis of 295 phenotypic features of 266 *Xanthomonas* strains and related strains and an improved taxonomy of the genus.', *International journal of systematic bacteriology*, 40(4), pp. 348–69.

Morais, T. P. *et al.* (2015) 'Occurrence and diversity of *Ralstonia solanacearum* populations in Brazil', *Bioscience Journal*, 31(6), pp. 1722–1737.

Morel, A. (2018) *Etude du rôle lors de l'infection et sur la défense des plantes hôtes des effecteurs de type III RipHI,2,3 et RipAX2 de Ralstonia pseudosolanacearum.*

Morel, A. *et al.* (2018) 'The eggplant AG91-25 recognizes the Type III-secreted effector RipAX2 to trigger resistance to bacterial wilt (*Ralstonia solanacearum* species complex).', *Molecular plant pathology*, pp. 0–3.

Morrison, E. N., Emery, R. J. N. and Saville, B. J. (2015) 'Phytohormone Involvement in the Ustilago maydis–Zea mays Pathosystem: Relationships between Abscissic Acid and Cytokinin Levels and Strain Virulence in Infected Cob Tissue.', *PLOS ONE*. Edited by W. Wang, 10(6), p. e0130945.

Mukhtar, M. S. *et al.* (2011) 'Independently evolved virulence effectors converge onto hubs in a plant immune system network.', *Science (New York, N.Y.)*, 333(6042), pp. 596–601.

Mur, L. A. J. *et al.* (2008) 'The hypersensitive response; the centenary is upon us but how much do we know?', *Journal of Experimental Botany*, 59(3), pp. 501–520.

Myburg, A. A., Lev-Yadun, S. and Sederoff, R. R. (2013) 'Xylem Structure and Function.', in *eLS*. Chichester, UK: John Wiley & Sons, Ltd.

Nakamura, S. *et al.* (2008) 'Effect of cadmium on the chemical composition of xylem exudate from oilseed rape plants (*Brassica napus* L.).', *Soil Science and Plant Nutrition*, 54(1), pp. 118–127.

Nakano, M. and Mukaihara, T. (2019) 'The type III effector RipB from *Ralstonia solanacearum* RSI000 acts as a major avirulence factor in *Nicotiana benthamiana* and other *Nicotiana* species.', *Molecular plant pathology*, 20(9), pp. 1237–1251.

Naseer, S. *et al.* (2012) 'Casparian strip diffusion barrier in *Arabidopsis* is made of a lignin polymer without suberin.', *Proceedings of the National Academy of Sciences of the United States of America*, 109(25), pp. 10101–6.

Nega, E. *et al.* (2003) 'Hot water treatment of vegetable seed — an alternative seed treatment method to control seed-borne pathogens in organic farming / Heißwasserbehandlung von Gemüsesaatgut — eine alternative Saatgutbehandlungsmethode zur Bekämpfung samenbürtiger Pathogene im', *Zeitschrift für Pflanzenkrankheiten und Pflanzenschutz / Journal of Plant Diseases and Protection*. Verlag Eugen Ulmer KG, 110(3), pp. 220–234.

Nelissen, H., Moloney, M. and Inzé, D. (2014) 'Translational research: from pot to plot.', *Plant Biotechnology Journal*, 12(3), pp. 277–285.

Newman, M.-A. *et al.* (2013) 'MAMP (microbe-associated molecular pattern) triggered immunity in plants.', *Frontiers in plant science*, 4, p. 139.

Nicolas, E. *et al.* (2015) 'The Tn3-family of Replicative Transposons.', *Microbiology spectrum*, 3(4).

Noël, L. *et al.* (2003) 'XopC and XopJ, two novel type III effector proteins from *Xanthomonas campestris* pv. *vesicatoria*.', *Journal of bacteriology*, 185(24), pp. 7092–102.

O'Malley, R. C., Barragan, C. C. and Ecker, J. R. (2015) 'A user's guide to the *Arabidopsis* T-DNA insertion mutant collections.', *Methods in molecular biology (Clifton, N.J.)*, 1284, pp. 323–42.

Oerke, E. C. (2006) 'Crop losses to pests.', *The Journal of Agricultural Science*, 144(1), pp. 31–43.

Oh, H.-S. and Collmer, A. (2005) 'Basal resistance against bacteria in *Nicotiana benthamiana* leaves is accompanied by reduced vascular staining and suppressed by multiple *Pseudomonas syringae* type III secretion system effector proteins.', *The Plant journal : for cell and molecular biology*, 44(2), pp. 348–59.

Oliva, R. *et al.* (2019) 'Broad-spectrum resistance to bacterial blight in rice using genome editing.', *Nature biotechnology*, 37(11), pp. 1344–1350.

Orth, K. *et al.* (2000) 'Disruption of signaling by *Yersinia* effector YopJ, a ubiquitin-like protein protease.', *Science (New York, N.Y.)*, 290(5496), pp. 1594–7.

Pecher, P. *et al.* (2019) 'Phytoplasma SAPII effector destabilization of TCP transcription factors differentially impact development and defence of *Arabidopsis* versus maize.', *PLOS Pathogens*. Edited by D. Mackey, 15(9), p. e1008035.

Pedras, M. S. C. and Abdoli, A. (2017) 'Pathogen inactivation of cruciferous phytoalexins: detoxification reactions, enzymes and inhibitors.', *RSC Advances*, 7(38), pp. 23633–23646.



Peeters, N., Guidot, A., *et al.* (2013) 'Ralstonia solanacearum, a widespread bacterial plant pathogen in the post-genomic era.', *Molecular Plant Pathology*, 14(7), pp. 651–662.

Peeters, N., Carrère, S., *et al.* (2013) 'Repertoire, unified nomenclature and evolution of the Type III effector gene set in the Ralstonia solanacearum species complex.', *BMC genomics*, 14, p. 859.

Peng, Y., van Wersch, R. and Zhang, Y. (2018) 'Convergent and Divergent Signaling in PAMP-Triggered Immunity and Effector-Triggered Immunity.', *Molecular plant-microbe interactions : MPMI*, 31(4), pp. 403–409.

Pérez-Brocal, V., Latorre, A. and Moya, A. (2013) 'Symbionts and pathogens: what is the difference?', *Current topics in microbiology and immunology*, 358, pp. 215–43.

Phan, H. T. T. *et al.* (2016) 'Differential effector gene expression underpins epistasis in a plant fungal disease.', *The Plant journal : for cell and molecular biology*, 87(4), pp. 343–54.

Pieterse, C. M. *et al.* (1998) 'A novel signaling pathway controlling induced systemic resistance in Arabidopsis.', *The Plant cell*, 10(9), pp. 1571–80.

Pieterse, C. M. J. *et al.* (2002) 'Signalling in Rhizobacteria-Induced Systemic Resistance in Arabidopsis thaliana.', *Plant Biology*, 4(5), pp. 535–544.

Postma, J. *et al.* (2016) 'Avr4 promotes Cf-4 receptor-like protein association with the BAK1/SERK3 receptor-like kinase to initiate receptor endocytosis and plant immunity.', *The New phytologist*, 210(2), pp. 627–42.

Poussier, S., Vandewalle, P. and Luisetti, J. (1999) 'Genetic Diversity of African and Worldwide Strains of *Ralstonia solanacearum* as Determined by PCR-Restriction Fragment Length Polymorphism Analysis of the *hrp* Gene Region', *Applied and Environmental Microbiology*, 65(5), pp. 2184 LP – 2194.

Prior, P. *et al.* (2016) 'Genomic and proteomic evidence supporting the division of the plant pathogen *Ralstonia solanacearum* into three species.', *BMC genomics*, 17, p. 90.

Purcell, A. H. and Hopkins, D. L. (1996) 'Fastidious xylem-limited bacterial plant pathogens.', *Annual review of phytopathology*, 34, pp. 131–51.

Qi, J. *et al.* (2017) 'Apoplastic ROS signaling in plant immunity.', *Current Opinion in Plant Biology*, 38, pp. 92–100.

Qian, W. *et al.* (2005) 'Comparative and functional genomic analyses of the pathogenicity of phytopathogen *Xanthomonas campestris* pv. *campestris*.', *Genome research*, 15(6), pp. 757–67.

Qin, J. *et al.* (2018) 'The plant-specific transcription factors CBP60g and SARD1 are targeted by a *Verticillium* secretory protein VdSCP41 to modulate immunity.', *eLife*, 7.

Qutob, D. *et al.* (2009) 'Copy Number Variation and Transcriptional Polymorphisms of *Phytophthora sojae* RXLR Effector Genes *Avr1a* and *Avr3a*.', *PLoS ONE*. Edited by F. M. Ausubel, 4(4), p. e5066.

Rahman, M. A., Abdullah, H. and Vanhaecke, M. (1999) 'Histopathology of Susceptible and Resistant *Capsicum annuum* Cultivars Infected with *Ralstonia solanacearum*.', *Journal of Phytopathology*, 147(3), pp. 129–140.

Rensink, W. A. and Buell, C. R. (2004) 'Arabidopsis to Rice. Applying Knowledge from a Weed to Enhance Our Understanding of a Crop Species.', *Plant Physiology*, 135(2), pp. 622–629.

Rep, M. *et al.* (2002) 'Mass Spectrometric Identification of Isoforms of PR Proteins in Xylem Sap of Fungus-Infected Tomato.', *Plant Physiology*, 130(2), pp. 904–917.

Reusche, M. *et al.* (2012) 'Verticillium Infection Triggers VASCULAR-RELATED NAC DOMAIN7-Dependent *de Novo* Xylem Formation and Enhances Drought Tolerance in Arabidopsis.', *The Plant Cell*, 24(9), pp. 3823–3837.

Rico, A. and Preston, G. M. (2008) '*Pseudomonas syringae* pv. *tomato* DC3000 uses constitutive and apoplast-induced nutrient assimilation pathways to catabolize nutrients that are abundant in the tomato apoplast.', *Molecular plant-microbe interactions : MPMI*, 21(2), pp. 269–82.

Robert-Seilaniantz, A., Grant, M. and Jones, J. D. G. (2011) 'Hormone Crosstalk in Plant Disease and Defense: More Than Just JASMONATE-SALICYLATE Antagonism', *Annual Review of Phytopathology*, 49(1), pp. 317–343.

Roberts, S. J. *et al.* (1999) 'Transmission from Seed to Seedling and Secondary Spread of *Xanthomonas campestris* pv. *campestris* in Brassica Transplants: Effects of Dose and Watering Regime', *European Journal of Plant Pathology*, 105(9), pp. 879–889.

Rodriguez, P. A. and Bos, J. I. B. (2013) 'Toward Understanding the Role of Aphid Effectors in Plant Infestation.', *Molecular Plant-Microbe Interactions*, 26(1), pp. 25–30.

Rohmer, L., Guttman, D. S. and Dangl, J. L. (2004) 'Diverse evolutionary mechanisms shape the type III effector virulence factor repertoire in the plant pathogen *Pseudomonas syringae*.', *Genetics*, 167(3), pp. 1341–60.

Rossier, O. *et al.* (1999) 'The *Xanthomonas* Hrp type III system secretes proteins from plant and mammalian bacterial pathogens.', *Proceedings of the National Academy of Sciences of the United States of America*, 96(16), pp. 9368–73.

Roux, B. *et al.* (2015) 'Genomics and transcriptomics of *Xanthomonas campestris* species challenge the concept of core type III effectome.', *BMC genomics*. BMC Genomics, 16(1), p. 975.

Le Roux, C. C. *et al.* (2015) 'A receptor pair with an integrated decoy converts pathogen disabling of transcription factors to immunity.', *Cell*. United States, 161(5), pp. 1074–1088.

Rufián, J. S. *et al.* (2018) 'Suppression of HopZ Effector-Trigged Plant Immunity in a Natural Pathosystem.', *Frontiers in Plant Science*, 9.

Russell, H. L. (1898) *A bacterial rot of cabbage and allied plants*. University of Wisconsin, Agricultural Experiment Station.

Ryals, J. A. *et al.* (1996) 'Systemic Acquired Resistance.', *The Plant Cell*, pp. 1809–1819.

Rybak, M. *et al.* (2009) 'Identification of *Xanthomonas citri* ssp. *citri* host specificity genes in a heterologous expression host.', *Molecular plant pathology*, 10(2), pp. 249–62.

Sabbagh, C. R. R. *et al.* (2019) 'Pangenomic type III effector database of the plant pathogenic *Ralstonia* spp.', *PeerJ*, 7, p. e7346.

Safni, I. *et al.* (2014) 'Polyphasic taxonomic revision of the *Ralstonia solanacearum* species complex: proposal to emend the descriptions of *Ralstonia solanacearum* and *Ralstonia syzygii* and reclassify current *R. syzygii* strains as *Ralstonia syzygii*', *International Journal of Systematic and Evolutionary Microbiology*, 64(Pt 9), pp. 3087–3103.

Safni, I., Subandiyah, S. and Fegan, M. (2018) 'Ecology, Epidemiology and Disease Management of *Ralstonia syzygii* in Indonesia.', *Frontiers in microbiology*, 9, p. 419.

Saile, E. *et al.* (1997) 'Role of Extracellular Polysaccharide and Endoglucanase in Root Invasion and Colonization of Tomato Plants by *Ralstonia solanacearum*.', *Phytopathology*, 87(12), pp. 1264–71.

Saitou, N. and Nei, M. (1987) 'The neighbor-joining method: a new method for reconstructing phylogenetic trees.', *Molecular biology and evolution*, 4(4), pp. 406–25.

Salgon, S. *et al.* (2017) 'Eggplant Resistance to the *Ralstonia solanacearum* Species Complex Involves Both Broad-Spectrum and Strain-Specific Quantitative Trait Loci.', *Frontiers in plant science*, 8, p. 828.

Sang, Y. and Macho, A. P. (2017) 'Analysis of PAMP-Triggered ROS Burst in Plant Immunity.', *Methods in molecular biology (Clifton, N.J.)*, 1578, pp. 143–153.

Schaad, N. W. (1981) 'Cruciferous Weeds as Sources of Inoculum of *Xanthomonas campestris* in Black Rot of Crucifers.', *Phytopathology*, 71(11), p. 1215.

Scheible, W.-R. *et al.* (2003) 'An Arabidopsis mutant resistant to thaxtomin A, a cellulose synthesis inhibitor from *Streptomyces* species.', *The Plant cell*, 15(8), pp. 1781–94.

Schell, M. A. (2000) 'Control of Virulence and Pathogenicity Genes of *Ralstonia solanacearum* by an Elaborate Sensory Network.', *Annual review of phytopathology*, 38, pp. 263–292.

Schellenberg, B., Ramel, C. and Dudler, R. (2010) 'Pseudomonas syringae Virulence Factor Syringolin A Counteracts Stomatal Immunity by Proteasome Inhibition.', *Molecular Plant-Microbe Interactions*, 23(10), pp. 1287–1293.

Schowalter, T. D. (2016) 'Species Interactions.', in *Insect Ecology*. Elsevier, pp. 249–290.

Schreiber, L. and Franke, R. B. (2011) 'Endodermis and Exodermis in Roots.', in *eLS*. Chichester, UK: John Wiley & Sons, Ltd.

Schulte, R. and Bonas, U. (1992) 'Expression of the *Xanthomonas campestris* pv. *vesicatoria* *hrp* gene cluster, which determines pathogenicity and hypersensitivity on pepper and tomato, is plant inducible.', *Journal of bacteriology*, 174(3), pp. 815–23.

Schultink, A. *et al.* (2017) 'Roq1 mediates recognition of the *Xanthomonas* and *Pseudomonas* effector proteins XopQ and HopQ1.', *The Plant journal : for cell and molecular biology*, 92(5), pp. 787–795.

Schultz, T., Gabrielson, R. L. and Olson, S. (1986) 'Control of *Xanthomonas campestris* pv. *campestris* in crucifer seed with slurry treatments of calcium hypochlorite.', *Plant disease*.

Sels, J. *et al.* (2008) 'Plant pathogenesis-related (PR) proteins: A focus on PR peptides.', *Plant Physiology and Biochemistry*, 46(11), pp. 941–950.

Serrano, M. *et al.* (2014) 'The cuticle and plant defense to pathogens.', *Frontiers in plant science*, 5, p. 274.

Shapiro, L. R. *et al.* (2018) 'An Introduced Crop Plant Is Driving Diversification of the Virulent Bacterial Pathogen *Erwinia tracheiphila*.', *mBio*. Edited by D. S. Guttman, 9(5).

Sharpee, W. C. and Dean, R. A. (2016) 'Form and function of fungal and oomycete effectors.', *Fungal Biology Reviews*, 30(2), pp. 62–73.

Shen, Q.-H. *et al.* (2007) 'Nuclear activity of MLA immune receptors links isolate-specific and basal disease-resistance responses.', *Science (New York, N.Y.)*, 315(5815), pp. 1098–103.

Shigaki, T., Nelson, S. C. and Alvarez, A. M. (2000) 'Symptomless Spread of Blight-inducing Strains of *Xanthomonas campestris* pv. *campestris* on Cabbage Seedlings in Misted Seedbeds.', *European Journal of Plant Pathology*, 106(4), pp. 339–346.

Shimizu, T. *et al.* (2010) 'Two LysM receptor molecules, CEBiP and OsCERK1, cooperatively regulate chitin elicitor signaling in rice.', *The Plant journal : for cell and molecular biology*, 64(2), pp. 204–14.

Shimono, M. *et al.* (2016) 'The *Pseudomonas syringae* Type III Effector HopGI Induces Actin Remodeling to Promote Symptom Development and Susceptibility during Infection', *Plant Physiology*. United States, 171(3), pp. 2239–2255.

Siamer, S. *et al.* (2011) 'Expressing the *Erwinia amylovora* type III effector DspA/E in the yeast *Saccharomyces cerevisiae* strongly alters cellular trafficking.', *FEBS Open Bio*, 1(1), pp. 23–28.

Siebrecht, S. *et al.* (2003) 'Nutrient translocation in the xylem of poplar--diurnal variations and spatial distribution along the shoot axis.', *Planta*, 217(5), pp. 783–93.

Singh, A., Lim, G.-H. and Kachroo, P. (2017) 'Transport of chemical signals in systemic acquired resistance.', *Journal of integrative plant biology*, 59(5), pp. 336–344.

Singh, D., Dhar, S. and Yadava, D. K. (2011) 'Genetic and pathogenic variability of Indian strains of *Xanthomonas campestris* pv. *campestris* causing black rot disease in crucifers.', *Current microbiology*, 63(6), pp. 551–60.

Singh, S. *et al.* (2018) 'Molecular breeding for resistance to black rot [*Xanthomonas campestris* pv. *campestris* (Pammel) Dowson] in Brassicas: recent advances.', *Euphytica*, 214(10), p. 196.

Skellam, E. (2017) 'The biosynthesis of cytochalasans.', *Natural product reports*, 34(11), pp. 1252–1263.

Spoel, S. H. *et al.* (2003) 'NPR1 modulates cross-talk between salicylate- and jasmonate-dependent defense pathways through a novel function in the cytosol.', *The Plant cell*, 15(3), pp. 760–770.

Spoel, S. H. *et al.* (2009) 'Proteasome-mediated turnover of the transcription coactivator NPR1 plays dual roles in regulating plant immunity.', *Cell*, 137(5), pp. 860–872.

Stergiopoulos, I. *et al.* (2010) 'Tomato Cf resistance proteins mediate recognition of cognate homologous effectors from fungi pathogenic on dicots and monocots.', *Proceedings of the National Academy of Sciences*, 107(16), pp. 7610–7615.

Stoodley, P. *et al.* (2002) 'Biofilms as complex differentiated communities.', *Annual review of microbiology*, 56, pp. 187–209.

Szabo, L. J. and Bushnell, W. R. (2001) 'Hidden robbers: The role of fungal haustoria in parasitism of plants.', *Proceedings of the National Academy of Sciences*, 98(14), pp. 7654–7655.

Takemoto, D., Jones, D. A. and Hardham, A. R. (2003) 'GFP-tagging of cell components reveals the dynamics of subcellular re-organization in response to infection of Arabidopsis by oomycete pathogens.', *The Plant journal : for cell and molecular biology*, 33(4), pp. 775–92.

Tamura, K. *et al.* (1994) 'Bacterial spot of crucifers caused by *Xanthomonas campestris* pv. *raphani*.', *Japanese Journal of Phytopathology*. The Phytopathological Society of Japan, 60(3), pp. 281–287.

Tan, K.-C. *et al.* (2015) 'Functional redundancy of necrotrophic effectors - consequences for exploitation for breeding.', *Frontiers in plant science*, 6, p. 501.

Tan, K.-C. and Oliver, R. P. (2017) 'Regulation of proteinaceous effector expression in phytopathogenic fungi.', *PLoS pathogens*, 13(4), p. e1006241.

Tans-Kersten, J., Huang, H. and Allen, C. (2001) '*Ralstonia solanacearum* needs motility for invasive virulence on tomato.', *Journal of bacteriology*, 183(12), pp. 3597–605.

Tansirichaiya, S., Rahman, M. A. and Roberts, A. P. (2019) 'The Transposon Registry.', *Mobile DNA*, 10(1), p. 40.

Tasset, C. C. C. *et al.* (2010) 'Autoacetylation of the *Ralstonia solanacearum* effector PopP2 targets a lysine residue essential for RRS1-R-mediated immunity in Arabidopsis.', *PLoS pathogens*. United States, 6(11), p. e1001202.

Teper, D. *et al.* (2014) '*Xanthomonas euvesicatoria* type III effector XopQ interacts with tomato and pepper 14-3-3 isoforms to suppress effector-triggered immunity.', *The Plant journal : for cell and molecular biology*, 77(2), pp. 297–309.

Thomma, B. P. H. J. *et al.* (2005) '*Cladosporium fulvum* (syn. *Passalora fulva*), a highly specialized plant pathogen as a model for functional studies on plant pathogenic Mycosphaerellaceae.', *Molecular plant pathology*, 6(4), pp. 379–93.

Thulasi Devendrakumar, K., Li, X. and Zhang, Y. (2018) 'MAP kinase signalling: interplays between plant PAMP- and effector-triggered immunity.', *Cellular and Molecular Life Sciences*, 75(16), pp. 2981–2989.

Tjou-Tam-Sin, N. N. A., van de Bilt, J. L. J., Westenberg, M., Gorkink-Smits, P. P. M. A., *et al.* (2017) 'Assessing the Pathogenic Ability of *Ralstonia pseudosolanacearum* (*Ralstonia solanacearum* Phylotype I) from Ornamental *Rosa* spp. Plants.', *Frontiers in Plant Science*, 8.

Tjou-Tam-Sin, N. N. A., van de Bilt, J. L. J., Westenberg, M., Bergsma-Vlami, M., *et al.* (2017) 'First Report of Bacterial Wilt Caused by *Ralstonia solanacearum* in Ornamental *Rosa* sp.', *Plant Disease*, 101(2), pp. 378–378.

Tokuda, G. (2019) 'Plant cell wall degradation in insects: Recent progress on endogenous enzymes revealed by multi-omics technologies.', in, pp. 97–136.

Tsuda, K. and Somssich, I. E. (2015) 'Transcriptional networks in plant immunity.', *New Phytologist*, 206(3), pp. 932–947.

Turner, P., Barber, C. and Daniels, M. (1985) 'Evidence for clustered pathogenicity genes in *Xanthomonas campestris* pv. *campestris*.', *Molecular and General Genetics MGG*, 199(2), pp. 338–343.

Uhse, S. and Djamei, A. (2018) 'Effectors of plant-colonizing fungi and beyond.', *PLOS Pathogens*. Edited by C. Zipfel, 14(6), p. e1006992.

Underwood, W. (2012) 'The Plant Cell Wall: A Dynamic Barrier Against Pathogen Invasion.', *Frontiers in Plant Science*, 3.

Üstün, S. *et al.* (2016) 'The Proteasome Acts as a Hub for Plant Immunity and Is Targeted by *Pseudomonas* Type III Effectors.', *Plant physiology*, 172(3), pp. 1941–1958.

Vailleau, F. *et al.* (2007) 'Characterization of the interaction between the bacterial wilt pathogen *Ralstonia solanacearum* and the model legume plant *Medicago truncatula*.', *Molecular plant-microbe interactions : MPMI*, 20(2), pp. 159–67.

Valls, M., Genin, S. and Boucher, C. (2006) 'Integrated Regulation of the Type III Secretion System and Other Virulence Determinants in *Ralstonia solanacearum*.', *PLoS Pathogens*, 2(8), p. e82.

Vauterin, L. *et al.* (1995) 'Reclassification of *Xanthomonas*.', *International Journal of Systematic and Evolutionary Microbiology*. Microbiology Society, 45(3), pp. 472–489.

Verma, S., Nizam, S. and Verma, P. K. (2013) 'Biotic and Abiotic Stress Signaling in Plants.', in *Stress Signaling in Plants: Genomics and Proteomics Perspective, Volume I*. New York, NY: Springer New York, pp. 25–49.

Vicente, J. G. *et al.* (2001) 'Identification and Origin of *Xanthomonas campestris* pv. *campestris* Races and Related Pathovars.', *Phytopathology*, 91(5), pp. 492–9.

Vicente, J. G. and Holub, E. B. (2013) '*Xanthomonas campestris* pv. *campestris* (cause of black rot of crucifers) in the genomic era is still a worldwide threat to brassica crops.', *Molecular*

*plant pathology*, 14(1), pp. 2–18.

Vieira, P. and Gleason, C. (2019) 'Plant-parasitic nematode effectors — insights into their diversity and new tools for their identification', *Current Opinion in Plant Biology*, 50, pp. 37–43.

Vlot, A. C., Dempsey, D. A. and Klessig, D. F. (2009) 'Salicylic Acid, a multifaceted hormone to combat disease.', *Annual review of phytopathology*, 47, pp. 177–206.

Vogel, C. and Marcotte, E. M. (2012) 'Insights into the regulation of protein abundance from proteomic and transcriptomic analyses.', *Nature reviews. Genetics*, 13(4), pp. 227–32.

Vorhölter, F. J., Niehaus, K. and Pühler, A. (2001) 'Lipopolysaccharide biosynthesis in *Xanthomonas campestris* pv. *campestris*: a cluster of 15 genes is involved in the biosynthesis of the LPS O-antigen and the LPS core.', *Molecular genetics and genomics: MGG*, 266(1), pp. 79–95.

Voth, D. E., Broederdorf, L. J. and Graham, J. G. (2012) 'Bacterial Type IV secretion systems: versatile virulence machines.', *Future microbiology*, 7(2), pp. 241–257.

Walley, J. W. *et al.* (2008) 'The chromatin remodeler SPLAYED regulates specific stress signaling pathways.', *PLoS pathogens*, 4(12), p. e1000237.

Wang, A. and Krishnaswamy, S. (2012) 'Eukaryotic translation initiation factor 4E-mediated recessive resistance to plant viruses and its utility in crop improvement.', *Molecular plant pathology*, 13(7), pp. 795–803.

Wang, B. *et al.* (2017) 'Puccinia striiformis f. sp. tritici microRNA-like RNA 1 (Pst-milR1), an important pathogenicity factor of Pst, impairs wheat resistance to Pst by suppressing the wheat pathogenesis-related 2 gene.', *New Phytologist*, 215(1), pp. 338–350.

Wang, C. *et al.* (2014) 'Free radicals mediate systemic acquired resistance.', *Cell reports*, 7(2), pp. 348–355.

Wang, G. *et al.* (2015) 'The Decoy Substrate of a Pathogen Effector and a Pseudokinase Specify Pathogen-Induced Modified-Self Recognition and Immunity in Plants', *Cell Host & Microbe*, 18(3), pp. 285–295.

Wang, J. *et al.* (2002) 'Brefeldin A, a cytotoxin produced by *Paecilomyces* sp. and *Aspergillus clavatus* isolated from *Taxus mairei* and *Torreya grandis*.', *FEMS immunology and medical microbiology*, 34(1), pp. 51–7.

Wang, J., Hu, M., Wang, Jia, *et al.* (2019) 'Reconstitution and structure of a plant NLR resistosome conferring immunity.', *Science (New York, N.Y.)*, 364(6435).

Wang, M. *et al.* (2013) 'The critical role of potassium in plant stress response.', *International journal of molecular sciences*, 14(4), pp. 7370–90.

Wang, M. *et al.* (2016) 'Bidirectional cross-kingdom RNAi and fungal uptake of external RNAs confer plant protection.', *Nature plants*, 2, p. 16151.

Wang, N., Zhao, P., *et al.* (2019) 'A whitefly effector Bsp9 targets host immunity regulator

WRKY33 to promote performance.’, *Philosophical Transactions of the Royal Society B: Biological Sciences*, 374(1767), p. 20180313.

Wang, N., Wang, L., *et al.* (2019) ‘Plant Root Exudates Are Involved in *Bacillus cereus* ARI56 Mediated Biocontrol Against *Ralstonia solanacearum*.’, *Frontiers in microbiology*, 10, p. 98.

Wang, X. *et al.* (2015) ‘TCP transcription factors are critical for the coordinated regulation of isochorismate synthase 1 expression in *Arabidopsis thaliana*.’, *The Plant journal: for cell and molecular biology*, 82(1), pp. 151–62.

Wang, Z., Cui, D., Liu, C., *et al.* (2019) ‘TCP transcription factors interact with ZED1-related kinases as components of the temperature-regulated immunity.’, *Plant, cell & environment*, 42(6), pp. 2045–2056.

van Wees, S. C. M. *et al.* (2000) ‘Enhancement of induced disease resistance by simultaneous activation of salicylate- and jasmonate-dependent defense pathways in *Arabidopsis thaliana*.’, *Proceedings of the National Academy of Sciences*, 97(15), pp. 8711–8716.

Wei, Z. *et al.* (2013) ‘The congeneric strain *Ralstonia pickettii* QL-A6 of *Ralstonia solanacearum* as an effective biocontrol agent for bacterial wilt of tomato.’, *Biological Control*, 65(2), pp. 278–285.

Wei, Z. M. and Beer, S. V (1995) ‘*hrpL* activates *Erwinia amylovora hrp* gene transcription and is a member of the ECF subfamily of sigma factors.’, *Journal of bacteriology*, 177(21), pp. 6201–6210.

Weiberg, A. *et al.* (2013) ‘Fungal small RNAs suppress plant immunity by hijacking host RNA interference pathways.’, *Science (New York, N.Y.)*, 342(6154), pp. 118–23.

Weigel, D. and Glazebrook, J. (2002) *Arabidopsis: A Laboratory Manual*. New York, NY: Cold Spring Harbor Laboratory Press.

Wengelnik, K., Van den Ackerveken, G. and Bonas, U. (1996) ‘*HrpG*, a key *hrp* regulatory protein of *Xanthomonas campestris* pv. *vesicatoria* is homologous to two-component response regulators.’, *Molecular plant-microbe interactions: MPMI*, 9(8), pp. 704–12.

Wengelnik, K., Rossier, O. and Bonas, U. (1999) ‘Mutations in the regulatory gene *hrpG* of *Xanthomonas campestris* pv. *vesicatoria* result in constitutive expression of all *hrp* genes.’, *Journal of bacteriology*, 181(21), pp. 6828–31.

Weßling, R. *et al.* (2014) ‘Convergent targeting of a common host protein-network by pathogen effectors from three kingdoms of life’, *Cell host & microbe*, 16(3), pp. 364–375.

West, J. S., Atkins, S. D. and Fitt, B. D. L. (2009) ‘Detection of Airborne Plant Pathogens; Halting Epidemics Before they Start.’, *Outlooks on Pest Management*, 20(1), pp. 11–14.

Wicker, E. *et al.* (2012) ‘Contrasting recombination patterns and demographic histories of the plant pathogen *Ralstonia solanacearum* inferred from MLSA.’, *The ISME journal*, 6(5), pp. 961–74.



Wicklow, D. T., Jordan, A. M. and Gloer, J. B. (2009) 'Antifungal metabolites (monorden, monocillins I, II, III) from *Colletotrichum graminicola*, a systemic vascular pathogen of maize.', *Mycological Research*, 113(12), pp. 1433–1442.

Wight, W. D. *et al.* (2009) 'Biosynthesis and role in virulence of the histone deacetylase inhibitor depudecin from *Alternaria brassicicola*.', *Molecular plant-microbe interactions : MPMI*, 22(10), pp. 1258–67.

Williams, P. H. (1980) 'Black Rot: A Continuing.', *Plant Disease*, 64(8), p. 736.

Wittstock, U. *et al.* (2003) 'Chapter five Glucosinolate hydrolysis and its impact on generalist and specialist insect herbivores.', in, pp. 101–125.

Wittstock, U. and Gershenzon, J. (2002) 'Constitutive plant toxins and their role in defense against herbivores and pathogens.', *Current Opinion in Plant Biology*, 5(4), pp. 300–307.

Van Der Wolf, J. M. and Van Der Zouwen, P. S. (2010) 'Colonization of Cauliflower Blossom (*Brassica oleracea*) by *Xanthomonas campestris* pv. *campestris*, via Flies (*Calliphora vomitoria*) Can Result in Seed Infestation.', *Journal of Phytopathology*, 158(11–12), pp. 726–732.

Wu, C.-H. *et al.* (2017) 'NLR network mediates immunity to diverse plant pathogens.', *Proceedings of the National Academy of Sciences*, 114(30), pp. 8113–8118.

Wulff, E. G. *et al.* (2002) 'Biological Control of Black Rot (*Xanthomonas Campestris* Pv. *campestris*) of Brassicas with an Antagonistic Strain of *Bacillus Subtilis* in Zimbabwe', *European Journal of Plant Pathology*, 108(4), pp. 317–325.

Xi'ou, X. *et al.* (2015) 'Functional Characterization of a Putative Bacterial Wilt Resistance Gene (*RE-bw*) in Eggplant.', *Plant Molecular Biology Reporter*, 33(4), pp. 1058–1073.

Xu, M. *et al.* (2017) 'Translation Initiation Factor eIF4E and eIFiso4E Are Both Required for Peanut stripe virus Infection in Peanut (*Arachis hypogaea* L.).', *Frontiers in microbiology*, 8, p. 338.

Xu, R.-Q. *et al.* (2008a) 'AvrACXcc8004, a Type III Effector with a Leucine-Rich Repeat Domain from *Xanthomonas campestris* Pathovar *campestris* Confers Avirulence in Vascular Tissues of *Arabidopsis thaliana* Ecotype Col-0.', *Journal of Bacteriology*, 190(1), pp. 343–355.

Xu, R.-Q. *et al.* (2008b) 'AvrAC<sub>Xcc8004</sub>, a Type III Effector with a Leucine-Rich Repeat Domain from *Xanthomonas campestris* Pathovar *campestris* Confers Avirulence in Vascular Tissues of *Arabidopsis thaliana* Ecotype Col-0.', *Journal of Bacteriology*, 190(1), pp. 343–355.

Yabuuchi, E. *et al.* (1995) 'Transfer of two *Burkholderia* and an *Alcaligenes* species to *Ralstonia* gen. Nov.: Proposal of *Ralstonia pickettii* (Ralston, Palleroni and Doudoroff 1973) comb. Nov., *Ralstonia solanacearum* (Smith 1896) comb. Nov. and *R. solanacearum* s. str.', *Microbiology and immunology*, 39(11), pp. 897–904.

Yadeta, K. A. and Thomma, B. P. H. J. (2013) 'The xylem as battleground for plant hosts and vascular wilt pathogens.', *Frontiers in Plant Science*, 4.

Yan, X. *et al.* (2019) 'A type III effector XopL<sub>8004</sub> is vital for *Xanthomonas campestris*

pathovar *campestris* to regulate plant immunity.', *Research in Microbiology*, 170(3), pp. 138–146.

Yang, L. *et al.* (2017) 'Pseudomonas syringae Type III Effector HopBB1 Promotes Host Transcriptional Repressor Degradation to Regulate Phytohormone Responses and Virulence.', *Cell host & microbe*, 21(2), pp. 156–168.

Yu, K. *et al.* (2013) 'A feedback regulatory loop between G3P and lipid transfer proteins DIR1 and AZI1 mediates azelaic-acid-induced systemic immunity.', *Cell reports*, 3(4), pp. 1266–78.

Yu, S. L. *et al.* (2011) 'Peanut genetics and breeding in China.', *Shanghai Scientific and Technology Press, Shanghai, China*.

Yun, M. H. *et al.* (2006) 'Xanthan induces plant susceptibility by suppressing callose deposition.', *Plant physiology*, 141(1), pp. 178–87.

Zangerl, A. R. and Rutledge, C. E. (1996) 'The Probability of Attack and Patterns of Constitutive and Induced Defense: A Test of Optimal Defense Theory.', *The American Naturalist*. The University of Chicago Press, 147(4), pp. 599–608.

Zhang, J. Z., Creelman, R. A. and Zhu, J.-K. (2004) 'From Laboratory to Field. Using Information from Arabidopsis to Engineer Salt, Cold, and Drought Tolerance in Crops.', *Plant Physiology*, 135(2), pp. 615–621.

Zhang, W. *et al.* (2018) 'Different Pathogen Defense Strategies in Arabidopsis: More than Pathogen Recognition.', *Cells*, 7(12).

Zhang, Z.-M. *et al.* (2017) 'Mechanism of host substrate acetylation by a YopJ family effector.', *Nature plants*, 3, p. 17115.

Zheng, X.-Y. *et al.* (2012) 'Coronatine promotes *Pseudomonas syringae* virulence in plants by activating a signaling cascade that inhibits salicylic acid accumulation.', *Cell host & microbe*, 11(6), pp. 587–96.

Zhu, Z. *et al.* (2011) 'Derepression of ethylene-stabilized transcription factors (EIN3/EIL1) mediates jasmonate and ethylene signaling synergy in Arabidopsis.', *Proceedings of the National Academy of Sciences of the United States of America*, 108(30), pp. 12539–44.

Zumaquero, A. *et al.* (2010) 'Analysis of the role of the type III effector inventory of *Pseudomonas syringae* pv. *phaseolicola* 1448a in interaction with the plant.', *Journal of bacteriology*, 192(17), pp. 4474–88.

Zuo, J., Niu, Q.-W. and Chua, N.-H. (2000) 'An estrogen receptor-based transactivator XVE mediates highly inducible gene expression in transgenic plants.', *The Plant Journal*, 24(2), pp. 265–273.

# Annexes

**Table A.1. Putative Arabidopsis targets of T3Es from Xcc8004.** Table showing the 52 identified putative targets of Xcc8004 T3Es with their description and degree as determined in the EffectorK database.

Accession	Gene symbol and description	Degree <sup>a</sup>	Interacting Xop(s)
ATIG10850	Leucine-rich repeat protein kinase family protein	1	XopAL2
ATIG11090	(MAGL1) Alpha/beta-hydrolases superfamily protein	4	AvrXccA1, XopJ, XopK, XopR
ATIG13320	(PP2AA3) Protein phosphatase 2A subunit A3	3	XopAC, XopJ
ATIG22920	(CSN5A) COP9 signalosome 5A	37	XopAC
ATIG25490	(RCN1) Roots curl in NPA 1	7	XopAC
ATIG25550	(HHO3) HRS1 homolog 3	3	XopK
ATIG27090	Glycine-rich protein	1	XopK
ATIG52200	PLAC8 family protein	1	XopAC
ATIG52870	Peroxisomal membrane 22 kDa (Mpv17/PMP22) family protein	2	XopH, XopR
ATIG54060	(ASIL1) Member of the trihelix DNA binding protein family	6	AvrXccA1, XopJ
ATIG55170	DNA double-strand break repair protein	2	XopR
ATIG58100	(TCP8) TCP domain protein 8	13	AvrBsl, AvrXccA1, XopA, XopAC, XopAG, XopAL1, XopAM, XopG, XopK, XopP, XopR, XopX1, XopX2
ATIG60990	(IBA57.2) Chloroplast-localized COG0354	1	XopAC
ATIG71230	(CSN5B) COP9 signalosome 5B	8	AvrBsl, XopAC, XopG, XopK
ATIG76850	(SEC5A) Exocyst complex component SEC5 A	4	XopK
ATIG78040	Pollen Ole e 1 allergen and extensin family protein	2	XopAC
AT2G17290	(CPK6) Calcium dependent protein kinase 6	3	XopAC, XopJ, XopK
AT2G18230	(PPa2) Pyrophosphorylase 2	1	XopK
AT2G19650	Cysteine/Histidine-rich C1 domain family protein	2	XopAC
AT2G24020	(STIC2) Suppressor of TIC40	1	XopA
AT2G45680	(TCP9) TCP domain protein 9	15	XopAL1, XopK
AT3G02870	(VTC4) L-galactose-1-phosphate phosphatase	2	XopAC, XopK
AT3G08530	(CHC2) Clathrin heavy chain 2	11	XopL, XopR
AT3G09250	Nuclear transport factor 2 (NTF2) family protein	1	XopK
AT3G10260	(RTNLB8) Reticulon-like B 8	1	XopK
AT3G12920	(BRG3) BOI-related gene 3	7	XopAC, XopAG, XopAL1
AT3G14180	(ASIL2) Sequence-specific DNA binding transcription factor	2	XopK, XopR
AT3G15950	(NAI2) Similar to TSK-associating protein 1 (TSA1)	1	XopAC
AT3G25800	(PP2AA2) Protein phosphatase 2A subunit A2	3	XopAC
AT3G27960	(KLCR2) Kinesin light chain-related 2	21	XopAC, XopAG, XopF, XopZ
AT3G28670	Oxidoreductase, zinc-binding dehydrogenase family protein	4	XopJ, XopK, XopR, XopX2
AT3G46670	(UGT76E11) UDP-glucosyl transferase 76E11	3	XopK, XopP, XopX2
AT3G51090	Coiled-coil 90B-like protein (DUF1640)	3	XopAC, XopK, XopR
AT3G53990	(ATUSP) Universal stress protein	1	XopAC
AT3G54000	TIP41-like protein	3	XopAL1
AT3G58040	(SINAT2) Seven in absentia of Arabidopsis 2	1	XopAC
AT4G01090	Hypothetical protein	9	XopAG, XopR
AT4G09060	Hypothetical protein	3	XopK

AT4G17680	SBP (S-ribonuclease binding protein) family protein	16	XopAC, XopAG, XopALI, XopP
AT4G26660	Kinesin-like protein	2	XopR
AT4G38580	(FP6) Farnesylated protein 6	1	XopK
AT5G02020	(SIS) Salt induced serine rich	2	XopR
AT5G08070	(TCP17) TCP domain protein 17	7	XopAC, XopK, XopR
AT5G13890	Plant viral-response family protein (DUF716)	2	XopAC, XopJ
AT5G15790	RING/U-box superfamily protein	1	XopK
AT5G26720	Ubiquitin carboxyl-terminal hydrolase-like protein	4	XopAC, XopJ, XopK
AT5G37890	(SINAL7) SINA-like 7	1	XopAM
AT5G42050	(NRP) Asparagine rich protein	1	XopAC
AT5G42270	(VAR1) Variegated 1	1	XopAC
AT5G51110	(SDIRIP1) SDIRI-interacting protein 1	3	XopK
AT5G51440	(HSP23.5) HSP20-like chaperones superfamily protein	7	XopAC, XopALI
AT5G63790	(NAC102) NAC domain containing protein 102	1	XopAC

<sup>a</sup> Effector degree (number of interacting effector proteins) in EffectorK database including 23 species, not only *Xanthomonas campestris* pv. *campestris*.

**Table A.2. Putative Arabidopsis targets of T3Es from *RpsGM1000*.** Table showing the 176 identified putative targets of *RpsGM1000* T3Es with their description and degree as determined in the EffectorK database.

Accession	Gene symbol and description	Degree <sup>a</sup>	Interacting Rip(s)
ATIG04260	(MPI7) CaMV movement protein interacting protein 7	6	RipA1, RipA4, RipD, RipG4, RipG6, RipOI
ATIG05410	CDPK adapter, putative (DUF1423)	4	RipAD, RipAE, RipOI, RipVI
ATIG05960	ARM repeat superfamily protein	1	RipAJ
ATIG06390	(GSK1) GSK3/shaggy-like protein kinase 1	2	RipA3, RipS3
ATIG06510	Forkhead-associated domain protein	4	RipAE
ATIG07350	(SR45a) Serine/arginine rich-like protein 45A	6	RipA2, RipA3, RipAE, RipS3, RipVI, RipY
ATIG09660	RNA-binding KH domain-containing protein	2	RipAE, RipOI
ATIG13320	(PP2AA3) Protein phosphatase 2A subunit A3	3	RipAJ
ATIG14340	(BPL3) ACD11 binding partner, negatively regulates ROS-mediated defense response	5	RipA1, RipG4
ATIG17720	(ATB BETA) Type 2A protein serine/threonine phosphatase	1	RipAJ
ATIG20140	(SK4) SKP1-like 4	2	RipG1
ATIG22070	(TGA3) TGA1A-related gene 3	1	RipOI
ATIG22300	(GRF10) General regulatory factor 10	2	RipAE, RipAJ
ATIG22550	(NPF5.16) Tonoplast localized low affinity nitrogen transporter	1	RipAJ
ATIG22920	(CSN5A) COP9 signalosome 5A	37	RipAJ, RipOI
ATIG24590	(DRNL) Dornroschen-like	2	RipAE, RipOI
ATIG25490	(RCN1) Roots curl in NPA 1	7	RipAJ
ATIG26470	(SNS1) SNRK2 substrate 1	2	RipG5, RipOI
ATIG26660	Prefoldin chaperone subunit family protein	1	RipG1
ATIG27300	Transmembrane protein	4	RipA1
ATIG30860	RING/U-box superfamily protein	5	RipAE, RipH3, RipS3, RipVI
ATIG50710	(AUG4) HAUS augmin-like complex subunit	1	RipOI
ATIG55190	(PRA7) PRA1 (Prenylated rab acceptor) family protein	5	RipA1, RipA4, RipG6
ATIG68810	(ABS5) Basic helix-loop-helix (bHLH) DNA-binding superfamily protein	3	RipAE, RipG4, RipOI
ATIG71230	(CSN5B) COP9 signalosome 5B	8	RipAJ, RipAM, RipOI
ATIG72210	(BHLH096) Basic helix-loop-helix (bHLH) superfamily protein	4	RipAD, RipG4, RipH3, RipOI
ATIG72340	NagB/RpiA/CoA transferase-like superfamily protein	4	RipAE, RipOI, RipS3, RipVI
ATIG73030	(VPS46.2) ESCRT-related protein	1	RipH2
ATIG73500	(MKK9) MAP kinase kinase 9	1	RipG7
ATIG75950	(SKP1) S phase kinase-associated protein 1	7	RipG1, RipG5, RipG7
ATIG78300	(GRF2) General regulatory factor 2	1	RipAJ
ATIG79070	SNARE-associated protein-like protein	2	RipAK, RipP2
ATIG80040	Ubiquitin system component Cue	1	RipOI
ATIG80940	Snfl kinase interactor-like protein	2	RipAE, RipVI
AT2G03190	(SK16) SKP1-like 16	2	RipG1
AT2G05260	Alpha/beta-hydrolases superfamily protein	1	RipOI
AT2G17990	(AtCAP2) Calcium-dependent protein kinase 1 adaptor protein 2	6	RipA5, RipAD, RipAE, RipOI, RipS3, RipVI
AT2G21380	(KIN7.2) Kinesin motor family protein	3	RipAE, RipVI
AT2G23290	(MYB70) MYB domain protein 70	8	RipAD, RipAE, RipVI

AT2G23760	(BLH4) Member of the BEL family of homeodomain proteins	3	RipAE, RipAK, RipOI
AT2G25700	(SK3) SKPI-like 3	2	RipGI, RipG7
AT2G26560	(PLA2A) Phospholipase A 2A	1	RipG3
AT2G27820	(PDI) Prephenate dehydratase 1	3	RipAE, RipS3, RipVI
AT2G31070	(TCP10) TCP domain protein 10	3	RipAJ, RipOI
AT2G34090	(MEE18) Maternal effect embryo arrest 18	3	RipAE, RipAJ, RipOI
AT2G35330	(PIRI) PP2CA interacting RING finger protein 1	1	RipAJ
AT2G36410	Transcriptional activator (DUF662)	3	RipAE, RipP2, RipVI
AT2G37630	(ASI) Asymmetric leaves 1, a MYB-domain protein	2	RipAE, RipPI
AT2G39450	(MTP11) Golgi-localized manganese transporter	1	RipAI
AT2G41350	(AUG1) Augmin 1	5	RipAE
AT2G42790	(CSY3) Peroxisomal citrate synthase	4	RipAE, RipOI, RipP2, RipS3
AT2G44950	(HUB1) Histone mono-ubiquitination 1	4	RipAE
AT2G45680	(TCP9) TCP domain protein 9	15	RipAE, RipAJ, RipAK, RipAW, RipG4, RipOI, RipP2
AT2G46550	Transmembrane protein	1	RipA2
AT3G01670	(SEOA) Sieve element occlusion A	4	RipAE, RipS3
AT3G02520	(GRF7) General regulatory factor 7	2	RipAD, RipAJ
AT3G05545	RING/U-box superfamily protein	2	RipAE, RipVI
AT3G07780	(OBE1) Oberon 1	12	RipAI, RipA3, RipA4, RipA5, RipAD, RipAE, RipS3, RipVI
AT3G08530	(CHC2) Clathrin heavy chain 2	11	RipAD, RipAE
AT3G11410	(PP2CA) Protein phosphatase 2CA	3	RipAE, RipAJ, RipOI
AT3G11590	Golgin family A protein	7	RipAE, RipH2, RipS3, RipVI
AT3G12140	(EML1) EMSY-like 1	1	RipAE
AT3G12920	(BRG3) BOI-related gene 3	7	RipAI, RipAE, RipOI, RipVI
AT3G13720	(PRA8) PRA1 (Prenylated rab acceptor) family protein	6	RipAI, RipA4, RipD, RipG6
AT3G16310	Mitotic phosphoprotein N end (MPPN) family protein	3	RipAI, RipH2
AT3G17310	(DRM3) Domains Rearranged Methyltransferase3	1	RipAE
AT3G18490	(ASPG1) Aspartic protease in guard cell 1	1	RipAJ
AT3G21140	Pyridoxamine 5-phosphate oxidase family protein	3	RipAE, RipAK, RipOI
AT3G21175	(ZML1) ZIM-like 1	1	RipAJ
AT3G21330	Basic helix-loop-helix (bHLH) DNA-binding superfamily protein	2	RipH2, RipOI
AT3G21810	Zinc finger C-x8-C-x5-C-x3-H type family protein	4	RipAE, RipH3, RipS3, RipVI
AT3G22960	(PKP-ALPHA) Pyruvate kinase alpha subunit	2	RipAE, RipVI
AT3G23220	(ESE1) Ethylene and salt inducible 1	1	RipVI
AT3G25710	(BHLH32) Basic helix-loop-helix 32	4	RipAE, RipG4, RipOI
AT3G25800	(PP2AA2) Protein phosphatase 2A subunit A2	3	RipAJ
AT3G27010	(TCP20) TCP domain protein 20	7	RipOI
AT3G27960	(KLCR2) Kinesin light chain-related 2	21	RipAI, RipA2, RipA4, RipA5, RipAD, RipAE, RipG4, RipOI, RipS3, RipS6, RipVI
AT3G43590	Zinc knuckle (CCHC-type) family protein	2	RipA3, RipAE
AT3G44720	(ADT4) Arogenate dehydratase 4	3	RipAE, RipOI
AT3G48150	(APC8) Anaphase-promoting complex subunit 8	18	RipAE, RipAK, RipOI, RipS3, RipVI

AT3G48550	SHOOT GRAVITROPISM-like protein	3	RipAE, RipOI
AT3G49580	(LSU1) Response to low sulfur 1	21	RipA1, RipA2, RipA4, RipAD, RipAE, RipAV, RipAW, RipG4, RipOI, RipS3, RipVI
AT3G49760	(bZIP5) Basic leucine-zipper 5	2	RipAK, RipW
AT3G50910	Netrin receptor DCC	3	RipA1, RipVI
AT3G50940	P-loop containing nucleoside triphosphate hydrolases superfamily protein	2	RipA1, RipG6
AT3G52890	(KIPK) KCBP-interacting protein kinase	1	RipAE
AT3G54000	TIP41-like protein	3	RipAK, RipOI
AT3G54230	(SUA) Suppressor of ABI3-5	3	RipAE, RipAO
AT3G54390	Sequence-specific DNA binding transcription factor	3	RipH3, RipS3
AT3G60630	(HAM2) Hairy meristem 2	1	RipOI
AT4G00270	(GeBP) GLI enhancer binding protein	6	RipA2, RipAE, RipAX2, RipP2, RipS3, RipVI
AT4G01090	Hypothetical protein	9	RipA2, RipAE, RipS3, RipVI
AT4G02590	(UNE12) Unfertilized embryo sac 12	5	RipOI
AT4G03415	(PP2C52) Myristoylated 2C-type protein phosphatase	1	RipAJ
AT4G04020	(FIB) Fibrillin precursor protein	3	RipAJ
AT4G04890	(PDF2) Protodermal factor 2	1	RipOI
AT4G08150	(KNAT1) KNOTTED-like from Arabidopsis thaliana 1	7	RipA5, RipAE, RipOI, RipS3, RipVI
AT4G09000	(GRF1) General regulatory factor 1	1	RipAJ
AT4G09060	Hypothetical protein	3	RipAE, RipOI
AT4G10480	Nascent polypeptide-associated complex (NAC), alpha subunit family protein	1	RipH2
AT4G10750	Phosphoenolpyruvate carboxylase family protein	1	RipAE
AT4G15930	Dynein light chain type I family protein	1	RipAD
AT4G17220	(MAP70-5) Microtubule associated protein 70-5	2	RipAE
AT4G17680	SBP (S-ribonuclease binding protein) family protein	16	RipAD, RipAE, RipAK, RipOI
AT4G18910	(NIP1;2) NOD26-like intrinsic protein 1;2	1	RipAJ
AT4G19030	(NLMI) NOD26-like major intrinsic protein 1	4	RipA1
AT4G19700	(BOI) Botrytis Susceptible 1 Interactor	8	RipAE, RipAK, RipOI, RipVI
AT4G23050	PAS domain-containing protein tyrosine kinase family protein	4	RipAE, RipH3, RipOI, RipVI
AT4G23870	Hypothetical protein	1	RipAJ
AT4G24840	(COG2) Conserved oligomeric Golgi complex 2	10	RipAE, RipH3, RipOI, RipVI
AT4G25660	PPPDE putative thiol peptidase family protein	3	RipA1, RipG6, RipOI
AT4G25680	PPPDE putative thiol peptidase family protein	1	RipOI
AT4G25920	(ATDOA9) DUF295 organellar A9	2	RipAE
AT4G26455	(WIPI) WPP domain interacting protein 1	2	RipA1, RipAE
AT4G26660	Kinesin-like protein	2	RipAE
AT4G26750	(EXT-like) Extensin-like	2	RipA3, RipAO
AT4G28640	(IAA1) IAA inducible II	5	RipAE, RipVI
AT4G29780	Expression of the gene is affected by multiple stresses	1	RipAE
AT4G29790	Serine/arginine repetitive matrix protein	1	RipAW
AT4G31430	(KAKU4) Plant-specific protein that physically interacts with CRWN1 and its homolog CRWN4	1	RipA1
AT4G32190	(PIII) Protein involved in starch initiation	3	RipAE, RipG1
AT4G32570	(TIFY8) TIFY domain protein 8	3	RipAE, RipOI



AT4G35090	(CAT2) Peroxisomal catalase	2	RipAK, RipOI
AT4G36930	(SPT) Spatula, member of bHLH protein family	1	RipOI
AT4G39050	(KIN7.4) Kinesin motor family protein	10	RipAD, RipGI
AT5G02020	(SIS) Salt induced serine rich	2	RipOI
AT5G02150	(Fes1C) One of the Arabidopsis orthologs of the human Hsp70-binding protein 1 (HspBP-1)	4	RipAE, RipOI
AT5G06530	(ABCG22) ATP-binding cassette G22	1	RipAJ
AT5G06560	(MYOB7) Myosin-binding protein	2	RipAI, RipVI
AT5G06780	(EML2) EMSY-like 2	4	RipAE
AT5G07380	Hypothetical protein	1	RipP2
AT5G08070	(TCP17) TCP domain protein 17	7	RipAE, RipAJ, RipAK, RipOI
AT5G08330	(TCP21) TCP domain protein 21	7	RipAJ
AT5G13810	Glutaredoxin family protein	4	RipAE, RipOI
AT5G16550	(LDIP) LDAP interacting protein	2	RipAI, RipA5
AT5G17490	(RGL3) RGA-like protein 3	3	RipAK, RipOI
AT5G19390	(HGAP2) Protein with similarity to REN1, a Rho GTPase activating protein	4	RipAE, RipH3, RipS3, RipVI
AT5G20130	Sulfate adenylyltransferase subunit	1	RipAJ
AT5G22310	Trichohyalin-like protein	7	RipAE, RipH2, RipVI
AT5G22570	(WRKY38) WRKY DNA-binding protein 38	1	RipAE
AT5G22920	((RZPF34) RING/Zn-finger protein 34) RING ZINC-FINGER PROTEIN 34 (RZPF34)	1	RipOI
AT5G24170	Got1/Sft2-like vesicle transport protein family	1	RipAI
AT5G26720	Ubiquitin carboxyl-terminal hydrolase-like protein	4	RipAJ
AT5G26751	(SK II) SHAGGY-related kinase II	2	RipA2, RipS3
AT5G28300	(GT2L) GT-2-like protein	1	RipAE
AT5G28900	Calcium-binding EF-hand family protein	4	RipAI, RipA3, RipAK, RipOI
AT5G38110	(ASFIB) Anti-silencing function 1B	1	RipAJ
AT5G38470	(RAD23D) Raduatuib sensitive 23 D	2	RipW
AT5G38480	(GRF3) General regulatory factor 3	1	RipAJ
AT5G41410	(BEL1) Homeodomain protein required for ovule identity	3	RipAE, RipAK, RipOI
AT5G42190	(SKPIB) Similar to SKPI	7	RipGI, RipG5
AT5G42480	(ARC6) Accumulation and replication of chloroplasts 6	10	RipAI, RipAE, RipAW, RipB, RipG4, RipH2, RipH3, RipOI, RipS3
AT5G44090	Calcium-binding EF-hand family protein	1	RipA4
AT5G44160	(NUC) Nutcracker	1	RipAE
AT5G47790	SMAD/FHA domain-containing protein	1	RipAJ
AT5G48370	Thioesterase/thiol ester dehydrase-isomerase superfamily protein	6	RipAE, RipAX2, RipOI
AT5G51110	(SDIRIP1) SDIRI-interacting protein 1	3	RipOI
AT5G51440	(HSP23.5) HSP20-like chaperones superfamily protein	7	RipAE, RipAK, RipAW, RipH3, RipOI
AT5G53060	(RCF3) Regulator of CBF gene expression 3	2	RipA3, RipVI
AT5G53330	Ubiquitin-associated/translation elongation factor EF1B protein	4	RipAD, RipAE, RipS3, RipVI
AT5G53620	RNA polymerase II degradation factor	1	RipOI
AT5G55620	Hypothetical protein	1	RipG7
AT5G56140	RNA-binding KH domain-containing protein	2	RipAE, RipVI
AT5G57210	Ypt/Rab-GAP domain of gyp1p superfamily protein	4	RipAE, RipOI
AT5G58690	(PLC5) Phosphatidylinositol-specific phospholipase C5	1	RipAJ

AT5G58720	SMR (Small MutS Related) domain-containing protein	5	RipAE, RipV1
AT5G58960	(GIL1) Gravitropic in the light 1	3	RipAE, RipS3, RipV1
AT5G59210	Myosin heavy chain-like protein	1	RipAE
AT5G59610	(DJC73) Chaperone DnaJ-domain superfamily protein	1	RipP2
AT5G59730	(EXO70H7) Exocyst subunit EXO70 family protein H7	1	RipG7
AT5G61010	(EXO70E2) Exocyst subunit EXO70 family protein E2	6	RipAD, RipAE, RipS3, RipV1
AT5G63310	(NDPK2) Nucleoside diphosphate kinase 2	1	RipH3
AT5G63510	(GAMMA CAL1) Gamma carbonic anhydrase-like protein 1	1	RipG7
AT5G65410	(HB25) Homeobox protein 25	1	RipAJ
AT5G66480	Bacteriophage N4 adsorption B protein	5	RipAI, RipVI
AT5G66770	GRAS family transcription factor	1	RipOI

---

<sup>a</sup> Effector degree (number of interacting effector proteins) in EffectorK database including 23 species, not only *Ralstonia pseudosolanacearum*.

**Table A.3. Putative targets of orthologous T3Es from *Xcc8004* and *RpsGM11000*.** For each T3E from the set of orthologs between *Xcc8004* and *RpsGM11000*, the number of identified targets (if any) is presented. Common targets of both members of each orthologous groups are also indicated.

Accession	Gene symbol	Mutant line	Given name	Origin
AT1G13320	PP2AA3	SALK_014113	MGF316	A. Delong (Brown University)
AT1G13320	PP2AA3	SALK_099550	MGF318	A. Delong (Brown University)
AT1G22920	CSN5A	SALK_063436	MGF323	V. Decroocq (BFP, Bordeaux)
AT1G22920	CSN5A	SALK_027705	MGF336	V. Decroocq (BFP, Bordeaux)
AT1G25490	RCN1	SALK_059903	MGF309	A. Delong (Brown University)
AT1G25490	RCN1	SALK_059903	MGF358	NASC
AT1G71230	CSN5B	SALK_007134	MGF327	V. Decroocq (BFP, Bordeaux)
AT1G71230	CSN5B	SALK_007134	MGF349	NASC
AT2G45680	TCP9	SALK_143587	MGF241	R. Immink (Wageningen University)
AT2G45680	TCP9	WiscDsLox384D1	MGF301	NASC
AT2G45680	TCP9	SALK_035853	MGF376	NASC
AT3G08530	CHC2	SAIL_601_A09	MGF452	R. Berthomé (LIPM, Toulouse)
AT3G08530	CHC2	SAIL_720_D10	MGF453	R. Berthomé (LIPM, Toulouse)
AT3G12920	BRG3	GK-661B07.01	MGF346	NASC
AT3G12920	BRG3	SAIL_261_G05	MGF362	NASC
AT3G12920	BRG3	SAIL_302_F07	MGF366	NASC
AT3G25800	PP2AA2	SALK_037095	MGF311	A. Delong (Brown University)
AT3G25800	PP2AA2	SALK_042724	MGF371	A. Delong (Brown University)
AT3G27960	KLCR2	SALK_142719	MGF283	NASC
AT3G27960	KLCR2	SALK_148296	MGF354	NASC
AT3G54000	-	WiscDsLox247H12	MGF294	NASC
AT4G01090	-	SALK_087137	MGF280	NASC
AT4G09060	-	SALK_143698	MGF284	NASC
AT4G09060	-	SAIL_134_D02	MGF286	NASC
AT4G17680	-	SAIL_1281_C06	MGF291	NASC
AT4G17680	-	SAIL_420_E12	MGF341	NASC
AT4G26660	-	SALK_025234	MGF262	NASC
AT4G26660	-	SALK_086971	MGF268	NASC
AT5G02020	SIS	SALK_064028	MGF249	A. Polle (Gottingen University)
AT5G02020	SIS	SALK_040413	MGF370	NASC
AT5G08070	TCPI7	SALK_148580	MGF274	NASC
AT5G08070	TCPI7	SALK_147288	MGF360	NASC
AT5G26720	-	SALK_022204	MGF255	NASC
AT5G51110	SDIRIP1	GK-453C08.01	MGF254	NASC
AT5G51440	HSP23.5	SALK_118536	MGF271	NASC

**Table A.4. List of bacterial strains used in this study.** List of bacterial strains used in this study with the internal collection code, description and resistance marker classified by experimental use.

Code	Description	Species <sup>a</sup>	Strain	Resistance <sup>b</sup>
<b>Pathogenicity assays</b>				
MC40	WT	<i>Xcc</i>	8004	Rif
MC44	$\Delta xopAC$	<i>Xcc</i>	8004	Rif
LNL996	$\Delta xopAG$	<i>Xcc</i>	8004	Rif
LNL645	$\Delta xopQ$	<i>Xcc</i>	8004	Rif
LNL812	$\Delta xopP$ - <i>xopALl</i>	<i>Xcc</i>	8004	Rif
LNL649	$\Delta xopAM$	<i>Xcc</i>	8004	Rif
EG67	$\Delta xopG$	<i>Xcc</i>	8004	Rif
MGF172	$\Delta hrpW$	<i>Xcc</i>	8004	Rif
MGF170	$\Delta xopAG\Delta xopQ\Delta xopP\Delta xopAM\Delta xopG\Delta hrpW$	<i>Xcc</i>	8004	Rif
MGF195	$\Delta xopAG\Delta xopAG$	<i>Xcc</i>	8004	Rif
MGF284	$\Delta xopAG\Delta xopAG::xopAG$	<i>Xcc</i>	8004	Rif
GM11000	WT	<i>Rps</i>	GM11000	-
GRS174	$\Delta ripOI$	<i>Rps</i>	GM11000	Gm
<b>Generation of transgenic Arabidopsis lines</b>				
LNI310	pER8- <i>hrpW</i>	<i>Atu</i>	GV3101	Rif/Gm/Spc
LNI313	pER8- <i>xopAG</i>	<i>Atu</i>	GV3101	Rif/Gm/Spc
LNI317	pER8- <i>xopAM</i>	<i>Atu</i>	GV3101	Rif/Gm/Spc
LNI257	pER8- <i>xopG</i>	<i>Atu</i>	GV3101	Rif/Gm/Spc
LNI263	pER8- <i>xopP</i>	<i>Atu</i>	GV3101	Rif/Gm/Spc
LNI264	pER8- <i>xopQ</i>	<i>Atu</i>	GV3101	Rif/Gm/Spc
MGF149	pER8- <i>xopJ6</i>	<i>Atu</i>	GV3101	Rif/Gm/Spc
MGF30	pER8- <i>ripAXI</i>	<i>Atu</i>	GV3101	Rif/Gm/Spc
MGF32	pER8- <i>ripAX2</i>	<i>Atu</i>	GV3101	Rif/Gm/Spc
MGF34	pER8- <i>ripB</i>	<i>Atu</i>	GV3101	Rif/Gm/Spc
MGF36	pER8- <i>ripHI</i>	<i>Atu</i>	GV3101	Rif/Gm/Spc
MGF38	pER8- <i>ripH2</i>	<i>Atu</i>	GV3101	Rif/Gm/Spc
MGF40	pER8- <i>ripH3</i>	<i>Atu</i>	GV3101	Rif/Gm/Spc
MGF42	pER8- <i>ripOI</i>	<i>Atu</i>	GV3101	Rif/Gm/Spc
MGF44	pER8- <i>ripR</i>	<i>Atu</i>	GV3101	Rif/Gm/Spc
MGF46	pER8- <i>ripW</i>	<i>Atu</i>	GV3101	Rif/Gm/Spc
<b>ROS burst measurement</b>				
NPI20	pMDC43- <i>RanBPI</i>	<i>Atu</i>	GV3101	Rif/Tc/Kan
MGF188	pMDC43- <i>xopP</i>	<i>Atu</i>	GV3101	Rif/Tc/Kan
MGF182	pMDC43- <i>xopAG</i>	<i>Atu</i>	GV3101	Rif/Tc/Kan
MGF186	pMDC43- <i>ripOI</i>	<i>Atu</i>	GV3101	Rif/Tc/Kan
MGF184	pMDC43- <i>xopJ6</i>	<i>Atu</i>	GV3101	Rif/Tc/Kan
<b>Microscopy</b>				
MGF249	pBIN- <i>xopAG</i> -CFP	<i>Atu</i>	C58	Tc/Kan
MGF241	pBIN- <i>xopAG</i> -YFP	<i>Atu</i>	C58	Tc/Kan
MGF244	pBIN- <i>ripOI</i> -CFP	<i>Atu</i>	C58	Tc/Kan
MGF242	pBIN- <i>ripOI</i> -YFP	<i>Atu</i>	C58	Tc/Kan
MGF259	pBIN- <i>BRG3</i> -CFP	<i>Atu</i>	C58	Tc/Kan
MGF257	pBIN- <i>BRG3</i> -YFP	<i>Atu</i>	C58	Tc/Kan
MGF283	pAM-PAT-35S- <i>GFP</i>	<i>Atu</i>	GV3101	Gm/Cb
<b>Regulation/translocation assays</b>				
EL308	WT	<i>Xcc</i>	CN06	Rif
MGF166	pAIO-J6	<i>Xcc</i>	CN06	Rif
MGF159	$\Delta hrpV$ pAIO-J6	<i>Xcc</i>	CN06	Rif
MGF157	<i>hrpG*</i> pAIO-J6	<i>Xcc</i>	CN06	Rif
MGF161	<i>hrpG*</i> $\Delta hrpV$ pAIO-J6	<i>Xcc</i>	CN06	Rif
MGF198	pAIO-W	<i>Xcc</i>	CN06	Rif
MGF200	$\Delta hrpV$ pAIO-W	<i>Xcc</i>	CN06	Rif
MGF202	<i>hrpG*</i> pAIO-W	<i>Xcc</i>	CN06	Rif
MC40	WT	<i>Xcc</i>	8004	Rif
LNL619	$\Delta avrBsl$	<i>Xcc</i>	8004	Rif

<sup>a</sup> *Xcc*: *X. campestris* pv. *campestris*; *Rps*: *R. pseudosolanacearum*; *Atu*: *A. tumefaciens*.

<sup>b</sup> Rif: rifampicin; Gm: gentamycin; Spc: spectinomycin; Tc: tetracycline; Kan: kanamycin; Cb: carbenicillin.

**Table A.5. List of primers used in this study.** List of primers used in this study with the internal collection code, description and sequence (5' to 3') classified by experimental use.

Code	Description	Sequence (5' to 3')
<b>Genotyping of T-DNA lines</b>		
MGF53	GABI_453C08_LP	CCCAAAAATATAGAAAAGCCAATG
MGF54	GABI_453C08_RP	TAATGTCCGGCAAATTTGAAG
MGF55	SALK_022204_LP	GAGGTCTCATCACACGAAAGC
MGF56	SALK_022204_RP	TTTTGTTTTGAGTCCAAAGGC
MGF57	SALK_025234_LP	TTTCCGTTGCAGAGTTTGAAG
MGF58	SALK_025234_RP	TGTCCTGAATTTTCGATTCGACC
MGF59	SALK_0404I3_LP	TGTACCTGCAAAATCCGAAAC
MGF60	SALK_0404I3_RP	ATTATGGAAGACCCCAACAAGC
MGF61	SALK_040760_LP	ACATTCTTCACGGTTCGTTTG
MGF62	SALK_040760_RP	CAACGTGGAACACCAAGTATCC
MGF64	LB (SALK)	ATTTTGCCGATTTCGGAAC
MGF65	SALK_08697I_LP	CGCAACTAGGAAGCTGTGATC
MGF66	SALK_08697I_RP	AAGCGAGAACAGGTTCCTAGG
MGF67	SALK_087I37_LP	GAGTGTGAGATTCAGAGCGG
MGF68	SALK_087I37_RP	CAAAGATCATCTACTTCGCGG
MGF69	SALK_142719_LP	TGCAAGTAGGGAAGAAGTCATC
MGF70	SALK_142719_RP	ACCAAGCTCAGGACTCTCCTC
MGF71	SALK_143698_LP	GGAAATGAGTGGTGAAAACATG
MGF72	SALK_143698_RP	TCAATCAAATCCCAGAAAACG
MGF73	SALK_123484_LP	TCAATCCCTCAGCCAGATATG
MGF74	SALK_123484_RP	CACCTCGAGTGTATCTTCGGC
MGF75	SALK_118536_LP	CTTCGCATCGAATCTCTCATC
MGF76	SALK_118536_RP	CCTACTCGTAACCTCCGTCC
MGF77	SALK_148580_LP	TCTTTGGATCCTCAGATCTTCC
MGF78	SALK_148580_RP	ATGTACCTTTGCTCGCATCAG
MGF79	SAIL_108_D03_LP	AGCGAGTGCAGCTCTGTTTAC
MGF80	SAIL_108_D03_RP	AAGAAGACCACCTCCAGTTCC
MGF81	SAIL_134_D02_LP	TTGAGGTGGATATCAATGGG
MGF82	SAIL_134_D02_RP	TGCTCAGCTTTAGCGAGATTG
MGF83	SAIL_128I_C06_LP	AATCCCAACCACTATGGACC
MGF84	SAIL_128I_C06_RP	AAAACGGTGATGATTGAATGG
MGF85	WiscDsLox247HI2_LP	AACAAATCAAACCTTGCCACG
MGF86	WiscDsLox247HI2_RP	ATGACATAACCATCTGCCGAG
MGF87	WiscDsLox384DI_LP	GGCGGGAAAAGCTAATAACTG
MGF88	WiscDsLox384DI_RP	CTGGACCCCATTTGTACAGATG
MGF92	LB (SAIL)	TAGCATCTGAATTTTCATAACCAATCTCGATACAC
MGF93	LB (GABI KIT)	ATATTGACCATCATACTCATTGC
MGF97	SALK_14663I_LP	ATGTGTTTGTGTCAGGAGGAG
MGF98	SALK_14663I_RP	TCAGGATCGATGTAGAGCACC
MGF99	SALK_064028_LP	TGTGGCAACTACCGACCTTAG
MGFI00	SALK_064028_RP	TCGAAATCGAAATGGAAACAG
MGFI01	SM_3_29639_LP	TGAATCTGTTTTTCTCCATCC
MGFI02	SM_3_29639_RP	CTCGAAGCAGCAAAAGATGAC
MGFI03	SM_3_2315I_LP	CAGCAAAACCTAGATTTCTTG
MGFI04	SM_3_2315I_RP	TTGTTGGTGATGTCGTATTG
MGFI05	SALK_147288_LP	TCTTTGGATCCTCAGATCTTCC
MGFI06	SALK_147288_RP	ATGTACCTTTGCTCGCATCAG
MGFI07	SALK_143587_LP	AACCTTAAAAATCCCGACGAC
MGFI08	SALK_143587_RP	GGACCATGACTTAGAGAGGGC
MGFI09	SALK_016203_LP	AAATTTCTTGAACCCACCACC
MGFI10	SALK_016203_RP	CCACCTGCAAGTTCAAACAAC
MGFI12	SALK_0141I3_LP	TATTTCCAAACTTTGGGGGAC
MGFI13	SALK_0141I3_RP	ATGGACACAGCTTGAAGATGG
MGFI14	SALK_099550_LP	GCACCAAGCTTCTCATCAAAG
MGFI15	SALK_099550_RP	GACCGAGCCAACTAGGTAAG
MGFI16	SALK_063436_LP	CCCTCCCAAGTTTAAATCG
MGFI17	SALK_063436_RP	ATGCCAAATCTATGTGTGCC
MGFI18	SALK_027705_LP	ACGATGTAATCATGGGCTCTG
MGFI19	SALK_027705_RP	TCACCTTCTGGATCTCCTTTG
MGFI20	GABI_444C0I_LP	AGACTTTGAACGATCCTCGTG
MGFI21	GABI_444C0I_RP	CTGTGGCTCCTTCTGATCTTG
MGFI22	SALK_027705_LP	ACGATGTAATCATGGGCTCTG
MGFI23	SALK_027705_RP	TCACCTTCTGGATCTCCTTTG
MGFI24	SALK_059903_LP	GCACAAATCCTATTGGCTTG
MGFI25	SALK_059903_RP	AGTTAGAACCATGGAACGCAC

MGFI26	SALK_059903_LP	GCACAAATCCTATTTGGCTTG
MGFI27	SALK_059903_RP	AGTTAGAACCATGGAACGCAC
MGFI28	SAIL_656_FII_LP	TGGATTGTAATGAGCTGTCCC
MGFI29	SAIL_656_FII_RP	TTGAAGCTGATGATGAACCC
MGFI30	SALK_007134_LP	AATCCCCGAAGTAACATTTTTG
MGFI31	SALK_007134_RP	CATTACCCAGCAGTGGAGAAAG
MGFI32	SALK_035853_LP	TGTGACCGGTTTAATCAAAGG
MGFI33	SALK_035853_RP	TTCTTCAACCTTCGTGTGAC
MGFI34	GABI_661B07_LP	AACCAACGATACAGTCCGTTG
MGFI35	GABI_661B07_RP	GGAAATGACATTGAAAGTGGG
MGFI36	SAIL_261_G05_LP	TTGGCAGACAAGAGTGTGTTG
MGFI37	SAIL_261_G05_RP	GCTAACTTCCACCGTTCTTCC
MGFI38	SAIL_302_F07_LP	AACCAACGATACAGTCCGTTG
MGFI39	SAIL_302_F07_RP	TCGTGTTCCATCATCATCATC
MGFI40	SALK_042724_LP	CGATGTTACGTGCCCTCTTAC
MGFI41	SALK_042724_RP	TCTACCGAATGACCATTTTGC
MGFI42	SALK_037095_LP	AGCTGCTATGCGTACTTCAGC
MGFI43	SALK_037095_RP	ATGATCGATGAGCCGTTGTAC
MGFI44	SALK_148296_LP	GTTCTTGGAGTCGGTTTTAGG
MGFI45	SALK_148296_RP	GTCCAGGCGGAGTTTATTTTC
MGFI46	SAIL_420_EI2_LP	TCGCAAAAATAGAATCATATAAAGATG
MGFI47	SAIL_420_EI2_RP	AAGAAGCGGAGTTGGAGAAAG
MGFI48	SALK_147288_LP	TCCTTGGATCCTCAGATCTTCC
MGFI49	SALK_147288_RP	ATGTACCTTTGCTCGCATCAG
MGFI50	SALK_026434_LP	TCAGCTAGGAAGTTAGCTGCG
MGFI51	SALK_026434_RP	AATGCTCAAAGAAACATCCCC
MGFI52	SALK_059068_LP	TTTCTCAACCATCACTCTCGC
MGFI53	SALK_059068_RP	ATGCTAAATCTGGCAATGGAC
MGFI54	SALK_035853_LP	TGTGACCGGTTTAATCAAAGG
MGFI55	SALK_035853_RP	TTCTTCAACCTTCGTGTGAC
MGFI56	SALK_044149_LP	CTAGCATGTCCCTCGTCTCTG
MGFI57	SALK_044149_RP	ACCCGAGAGGATATGGTGATC
MGFI58	SALK_066339_LP	TTCCGGTTTCACTTTTTTCATG
MGFI59	SALK_066339_RP	TGAGGATCCGTCGATATCTTG
MGFI60	SALK_098769_LP	TACAAGTTTGCGAATCCAAC
MGFI61	SALK_098769_RP	ATTCCAATTCTCGCTTACC
MGFI62	SALK_024167_LP	GCTTGTGTAAAATCGTTGGG
MGFI63	SALK_024167_RP	AAATAGCAGAGATTGCCTCCC
MGFI64	SALK_114731_LP	CTTGGCTTCAACACCAGTCTC
MGFI65	SALK_114731_RP	CACACCACATCAGAATTGGTG
MGFI66	SALK_024983_LP	TCACCTCCAATTCATTCCAAG
MGFI67	SALK_024983_RP	AGGAGAAGCGGAGGTTGATAG
MGFI68	SALK_131837_LP	TTTAAACCAATCGAGTGTGCC
MGFI69	SALK_131837_RP	ACCTGGTAGAAATCAATGGGG
MGFI70	SAIL_580_C03_LP	ACCATAGTCATCTGCCACCTG
MGFI71	SAIL_580_C03_RP	TGCTGAGTCACTTTTGACACG
MGFI72	WiscDsLox319F06_LP	CTTTCTTTCCCTTTTTGGGTG
MGFI73	WiscDsLox319F06_RP	TGAGGATCCGTCGATATCTTG
MGFI74	SAIL_177_G12_LP	CGCCACTGAAACTGAGAAAAG
MGFI75	SAIL_177_G12_RP	TAGTGAGTTCATAATGGCGG
MGFI76	SAIL_693_G04_LP	ATCAGCAACGGACATTTCAC
MGFI77	SAIL_693_G04_RP	TAAATGGTTTAAAGCGGTGTGC
<b>Genotyping of pER8-T3E lines</b>		
LNL370	pER8- <i>hrpW</i> -Fw	TTTGGTCTCAAGGTATGCTGACGTACTGCATGCAAC
LNL371	pER8- <i>hrpW</i> -Rv	TTTGGTCTCACATACACCATCGGGGCAGGGCCTCAC
LNL448	pER8- <i>xopAG</i> -Fw	TTTGGTCTCAAGGTGTGGCAGACAACTTCTTTCTTTTC
LNL449	pER8- <i>xopAG</i> -Rv	TTTGGTCTCACATACCTTGAGGCAGGCAAGGTTGGTG
LNL412	pER8- <i>xopAM</i> -Fw	TTTGGTCTCAAGGTATGACCTTACCGGATTCGATC
LNL413	pER8- <i>xopAM</i> -Rv	TTTGGTCTCACATACCCGACGCGCCAGACACGCCTC
LNL396	pER8- <i>xopG</i> -Fw	TTTGGTCTCAAGGTGTGAATCGGAGCCCTGGTGTG
LNL397	pER8- <i>xopG</i> -Rv	TTTGGTCTCACATACACCATTTCTCCGCACGAATAC
MGF32	pER8- <i>xopJ6</i> -Fw	TTTGGTCTCAAGGTATGACAGACTGGACAAACTATCG
MGF33	pER8- <i>xopJ6</i> -Rv	TTTGGTCTCACATACCCGAGGAGCAAAAGGCTCATTTTGC
LNL408	pER8- <i>xopP</i> -Fw	TTTGGTCTCAAGGTATGCATCGTGTGCAATGATC
LNL409	pER8- <i>xopP</i> -Rv	TTTGGTCTCACATACCTTGGCCTTGCTAAGCGCTTTTC
LNL410	pER8- <i>xopQ</i> -Fw	TTTGGTCTCAAGGTATGGATTCCATCAGGCATCG
LNL411	pER8- <i>xopQ</i> -Rv	TTTGGTCTCACATACACTGAGCTCCCGCAGCACCGCTG
MGFI0	pER8- <i>ripAXI</i> -Fw	AAGCGCTCGACATCATCAAC
MGFI1	pER8- <i>ripAXI</i> -Rv	AGGTCATGCTGCTGTGACTC
MGFI2	pER8- <i>ripAX2</i> -Fw	ATGCGGGCAAAGTAAACGAG
MGFI3	pER8- <i>ripAX2</i> -Rv	TGATGCTGGTCTTGGGGTTC

MGF14	pER8- <i>ripB</i> -Fw	GAAGGACCACGCCAAGTTCC
MGF15	pER8- <i>ripB</i> -Rv	GCGAAATCGGTCGTGTTGTTG
MGF16	pER8- <i>ripHI</i> -Fw	GCTTGGCTTGCTGAGTTTAC
MGF17	pER8- <i>ripHI</i> -Rv	AACGTCAGCCTCCATAGCTG
MGF18	pER8- <i>ripH2</i> -Fw	ACTGACGCAACAGAGGCTAC
MGF19	pER8- <i>ripH2</i> -Rv	CCACCACAGCAGCAGATGTC
MGF20	pER8- <i>ripH3</i> -Fw	GTCTGGACCAGCAGAGGAAG
MGF21	pER8- <i>ripH3</i> -Rv	CCCCTCTAGCAACCACTCC
MGF22	pER8- <i>ripOI</i> -Fw	ACACGATCGCCAACCATTTT
MGF23	pER8- <i>ripOI</i> -Rv	GGCACTGAACGTTGTTTCGAC
MGF28	pER8- <i>ripR</i> -Fw	ATTCAACATCCCGAATTCCG
MGF29	pER8- <i>ripR</i> -Rv	CAGATCTCGGTCAGGCGATAC
MGF26	pER8- <i>ripW</i> -Fw	ACGCCCAAAGTGGAGATCAC
MGF27	pER8- <i>ripW</i> -Rv	GACTTGGCTCTTGTCGGGAG
<b>qRT-PCR</b>		
MGF43	<i>OXA1</i> -Fw	TACCTGATCTGCCTCCACCT
MGF44	<i>OXA1</i> -Rv	AACAGGACTCAGCGATGTTG
MGF47	<i>GAPC2</i> -Fw	AGGTCAAGCATTTTCGATGC
MGF48	<i>GAPC2</i> -Rv	AACGATAAGGTCAACGACACG
MGF40	<i>xopAG</i> -Fw	TCAAGCGTGCGTGGTTGATGC
MGF41	<i>xopAG</i> -Rv	GCAGACTTCATGGAGATGGCG
MGF51	<i>ripOI</i> -Fw	TCGGTCAATCCCTTCAGGCTG
MGF23	<i>ripOI</i> -Rv	GGCACTGAACGTTGTTTCGAC
MGF231	<i>ripHI</i> -Fw	GGCTGCTGGTCCATCTGTTT
MGF232	<i>ripHI</i> -Rv	CAACGATGTCAACCAAGCTG
MGF49	<i>ripH2</i> -Fw	GTGCCAGTTGACTCAGAGAC
MGF19	<i>ripH2</i> -Rv	CCACCACAGCAGCAGATGTC
MGF50	<i>ripH3</i> -Fw	GCTATGCAGACAGCTCATGG
MGF21	<i>ripH3</i> -Rv	CCCCTCTAGCAACCACTCC
LNL370	<i>hrpW</i> -Fw	GCTGACGTACTGCATGCAAC
LNL371	<i>hrpW</i> -Rv	ACCATCGGGGCAGGGCCTCAC
LNL396	<i>xopG</i> -Fw	TGAAGTGGAGCCCTGGTGTG
LNL697	<i>xopG</i> -Rv	ACCATTCTCCGCACGAATAC
MGF38	<i>xopP</i> -Fw	GTGTACGAACCATGGCGCAG
MGF39	<i>xopP</i> -Rv	GCTGAAGATGAGCGAGGTTGC
MGF36	<i>xopQ</i> -Fw	CCATGGCCTTCGACCAGATC
MGF37	<i>xopQ</i> -Rv	TCACCTGCTCCACAACGCTG
I6SL (EL)	<i>I6S</i> -Fw	TGACGGTACCCAAGAATAAGCA
I6SR (EL)	<i>I6S</i> -Rv	ACGCTTGACCCCTTCGTATTA
J6F (EL)	<i>xopJ6</i> -Fw	GTGGAGGAAAGACGAGACAGC
J6R (EL)	<i>xopJ6</i> -Rv	CAGTGCAGAGACATGGAAA
<b>Clonings</b>		
MGF229	AttB1- <i>BRG3</i>	GGGGACAAGTTTGTACAAAAAAGCAGGCTTCATGGCCGTTGAAGCTCACC
MGF230	AttB2- <i>BRG3</i> (no stop codon)	GGGGACCACTTTGTACAAAGAAAGCTGGGTGAGAGGAAAGATTAAACATGTAGAC
MGF3	Deletion of <i>xopP</i> - L fragment - 1F	TTTGGTCTCAAGGTGTGCGCTGGCTGCATCGATCG
MGF4	Deletion of <i>xopP</i> - L fragment - 2R	TTTGGTCTCACATAAGGAAAGCTCCAGAAATTGCG
MGF5	Deletion of <i>xopP</i> - R fragment - 2F	TTTGGTCTCATATGTGTTTCGCTGCGCTCTATTGAC
MGF6	Deletion of <i>xopP</i> - R fragment - 3R	TTTGGTCTCACTTGAAGCGAGTTAATCGACCGTGC
MGF7	Deletion of <i>xopP</i> - internal F	GTGGGATGCATTATCCGTCGACG
LN334	Deletion of <i>hrpW</i> - R fragment - 1F	TTTGGTCTCAAGGTAGCAAGTTCCGGAAGAAGAAG
LN335	Deletion of <i>hrpW</i> - R fragment - 2R	TTTGGTCTCACATAGCTCATGATCACC GCGGTCAG
MGF8	Deletion of <i>hrpW</i> - R fragment - 2F	TTTGGTCTCATATGCTGCACATCGCGTACTACGTC
MGF9	Deletion of <i>hrpW</i> - R fragment - 3R	TTTGGTCTCACTTGATCGAACGCACGCTTCAG
LN338	Deletion of <i>hrpW</i> - internal F	CGCAGCCTTGCGTCTCCGCTGTG
MGF32	<i>xopJ6</i> (1-300) flanked by BsaI sites - Fw	TTTGGTCTCAAGGTATGACAGACTGGACAAACTATCG
MGF33	<i>xopJ6</i> (1-300) flanked by BsaI sites - Rv	TTTGGTCTCACATACCGGAGGAGCAAAGGCTCATTTTGC
MGF214	563bp upstream <i>xopAG</i> + BamHI site	CGGAGGATCCCTGCAGCACACACCTGGATCG
MGF215	100bp downstream <i>xopAG</i> + HindIII site	GCCTAAGCTTCCAGGAAAAGGTGCCTAAAGACG

The time between the writing of the present thesis and its defense was extraordinarily extended because of the strict confinement measures imposed due to the COVID19 pandemics. During this extension, two articles were written: a review about the functions of *Ralstonia solanacearum* T3Es and an opinion piece about the collective action of effectors. Both articles are included in the present thesis as the following two annexes.

## **ANNEX 1: The large, diverse, and robust arsenal of *Ralstonia solanacearum* type III effectors and their in planta functions**

This review compiles all the available functional information about RSSC T3Es. My contribution was the compilation of the data together with David Landry, with whom I share the first authorship, redaction of the article and proof after its acceptance. It was published as a microreview in *Molecular Plant Pathology* (submission date: 28/04/2020; acceptance date: 22/06/2020). The review, as published (doi: 10.1111/mpp.12977), is attached.



# The large, diverse, and robust arsenal of *Ralstonia solanacearum* type III effectors and their in planta functions

David Landry  | Manuel González-Fuente  | Laurent Deslandes  | Nemo Peeters 

Laboratoire des Interactions Plantes Micro-organismes (LIPM), INRAE, CNRS, Université de Toulouse, Castanet-Tolosan, France

## Correspondence

Nemo Peeters, Laboratoire des Interactions Plantes Micro-organismes (LIPM), INRAE, CNRS, Université de Toulouse, F-31326 Castanet-Tolosan, France.  
Email: nemo.peeters@inrae.fr

## Funding information

Agence Nationale de la Recherche, Grant/Award Number: ANR-10-LABX-41 and ANR-11-IDEX-0002-02

## Abstract

The type III secretion system with its delivered type III effectors (T3Es) is one of the main virulence determinants of *Ralstonia solanacearum*, a worldwide devastating plant pathogenic bacterium affecting many crop species. The pan-effectome of the *R. solanacearum* species complex has been exhaustively identified and is composed of more than 100 different T3Es. Among the reported strains, their content ranges from 45 to 76 T3Es. This considerably large and varied effectome could be considered one of the factors contributing to the wide host range of *R. solanacearum*. In order to understand how *R. solanacearum* uses its T3Es to subvert the host cellular processes, many functional studies have been conducted over the last three decades. It has been shown that *R. solanacearum* effectors, as those from other plant pathogens, can suppress plant defence mechanisms, modulate the host metabolism, or avoid bacterial recognition through a wide variety of molecular mechanisms. *R. solanacearum* T3Es can also be perceived by the plant and trigger immune responses. To date, the molecular mechanisms employed by *R. solanacearum* T3Es to modulate these host processes have been described for a growing number of T3Es, although they remain unknown for the majority of them. In this microreview, we summarize and discuss the current knowledge on the characterized *R. solanacearum* species complex T3Es.

## KEYWORDS

effectome, immunity, *Ralstonia solanacearum*, susceptibility, targets, type III effectors, virulence

## 1 | INTRODUCTION

Bacteria from the *Ralstonia solanacearum* species complex (RSSC) are soilborne plant pathogens responsible for bacterial wilt on more than 250 species, moko and blood diseases of banana, brown rot of potato, and Sumatra disease on clove trees (Peeters *et al.*, 2013a). Due to its aggressiveness, broad host range, widespread

geographical distribution, and long-lasting persistence on the soil, *Ralstonia* ranks among the most devastating plant pathogenic bacteria (Mansfield *et al.*, 2012). For a successful infection, RSSC bacteria rely on different virulence determinants, including the production of exopolysaccharides and phytohormones, secretion of cell wall-degrading enzymes, detoxification, and nutrient-scavenging systems and motility (Genin and Denny, 2012). However, the main virulence

David Landry and Manuel González-Fuente contributed equally to this work.

This is an open access article under the terms of the Creative Commons Attribution License, which permits use, distribution and reproduction in any medium, provided the original work is properly cited.

© 2020 The Authors. *Molecular Plant Pathology* published by British Society for Plant Pathology and John Wiley & Sons Ltd

determinant of RSSC bacteria is the type III secretion system (T3SS), a “molecular syringe” that allows the translocation of several type III effector proteins (T3Es) directly into the host cell (Coll and Valls, 2013). These T3Es, referred to as *Ralstonia* injected proteins (Rips), are able to subvert the defences and modify the metabolism of the host to promote virulence.

## 2 | THE RSSC TYPE III EFFECTOME, A LARGE AND VARIED ARSENAL

Since the first RSSC T3E genes were cloned in the 1990s (Carney and Denny, 1990; Arlat *et al.*, 1994; Guéron *et al.*, 2000), different approaches have been conducted to systematically identify at the genome scale the full T3E repertoire of several RSSC strains. Two main strategies were undertaken: (a) sequence-based approaches, searching for sequence homology with previously described effector genes and/or for the presence of certain 25-nucleotide *cis* elements in their promoters, the *hrp<sub>II</sub>* box or the plant-inducible promoter (PIP) box motifs (Salanoubat *et al.*, 2002; Cunnac *et al.*, 2004a; Gabriel *et al.*, 2006; Peeters *et al.*, 2013b; Sabbagh *et al.*, 2019), and (b) regulation-based strategies, exploiting that T3E gene expression is controlled by HrpB, an AraC family member of transcriptional regulators (Genin *et al.*, 1992; Cunnac *et al.*, 2004a). Regulation-based strategies include gene expression studies (Cunnac *et al.*, 2004b; Occhialini *et al.*, 2005) and genetic screens using random transposon-insertion mutagenesis (Mukaihara *et al.*, 2004). Verification of the T3SS-dependency of the secretion or translocation is typically required to confirm the bona fide T3E status of *in silico* predicted or candidate T3Es (Lonjon *et al.*, 2018). Most translocation analyses exploit the adenylate cyclase (Cya) reporter system (Cunnac *et al.*, 2004b; Mukaihara and Tamura, 2009; Mukaihara *et al.*, 2010). T3SS-dependent secretion analyses compare the secreted proteins, detected by immunoblotting or mass spectrometry, of wild-type compared to *hrp* mutant strains (Tamura *et al.*, 2005; Solé *et al.*, 2012; Lonjon *et al.*, 2016; Sabbagh *et al.*, 2019).

A recent genomic study on 140 RSSC strains identified the pan-effectome of the species complex, consisting of 102 T3E and 16 hypothetical T3E genes (Sabbagh *et al.*, 2019). RSSC strains carry on average 64 T3E genes (minimum 45 in *R. syzygii* subsp. *syzygii* strain R24 and maximum 76 in *R. pseudosolanacearum* strain Rs-10-244). This contrasts with other plant pathogenic bacteria such as *Pseudomonas syringae* and *Xanthomonas campestris*, with an average of 31 (min. 3, max. 53) and 23 (min. 12, max. 28) T3E genes, respectively (Roux *et al.*, 2015; Dillon *et al.*, 2019). The existence of several paralog families, such as the RipG (former GALA), RipS (SKWP), RipA (AWR), RipH (HLK), or RipP (PopP) families, can be considered as a remarkable feature of the RSSC. Not a single known RSSC strain does not carry multiple copies of these paralog T3E families. This contributes to the large size of the RSSC pan-effectome. The T3E repertoires of different RSSC strains are quite diverse, with only 16 core T3Es (i.e., T3Es present in at least 95% of sequenced strains), which represents 13.6% of the RSSC pan-effectome (Sabbagh *et al.*, 2019). This core-effectome is larger than in *P. syringae* (four core T3Es, 5.7%

of its pan-effectome) or *X. campestris* (three core T3Es, 8.6% of its pan-effectome) (Roux *et al.*, 2015; Dillon *et al.*, 2019). Several studies have tried to connect the T3E diversity to the host specificity of RSSC strains (Ailloud *et al.*, 2015; Cho *et al.*, 2019; Sabbagh *et al.*, 2019). Although some host specificity determinants could be identified, the power of such studies has usually been largely limited by the lack of exhaustive strain host range empirical data.

## 3 | MANY T3ES, BUT FOR WHAT PURPOSE?

As model root and vascular plant pathogens, RSSC bacteria are among the pathogens with a larger number of functionally characterized T3Es. Some effectome-scale experiments have tried to shed light on the function of RSSC T3Es through systematic determination of their ability to induce a hypersensitive response (HR; Wroblewski *et al.*, 2009), inhibit plant defences (Nakano and Mukaihara, 2019a), or identify their plant targets (González-Fuente *et al.*, 2020). However, most of our current knowledge on effector function comes from smaller-scale experiments in which often one or a few T3Es are studied. To date, we have counted more than 50 different RSSC T3Es that have been characterized with varying degrees of detail (Figure 1 and Table 1). One of the main factors complicating this task is the observed genetic redundancy among different RSSC T3Es (Angot *et al.*, 2006; Solé *et al.*, 2012; Chen *et al.*, 2014). This redundancy is likely to ensure a more robust virulence strategy for the bacteria (Ghosh and O'Connor, 2017), although it makes the functional dissection of single effectors more complicated, particularly for the paralog families. Nevertheless, some members of these families can still have specific and nonredundant functions (Angot *et al.*, 2006; Turner *et al.*, 2009; Wang *et al.*, 2016).

Similar to other pathogens, RSSC T3Es collectively contribute to the pathogen fitness in the plant through different and not always well-characterized mechanisms (Toruño *et al.*, 2016). These include the interference with the plant basal defence responses, alteration of the plant metabolism, and avoidance of the specific recognition of other T3Es. However, some RSSC T3Es can also be recognized by specific plant genotypes and induce strong immune responses.

### 3.1 | Interference with plant basal immunity

The subversion of basal defences is one of the most studied functions of pathogen effectors. Several RSSC T3Es are known to interfere with different host cellular processes involved in these basal defence responses. RipP2 (former PopP2) relies on its acetyltransferase activity to acetylate the WRKY domain of the plant homonymous transcription factors, which prevents their association with DNA and subsequent expression of defence-related genes (Le Roux *et al.*, 2015). RipAY is selectively activated by eukaryotic thioredoxins to degrade the host glutathione, which plays an important role in plant immunity (Fujiwara *et al.*, 2016, 2020; Mukaihara *et al.*, 2016; Sang *et al.*, 2018). RipAR and RipAW rely on their E3 ubiquitin ligase

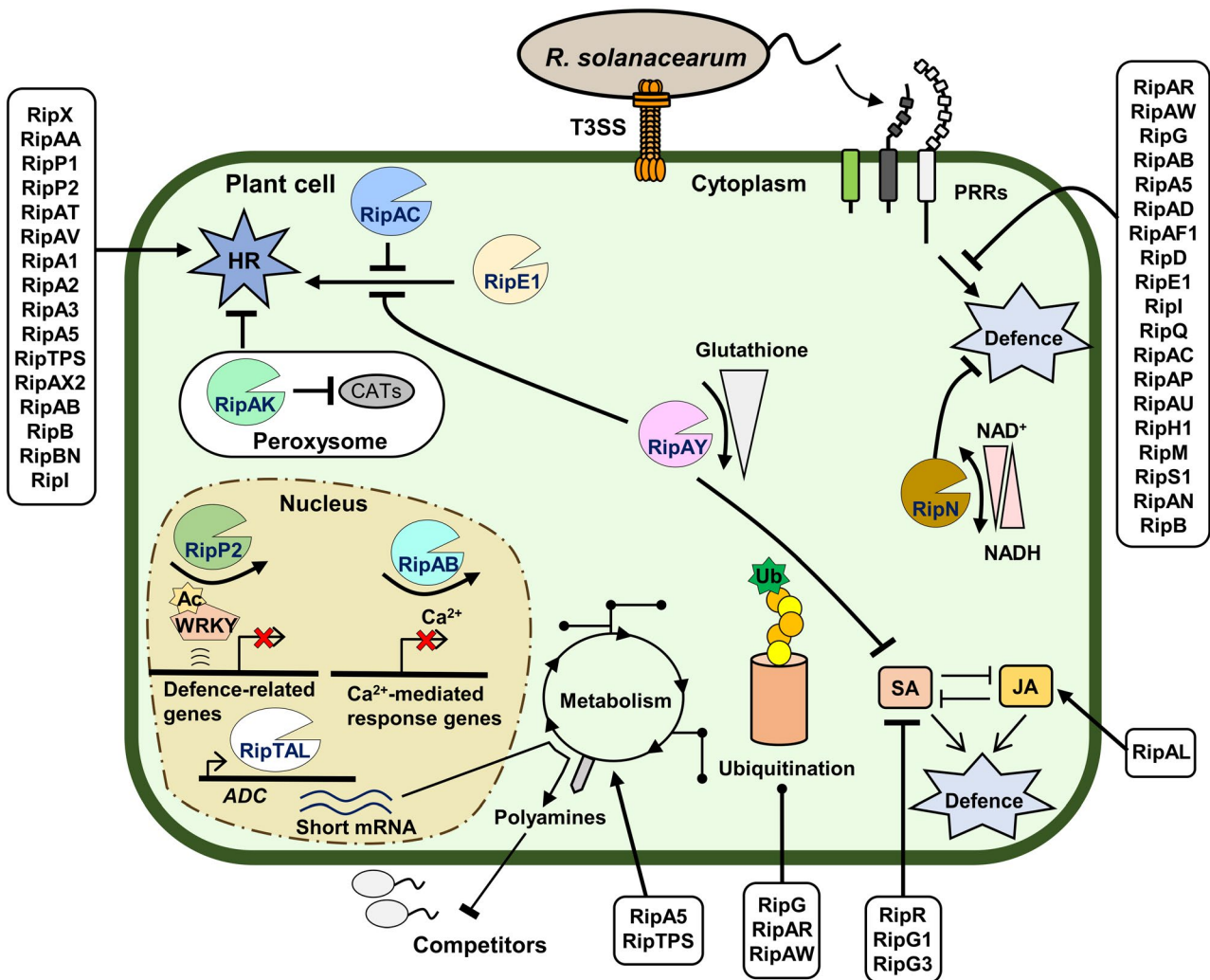


**FIGURE 1** *Ralstonia solanacearum* species complex (RSSC) bacteria deploy an arsenal of type III effectors (T3Es) to alter the plant metabolism and interfere with plant immune responses. During the infection process, conserved bacterial molecules are recognized by plant pattern recognition receptors (PRRs) at the surface of the host cell. They activate basal defence responses to prevent pathogen proliferation. However, RSSC bacteria translocate T3Es into the plant cell to subvert the plant defences and accommodate the bacterial needs. T3Es act on different host pathways. RipAY and RipN alter the glutathione level and NADH/NAD<sup>+</sup> ratio, respectively. RipAY, RipR, RipAL, RipG1, and RipG3 target the hormone synthesis and signalling level. Different RipG family members, RipAR and RipAW, interfere with ubiquitination processes. The metabolism is also manipulated by RSSC T3Es. RipA5, RipTPS, and RipTAL are able to modulate certain metabolic pathways. RipTAL binds to the plant DNA, activating the expression of shorter and more efficiently translated transcripts of *arginine decarboxylase* (ADC) genes, key enzymes in the biosynthesis of polyamines. This boost in the polyamine level could prevent the proliferation of *Ralstonia* niche competitors. RipP2 relies on its acetyltransferase activity to acetylate defensive WRKY transcription factors, inhibiting their DNA-binding activities and preventing subsequent expression of defence-related genes. The nuclear T3E RipAB inhibits the expression of Ca<sup>2+</sup>-related defence genes. In addition to these functionally characterized RSSC T3Es, other effectors involved in dampening of basal defence through as yet unknown mechanisms have been identified: RipAR, RipAW, RipG family, RipAB, RipA5, RipAD, RipAF1, RipD, RipE1, RipI, RipQ, RipAC, RipAP, RipAU, RipH1, RipM, RipS1, RipAN, and RipB. RSSC T3Es can also be perceived in planta by intracellular immune-Nod-like receptors (NLRs), leading to the activation of specific defence mechanisms, often associated with an HR. RipE1, RipAA, RipP1, RipX, RipP2, RipAT, RipAV, RipA1-A5, RipTPS, RipAX2, RipAB, RipB, RipBN, and RipI also induce HR on several hosts. Some T3Es can modulate the activity of others and prevent their recognition by the plant surveillance system. Indeed, peroxisome-localized RipAK suppresses effector-triggered HR by inhibiting host catalase activities (CATs). RipAY and RipAC inhibit RipE1-mediated HR

activity to inhibit plant defence responses (Nakano *et al.*, 2017). Also linked to ubiquitination, the RipG (former GALA) family of T3Es presents a eukaryotic F-box domain required for the interaction with *Arabidopsis* components of the Skp, Cullin, F-box containing (SCF) complex contributing to *Ralstonia* virulence (Angot *et al.*, 2006; Remigi *et al.*, 2011). RipAL is a chloroplastic effector with a

lipase domain required for the induction of jasmonic acid (JA) production and suppression of salicylic acid (SA) signalling (Nakano and Mukaiyara, 2018). The inhibition of SA-mediated defences seems also to be the role of RipR (former PopS) and RipG1 and RipG3, although the molecular mechanisms behind this inhibition still remain unknown (Jacobs *et al.*, 2013; Medina-Puche *et al.*, 2019). RipAB

**TABLE 1** List of functionally characterized *Ralstonia solanacearum* species complex type III effectors

Effector <sup>a</sup>	Functional annotation <sup>b</sup>	Homologs <sup>c</sup>	Subcellular localization	PAMP-triggered immunity inhibition <sup>d</sup>	Description	Reference(s)
RipA (AWR) family						
RipA1			Cytoplasm (RipA1 and RipA4 also plasma membrane)	(+)	Collective contribution to virulence in eggplant and tomato and negative contribution to virulence in <i>Arabidopsis thaliana</i>	Cunnac <i>et al.</i> (2004b), Solé <i>et al.</i> (2012)
RipA2			Cytoplasm and plasma membrane		Cell death in <i>Nicotiana benthamiana</i>	Solé <i>et al.</i> (2012), Jeon <i>et al.</i> (2020)
RipA4			Cytoplasm		Major contribution to virulence in tomato, eggplant and <i>Arabidopsis</i> and cell death in different <i>Nicotiana</i> spp.	Cunnac <i>et al.</i> (2004b), Solé <i>et al.</i> (2012)
RipA5			Cytoplasm	+	Cell death in <i>Nicotiana glutinosa</i>	Solé <i>et al.</i> (2012)
			Cytoplasm		Inhibition of TOR pathway in yeast and in <i>N. benthamiana</i> , negative contribution to virulence in <i>A. thaliana</i> and cell death in different <i>Nicotiana</i> spp.	Solé <i>et al.</i> (2012), Popa <i>et al.</i> (2016), Nakano and Mukaihara (2019a)
RipAA (AvrA)					Cell death in pepper and different <i>Nicotiana</i> spp., contribution to virulence in <i>Medicago truncatula</i> and bacterial fitness in tomato	Carney and Denny (1990), Robertson <i>et al.</i> (2004), Pouemyro <i>et al.</i> (2009), Turner <i>et al.</i> (2009), Wroblewski <i>et al.</i> (2009), Macho <i>et al.</i> (2010), Chen <i>et al.</i> (2018)
RipAB	Nuclear localization signal		Nucleus	+	Contribution to virulence in potato and cell death in <i>N. benthamiana</i> only when localized in the nucleus	Zheng <i>et al.</i> (2019)
RipAC (PopC)	Leucine-rich repeat domain	XopL/ XopAE (X)	Nucleus and cytoplasm	+	Contribution to virulence in <i>A. thaliana</i> and tomato and bacterial fitness in eggplant and suppression of SGT1-dependent immune response in <i>A. thaliana</i> and <i>N. benthamiana</i>	Macho <i>et al.</i> (2010), Nakano and Mukaihara (2019a), Yu <i>et al.</i> (2020)
RipAD		XopV (X)	Cytoplasm and chloroplasts	+	Inhibition of flg22-induced reactive oxygen species production in <i>N. benthamiana</i>	Jeon <i>et al.</i> (2020)
RipAF1	Putative ADP-ribosyltransferase	HopF2 (P)	Nucleus and cytoplasm	+	Contribution to bacterial fitness in eggplant and inhibition of flg22-induced reactive oxygen species production in <i>N. benthamiana</i>	Macho <i>et al.</i> (2010), Jeon <i>et al.</i> (2020)
RipAK			Peroxisomes		Contribution to bacterial fitness in eggplant and inhibition of plant catalase activity to inhibit plant defence responses in <i>A. thaliana</i> and <i>Nicotiana tabacum</i>	Macho <i>et al.</i> (2010), Sun <i>et al.</i> (2017)
RipAL	Putative lipase domain	Lipase (X)	Chloroplasts	+	Induction of jasmonic acid production to inhibit salicylic acid signalling in <i>A. thaliana</i> and pepper	Nakano and Mukaihara (2018, 2019a)

(Continues)

TABLE 1 (Continued)

Effector <sup>a</sup>	Functional annotation <sup>b</sup>	Homologs <sup>c</sup>	Subcellular localization	PAMP-triggered immunity inhibition <sup>d</sup>	Description	Reference(s)
RipAM				+	Contribution to virulence in potato	Zheng <i>et al.</i> (2019)
RipAN				+	Contribution to virulence in potato	Zheng <i>et al.</i> (2019), Nakano and Mukaihara (2019a)
RipAP	Ankyrin repeats			+	Inhibition of flg22-induced reactive oxygen species production in <i>N. benthamiana</i>	Nakano and Mukaihara (2019a)
RipAR	Ubiquitin ligase domain		Cytoplasm	+	Inhibition of PAMP-triggered immunity depending on its E3 ubiquitin ligase activity	Nakano <i>et al.</i> (2017)
RipAT					Hypersensitive response in lettuce and certain pepper and tomato cultivars	Wroblewski <i>et al.</i> (2009)
RipAU				+	Inhibition of flg22-induced reactive oxygen species production in <i>N. benthamiana</i>	Nakano and Mukaihara (2019a)
RipAV		HopAV1 (P)			Contribution to bacterial fitness in eggplant and hypersensitive response in lettuce and certain pepper and tomato cultivars	Wroblewski <i>et al.</i> (2009), Macho <i>et al.</i> (2010)
RipAW	Ubiquitin ligase domain		Cytoplasm	+	Inhibition of PAMP-triggered immunity depending on its E3 ubiquitin ligase activity	Nakano <i>et al.</i> (2017, 2019a)
RipAX2 (Rip36)	Zn-binding motif	HopH1 (P), XopG (X)			Avirulence in wild and cultivated eggplant	Nahar <i>et al.</i> (2014), Morel <i>et al.</i> (2018)
RipAY	$\gamma$ -glutamyl cyclotransferases		Nucleus and cytoplasm	+	Contribution to bacterial fitness in eggplant, depletion of glutathione in yeast, eggplant and <i>A. thaliana</i> , inhibition of salicylic acid-mediated defences in <i>A. thaliana</i> and <i>N. benthamiana</i> and suppression of RipE1-mediated hypersensitive response in <i>N. benthamiana</i>	Macho <i>et al.</i> (2010), Fujiwara <i>et al.</i> (2016, 2020), Mukaihara <i>et al.</i> (2016), Sang <i>et al.</i> (2018, 2020)
RipB	Inosine-uridine nucleoside N-ribosylhydrolase	HopQ1 (P), XopQ (X)			Roq1-mediated resistance	Nakano and Mukaihara (2019b)
RipBH		Espl2 (Sa), ShET2 (Y)			Contribution to virulence in potato	Zheng <i>et al.</i> (2019)
RipBN	Putative cysteine protease	AvrRpt2 (P)			Ptr1-mediated resistance	Mazo-molina <i>et al.</i> (2019)
RipD		HopD1 (P), XopB (X)	Endoplasmic reticulum	+	Contribution to bacterial fitness in eggplant, tomato, and bean and inhibition of flg22-induced reactive oxygen species production in <i>N. benthamiana</i>	Macho <i>et al.</i> (2010), Jeon <i>et al.</i> (2020)

(Continues)

TABLE 1 (Continued)

Effector <sup>a</sup>	Functional annotation <sup>b</sup>	Homologs <sup>c</sup>	Subcellular localization	PAMP-triggered immunity inhibition <sup>d</sup>	Description	Reference(s)
RipE1	Transglutaminase protein family	HopX1 (P), XopE (X)		+	Induction of salicylic acid and jasmonic acid synthesis to trigger immunity in <i>N. benthamiana</i> and <i>A. thaliana</i>	Nakano and Mukaihara (2019a), Sang et al. (2020)
RipF1 (PopF1)	Translocator of T3E	NopX (B/Si)			Important for the translocation of effector	Meyer et al. (2006)
RipF2 (PopF2)	Translocator of T3E	NodX (B/Si)			Important for the translocation of effector	Meyer et al. (2006)
RipG (GALA) family	F-box			(+)	Collective contribution to virulence in <i>A. thaliana</i> , tomato, and eggplant, interaction with SKP1-like proteins (except RipG3 and RipG4)	Angot et al. (2006), Remigi et al. (2011), Wang et al. (2016)
RipG1	F-box and N-myristoylation domains		Chloroplasts and plasma membrane	+	Inhibition of flg22-induced salicylic acid-dependent defence responses in <i>N. benthamiana</i> and <i>A. thaliana</i>	Medina-Puche et al. (2019)
RipG3	F-box and N-myristoylation domains		Chloroplasts	+	Inhibition of flg22-induced salicylic acid-dependent defence responses in <i>N. benthamiana</i> and <i>A. thaliana</i>	Medina-Puche et al. (2019)
RipG4	F-Box			+	Inhibition of callose deposition in <i>A. thaliana</i>	Remigi et al. (2011)
RipG7	F-Box				Essential for virulence in late stages of infection in <i>M. truncatula</i>	Angot et al. (2006), Turner et al. (2009), Wang et al. (2016)
					Interaction with <i>A. thaliana</i> ASK1, 2, 11, and 13, and <i>M. truncatula</i> MSKa	
RipH (HLK) family		XopP (X)		(+)	Collective contribution to virulence in tomato	Chen et al. (2014), Nakano and Mukaihara (2019a)
RipI			Nucleus	+	Cell death in yeast and <i>N. benthamiana</i> , through interaction with bHLH93 transcription factor, and immune responses in tomato	Deng et al. (2016), Nakano and Mukaihara (2019a), Zhuo (2020)
RipM				+	Inhibition of flg22-induced reactive oxygen species production in <i>N. benthamiana</i>	Nakano and Mukaihara (2019a)
RipN	Nudix hydrolase domain		Nucleus and endoplasmic reticulum	+	Alteration of the plant NADH/NAD <sup>+</sup> ratio and suppression of PAMP-triggered immunity defences in <i>A. thaliana</i>	Sun et al. (2019)
RipP1 (PopP1)	Putative acetyltransferase	HopZ2 (P), XopJ4 (X)			Avirulence factor in different <i>Nicotiana</i> spp. (major contribution in <i>N. glutinosa</i> ) and in <i>Petunia</i> lines	Lavie et al. (2002), Pouemyro et al. (2009), Chen et al. (2018)

(Continues)



TABLE 1 (Continued)

Effector <sup>a</sup>	Functional annotation <sup>b</sup>	Homologs <sup>c</sup>	Subcellular localization	PAMP-triggered immunity inhibition <sup>d</sup>	Description	Reference(s)
RipP2 (PopP2)	Acetyltransferase	AvrA (Sa), HopZ4 (P), VopA (V), YopJ (Y)	Nucleus	+	Acetylation of WRKY transcription factors to inhibit PAMP-triggered immunity defences and RRS1-R to induce effector-triggered immunity in <i>A. thaliana</i> , avirulence factor in eggplant and contribution to virulence in <i>A. thaliana</i> and to bacterial fitness in tomato, eggplant, and bean	Deslandes <i>et al.</i> (2003), Tasset <i>et al.</i> (2010), Macho <i>et al.</i> (2010), Le Roux <i>et al.</i> (2015), Sarris <i>et al.</i> (2015), Xiao <i>et al.</i> (2015)
RipQ		HopAA1 (P)		+	Inhibition of flg22-induced reactive oxygen species production in <i>N. benthamiana</i>	Nakano and Mukaihara (2019a)
RipR (PopS)		AvrE/ HopR1 (P), DspA/E (E), XopAM (X)			Inhibition of salicylic acid-dependent defences and contribution to virulence in <i>Solanum</i> spp. and to bacterial fitness in eggplant	Macho <i>et al.</i> (2010), Jacobs <i>et al.</i> (2013)
RipS1 (SKWP1)		XopAD (X)		+	Inhibition of flg22-induced reactive oxygen species production in <i>N. benthamiana</i>	Nakano and Mukaihara (2019a)
RipS4 (SKWP4)		XopAD (X)			Contribution to bacterial fitness in eggplant	Macho <i>et al.</i> (2010)
RipTAL (BrG11)	Transcription activator-like protein	AvrBs3/TAL family (X)	Nucleus		Specific binding on DNA from different hosts and induction of synthesis of polyamines in <i>Solanum</i> spp., possibly to inhibit the proliferation of competitors, and contribution to bacterial fitness in eggplant	Macho <i>et al.</i> (2010), de Lange <i>et al.</i> (2013), Wu <i>et al.</i> (2019)
RipTPS	Trehalose-6-phosphate-synthase	Trehalose-6-phosphate synthase (A/X)			Synthesis of trehalose-6-phosphate in yeast and enzymatic activity-independent hypersensitive response in <i>N. tabacum</i>	Pouemyro <i>et al.</i> (2014)
RipX (PopA)	Hairpin-like protein		Nucleus and plasma membrane		Hypersensitive response in <i>Petunia</i> , <i>N. tabacum</i> and <i>N. benthamiana</i> by affecting negatively the transcription of <i>atpA</i> gene for the latter and formation of ion-conducting pores in vitro	Arlat <i>et al.</i> (1994), Belbahri <i>et al.</i> (2002), Racapé <i>et al.</i> (2005), Sun <i>et al.</i> (2020)
RipY					Contribution to bacterial fitness in eggplant	Macho <i>et al.</i> (2010)

<sup>a</sup>Former name in parentheses.<sup>b</sup>Proven or putative functional annotation.<sup>c</sup>Homologs characterized in other bacterial genera. A, *Acidovorax*; B, *Bradyrhizobium*; E, *Erwinia*; P, *Pseudomonas*; Sa, *Salmonella*; Sj, *Sinorhizobium*; V, *Vibrio*; X, *Xanthomonas*; Y, *Yersinia*.<sup>d</sup>Indicated only when the ability to inhibit any classical PAMP-triggered immunity (PTI) response has been proven. In parentheses when only some members of a paralog T3E family members inhibit PTI responses.

(former PopB) down-regulates the calcium signalling pathway and inhibits the plant basal defences (Zheng *et al.*, 2019). Finally, RipN contains a Nudix hydrolase domain required to alter the NADH/NAD<sup>+</sup> ratio in planta and to inhibit the plant defence responses (Sun *et al.*, 2019).

In addition to these functionally characterized RSSC T3Es, other basal defence inhibiting T3Es have been identified in large-scale screenings. Sixteen additional RSSC T3Es have been reported as suppressors of the flg22-induced reactive oxygen species (ROS) production, a marker typically associated with pathogen-associated molecular pattern (PAMP)-triggered immunity (Sang and Macho, 2017): RipA5 (former AWR5), RipAD, RipAF1, RipD, RipE1, RipI, RipQ, RipAC (former PopC), RipAL, RipAP, and RipAU; and to a lesser extent RipH1 (former HLK1), RipM, RipS1 (former SKWP1), RipAN, and RipB (Nakano and Mukaiharu, 2019a; Jeon *et al.*, 2020).

### 3.2 | Targeting plant metabolism

Plant pathogenic bacterial T3Es can also interfere with different host metabolic processes to promote the bacterial survival, release nutrients, and facilitate the infection (Macho, 2016). RSSC bacteria thrive in the xylem, manipulating the composition of the xylem sap (Lowe-Power *et al.*, 2018). This manipulation can occur through different mechanisms, including the T3SS, as RSSC bacteria are able to inject T3Es into living cells surrounding the vasculature (Vasse *et al.*, 2000; Henry *et al.*, 2017). Indeed, some RSSC T3Es display different activities that could modulate the plant metabolism. One of the better characterized examples is RipTAL (former Brg11), which presents homology with *Xanthomonas* spp. transcription activator-like (TAL) effectors (de Lange *et al.*, 2013). RipTAL induces the expression of plant genes involved in the synthesis of polyamines, evading their native translational regulation mechanisms (Wu *et al.*, 2019). It is hypothesized that this RipTAL-induced boost of the plant polyamine levels prevents the proliferation of possible *Ralstonia* competitors (Wu *et al.*, 2019). RipA5 acts as an inhibitor of the conserved target of rapamycin (TOR) pathway in yeast and plant cells (Popa *et al.*, 2016). As a key regulator of the switch between growth and stress responses (Dobrenel *et al.*, 2016), RipA5-mediated inhibition of the plant TOR pathway leads to reduced nitrate reductase activity (Popa *et al.*, 2016). Lastly, RipTPS possesses trehalose-6-phosphate synthase activity in yeast (Poueymiro *et al.*, 2014). As trehalose-6-phosphate is a key regulatory molecule in plant metabolism (Baena-González and Lunn, 2020), RipTPS could potentially interfere with this regulation but so far this activity has not been shown in planta.

### 3.3 | Contribution to virulence through (as of yet) unknown mechanisms

In addition to the beforementioned RSSC T3Es for which functional roles could be assigned, other T3E genes have been also identified as contributors to bacterial virulence on different hosts. These

additional T3E genes have been identified through pathogenicity or competitive index assays with single or multiple gene mutants. These tests allow us to pinpoint the involvement in virulence but do not provide further information about the underlying molecular mechanisms. This is the case for RipA2 and RipD, which contribute to virulence in tomato (Cunnac *et al.*, 2004b), or RipAA and RipG7, important in the early and late stages of infection of the model legume species *Medicago truncatula*, respectively (Turner *et al.*, 2009; Wang *et al.*, 2016). RipAC, RipAF1, RipAK, RipAV, RipAY, RipD, RipP2, RipR, RipS4, RipY, and RipTAL contribute to bacterial fitness in eggplant (Macho *et al.*, 2010). For RipD and RipP2, this contribution to fitness was also demonstrated in tomato and bean, and in the case of RipAA, exclusively in tomato (Macho *et al.*, 2010). The RipA family members contribute collectively to virulence in both eggplant and tomato (Solé *et al.*, 2012), and the RipH family members also contribute to virulence in tomato (Chen *et al.*, 2014). RipAM, RipAN, and RipBH contribute significantly to virulence in potato (Zheng *et al.*, 2019), and RipAC acts similarly in tomato (Yu *et al.*, 2020).

### 3.4 | Effectors triggering plant immune responses

Through evolution, plants have evolved mechanisms to recognize specific RSSC T3Es and induce a strong defence response often associated with a hypersensitive response (HR) (Balint-Kurti, 2019). This is precisely what was observed on petunia with RipX (former PopA), the first RSSC T3E to have been characterized (Arlat *et al.*, 1994). This same phenotype was later observed in tobacco (Belbahri *et al.*, 2002; Racapé *et al.*, 2005), and could be explained by a RipX-mediated inhibition of the gene expression of the ATP synthase F1 subunit  $\alpha$  (Sun *et al.*, 2020). RipAA and RipP1 (former AvrA and PopP1, respectively) trigger strong HRs in diverse *Nicotiana* spp. (Carney and Denny, 1990; Robertson *et al.*, 2004; Poueymiro *et al.*, 2009; Chen *et al.*, 2018). Additionally, RipP1 also triggers anHR on petunia St40 line (Lavie *et al.*, 2002), and RipAA, in pepper CW300 and RNAKy accessions (Wroblewski *et al.*, 2009). RipP2 was the first RSSC T3E for which the corresponding immune receptor was identified in *Arabidopsis*: Recognition of *R. solanacearum* 1 (RRS1) (Deslandes *et al.*, 1998; Deslandes *et al.*, 2003). It was later shown that this recognition also involves the Resistance to *Pseudomonas syringae* 4 (RPS4) immune receptor (Gassmann *et al.*, 1999; Narusaka *et al.*, 2009; Williams *et al.*, 2014). The RPS4/RRS1-dependent immunity is activated by RipP2 acetylation of RRS1 C-terminal WRKY domain representing an integrated decoy that mimics RipP2 virulence targets (Tasset *et al.*, 2010; Le Roux *et al.*, 2015; Sarris *et al.*, 2015). RipAT and RipAV induce HR-like phenotypes when expressed in most lettuce and certain pepper and tomato cultivars (Wroblewski *et al.*, 2009). RipA1, RipA2, RipA3, and RipA5 trigger HRs with varying intensities on different *Nicotiana* spp. (Solé *et al.*, 2012; Jeon *et al.*, 2020). RipTPS produces an HR specifically on *N. tabacum* independently of its enzymatic activity (Poueymiro *et al.*, 2014). RipAX2 (former Rip36) elicits immunity on wild and cultivated eggplants in a Zn-finger domain-dependent (Nahar *et al.*, 2014) and



independent (Morel *et al.*, 2018) manner, respectively. RipAB triggers an HR in *N. benthamiana* but only when localized in the nucleus (Zheng *et al.*, 2019). RipB induces chlorosis in different *Nicotiana* spp. in a Recognition of XopQ1 (Roq1)-dependent manner (Nakano and Mukaihara, 2019b). RipBN triggers resistance in tomato in a *Pseudomonas tomato* race 1 (Ptr1)-dependent manner (Mazo-Molina *et al.*, 2019). RipE1 triggers immune responses mediated by both SA and JA in *N. benthamiana* and *Arabidopsis* (Sang *et al.*, 2020). RipE1 also triggers an HR in *N. tabacum* and *N. benthamiana* in a Suppressor of G2 allele of *skp1* (SGT1)-dependent manner for the latter (Jeon *et al.*, 2020). Last, RipI triggers immune responses in tomato and cell death in yeast and *N. benthamiana*, the latter through interaction with the plant basic helix-loop-helix 93 (bHLH93) transcription factor (Deng *et al.*, 2016; Zhuo *et al.*, 2020).

### 3.5 | Effectors preventing other effectors to be recognized in planta

The recognition of RSSC T3Es and subsequent strong immune responses can also be counteracted through the action of other T3Es, sometimes referred as “meta-effectors” (Kubori *et al.*, 2010). This could allow the bacteria to conserve effectors with potent virulence functions for which a given host has already developed specific recognition capabilities. This is the case for RipAY, which can inhibit the previously mentioned RipE1-triggered immunity (Sang *et al.*, 2020). RipAY inhibits RipE1-mediated activation of the SA signalling pathway probably through degradation of the plant cellular glutathione (Mukaihara *et al.*, 2016; Sang *et al.*, 2018, 2020). It has also been proposed that RipAC suppresses RipE1-triggered immunity, inhibiting in this case SGT1-mediated MAPK activation (Yu *et al.*, 2020). RipAK is able to prevent *Ralstonia*-induced HR in *N. tabacum* by inhibiting plant catalase activity (Sun *et al.*, 2017). Whether this HR is induced by RipAA, RipB, and/or RipP1, responsible for RSSC incompatibility in *N. tabacum* (Poueymiro *et al.*, 2009; Nakano and Mukaihara, 2019b), is still unknown.

## 4 | CONCLUSIONS AND PERSPECTIVES

In this microreview, we have summarized the current knowledge about RSSC T3Es. Despite being one of the largest and most studied bacterial plant pathogen effectomes, a majority of RSSC T3Es remain poorly characterized to date. This will undoubtedly change in the near future as more and more RSSC T3Es are currently being characterized by several research groups worldwide. Nevertheless, from what is currently known, we can already see that the large RSSC effectome is highly diversified in terms of molecular functions, subcellular localizations, and host-targeted processes. RSSC T3Es act in the host plasma membrane, cytoplasm, nucleus, chloroplasts, or peroxisomes, and interfere with the plant gene expression regulation at the transcriptional and translational level, metabolism, ubiquitination, phytohormone production and signalling, redox homeostasis, and calcium signalling. This functional repertoire, coupled with genetic

and functional redundancy, confers RSSC bacteria with a strong, varied, and robust set of weaponry against their hosts. It is thus tempting to hypothesize that this T3E diversity contributes to the adaptability of *Ralstonia* as a species complex to a wide range of plant hosts. It should also be noted that this large cornucopia of T3Es could be a key factor in the appearance of RSSC strains adapted to new host plants, like the recently identified strains virulent on cucurbitaceous crops (Wicker *et al.*, 2007), coffee plant (Lopes *et al.*, 2015), fig tree (Jiang *et al.*, 2016), African daisy (Weibel *et al.*, 2016), and roses (Tjou-Tam-Sin *et al.*, 2017). Future work will help to elucidate whether the so far uncharacterized T3Es target similar processes to those previously described or if, on the contrary, they interfere with completely different plant processes. This is key to understanding whether the strength of RSSC effectomes comes from its high diversity (i.e., RSSC bacteria target simultaneously many different plant processes) or from its redundancy (i.e., RSSC bacteria target a few key plant processes with redundant T3Es). The characterization of new T3Es will also allow the plant processes that RSSC bacteria specifically target to be determined to establish a successful infection. Interestingly, 9 out of the 16 RSSC core T3Es have been shown to contribute to virulence in different hosts: RipA2, RipAB, RipAM, RipAN, RipAY, RipG5, RipG6, RipH2, and RipR. From these nine T3Es, functional information is only available for five of them: RipG5 and RipG6 interact with components of the E3 ubiquitin ligase complex (Angot *et al.*, 2006; Remigi *et al.*, 2011), RipR inhibits SA-mediated defence responses (Jacobs *et al.*, 2013), RipAY degrades plant glutathione (Fujiwara *et al.*, 2016, 2020; Mukaihara *et al.*, 2016; Sang *et al.*, 2018), and RipAB down-regulates the calcium signalling pathway (Zheng *et al.*, 2019). These different processes, together with the unknown ones targeted by the other core T3Es, could represent the minimum plant processes that *Ralstonia* needs to modulate. This “basal arsenal” could be complemented with accessory T3Es that could have additive effects, targeting the same or different processes. However, this characterization might prove quite complex as these plant processes, and their modulation by *Ralstonia* T3Es, might vary substantially among different organs and host species. The diverse, and sometimes large, host range of RSSC strains and the functional diversity and redundancy of its effectome are therefore some of the causes of RSSC adaptability and aggressiveness, but also some of the major factors complicating its systematic and exhaustive study. A valuable tool that will open a wide variety of possibilities in the decipherment of RSSC T3E functions is the generation of a strain devoid of all its effectors, as has been performed on the *P. syringae* strain DC3000 (Cunnac *et al.*, 2011). This should be completed soon on the RSSC strain OE1-1 (K. Onishi, Kochi University, Japan, personal communication). The fact that RSSC bacteria can infect both model and agronomically important crop species confers a practical perspective to this information gathered over the last decades. This should certainly contribute to the design of effective and sustainable control measures against the devastating RSSC.

### ACKNOWLEDGMENTS

D.L. and M.G.F. were supported by PhD fellowships from the French Ministry of National Education and Research and the French


Laboratory of Excellence project "TULIP" (ANR-10-LABX-41; ANR-11-IDEX-0002-02), respectively. The LIPM is supported by the French Laboratory of Excellence project "TULIP" (ANR-10-LABX-41; ANR-11-IDEX-0002-02). None of the coauthors have a conflict of interest to declare. We would like to thank our colleague Stephane Genin for critically reading this work.

## DATA AVAILABILITY STATEMENT

Data sharing is not applicable to this article as no new data were created or analysed in this study.

## ORCID

David Landry  <https://orcid.org/0000-0002-6147-8580>

Manuel González-Fuente  <https://orcid.org/0000-0003-2960-2657>

Laurent Deslandes  <https://orcid.org/0000-0003-1974-5144>

Nemo Peeters  <https://orcid.org/0000-0002-1802-0769>

## REFERENCES

- Ailloud, F., Lowe, T., Cellier, G., Roche, D., Allen, C. and Prior, P. (2015) Comparative genomic analysis of *Ralstonia solanacearum* reveals candidate genes for host specificity. *BMC Genomics*, 16, 270.
- Angot, A., Peeters, N., Lechner, E., Vailleau, F., Baud, C., Gentzbittel, L. et al. (2006) *Ralstonia solanacearum* requires F-box-like domain-containing type III effectors to promote disease on several host plants. *Proceedings of the National Academy of Sciences of the United States of America*, 103, 14620–14625.
- Arlat, M., Van Gijsegem, F., Huet, J.C., Pernollet, J.C. and Boucher, C.A. (1994) PopA1, a protein which induces a hypersensitivity-like response on specific *Petunia* genotypes, is secreted via the Hrp pathway of *Pseudomonas solanacearum*. *EMBO Journal*, 13, 543–553.
- Baena-González, E. and Lunn, J.E. (2020) SnRK1 and trehalose 6-phosphate – Two ancient pathways converge to regulate plant metabolism and growth. *Current Opinion in Plant Biology*, 55, 52–59.
- Balint-Kurti, P. (2019) The plant hypersensitive response: concepts, control and consequences. *Molecular Plant Pathology*, 20, 1163–1178.
- Belbahri, L., Boucher, C., Candresse, T., Nicole, M., Ricci, P. and Keller, H. (2002) A local accumulation of the *Ralstonia solanacearum* PopA protein in transgenic tobacco renders a compatible plant–pathogen interaction incompatible. *The Plant Journal*, 28, 419–430.
- Carney, B.F. and Denny, T.P. (1990) A cloned avirulence gene from *Pseudomonas solanacearum* determines incompatibility on *Nicotiana tabacum* at the host species level. *Journal of Bacteriology*, 172, 4836–4843.
- Chen, L., Shirota, M., Zhang, Y., Kiba, A., Hikichi, Y. and Ohnishi, K. (2014) Involvement of HLK effectors in *Ralstonia solanacearum* disease development in tomato. *Journal of General Plant Pathology*, 80, 79–84.
- Chen, L., Dahal, A., Zhang, Y., Rokunuzzaman, M., Kiba, A., Hikichi, Y. et al. (2018) Involvement of avirulence genes *avrA* and *popP1* of Japanese *Ralstonia solanacearum* strains in the pathogenicity to tobacco. *Physiological and Molecular Plant Pathology*, 102, 154–162.
- Cho, H., Song, E.-S., Heu, S., Baek, J., Lee, Y.K., Lee, S. et al. (2019) Prediction of host-specific genes by pan-genome analyses of the Korean *Ralstonia solanacearum* species complex. *Frontiers in Microbiology*, 10, 506.
- Coll, N.S. and Valls, M. (2013) Current knowledge on the *Ralstonia solanacearum* type III secretion system. *Microbial Biotechnology*, 6, 614–620.
- Cunnac, S., Boucher, C. and Genin, S. (2004a) Characterization of the cis-acting regulatory element controlling HrpB-mediated activation of the Type III secretion system and effector genes in *Ralstonia solanacearum*. *Journal of Bacteriology*, 186, 2309–2318.
- Cunnac, S., Occhialini, A., Barberis, P., Boucher, C. and Genin, S. (2004b) Inventory and functional analysis of the large Hrp regulon in *Ralstonia solanacearum*: identification of novel effector proteins translocated to plant host cells through the type III secretion system. *Molecular Microbiology*, 53, 115–128.
- Cunnac, S., Chakravarthy, S., Kvitko, B.H., Russell, A.B., Martin, G.B. and Collmer, A. (2011) Genetic disassembly and combinatorial reassembly identify a minimal functional repertoire of type III effectors in *Pseudomonas syringae*. *Proceedings of the National Academy of Sciences of the United States of America*, 108, 2975–2980.
- Deng, M.-Y., Sun, Y.-H., Li, P., Fu, B., Shen, D. and Lu, Y.-J. (2016) The phytopathogenic virulent effector protein RipI induces apoptosis in budding yeast *Saccharomyces cerevisiae*. *Toxicon*, 121, 109–118.
- Deslandes, L., Pileur, F., Liaubet, L., Camut, S., Can, C. and Williams, K. et al. (1998) Genetic characterization of RRS1, a recessive locus in *Arabidopsis thaliana* that confers resistance to the bacterial soil-borne pathogen *Ralstonia solanacearum*. *Molecular Plant-Microbe Interactions*, 11, 659–667.
- Deslandes, L., Olivier, J., Peeters, N., Feng, D.X., Khounloham, M., Boucher, C. et al. (2003) Physical interaction between RRS1-R, a protein conferring resistance to bacterial wilt, and PopP2, a type III effector targeted to the plant nucleus. *Proceedings of the National Academy of Sciences of the United States of America*, 100, 8024–8029.
- Dillon, M.M., Almeida, R.N.D., Laflamme, B., Martel, A., Weir, B.S., Desveaux, D. et al. (2019) Molecular evolution of *Pseudomonas syringae* type III secreted effector proteins. *Frontiers in Plant Science*, 10, e00418.
- Dobrenel, T., Caldana, C., Hanson, J., Robaglia, C., Vincentz, M., Veit, B. et al. (2016) TOR signaling and nutrient sensing. *Annual Review of Plant Biology*, 67, 261–285.
- Fujiwara, S., Kawazoe, T., Ohnishi, K., Kitagawa, T., Popa, C., Valls, M. et al. (2016) RipAY, a plant pathogen effector protein, exhibits robust  $\gamma$ -glutamyl cyclotransferase activity when stimulated by eukaryotic thioredoxins. *Journal of Biological Chemistry*, 291, 6813–6830.
- Fujiwara, S., Ikejiri, A., Tanaka, N. and Tabuchi, M. (2020) Characterization of the mechanism of thioredoxin-dependent activation of  $\gamma$ -glutamylcyclotransferase, RipAY, from *Ralstonia solanacearum*. *Biochemical and Biophysical Research Communications*, 523, 759–765.
- Gabriel, D.W., Allen, C., Schell, M., Denny, T.P., Greenberg, J.T., Duan, Y.P. et al. (2006) Identification of open reading frames unique to a select agent: *Ralstonia solanacearum* race 3 biovar 2. *Molecular Plant-Microbe Interactions*, 19, 69–79.
- Gassmann, W., Hinsch, M.E. and Staskawicz, B.J. (1999) The *Arabidopsis* RPS4 bacterial-resistance gene is a member of the TIR-NBS-LRR family of disease-resistance genes. *The Plant Journal*, 20, 265–277.
- Genin, S. and Denny, T.P. (2012) Pathogenomics of the *Ralstonia solanacearum* species complex. *Annual Review of Phytopathology*, 50, 67–89.
- Genin, S., Gough, C.L., Zischek, C. and Boucher, C.A. (1992) Evidence that the *hrpB* gene encodes a positive regulator of pathogenicity genes from *Pseudomonas solanacearum*. *Molecular Microbiology*, 6, 3065–3076.
- Ghosh, S. and O'Connor, T.J. (2017) Beyond paralogs: the multiple layers of redundancy in bacterial pathogenesis. *Frontiers in Cellular and Infection Microbiology*, 7, 467.
- González-Fuente, M., Carrère, S., Monachello, D., Marsella, B.G., Cazalé, A.C., Zischek, C. et al. (2020) EffectorK, a comprehensive resource to mine for pathogen effector targets in the *Arabidopsis* proteome. *Molecular Plant Pathology*, [in press]. <https://doi.org/10.1111/mpp.12965>
- Gueneron, M., Timmers, A.C.J., Boucher, C. and Arlat, M. (2000) Two novel proteins, PopB, which has functional nuclear localization signals, and PopC, which has a large leucine-rich repeat domain, are secreted through the hrp-secretion apparatus of *Ralstonia solanacearum*. *Molecular Microbiology*, 36, 261–277.
- Henry, E., Toruño, T.Y., Jauneau, A., Deslandes, L. and Coaker, G. (2017) Direct and indirect visualization of bacterial effector

- delivery into diverse plant cell types during infection. *The Plant Cell*, 29, 1555–1570.
- Jacobs, J.M., Milling, A., Mitra, R.M., Hogan, C.S., Ailloud, F., Prior, P. et al. (2013) *Ralstonia solanacearum* requires PopS, an ancient AvrE-family effector, for virulence and to overcome salicylic acid-mediated defenses during tomato pathogenesis. *mBio*, 4, e00875-13.
- Jeon, H., Kim, W., Kim, B., Lee, S., Jayaraman, J., Jung, G. et al. (2020) *Ralstonia solanacearum* type III effectors with predicted nuclear localization signal localize to various cell compartments and modulate immune responses in *Nicotiana* spp. *The Plant Pathology Journal*, 36, 43–53.
- Jiang, Y., Li, B., Liu, P., Liao, F., Weng, Q. and Chen, Q. (2016) First report of bacterial wilt caused by *Ralstonia solanacearum* on fig trees in China. *Forest Pathology*, 46, 256–258.
- Kubori, T., Shinzawa, N., Kanuka, H. and Nagai, H. (2010) *Legionella* metaeffector exploits host proteasome to temporally regulate cognate effector. *PLoS Pathogens*, 6, e1001216.
- de Lange, O., Schreiber, T., Schandry, N., Radeck, J., Braun, K.H., Koszinowski, J. et al. (2013) Breaking the DNA-binding code of *Ralstonia solanacearum* TAL effectors provides new possibilities to generate plant resistance genes against bacterial wilt disease. *New Phytologist*, 199, 773–786.
- Lavie, M., Shillington, E., Eguiluz, C., Grimsley, N. and Boucher, C. (2002) PopP1, a new member of the YopJ/AvrRxv family of type III effector proteins, acts as a host-specificity factor and modulates aggressiveness of *Ralstonia solanacearum*. *Molecular Plant-Microbe Interactions*, 15, 1058–1068.
- Le Roux, C., Huet, G., Jauneau, A., Camborde, L., Trémousaygue, D., Kraut, A. et al. (2015) A receptor pair with an integrated decoy converts pathogen disabling of transcription factors to immunity. *Cell*, 161, 1074–1088.
- Lonjon, F., Turner, M., Henry, C., Rengel, D., Lohou, D., van de Kerkhove, Q. et al. (2016) Comparative secretome analysis of *Ralstonia solanacearum* type 3 secretion-associated mutants reveals a fine control of effector delivery, essential for bacterial pathogenicity. *Molecular & Cellular Proteomics*, 15, 598–613.
- Lonjon, F., Peeters, N., Genin, S. and Vailleau, F. (2018) In vitro and in vivo secretion/translocation assays to identify novel *Ralstonia solanacearum* type 3 effectors. In: Medina, C. and López-Baena, F.J. (Eds.) *Host-Pathogen Interactions. Methods and Protocols. Methods in Molecular Biology* vol. 1734. New York, NY: Springer-Link. pp. 209–222.
- Lopes, C.A., Rossato, M. and Boiteux, L.S. (2015) The host status of coffee (*Coffea arabica*) to *Ralstonia solanacearum* phylo type I isolates. *Tropical Plant Pathology*, 40, 1–4.
- Lowe-Power, T.M., Hendrich, C.G., von Roepenack-Lahaye, E., Li, B., Wu, D., Mitra, R. et al. (2018) Metabolomics of tomato xylem sap during bacterial wilt reveals *Ralstonia solanacearum* produces abundant putrescine, a metabolite that accelerates wilt disease. *Environmental Microbiology*, 20, 1330–1349.
- Macho, A.P. (2016) Subversion of plant cellular functions by bacterial type-III effectors: beyond suppression of immunity. *New Phytologist*, 210, 51–57.
- Macho, A.P., Guidot, A., Barberis, P., Beuzón, C.R. and Genin, S. (2010) A competitive index assay identifies several *Ralstonia solanacearum* type III effector mutant strains with reduced fitness in host plants. *Molecular Plant-Microbe Interactions*, 23, 1197–1205.
- Mansfield, J., Genin, S., Magori, S., Citovsky, V., Sriariyanum, M., Ronald, P. et al. (2012) Top 10 plant pathogenic bacteria in molecular plant pathology. *Molecular Plant Pathology*, 13, 614–629.
- Mazo-Molina, C., Mainiero, S., Hind, S.R., Kraus, C.M., Vachev, M., Maviane-Macia, F. et al. (2019) The *Ptr1* locus of *Solanum lycopersicoides* confers resistance to race 1 strains of *Pseudomonas syringae* pv. *tomato* and to *Ralstonia pseudosolanacearum* by recognizing the type III effectors AvrRpt2 and RipBN. *Molecular Plant-Microbe Interactions*, 32, 949–960.
- Medina-Puche, L., Tan, H., Dogra, V., Wu, M., Rosas-Díaz, T., Wang, L. et al. (2019) A novel pathway linking plasma membrane and chloroplasts is co-opted by pathogens to suppress salicylic acid-dependent defenses. *bioRxiv*. <https://doi.org/10.1101/837955> [preprint].
- Meyer, D., Cunnac, S., Guéron, M., Declercq, C., Van Gijsegem, F., Lauber, E. et al. (2006) PopF1 and PopF2, two proteins secreted by the type III protein secretion system of *Ralstonia solanacearum*, are translocators belonging to the HrpF/NopX family. *Journal of Bacteriology*, 188, 4903–4917.
- Morel, A., Guinard, J., Lonjon, F., Sujeeun, L., Barberis, P., Genin, S. et al. (2018) The eggplant AG91-25 recognizes the type III-secreted effector RipAX2 to trigger resistance to bacterial wilt (*Ralstonia solanacearum* species complex). *Molecular Plant Pathology*, 19, 2459–2472.
- Mukaihara, T. and Tamura, N. (2009) Identification of novel *Ralstonia solanacearum* type III effector proteins through translocation analysis of hrpB-regulated gene products. *Microbiology*, 155, 2235–2244.
- Mukaihara, T., Tamura, N., Murata, Y. and Iwabuchi, M. (2004) Genetic screening of Hrp type III-related pathogenicity genes controlled by the HrpB transcriptional activator in *Ralstonia solanacearum*. *Molecular Microbiology*, 54, 863–875.
- Mukaihara, T., Tamura, N. and Iwabuchi, M. (2010) Genome-wide identification of a large repertoire of *Ralstonia solanacearum* type III effector proteins by a new functional screen. *Molecular Plant-Microbe Interactions*, 23, 251–262.
- Mukaihara, T., Hatanaka, T., Nakano, M. and Oda, K. (2016) *Ralstonia solanacearum* type III effector RipAY is a glutathione-degrading enzyme that is activated by plant cytosolic thioredoxins and suppresses plant immunity. *mBio*, 7, e00359-16.
- Nahar, K., Matsumoto, I., Taguchi, F., Inagaki, Y., Yamamoto, M., Toyoda, K. et al. (2014) *Ralstonia solanacearum* type III secretion system effector Rip36 induces a hypersensitive response in the nonhost wild eggplant *Solanum torvum*. *Molecular Plant Pathology*, 15, 297–303.
- Nakano, M. and Mukaihara, T. (2018) *Ralstonia solanacearum* type III effector RipAL targets chloroplasts and induces jasmonic acid production to suppress salicylic acid-mediated defense responses in plants. *Plant & Cell Physiology*, 59, 2576–2589.
- Nakano, M. and Mukaihara, T. (2019a) Comprehensive identification of PTI suppressors in type III effector repertoire reveals that *Ralstonia solanacearum* activates jasmonate signaling at two different steps. *International Journal of Molecular Sciences*, 20, 5992.
- Nakano, M. and Mukaihara, T. (2019b) The type III effector RipB from *Ralstonia solanacearum* RS1000 acts as a major avirulence factor in *Nicotiana benthamiana* and other *Nicotiana* species. *Molecular Plant Pathology*, 20, 1237–1251.
- Nakano, M., Oda, K. and Mukaihara, T. (2017) *Ralstonia solanacearum* novel E3 ubiquitin ligase (NEL) effectors RipAW and RipAR suppress pattern-triggered immunity in plants. *Microbiology*, 163, 992–1002.
- Narusaka, M., Shirasu, K., Noutoshi, Y., Kubo, Y., Shiraiishi, T., Iwabuchi, M. et al. (2009) RRS1 and RPS4 provide a dual Resistance-gene system against fungal and bacterial pathogens. *The Plant Journal*, 60, 218–226.
- Occhialini, A., Cunnac, S., Reymond, N., Genin, S. and Boucher, C. (2005) Genome-wide analysis of gene expression in *Ralstonia solanacearum* reveals that the *hrpB* gene acts as a regulatory switch controlling multiple virulence pathways. *Molecular Plant-Microbe Interactions*, 18, 938–949.
- Peeters, N., Guidot, A., Vailleau, F. and Valls, M. (2013a) *Ralstonia solanacearum*, a widespread bacterial plant pathogen in the post-genomic era. *Molecular Plant Pathology*, 14, 651–662.
- Peeters, N., Carrère, S., Anisimova, M., Plener, L., Cazalé, A.-C. and Genin, S. (2013b) Repertoire, unified nomenclature and evolution of the type III effector gene set in the *Ralstonia solanacearum* species complex. *BMC Genomics*, 14, 859.
- Popa, C., Li, L., Gil, S., Tatjer, L., Hashii, K., Tabuchi, M. et al. (2016) The effector AWR5 from the plant pathogen *Ralstonia solanacearum* is an inhibitor of the TOR signalling pathway. *Scientific Reports*, 6, 27058.
- Poueymiro, M., Cunnac, S., Barberis, P., Deslandes, L., Peeters, N., Cazale-Noel, A.C. et al. (2009) Two type III secretion system effectors from



- Ralstonia solanacearum* GM1000 determine host-range specificity on tobacco. *Molecular Plant-Microbe Interactions*, 22, 538–550.
- Poueymiro, M., Cazalé, A.C., François, J.M., Parrou, J.L., Peeters, N. and Genin, S. (2014) A *Ralstonia solanacearum* type III effector directs the production of the plant signal metabolite trehalose-6-phosphate. *mBio*, 5, e02065-14.
- Racapé, J., Belbahri, L., Engelhardt, S., Lacombe, B., Lee, J., Lochman, J. et al. (2005) Ca<sup>2+</sup>-dependent lipid binding and membrane integration of PopA, a harpin-like elicitor of the hypersensitive response in tobacco. *Molecular Microbiology*, 58, 1406–1420.
- Remigi, P., Anisimova, M., Guidot, A., Genin, S. and Peeters, N. (2011) Functional diversification of the GALA type III effector family contributes to *Ralstonia solanacearum* adaptation on different plant hosts. *New Phytologist*, 192, 976–987.
- Robertson, A.E., Wechter, W.P., Denny, T.P., Fortnum, B.A. and Kluepfel, D.A. (2004) Relationship between avirulence gene (*avrA*) diversity in *Ralstonia solanacearum* and bacterial wilt incidence. *Molecular Plant-Microbe Interactions*, 17, 1376–1384.
- Roux, B., Bolot, S., Guy, E., Denancé, N., Lautier, M., Jardinaud, M.-F. et al. (2015) Genomics and transcriptomics of *Xanthomonas campestris* species challenge the concept of core type III effectome. *BMC Genomics*, 16, 975.
- Sabbagh, C.R.R., Carrere, S., Lonjon, F., Vailleau, F., Macho, A.P., Genin, S. et al. (2019) Pangenomic type III effector database of the plant pathogenic *Ralstonia* spp. *PeerJ*, 7, e7346.
- Salanoubat, M., Genin, S., Artiguenave, F., Gouzy, J., Mangenot, S., Arlat, M. et al. (2002) Genome sequence of the plant pathogen *Ralstonia solanacearum*. *Nature*, 415, 497–502.
- Sang, Y. and Macho, A.P. (2017) Analysis of PAMP-triggered ROS burst in plant immunity. *Methods in Molecular Biology*, 1578, 143–153.
- Sang, Y., Wang, Y., Ni, H., Cazalé, A.C., She, Y.M., Peeters, N. et al. (2018) The *Ralstonia solanacearum* type III effector RipAY targets plant redox regulators to suppress immune responses. *Molecular Plant Pathology*, 19, 129–142.
- Sang, Y., Yu, W., Zhuang, H., Wei, Y., Derevnina, L., Yu, G. et al. (2020) Intra-strain elicitation and suppression of plant immunity by *Ralstonia solanacearum* type-III effectors in *Nicotiana benthamiana*. *Plant Communications*, 1, 100025.
- Sarris, P.F., Duxbury, Z., Huh, S.U., Ma, Y., Segonzac, C., Sklenar, J. et al. (2015) A plant immune receptor detects pathogen effectors that target WRKY transcription factors. *Cell*, 161, 1089–1100.
- Solé, M., Popa, C., Mith, O., Sohn, K.H., Jones, J.D., Deslandes, L. et al. (2012) The *avr* gene family encodes a novel class of *Ralstonia solanacearum* type III effectors displaying virulence and avirulence activities. *Molecular Plant-Microbe Interactions*, 25, 941–953.
- Sun, Y., Li, P., Deng, M., Shen, D., Dai, G., Yao, N. et al. (2017) The *Ralstonia solanacearum* effector RipAK suppresses plant hypersensitive response by inhibiting the activity of host catalases. *Cellular Microbiology*, 19, e12736.
- Sun, Y., Li, P., Shen, D., Wei, Q., He, J. and Lu, Y. (2019) The *Ralstonia solanacearum* effector RipN suppresses plant PAMP-triggered immunity, localizes to the endoplasmic reticulum and nucleus, and alters the NADH/NAD<sup>+</sup> ratio in *Arabidopsis*. *Molecular Plant Pathology*, 20, 533–546.
- Sun, T., Wu, W., Wu, H., Rou, W., Zhou, Y., Zhuo, T. et al. (2020) *Ralstonia solanacearum* elicitor RipX induces defense reaction by suppressing the mitochondrial *atpA* gene in host plant. *International Journal of Molecular Sciences*, 21, 2000.
- Tamura, N., Murata, Y. and Mukaiyama, T. (2005) Isolation of *Ralstonia solanacearum* *hrpB* constitutive mutants and secretion analysis of *hrpB*-regulated gene products that share homology with known type III effectors and enzymes. *Microbiology*, 151, 2873–2884.
- Tasset, C., Bernoux, M., Jauneau, A., Pouzet, C., Brière, C., Kieffer-Jacquiod, S. et al. (2010) Autoacetylation of the *Ralstonia solanacearum* effector PopP2 targets a lysine residue essential for RRS1-R-mediated immunity in *Arabidopsis*. *PLoS Pathogens*, 6, e1001202.
- Tjou-Tam-Sin, N.N.A., van de Bilt, J.L.J., Westenberg, M., Bergsma-Vlami, M., Korpershoek, H.J., Vermunt, A.M.W. et al. (2017) First report of bacterial wilt caused by *Ralstonia solanacearum* in ornamental *Rosa* sp. *Plant Disease*, 101, 378–378.
- Toruño, T.Y., Stergiopoulos, I. and Coaker, G. (2016) Plant-pathogen effectors: cellular probes interfering with plant defenses in spatial and temporal manners. *Annual Review of Phytopathology*, 54, 419–441.
- Turner, M., Jauneau, A., Genin, S., Tavella, M.J., Vailleau, F., Gentzblatt, L. et al. (2009) Dissection of bacterial wilt on *Medicago truncatula* revealed two type III secretion system effectors acting on root infection process and disease development. *Plant Physiology*, 150, 1713–1722.
- Vasse, J., Genin, S., Frey, P., Boucher, C. and Brito, B. (2000) The *hrpB* and *hrpG* regulatory genes of *Ralstonia solanacearum* are required for different stages of the tomato root infection process. *Molecular Plant-Microbe Interactions*, 13, 259–267.
- Wang, K., Remigi, P., Anisimova, M., Lonjon, F., Kars, I., Kajava, A. et al. (2016) Functional assignment to positively selected sites in the core type III effector RipG7 from *Ralstonia solanacearum*. *Molecular Plant Pathology*, 17, 553–564.
- Weibel, J., Tran, T.M., Bocsanczy, A.M., Daughtrey, M., Norman, D.J., Mejia, L. et al. (2016) A *Ralstonia solanacearum* strain from Guatemala infects diverse flower crops, including new asymptomatic hosts vinca and sutera, and causes symptoms in geranium, Mandevilla vine, and new host African daisy (*Osteospermum ecklonis*). *Plant Health Progress*, 17, 114–121.
- Wicker, E., Grassart, L., Coranson-Beaudu, R., Mian, D., Guilbaud, C., Fegan, M. et al. (2007) *Ralstonia solanacearum* strains from Martinique (French West Indies) exhibiting a new pathogenic potential. *Applied and Environmental Microbiology*, 73, 6790–6801.
- Williams, S.J., Sohn, K.H., Wan, L., Bernoux, M., Sarris, P.F., Segonzac, C. et al. (2014) Structural basis for assembly and function of a heterodimeric plant immune receptor. *Science*, 344, 299–303.
- Wroblewski, T., Caldwell, K.S., Piskurewicz, U., Cavanaugh, K.A., Xu, H., Kozik, A. et al. (2009) Comparative large-scale analysis of interactions between several crop species and the effector repertoires from multiple pathovars of *Pseudomonas* and *Ralstonia*. *Plant Physiology*, 150, 1733–1749.
- Wu, D., von Roepenack-Lahaye, E., Buntru, M., de Lange, O., Schandry, N., Pérez-Quintero, A.L. et al. (2019) A plant pathogen type III effector protein subverts translational regulation to boost host polyamine levels. *Cell Host & Microbe*, 26, 638–649.e5.
- Xiao, X., Cao, B., Li, G., Lei, J., Chen, G., Jiang, J., Cheng, Y. (2015) Functional characterization of a putative bacterial wilt resistance gene (*RE-bw*) in eggplant. *Plant Molecular Biology Reporter*, 33, 1058–1073.
- Yu, G., Xian, L., Xue, H., Yu, W., Rufian, J., Sang, Y. et al. (2020) A bacterial effector protein prevents MAPK-mediated phosphorylation of SGT1 to suppress plant immunity. *bioRxiv*. <https://doi.org/10.1101/641241> [preprint].
- Zheng, X., Li, X., Wang, B., Cheng, D., Li, Y., Li, W. et al. (2019) A systematic screen of conserved *Ralstonia solanacearum* effectors reveals the role of RipAB, a nuclear-localized effector that suppresses immune responses in potato. *Molecular Plant Pathology*, 20, 547–561.
- Zhuo, T., Wang, X., Chen, Z., Cui, H., Zeng, Y. and Chen, Y. et al. (2020) The *Ralstonia solanacearum* effector RipI induces a defence reaction by interacting with the bHLH93 transcription factor in *Nicotiana benthamiana*. *Molecular Plant Pathology*, 21, 999–1004.

**How to cite this article:** Landry D, González-Fuente M, Deslandes L, Peeters N. The large, diverse, and robust arsenal of *Ralstonia solanacearum* type III effectors and their in planta functions. *Molecular Plant Pathology*. 2020;00:1–12. <https://doi.org/10.1111/mpp.12977>

## ANNEX 2: From effectors to effectomes: Are functional studies of individual effectors enough to decipher plant pathogen infectious strategies?

This opinion piece discusses the advances, challenges and limitations in the collective study of effectomes rather than effectors with a focus on the generation of polymutants and synthetic biology as promising strategies. It was submitted to PLOS Pathogens (submission date: 20/07/2020). The submitted draft is attached.

Arroyo-Velez et al

# **From effectors to effectomes: Are functional studies of individual effectors enough to decipher plant pathogen infectious strategies?**

Noe Arroyo Velez<sup>1,§</sup>, Manuel González Fuente<sup>1,§</sup>, Nemo Peeters<sup>1</sup>, Emmanuelle Lauber<sup>1</sup>, Laurent D. Noël<sup>1\*</sup>

<sup>1</sup>LIPM, Université de Toulouse, INRAE, CNRS, F-31326 Castanet-Tolosan, France

<sup>§</sup> Equal contributions

\*Author for correspondence: laurent.noel@inrae.fr

Effector proteins of plant pathogens are key virulence determinants secreted and often translocated inside plant cells where they subvert host immunity and physiology to the pathogen's benefit [1].

## **Achievements and limits of current effectors studies in plant pathogens**

A pathogen's effectome is the repertoire of all its effector proteins (Fig. 1A). To date, most effector proteins are studied individually, omitting the broader context in which they function as the effectome. Size and composition of effectomes vary greatly between pathogens, including at the intraspecific level, ranging from as little as four in *Erwinia amylovora* to hundreds of effector proteins per isolate in some fungi, nematodes and oomycetes [Fig. 2A, 2, 3-11]. These differences influence pathogen's virulence, lifestyle and host range [12-14]. Known effector functions are the result of a combination of experimental approaches, often low-throughput and based on *in vitro* or heterologous systems [Fig. 1B, Fig. 2C-D, 15]. Some effectome-scale screens have been conducted but these are still a compilation of individual effectors studies and thus present the same limitations as smaller-scale studies [16-20].

## **Evidences for effector-effector interferences within effectomes**

Studies of individual effector proteins intrinsically overlook their coordinated functions due to functional redundancy [21, 22], expression patterns dependent on infection stages or plant organ [23-25] and epistatic interactions within effectomes [26-29]. Therefore, effectome functions are usually not the sum of the individual effector functions (Fig. 1C) and dedicated experimental approaches would be needed to determine how effectomes function as a whole. Prerequisites are the knowledge of the effectome composition, an experimentally-manageable effectome size and a

genetically amenable pathogen. Consequently, functional characterization of effectomes is most advanced in bacteria [22, 26, 30, 31] and developing at an ever increasing pace in fungi or nematodes thanks to powerful genome editing tools [32, 33] and/or effector gene clustering [34].

### **Effectome functions depend on the plant target repertoire**

To achieve the functional characterization of effectomes we must take into account that effectors functions are host-dependent as they acquire their “functional sense” only in association with their plant cognate interactors (Fig. 2B). Effectors tend to target multiple highly connected host proteins [16, 20, 35, 36] but may also specifically interact with nucleic acids [37, 38] or metabolites from the pathogen or the host [39]. Therefore, the function of a full effectome largely depends on the host target repertoire, or “targetome”, as well as on the interactions among its components (Fig. 1C) as proposed [40]. Effector-mediated virulence is thus an emergent property resulting from interactions between a pathogen effectome and a susceptible host targetome [41]. Effectome and targetome diversity should therefore be carefully considered since it should unravel the complexity and the diversity of the molecular mechanisms underlying pathogen virulence and plant susceptibility.

### **Many lessons still to be learned from deconstructing effectomes**

Effector poly-mutants are interesting resources to unveil functions of effector families [17, 42-45] and effectomes [22, 26, 30]. Effector genes have to be deleted individually and sequentially. To date, the *Pseudomonas syringae* polymutant DC3000Δ36E is the only known mutant for a complex effectome in a plant pathogen [26]. In *P. syringae*, such effectome mutant has allowed significant discoveries not only in our understanding of the role of individual effectors but most importantly in the identification of functionally redundant effectors [22] and the definition of minimal effectome functions required to become a plant pathogen [26, 30, 31]. To reach its full potential, we believe that future mutagenesis should aim at partial random deconstruction of effectomes using highly efficient tools such as CRISPR-cas9 coupled to sensitive high-throughput pathogenicity assays on automated phenotyping infrastructures.

### **Synthetic effectomes to understand how effectomes really function**

Effectome mutants open the possibility to reconstruct synthetic effectomes and test for their function. The choice of the receiver strain and the composition and size of the minimal effectomes to be tested in infection tests have to be carefully considered (Fig. 2E). While environmental effectorless strains often require the introduction of a functional effector secretion-translocation machinery [46,

47], effectome mutants might still express and translocate yet unidentified effectors that could interfere with the characterization of synthetic effectomes [26, 30]. Because of functional redundancy between effectors, functional synthetic effectomes can include only a portion of an original effectome [e.g., 30]. Effectors originating from other strains, species, genera or even kingdoms could also be studied by such approaches as long as effector secretion-translocation happens [e.g., 48, 49, 50]. Though sometimes random [30], effector combinations have, up to now, been mostly based on gene families [45], gene clusters [30] or functional categories [22]. Yet, the combination of synthetic biology, next generation sequencing technologies and high throughput phenotyping methods now opens the avenue for the generation of large random effector libraries to be tested in minimal strains and their functional characterization on host or nonhost plants (Fig. 2F).

We believe that such holistic genetic approaches applied to effectomes should greatly advance our understanding of two basic questions: how do pathogens evolve and adapt to new hosts?

## Figure legends

**Figure 1:** Functions achieved by an effectome are more than the sole addition of the individual effector functions. (A) The effectome is the sum of the  $n$  individual effectors from a single pathogen strain. (B) Examples of functional studies which can be conducted for each of the  $n$  effector proteins of a given effectome. PTI, PAMP-triggered immunity; ETI, effector-triggered immunity; Y2H, yeast two-hybrid; co-IPs, co-immunoprecipitations; FRET, Foster resonance energy transfer. (C) Due to functional redundancies and epistatic interactions, the effectome function is different from the sum of individual effector functions. Importantly, effector and effectome functions will depend on the composition and diversity of effector targets present in the plant species and accession considered.

**Figure 2:** Diversity of both the microbial effectome and the plant target repertoire impacts the function of the effectome. (A) Effectomes are diverse at the intra- and inter-specific levels. (B) Individual effector can have one or multiple plant targets with either positive (arrowheads) or negative (blunt arrows) impacts. Hubs are plant proteins or functions which are targeted by multiple effectors. Some effectors might directly or indirectly affect the function of other effectors. To date, plant functions targeted by effectors are immunity, physiology and metabolism. Distinct plant targets are affected depending on the pathogen effectome. Target diversity implies that different plant accessions will respond differently to distinct effectomes. (C-E) Schematic representation of possible genetic manipulations of effectomes. The effectome of wild-type (WT) strain B (C) can be genetically manipulated by deleting individual (D) or multiple effector genes yielding an effectome mutant (E). Effectorless strains found in the environment can also be used and complemented with the appropriate



effector secretion-translocation machinery if missing. Examples of random or informed libraries corresponding to an effector combinatorial originating from strain B or any other strain could be reintroduced in an effectorless strain (E) and tested for functional complementations on host or nonhost plants of multiple cultivars (F). Each symbol represents a distinct effector produced by the pathogen. Members of a given effector protein family are represented with the same shape but different colours.

## Acknowledgements:

We are grateful to Jonathan Jacobs (Ohio State University, Ohio) for critically reading this manuscript. NAV and MGF were supported by PhD fellowships from the Mexican National Council of Science and Technology (CONACYT) and the French Laboratory of Excellence project ‘TULIP’ (ANR-10-LABX-41; ANR-11-IDEX-0002-02), respectively. EL, NP and LDN were supported by grants from the French National Research Agency (PAPTiCROPS ANR-16-CE21-0005-02 and NEPHRON ANR-18-CE20-0020-01). The LIPM is supported by the French Laboratory of Excellence project ‘TULIP’ (ANR-10-LABX-41; ANR-11-IDEX-0002-02). Authors benefited from the COST actions FA1208 SUSTAIN and CA16107 EuroXanth.

## References

1. Toruno TY, Stergiopoulos I, Coaker G. Plant-Pathogen Effectors: Cellular Probes Interfering with Plant Defenses in Spatial and Temporal Manners. *Annu Rev Phytopathol.* 2016;54:419-41. Epub 2016/07/01. doi: 10.1146/annurev-phyto-080615-100204. PubMed PMID: 27359369; PubMed Central PMCID: PMC5283857.
2. Kim KT, Jeon J, Choi J, Cheong K, Song H, Choi G, et al. Kingdom-Wide Analysis of Fungal Small Secreted Proteins (SSPs) Reveals their Potential Role in Host Association. *Front Plant Sci.* 2016;7:186. Epub 2016/03/01. doi: 10.3389/fpls.2016.00186. PubMed PMID: 26925088; PubMed Central PMCID: PMC4759460.
3. Nissinen RM, Ytterberg AJ, Bogdanove AJ, KJ VANW, Beer SV. Analyses of the secretomes of *Erwinia amylovora* and selected *hrp* mutants reveal novel type III secreted proteins and an effect of HrpJ on extracellular harpin levels. *Mol Plant Pathol.* 2007;8(1):55-67. Epub 2007/01/01. doi: 10.1111/j.1364-3703.2006.00370.x. PubMed PMID: 20507478.
4. Bogdanove AJ, Kim JF, Wei ZM, Kolchinsky P, Charkowski AO, Conlin AK, et al. Homology and functional similarity of an *hrp*-linked pathogenicity locus, *dspEF*, of *Erwinia amylovora* and the avirulence locus *avrE* of *Pseudomonas syringae* pathovar tomato. *Proc Natl Acad Sci U S A.* 1998;95(3):1325-30.
5. Zhao Y, He SY, Sundin GW. The *Erwinia amylovora avrRpt2EA* gene contributes to virulence on pear and *AvrRpt2EA* is recognized by Arabidopsis RPS2 when expressed in *pseudomonas syringae*. *Mol Plant*

- 137 Microbe Interact. 2006;19(6):644-54. Epub 2006/06/17. doi: 10.1094/MPMI-19-0644. PubMed PMID:  
138 16776298.
- 139 6. Schuster M, Schweizer G, Kahmann R. Comparative analyses of secreted proteins in plant pathogenic  
140 smut fungi and related basidiomycetes. Fungal Genet Biol. 2018;112:21-30. Epub 2017/01/17. doi:  
141 10.1016/j.fgb.2016.12.003. PubMed PMID: 28089076.
- 142 7. Dillon MM, Almeida RND, Laflamme B, Martel A, Weir BS, Desveaux D, et al. Molecular Evolution  
143 of *Pseudomonas syringae* Type III Secreted Effector Proteins. Front Plant Sci. 2019;10:418. Epub 2019/04/27.  
144 doi: 10.3389/fpls.2019.00418. PubMed PMID: 31024592; PubMed Central PMCID: PMC6460904.
- 145 8. Vieira P, Gleason C. Plant-parasitic nematode effectors - insights into their diversity and new tools for  
146 their identification. Curr Opin Plant Biol. 2019;50:37-43. Epub 2019/03/29. doi: 10.1016/j.pbi.2019.02.007.  
147 PubMed PMID: 30921686.
- 148 9. Roux B, Bolot S, Guy E, Denance N, Lautier M, Jardinaud MF, et al. Genomics and transcriptomics  
149 of *Xanthomonas campestris* species challenge the concept of core type III effectome. BMC Genomics.  
150 2015;16:975. doi: 10.1186/s12864-015-2190-0. PubMed PMID: 26581393; PubMed Central PMCID:  
151 PMC64652430.
- 152 10. Sabbagh CRR, Carrere S, Lonjon F, Vailleau F, Macho AP, Genin S, et al. Pangenomic type III  
153 effector database of the plant pathogenic *Ralstonia* spp. PeerJ. 2019;7:e7346. Epub 2019/10/04. doi:  
154 10.7717/peerj.7346. PubMed PMID: 31579561; PubMed Central PMCID: PMC6762002.
- 155 11. Badet T, Oggenfuss U, Abraham L, McDonald BA, Croll D. A 19-isolate reference-quality global  
156 pangenome for the fungal wheat pathogen *Zymoseptoria tritici*. BMC Biol. 2020;18(1):12. Epub 2020/02/13.  
157 doi: 10.1186/s12915-020-0744-3. PubMed PMID: 32046716; PubMed Central PMCID: PMC67014611.
- 158 12. Sarkar SF, Gordon JS, Martin GB, Guttman DS. Comparative genomics of host-specific virulence in  
159 *Pseudomonas syringae*. Genetics. 2006;174(2):1041-56. Epub 2006/09/05. doi: 10.1534/genetics.106.060996.  
160 PubMed PMID: 16951068; PubMed Central PMCID: PMC1602070.
- 161 13. Liao J, Huang H, Meusnier I, Adreit H, Ducasse A, Bonnot F, et al. Pathogen effectors and plant  
162 immunity determine specialization of the blast fungus to rice subspecies. eLife. 2016;5. Epub 2016/12/23. doi:  
163 10.7554/eLife.19377. PubMed PMID: 28008850; PubMed Central PMCID: PMC5182064.
- 164 14. Gaulin E, Pel MJC, Camborde L, San-Clemente H, Courbier S, Dupouy MA, et al. Genomics analysis  
165 of *Aphanomyces* spp. identifies a new class of oomycete effector associated with host adaptation. BMC Biol.  
166 2018;16(1):43. Epub 2018/04/20. doi: 10.1186/s12915-018-0508-5. PubMed PMID: 29669603; PubMed  
167 Central PMCID: PMC5907361.
- 168 15. Dalio RJD, Herlihy J, Oliveira TS, McDowell JM, Machado M. Effector Biology in Focus: A Primer  
169 for Computational Prediction and Functional Characterization. Mol Plant Microbe Interact. 2018;31(1):22-33.  
170 Epub 2017/10/13. doi: 10.1094/MPMI-07-17-0174-FI. PubMed PMID: 29023190.
- 171 16. Mukhtar MS, Carvunis AR, Dreze M, Epple P, Steinbrenner J, Moore J, et al. Independently evolved  
172 virulence effectors converge onto hubs in a plant immune system network. Science. 2011;333(6042):596-601.  
173 Epub 2011/07/30. doi: 10.1126/science.1203659. PubMed PMID: 21798943; PubMed Central PMCID:  
174 PMC3170753.

- 175 17. Chen S, Songkumarn P, Venu RC, Gowda M, Bellizzi M, Hu J, et al. Identification and  
176 characterization of in planta-expressed secreted effector proteins from *Magnaporthe oryzae* that induce cell  
177 death in rice. *Mol Plant Microbe Interact.* 2013;26(2):191-202. Epub 2012/10/06. doi: 10.1094/MPMI-05-12-  
178 0117-R. PubMed PMID: 23035914.
- 179 18. Popov G, Fraiture M, Brunner F, Sessa G. Multiple *Xanthomonas euvesicatoria* Type III Effectors  
180 Inhibit flg22-Triggered Immunity. *Mol Plant Microbe Interact.* 2016;29(8):651-60. Epub 2016/08/17. doi:  
181 10.1094/MPMI-07-16-0137-R. PubMed PMID: 27529660.
- 182 19. Robin GP, Kleemann J, Neumann U, Cabre L, Dallery JF, Lapalu N, et al. Subcellular Localization  
183 Screening of *Colletotrichum higginsianum* Effector Candidates Identifies Fungal Proteins Targeted to Plant  
184 Peroxisomes, Golgi Bodies, and Microtubules. *Front Plant Sci.* 2018;9:562. Epub 2018/05/18. doi:  
185 10.3389/fpls.2018.00562. PubMed PMID: 29770142; PubMed Central PMCID: PMC5942036.
- 186 20. González-Fuente M, Carrère S, Monachello D, Marsella BG, Cazalé A-C, Zischek C, et al. EffectorK,  
187 a comprehensive resource to mine for *Ralstonia*, *Xanthomonas* and other published effector interactors in the  
188 Arabidopsis proteome. *Mol Plant Pathol.* 2020;in press.
- 189 21. Friesen TL, Zhang Z, Solomon PS, Oliver RP, Faris JD. Characterization of the interaction of a novel  
190 *Stagonospora nodorum* host-selective toxin with a wheat susceptibility gene. *Plant Physiol.* 2008;146(2):682-  
191 93. Epub 2007/12/11. doi: 10.1104/pp.107.108761. PubMed PMID: 18065563; PubMed Central PMCID:  
192 PMCPMC2245837.
- 193 22. Kvitko BH, Park DH, Velasquez AC, Wei CF, Russell AB, Martin GB, et al. Deletions in the repertoire  
194 of *Pseudomonas syringae* pv. *tomato* DC3000 type III secretion effector genes reveal functional overlap among  
195 effectors. *PLoS Pathog.* 2009;5(4):e1000388. Epub 2009/04/22. doi: 10.1371/journal.ppat.1000388. PubMed  
196 PMID: 19381254; PubMed Central PMCID: PMC2663052.
- 197 23. Kleemann J, Rincon-Rivera LJ, Takahara H, Neumann U, Ver Loren van Themaat E, van der Does  
198 HC, et al. Sequential delivery of host-induced virulence effectors by appressoria and intracellular hyphae of  
199 the phytopathogen *Colletotrichum higginsianum*. *PLoS Pathog.* 2012;8(4):e1002643. Epub 2012/04/13. doi:  
200 10.1371/journal.ppat.1002643. PubMed PMID: 22496661; PubMed Central PMCID: PMCPMC3320591.
- 201 24. Wang Q, Han C, Ferreira AO, Yu X, Ye W, Tripathy S, et al. Transcriptional programming and  
202 functional interactions within the *Phytophthora sojae* RXLR effector repertoire. *Plant Cell.* 2011;23(6):2064-  
203 86. Epub 2011/06/10. doi: 10.1105/tpc.111.086082. PubMed PMID: 21653195; PubMed Central PMCID:  
204 PMCPMC3160037.
- 205 25. Skibbe DS, Doehleemann G, Fernandes J, Walbot V. Maize tumors caused by *Ustilago maydis* require  
206 organ-specific genes in host and pathogen. *Science.* 2010;328(5974):89-92. Epub 2010/04/03. doi:  
207 10.1126/science.1185775. PubMed PMID: 20360107.
- 208 26. Wei HL, Chakravarthy S, Mathieu J, Helmann TC, Stodghill P, Swingle B, et al. *Pseudomonas*  
209 *syringae* pv. *tomato* DC3000 Type III Secretion Effector Polymutants Reveal an Interplay between HopAD1  
210 and AvrPtoB. *Cell Host Microbe.* 2015;17(6):752-62. Epub 2015/06/13. doi: 10.1016/j.chom.2015.05.007.  
211 PubMed PMID: 26067603; PubMed Central PMCID: PMCPMC4471848.

- 212 27. Phan HT, Rybak K, Furuki E, Breen S, Solomon PS, Oliver RP, et al. Differential effector gene  
213 expression underpins epistasis in a plant fungal disease. *Plant J.* 2016;87(4):343-54. Epub 2016/05/03. doi:  
214 10.1111/tpj.13203. PubMed PMID: 27133896; PubMed Central PMCID: PMCPMC5053286.
- 215 28. Guo X, Zhong D, Xie W, He Y, Zheng Y, Lin Y, et al. Functional Identification of Novel Cell Death-  
216 inducing Effector Proteins from *Magnaporthe oryzae*. *Rice (N Y).* 2019;12(1):59. Epub 2019/08/08. doi:  
217 10.1186/s12284-019-0312-z. PubMed PMID: 31388773; PubMed Central PMCID: PMCPMC6684714.
- 218 29. Wei HL, Zhang W, Collmer A. Modular Study of the Type III Effector Repertoire in *Pseudomonas*  
219 *syringae* pv. *tomato* DC3000 Reveals a Matrix of Effector Interplay in Pathogenesis. *Cell Rep.*  
220 2018;23(6):1630-8. Epub 2018/05/10. doi: 10.1016/j.celrep.2018.04.037. PubMed PMID: 29742421.
- 221 30. Cunnac S, Chakravarthy S, Kvitko BH, Russell AB, Martin GB, Collmer A. Genetic disassembly and  
222 combinatorial reassembly identify a minimal functional repertoire of type III effectors in *Pseudomonas*  
223 *syringae*. *Proc Natl Acad Sci U S A.* 2011;108(7):2975-80. Epub 2011/02/02. doi: 10.1073/pnas.1013031108.  
224 PubMed PMID: 21282655; PubMed Central PMCID: PMCPMC3041132.
- 225 31. Wei HL, Collmer A. Defining essential processes in plant pathogenesis with *Pseudomonas syringae*  
226 pv. *tomato* DC3000 disarmed polymutants and a subset of key type III effectors. *Mol Plant Pathol.*  
227 2018;19(7):1779-94. Epub 2017/12/27. doi: 10.1111/mpp.12655. PubMed PMID: 29277959; PubMed Central  
228 PMCID: PMCPMC6638048.
- 229 32. Nodvig CS, Nielsen JB, Kogle ME, Mortensen UH. A CRISPR-Cas9 System for Genetic Engineering  
230 of Filamentous Fungi. *PLoS One.* 2015;10(7):e0133085. Epub 2015/07/16. doi:  
231 10.1371/journal.pone.0133085. PubMed PMID: 26177455; PubMed Central PMCID: PMCPMC4503723.
- 232 33. Friedland AE, Tzur YB, Esvelt KM, Colaiacovo MP, Church GM, Calarco JA. Heritable genome  
233 editing in *C. elegans* via a CRISPR-Cas9 system. *Nat Methods.* 2013;10(8):741-3. Epub 2013/07/03. doi:  
234 10.1038/nmeth.2532. PubMed PMID: 23817069; PubMed Central PMCID: PMCPMC3822328.
- 235 34. Kamper J, Kahmann R, Bolker M, Ma LJ, Brefort T, Saville BJ, et al. Insights from the genome of the  
236 biotrophic fungal plant pathogen *Ustilago maydis*. *Nature.* 2006;444(7115):97-101. Epub 2006/11/03. doi:  
237 10.1038/nature05248. PubMed PMID: 17080091.
- 238 35. Li H, Zhou Y, Zhang Z. Network Analysis Reveals a Common Host-Pathogen Interaction Pattern in  
239 *Arabidopsis* Immune Responses. *Front Plant Sci.* 2017;8:893. Epub 2017/06/15. doi:  
240 10.3389/fpls.2017.00893. PubMed PMID: 28611808; PubMed Central PMCID: PMCPMC5446985.
- 241 36. Ahmed H, Howton TC, Sun Y, Weinberger N, Belkhadir Y, Mukhtar MS. Network biology discovers  
242 pathogen contact points in host protein-protein interactomes. *Nat Commun.* 2018;9(1):2312. Epub 2018/06/15.  
243 doi: 10.1038/s41467-018-04632-8. PubMed PMID: 29899369; PubMed Central PMCID: PMCPMC5998135.
- 244 37. Boch J, Scholze H, Schornack S, Landgraf A, Hahn S, Kay S, et al. Breaking the code of DNA binding  
245 specificity of TAL-type III effectors. *Science.* 2009;326(5959):1509-12. Epub 2009/11/26. doi:  
246 10.1126/science.1178811. PubMed PMID: 19933107.
- 247 38. Moscou MJ, Bogdanove AJ. A simple cipher governs DNA recognition by TAL effectors. *Science.*  
248 2009;326(5959):1501. Epub 2009/11/26. doi: 10.1126/science.1178817. PubMed PMID: 19933106.

39. de Jonge R, van Esse HP, Kombrink A, Shinya T, Desaki Y, Bours R, et al. Conserved fungal LysM effector Ecp6 prevents chitin-triggered immunity in plants. *Science*. 2010;329(5994):953-5. Epub 2010/08/21. doi: 10.1126/science.1190859. PubMed PMID: 20724636.
40. Hajri A, Brin C, Hunault G, Lardeux F, Lemaire C, Manceau C, et al. A "repertoire for repertoire" hypothesis: repertoires of type three effectors are candidate determinants of host specificity in *Xanthomonas*. *PLoS One*. 2009;4(8):e6632. Epub 2009/08/15. doi: 10.1371/journal.pone.0006632. PubMed PMID: 19680562; PubMed Central PMCID: PMC2722093.
41. Casadevall A, Fang FC, Pirofski LA. Microbial virulence as an emergent property: consequences and opportunities. *PLoS Pathog*. 2011;7(7):e1002136. Epub 2011/08/05. doi: 10.1371/journal.ppat.1002136. PubMed PMID: 21814511; PubMed Central PMCID: PMC3141035.
42. Angot A, Peeters N, Lechner E, Vailleau F, Baud C, Gentzbittel L, et al. *Ralstonia solanacearum* requires F-box-like domain-containing type III effectors to promote disease on several host plants. *Proc Natl Acad Sci U S A*. 2006;103(39):14620-5. Epub 2006/09/20. doi: 10.1073/pnas.0509393103. PubMed PMID: 16983093; PubMed Central PMCID: PMC1600009.
43. Khrunyk Y, Munch K, Schipper K, Lupas AN, Kahmann R. The use of FLP-mediated recombination for the functional analysis of an effector gene family in the biotrophic smut fungus *Ustilago maydis*. *New Phytol*. 2010;187(4):957-68. Epub 2010/08/03. doi: 10.1111/j.1469-8137.2010.03413.x. PubMed PMID: 20673282.
44. Sole M, Popa C, Mith O, Sohn KH, Jones JD, Deslandes L, et al. The awr gene family encodes a novel class of *Ralstonia solanacearum* type III effectors displaying virulence and avirulence activities. *Mol Plant Microbe Interact*. 2012;25(7):941-53. Epub 2012/03/15. doi: 10.1094/MPMI-12-11-0321. PubMed PMID: 22414437.
45. Kay S, Boch J, Bonas U. Characterization of AvrBs3-like effectors from a Brassicaceae pathogen reveals virulence and avirulence activities and a protein with a novel repeat architecture. *Mol Plant Microbe Interact*. 2005;18(8):838-48. Epub 2005/09/02. doi: 10.1094/MPMI-18-0838. PubMed PMID: 16134896.
46. Collmer A, Badel JL, Charkowski AO, Deng WL, Fouts DE, Ramos AR, et al. *Pseudomonas syringae* Hrp type III secretion system and effector proteins. *Proc Natl Acad Sci U S A*. 2000;97(16):8770-7. Epub 2000/08/02. PubMed PMID: 10922033; PubMed Central PMCID: PMC34010.
47. Meline V, Delage W, Brin C, Li-Marchetti C, Sochard D, Arlat M, et al. Role of the acquisition of a type 3 secretion system in the emergence of novel pathogenic strains of *Xanthomonas*. *Mol Plant Pathol*. 2019;20(1):33-50. Epub 2018/08/05. doi: 10.1111/mpp.12737. PubMed PMID: 30076773; PubMed Central PMCID: PMC6430459.
48. Upadhyaya NM, Mago R, Staskawicz BJ, Ayliffe MA, Ellis JG, Dodds PN. A bacterial type III secretion assay for delivery of fungal effector proteins into wheat. *Mol Plant Microbe Interact*. 2014;27(3):255-64. Epub 2013/10/26. doi: 10.1094/MPMI-07-13-0187-FI. PubMed PMID: 24156769.
49. Sohn KH, Lei R, Nemri A, Jones JD. The downy mildew effector proteins ATR1 and ATR13 promote disease susceptibility in *Arabidopsis thaliana*. *Plant Cell*. 2007;19(12):4077-90. Epub 2008/01/01. doi: 10.1105/tpc.107.054262. PubMed PMID: 18165328; PubMed Central PMCID: PMC2217653.

- 287 50. Fabro G, Steinbrenner J, Coates M, Ishaque N, Baxter L, Studholme DJ, et al. Multiple candidate  
288 effectors from the oomycete pathogen *Hyaloperonospora arabidopsidis* suppress host plant immunity. PLoS  
289 Pathog. 2011;7(11):e1002348. Epub 2011/11/11. doi: 10.1371/journal.ppat.1002348. PubMed PMID:  
290 22072967; PubMed Central PMCID: PMC3207932.

291

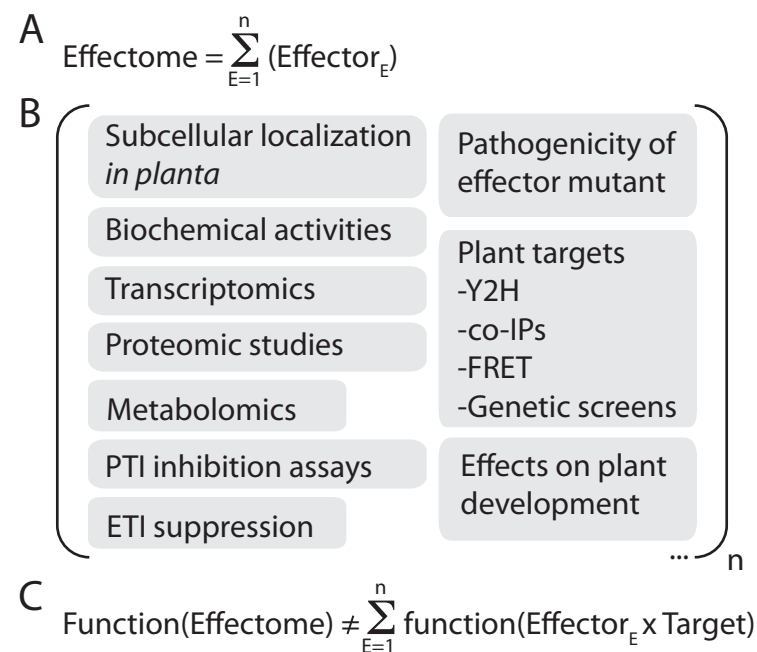


Figure 1: Functions achieved by an effectome are more than the sole addition of the individual effector functions. (A) The effectome is the sum of the  $n$  individual effectors from a single pathogen strain. (B) Examples of functional studies which can be conducted for each of the  $n$  effector proteins of a given effectome. PTI, PAMP-triggered immunity; ETI, effector-triggered immunity; Y2H, yeast two-hybrid; co-IPs, co-immunoprecipitations; FRET, Foster resonance energy transfer. (C) Due to functional redundancies and epistatic interactions, the effectome function is different from the sum of individual effector functions. Importantly, effector and effectome functions will depend on the composition and diversity of effector targets present in the plant species and accession considered.

## Figure 1

Arroyo Velez et al

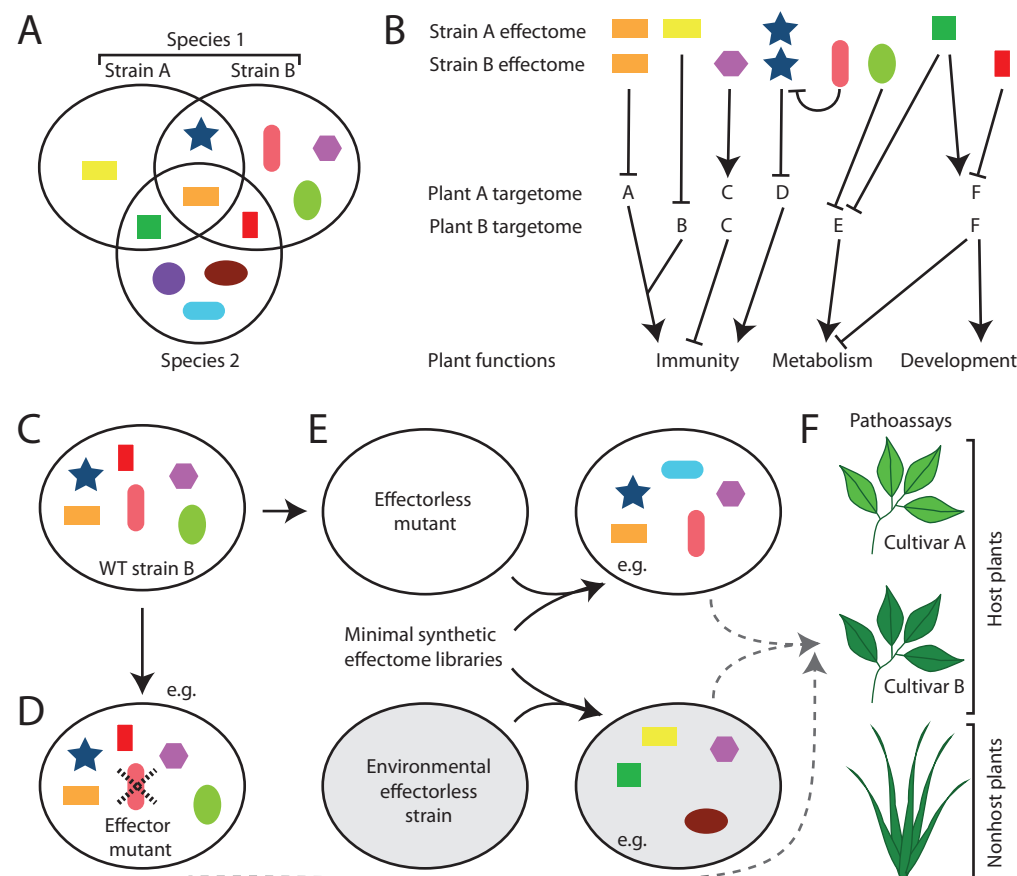


Figure 2: Diversity of both the microbial effectome and the plant target repertoire impacts the function of the effectome. (A) Effectomes are diverse at the intra- and inter-specific levels. (B) Individual effector can have one or multiple plant targets with either positive (arrowheads) or negative (blunt arrows) impacts. Hubs are plant proteins or functions which are targeted by multiple effectors. Some effectors might directly or indirectly affect the function of other effectors. To date, plant functions targeted by effectors are immunity, physiology and metabolism. Distinct plant targets are affected depending on the pathogen effectome. Target diversity implies that different plant accessions will respond differently to distinct effectomes. (C-E) Schematic representation of possible genetic manipulations of effectomes. The effectome of wild-type (WT) strain B (C) can be genetically manipulated by deleting individual (D) or multiple effector genes yielding an effectome mutant (E). Effectorless strains found in the environment can also be used and complemented with the appropriate effector secretion-translocation machinery if missing. Examples of random or informed libraries corresponding to an effector combinatorial originating from strain B or any other strain can be introduced in an effectorless strain (E) and tested for functional complementations on host or nonhost plants of multiple cultivars (F). Each symbol represents a distinct effector produced by the pathogen. Members of a given effector protein family are represented with the same shape but different colours.

**Figure 2**  
Arroyo Velez et al